frontiers | Research Topics

Mountainous forest ecosystems: Challenges and management implications

Edited by
Shreekar Pant, Jahangeer A. Bhat, Zishan Ahmad Wani,
K. V. Satish and Vikram S. Negi

Published in
Frontiers in Forests and Global Change

November 2023

ISSN 1664-8714
ISBN 978-2-8325-3891-3
DOI 10.3389/978-2-8325-3891-3

About Frontiers

Frontiers is more than just an open access publisher of scholarly articles: it is a pioneering approach to the world of academia, radically improving the way scholarly research is managed. The grand vision of Frontiers is a world where all people have an equal opportunity to seek, share and generate knowledge. Frontiers provides immediate and permanent online open access to all its publications, but this alone is not enough to realize our grand goals.

Frontiers journal series

The Frontiers journal series is a multi-tier and interdisciplinary set of open-access, online journals, promising a paradigm shift from the current review, selection and dissemination processes in academic publishing. All Frontiers journals are driven by researchers for researchers; therefore, they constitute a service to the scholarly community. At the same time, the *Frontiers journal series* operates on a revolutionary invention, the tiered publishing system, initially addressing specific communities of scholars, and gradually climbing up to broader public understanding, thus serving the interests of the lay society, too.

Dedication to quality

Each Frontiers article is a landmark of the highest quality, thanks to genuinely collaborative interactions between authors and review editors, who include some of the world's best academicians. Research must be certified by peers before entering a stream of knowledge that may eventually reach the public - and shape society; therefore, Frontiers only applies the most rigorous and unbiased reviews. Frontiers revolutionizes research publishing by freely delivering the most outstanding research, evaluated with no bias from both the academic and social point of view. By applying the most advanced information technologies, Frontiers is catapulting scholarly publishing into a new generation.

What are Frontiers Research Topics?

Frontiers Research Topics are very popular trademarks of the *Frontiers journals series*: they are collections of at least ten articles, all centered on a particular subject. With their unique mix of varied contributions from Original Research to Review Articles, Frontiers Research Topics unify the most influential researchers, the latest key findings and historical advances in a hot research area.

Find out more on how to host your own Frontiers Research Topic or contribute to one as an author by contacting the Frontiers editorial office: frontiersin.org/about/contact

Mountainous forest ecosystems: Challenges and management implications

Topic editors

Shreekar Pant — Baba Ghulam Shah Badshah University, India
Jahangeer A. Bhat — Fiji National University, Fiji
Zishan Ahmad Wani — Baba Ghulam Shah Badshah University, India
K. V. Satish — Banaras Hindu University, India
Vikram S. Negi — Govind Ballabh Pant National Institute of Himalayan Environment and Sustainable Development, India

Citation

Pant, S., Bhat, J. A., Wani, Z. A., Satish, K. V., Negi, V. S., eds. (2023). *Mountainous forest ecosystems: Challenges and management implications*.
Lausanne: Frontiers Media SA. doi: 10.3389/978-2-8325-3891-3

Table of contents

05 Editorial: Mountainous forest ecosystems: challenges and management implications
Shreekar Pant, Jahangeer A. Bhat, Zishan Ahmad Wani, K. V. Satish and Vikram S. Negi

08 Phyto-ecological analysis of *Phytolacca acinosa* Roxb. assemblages in Kashmir Himalaya, India
Junaid A. Magray, Bilal A. Wani, Tajamul Islam, Aijaz H. Ganie and Irshad A. Nawchoo

21 Conservation Priority Index of species, communities, and habitats for biodiversity conservation and their management planning: A case study in Gulmarg Wildlife Sanctuary, Kashmir Himalaya
Zishan A. Wani, Jahangeer A. Bhat, Vikram S. Negi, K. V. Satish, Sazada Siddiqui and Shreekar Pant

37 Ensemble modeling to predict the impact of future climate change on the global distribution of *Olea europaea* subsp. *cuspidata*
Sajid Khan and Susheel Verma

50 Water–energy, climate, and habitat heterogeneity mutually drives spatial pattern of tree species richness in the Indian Western Himalaya
Shinny Thakur, Rupesh Dhyani, Vikram S. Negi and Indra D. Bhatt

63 Floristic composition, biological spectrum, and phytogeographic distribution of the Bin Dara Dir, in the western boundary of Pakistan
Fazal Manan, Shujaul Mulk Khan, Zahir Muhammad, Zeeshan Ahmad, Abdullah Abdullah, Amjad ur Rahman, Heesup Han, Antonio Ariza-Montes, Nicolás Contreras-Barraza and António Raposo

79 Tree rings of *Rhododendron arboreum* portray signal of monsoon precipitation in the Himalayan region
Rupesh Dhyani, Amalava Bhattacharyya, Rajesh Joshi, Mayank Shekhar, Jagdish Chandra Kuniyal and Parminder Singh Ranhotra

91 Land use/land cover change and its implication on soil erosion in an ecologically sensitive Himachal Himalayan watershed, Northern India
Manthena Prashanth, Arun Kumar, Sunil Dhar, Omkar Verma, Shashi Kant Rai and Beena Kouser

108 Elevation, aspect, and habitat heterogeneity determine plant diversity and compositional patterns in the Kashmir Himalaya
Zishan A. Wani, Vikram S. Negi, Jahangeer A. Bhat, K. V. Satish, Ashish Kumar, Sajid Khan, Rupesh Dhyani, Sazada Siddiqui, Rahmah N. Al-Qthanin and Shreekar Pant

121 Vertical distribution differences of the understory herbs and their driving factors on shady and sunny slopes in high altitude mountainous areas
Jiahua Han, Huiyan Yin, Jie Xue, Zhiwei Zhang, Zhen Xing, Shunke Wang, Jingjing Chang, Xiaoqiang Chen and Bo Yu

133 Elevational patterns of soil nematode diversity, community structure and metabolic footprint in the Trikuta mountains of Northwestern Himalaya
Fozia Choudhary, Anil Bhardwaj, Iqra Sayeed, Shabir Ahmad Rather, Mohammad Abdul Hannan Khan and Ali Asghar Shah

148 Altitudinal gradient drives significant changes in soil physico-chemical and eco-physiological properties of *Rhododendron anthopogon*: a case study from Himalaya
Zahid Ahmed Mangral, Shahid Ul Islam, Lubna Tariq, Sharanjeet Kaur, Rameez Ahmad, Akhtar H. Malik, Shailendra Goel, Ratul Baishya, Saroj Kanta Barik and Tanvir Ul Hassan Dar

164 The effects of forest types and age groups on forest provisioning and supporting service value in Sanhu Nature Reserve, Northeast China
Qiang Liu, Yan Cheng, Fang Yu and Chunnan Fan

178 Effect of forest fire on tree diversity and regeneration in the forests of Uttarakhand, Western Himalaya, India
Himanshu Bargali, Dinesh Bhatt, Rakesh Chandra Sundriyal, Virendra Pratap Uniyal, Aseesh Pandey and Ram Ranjan

188 Modeling decline of mountain range forest using survival analysis
Thakur Dhakal, Ki Hwan Cho, Su-Jin Kim and Mu-Sup Beon

200 Dry matter dynamics and carbon flux along riverine forests of Gori valley, Western Himalaya
Soni Bisht, Surendra Singh Bargali, Kiran Bargali, Yashwant Singh Rawat and Gopal Singh Rawat

frontiers | Frontiers in Forests and Global Change

TYPE Editorial
PUBLISHED 25 October 2023
DOI 10.3389/ffgc.2023.1300020

Editorial: Mountainous forest ecosystems: challenges and management implications

Shreekar Pant[1], Jahangeer A. Bhat[2], Zishan Ahmad Wani[3]*, K. V. Satish[4] and Vikram S. Negi[5]

[1]Centre for Biodiversity Studies, Baba Ghulam Shah Badshah University, Rajouri, India, [2]Piramal Foundation for Education Leadership (State Transformation Program), Jammu and Kashmir, India, [3]Conservation Ecology Lab, Department of Botany, Baba Ghulam Shah Badshah University, Rajouri, India, [4]Remote Sensing Laboratory, Institute of Environment and Sustainable Development, Banaras Hindu University, Varanasi, India, [5]Center for Biodiversity Conservation and Management, G. B. Pant, National Institute of Himalayan Environment, Almora, Uttarakhand, India

OPEN ACCESS

EDITED AND REVIEWED BY
Susanna Nocentini,
University of Florence, Italy

*CORRESPONDENCE
Zishan Ahmad Wani
✉ zishanwani786@gmail.com

RECEIVED 23 September 2023
ACCEPTED 16 October 2023
PUBLISHED 25 October 2023

CITATION
Pant S, Bhat JA, Wani ZA, Satish KV and Negi VS (2023) Editorial: Mountainous forest ecosystems: challenges and management implications.
Front. For. Glob. Change 6:1300020.
doi: 10.3389/ffgc.2023.1300020

KEYWORDS

mountain ecosystems, species diversity, ecosystem services, threats, conservation

Editorial on the Research Topic
Mountainous forest ecosystems: challenges and management implications

Mountains have a rich natural and human history and are dynamic landscapes. Mountains provide the perfect environment for biodiversity to flourish due to their varied topography and isolated biogeography. In fact, mountainous regions are home to half of the 34 global diversity hotspots and one-third of the terrestrial biodiversity (Gebrehiwot et al., 2019). However, mountains are more vulnerable to environmental deterioration brought on by increasing weather extremes that disrupt hillslope stability, and raise the risk of landslides, which could have serious negative effects on soil fertility, water quality, sediment deposition, and human habitation as well as fatalities and property destruction (Karpouzoglou et al., 2020). An explicit investigation of patterns in species richness and knowledge of the factors influencing these patterns are essential for the conservation and management of biodiversity. In order to address issues related to biodiversity conservation and sustainable development, we have gathered 15 research articles in the present Research Topic that illustrate the ecology and management of mountain forest ecosystems.

Any area's floristic composition contains important data regarding the diversity and distribution of plants (Wani and Pant, 2023a). Additionally, it results in the accurate identification of plant species, aiding in their scientific and methodical conservation (Wani and Pant, 2023b). The floristic composition, biological spectrum, and phytogeographical components of Pakistan's western boundary along the Bin Dara were evaluated by Manan et al.. Understanding community structure, organization, and their response to changes in other environmental factors requires phyto-ecological studies. Magray et al. examined the relationships between the soil and phytosociological characteristics of *Phytolacca acinosa* communities. Understanding the patterns and processes of biodiversity depends on the analysis of species richness along a broad geographic gradient (Costa et al., 2023). Because of their sharp ecological gradients, mountain forest ecosystems are hotspots for biodiversity. Elevational gradient, slope, and aspect provide a singular opportunity to investigate how different plant species react to shifting environmental factors. Wani et al. concluded that floristic diversity should be studied not only with reference to elevational gradients but also with regards to aspects and habitats in their research article after analyzing the species diversity and distribution patterns with respect to altitude, aspect, and habitat types in the Kashmir Himalayas. Thakur et al. developed a species richness map by stacking the ranges of 51 tree species along an elevational gradient in the Western Himalaya using stacked species distribution models (SSDMs). For revealing the environmental gradient change law of plant diversity, it is crucial to comprehend the vertical distribution of undergrowth herbaceous plants in high altitude mountain areas (Chitale et al., 2014). However, it is still unclear how diversity and environmental factors interact as well as the species composition of herbaceous plants across various altitude gradients. Han et al. examined the variations in the vertical distribution of the understory herbs and the factors that influenced them on sunny and shady slopes at Sejila Mountain in southeast Tibet, which is located at an elevation of 2,000–3,300 m. High-altitude regions like the Himalaya, where numerous gradients coexist on a relatively small spatial scale, serve as the best natural laboratories for studying the ecological responses of plants. Along an altitudinal gradient in the Kashmir Himalaya, Mangral et al. examined the impact of soil physico-chemical and eco-physiological properties on the broadleaf evergreen woody shrub *Rhododendron anthopogon* D. Don. According to the study, *R. anthopogon* has enough soil physico-chemical plasticity and eco-physiological adaptability, which should be favorable for its survival in future climates, giving it an adaptive advantage and soon extending its range. By examining the abundance, composition, diversity and functional indices, and metabolic footprint of soil nematodes along an altitudinal gradient in the Trikuta mountain range of the Pir-Panjal to Shivalik Himalaya, Choudhary et al. in their Research Topic were able to decipher the elevational patterns of soil nematode community structure and trophic diversity.

The livelihoods of indigenous communities are being impacted by the fragile and perilous mountain ecosystems that are being threatened by a variety of anthropogenic disturbances and climate change (Nyaupane, 2022; Ridwan et al., 2023). Changes in land use and land cover (LULC) are among the major environmental issues facing the world today and present a grave threat to humankind. As evidenced by the numerous development initiatives undertaken in nearly every region of the world, LULC change is a key consideration in the majority of public initiatives (Haregeweyn et al., 2015). Using Landsat and Sentinel imageries for the years 1999, 2010, and 2020, Prashanth et al. estimated the soil loss in relation to long-term LULC change in the Dehar watershed, Himachal Himalaya, North India. In order to identify the pattern and contributing factors of deforestation in the Honam-Jeongmaek mountain range, Dhakal et al. examined the changes in land cover, the characteristics of the forest, and models of the forest decline over the past two decades. The composition, structure, and function of ecosystems can be affected in a variety of ways by forest fire, a natural ecological disturbance agent, at both the landscape and regional scales (Bargali et al., 2022). The main causes of forest fires, which have a negative impact on species diversity, nutrient dynamics, and regeneration potential as well as emit greenhouse gases that contribute to global climate warming, are, however, anthropogenic activities like dependence on non-timber forest products and the expansion of agricultural areas (Ray et al., 2019). Using Landsat 5, 7, and 8 satellite imagery to create fire frequency maps. Bargali et al. investigated the effects of forest fires on tree diversity and their regeneration in three forests in Uttarakhand, India. One of the key factors affecting the redistribution of species worldwide is climate change (Wani et al., 2022, 2023a). *Olea europaea* subsp. *cuspidata*, a wild olive subspecies, was the subject of Khan and Verma's global geographic occurrence data compilation and projection of potential distribution models in present and future climate scenarios. For the first time, Dhyani et al. reported a climatically sensitive tree ring chronology of the *Rhododendron arboreum*, a broadleaf tree from the Himalayan region, covering the period from 1732 to 2017 CE. They found that the climate during the monsoon season restricts the growth of this tree in this region.

Current global trends emphasize the value of protecting biodiversity and providing ecosystem services (Wani et al., 2023b). The value of forest ecosystem services is crucial for promoting the preservation of forest resources and sustainable development. The provisioning and supporting services offered by the forest ecosystem in Northeast China's Jilin Songhuajiang Sanhu National Nature Reserve were assessed by Liu et al.. In the Gori valley, Western Himalaya, Bisht et al. studied the dry matter dynamics and carbon flux along riverine forests. They came to the conclusion that riverine forests play a crucial role in acting as a significant sink for atmospheric carbon dioxide. It is crucial to comprehend how mountainous ecosystems work and how they should be managed. Setting conservation priorities requires specialized research on the evaluation and monitoring of biodiversity and the provision of ecosystem services in light of the dynamic nature of such ecosystems. In order to plan for the conservation and management of species, habitats, and communities in the Kashmir Himalayas of India, Wani et al. evaluated the Conservation Priority Index (CPI) of each. They also suggested a practical method for managing protected areas and preserving biodiversity.

Author contributions

SP: Conceptualization, Supervision, Writing—review & editing. JB: Writing—review & editing. ZW: Conceptualization, Writing—original draft, Writing—review & editing. KS: Writing—review & editing. VN: Writing—review & editing.

Conflict of interest

The authors declare that the research was conducted in the absence of any commercial or financial relationships that could be construed as a potential conflict of interest.

Publisher's note

References

Bargali, H., Calderon, L. P. P., Sundriyal, R. C., and Bhatt, D. (2022). Impact of forest fire frequency on floristic diversity in the forests of Uttarakhand, western Himalaya. *Trees Forests People* 9, 100300 doi: 10.1016/j.tfp.2022.100300

Chitale, V. S., Behera, M. D., and Roy, P. S. (2014). Future of endemic flora of biodiversity hotspots in India. *PLoS ONE* 9, e115264. doi: 10.1371/journal.pone.0115264

Costa, F. V. D., Viana-Júnior, A. B., Aguilar, R., Silveira, F. A., and Cornelissen, T. G. (2023). Biodiversity and elevation gradients: insights on sampling biases across worldwide mountains. *J. Biogeogr.* 50, 1879–1889. doi: 10.1111/jbi.14696

Gebrehiwot, K., Demissew, S., Woldu, Z., Fekadu, M., Desalegn, T., and Teferi, E. (2019). Elevational changes in vascular plants richness, diversity, and distribution pattern in Abune Yosef mountain range, Northern Ethiopia. *Plant Divers.* 41, 220–228. doi: 10.1016/j.pld.2019.06.005

Haregeweyn, N., Tsunekawa, A., Nyssen, J., Poesen, J., Tsubo, M., Meshesha, D., et al. (2015). Soil erosion and conservation in Ethiopia: a review. *Prog. Phys. Geogr.* 39, 750–774. doi: 10.1177/0309133315598725

Karpouzoglou, T., Dewulf, A., Perez, K., Gurung, P., Regmi, S., Isaeva, A., et al. (2020). From present to future development pathways in fragile mountain landscapes. *Environ. Sci. Policy* 114, 606–613. doi: 10.1016/j.envsci.2020.09.016

Nyaupane, G. P. (2022). "Himalayan vulnerabilities and resilience: climate change and natural disasters, shifting physical landscapes, and development," in *Tourism and Development in the Himalaya*. London: Routledge, 39–54.

Ray, T., Malasiya, D., Dar, J. A., Khare, P. K., Khan, M. L., Verma, S., et al. (2019). Estimation of greenhouse gas emissions from vegetation fires in Central India. *Clim. Chang. Environ. Sustain.* 7, 32–38. doi: 10.5958/2320-642X.2019.00005.X

Ridwan, Q., Wani, Z. A., Hanief, M., Pant, S., Shah, A. A., Siddiqui, S., et al. (2023). Indigenous knowledge and perception of local people towards biodiversity conservation in rajouri District of Jammu and Kashmir, India. *Sustainability* 15, 3198. doi: 10.3390/su15043198

Wani, Z. A., Fatima, T., Verma, O., Sharma, V., and Pant, S. (2023a). "Impacts of climate change on plants with special reference to the Himalayan Region," in *Climate Change Adaptation, Risk Management and Sustainable Practices in the Himalaya*. Cham: Springer International Publishing, 237–251.

Wani, Z. A., and Pant, S. (2023a). Assessment of floristic diversity and community characteristics of Gulmarg Wildlife sanctuary, Kashmir Himalaya. *Geol. Ecol. Landscap.* 2023, 1–21. doi: 10.1080/24749508.2023.2196767

Wani, Z. A., and Pant, S. (2023b). Status of biodiversity in a protected area of Kashmir Himalaya: Gulmarg wildlife sanctuary. *Nordic J. Botany* 2023, e03982. doi: 10.1111/njb.03982

Wani, Z. A., Ridwan, Q., Khan, S., Pant, S., Siddiqui, S., Moustafa, M., et al. (2022). Changing climatic scenarios anticipate dwindling of suitable habitats for endemic species of Himalaya—Predictions of ensemble modelling using *Aconitum heterophyllum* as a Model Plant. *Sustainability* 14, 8491. doi: 10.3390/su14148491

Wani, Z. A., Satish, K. V., Islam, T., Dhyani, S., and Pant, S. (2023b). Habitat suitability modelling of *Buxus wallichiana* Bail.: an endemic tree species of Himalaya. *Vegetos* 36, 583–590. doi: 10.1007/s42535-022-00428-w

frontiers | Frontiers in Forests and Global Change

TYPE Original Research
PUBLISHED 04 August 2022
DOI 10.3389/ffgc.2022.976902

OPEN ACCESS

EDITED BY
Zishan Ahmad Wani,
Baba Ghulam Shah Badshah University,
India

REVIEWED BY
Ishfaq Ahmad Wani,
Baba Ghulam Shah Badshah University,
India
Zeeshan Ahmad,
Quaid-i-Azam University, Pakistan

*CORRESPONDENCE
Junaid A. Magray
junaidmagray786@gmail.com

SPECIALTY SECTION
This article was submitted to
Forest Management,
a section of the journal
Frontiers in Forests and Global Change

RECEIVED 23 June 2022
ACCEPTED 13 July 2022
PUBLISHED 04 August 2022

CITATION
Magray JA, Wani BA, Islam T, Ganie AH and Nawchoo IA (2022) Phyto-ecological analysis of *Phytolacca acinosa* Roxb. assemblages in Kashmir Himalaya, India.
Front. For. Glob. Change 5:976902.
doi: 10.3389/ffgc.2022.976902

Phyto-ecological analysis of *Phytolacca acinosa* Roxb. assemblages in Kashmir Himalaya, India

Junaid A. Magray[1]*, Bilal A. Wani[1], Tajamul Islam[1], Aijaz H. Ganie[2] and Irshad A. Nawchoo[1]

[1]Plant Reproductive Biology, Genetic Diversity and Phytochemistry Research Laboratory, Department of Botany, University of Kashmir, Srinagar, India, [2]Department of Botany, University of Kashmir, Kargil, Ladakh

Phyto-ecological studies are essential in understanding community structure, organization and their response to changes in other environmental factors. In this study we analyzed the phytosociological and soil characteristics of *Phytolacca acinosa* communities and their correlation. 110 quadrats were laid across ten randomly selected sites in Kashmir Himalaya, India. Soil analysis was done using standard protocols. Overall, 161 species were recorded, belonging to 128 genera and 49 families. The species richness (SR) ranges from 27 to 83. Highest IVI was recorded for *Poa angustifolia* (60.06) and least for *Berberis lycium*, *Abies pindrow*, *Plectranthus ragosus*, and *Ailanthus altissima* (0.37 each). *P. acinosa* showed 100% random associations with other plant species. Soil properties varied significantly across the selected sites. Significant positive correlation was found between species richness (SR), Organic matter (OM) ($r = 0.79$), Organic carbon (OC) ($r = 0.79$) and Shannon–Wiener index (H) ($r = 0.92$). Nitrogen content also showed positive correlation with SR and H. Floristic composition of *P. acinosa* assemblages was governed by soil properties and habitat characteristics of sampling sites. Areas with highest floral diversity had high soil fertility while areas with low soil fertility possess lower diversity and need restoration. The knowledge may prove helpful in management of these habitats, boost conservation and mitigate the effects of changing climate.

KEYWORDS

climate change, community composition, Kashmir Himalaya, soil chemistry, species diversity

Introduction

Study of vegetation structure dynamics is a vital aspect of ecology that assists in understanding the function and overall structure of a community. Phytosociology or vegetation analysis is the science that deals with the study of the plant assemblages (communities), their characteristics, composition, classification, distribution, and relationships among species. Its primary goal is to delimit and characterize vegetation types based on the whole species (floristic) composition (Dengler, 2016). Phytosociological studies are important in understanding the population dynamics, habitat, species interaction and vegetation structure of an ecosystem (Collins et al., 2020). The vegetation of an area can be classified based on physiognomy and functional combination or on its component species that discriminate the physical appearance of vegetation (Mumshad et al., 2021). Plant communities are formed by those species which share the structural and floristic characteristics at certain level of environmental tolerance. Various biotic and abiotic factors of a region influence the plant population and vegetation heterogeneity (Jiao et al., 2019; Ocon et al., 2021). Furthermore, edaphic factors and topography complexity impact plant performance, vegetation composition and diversity (Chin and Kupfer, 2020). The phyto-ecological studies are essential in understanding the interrelationship between soil, environment and vegetation structure of a specific region. These investigations are vital in ascertaining the ecological status of species in a community (Ray and George, 2009), besides understanding the species diversity, organization of communities and in selecting valuable species from plant communities (Abinaya and Paulsamy, 2015; Wani Z. A. et al., 2022). The functional capacities of an ecosystem as well as its components are evaluated for ecological assessment. This involves assessment of phytosociological parameters (diversity, abundance, frequency, and important value index) of each species and anthropogenic threats to their habitat that may affect the functional and structural integrity of an ecosystem (Manoj et al., 2012).

Kashmir Himalaya, a scenic landscape of Indian sub-continent, an integral part of the Himalayan biodiversity hotspot. Himalayan region harbors stupendously diverse repository of plants with enormous economic and medicinal value (Aryal et al., 2018; Tali et al., 2019). This biodiversity is sustained by the steep climatic gradient characterized in Mountainous range of Himalaya (Rawal et al., 2018; Rana et al., 2021). In Himalayan ecosystems, floral diversity has a crucial role in maintaining ecological, functional integrity and serving indispensable ecosystem services that have enormous scientific utility (Ahmed et al., 2020). Apart from anthropogenic pressures that include deforestation, land cover change and urbanization, mountain ecosystems are also very sensitive to changing climate which eventually leads to the biodiversity loss (Khan S. M. et al., 2012; Paudel et al., 2018; Yadav et al., 2021). Therefore, for maintaining biodiversity and soil fertility, effective management strategies are mandatory. For the benefit of nature and humans, the United Nations Decade on Ecosystem Restoration (2021–2030) has emphasized restoration and protection of ecosystems across all continents. Healthy ecosystems have the ability to alleviate the effects of changing climate and prevent the loss of biodiversity. Phyto-ecological studies are important in understanding the relationship between vegetation, environment and plant responses toward changing climate (Chawla et al., 2012). Vegetation surveys and documentation will assist in monitoring and evaluating climate change that are vital for conservation and management initiatives (Malfasi and Cannone, 2020).

Phytolacca acinosa Roxb. (Phytolaccaceae) is a perennial herb distributed across Himalaya from Hazara to Bhutan. It is native to Himalaya, east and southeast Asia including Myanmar, China, Taiwan, Bhutan, Japan, Tibet, Vietnam, Manchuria, India, and Korea mostly growing along roadsides, inside forests and forest margins at the elevation of 500–3400 m (POWO., 2022). *P. acinosa* has immense medicinal importance and is widely used as a diuretic in Chinese folk medicine system and treatment of various diseases such as swelling, edema, indigestion, eye disorder, body ache, and sores (Ma et al., 2017; Basnet and Kalauni, 2020). *P. acinosa* contains many phytochemicals including tannins, flavonoids, polyphenol, triterpenoids, flavones, saponins, tannic and phenolic compounds (Lin et al., 2018; Ma et al., 2019; Tao et al., 2020). It also exhibits substantial antibacterial, antifungal, antiviral and anti-inflammatory activities (He et al., 2004; Manzoor et al., 2017; Abekura et al., 2019). Keeping in view the medicinal importance of the plant species the phytosociology in relation to soil and ecological parameters were carried out. The data generated will not only be helpful for the management of the species but also the habitats as well, which may prove helpful in conservation of this valuable plant species as well help in restoration of these habitats and mitigate the impacts of climate change.

The aim of our study was to address the following specific questions; (i) the composition of plant assemblages associated with *Phytolacca acinosa* in the Kashmir Himalaya (ii) soil parameters of the study sites (iii) variability of the ecological parameters of associated communities of the *P. acinosa* and (iv) the correlation between phytosociological and soil parameters in *P. acinosa* assemblages across the selected sites of Kashmir Himalaya.

Materials and methods

Study area

The current study was conducted in Kashmir Himalaya, India, situated between 32°20’ to 34°50’ N latitude and 73°55’ to 75°35’ E longitude (Tali et al., 2015) encompassing an area of around 15,948 sq. km. The region is a part of the northwest Himalaya in India and comprises of a deep oval shaped valley, bounded by high mountain ranges; the Lesser or Middle Himalaya, known as the Pir Panjal Range, separates the Valley from the Jammu region in the south and southwest, while the Greater Himalaya separates it from the Ladakh region in the north and east (**Figure 1**). The altitudinal gradient of the valley ranges from 1500 to

1800 m (asl), whereas the average elevation of the adjacent mountains' ranges from 3000 to 4000 m, with Kolahoi (5420 m) (Romshoo et al., 2020) being the highest peak. Climate of this region exhibits resemblance with continental-Mediterranean type found along temperate latitudes and is characterized by well-defined seasonality. The mean annual temperature of the region varies from a maximum of 35°C in summer to minimum of −10°C during winter (Zaz et al., 2019) and receives an annual precipitation of roughly 1200 mm predominantly in the form of snow (Romshoo et al., 2020). The vegetation of the area is temperate; subalpine and alpine type harboring enormous floristic diversity.

Selection of sites

Extensive field surveys were carried out across Kashmir Himalaya and 10 sites were selected based on the presence, abundance and availability of the natural populations of *P. acinosa* (**Figure 1**). The selected sites vary visually in vegetation structure and composition. The geo-coordinates and habitat characteristics are given in **Table 1**.

Vegetation sampling

The phytosociological studies were carried out during 2020–2021 across selected sites using the quadrat method (Curtis and McIntosh, 1950). The vegetation diversity was analyzed by using random sampling technique to give the best representation of the floristic composition. A total of 10 study sites (with 110 quadrats) were selected for vegetation sampling. At each site, 8–10 quadrats of 3 m × 3 m size with *P. acinosa* at center of each quadrat were randomly laid out for sampling. Additional quadrats were laid to distinguish possible unrecognized communities. The shape of quadrat was primarily square but at some instances was modified as per requirement to obtain a homogeneous and representative portrayal of vegetation, e.g., rectangular plots along water streams (Walentowski et al., 2018). Phytosociological characteristics i.e., abundance, frequency, density, relative abundance, relative frequency, relative density, and Importance Value Index (IVI) were a determined at every site for *P. acinosa* along with constituent plant species (Noreen et al., 2019; Kamran et al., 2020). Distribution levels were noted for other associated species available in the study area. The species richness (SR) was calculated as the total number of species present in a sampling site. Moreover, species diversity was determined using diversity indices such as Simpson's index (1/D) (Simpson, 1949), Jaccard's index (J) (Chao et al., 2005), and Shannon–Wiener index (H) (Shannon and Weaver, 1963). All the collected specimens were identified with the help of experts and by perusal the existing literature and online flora (POWO., 2022).

Soil sampling and analysis

For soil analysis, composite soil samples were collected from rhizosphere up to a depth of 15cm from each selected site in triplicates, correctly labeled, air dried in laboratory, and then sieved to remove gravel and debris (Khan et al., 2017; Iqbal et al., 2021). The soil properties—available nitrogen (N), potassium (K), phosphorus (P), soil organic carbon (OC), organic matter (OM), and soil pH were analyzed. The soil samples were analyzed at Soil Testing Laboratory of State Agriculture Department, Lal Mandi, Srinagar, Jammu and Kashmir, India.

The pH of soil was estimated in 1:5 soil–water suspensions using a digital pH meter (Khan W. et al., 2012). Likewise, OC in soil was assessed by rapid titration method of Walkley and Black (1934). At each study site, other chemical parameters of soil including available N, K, and P were analyzed using already set methodology of Subbiah and Asija (1956); Black (1968) (flame photometric method); and Olsen et al. (1954) (spectrophotometer method), respectively. Soil organic matter (OM) was computed by multiplying a factor of 1.724 to soil OC (Davies, 1974).

Statistical analysis

All the collected data was analyzed to evaluate the phytosociological attributes of each species, their relationships and effect of various soil properties on the vegetation attributes of the selected area. For further analysis the data related to plant assemblages at all sites (quadrats) was sorted in MS EXCEL as per software requirements. To appraise the impact of edaphic factors on species composition and distribution pattern, the species and soil data were analyzed using correlation analysis in Origin pro 2021b software (version 9.0). The data matrix of species was subjected for cluster analysis to visualize the similarity among the study sites. Bray–Curtis index was employed to estimate the degree of similarity in species composition between the ten selected sites (Ismail and ELawad, 2015) using PAST software (version 4.09). The similarity dendrogram obtained from the result of cluster analysis was plotted. The plant (vegetation) data was also quantitatively analyzed for the determination of frequency, density, abundance as per Mishra et al. (2017); and Curtis and McIntosh (1950) and important value index (IVI) of *P. acinosa* and associated species at each study site. The IVI of each species was computed by adding up the relative frequency, relative density, and relative abundance following Phillips (1959). Data regarding composition and structure of the natural habitats harboring populations of *P. acinosa* was recorded across all the selected sites. The sampling was carried out during the flowering period and the data pertaining to *P. acinosa* assemblages along with the associated plant species was collected from 10 study sites (**Table 1**). The community composition was analyzed

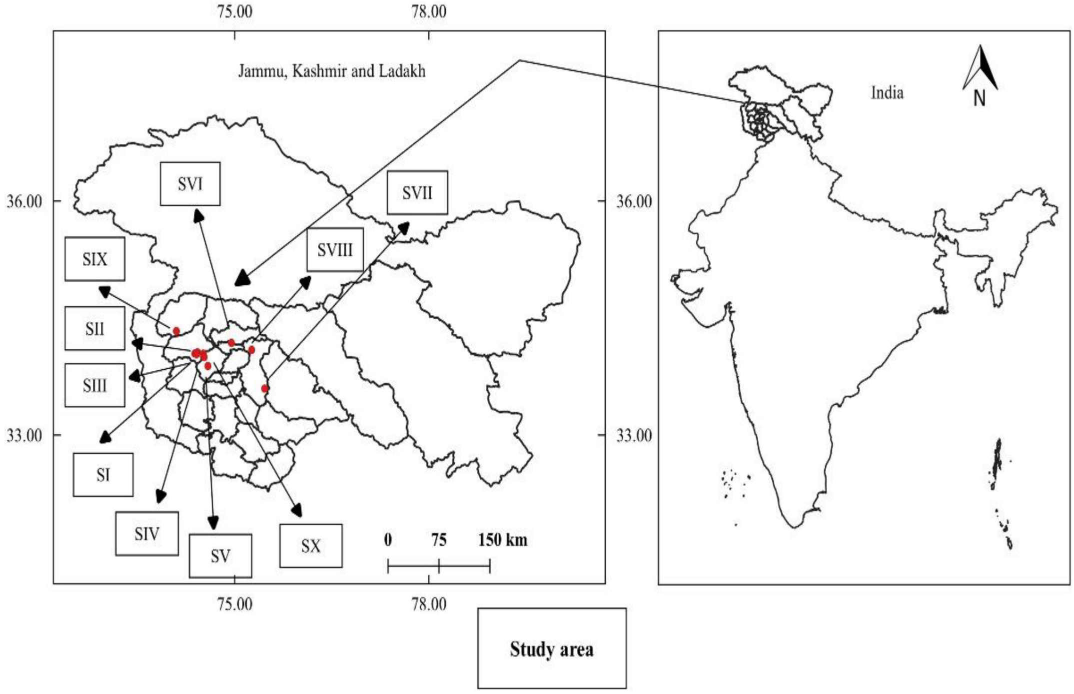

FIGURE 1
Map showing the study area and sampling sites in Kashmir Himalaya, India. (SI–Tangmarg; SII–Gulmarg; SIII–Drung; SIV–Gogaldara; SV–Doodhpathri; SVI–Dara Harwan; SVII–Daksum; SVIII–Pahalgam; SIX–Bangus; SX–Khag).

Table 1 Geo-coordinates, altitude and habitat characteristics of the study sites across Kashmir Himalaya, India.

Study sites	Latitude (N)	Longitude (E)	Altitude (m asl)	Habitat
Tangmarg (SI)	34.06085°	74.42472°	1,950	Open rocky slope
Gulmarg (SII)	34.04557°	74.38441°	2,700	Partial shady and slope
Drung (SIII)	34.03783°	74.41106°	2,250	Shady, inside forest
Gogaldara (SIV)	34.04317°	74.51425°	2,400	Shady slope
Doodhpathri (SV)	33.88613°	74.58712°	2,600	Open slope
Dara, Harwan (SVI)	34.18201°	74.94989°	2,150	Rocky slope, both open and shade
Daksum (SVII)	33.59575°	75.46383°	2,900	Shady slope and little moist
Pahalgam (SVIII)	34.09216°	75.26322°	2,800	Partial shady slope
Bangus (SIX)	34.33333°	74.09972°	2,500	Partial shady along roadside
Khag (SX)	34.00011°	74.52829°	2,000	Open along roadside

using cooccur package (version 4.0.3) in which co-occurrence data matrix (presence/absence) was envisaged by probabilistic hypergeometric co-occurrence model employed in R Core Team (2020) (Griffith et al., 2016). To extract the species pairings and associated probabilities, we use the *prob table()* function to retrieve the results element of the cooccur object.

Results

In the present study, 161 plant species were recorded belonging to 128 genera and 49 families (Supplementary Material 1, Figure 2). Out of these plant species, herbs were dominant with 84.47% followed by trees (7.45%), shrubs (5.59%), climber (1.24%), and Fern (1.24%). However, the contribution of different families to the floristic diversity was disproportionate: only 7 families contributed half (50%) of the species pool, while the remaining 50% of the species were contributed by the rest of the 41 families. In terms of the species number, Asteraceae was found as the largest family with 25 species followed by Lamiaceae (13 species), Poaceae and Rosaceae (10 species each), Polygonaceae (8 species), Fabaceae and Caryophyllaceae (7 species each), Ranunculaceae (7 species). There were 21 families represented by a single species recorded at different sites of Kashmir Himalaya (**Figure 2**). The natural vegetation of a particular region reflects the interaction amongst the associated fauna and flora, edaphic and other environmental factors. The calculated IVI values were used to assign the dominance of species. The highest IVI was recorded for *P. angustifolia* and least for *B. lycium*, *A. pindrow*, *P. ragosus*, and *A. altissima.* Based on IVI, *Poa angustifolia* (IVI 60.06), *C. dactylon* (53.60), *P.* pratensis (16.70)*, U. dioica* (30.73)*, C. iberica* (25.04)*, T. repens* (15.17), *G. nepalense* (24.58), *F. nubicola* (14.08), *and P. aviculare* (19.45) were the dominant species in *P. acinosa* communities across different sampling sites. *P. acinosa* secured highest and lowest IVI of 11.33 and 4.82 in site II and site X, respectively. Habit-wise, herbaceous flora was dominant with 136 species followed by arboreal flora (12 species), shrubs (9 species), climbers (2 species) and ferns (2 species).

The plant species richness ranged from 27 to 83 and differed between different study sites. *C. dactylon* and *U. dioica* were the most common species found across most of the sites. The Shannon-Wiener diversity index (H) was highest at (SVIII)- (4.12). Khag (SX) reported the lowest value of Shanon (H) (2.68), Simpson (1/D) (0.81) and Jaccard's (J) index (0.9), respectively. The results of current study highlighted variations in species richness (SR) and plant community composition associated with the variability in soil properties across the sampling sites. The highest species richness was found at site SVII (Daksum) while the lowest i.e., 27 species were listed at site SX (Khag).

The phytosociological and soil parameters of selected sites

Site SI (Tangmarg)

The site SI was relatively less diverse having a low value of shannon-weiner index (0.88). Out of 31 plant species, *Cynodon dactylon* with IVI 53.60 was the dominant one followed by *Urtica dioica* (IVI 30.73) and *Centaurea iberica* (25.04). *Berberis lycium* and *Stipa sibirica* were the rare species having IVI 2.25 and 2.77, respectively. *P. acinosa* recorded an IVI of 10.55. The species composition reflects the presence of 30 herbs and a single tree species. The soil at site I was less acidic (pH–6.68) (**Table 2**). The average OC content at Site I was 3.57% and OM was 6.16%. The value of N, P, and K was 0.02%, 132.43 and 596.59 kg ha^{-1}, respectively.

Site SII (Gulmarg)

The vegetation analysis of the *P. acinosa* communities at Site SII (Gulmarg) revealed rich species diversity. This site has high species richness of 68, with *C. dactylon* (IVI 17.18) being the dominant species followed by *P. pratensis* (IVI 15.40) while *R. webbiana* (IVI 1.24) was recorded as rare species. *P. acinosa* secured the lowest IVI of 4.82 at Gulmarg. Herbs represent 89.71%, shrubs and trees 4.41% each and climbers 1.47% of the total vegetation. The average pH (acidity) and OC of the soil was 5.71 and 6.55%, respectively. Besides, the mean value of N, P, and K were calculated as 0.04%, 234.83 kg ha^{-1} and 443.15 kg ha^{-1}, respectively.

Site SIII (Drung)

The Site SIII has an altitude of 2200m asl and *P. angustifolia* having IVI 60.06 was the dominant species followed by *C. dactylon* (IVI 44.03) while *R. canina* and *R. fruticosa* each with IVI 2.43 were rare species. A total of 32 species were recorded. Among these 3.13% were trees, 9.38% shrubs, and 87.50% herbs. The value of the soil pH was 6.32 (**Table 2**) indicating slightly less acidic nature of soil. Further, the mean value of soil chemical properties including K, P, N, OM and OC was 568.59 kg ha^{-1}, 100.8 kg ha^{-1}, 0.04, 6.92, and 4.02%, respectively.

Site SIV (Gogaldara)

The plant community of sampling Site SIV is represented by 49 species. *C. dactylon* and *P. angustifolia* were the dominant species whereas *E. canadensis* was rare species based on calculated IVI. Vegetation was a blend of herbs (95.92%) shrubs (2.04%) and trees (2.04%). The mean soil pH and OC content was 6.05 and 6.58%, respectively. Moreover, the mean value of P and N in soil was recorded as 146.20 kg ha^{-1}, and 0.045%, respectively.

Site SV (Doodhpathri)

At Doodhpathri, 33 species were found and *T. repens* was the dominant, followed by *U. dioica*. The lowest IVI of 2.47 was calculated for *A. acuminata*. The vegetation was composed of 32 herbs and a single shrub. The soil of Site V was less acidic having pH (6.19). The mean OC and OM content present in soil was 2.24% and 3.86%, respectively. Soil of this site also had maximum average value of 619.36 kg ha^{-1} for K (**Table 2**).

Site SVI (Dara)

Site SVI harbors unique and ample floristic diversity with species richness of 68 with herbs, shrubs and trees accounting for 82.35, 8.82, and 8.82%, respectively. *U. dioica* was the dominant species of this area followed by *V. odorata*. The calculated IVI of *P. acinosa* was 4.68. This site has lower content of OM (5.40%) and OC (3.13%) in soil (**Table 2**). Furthermore, the average P, K, and N content at this site was 74.84 kg ha^{-1}, 385.21 kg ha^{-1}, and 0.03%, respectively.

Site SVII (Daksum)

Site SVII (Daksum) has a high species diversity having Shanon-weiner index of 3.99 and registered the highest species richness (83). Based on calculated IVI, *P. aviculare* (19.45) and *P. pratensis* (16.70) were the dominant species of this area. *A. pindrow*, *B. lycium*, *P. ragosus* had lowest IVI. The area is dominated by herbs (90.36%) followed by trees (6.02%)

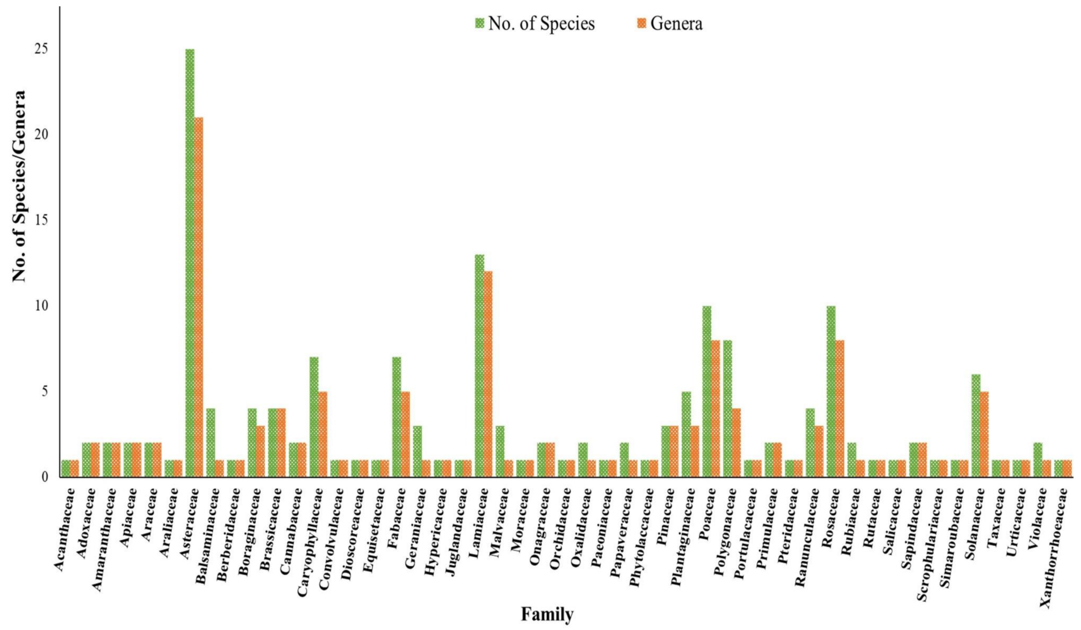

FIGURE 2

Number of species and genera present in different families recorded across study sites.

Table 2 Soil chemical properties and floral diversity parameters of selected study sites in Kashmir Himalaya (OC–organic carbon, OM–organic matter, N–Nitrogen, P–phosphorus, K–potassium; SR–species richness, H–Shanon-weiner index, J–Jaccard's index of evenness, 1/D–Simpson's index).

Site	pH	OC (%)	OM (%)	N (%)	P (Kgha^{-1})	K (Kgha^{-1})	SR	H	J	1/D
SI	6.68 ± 0.02*	3.57 ± 0.02	6.16 ± 0.03	0.02 ± 0.012	132.43 ± 12.37	596.59 ± 37.89	31	3.01	0.88	0.92
SII	5.71 ± 0.02	6.55 ± 0.19	11.30 ± 0.02	0.04 ± 0.004	234.83 ± 12.43	443.15 ± 16.48	68	4.05	0.96	0.98
SIII	6.32 ± 0.02	4.02 ± 0.02	6.92 ± 0.06	0.04 ± 0.003	100.80 ± 9.59	568.59 ± 22.63	32	2.9	0.84	0.91
SIV	6.05 ± 0.05	6.58 ± 0.02	11.34 ± 0.10	0.045 ± 0.001	146.2 ± 11.98	543.20 ± 19.54	49	3.62	0.94	0.97
SV	6.19 ± 0.01	2.24 ± 0.01	3.86 ± 0.02	0.032 ± 0.002	154.78 ± 5.67	619.36 ± 23.73	33	3.35	0.96	0.96
SVI	6.92 ± 0.05	3.13 ± 0.02	5.40 ± 0.03	0.03 ± 0.004	74.84 ± 8.76	385.21 ± 11.05	68	3.92	0.93	0.98
SVII	5.54 ± 0.03	12.39 ± 0.09	21.36 ± 0.02	0.05 ± 0.007	177.63 ± 13.24	605.55 ± 38.33	83	3.99	0.9	0.97
SVIII	5.89 ± 0.08	10.59 ± 0.02	18.26 ± 0.09	0.08 ± 0.030	77.88 ± 6.41	552.53 ± 17.17	76	4.12	0.95	0.98
SIX	6.76 ± 0.07	6.21 ± 0.02	10.71 ± 0.02	0.05 ± 0.002	43.25 ± 8.35	289.78 ± 10.05	39	3.51	0.96	0.96
SX	6.46 ± 0.05	1.16 ± 0.01	2.00 ± 0.02	0.03 ± 0.004	111.10 ± 9.74	473.76 ± 15.88	27	2.68	0.81	0.91

*Mean ± SD.

and shrubs (3.61%). The soil was most acidic having pH of 5.84 and quite rich in chemical properties with highest average value of OM and OC content (12.39% and 21.36%), respectively (Table 2). The average value calculated for P, K and N were also high (177.63 kg ha^{-1} and 605.55 kg ha^{-1}, and 0.05%, respectively).

Site SVIII (Pahalgam)

Phytosociological studies at site SVIII (Pahalgam) revealed the presence of second highest number of species (76) associated with the *P. acinosa* comprising of 96.05% herbs, 2.63% trees and 1.32% shrubs. *T. repens* (IVI 12.38) and *I. heterantha and R. pseudoacacia* (IVI 0.43 each) were the dominant and rare species, respectively. The soil of site VIII had second lowest average pH of 5.89 and highest nitrogen content of 0.08%. The soils also share a rich proportion of OC, OM and K content (10.59%, 18.26%, and 552.53 kg ha^{-1}, respectively) (Table 2).

Site SIX (Bangus)

The Site SIX has a species richness of 39 mostly comprised of herbs (97.44%) and shrubs (2.56%). The highest IVI was recorded for *C. dactylon* and lowest IVI for *S. chrysanthemoides, A. accuminata and T. farfara.* The average calculated pH, OC and OM of the soil was 6.76, 6.21% and 10.71%, respectively.

The site had the average N content of 0.05% and recorded the lowest value of P content (43.25 kg ha^{-1}) (**Table 2**).

Site SX (Khag)

At Site SX the plant community was represented by lowest number of species having species richness of 27. As per IVI calculated, *U. dioica* was the dominant species followed by *P. pratensis* while as *A. pindrow*, *R. pseudoacacia* and *P. wallichiana* were rare species. The Vegetation found in this site was a blend of all the growth forms: herbs (59.23%), trees (25.93%) and shrubs (14.81%). The soil had nitrogen content of 0.74% and average calculated pH and OM was 6.76. The site has lowest average value of OM (2.00%) and OC (1.16%) (**Table 2**). Moreover, the value recorded for N, P and K was 0.03%, 111.10 kg ha^{-1} and 473.76 kg ha^{-1}, respectively.

The present study revealed that plant community composition and species distribution pattern is considerably regulated by the amount and availability of soil nutrients. The correlation plot (**Figure 3**) indicated that species richness is positively correlated with OC, OM, N, P, Shannon diversity (H) and Simpson diversity (1/D) ($r = 0.79, 0.79, 0.58, 0.24, 0.92$, and 0.79, respectively), but the resultant correlation was significant only between species richness and OC, OM, Shannon diversity and Simpson index ($p < 0.05$). Similarly, species richness is negatively correlated with pH ($r = -0.56$), but the correlation was non-significant. In addition, positive correlation was found between Shannon diversity index and Simpson diversity index ($r = 0.95$; $p < 0.05$). A negative corelation was found between potassium and species diversity. SR increased significantly with increasing OC and OM content of soils.

Community composition and association

On the basis of community composition, a total of 161 plant species were reported to be associated with *P. acinosa.* Out of the 12880 species pair combinations, 8006 pairs (62.16%) were eliminated from the analysis as expected co-occurrence was < 1 and 4874 pairs were analyzed. The findings show that the majority of the classifiable species combinations were truly random. The significant non-random associations were mostly positive (524 positive compared to 153 negative).

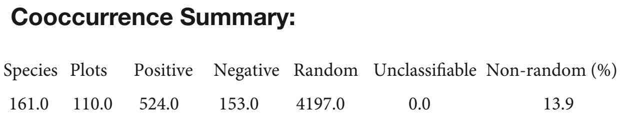

Cooccurrence Summary:

Species	Plots	Positive	Negative	Random	Unclassifiable	Non-random (%)
161.0	110.0	524.0	153.0	4197.0	0.0	13.9

The plant of interest (*Phytolacca acinosa*) shows 100% random associations with other species i.e., observed frequency of co-occurrence is not significantly different and roughly equal to expected. Visualizations of all pairwise combinations of species and their co-occurrence signals (positive, negative, and random) (**Figure 4**). The plot removes any species with non-significant negative or positive correlations, and then ranks the remaining species from the most negative to the most positive relationships (left to right).

Cluster analysis

The cluster analysis revealed highest similarity of 71.39% among SVII (Daksum) at 2900 m asl and SVIII (Pahalgam) at 2800 m asl. On the other hand, site III (Drung) at 2200 m asl inside coniferous forest m asl and site X (Khag) 2000 m asl in disturbed roadside habitat showed the least similarity (37.01%) (**Figure 5**).

Discussion

During this study, total 161 plant species from 128 genera belonging to 49 plant families were documented from the selected sites of Kashmir Himalaya, India. The dominant families in the region were Asteraceae and Lamiaceae, followed by Rosaceae. The studies are in accordance with Altaf et al. (2021) and Nafeesa et al. (2021), who also recorded the dominance of these families in Kashmir Himalaya. The dominance of the Asteraceae and Lamiaceae families in the Himalayan region is due to their larger ecological amplitude, high adaptive capacity, larger seed output, and presence of different reproductive strategies in diverse environmental conditions (Haq et al., 2021; Sofi et al., 2022; Wani I. A. et al., 2022).

The IVI gives an idea of socio-ecological interaction of species' and dominance pattern in a population (Wani I. A. et al., 2022). Across the study sites, analysis of IVI unveiled diverse species combinations with distinct dominants and co-dominants. The IVI of the constituent species exhibited considerable degree of variation ranging between 0.37 to 60.06. *P. angustifolia, P. pratensis, C. dactylon, U. dioica, C. iberica, T. repens, G. nepalense, F. nubicola and P. aviculare* have scored highest IVI (more dominant) reflecting their better adaptive mechanism to the conditions of the region (Ge et al., 2005; Shaheen et al., 2012). The majority of dominating species in the selected sites belonged to the Poaceae family. The higher seed vigor, germination, survivability and different means for vegetative reproduction assist these species for their stronger perpetuation (Ismail and ELawad, 2015). The studied species, *P. acinosa* has IVI ranging between 4.82 (Gulmarg)-11.33 (Khag) reflecting that this species had less perpetuation in the community of Gulmarg while better adaptation in Khag than the other associated species. Community characteristics of plants are highly impacted by the pressure exerted by overgrazing, trampling and varying environmental conditions.

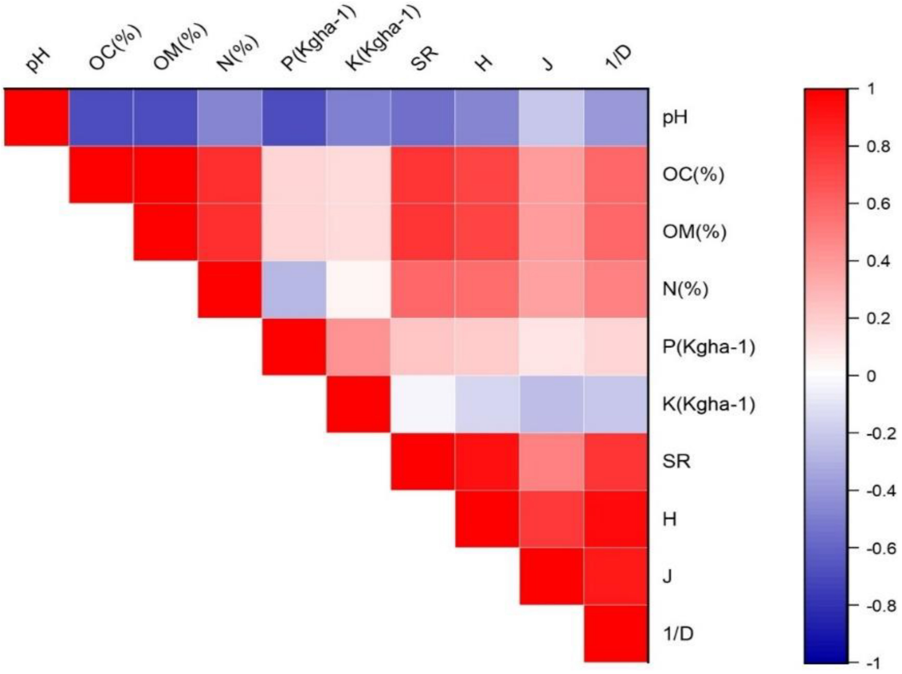

FIGURE 3
Correlation plot between vegetation and soil parameters. Statistical significance $p < 0.05$.

These differences in IVI across the sites may be attributed to surrounding environmental conditions and the anthropogenic activities which have already been reported from this area (Ganie et al., 2019). The IVI value of any species is an outcome of prevailing micro environmental conditions as well (Abinaya and Paulsamy, 2015).

The soil across sampling sites was acidic in nature with pH ranging between 5.54 to 6.92. Gairola et al. (2012), also suggested that for steady supply of nutrients the pH of forest soils should be slightly acidic. It has also been reported that the acidic nature of forest soils may be due to the basic cation uptake of by tree roots (Fujii et al., 2018). The pH of soil differed significantly across the study sites ($F = 1.976$, $p = 0.051$). This change in pH may be attributed to altitudinal differences among sites (Wani I. A. et al., 2022). There is significant negative correlation ($r = -0.7$, $p < 0.05$) between available P content and pH at the study sites (**Figure 3**). This is because crystalline and amorphous forms of Al and Fe couple with inorganic P compounds depending on pH of soil (Hedley et al., 1982). Organic matter (OM) is a major constituent of the forest floor supporting microbiological diversity and guarantees a long-term supply of nutrients through decomposition. OM provides a significant portion of soil carbon (C) and regulates soil characteristics (Mishra et al., 2018). Significant variation in both OC ($F = 8244.371$, $p < 0.05$) and OM ($F = 45985.584$, $p < 0.05$) was found across the study sites, with highest values at SVII (Daksum). This is consistent with the results depicted by Powers and Schlesinger (2002) who reported that soil carbon content varies across different habitats and elevation. According to Agren et al. (2013), litter decomposition is region specific and has a strong correlation with OM mineralization. In addition, other factors such as, species richness (SR) also contributes to the accumulation of OM. Available nitrogen (N) exhibited a significantly positive correlation with OC and OM content ($r = 0.8$, $p < 0.05$) (**Figure 3**). It has been reported that humus content is directly proportional to the amount of essential nutrients in soil. OC and phosphorous (P) content were negatively correlated (Gupta and Sharma, 2009). The nitrogen (N) content is dependent on the amount of OM in the soil (Jha et al., 1984). No significant variation was observed in the N content (%) ($F = 1.828$, $p > 0.05$) between the study sites (**Table 2**). N showed a positive correlation with potassium (K) (**Figure 3**). Previous studies carried out by Gupta and Sharma, (Gupta and Sharma, 2009); Mishra et al. (2017) also reported a positive correlation between N and K, which in turn are directly related to OM.

The P content varied significantly ($F = 3.556$, $p < 0.05$) ranging from 43.25 kg/ha^{-1} (SIX) to 77.88 kg/ha^{-1} (SVIII) across the study sites. Highest K content was recorded at SV (619.36 kg ha^{-1}) while SVIII had the lowest content (77.88 kg ha^{-1}). The potassium content in soil is proportional to the parent rock compositions. As the degree of weathering is regulated by altitude and accompanying climatic conditions, variations in K content may be related to habitat features and

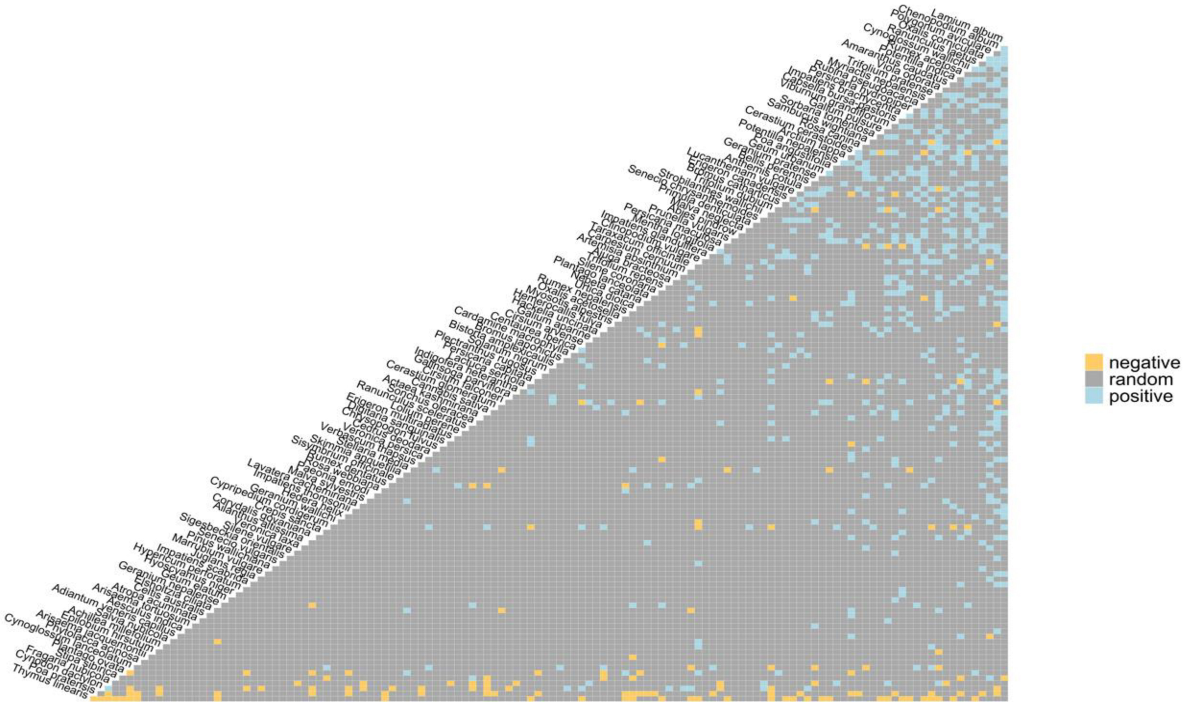

FIGURE 4
Heat map (co-occurrence plot) portraying the significant random negative and positive species relationships.

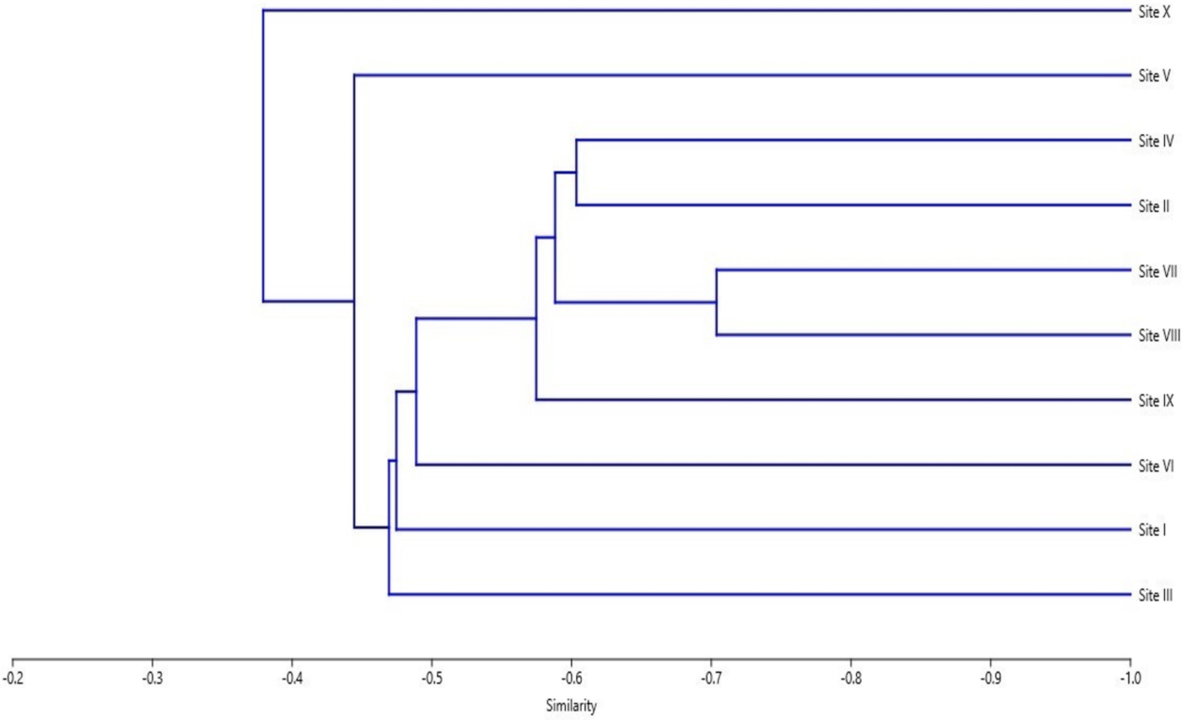

FIGURE 5
Bray-Curtis (Similarity) index among selected sites of the study area.

altitude (Mishra et al., 2017). Further, OC shows a positive correlation with K ($r = 0.15$) and N ($r = 0.8$), but this correlation was significant between OC and N ($p < 0.05$) (**Figure 3**). Owing to the fact that availability of K is maintained through decomposition of organic matter (Basumatary and Bordoloi, 1992), therefore a positive correlation is present between organic carbon and macronutrients (nitrogen and potassium) as both are dependent on the humus content in soil (Mishra et al., 2017).

A sturdy relationship was found between floristic diversity associated with *P. acinosa* and soil parameters across different sites in Kashmir Himalaya. Our results corroborate previous investigations of edaphic factors (Figueiredo et al., 2018; Jucker et al., 2018; Hofhansl et al., 2020), which found that vegetation attributes changed in relation to the regional variation of soil physico-chemical properties across different areas. Plant species composition and distribution is influenced by the soil characteristics (Yang et al., 2018). Across different sites soil properties such as, Ph, OC, OM among others show significant differences, that eventually impact the plant species composition (Rahman et al., 2022). The community composition and species distribution pattern is also regulated by the soil organic matter. Water holding capacity and colloidal nature of soil subsequently increased in plant communities with increase in OM content (Mumshad et al., 2021; Wani I. A. et al., 2022). Higher values of phytosociological parameters across the study sites can be attributed to the favorable soil chemical properties.

The highest degree of similarity (71.39%) was recorded between SVII and SVIII (**Figure 5**), as both sites had almost similar soil characteristics and relatively similar altitudes. SI (fertile forest soil) and SIII (rocky soil) exhibited least similarity (37.01%) which can be ascribed to the variation in habitat characteristics, altitude and soil properties between the two sites, the vegetation composition changed in relation to the regional variation of soil properties and elevation across different areas (Ismail and ELawad, 2015). The presence of entirely random association with other plants (**Figure 4**) revealed that *P. acinosa* inhabit distinct habitats and co-associates in a natural community within a specific geographical area (Gulzar et al., 2022).

Our study has revealed that the change in soil properties leads to subsequent changes in plant communities, especially in terms of species diversity, richness and cooccurrence patterns. Since the plant species respond individually to changing climatic and soil conditions, plant community composition is thus likely to be modified (Lafleur et al., 2010). Environmental factors like soil moisture, temperature and elevation governs the vegetation patterns and soil physico-chemical properties to a greater extent (Solon et al., 2007; Hamid et al., 2021). This interpretation is supported by differentiation in community composition and structural features such as number of species, co-occurrence patterns, and diversity indices. The species richness varied in relation to the combined pattern of edaphic factors like OC, OM, N, and pH, with the number of species being substantially higher where these soil properties except pH were high, and vice-versa (Solon et al., 2007). The present study also reflected that SVII (Daksum) has highest species richness (83), OC (12.39%) and OM (21.36%) content while SX (Khag) had lowest species richness (27), OC (1.16%) and OM (2.00%). Floristic composition and soil fertility of a particular site is largely affected by the anthropogenic activities. The sites with undisturbed and fertile soils have quite rich species diversity and the sites with poor and disturbed soils support minimum plant diversity. The sites characterized by fertile soils, higher floristic diversity and productivity act as potential areas of carbon sequestration (Mishra et al., 2017). Therefore, proper management of such areas will not only help in mitigating the climate change, but also allow the sustainable provisioning of ecosystem services and conservation of floristic diversity. Besides, the sites with the low soil fertility and species diversity need better management strategies for the restoration and plant species conservation.

Since community composition and distribution of plant species is partly under the control of climatic variables like average precipitation and temperature, the projected global climate change is likely to alter the composition and distribution pattern of vegetation (Chen et al., 2011; Brown and Vellend, 2014). Moreover, as soil processes and properties are partially governed by climatic variables, the climate change is also likely to modify soil properties (Gelybo et al., 2018). Floristic composition is influenced by soil physicochemical properties, and any modification in soil factors due to the changing climate leads to the variation in vegetation responses (Lafleur et al., 2010). Hence, relationship between climate, vegetation and soil properties are complex, multi-scale, and multi-aspect in nature. The study of plant-soil systems has become important in understanding plant community composition, population dynamics, and ecosystems functioning. Soil microclimate and other environmental factors that contribute to plant–soil system effect ecosystem composition, species diversity and possibly play a role in the evolution of species (van der Putten et al., 2016). Therefore, a better understanding of ecological and evolutionary repercussions of soil-vegetation interactions might assist in projecting and mitigating the effects of human-induced global climate change, and land use change for the better sustainable future.

Conclusion

The present study indicates that *Phytolacca acinosa* displays a broad range of habitats reflecting its diverse phytosociological amplitude and tolerance to existing environmental conditions. The phytosociological characteristics reveals that in *P. acinosa* communities; *Poa angustifolia, P. pratensis, and Cynadon dactylon* were the dominant species. The findings of present study emphasis on the significance of relationship between soil parameters, vegetation characteristics and plant associations for better understanding of communities' functioning. The lower IVI values of *P. acinosa* than associated plant species divulge its lesser ecological importance and perpetuation in the assemblages, hence needs conservation strategies. Moreover, the soil paraments plays a vital role in the establishment of plant communities with response to environmental conditions. The good soil properties and phytosociological attributes at some sites reflects the relatively stable nature of these sites and vice versa. All these parameters must be taken into consideration while studying species distribution pattern, community characteristics and association in a particular region. From our study it can be concluded that the knowledge of both species diversity and soil properties in different ecosystems can improve conservation efforts and ensure better management strategies for the restoration of degraded habitats over a period of time. In future, similar studies will help in understanding the community ecology their conservation strategies and restoration efforts, to ensure prolonged supply of ecosystem functioning and processes.

Data availability statement

The original contributions presented in this study are included in the article/**Supplementary material**, further inquiries can be directed to the corresponding author.

Author contributions

JM: methodology, data collection, and writing - original draft. BW: data collection. TI: curation and analysis, software, and visualization. AG: conceptualization and supervision, methodology, validation, and writing - original draft. IN: conceptualization, supervision, investigation, validation, and writing - review. All authors contributed to the article and approved the submitted version.

Funding

JM and BW acknowledged the Maulana Azad National Fellowship (MANF) for funding under MANF-201920-JKO416200268 and MANF-2018-19-JAM-100111, respectively and also TI acknowledged the University Grants Commission (UGC) under 924/(CSIRNET JUNE-2019) for providing financial assistance as Junior Research Fellowship.

Acknowledgments

The authors are thankful to the Head, Department of Botany, University of Kashmir. Colleagues at PRBGPR Laboratory, University of Kashmir are acknowledged for their kind support during the present study. We also thank to the Sajad A. Wani for giving valuable suggestion regarding the manuscript.

Conflict of interest

The authors declare that the research was conducted in the absence of any commercial or financial relationships that could be construed as a potential conflict of interest.

Publisher's note

Supplementary material

The Supplementary Material for this article can be found online at: https://www.frontiersin.org/articles/10.3389/ffgc.2022.976902/full#supplementary-material

References

Abekura, F., Park, J., Kwak, C. H., Ha, S. H., Cho, S. H., Chang, Y. C., et al. (2019). Esculentoside B inhibits inflammatory response through JNK & downstream NF-κB signaling pathway in LPS-triggered murine macrophage RAW 264.7 cells. *Int. Immunopharmacol.* 68, 156–163. doi: 10.1016/j.intimp.2019.01.003

Abinaya, G., and Paulsamy, S. (2015). Phytosociological analysis of the medicinal plant species, Thalictrum javanicum Blume in thottabetta, nilgiris, the western ghats. *Kongunadu Res. J.* 2, 56–62. doi: 10.26524/krj68

Agren, G. I., Hyvönen, R., Berglund, S. L., and Hobbie, S. E. (2013). Estimating the critical N: c from litter decomposition data and its relation to soil organic matter stoichiometry. *Soil Biol. Biochem.* 67, 312–318. doi: 10.1016/j.soilbio.2013.09.010

Ahmed, M. J., Murtaza, G., Shaheen, H., and Habib, T. (2020). Distribution pattern & associated flora of jurinea dolomiaea in the western Himalayan highlands of Kashmir: an indicator endemic plant of alpine phytodiversity. *Ecol. Indic.* 116:106461. doi: 10.1016/j.ecolind.2020.106461

Altaf, A., Haq, S. M., Shabnum, N., and Jan, H. A. (2021). Comparative assessment of PHYTO diversity in tangmarg forest division in Kashmir Himalaya, India. *Acta. Ecol. Sin.* *VP, doi: 10.1016/j.chnaes.2021.04.009

Aryal, K. P., Poudel, S., Chaudhary, R. P., Chettri, N., Chaudhary, P., Ning, W., et al. (2018). Diversity and use of wild and non-cultivated edible plants in the Western Himalaya. *J. Ethnobiol. Ethnomed.* 14:10. doi: 10.1186/s13002-018-0211-1

Basnet, A., and Kalauni, S. K. (2020). Phytochemical screening and biological activity analysis of some selected medicinal plants of Ilam district of Nepal. *Curr. Perspect. Med. Aromat. Plants* 3, 61–73. doi: 10.38093/cupmap.765409

Basumatary, A., and Bordoloi, P. K. (1992). Forms of potassium in some soils of Assam in relation to soil properties. *J. Indian Soc. Soil Sci.* 40, 443–446.

Black, C. A. (1968). *Soil Plant Relationships*, 2 ed Edn. New York, NY: Wiley & Sons, 405–653.

Brown, C. D., and Vellend, M. (2014). Non-climatic constraints on upper elevational plant range expansion under climate change. *Proc. Biol. Sci.* 281:20141779. doi: 10.1098/rspb.2014.1779

Chao, A., Chazdon, R. L., Colwell, R. K., and Shen, T. J. (2005). A new statistical approach for assessing similarity of species composition with incidence & abundance data. *Ecol. Lett.* 8, 148–159. doi: 10.1111/j.1461-0248.2004.00707.x

Chawla, A., Yadav, P. K., Uniyal, S. K., Kumar, A., Vats, S. K., Kumar, S., et al. (2012). Long-term ecological and biodiversity monitoring in the western Himalaya using satellite remote sensing. *Curr. Sci.* 102, 1143–1156.

Chen, I. C., Hill, J. K., Ohlemüller, R., Roy, D. B., and Thomas, C. D. (2011). Rapid range shifts of species associated with high levels of climate warming. *Science* 333, 1024–1026. doi: 10.1126/science.1206432

Chin, E. Y., and Kupfer, J. A. (2020). Identification of environmental drivers in urban greenway communities. *Urban For. Urban Green.* 47:126549. doi: 10.1016/j.ufug.2019.126549

Collins, S. L., Chung, Y. A., Baur, L. E., Hallmark, A., Ohlert, T. J., and Rudgers, J. A. (2020). Press–pulse interactions and long-term community dynamics in a Chihuahuan Desert grassland. *J. Veg. Sci.* 31, 722–732. doi: 10.1111/jvs.12881

Curtis, J. T., and McIntosh, R. P. (1950). The interrelations of certain analytic and synthetic phytosociological characters. *Ecology* 31, 434–455. doi: 10.2307/1931497

Davies, B. E. (1974). Loss-on-ignition as an estimate of soil organic matter. *Soil Sci. Soc. Am. J.* 38, 150–151. doi: 10.2136/sssaj1974.03615995003800010046x

Dengler, J. (2016). "Phytosociology," in *International Encyclopedia of Geography: People, the Earth, Environment & Technology: People, the Earth, Environment & Technology*, eds N. Castree, M. F. Goodchild, A. Kobayashi, W. Liu, and R. A. Marston (Hoboken, NJ: John Wiley & Sons), 1–6. *. doi: 10.1002/9781118786352.wbieg0136

Figueiredo, F. O., Zuquim, G., Tuomisto, H., Moulatlet, G. M., Balslev, H., and Costa, F. R. (2018). Beyond climate control on species range: the importance of soil data to predict distribution of Amazonian plant species. *J. Biogeogr.* 45, 190–200. doi: 10.1111/jbi.13104

Fujii, K., Shibata, M., Kitajima, K., Ichie, T., Kitayama, K., and Turner, B. L. (2018). Plant–soil interactions maintain biodiversity and functions of tropical forest ecosystems. *Ecol. Res.* 33, 149–160. doi: 10.1007/s11284-017-1511-y

Gairola, S., Sharma, C. M., Ghildiyal, S. K., and Suyal, S. (2012). Chemical properties of soils in relation to forest composition in moist temperate valley slopes of Garhwal Himalaya, India. *Environmentalist* 32, 512–523. doi: 10.1007/s10669-012-9420-7

Ganie, A. H., Tali, B. A., Khuroo, A. A., Reshi, Z. A., and Nawchoo, I. A. (2019). Impact assessment of anthropogenic threats to high-valued medicinal plants of Kashmir Himalaya, India. *J. Nat. Conserv.* 50:125715. doi: 10.1016/j.jnc.2019.125715

Ge, X. J., Zhang, L. B., Yuan, Y. M., Hao, G., and Chiang, T. Y. (2005). Strong genetic differentiation of the East-Himalayan *Megacodon stylophorus* (Gentianaceae) detected by inter-simple sequence repeats (ISSR). *Biodivers. Conserv.* 14, 849–861. doi: 10.1007/s10531-004-0655-6

Gelybo, G., Tóth, E., Farkas, C., Horel, A., Kasa, I., and Bakacsi, Z. (2018). Potential impacts of climate change on soil properties. *Agrokémia és Talajtan* 67, 121–141. doi: 10.1556/0088.2018.67.1.9

Griffith, D. M., Veech, J. A., and Marsh, C. J. (2016). Cooccur: probabilistic species co-occurrence analysis in R. *J. Stat. Softw.* 69, 1–17. doi: 10.18637/jss.v069.c02

Gulzar, R., Banday, F. A., Rather, Z. A., Rashid, I., and Khuroo, A. A. (2022). Naturalisation of ranunculus repens in Kashmir Himalaya: floristic and ecological aspects. *Plant Biosyst.* 1–7. doi: 10.1080/11263504.2022.2036847

Gupta, M. K., and Sharma, S. D. (2009). Effect of tree plantation on soil properties, profile morphology & productivity index-II. Poplar in Yamunanagar district of Haryana. *Ann. For.* 17, 43–70.

Hamid, M., Khuroo, A. A., Malik, A. H., Ahmad, R., and Singh, C. P. (2021). Elevation & aspect determine the differences in soil properties and plant species diversity on Himalayan mountain summits. *Ecol. Res.* 36, 340–352. doi: 10.1111/1440-1703.12202

Haq, S. M., Calixto, E. S., Rashid, I., and Khuroo, A. A. (2021). Human-driven disturbances change the vegetation characteristics of temperate forest stands: a case study from Pir Panchal mountain range in Kashmir Himalaya. *Trees For. People* 6:100134. doi: 10.1016/j.tfp.2021.100134

He, Y. W., Pan, Y. F., Wang, P., and Guo, J. S. (2004). The effects of Poke weed antiviral protein on replication of HCV. *Chin. Hepatol.* 7, 233–236.

Hedley, M. J., Stewart, J. W. B., and Chauhan, B. (1982). Changes in inorganic and organic soil phosphorus fractions induced by cultivation practices and by laboratory incubations. *Soil Sci. Soc. Am. J.* 46, 970–976. doi: 10.2136/sssaj1982.03615995004600050017x

Hofhansl, F., Chacon-Madrigal, E., Fuchslueger, L., Jenking, D., Morera-Beita, A., Plutzar, C., et al. (2020). Climatic and edaphic controls over tropical forest diversity and vegetation carbon storage. *Sci. Rep.* 10, 1–11. doi: 10.1038/s41598-020-61868-5

Iqbal, M., Khan, S. M., Ahmad, Z., Hussain, M., Nasar, S., Shah, S. K., et al. (2021). Vegetation classification of the margalla foothills, islamabad under the influence of edaphic factors & anthropogenic activities using modern ecological tools. *Pakistan J. Bot.* 53, 10–30848. doi: 10.30848/PJB2021-5(22)

Ismail, I. M., and ELawad, A. A. (2015). Phytosociological analysis and species diversity of herbaceous layer in rashad and Alabassia Localities, South Kordofan State, Sudan. *Jordan J. Biol. Sci.* 147, 1–7. doi: 10.12816/0027562

Jha, M. N., Rathore, R. K., and P&e, P. (1984). Soil factor affecting the natural regeneration of silver fir & spruce in Himachal Pradesh. *Indian For.* 110, 293–298.

Jiao, S., Li, J., Li, Y., Jia, J., and Xu, Z. (2019). Soil C, N, & P distribution as affected by plant communities in the yellow river delta, China. *PLoS One* 14:e0226887. doi: 10.1371/journal.pone.0226887

Jucker, T., Bongalov, B., Burslem, D. F., Nilus, R., Dalponte, M., Lewis, S. L., et al. (2018). Topography shapes the structure, composition and function of tropical forest landscapes. *Ecol. Lett.* 21, 989–1000. doi: 10.1111/ele.12964

Kamran, S., Khan, S. M., Ahmad, Z., Ur Rahman, A., Iqbal, M., Manan, F., et al. (2020). The role of graveyards in species conservation and beta diversity: a vegetation appraisal of sacred habitats from Bannu, Pakistan. *J. For. Res.* 31, 1147–1158. doi: 10.1007/s11676-019-00893-1

Khan, M., Khan, S. M., Ilyas, M., Alqarawi, A. A., Ahmad, Z., and Abd_Allah, E. F. (2017). Plant species and communities assessment in interaction with edaphic & topographic factors; an ecological study of the mount Eelum district Swat, Pakistan. *Saudi J. Biol. Sci.* 24, 778–786. doi: 10.1016/j.sjbs.2016.11.018

Khan, S. M., Page, S., Ahmad, H., Shaheen, H., and Harper, D. M. (2012). Vegetation dynamics in the Western Himalayas, diversity indices and climate change. *Sci. Technol. Dev. J.* 31, 232–243.

Khan, W., Ahmad, H., Haq, F., Islam, M., and Bibi, F. (2012). Present status of moist temperate vegetation of Thandiani forests district Abbottabad Pakistan. *Int. J. Biosci.* 10, 80–88.

Lafleur, B., Pare, D., Munson, A. D., and Bergeron, Y. (2010). Response of northeastern North American forests to climate change: will soil conditions constrain tree species migration? *Environ. Rev.* 18, 279–289. doi: 10.1139/A10-013

Lin, D. U., Wang, J. X., Wang, F., Zhou, H. Y., and Wei, D. U. (2018). Triterpenoid saponins from roots of *Phytolacca acinosa*. *China J. Chin. Materia Med.* 43, 2552–2556.

Ma, X. P., Lou, H. Y., Zhang, W. F., Song, J. R., Li, Y., and Pan, W. D. (2019). Triterpenoids from *Phytolacca acinosa*. *Chem. Nat. Compd.* 55, 292–295. doi: 10.1007/s10600-019-02670-2

Ma, X. P., Zhang, W. F., Yi, P., Lan, J. J., Xia, B., Jiang, S., et al. (2017). Novel flavones from the root of *Phytolacca acinosa* Roxb. *Chem. Biodivers.* 14:e1700361. doi: 10.1002/cbdv.201700361

Malfasi, F., and Cannone, N. (2020). Climate warming persistence triggered tree ingression after shrub encroachment in a high alpine tundra. *Ecosystems* 23, 1657–1675. doi: 10.1007/s10021-020-00495-7

Manoj, K., Nandakumar, M. K., Remya, M. P., Shinila, K., and Lakshmi, P. D. (2012). Phytosociological analysis of riparian tree species of Alakyam stream; Pariyaram, Kerala, India. *Int. J. Environ. Sci.* 2, 1895–1903.

Manzoor, N., Wani, I., Singh, K. P., and Pal, A. (2017). In-vitro antimicrobial activity phytochemical screening of *Phytolacca acinosa* in Kashmir Valley. *Int. J. Sci. Res.* 6, 102–106.

Mishra, G., Das, P. K., Borah, R., and Dutta, A. (2017). Investigation of phytosociological parameters & physico-chemical properties of soil in tropical semi-evergreen forests of Eastern Himalaya. *J. For. Res.* 28, 513–520. doi: 10.1007/s11676-016-0330-2

Mishra, G., Giri, K., and Pandey, S. (2018). Role of Alnus nepalensis in restoring soil fertility: a case study in Mokokchung, Nagaland. *Nat. Acad. Sci. Lett.* 41, 265–268. doi: 10.1007/s40009-018-0668-4

Mumshad, M., Ahmad, I., Khan, S. M., Rehman, K., Islam, M., Sakhi, S., et al. (2021). Phyto-ecological studies and distribution pattern of plant species and communities of Dhirkot, Azad Jammu and Kashmir, Pakistan. *PLoS One* 16:e0257493. doi: 10.1371/journal.pone.0257493

Nafeesa, Z., Haq, S. M., Bashir, F., Gaus, G., Mazher, M., Anjum, M., et al. (2021). Observations on the floristic, life-form, leaf-size spectra and habitat diversity of vegetation in the Bhimber hills of Kashmir Himalayas. *Acta Ecol. Sin.* 41, 228–234. doi: 10.1016/j.chnaes.2021.03.003

Noreen, I., Khan, S. M., Ahmad, Z., Rahman, I. U., Tabassum, A. B., and Abd_Allah, E. F. (2019). Response of different plant species to pollution emitted from oil and gas plant with special reference to heavy metals accumulation. *Pakistan J. Bot.* 51, 1231–1240. doi: 10.30848/PJB2019-4(39)

Ocon, J. P., Ibanez, T., Franklin, J., Pau, S., Keppel, G., Rivas-Torres, G., et al. (2021). Global tropical dry forest extent and cover: a comparative study of bioclimatic definitions using two climatic data sets. *PLoS One* 16:e0252063. doi: 10.1371/journal.pone.0252063

Olsen, S. R., Watanabe, F. S., Cosper, H. R., Larson, W. E., and Nelson, L. B. (1954). Residual phosphorus availability in long-time rotations on calcareous soils. *Soil Sci.* 78, 141–152. doi: 10.1097/00010694-195408000-00008

Paudel, P. K., Sipos, J., and Brodie, J. F. (2018). Threatened species richness along a Himalayan elevational gradient: quantifying the influences of human population density, range size, and geometric constraints. *BMC Ecology* 18:6. doi: 10.1186/s12898-018-0162-3

Phillips, E. A. (1959). *Methods of vegetation study*. New York, NY: Holt, Rhinehart and Winston, 107.

Powers, J. S., and Schlesinger, W. H. (2002). Relationships among soil carbon distributions and biophysical factors at nested spatial scales in rain forests of northeastern Costa Rica. *Geoderma* 109, 165–190. doi: 10.1016/S0016-7061(02)00147-7

POWO. (2022). *Plants of the World Online*. Available from: http://www.plantsoftheworldonline.org/ (accessed 13 March 2022)

R Core Team (2020). *R: A Language and Environment for Statistical Computing*. Vienna: R Foundation for Statistical Computing.

Rahman, I. U., Hart, R. E., Ijaz, F., Afzal, A., Iqbal, Z., Calixto, E. S., et al. (2022). Environmental variables drive plant species composition & distribution in the moist temperate forests of Northwestern Himalaya, Pakistan. *PloS One* 17:e0260687. doi: 10.1371/journal.pone.0260687

Rana, S. K., Rana, H. K., Luo, D., and Sun, H. (2021). Estimating climate-induced 'Nowhere to go'range shifts of the Himalayan Incarvillea Juss. using multi-model median ensemble species distribution models. *Ecol. Indic.* 121:107127. doi: 10.1016/j.ecolind.2020.107127

Rawal, R. S., Rawal, R., Rawat, B., Negi, V. S., and Pathak, R. (2018). Plant species diversity & rarity patterns along altitude range covering treeline ecotone in Uttarakhand: conservation implications. *Trop. Ecol.* 59, 225–239.

Ray, J. G., and George, J. (2009). Phytosociology of roadside communities to identify ecological potentials of tolerant species. *J. Ecol. Nat. Environ.* 1, 184–190.

Romshoo, S. A., Bashir, J., and Rashid, I. (2020). Twenty-first century-end climate scenario of Jammu & Kashmir Himalaya. India, using ensemble climate models. *Clim. Change* 162, 1473–1491. doi: 10.1007/s10584-020-02787-2

Shaheen, H., Shinwari, Z. K., Qureshi, R. A., and Ullah, Z. (2012). Indigenous plant resources & their utilization practices in village populations of Kashmir himalayas. *Pakistan J. Bot.* 44, 739–745.

Shannon, C. E., and Weaver, W. W. (1963). *The Mathematical Theory of Communication*. Urbana: University of Illinois Press, 117.

Simpson, E. H. (1949). Measurement of diversity. *Nature* 163, 688–688. doi: 10.1038/163688a0

Sofi, I. I., Zargar, S. A., Ganie, A. H., and Shah, M. A. (2022). Distribution dynamics of *Arnebia Euchroma* (Royle) IM Johnst. and associated plant communities in Trans-Himalayan Ladakh region in relation to local livelihoods under climate change. *Trees For. People* 7:100213. doi: 10.1016/j.tfp.2022.100213

Solon, J., Degorski, M., and Roo-Zielinska, E. (2007). Vegetation response to a topographical-soil gradient. *Catena* 71, 309–320. doi: 10.1016/j.catena.2007.01.006

Subbiah, B. V., and Asija, C. L. (1956). A rapid procedure for the estimation of available nitrogen in soils. *Curr. Sci.* 25, 256–260.

Tali, B. A., Ganie, A. H., Nawchoo, I. A., Wani, A. A., and Reshi, Z. A. (2015). Assessment of threat status of selected endemic medicinal plants using IUCN regional guidelines: a case study from Kashmir Himalaya. *J. Nat. Conserv.* 23, 80–89. doi: 10.1016/j.jnc.2014.06.004

Tali, B. A., Khuroo, A. A., Ganie, A. H., and Nawchoo, I. A. (2019). Diversity, distribution & traditional uses of medicinal plants in Jammu & Kashmir (J&K) state of Indian Himalayas. *J. Herb. Med.* 17:100280. doi: 10.1016/j.hermed.2019.100280

Tao, Y., Jiang, E., and Cai, B. (2020). Development of an ultra-high-performance liquid chromatography coupled with triple quadrupole mass spectrometry method for comparative pharmacokinetics of six triterpenoids in rat plasma and application to different forms of *Phytolacca acinosa*. *J. Sep. Sci.* 43, 1248–1255. doi: 10.1002/jssc.201901140

van der Putten, W. H., Bradford, M. A., Pernilla Brinkman, E., van de Voorde, T. F., and Veen, G. F. (2016). Where, when and how plant–soil feedback matters in a changing world. *Funct. Ecol.* 30, 1109–1121. doi: 10.1111/1365-2435.12657

Walentowski, H., Aas, G., Göllner, A., Ahl, L., and Feulner, M. (2018). Phytosociological studies of *Malus sylvestris* in North Hesse and upper Franconia. Germany. *Tuexenia* 38, 97–110.

Walkley, A., and Black, I. A. (1934). An examination of the degtjareff method for determining soil organic matter, and a proposed modification of the chromic acid titration method. *Soil Sci.* 37, 29–38. doi: 10.1097/00010694-193401000-00003

Wani, I. A., Verma, S., Gupta, R., Ganaie, M. M., Nigam, G., Shafik, H. M., (2022). Nutrient analysis and species diversity of alpine grasslands: a comparative analysis of less studied biodiversity hotspots. *Sustainability* 14:887. doi: 10.3390/su14020887

Wani, Z. A., Islam, T., Satish, K. V., Ahmad, K., Dhyani, S., and Pant, S. (2022). Cultural value and vegetation structure of *Buxus wallichiana* Bail. in Rajouri-Poonch region of Indian Himalayan region (VSI: Mountainous regions). *Trees, For. People* 7:100182. doi: 10.1016/j.tfp.2021.100182

Yadav, R. R., Negi, P. S., and Singh, J. (2021). Climate change and plant biodiversity in Himalaya. India. *Proc. Indian Natl Sci. Acad.* 87, 234–259. doi: 10.1007/s43538-021-00034-5

Yang, Y. S., Zhang, L., Li, H. Q., He, H. D., Wei, Y. X., Luo, J., et al. (2018). Soil physicochemical properties and vegetation structure along an elevation gradient and implications for the response of alpine plant development to climate change on the northern slopes of the Qilian Mountains. *J. Mt. Sci.* 15, 1006–1019. doi: 10.1007/s11629-017-4637-z

Zaz, S. N., Romshoo, S. A., Krishnamoorthy, R. T., and Viswanadhapalli, Y. (2019). Analyses of temperature and precipitation in the Indian Jammu and Kashmir region for the 1980–2016 period: implications for remote influence and extreme events. *Atmos. Chem. Phys.* 19, 15–37. doi: 10.5194/acp-19-15-2019

frontiers | Frontiers in Forest and Global Change

TYPE Original Research
PUBLISHED 25 August 2022
DOI 10.3389/ffgc.2022.995427

EDITED BY
Yashwant Singh Rawat,
Federal Technical and Vocational
Education and Training Institute
(FTVETI), Ethiopia

REVIEWED BY
Mohd Tariq,
Parul University, India
Zeeshan Ahmad,
Quaid-i-Azam University, Pakistan

*CORRESPONDENCE
Shreekar Pant
shreekarpant.2@gmail.com

SPECIALTY SECTION
This article was submitted to
Forest Management,
a section of the journal
Frontiers in Forests and Global Change

RECEIVED 15 July 2022
ACCEPTED 28 July 2022
PUBLISHED 25 August 2022

CITATION
Wani ZA, Bhat JA, Negi VS, Satish KV, Siddiqui S and Pant S (2022) Conservation Priority Index of species, communities, and habitats for biodiversity conservation and their management planning: A case study in Gulmarg Wildlife Sanctuary, Kashmir Himalaya.
Front. For. Glob. Change 5:995427.
doi: 10.3389/ffgc.2022.995427

Conservation Priority Index of species, communities, and habitats for biodiversity conservation and their management planning: A case study in Gulmarg Wildlife Sanctuary, Kashmir Himalaya

Zishan A. Wani[1], Jahangeer A. Bhat[2], Vikram S. Negi[3], K. V. Satish[4], Sazada Siddiqui[5] and Shreekar Pant[6]*

[1]Conservation Ecology Lab, Department of Botany, Baba Ghulam Shah Badshah University, Rajouri, Jammu and Kashmir, India, [2]College of Horticulture and Forestry Rani Lakshmi Bai Central Agricultural University, Jhansi, UP, India, [3]Center for Biodiversity Conservation and Management, G. B. Pant, National Institute of Himalayan Environment, Almora, Uttarakhand, India, [4]Remote Sensing Laboratory, Institute of Environment and Sustainable Development, Banaras Hindu University, Varanasi, India, [5]Department of Biology, College of Science, King Khalid University, Abha, Saudi Arabia, [6]Centre for Biodiversity Studies, Baba Ghulam Shah Badshah University, Rajouri, Jammu and Kashmir, India

The present study is an attempt to evaluate the Conservation Priority Index (CPI) of species, habitats, and communities for their conservation and management planning in the Kashmir Himalayas in India. The present study is an attempt to prioritize 361 plant species, 18 plant communities (10 within the forest zone and 08 within the alpine zone), and 07 habitats for conservation planning. Out of the total plant species recorded, 06 species were categorized as critically endangered, 20 endangered, 28 vulnerable, and 98 species to be near threatened. Amongst the forest and alpine communities, *Abies pindrow* community and *Juniperus squamata-Rhododendron anthopogon* mixed community showed the maximum CPI values. Amongst the habitats, dry habitats showed the maximum CPI in the sanctuary. The study found that the threatened species positively correlated with the native and endemic species indicating that these species were rigorously affected due to biotic and abiotic stresses. Based on the results of the present study, we propose a practical method for biodiversity conservation and management of protected areas. The approach employs a variety of qualitative and quantitative features to compute CPI in conjunction with phytosociological data. This kind of study will be immensely helpful to forest officials, policy makers, conservators, and researchers for planning better strategies to conserve and manage particular species, communities, and even habitats in protected areas.

KEYWORDS

Himalayan region, plant community, Conservation Priority Index, endemism, threatened species

Introduction

Asia is home to one of the largest, most elevated, and most highly populated mountain ranges in the world. This mountain range is called the Himalayas (Rana et al., 2021). The Himalayas designated as a global biodiversity hotspot underlines their significance as a storehouse for unique flora and fauna (Allen et al., 2010). A high degree of endemism in the area suggests the presence of numerous important eco-regions and ecosystems with global significance (Dhar, 2002). Himalayan forests serve as a significant "sink" for carbon dioxide and further provide a livelihood to a sizable population both upstream and downstream (Reddy et al., 2016; Chakraborty et al., 2017; Negi et al., 2018a). Therefore, India's National Action Plan on Climate Change (NAPCC) considered this region vital for preserving the ecological security of India (Negi et al., 2019). However, the Himalayan ecosystems are highly vulnerable and are degrading due to various biotic and abiotic stresses (Wani et al., 2022). Overall, climate change is a leading cause of ecological changes and biodiversity loss, although species invasions are also one of the important factors contributing to changes in forest productivity and biodiversity loss, especially native and endemic species (Behera et al., 2019; Negi et al., 2021; Wani et al., 2021). Besides these factors, the forests of the Himalayan region are now becoming vulnerable due to increasing anthropogenic disturbances like deforestation, unsustainable fuel wood, timber collection, and agricultural expansion (Negi and Maikhuri, 2017; Thakur et al., 2022). Therefore, detailed information on species, communities, and habitats is necessary to create effective conservation and management plans for these biodiversity-rich places.

Protected Areas (PA) are recognized as areas with high biodiversity, and as a result, receive special consideration and increased focus on biodiversity conservation and management (Rawat and Adhikari, 2015). A number of studies have, therefore, highlighted the contribution of PAs in the conservation of biodiversity and also in preventing threatened species from extinction risk (Karanth et al., 2010; Oldekop et al., 2016). However, recent studies conducted around the world have shown that biodiversity and other ecosystem products and services continue to be lost despite constant growth in the number of areas covered under PAs (Jenkins and Joppa, 2009; McDonald and Boucher, 2011). According to IPBES (2019), up to one million species of plants and animals are threatened by the risk of extinction. The most recent update of the IUCN Red List includes 142, 577 species [International Union for Conservation of Nature (IUCN), 2022] representing ∼7% of the biodiversity of the planet (Ronsted et al., 2022). The irony is that most plant species lack global risk assessment, and the lack of knowledge of which plant species are at risk of extinction limits our ability to frame conservation and management policies (Nic Lughadha et al., 2020). Therefore, the first stage in conservation planning in every region is to establish priorities, criteria, and indicators (Mirtl et al., 2018; Negi et al., 2019). The criteria and indicators approach offers a mechanism for evaluating changes in specific forestry circumstances, and this knowledge helps forest managers plan pertinent conservation policies (Rawat et al., 2008). Additionally, vulnerability mapping of certain species and forests is needed, especially in the Himalayan region, for the implementation of ground-level management plans (Thakur et al., 2020, 2022). Further, to manage and conserve biodiversity in the face of ongoing global change, it is necessary to have enough data to evaluate the status and trends of species ranges, their population, community makeup, and habitat types (Oliver et al., 2021). Species richness has been the main focus of conservation studies and is still widely used (Bano et al., 2018). For instance, conservation planning has historically given priority to some regions over others using the information on richness mixed with various metrics (such as endemism or rarity) (Cadotte and Tucker, 2018). However, to assess the state and trends of species distributions and manage biodiversity in the face of continuing global change, sufficient evidence is required (Oliver et al., 2021). The status and trends of species populations and distributions, communities, and different types of habitats directly linked to the ecological value of those variables are crucial for conservation and management (Bland et al., 2015).

To prevent species extinction, broad, ecosystem-based conservation strategies are also required, which do not rely on taxonomic information or the determination of individual species but on the community composition and habitat types. Thus, developing a Conservation Priority Index of unique species, communities, and habitats at local, regional, national, and global levels is an important step in conservation and management planning. Species richness, nativity, and endemism are a few of the qualities that help prioritize species, communities, and habitats (Pant and Samant, 2007). In Kashmir Himalaya, few efforts have been made to prioritize species for conservation, but most of these studies primarily focused to prioritize medicinal or economically important plants (Dar and Naqshi, 2001; Baig et al., 2014; Tali et al., 2015, 2018; Haq et al., 2019, 2021). However, no attempt has been made to prioritize species, habitats, and communities for conservation and management within the protected area networks of Kashmir Himalaya. Keeping these research gaps in consideration, the present study attempts to evaluate the Conservation Priority Index (CPI) of species, habitats, and communities in Gulmarg Wildlife Sanctuary (GWLS), in order to find out which species, communities, and habitats should be prioritized for conservation and management planning within the sanctuary.

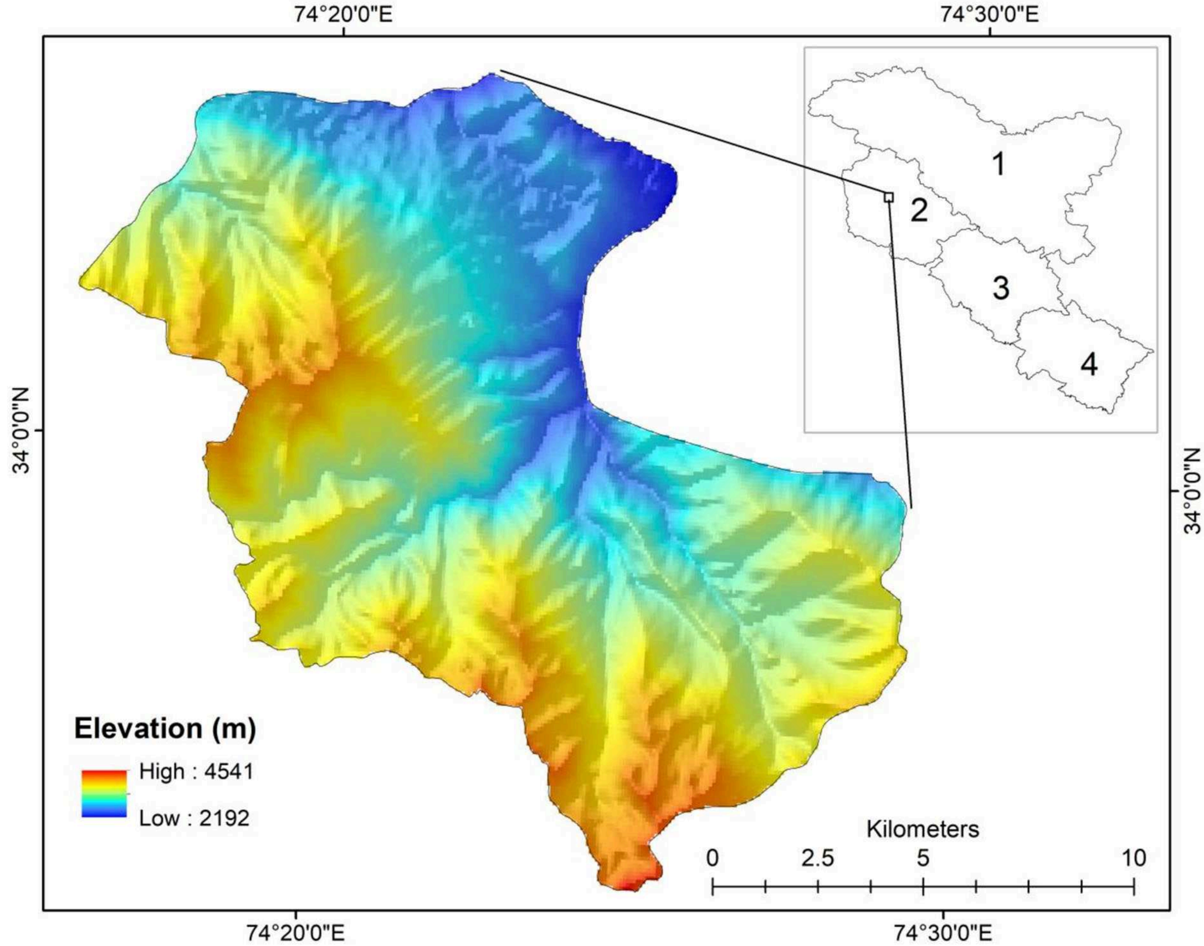

FIGURE 1
Location map of Gulmarg Wildlife Sanctuary.

Materials and methods

Study area

Gulmarg Wildlife Sanctuary (GWLS) stretches between 74°17′ to 74°79′ N latitude and 34°55′ to 34°60′ E longitude in District of Baramulla situated in Jammu and Kashmir (Figure 1). It covers an area of 180 km^2, out of which 60 and 120 km^2 of the areas are under forest and alpine zones, respectively, with an altitudinal range of 2,300–4,200m asl. GWLS has two administrative units: Ferozpora/Tangmarg and Block Gulmarg and are divided into 20 compartments numbering 31–41 (Lower elevation compartments) and 50–58 (Upper elevation compartments), respectively. The mountains in this Himalayan region maintain their glaciation above 3,700 m almost all year round, and the sanctuary has a wet temperate climate with a well-balanced supply of moisture. As a result, the area above 3,700 m asl represents the nival zone and fits well with the climatological concept of the snowline developed for mesic mountains (Gottfried et al., 2011). Geologically, the region is made up of Triassic Limestone rocks, Panjal Traps volcanic rocks, Salkhala Series metamorphic rocks associated with granitic intrusions, and Karewa Group sediments (Dar et al., 2014). Since the area is entirely mountainous, the topography is very uneven. The vegetation is affected at all levels by a number of topographic elements, including altitude, slope steepness, exposure to light and wind, and the direction of mountain chains (Nanda et al., 2019). Coniferous temperate mountain forests of Blue Pine (*Pinus wallichiana*), sub-alpine forests of Silver Fir (*Abies pindrow*), and Himalayan Birch (*Betula utilis*), then alpine scrub and meadows, make up the majority of the vegetation of Gulmarg (Khuroo et al., 2015). Additionally, the sanctuary is home to numerous medicinal plants and nomadic groups like the Gujjars and Bakerwals (Wani and Pant, 2020).

Data collection and analysis

Field visits and surveys were carried out for the qualitative and quantitative assessment of the plant species within the forest, as well as the alpine zone, of the study area in different seasons from May 2018 to June 2022. A total of 123 sites (63 in the forest zone and 60 in the alpine zone) were selected to cover all the possible aspects and habitats along the altitudinal gradient (2,300–4,200m asl). Habitats were identified on the basis of physical features and the dominant vegetation of the sites. The sites having closed canopy along with a high proportion of organic matter and moisture were considered shady moist habitats. Sites having an open canopy with a low proportion of organic matter and moisture were classified as dry habitats whereas sites having an open canopy with high moisture and humus were classified as moist habitats. The sites with high anthropogenic pressures (assessed in terms of trampling, the quantity of animal and human wastes, and distance from the residential areas) were considered exposed habitats. Quantitative assessment was carried out using a stratified random sampling method after laying out a plot of 50 × 50 m at each site. For the assessment of plant species within each plot, 10 random quadrats of 10 × 10 m were laid for trees, 10 quadrats of 5 × 5 m for shrubs, and 20 quadrats of 1 × 1 m for herbs nested in the same plot following standard sampling methods (Curtis and Intosh, 1950; Mishra, 1968; Samant et al., 2002; Rawal et al., 2018). The plant specimens from each plot were collected and relevant information (altitudinal range, habitat, and growth forms) were recorded in a field book. Each collected specimen was later identified up to the species level with the help of local and regional floras (Dhar and Kachroo, 1983; Bhat, 1984; Naqshi et al., 1984; Singh and Kachroo, 1994; Singh et al., 2002). Accepted nomenclature and families of the species were retrieved from the Plants of the World Online database (https://powo.science.kew.org). Forest communities were delineated on the basis of the Importance Value Index (IVI) following the study of Mishra (1991). Sites having ≥50% of the total IVI contributed by a single species were categorized as pure communities of that species whereas sites having ≥50% of the total IVI contributed by two or more species were categorized as mixed communities of those species. Using the same criteria, communities in the alpine zone were identified on the basis of relative density instead of IVI following Rana and Samant (2009).

The nativity and endemism of the species were determined (Dhar and Samant, 1993; Samant et al., 1996; Samant and Dhar, 1997; Khuroo et al., 2007, 2010). Plant species having their origins in the Himalayan region were considered native and the rest were considered non-natives, while the plant species having their distribution limited to the Himalayan region were considered endemics (Samant et al., 1998). Furthermore, the threat status of the plant species was assessed following the study of Rana and Samant (2010) using the parameters viz., population size, habitat specificity, altitudinal range, nativity, and endemism. Furthermore, information regarding the use values of the plant species was collected through interviews and discussions with knowledgeable persons from the surrounding villages of the sanctuary.

CPI was calculated to assess the site-specific threat status at species, habitat, and community levels (Rana and Samant, 2009, 2010; Singh and Samant, 2010; Rana et al., 2020). The CPI value of plant species was calculated as the cumulative values of six attributes *viz.*, altitudinal range, habitat specificities, use values, population size, nativity and endemism, and extraction trend following Rana and Samant (2010). The attributes used for each species were given grades/marks, with a maximum of 10 points, moderate of 6 points, and minimum of 2 points (Table 1). The species having ≥75% of total CPI (i.e., ≥45 out of 60) were categorized as Critically Endangered; 65–74% as Endangered; 55–64% as Vulnerable; 45–54% as Near Threatened, and ≤44% as Least Concerned, following Rana and Samant (2010) with some modifications. Based on the representative sites, range of altitudes, species richness, native species, endemic species, useful species, and threatened species, the CPI of habitats and communities was calculated (Rana and Samant, 2009). The CPI of habitats and communities is the aggregate value of all these attributes, the value of which ranges from 2 to 10 (Table 2). The species, habitats, and communities satisfying all the attributes in the highest grade resulted in the highest aggregate values while attributes with the lowest grade resulted in the lowest aggregate values. Correlation of the total species with a number of native and endemic species, number of users with threatened species, and number of native and endemic species with threatened species in the forest, as well as the alpine zone, was calculated using Microsoft Excel 2010.

Results

Species diversity and phytogeographic affinities

A total of 361 plant species belonging to 73 families and 210 genera were recorded (Supplementary Table S1). Asteraceae was the dominant family with 56 species followed by Lamiaceae (22 species), Rosaceae (21 species), and Ranunculaceae (19 species). Ten most dominant families are presented in Figure 2. A total of 184 plant species were found native and 81 species endemic to the Himalayan region. Non-native species have different phytogeographic affinities with major contributions from Asia, Eurasia, and Europe (Figure 3). A total of 158 plant species were found to be utilized by the local people for various purposes i.e., food, fodder, medicine, fuel wood, and timber. Among the unique and high-value medicinal plants were *Achillea millifolium*, *Angelica glauca*, *Artemisia absinthium*, *Bergenia ciliata*, *Colchicum luteum*, *Dolomiaea costus*, *Fritillaria roylei*,

TABLE 1 Attributes used for calculating the CPI of plant species in GWLS.

Score	Range of altitude (m)	Habitat	Use values	Population size	Native/Endemic	Extraction trend
2	>1,000	>3	<3	>250 Ind/>5 Locations	Non-native	No extraction
6	500–1,000	2–3	3–4	51–250 Ind/5 Locations	Native	Self-use
10	<1,000	1	>4	≤50 Ind/2 Locations	Native and Endemic	Commercial

TABLE 2 Attributes used to calculate the CPI of communities and habitats.

Score	Sites	Altitudinal range (m)	Habitats*	Total species %	Native species %	Endemic species %	Useful species %	Threatened species %
10	1	<200	1	>35	>35	>35	>35	>35
8	2	200–400	2	30–35	30–35	30–35	30–35	30–35
6	3	400–600	3	25–30	25–30	25–30	25–30	25–30
4	4	600–800	4	20–25	20–25	20–25	20–25	20–25
2	>4	>800	>4	<20	<20	<20	<20	<20

*Not used for CPI calculation of habitats.

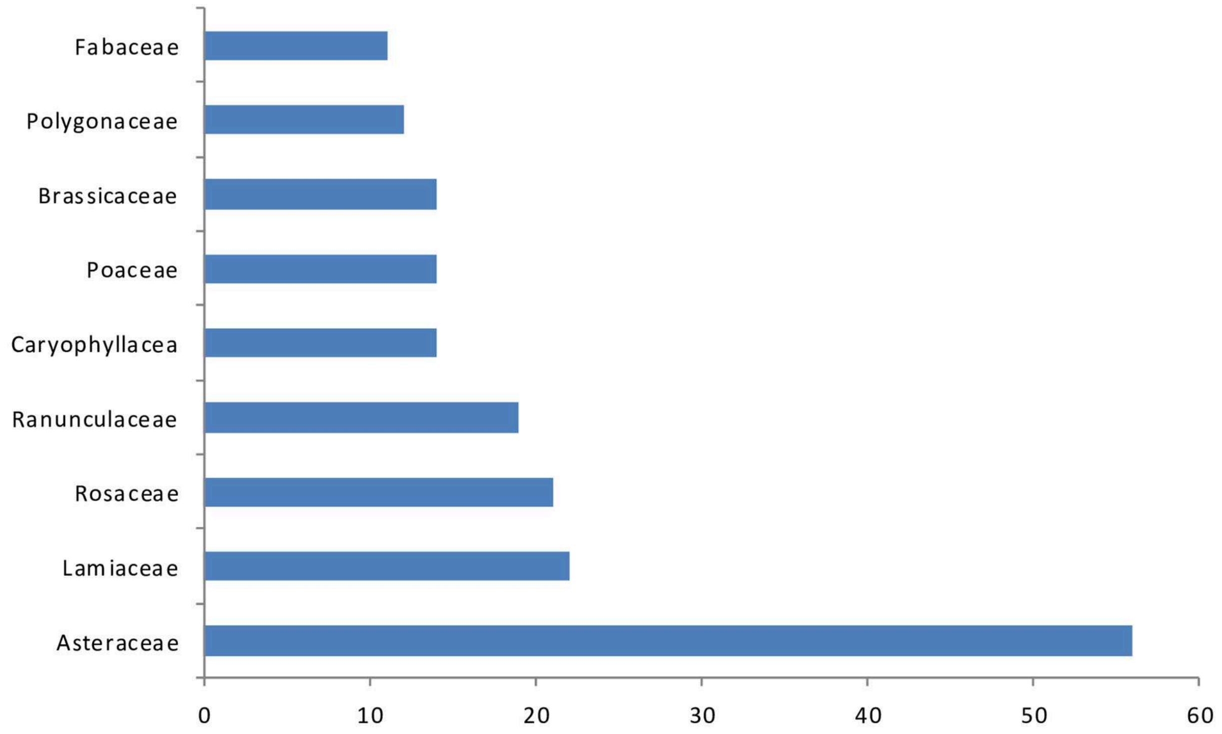

FIGURE 2
Ten dominant plant families in GWLS.

Hyoscyamus niger, *Inula racemosa*, *Lamium album*, *Picrorhiza kurroa*, *Podophyllum hexandrum*, *Trillium govanianum*, and *Thymus linearis*. Medicinal plants like *Aconitum heterophyllum*, *Angelica glauca*, *Dolomiaea costus*, *Fritillaria roylei*, *Picrorhiza kurroa*, *Rheum webbiana*, and *Trillium govanianum* are used highly for commercial purposes. Prominent wild edibles used by the local inhabitants include *Taraxacum sect. Taraxacum*, *Berberis lycium*, *Capsella bursa-pastrosis*, *Dipsacus innermis*, *Dioscorea deltoidea*, *Rheum webbiana*, *Malva neglecta*, *Fragaria nubicola*, and *Viburnum grandiflorum*.

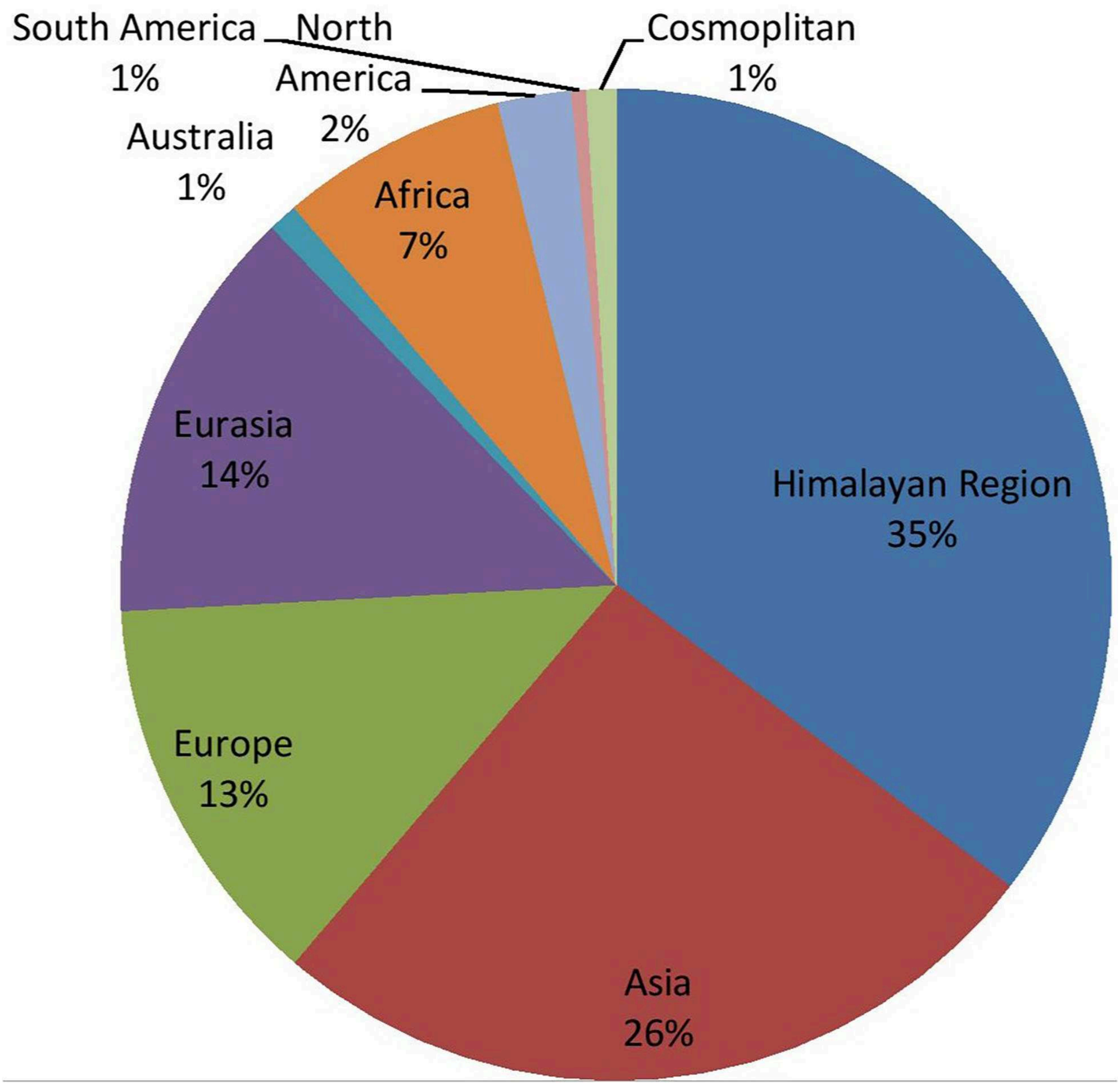

FIGURE 3
Phytogeographic affinities of the recorded plant species from GWLS.

Habitat and community diversity

The study revealed a total of seven habitats including shady, moist, dry, bouldary, rocky, riverine, moist, and exposed throughout GWLS. A total of 18 plant communities were identified including 10 forest communities and 8 alpine communities. Ten plant communities delineated from the forest zone include *Abies pindrow* community, *Pinus wallichiana* community, *A. pindrow-P. wallichiana* mixed community, *P. wallichiana-Cedrus deodara* mixed community, *A. pindrow-Picea smithiana* mixed community, *A. pindrow-Picea smithiana* mixed community, *Aesculus indica-Taxus wallichiana* mixed community, *Taxus wallichiana-Prunus cornuta-Aesculus indica* mixed community, *Abies pindrow-Acer cesium* mixed community, and *Betula utilis* community. Eight plant communities delineated from the alpine zone include *Viburnum grandiflorum* community, *Salix denticulata* community, *Rhododendron campanulatum* community, *Juniperus squamata* community, *Juniperus squamata-Rhododendron anthopogon* mixed community, *Bistorta affinis- Saussurea acktinsonii-Bergenia stracheyi* mixed community, *Rhododendron anthopogon* community, and *Bistorta affinis-Swertia petiolata* mixed community.

Prioritization of communities and habitats for conservation

Site representation

Amongst habitats, dry habitats represented maximum sites (27) followed by bouldary (22), shady moist (20), exposed (17), riverine (13), rocky (16), and moist (6). Amongst forest communities, *Abies pindrow* community was represented at maximum sites (16 sites) followed by *Pinus wallichiana* community (9 sites), *Betula utilis* community (7 sites each) *Abies pindrow-Pinus wallichiana* mixed, *Pinus wallichiana–Cedrus deodara* mixed (6 each). The rest of the communities were represented at <6 sites. Amongst alpine communities, *Juniperus squamata-Rhododendron anthopogon* mixed community represented maximum sites (21) followed *Bistorta affinis- Saussurea acktinsonii-Bergenia stracheyi* mixed community (13) and *Bistorta affinis-Swertia petiolata* mixed and *Rhododendron anthopogon* community (7 sites each) and *Viburnum grandiflorum* (6 sites). *Juniperus squamata, Salix denticulata, and*

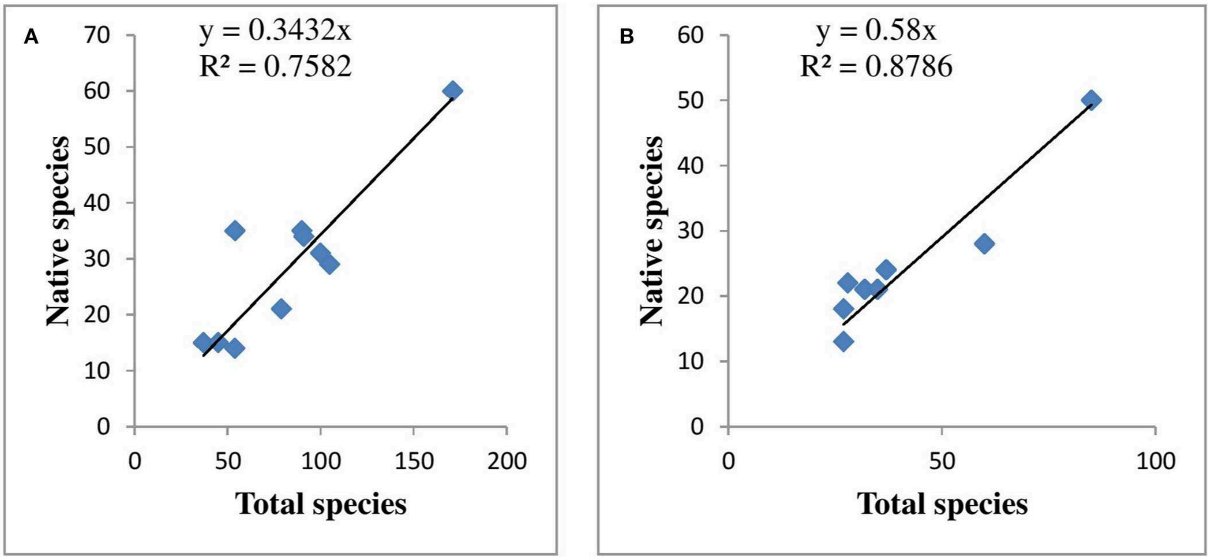

FIGURE 4
Correlation between total species and native species **(A)** forest zone **(B)** alpine zone.

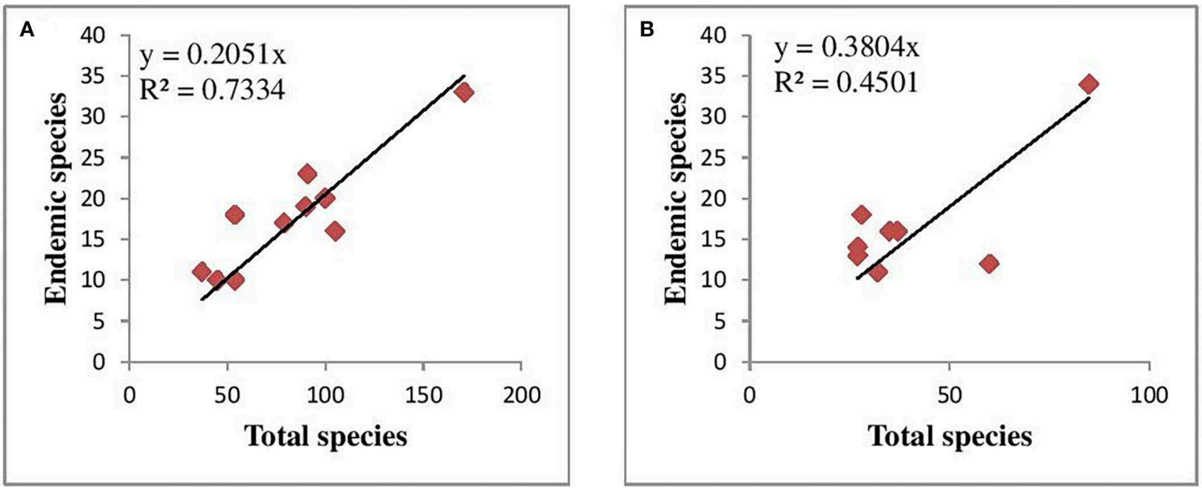

FIGURE 5
Correlation between total species and endemic specie **(A)** forest zone **(B)** alpine zone.

Rhododendron campanulatum communities were represented at <4 sites.

Altitudinal distribution

Amongst the habitats, bouldary habitats showed a wide distribution range followed by dry riverine and rocky habitats. Amongst the forest communities, the distribution range was maximum (2,300–3,000) for *Abies pindrow* community followed by *Pinus wallichiana-Abies pindrow* mixed (2,400–2,700) and *Pinus wallichiana* (2,300–2,600) and *Betula utilis* (2,300–3,500). Amongst alpine communities, the altitudinal range was maximum for the *Juniperus squamata-Rhododendron anthopogon* mixed community (3,400–3,900) followed by *Bistorta affinis- Saussurea acktinsonii- Bergenia stracheyi* mixed (3,350–3,700) community. *Rhododendron campanulatum* and *Salix denticulata* communities were having the least altitudinal ranges.

Species richness

Amongst habitats, species richness was highest (34.1%) in a dry habitat, followed by shady moist (32.7%), bouldary (29.7%), rocky (27.8%), riverine (22.3%), exposed (20.3%), and moist (13.4%). Amongst the forest communities, species richness was found maximum in *Abies pindrow* community

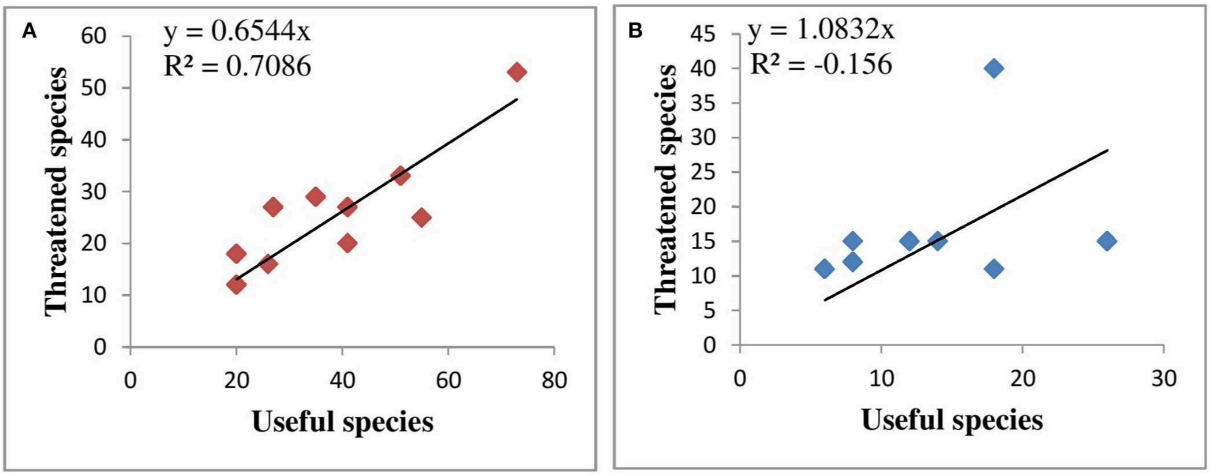

FIGURE 6
Correlation between useful species and threatened species **(A)** forest zone **(B)** alpine zone.

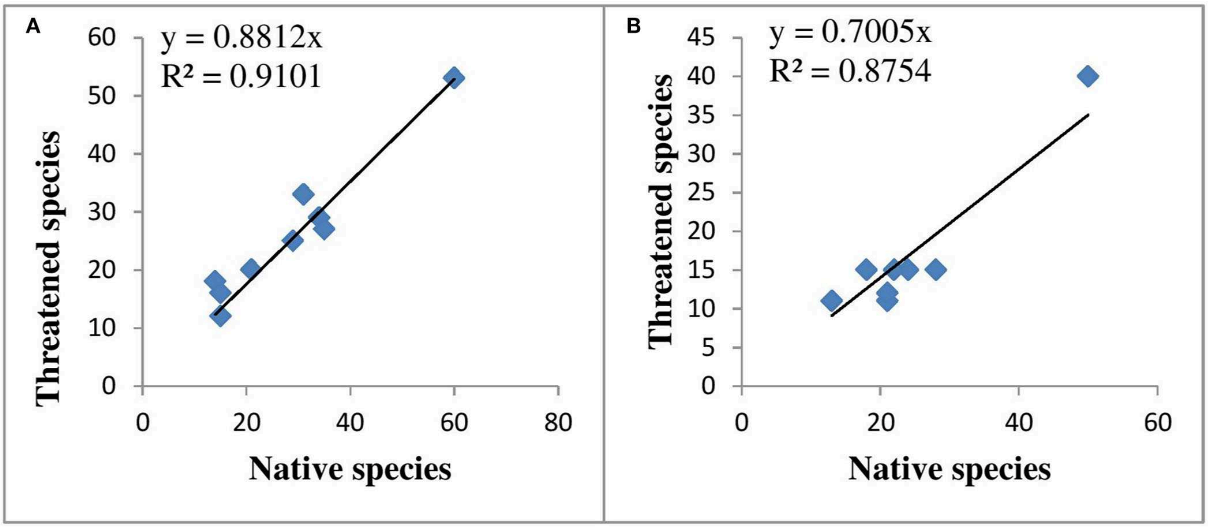

FIGURE 7
Correlation of native species and threatened species **(A)** forest zone **(B)** alpine zone.

(46.8%), followed by *Pinus wallichiana* community (28.9%), *Pinus wallichiana-Abies pindrow* mixed community (27.5%), and *Abies pindrow-Picea smithiana* mixed community (24.7%). Amongst the alpine communities, species richness was maximum in *Juniperus squamata-Rhododendron anthopogon* mixed community (23.4%) followed by *Viburnum grandiflorum* community (16.5%), *Juniperus squamata* community (10.1%) and *Bistorta affinis- Saussurea acktinsonii- Bergenia stracheyi* mixed community (9.6%).

Distribution of native and endemic species

Amongst the habitats, dry habitats exhibit maximum native species (35.5%) followed by bouldary (35.1%), shady moist (31.1%), rocky (25.6%), exposed (19.5%), riverine (13.5%), and moist (12.8%). Dry habitats exhibit maximum endemic species (44.4%) followed by shady moist (41.9%), bouldary (35.8%), exposed (29.6%), rocky (22.2%), riverine (16.1%), and moist (12.8%). Amongst the forest communities, maximum native species were found in the *Abies pindrow* community (40.52%) followed by *Abies pindrow-Picea smithiana* mixed community and *Betula utilis* (23.6% each), *Abies pindrow-Acer cesium* mixed community (22.9%), and *Pinus wallichiana* community (20.9%). Maximum endemic species were found in *Abies pindrow* community (40.7%) followed by *Abies pindrow-Acer cesium* mixed (28.3%), and *Abies pindrow-Pinus wallichiana* mixed (24.6%). Amongst alpine communities, maximum native, as well as endemic species (33.7% native and 41.9% endemic), were found in *Juniperus squamata-Rhododendron anthopogon* mixed community followed by *Viburnum grandiflorum* community (18.9% native and 14.8% endemic), and *Rhododendron anthopogon* community (14.8% native and 22.2% endemic).

Distribution of useful species

Maximum useful species were distributed in bouldary habitats (38.5%) followed by dry (37.9%), shady moist (34.8%), rocky (34.1%), exposed (29.5%), riverine (22.7%), and moist habitats (19.6%). Amongst the forest communities, the maximum number of useful species were distributed in *Abies pindrow* community (46.2%) followed by *Pinus wallichiana* communities (35.4%), *Abies pindrow-Pinus wallichiana* mixed communities (32.9%), and *Abies pindrow-Picea smithiana* mixed community (25.9%). Amongst alpine communities, the maximum number of useful species were distributed in *Viburnum grandiflorum* community (16.4%) followed by *Juniperus squamata-Rhododendron anthopogon* mixed and *Salix denticulata* communities (11.3%), and *Juniperus squamata* community (8.8%).

Distribution of threatened species

Amongst habitats, maximum threatened species were distributed in rocky habitats (34.6%) followed by bouldary (32.6%), shady moist (30.7%), dry (25.0%), exposed (23.0%), moist (15.3), and riverine (13.4%). Amongst forest communities, maximum threatened species were distributed in *Abies pindrow* community (34.8%) followed by *Abies pindrow-Pinus wallichiana* mixed (21.7%), *Abies pindrow-Acer cesium* mixed (19.0%), *Abies pindrow-Picea smithiana* mixed and *Betula utilis* community (17.7% each). Amongst alpine communities, maximum threatened species were distributed in *Juniperus squamata-Rhododendron anthopogon* mixed community (26.3%) followed by *Viburnum grandiflorum*, *Juniperus squamata* and *Rhododendron anthopogon* communities (9.8% each). A significant positive correlation is found between the total species and native species in the forest zone (0.87, $p < 0.01$,

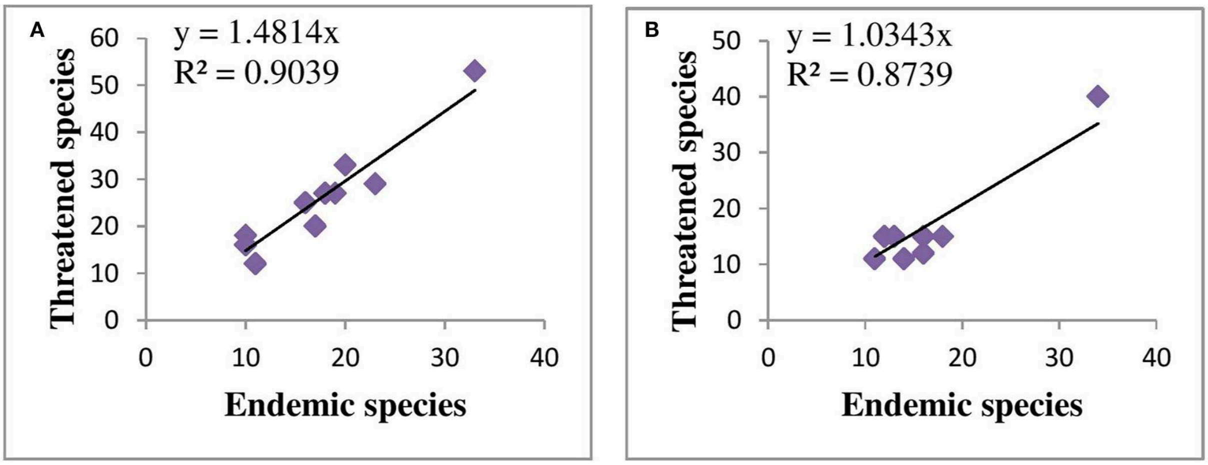

FIGURE 8
Correlation of endemic species and threatened species **(A)** forest zone **(B)** alpine zone.

TABLE 3 Calculated CPI value of different habitats within GWLS.

Habitats	Sites	Altitudinal range (m)	Total species %	Native species %	Endemic species %	Useful species %	Threatened species %	CPI
Shady moist	20	2,300–2,900	32.7	31.1	41.9	34.8	30.7	46
Rocky	16	2,300–3,800	27.8	25.6	22.2	34.1	34.6	36
Bouldary	22	2,500–4,200	29.7	35.1	35.8	38.5	32.6	48
Dry	27	2,400–3,600	34.1	35.1	44.4	37.9	25.0	50
Riverine	13	2,300–3,800	22.3	13.5	16.1	22.7	13.4	18
Exposed	17	2,300–4,200	20.3	19.5	29.6	29.5	23.0	26
Moist	6	2,700–3,200	13.4	12.8	14.8	19.6	15.3	18

TABLE 4 Calculated CPI of different delineated forest communities within GWLS.

Community	RS	H	AR	SR%	N%	EN%	US%	Th%	CPI
Forest communities									
Abies pindrow	16	5	2,300–3,000	46.8	40.54	40.74	46.20	34.8	56
Pinus wallichiana	9	4	2,300-2,600	28.9	19.5	20.9	35.4	16.4	38
Abies pindrow-Pinus wallichiana mixed	6	3	2,400–2,700	27.5	20.9	24.6	32.9	21.7	42
Pinus wallichiana-Cedrus deodara mixed	6	3	2,350–2,600	22.0	14.1	20.9	25.9	13.1	36
Abies pindrow-Picea smithiana mixed	5	2	2,400–2,550	24.7	23.6	24.4	25.9	17.7	40
Aesculus indica-Pinus wallichiana mixed	2	1	2,400–2,500	10.1	10.1	13.5	12.6	7.8	38
Aesculus indica-Taxus wallichiana mixed	2	2	2,500–2,700	14.8	9.4	12.3	15.1	11.8	36
Taxus wallichiana-Prunus cornuta-Aesculus indica mixed	5	3	2,450–2,600	12.3	10.1	12.3	16.4	10.5	28
Abies pindrow-Acer cesium mixed	5	4	2,750–2,950	25.0	22.9	28.3	22.1	19.0	38
Betula utilis	7	2	3,200–3,500	14.8	23.6	22.2	17.0	17.7	32
Alpine communities									
Viburnum grandiflorum	6	2	3,000–3,200	16.5	18.9	14.8	16.4	9.8	28
Salix denticulate	1	1	3,170	8.8	14.1	13.5	11.3	7.2	40
Rhododendron campanulatum	2	1	3,230	7.4	12.1	16.0	7.5	8.5	38
Juniperus squamata	3	1	3,350	10.1	16.2	19.7	8.8	9.8	36
Juniperus squamata-Rhododendron anthopogon mixed	21	3	3,400–3,900	23.4	33.7	41.9	11.3	26.3	44
Bistorta affinis- Saussurea acktinsonii- Bergenia stracheyi mixed	13	3	3,350–3,700	9.6	14.1	19.7	5.0	7.8	26
Rhododendron anthopogon	7	2	3,800–4,050	7.7	14.8	22.2	5.0	9.8	28
Bistorta affinis-Swertia petiolata	7	3	3,900–4,200	7.4	8.1	17.2	3.7	7.2	26

RS, Representative sites; H, Habitat; AR, Altitudinal range; SR, Species richness; N, Nativity; EN, Endemism; US, Useful species; Th, Threatened species; CPI, Conservation Priority Index.

R^2 0.75) and alpine zone (0.94, $p < 0.01$, $R^2 = 0.87$) (Figure 4) and there is also a significant positive correlation between the total species and endemic species in the forest (0.90, $p < 0.01$, $R^2 = 0.73$) and alpine zones (0.75, $p < 0.01$, $R^2 = 0.45$) (Figure 5). A significant positive correlation is found between the number of useful species and the number of threatened species in the forest ($r = 0.85$, $p < 0.01$, $R^2 = 0.70$), as well in the alpine zone ($r = 0.830$, $p < 0.01$, $R^2 = -0.15$) (Figure 6). Further, a significant positive correlation is found between the number of threatened species and native species in the forest zone ($r = 0.96$, $p < 0.01$, $R^2 = 0.91$) and in alpine zone ($r = 0.94$, $p < 0.01$, $R^2 = 0.87$) (Figure 7) and endemic species in forest zone ($r = 0.95$, $p < 0.01$, $R^2 = 0.90$) and in the alpine zone ($r = 0.95$, $p < 0.01$, $R^2 = 0.87$) (Figure 8).

Conservation priority index

Based on the threat assessment of the species, 6 plant species were assessed to be critically endangered, 20 endangered, 28 vulnerable, and 98 plant species were assessed to be near threatened. Rests of the species were assessed to be the least concern in the study area (Supplementary Table S1). Amongst the habitats, dry habitats showed the maximum CPI (50) followed by bouldary (48), shady moist (46), and rocky (36) habitats (Table 3). Amongst forest communities, *Abies pindrow* community showed maximum CPI value (56), followed by *Abies pindrow-Pinus wallichiana* mixed community (42), *Abies pindrow-Picea smithiana* mixed community (40) (Table 4). Amongst alpine communities, *Juniperus squamata-Rhododendron* *anthopogon* mixed community showed maximum CPI value (44), followed by *Salix denticulata* (40), *Rhododendron campanulatum* (38), and *Juniperus squamata* community (36) (Table 4).

Discussion

Species richness recorded during the present study was higher than in earlier reports from the Indian Himalayan region (Singh et al., 2007; Chawla et al., 2008; Dar and Sundarapandian, 2016; Pandey et al., 2018; Haq et al., 2019, 2021; Ahmad et al., 2020). Asteraceae, Lamiaceae, Rosaceae, and Ranunculaceae were reported to be dominant contributing maximum species. These families have been reported as dominant in Indian Himalayas in earlier studies also (Samant et al., 2007; Dar and Khuroo, 2012; Haq et al., 2019; Ahmad et al., 2021; Altaf et al., 2021). As a large number of species has become threatened in Kashmir Himalaya over the decades due to various anthropogenic disturbances (Hamid et al., 2020), the rich floristic diversity of the native, endemic, economically important, and threatened species in the GWLS signifies the enormous conservation and socio-economic values of the sanctuary.

A significant positive correlation was found between the total species and native species in the forest and alpine zones. There is also a significant positive correlation between the total species and endemic species in the forest and alpine zones which indicate that as the number of species increases there is an increase in the number of native and endemic species. The correlation between the number of useful species and the number of threatened species in the forest was much strong than in the alpine zone indicating that the number of threatened species was higher in forest communities having biotic/abiotic pressures. It is obvious that an increased number of useful species in a community will lead to a burden on

FIGURE 9
Notable threatened plants of GWLS **(A)** *Podophyllum hexandrum* **(B)** *Aconitum heterophyllum* **(C)** *Trillium govanianum* **(D)** *Phytolacca acinosa* **(E)** *Arisaema jacquemontii* **(F)** *Dioscorea deltoidea* **(G)** *Rhododendron campanulatum* **(H)** *Arisaema propinquum* **(I)** *Hyoscyamus niger*.

TABLE 5 Threat status of some prioritized plant species as per previous studies.

Taxa	Nayar and Sastry (1988)	Walter and Gillett (1998)	Molur and Walker (1998)	Dar and Naqshi (2001)	Rao et al. (2003)	Tali et al. (2015)	International Union for Conservation of Nature (IUCN) (2022)	Present study
Ulmus wallichiana	–	EN	–	EN	EN	–	VUL	VUL
Berberis lycium	–	–	EN	–	–	–		EN
Aconitum heterophyllum	–	EN	CR	EN	–	–	EN	EN
Aconitum violaceum	–	–	CR	–	–	–	VUL	VUL
Aquilegia nivalis	–	EN	–	VUL	EN	EN	–	EN
Atropa acuminata	–	–	CR	VUL	–	EN	EN	EN
Dioscorea deltoidea	VUL	–	CR	–	–		–	EN
Dolomiaea costus	EN	EN	CR	VUL	EN	–	CR	CR
Acer cesium	VUL	–	–	–	VUL	–	–	NT
Angelica glauca	–	EN	–	–	–		–	EN
Fritillaria roylei	–		CR	R	–	VUL	–	CR
Inula racemosa	VUL	VUL	–	R	–	–	–	VUL
Trillium govanianum	–	–	–	–	–	–	EN	CR
Eremerus himalaicus	R	–	–	–	–	–	–	CR
Hyoscyamus niger	–	–	–	R	–	–	–	VUL
Meconopsis latifolia	VUL	VUL		EN	VUL			EN
Picrorhiza kurrooa	VUL	–	–	EN	–	–	–	CR
Rhododendron campanulatum	–	–	–	VUL	–	–	–	CR

CR, Critically Endangered; EN, Endangered; VUL, Vulnerable; R, Rare.

the unique species, resulting in their declining population. Further, a significant positive correlation between the number of threatened species and native species in the forest zone and in the alpine zone and endemic species in the forest zone and in the alpine zone indicated that the native and endemic plant species were rigorously affected due to biotic and abiotic stresses (Rana et al., 2020). Anthropogenic disturbances coupled with climate change promote biological invasions in mountain ecosystems and thus pose threat to native and endemic species and are a global concern (Ahmad et al., 2021; Li et al., 2021). Endemic species are specialist species and have narrow niche widths and thus narrow environmental tolerance (Mills et al., 2020).

Conservation prioritization of species, habitats, and communities is a prerequisite for biodiversity conservation and management planning in the protected area (Singh and Samant, 2010). Based on the CPI value of species in the present study, 41.8% of species were categorized as threatened and near threatened in the study area. Some of the plants assessed to be threatened in GWLS are given in Figure 9. Some of these plant species have been categorized as threatened in some previous studies also (Table 5). However, Hamid et al. (2020) pointed out that many plant species like *Betula utilis*, *Colchicum luteum*, *Podophyllum hexandrum*, *Rheum webbianum*, *Taxus wallichiana*, and *Valeriana jatamansii* have not been included in the threatened lists despite of their dwindling populations and thus recommended their immediate categorization as per the IUCN criteria.

Among the forest community, *Abies pindrow* community and *Abies pindrow-Pinus wallichiana* mixed community, whereas among alpine communities, *Juniperus squamata-Rhododendron anthopogon* mixed and *Salix denticulata* community with high CPI values indicated the need for conservation (Figure 10). Furthermore, dry, bouldary, and shady moist habitats with high CPI value reveal that the proper management of these habitats would help in maintaining the natural ecosystems and conservation of species of the area, as the habitat fragmentation and degradation are considered as one of the primary drivers of species extinction (Tilman et al., 2001; Ganie et al., 2019; Quan et al., 2021; Su et al., 2022). The prioritized habitats and communities not only have higher species richness, but also possess the premier number of native, endemic, economically important, and threatened species. Thus, any alteration in these communities and habitats will lead to an alteration in their species composition; the consequences of which may be the loss of native, endemic, and threatened species (Mehta et al., 2020). Further, the communities were identified on the basis of the dominance of one or more species pointing out that any alteration in such dominant species will alter the composition of these communities. Therefore, the regeneration dynamics of such dominant species need to be analyzed thoroughly for conservation and management

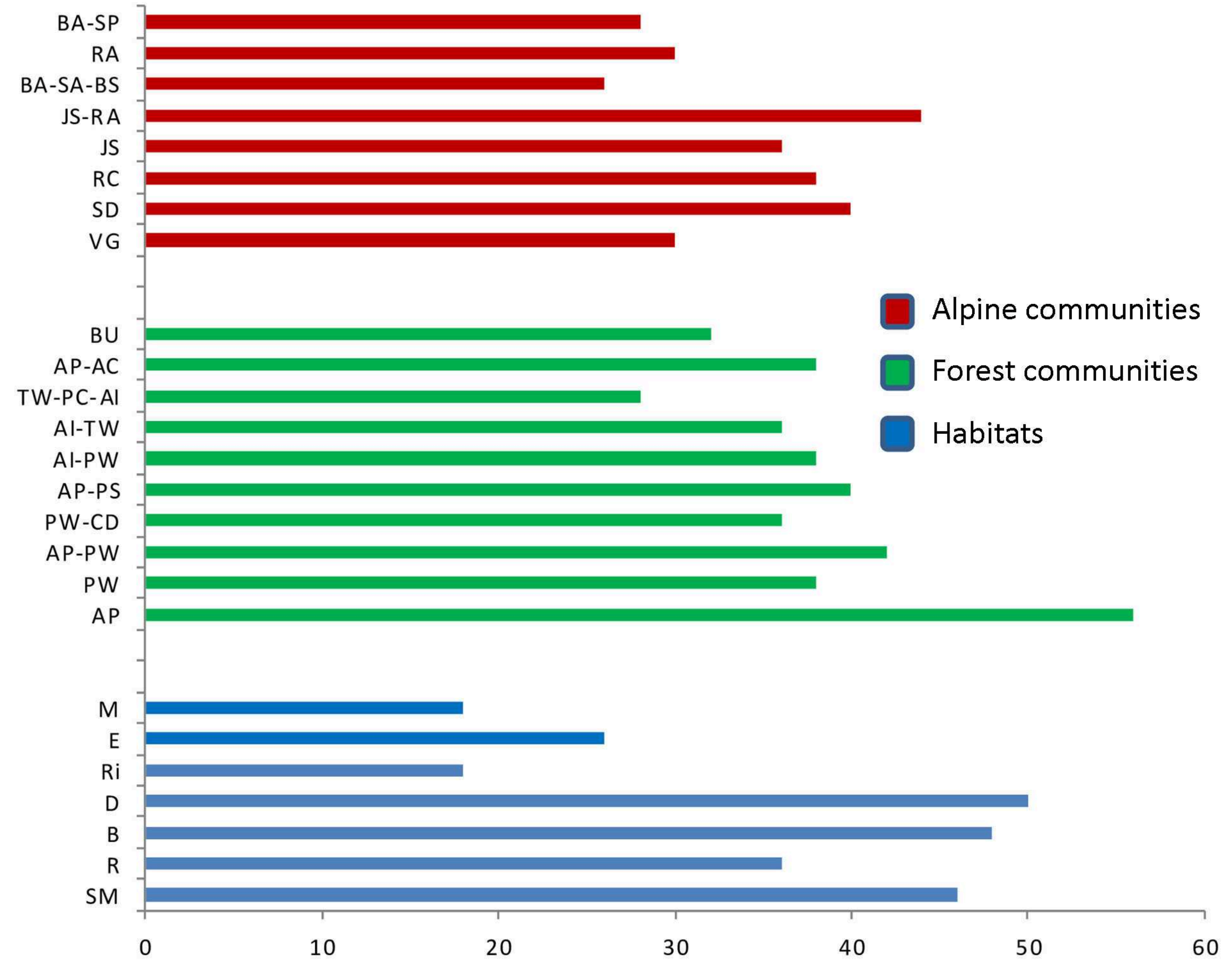

FIGURE 10
CPI of delineated alpine and forest communities and habitats; BA-SP, *Bistorta affinis-Swertia petiolata* community; RA, *Rhododendron anthopogon* community; BA-SA-BS, *Bistorta affinis-Saussurea acktinsonii-Bergenia stracheyi* community; *Juniperus squamata-Rhododendron anthopogon* community; *Juniperus squamata* community; *Rhododendron campanulatum* community; *Salix denticulata* community; *Viburnum grandiflorum* community; AP, *Abies pindrow* community; PW, *Pinus wallichiana* community; AP-PW, *Abies pindrow-Pinus wallichiana* community; PW-CD, *Pinus wallichiana-Cedrus deodara* community; AP-PS, *Abies pindrow-Picea smithiana* community; AI-PW, *Aesculus indica-Pinus wallichiana* community; AI-TW, *Aesculus indica-Taxus wallichiana* community; TW-PC-AI, *Taxus wallichiana-Prunus cornuta-Aesculus indica* community; AP-AC, *Abies pindrow-Acer cesium* community; BU, *Betula utilis* community; M, Moist; E, Exposed; Ri, Riverine; D, Dry; B, Bouldary; R, Rocky; SM, Shady Moist.

planning. Further, regular monitoring of the prioritized habitats and communities is desirable to comprehend the structural and functional alterations in the natural vegetation due to various biotic and abiotic stresses as suggested by previous studies (Negi et al., 2018b, 2019).

At the local level, proper application of the IUCN criteria is necessary for assessing the conservation status of taxonomic units (Rodrigues et al., 2006; Miller et al., 2007; Abeli et al., 2009). The comprehensive method used in this study includes IUCN criteria that are suitable in the local context (Dunn et al., 1999; Keller and Bollmann, 2004; Gauthier et al., 2010). The current work proposes a practical method for managing protected areas based on scientific site-specific techniques (species, habitats, and communities), which employs a variety of qualitative and quantitative features to compute CPI in conjunction with phytosociological data. However, it is well-established that such research is useless unless the findings of these studies are used by forest managers and policymakers for implementing biodiversity conservation and management policies.

Conclusion

The present study attempts to assess the floristic diversity of forest and alpine communities in GWLS. Further, the study attempts to prioritize the species, habitats, and communities for conservation and management strategies. A number of species were assessed to be threatened within the study area and out of which many species are on the IUCN's Red List of species. Further, the prioritized habitats and communities in GWLS are not only rich in species number, but also possess a greater number of native, endemic, and threatened species. Therefore, any type of negative impact on such habitats and communities, in turn will affect the survival of such precious species. Long-term monitoring using the quadrat method for all the growth forms of the georeferenced plots representing the prioritized habitats and communities is required. Further, tourist influx should be limited as per the carrying capacity of the sanctuary, and guidelines for the visitors should be framed in order to reduce the trampling of herbaceous flora inside the sanctuary. Thus, the present study has developed baseline information for initiating conservation and management planning.

Data availability statement

The original contributions presented in the study are included in the article/Supplementary material, further inquiries can be directed to the corresponding author/s.

Author contributions

ZW: conceptualization, methodology, data collection, curation and analysis, investigation, and writing original draft. JB and VN: writing the review and validation. KS: writing the review. SS: writing the review and funding acquisition. SP: conceptualization, supervision, validation, and writing the review. All authors contributed to the article and approved the submitted version.

Funding

The authors extend their appreciation to the Deanship of Scientific Research at King Khalid University for funding this work through a Large Group Research Project under grant number (RGP2/90/44).

Conflict of interest

The authors declare that the research was conducted in the absence of any commercial or financial relationships that could be construed as a potential conflict of interest.

Publisher's note

Supplementary material

The Supplementary Material for this article can be found online at: https://www.frontiersin.org/articles/10.3389/ffgc.2022.995427/full#supplementary-material

References

Abeli, T., Gentili, R., Rossi, G., Bedini, G., and Foggi, B. (2009). Can the IUCN criteria be effectively applied to peripheral isolated plant populations? *Biodivers. Conserv*. 18, 3877–3890. doi: 10.1007/s10531-009-9685-4

Ahmad, M., Sharma, P., Rathee, S., Singh, H. P., Batish, D. R., Lone, G. R., et al. (2021). Niche width analyses facilitate identification of high-risk endemic species at high altitudes in western Himalayas. *Ecol. Indcat.* 126, 107653. doi: 10.1016/j.ecolind.2021.107653

Ahmad, M., Uniyal, S. K., Batish, D. R., Singh, H. P., Jaryan, V., Rathee, S., et al. (2020). Patterns of plant communities along vertical gradient in Dhauladhar Mountains in Lesser Himalayas in North-Western India. *Sci. Tot. Environ.* 716, 136919. doi: 10.1016/j.scitotenv.2020.136919

Allen, D. J., Molur, S., and Daniel, B. A. (2010). *The Status and Distribution of Freshwater Biodiversity in the eastern Himalaya. International Union for Conservation of Nature and Natural Resources*. Cambridge; Gland: IUCN.

Altaf, A., Haq, S. M., Shabnum, N., and Jan, H. A. (2021). Comparative assessment of Phyto diversity in Tangmarg Forest division in Kashmir Himalaya, India. *Acta Ecol. Sin.* doi: 10.1016/j.chnaes.2021.04.009

Baig, B. A., Ramamoorthy, D., and Wani, B. A. (2014). Population status and conservation prioritization of some threatened medicinal plants of Kashmir Himalayas. *Int. J. Appl. Biol. Pharm. Technol.* 5.

Bano, S., Khan, S. M., Alam, J., Alqarawi, A. A., Abd Allah, E. F., Ahmad, Z., et al. (2018). Eco-Floristic studies of native plants of the Beer Hills along the Indus River in the districts Haripur and Abbottabad, Pakistan. *Saudi J. Biol. Sci.* 25, 801–810. doi: 10.1016/j.sjbs.2017.02.009

Behera, M. D., Behera, S. K., and Sharma, S. (2019). Recent advances in biodiversity and climate change studies in India. *Biodivers. Conserv.* 28, 1943–1951. doi: 10.1007/s10531-019-01781-0

Bhat, N. A. (1984). *Floristic Composition of Gulmarg (Baramulla)* (Ph. D. Thesis). University of Kashmir, Srinagar.

Bland, L. M., Collen, B., Orme, C. D. L., and Bielby, J. (2015). Predicting the conservation status of data- deficient species. *Conserv. Biol.* 29, 250–259. doi: 10.1111/cobi.12372

Cadotte, M. W., and Tucker, C. M. (2018). Difficult decisions: strategies for conservation prioritization when taxonomic, phylogenetic and functional diversity are not spatially congruent. *Biol. Conserv*. 225, 128–133. doi: 10.1016/j.biocon.2018.06.014

Chakraborty, A., Joshi, P. K., and Sachdeva, K. (2017). Capturing forest dependency in the central Himalayan region: variations between Oak (*Quercus* spp.) and Pine (*Pinus* spp.) dominated forest landscapes. *Ambio*. 47, 504–522. doi: 10.1007/s13280-017-0947-1

Chawla, A., Rajkumar, S., Singh, K. N., Lal, B., and Singh, R. D. (2008). Plant Species Diversity along an Altitudinal Gradient of Bhabha Valley in Western Himalaya. *J. Moun. Sci.* 5, 157–177. doi: 10.1007/s11629-008-0079-y

Curtis, J. T., and Intosh, M. C. (1950). The Inter relation of certain analytic and phytosociological character. *Ecology* 31, 434–445. doi: 10.2307/1931497

Dar, G. H., and Khuroo, A. A. (2012). Floristic diversity in the Kashmir Himalaya: progress, problems and prospects. *Sains Malay.* 42, 1377–1386.

Dar, G. H., and Naqshi, A. R. (2001). Threatened flowering plants of the Kashmir Himalaya – a checklist. *Orien. Sci.* 6, 23–53.

Dar, J. A., and Sundarapandian, S. (2016). Patterns of plant diversity in seven temperate forest types of Western Himalaya, India. *J. Asia Pac. Biodivers.* 9, 280–292. doi: 10.1016/j.japb.2016.03.018

Dar, R. A., Rashid, I., Romshoo, S. A., and Marazi, A. (2014). Sustainability of winter tourism in a changing climate over Kashmir Himalaya. *Environ. Mon. Asses.* 186, 2549–2562. doi: 10.1007/s10661-013-3559-7

Dhar, U. (2002). Conservation implications of plant endemism in high-altitude Himalaya. *Curr. Sci.* 82, 141–148.

Dhar, U., and Kachroo, P. (1983). Alpine flora of Kashmir Himalaya, Scientific Publishers, Jodhpur. *India.* doi: 10.2307/2805987

Dhar, U., and Samant, S. S. (1993). Endemic diversity of Indian Himalaya I. Ranunculaceae and II. Paeoniaceae. *J, Biogeogra.* 20, 659–668. doi: 10.2307/2845521

Dunn, E. H., Hussell, D. J. T., and Welsh, D. A. (1999). Priority-setting tool applied to Canada's land birds based on concern and responsibility of species. *Conserv. Biol.* 13, 1404–1415. doi: 10.1046/j.1523-1739.1999.98400.x

Ganie, A. H., Tali, B. A., Khuroo, A. A., Reshi, Z. A., and Nawchoo, I. A. (2019). Impact assessment of anthropogenic threats to high-valued medicinal plants of Kashmir Himalaya, India. *J. Nat. Conserv* 50, 125715. doi: 10.1016/j.jnc.2019.125715

Gauthier, P., Debussche, M., and Thompson, J. D. (2010). Regional priority setting for rare species based on a method combining three criteria. *Biol. Conserv.* 143, 1501–1509. doi: 10.1016/j.biocon.2010.03.032

Gottfried, M., Hantel, M., Maurer, C., Toechterle, R., Pauli, H., and Grabherr, G. (2011). Coincidence of the alpine–nival ecotone with the summer snowline. *Environ. Res. Lett.* 6, 014013. doi: 10.1088/1748-9326/6/1/014013

Hamid, M., Khuroo, A. A., Ahmad, R., Rasheed, S., Malik, A. H., and Dar, G. H. (2020). "Threatened flora of Jammu and Kashmir state," in *Biodiversity of the Himalaya: Jammu and Kashmir state*, eds G. H. Dar and A. A. Khuroo (Singapore: Springer Nature). 957–995. doi: 10.1007/978-981-32-9174-4_37

Haq, S. M., Malik, A. H., Khuroo, A. A., and Rashid, I. (2019). Floristic composition and biological spectrum of Keran-a remote valley of northwestern Himalaya. *Acta Ecol. Sin.* 39, 372–379. doi: 10.1016/j.chnaes.2018.12.001

Haq, S. M., Shah, A. A., Yaqoob, U., and Hassan, M. (2021). Floristic quality assessment index of the Dagwan stream in Dachigam National Park of Kashmir Himalaya. *Proc. Natl. Acad. Sci. India Sect. B Biol. Sci.* 91, 657–664. doi: 10.1007/s40011-021-01247-w

International Union for Conservation of Nature (IUCN) (2022). *The IUCN Red List of threatened species (Version 2021-3).* Available online at: https://www.iucnredlist.org. (accessed May 18, 2021–November 23, 2021).

IPBES (2019). *Global assessment report on biodiversity and ecosystem services of the Intergovernmental Science-Policy Platform on Biodiversity and Ecosystem Services.* IPBES Secretariat.

Jenkins, C. N., and Joppa, L. (2009). Expansion of the global terrestrial protected area system. *Biol. Conserv.* 142, 2166–2174. doi: 10.1016/j.biocon.2009.04.016

Karanth, K. K., Nichols, J. D., Ullas., Karanth, K., Hines, J. E., and Christensen, N. L. (2010). The shrinking ark: patterns of large mammal extinctions in India. *Proc. R. Soc. B Biol. Sci.* 277, 1971–1979. doi: 10.1098/rspb.2010.0171

Keller, V., and Bollmann, K. (2004). From red lists to species of conservation concern. *Conserv. Biol.* 18, 1636–1644. doi: 10.1111/j.1523-1739.2004.00464.x

Khuroo, A. A., Hamid, M., and Malik, A. H. (2015). Himadri site in Kashmir Himalaya. *ENVIS Newsl. Him. Ecol.* 12, 4.

Khuroo, A. A., Rashid, I., Reshi, Z., Dar, G. H., and Wafai, B. A. (2007). The alien flora of Kashmir Himalaya. *Biol. Inv.* 9, 269–292. doi: 10.1007/s10530-006-9032-6

Khuroo, A. A., Weber, E., Malik, A. H., Dar, G. H., and Reshi, Z. A. (2010). Taxonomic and biogeographic patterns in the native and alien woody flora of Kashmir Himalaya, India. *Nord. J. Bot.* 28, 685–696. doi: 10.1111/j.1756-1051.2010.00750.x

Li, W., Shi, Y., Zhu, D., Wang, W., Liu, H., Li, J., et al. (2021). Fine root biomass and morphology in a temperate forest are influenced more by the nitrogen treatment approach than the rate. *Ecol. Indicat.* 130, 108031. doi: 10.1016/j.ecolind.2021.108031

McDonald, R. I., and Boucher, T. M. (2011). Global development and the future of the protected area strategy. *Biol. Conserv.* 144, 383–392. doi: 10.1016/j.biocon.2010.09.016

Mehta, P., Sekar, K. C., Bhatt, D., Tewari, A., Bisht, K., Upadhyay, S., et al. (2020). Conservation and prioritization of threatened plants in Indian Himalayan Region. *Biodivers. Conserv.* 29, 1723–1745. doi: 10.1007/s10531-020-01959-x

Miller, R. M., Rodríguez, J. P., Aniskowicz-Fowler, T., Bambaradeniya, C., Boles, R., Eaton, M. A., et al. (2007). National threatened species listing based on IUCN criteria and regional guidelines: current status and future perspectives. *Conserv. Biol.* 21, 684–686. doi: 10.1111/j.1523-1739.2007.00656.x

Mills, C. G., Allen, R. J., and Blythe, R. A. (2020). Resource spectrum engineering by specialist species can shift the specialist-generalist balance. *Theor. Ecol.* 13, 149–163. doi: 10.1007/s12080-019-00436-8

Mirtl, M., Borer, E. T., Djukic, I., Forsius, M., Haubold, H., Hugo, W., et al. (2018). Genesis, goals and achievements of long-term ecological research at the global scale: a critical review of ILTER and future directions. *Sci. Tot. Environ.* 626, 1439–1462. doi: 10.1016/j.scitotenv.2017.12.001

Mishra, K. C. (1991). *Manual of Plant Ecology.* Oxford: Oxford and IBH Publishing, 508.

Mishra, R. (1968). *Ecological Work Book.* Calcutta: Oxford and IBH Publishing Company.

Molur, S., and Walker, S. (1998). *Report of the workshop "conservation, assessment and management plan for selected medicinal plants of northern, northeastern and central India" (BCPP Endangered Species Project) Zoo Outreach Organisation.* Conservation Breeding Specialist Group, India, Coimbatore, India, 62.

Nanda, A. B., Nelofar., and Lone, R. A. (2019). Study of phenology of woody flora of Gulmarg and its neighbourhood for landscape use. *J. Sci. Res. Rep.* 22, 1–7. doi: 10.9734/jsrr/2019/v22i430095

Naqshi, A. R., Malla, M. Y., and Dar, G. H. (1984). Plants of Gulmarg. *J. Ecol. Tax. Bot.* 5, 709–741.

Nayar, M. P., and Sastry, A. R. K. (1988). *Red Data Book of Indian plants*, vols 1–3. Calcutta: BSI.

Negi, V. S., Giri, L., and Sekar, K. C. (2018b). Floristic diversity, community composition and structure in Nanda Devi National Park after prohibition of human activities, Western Himalaya, India. *Curr. Sci.* 115, 1056–1064. doi: 10.18520/cs/v115/i6/1056-1064

Negi, V. S., Joshi, B. C., Pathak, R., Rawal, R. S., and Sekar, K. C. (2018a). Assessment of fuel wood diversity and consumption patterns in cold desert part of Indian Himalaya: implication for conservation and quality of life. *J. Clean Prod.* 196, 23–31. doi: 10.1016/j.jclepro.2018.05.237

Negi, V. S., and Maikhuri, R. K. (2017). Forest resources consumption pattern in Govind wildlife sanctuary, western Himalaya, India. *J. Environ. Plan Manag.* 60, 1235–1252. doi: 10.1080/09640568.2016.1213707

Negi, V. S., Pathak, R., Rawal, R. S., Bhatt, I. D., and Sharma, S. (2019). Long-term ecological monitoring on forest ecosystems in Indian Himalayan Region: criteria and indicator approach. *Ecol. Ind.* 102, 374–381. doi: 10.1016/j.ecolind.2019.02.035

Negi, V. S., Tiwari, D. C., Singh, L., Thakur, S., and Bhatt, I. D. (2021). Review and synthesis of climate change studies in the Himalayan region. *Environ. Dev. Sust.* 10471–10502. doi: 10.1007/s10668-021-01880-5

Nic Lughadha, E., Bachman, S. P., Leao, T. C., Forest, F., Halley, J. M., Moat, J., et al. (2020). Extinction risk and threats to plants and fungi. *Plants Peo Plan* 2, 389–408. doi: 10.1002/ppp3.10146

Oldekop, J. A., Holmes, G., Harris, W. E., and Evans, K. L. (2016). A global assessment of the social and conservation outcomes of protected areas. *Conserv. Biol.* 30, 133–141. doi: 10.1111/cobi.12568

Oliver, R. Y., Meyer, C., Ranipeta, A., Winner, K., and Jetz, W. (2021). Global and national trends, gaps, and opportunities in documenting and monitoring species distributions. *PLoS Biol.* 19, e3001336. doi: 10.1371/journal.pbio.3001336

Pandey, A., Rai, S., and Kumar, D. (2018). Changes in vegetation attributes along an elevation gradient towards timberline in Khangchendzonga National Park, Sikkim. *Trop. Ecol.* 59, 259–271.

Pant, S., and Samant, S. S. (2007). Assessment of plant diversity and prioritization of communities for conservation in Mornaula Reserve Forest. *Appl. Ecol. Environ. Res.* 5, 123–138. doi: 10.15666/aeer/0502_123138

Quan, Q., Gao, S., Shang, Y., and Wang, B. (2021). Assessment of the sustainability of Gymnocypris eckloni habitat under river damming in the source region of the Yellow River. *Sci. Total Environ.* 778, 146312. doi: 10.1016/j.scitotenv.2021.146312

Rana, D., Kapoor, K. S., Samant, S. S., and Bhatt, A. (2020). Plant species conservation priority index for preparing management strategies: a case study from the Western Himalayas of India. *Small Scale For.* 19, 461–481. doi: 10.1007/s11842-020-09447-4

Rana, M. S., and Samant, S. S. (2009). Prioritization of habitats and communities for conservation in the Indian Himalayan Region: a state-of-the-art approach from Manali Wildlife Sanctuary. *Curr. Sci.* 97, 326–335.

Rana, M. S., and Samant, S. S. (2010). Threat categorisation and conservation prioritisation of floristic diversity in the Indian Himalayan region: a state of art approach from Manali Wildlife Sanctuary. *J. Natl. Conserv.* 18, 159–168. doi: 10.1016/j.jnc.2009.08.004

Rana, S. K., Rawal, R. S., Dangwal, B., Bhatt, I. D., and Price, T. D. (2021). 200 years of research on Himalayan biodiversity: trends, gaps, and policy implications. *Front. Ecol. Evol.* 8, 603422. doi: 10.3389/fevo.2020.603422

Rao, C. S., Suresh, B. L., and Suresh, G. (2003). *Red list of threatened Vascular Plant Species in India.* ENVIS, Botanical Survey of India, Howrah, Ministry of Environment and Forests, Government of India.

Rawal, R. S., Rawal, R., Rawat, B., Negi, V. S., and Pathak, R. (2018). Plant species diversity and rarity patterns along elevation range covering treeline ecotone in Uttarakhand: conservation implications. *Trop. Ecol.* 59, 1–15.

Rawat, G. S., and Adhikari, B. S. (eds.). (2015). *Ecology and Management of Grassland Habitats in India, ENVIS Bulletin: Wildlife and Protected Areas.* Vol. 17, Wildlife Institute of India, Dehradun, India

Rawat, T. S., Menaria, B. L., Dugaya, D., and Kotwal, P. C. (2008). Sustainable forest management in India. *Curr. Sci.* 94, 996–1002.

Reddy, C. S., Jha, C. S., Dadhwal, V. K., Krishna, P. H., Pasha, S. V., Satish, K. V., et al. (2016). Quantification and monitoring of deforestation in India over eight decades (1990-2013). *Biodivers. Conserv.* 25, 93–116. doi: 10.1007/s10531-015-1033-2

Rodrigues, A. S. L., Pilgrim, J. D., Lamoreux, J. F., Hofman, M., and Brooks, T. M. (2006). The value of the IUCN Red List for conservation. *Trend Ecol. Evol.* 21, 71–76. doi: 10.1016/j.tree.2005.10.010

Ronsted, N., Walsh, S. K., Clark, M., Edmonds, M., Flynn, T., Heintzman, S., et al. (2022). Extinction risk of the endemic vascular flora of Kauai, Hawaii, based on IUCN assessments. *Conserv. Biol.* e13896. doi: 10.1111/cobi.13896

Samant, S. S., Butola, J. S., and Sharma, A. (2007). Assessment of diversity, distribution, conservation status and preparation of management plan for medicinal plants in the catchment areas of Parbati Hydroelectric Power Project Stage –III in Northwestern Himalaya. *J. Moun Sci.* 4, 34–56. doi: 10.1007/s11629-007-0034-3

Samant, S. S., and Dhar, U. (1997). Diversity, endemism and economic potential of wild edible plants of Indian Himalaya. *Int. J. Sust. Dev. World Ecol.* 4, 179–191. doi: 10.1080/13504509709469953

Samant, S. S., Dhar, U., and Palni, L. M. S. (1998). *Medicinal Plants of Indian Himalaya.* Almora, India, Gyanodaya Prakashan.

Samant, S. S., Dhar, U., and Rawal, R. S. (1996). "Conservation of rare endangered plants. The context of Nanda Devi Biosphere Reserve," in *Conservation and Management of Biological Resources in Himalaya*, eds P. S. Ramakrishnan, A. N. Purohit, K. G. Saxena, K.S. Rao, and R. K. Maikhuri (New Delhi: Oxford and IBH Publishing Company Private Limited), 521–545.

Samant, S. S., Joshi, H. C., Arya, S. C., and Pant, S. (2002). *Studies on the structure, composition and changes of vegetation in Nanda Devi Biosphere Reserve, West Himalaya.* New Delhi: Final Technique submitted to Ministry of Environment and Forests.

Singh, A., and Samant, S. S. (2010). Conservation prioritization of habitats and forest communities in the Lahaul valley of proposed cold desert biosphere reserve, north western Himalaya, India. *Appl. Ecol. Environ. Res.* 8, 101–107. doi: 10.15666/aeer/0802_101117

Singh, J. B., and Kachroo, P. (1994). *Forest Flora of Pir Panjal Range (North Western Himalaya).* Dehradun: Bishen Singh Mahendra Pal Singh.

Singh, K. N., Lal, B., Singh, R. D., Todaria, N. P., and Ahuja, P. S. (2007). Species richness, distribution pattern and conservation status of higher plants in the Spiti cold desert of trans-Himalaya, India. *I. J. Biodivers. Sci. Manag.* 3, 223–233. doi: 10.1080/17451590709618176

Singh, N. P., Singh, D. K., and Uniyal, B. P. (2002). *Flora of Jammu and Kashmir.* Calcutta: Botanical Survey of India.

Su, N., Jarvie, S., Yan, Y., Gong, X., Li, F., Han, P., et al. (2022). Landscape context determines soil fungal diversity in a fragmented habitat. *Catena* 213. doi: 10.1016/j.catena.2022.106163

Tali, B. A., Ganie, A. H., Nawchoo, I. A., Wani, A. A., and Reshi, Z. A. (2015). Assessment of threat status of selected endemic medicinal plants using IUCN regional guidelines: a case study from Kashmir Himalaya. *J. Natl. Conserv.* 23, 80–89. doi: 10.1016/j.jnc.2014.06.004

Tali, B. A., Khuroo, A. A., Nawchoo, I. A., and Ganie, A. H. (2018). Prioritizing conservation of medicinal flora in the Himalayan biodiversity hotspot: an integrated ecological and socioeconomic approach. *Environ. Conserv* 46, 147–154. doi: 10.1017/S0376892918000425

Thakur, S., Negi, V. S., Dhyani, R., Bhatt, I. D., and Yadava, A. K. (2022). Influence of environmental factors on tree species diversity and composition in the Indian western Himalaya. *For. Ecol. Manag.* 503, 119746. doi: 10.1016/j.foreco.2021.119746

Thakur, S., Negi, V. S., Pathak, R., Dhyani, R., Durgapal, K., and Rawal, R. S. (2020). Indicator based integrated vulnerability assessment of community forests in Indian west Himalaya. *For. Ecol. Manag.* 457, 117674. doi: 10.1016/j.foreco.2019.117674

Tilman, D., Fargione, J., Wolff, B., Antonio, C., Dobson, A., Howarth, R., et al. (2001). Forecasting agriculturally driven global environmental change. *Science* 292, 281–284 doi: 10.1126/science.1057544

Walter, K. S., and Gillett, H. J. (1998). *IUCN Red List of Threatened Plants. Compiled by the World Conservation Monitoring Centre.* Gland/Cambridge: IUCN – The World Conservation Union.

Wani, Z. A., and Pant, S. (2020). Ethnomedicinal study of plants used to cure skin diseases and healing of wounds in Gulmarg Wildlife Sanctuary (GWLS), Jammu and Kashmir. *Ind. J. Trad. Knowl.* 19, 327–334.

Wani, Z. A., Pant, S., and Sharma, V. (2021). "Diversity, distribution and status of weed species of Northwest Himalaya," in *Bioremediation using weeds, Energy, Environment and Sustainability*, eds D. Pant, Bhatia, S. K., Patel, A. K., and Giri, A. (Singapore: Springer), 3–36. doi: 10.1007/978-981-33-6552-0_1

Wani, Z. A., Satish, K. V., Islam, T., Dhyani, S., and Pant, S. (2022). Habitat suitability modelling of *Buxus wallichiana* Bail.; an endemic tree species of Himalaya. *Vegetos.* doi: 10.1007/s42535-022-00428-w

frontiers | Frontiers in Forests and Global Change

TYPE Original Research
PUBLISHED 20 September 2022
DOI 10.3389/ffgc.2022.977691

OPEN ACCESS

EDITED BY
Vikram S. Negi,
Govind Ballabh Pant National Institute of Himalayan Environment and Sustainable Development, India

REVIEWED BY
Kailash Gaira,
Govind Ballabh Pant National Institute of Himalayan Environment and Sustainable Development, India
Harshit Pant Jugran,
Govind Ballabh Pant National Institute of Himalayan Environment and Sustainable Development, India

*CORRESPONDENCE
Susheel Verma
eremurus@rediffmail.com
Sajid Khan
sajidkhan717@gmail.com

SPECIALTY SECTION
This article was submitted to Forest Management, a section of the journal Frontiers in Forests and Global Change

RECEIVED 24 June 2022
ACCEPTED 22 August 2022
PUBLISHED 20 September 2022

CITATION
Khan S and Verma S (2022) Ensemble modeling to predict the impact of future climate change on the global distribution of *Olea europaea* subsp. *cuspidata*.
Front. For. Glob. Change 5:977691.
doi: 10.3389/ffgc.2022.977691

Ensemble modeling to predict the impact of future climate change on the global distribution of *Olea europaea* subsp. *cuspidata*

Sajid Khan[1]* and Susheel Verma[1,2]*

[1]Conservation and Molecular Biology Laboratory, Department of Botany, Baba Ghulam Shah Badshah University, Rajouri, India, [2]Department of Botany, University of Jammu, Jammu, India

Climate change is one of the significant factors influencing global species redistribution. As a result, a better understanding of the species' possible range change in future climate conditions is needed. Therefore, this study compiles global geographic occurrence data of a wild olive sub-species, *Olea europaea* subsp. *cuspidate*, and projected potential distribution models in current and future climate scenarios. This study using ensemble modeling predicted that the species will undergo a significant decrease in habitat suitability under future climatic conditions with a contraction ranging from ca. 41 and 42% under RCP4.5 2050 and to about 56 and 61% under RCP8.5 2070 for committee averaging and weighted mean, respectively. More specifically, there will be a decrease in habitat suitability in regions of the southeastern part of the United States in North America; coastal regions in South America; coastal regions in the majority of eastern Africa; coastal parts of Spain, France, Italy, and Greece in Europe; coastal parts of Yemen and Saudi Arabia; the southeastern parts of Pakistan and the southern part of China in Asia; and southwestern and eastern parts of Australia when compared to current habitat suitability. The results of this ensemble modeling could be extremely valuable in identifying cultivation hotspots for the effective restoration and protection of this olive lineage under future climatic conditions.

KEYWORDS

***Olea europaea* subsp. *cuspidata*, species distribution modeling, climate change, global distribution, habitat suitability**

Introduction

Climate change is one of the key components determining the species' range redistribution (Parmesan et al., 2011; Pacifici et al., 2015). As such, changing climatic conditions will likely expand or shrink the species' geographic ranges (Chen et al., 2011; Palmer et al., 2015). Adding to the worries are the consequences of global warming, which are expected to exacerbate in the next 50 years (Ahmad et al., 2019a).

The Intergovernmental Panel on Climate Change Sixth Assessment Report (IPCC, 2021) states that the ongoing climate warming has caused the pole-ward shift of numerous plant and animal species in both the southern and the northern hemisphere and the growing season, especially in the northern hemisphere extratropics, has expanded by 2 days each decade since the 1950s. A plethora of research studies have reported that recent anthropogenic-induced ecological changes are responsible for species range shifts (Malhi et al., 2020), changes in phenology (Negi et al., 2021), and species extinctions (Román-Palacios and Wiens, 2020). However, there is still a dearth of information about the biological dynamics of these shifting climatic impacts and documentation of climate change hotspots of vulnerability and resilience (Bellard et al., 2012). Furthermore, rising global temperatures have resulted in significant climatic zone shifts in several areas around the globe, including the substantial expansion of arid climatic zones and the shrinkage of polar climatic zones (IPCC, 2019). As a result, many native species have experienced a substantial shift in their geographical ranges, abundances, and seasonality of activities (Weiskopf et al., 2020). All these negative consequences act as barriers to the management and conservation of biodiversity (Thomas et al., 2004; Butchart et al., 2010; Cook et al., 2012; IPCC, 2012; Pacifici et al., 2017; Pecl et al., 2017; Convention on Biological Diversity, 2020).

As ecology and conservation disciplines require a robust understanding of species distribution and habitat requirements, species distribution models (SDM) are, therefore, one of the essential techniques for spatio-temporal predictions of biodiversity at the biogeographic scale (Alvarado-Serrano and Knowles, 2014; Naimi, 2015; Srivastava et al., 2019). SDM projections can be used to develop sustainable management plans to help minimize the effects of climate change (Pyke and Fischer, 2005; Schorr et al., 2012; Porfirio et al., 2014). However, one major disadvantage of these distribution models is that there are already a large number of modeling algorithms available, and this number is expanding all the time, making it difficult to choose the optimal methodology (Elith et al., 2010; Ahmad et al., 2019b). To overcome this problem, the ensemble modeling technique implemented in the biomod2 package provides a valuable platform for determining the species' current distribution and predicting their future potential Spatio-temporal distributions under changing climatic scenarios (Gillard et al., 2017; Thuiller et al., 2019).

RCPs (representative concentration pathways) represent greenhouse gas emissions, atmospheric concentrations, air pollutant emissions, and land use in the twenty-first century (Vuuren et al., 2011). Based on the mitigation scenarios' trajectory, four (RCPs) have been described (IPCC, 2014). In order to identify suitable habitats for species in the 2050s and 2070s, the model was thus trained using current climate data and projected onto future climate change bioclimatic datasets for all RCPs scenarios. Therefore, to estimate the impact of climate change on species distribution, multiple scenarios based on various RCPs must be examined (Araujo and Rahbek, 2006; Parmesan, 2006; Beaumont et al., 2007; Bellard et al., 2012). This paper is based on the global distribution modeling of *Olea europaea* subsp. *cuspidata* (synonyms—*Olea ferruginea, Olea africana, Olea chrysophylla*) using an ensemble modeling approach. It is a wild species of olive lineage (Green, 2002) and is believed to be of Mediterranean origin (De Candolle, 1882) and a prominent part of Mediterranean vegetation (De Ollas et al., 2019). However, the species is introduced into Australia, New Zealand, and the Pacific islands as a rootstock for cultivated olive (Besnard et al., 2014). Due to over-exploitation, Ethiopia's species is extremely threatened (Negash, 2010). It is used for various purposes, including quality fuel wood and furniture (Negash, 2010), and is also a valuable source of natural antioxidants and bioactive materials (Long et al., 2010). It has numerous medicinal and anti-bacterial properties (Masoko and Makgapeetja, 2015). Therefore, climate change affects livelihoods and economic security, particularly in communities, along with its distribution range. More specifically, we aim to address the following key questions: (1) What is the current distribution of *Olea europaea* subsp. *cuspidata*? (2) What will be the future potential distribution of this species under different climate change scenarios? and (3) what are the key bioclimatic variables affecting the distribution of this species?

Materials and methods

Species distribution data

Occurrence data for *Olea europaea* subsp. *cuspidata* was downloaded primarily from the Global Biodiversity Information Facility (GBIF, 2021) using the gbif function from the dismo package (Hijmans et al., 2020), Botanical Information and Ecology Network Database (BIEN; accessed on 01 August 2021) using the BIEN_occurrence_species function from BIEN package (Maitner et al., 2018) and was further supplemented with intensive field surveys carried by the authors from North Western India and Herbarium records from Forest Research Institute (FRI) Dehradun and various centers of Botanical Survey of India (BSI Dehradun, BSI Kolkatta, and HAWHRC Solan). A total of 4,599 georeferenced occurrence points were obtained from the above-mentioned sources for *Olea europaea* subsp. *cuspidata*. The obtained occurrence dataset was subsequently processed to exclude any locations that fell into the oceans. As a result, 4,461 points were retained. Furthermore, it is a well-known fact that distribution data is frequently skewed toward locations that are geographically user-friendly and easily accessible (Hijmans et al., 2005). This can manifest itself in the form of geographical sample bias (Ahmad et al., 2019a). We employed spatial thinning to minimize spatial autocorrelation and sample bias by dividing the entire region into 10 × 10 km grid cells and selecting a single occurrence point from each cell with one or more occurrence points. After geographic thinning, the final dataset for modeling the distribution of *Olea europaea* subsp. *cuspidata* in this study consisted of 776 georeferenced points.

Environmental data

We used the current climatic factors from the WorldClim database, version 1.4 (Hijmans et al., 2005) (http://www.worldclim.org) to estimate the global current potential distribution of *Olea europaea* subsp. *cuspidata*. Between 1950 and 2000, these climatic variables indicated the minimum, maximum, and average values of monthly, quarterly, and annual ambient temperatures and precipitation data. These environmental variables had a spatial resolution of 2.5 arc seconds (∼4.5 km resolution at the equator). These bioclimatic variables often show a higher degree of collinearity, resulting in poor misleading model performance (Ahmad et al., 2019a). As a result, we used Pearson's correlation analysis to choose only one variable from each pair of strongly associated variables with a correlation coefficient (i.e., $r > 0.75$ or -0.75) before modeling. A total of 10 variables were retained after correlation analysis for modeling the distribution of target species under present climate conditions (Table 1). The Intergovernmental Panel on Climate Change (IPCC) fifth assessment report (AR5) (Moss, 2010) provided Hadley Global Environment Model 2-Earth System (HADGEM2-ES) simulations for two representative concentration pathways (RCP4.5 and RCP8.5) for the two time periods (i.e., 2050 and 2070) for predicting the future potential distribution of the *Olea europaea* subsp. *cuspidata*. RCPs provide climate change trajectories by describing scenarios based on assumptions about socio-economic conditions, greenhouse gas emissions, and the concentration of air pollutants (Albuquerque et al., 2019). The same set of environmental variables used to estimate the current distribution of the examined species was also used to predict their future distributions.

TABLE 1 Bioclimatic variables selected for modeling the distribution of *Olea europaea* subsp. *cuspidata* in the present study.

Description of bioclimatic variables	Units	Temporal scale
Annual mean temperature (BIO-1)	Degree Celsius	Annual
Mean diurnal range (BIO-2)	Degree Celsius	Variation
Isothermality (BIO-3)	Dimensionless	Variation
Max temperature of warmest month (BIO-5)	Degree Celsius	Month
Min temperature of coldest month (BIO-6)	Degree Celsius	Month
Mean temperature of wettest quarter (BIO-8)	Degree Celsius	Quarter
Mean temperature of driest quarter (BIO-9)	Degree Celsius	Quarter
Annual mean precipitation (BIO-12)	Millimeter	Annual
Precipitation of driest month (BIO-14)	Millimeter	Month
Precipitation of coldest quarter (BIO-19)	Millimeter	Quarter

Modeling technique

We performed the ensemble distribution modeling using the nine algorithms implemented in the biomod2 package (Thuiller et al., 2009, 2020). We performed the ensemble distribution modeling using the nine algorithms as implemented in the biomod2 package (Thuiller et al., 2009, 2020), which include: the Generalized Linear Model (GLM) (McCullagh and Nelder, 1989), the Generalized Additive Models (GAM) (Hastie and Tibshirani, 1990), Generalized Boosted Models (GBM) (Ridgeway, 1999), Classification Tree Analysis (CTA) (Breiman et al., 1984), Flexible Discriminant Analysis (FDA) (Hastie et al., 1994), Artificial Neural Networks (ANN) (Ripley, 1996), Maximum Entropy (MAXENT) (Phillips et al., 2006), Random Forest (RF) (Breiman, 2001), and Surface Response Envelope (SRE) (Busby, 1991). As the different algorithms used for distribution modeling require both presence and absence data types, it is impossible to obtain the actual absence data throughout the study region. Therefore, in this study, we randomly generated an equal number of pseudo-absences to that of presence points within the study area, as recommended by Barbet-Massin et al. (2012) and Guisan et al. (2017). We built the models using 80% of the data (training set) and evaluated the model performance with the rest of the 20% of the data (evaluation set). We generated each of the models three times. We preferred two evaluation metrics to evaluate the accuracy of the models: the area under the curve (AUC) of receiver operating characteristics (ROC) and true skills statistics (TSS) (Allouche et al., 2006; Rather et al., 2022; Wani et al., 2022a). We built the final ensemble models for each climate scenario and time period based on both the committee averaging and weighted mean separately; finally, for creating the final ensemble models, only those models with a TSS score of ≥ 0.8 were used.

Variable importance

To assess the relative impact of each climate condition in determining the distribution of selected plant species, we employed the permutation approach (Elith et al., 2005).

Predictions are made from a particular algorithm after changing only one target variable, while the rest of the variables are maintained statically in this method. The variable relevance estimations are obtained as the difference between the original forecast and the permuted variable prediction divided by one minus the correlation score (1-correlation score) (Ahmad et al., 2019a). As a result, high values indicate that the predictor variable is more important in the model, while a value of 0 indicates that the variable is not important in the model.

Species range change

In order to visualize and measure the range change of the target plant species under future climatic conditions, we used the same biomod range size function as that implemented in the biomod2 package (Guisan et al., 2017). This function provides a summary statistic on species range change, and the prediction map shows the gain or loss of suitable conditions for the studied plant species, according to Guisan et al. (2017). Interestingly, detailed information on four absolute metrics related to "species loss" (i.e., loss of suitable habitat by the studied species under future climate change), "species absence" (i.e., amount of area not occupied by the studied species under current and future climatic scenarios), "stable" (i.e., the amount of area occupied by the studied species both under current and future climatic scenarios) and "gain" (i.e., a gain of suitable habitat by the studied species under future climate change) can be obtained (Guisan et al., 2017). Lastly, from the above four absolute metrics, three additional relative metrics can be calculated, including "percentage loss" (i.e., percentage of currently suitable areas predicted to be lost and is calculated as [loss/(loss + stable)]; "percentage gain" (i.e., percentage of new habitats predicted to be suitable when compared with the species' current distribution size and is calculated as [gain/(loss + stable)]; and "range change," i.e., the overall output of predictions and is calculated as (percentage gain-percentage loss) (Kumari et al., 2022; Wani et al., 2022b).

Results

Model evaluation

The final ensemble models developed had an AUC of 0.991 and a TSS of 0.913 in terms of committee averaging. Similarly, the ensemble models developed had an AUC of 0.992 and a TSS of 0.908 in terms of weighted mean. Both of these scores indicate that our final model had predicted the distribution of the *Olea europaea* subsp. *cuspidata* with higher accuracy. When evaluated against the individual algorithms, the predictive accuracy was again excellent but varied, with RF, GBM, GLM, and GLM performing fairly well, followed by FDA, CTA, and Maxent. Phillips, when compared to the rest of the algorithms, the SRE and ANN had the lowest accuracy (Figure 1).

Variable importance

The performance of the selected bioclimatic variables varied significantly among the different algorithms (Table 2). In particular, the most significant variables governing the distribution of *Olea europaea* subsp. *cuspidata* were BIO-01 (annual mean temperature) with importance scores ranging from 0.13 (in the case of RF) to 0.86 (in the case of GLM) (mean score = 0.46), followed by BIO-05 (max temperature of warmest month) with importance scores ranging from 0.02 (for GBM) to 0.43 (for GLM) (mean score = 0.20) and BIO-03 (Isothermality) with importance scores ranging from 0.08 (for GAM) to 0.31 (for MAXENT.Phillips) (mean score = 0.17). The rest of the variables had diverse responses over different algorithms, therefore their influence on governing *Olea europaea* subsp. *cuspidata* potential distribution was extremely variable (Table 2).

Current distribution

The final ensemble model reveals that under current climatic conditions, the areas having highly suitable and optimal climatic conditions for the growth of *Olea europaea* subsp. *cuspidata* are majority parts of Mexico, the southeastern part of the United States in North America; coastal parts of Columbia, Ecuador, and Peru, major parts of Chile, central, eastern and southern parts of Argentina, majority of Uruguay, and southern and eastern parts of Brazil in South America; coastal parts of western Sahara, Morocco, Libya and Egypt, majority of Ethiopia, Kenya, almost entire of Zimbabwe, Namibia, Botswana, Madagascar, and South Africa in Africa; western coastal parts of Portugal, Spain, France, United Kingdom, Italy, and Turkey in Europe; coastal parts of Yemen and Saudi Arabia, the southeastern part of Pakistan, North Western Himalayan states of Jammu and Kashmir, Himachal Pradesh, Uttarakhand, and Arunachal Pradesh, Bhutan and Nepal, Northwestern part of Myanmar, the northern part of Thailand, the southern part of China in Asia; Central, southern, eastern, western and southern western parts of Australia and major parts of New Zealand in Australasia (Figure 2).

Future potential distribution

The predictions of the future ensemble models showed that there will be a decrease in the habitat suitability for *Olea europaea* Subsp. *cuspidata* under all the future climatic

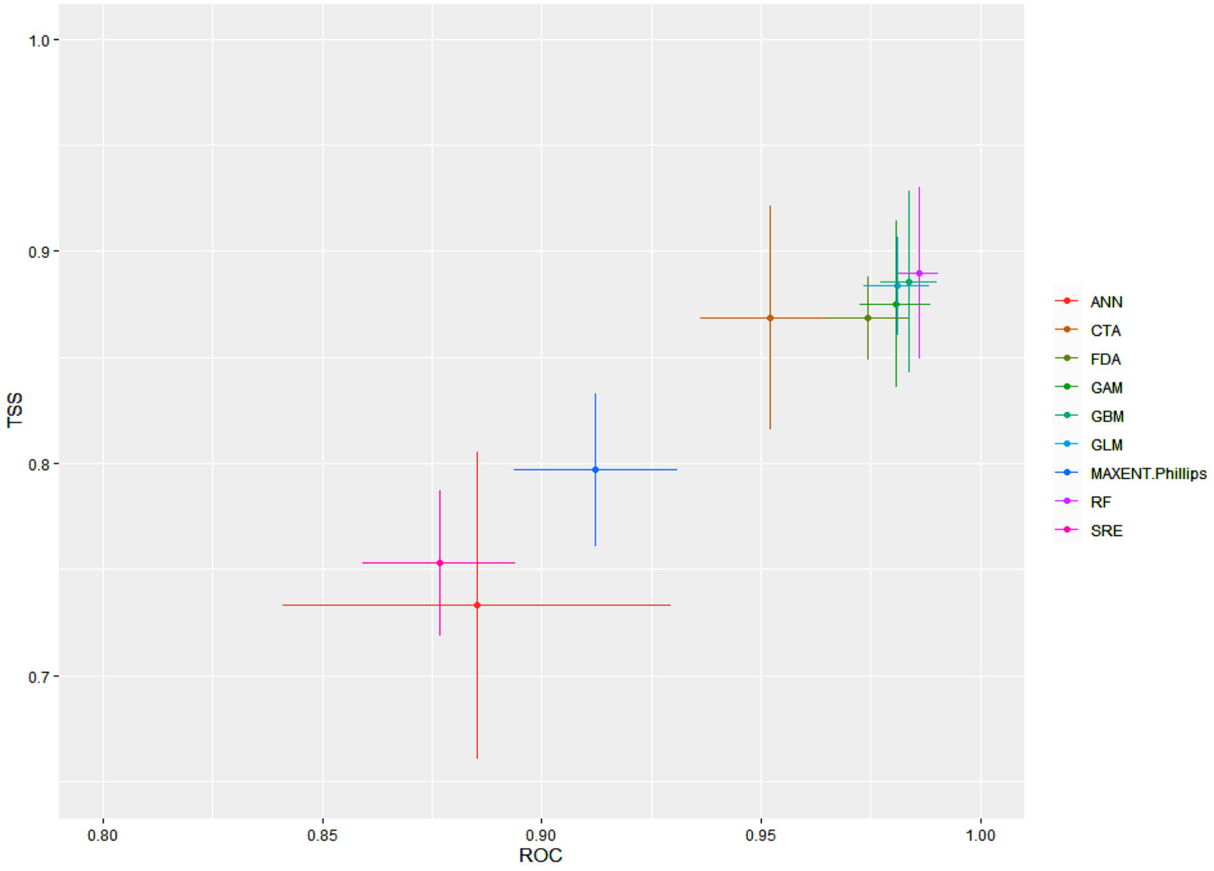

FIGURE 1
For *Olea europaea* subsp. *cuspidata*, mean model evaluation scores by algorithms according to two separate evaluation metrics, ROC (AUC) and TSS.

TABLE 2 The relevance scores of the selected bioclimatic variables, both overall and by the algorithm.

	GLM	GBM	GAM	CTA	ANN	SRE	FDA	RF	MAXENT. Phillips	Mean
bio_01	0.86	0.21	0.68	0.69	0.41	0.35	0.59	0.13	0.19	0.46
bio_02	0.13	0.00	0.08	0.02	0.23	0.13	0.00	0.00	0.02	0.07
bio_03	0.13	0.15	0.08	0.28	0.14	0.25	0.11	0.13	0.31	0.17
bio_05	0.43	0.02	0.40	0.10	0.25	0.23	0.08	0.05	0.22	0.20
bio_06	0.14	0.00	0.10	0.00	0.65	0.30	0.02	0.04	0.06	0.15
bio_08	0.03	0.00	0.05	0.01	0.11	0.20	0.00	0.02	0.11	0.06
bio_09	0.12	0.01	0.09	0.12	0.34	0.33	0.04	0.04	0.05	0.13
bio_12	0.10	0.02	0.08	0.08	0.26	0.18	0.06	0.03	0.16	0.11
bio_14	0.02	0.00	0.02	0.02	0.08	0.12	0.01	0.01	0.14	0.05
bio_19	0.16	0.01	0.08	0.01	0.25	0.14	0.02	0.01	0.06	0.08

scenarios. However, some of the currently suitable areas will consistently remain suitable in future climates also, such as the central part of Mexico, southern and central parts of the United States in North America; coastal parts of Columbia, Ecuador, and Peru, and major parts of Chile, central, eastern and southern parts of Argentina, southern and eastern parts of Brazil in South America; certain parts of Ethiopia, Kenya and Tanzania, eastern Madagascar and Southern parts of Namibia and South Africa in Africa; major parts of Spain, France, United Kingdom, Italy Germany,

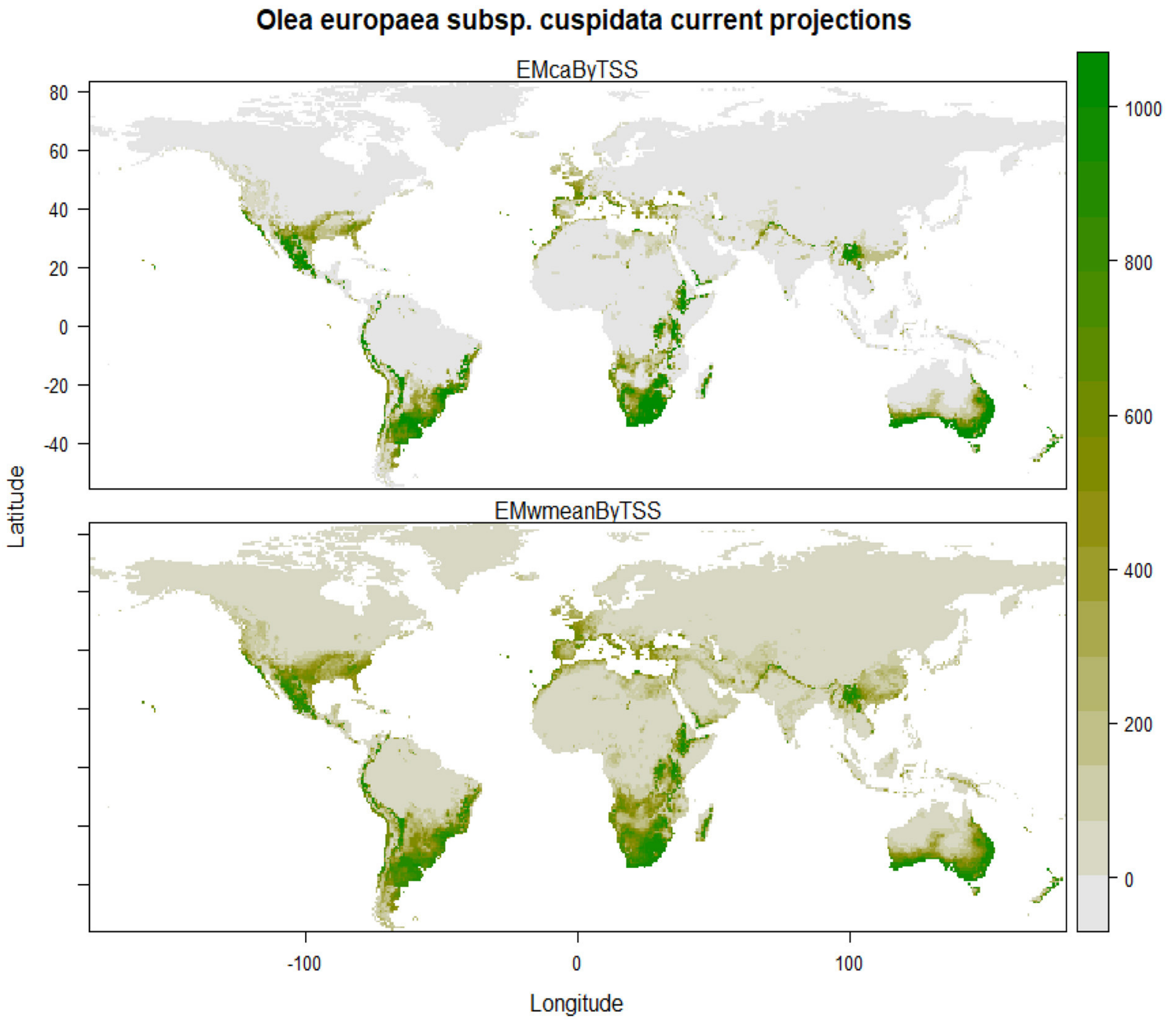

FIGURE 2
Plot showing the geographic projections using the committee average (above) and weighted mean (below) ensemble models for *Olea europaea* subsp. *cuspidata* under current climatic conditions.

and Turkey in Europe; North Eastern Himalayan states of Jammu and Kashmir, Himachal Pradesh, Uttarakhand, and Arunachal Pradesh, Bhutan and Nepal, Northwestern part of Myanmar, the northern part of Thailand in Asia; southern parts of Australia and entire of New Zealand in Australasia (Figure 3).

Species range change

The results of the range change analysis once again indicated that *Olea europaea* subsp. *cuspidata* will undergo significant range changes under future climatic conditions and ranges from −40.52 and −42.11% under RCP4.5 2050 for committee averaging and weighted mean, respectively, to −56.16 and −60.80% under RCP8.5 2070 for committee averaging and weighted mean, respectively (Table 3). This range change will be governed mostly by habitat loss in future climatic scenarios. More specifically, there will be a reduction in suitable areas for *Olea europaea* Subsp. *cuspidata* by about 50.05 and 49.99% (under RCP4.5 2050), 54.20 and 55.04% (RCP4.5 2070), 55.90 and 56.52% (RCP8.5 2050), and 69.17 and 71.11% (under RCP8.5 for the year 2070) for committee averaging and weighted mean, respectively, when compared to current habitat suitability (Table 3). The areas that are likely to become unsuitable in the future include the majority parts of Mexico and the southeastern part of the United States in North America; Northern

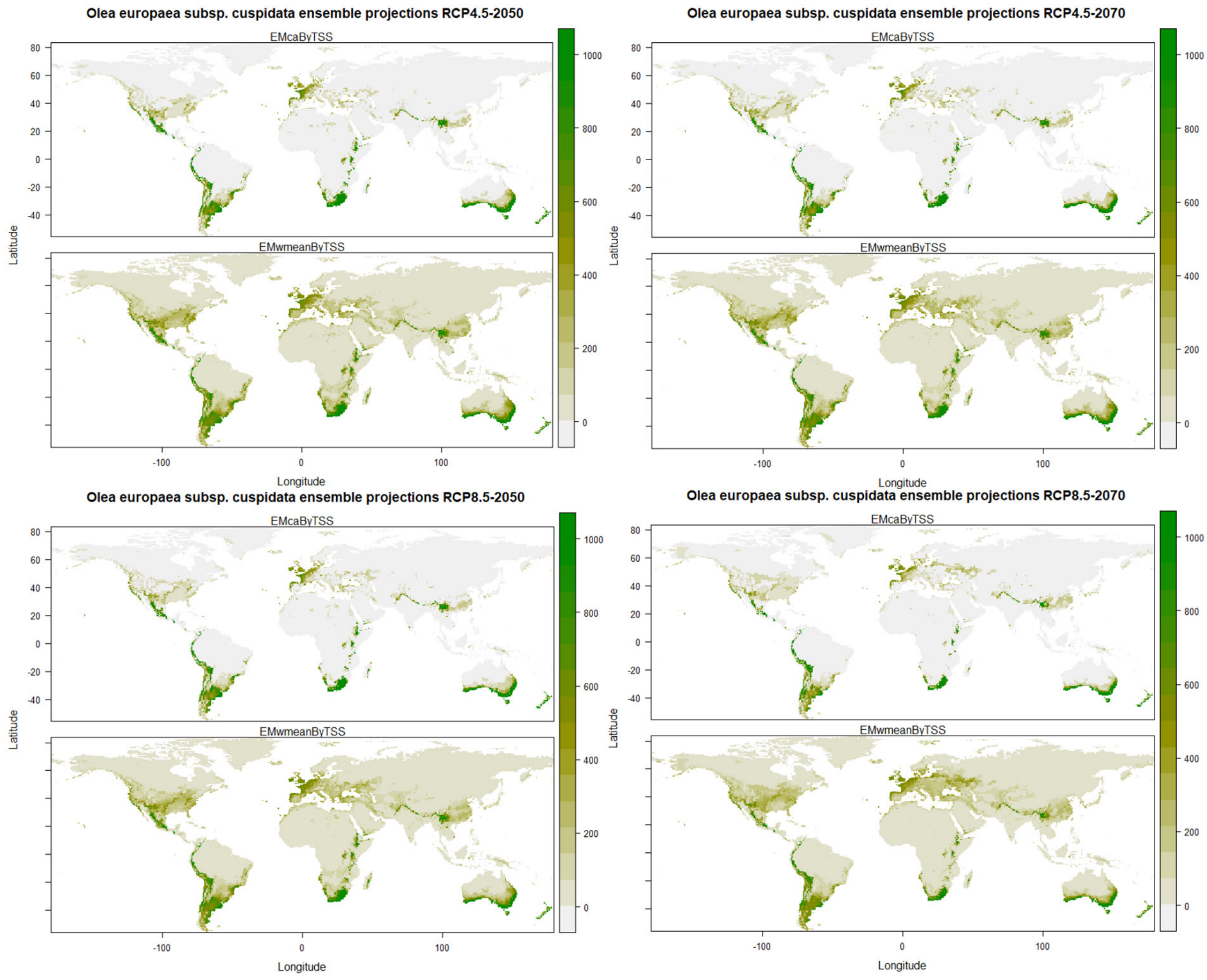

FIGURE 3
Plots of the predicted habitat suitability for *Olea europaea* subsp. *cuspidata* under future climate change scenarios.

Chile, east and central parts of Argentina, certain parts of southern and eastern Brazil in South America; coastal parts of Ecuador and Columbia, central parts of Ethiopia, Kenya and Tanzania, parts of Madagascar and central parts of Namibia and South Africa in Africa; coastal parts of Spain, France, Italy and Greece in Europe; coastal parts of Yemen and Saudi Arabia, the southeastern part of Pakistan and southern part of China in Asia; southwestern and eastern parts of Australia (Figure 4). In contrast, some of the currently unsuitable areas become increasingly suitable for future climate with a range expansion of 9.53 and 7.88% (under RCP4.5 2050), 10.61 and 8.58% (RCP4.5 2070), 11.65 and 9.63% (RCP8.5 2050), and 13.01 and 10.31% (under RCP8.5 2070) for committee averaging and weighted mean, respectively, when compared to current habitat suitability for (Table 3). These expanding suitability areas include a certain portion of the southern United States, most of the parts of Chile, some parts of Indian Himalayan states, North Eastern Himalayan states of Jammu and Kashmir, Uttarakhand, Sikkim, and Arunachal Pradesh, as well as certain parts of Bhutan and Nepal and southern China (Figure 4).

Discussion

This study employed two evaluation metrics to assess the predictive performance of our model run: threshold-independent Area under the Curve (AUC) and threshold-dependent True Skill Statistics (TSS). These criteria are frequently used in ecology to evaluate habitat modeling performance (Allouche et al., 2006). The AUC is extensively

TABLE 3 Summary of the range change statistics in terms of pixels for the *Olea europaea* subsp. *cuspidata* under climate change scenarios compared to current climatic conditions.

Scenario	Ensemble type	Loss	Absent	Stable	Gain	Loss (%)	Gain (%)	Range change (%)
RCP4.5 2050	Committee averaging	356,499	8,087,753	355,798	67,883	50.05	9.53	−40.52
RCP4.5 2070	Committee averaging	386,078	8,080,091	326,219	75,545	54.20	10.61	−43.60
RCP8.5 2050	Committee averaging	398,162	8,072,658	314,135	82,978	55.90	11.65	−44.25
RCP8.5 2070	Committee averaging	492,706	8,062,965	219,591	92,671	69.17	13.01	−56.16
RCP4.5 2050	Weighted mean	271,335	8,282,368	271,478	42,752	49.99	7.88	−42.11
RCP4.5 2070	Weighted mean	298,740	8,278,568	244,073	46,552	55.04	8.58	−46.46
RCP8.5 2050	Weighted mean	306,776	8,272,834	236,037	52,286	56.52	9.63	−46.88
RCP8.5 2070	Weighted mean	385,985	8,269,150	156,828	55,970	71.11	10.31	−60.80

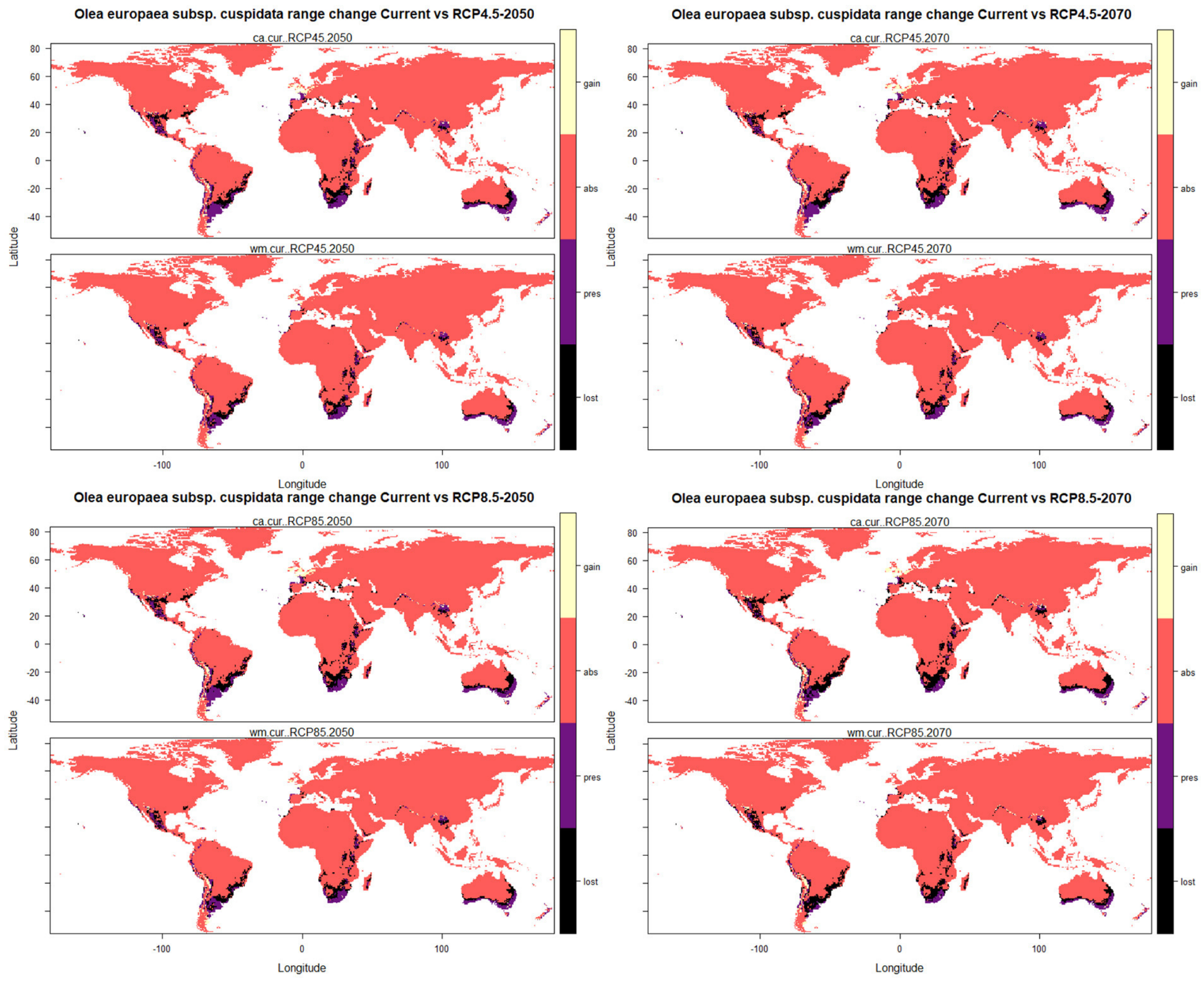

FIGURE 4
Plots of the predicted range changes for *Olea europaea* subsp. *cuspidata* between current and future climatic conditions.

used to evaluate the accuracy of habitat suitability models, while TSS normalizes total accuracy (Allouche et al., 2006; Becerra-López et al., 2017). The threshold-independent AUC and threshold-dependent TSS performance scores for *Olea europaea* subsp. *cuspidata* were 0.991 and 0.913 for committee averaging and 0.992 and 0.908 for weighted mean, respectively. The consistent results obtained prove the model's improved performance.

Environmental conditions influence the distribution of a plant species. This impact is because climate variables such as temperature and precipitation impact species' physiological and reproductive capabilities (Sharma and Raghubanshi, 2006). Several critical biological processes of a species are synchronized by these climate-based characteristics, including dispersion ability, home range size (Bradley and Mustard, 2006), and the ability to survive under unfavorable conditions (Morris et al., 2019). However, this does not hold true for all cases, as other edaphic and topographic factors and interactions among the biotic and abiotic environments significantly impact the species distribution (Norberg et al., 2019). However, when the modeling is performed over large-scale areas such as the whole globe or continents, climatic conditions are reported as the sole determinants for evaluating the degree of distribution of the organisms (Waltari et al., 2014). Earlier SDM studies conducted on *Olea europaea* subsp. *cuspidata* in Asia have reported a loss of suitable habitat, particularly in low elevations, and a shifting distribution toward high altitudes (Ashraf et al., 2016, 2017). The other two wild olive subspecies, *O. europaea* subsp. *europaea* var. *sylvestris*, are predicted to increase habitat suitability, while *O. europaea* subsp. *maroccana* shows substantial contraction in future climate (Kassout et al., 2022). This suggests that plant species behave differently in future climate projections, even at the subspecies level.

The species' distribution range reflects its adaptation to the Mediterranean-type climate of the world. Such a climate is considered one of the most vulnerable zones to global warming (Almeida et al., 2022; Kassout et al., 2022). The current distribution range is stretched across many regions of all the continents, especially prominent parts of the southern hemisphere. During the last few decades, 90 percent of the net global ocean heat gain was concentrated in the southern hemisphere (Rathore et al., 2018). Several meteorological alterations have been observed in the southern hemisphere during the past several decades (Solman and Orlanski, 2016). Certain precipitation-related variables influencing this plant species' distribution have been identified (Deblauwe et al., 2016; Amiri et al., 2020). The distribution of this plant in coastal parts of Western Sahara, Morocco, Libya, and Egypt, the majority of Ethiopia, Kenya, and almost the entire country of Zimbabwe, Namibia, Botswana, Madagascar, and South Africa in Africa reflects its adaptability in the relatively low precipitation-dominated area. These findings are consistent with model-based predictions made by several other researchers, who identified temperature and precipitation-derived variables as the primary determinants of plant distribution (Woodward et al., 2004; Priyanka and Joshi, 2013; Manzoor et al., 2018; Panda and Behera, 2018; Thapa et al., 2018; Xu et al., 2021).

The study is a pioneering but crucial step in looking into the impact of climate change on the current distribution and the possible range of suitable habitats of *Olea europaea* subsp. *cuspidata* on a global scale. The study's findings show that temperature-related bioclimatic variables play a vital role in this species' distribution (Figures 2, 3), with BIO-1 (Annual Mean Temperature) being the most important explanatory variable, followed by BIO-5 (Max Temperature of Warmest Month) and BIO-3 (Annual Mean Temperature) (Isothermality). These variables are expected to alter significantly under the RCP8.5 scenario, causing substantial portions of the current distribution area to become unsuitable by 2050. This study predicts more range contraction under RCP8.5 by 2070, a comparatively more extreme scenario. On the other hand, rainfall patterns in many regions of the world are expected to result in a more widespread variable and extended dry spells. According to a recent climate precipitation trend analysis for the previous few decades, the total amount of annual precipitation is escalating along with increasing trends in consecutive dry days (CDD) (Mudelsee, 2018; Parey, 2019; Dad et al., 2021). Under the predicted importance of rainfall patterns for *Olea europaea* subsp. *cuspidata*, future extreme climate events may put additional stress on already established populations and restrict its spread to places that would be unsuitable under current climatic conditions (Kelly and Goulden, 2008).

Future climate change is expected to impair total habitat suitability for this species, with more than a quarter of suitable habitat predicted to be lost by 2070 under RCP8.5. In fact, our findings are consistent with other reports that have found a decline in the worldwide and regional species distribution as a result of climate change (Rabasa et al., 2013; Panda and Behera, 2018; Moraira et al., 2020; Zu et al., 2021). In a recent study investigating the future predictions for the spread of invasive species under the influence of climate change in South Africa, Bezeng et al. (2017) discovered a range reduction for more than 80 species. Our predicted model for the future distribution of this species corresponds with the results of Ghafoor et al. (2021), which experimentally established the reduced seed germination and vegetative growth in *Olea europaea* subsp. *cuspidate*, and predicted that climate change will significantly influence olive ecophysiology, leading to species composition changes and shifting distribution (Brito et al., 2019). In the southeast of Australia, where the species is predicted to lose its habitat substantially, vegetation type has been demonstrated to have a substantial impact on fire response to warmer temperatures, with wetter, coastal temperate forests being more likely to experience increased fire frequency (Bradstock et al., 2014). Similar observations were recorded about the distribution pattern of 292 naturalized alien species in Australia, which has been observed to be affected under future climate change scenarios (Duursma et al., 2013). Several cases of vegetation and disturbance regimes, local plant extinctions, phenological changes in reproduction, and altered biotic interactions have been observed in Australia, posing a threat to communities and endangered species (Hoffmann et al., 2018). Another most affected region in terms of habitat loss is *Olea europaea* subsp. *cuspidata* is predicted to be in sub-Saharan Africa. According to projections, countries like South Africa, Namibia, and Botswana will face temperatures greater than the global average by 2050 (Davis-Reddy and Vincent, 2017). In addition, rainfall in Southern Africa is anticipated to drop by nearly 10% by 2050 (IPCC, 2014). Our results agree with several other studies which have found that climate change has affected the habitat suitability of several other plant species (Bradley et al., 2009; Taylor et al., 2012; Wan et al., 2016; Manzoor et al., 2018). The availability of moisture and the low temperatures associated with these regions may promote future distribution feasible in the context of climate change (Chen et al., 2011; Fei et al., 2017; Panda and Behera, 2018; Rathore et al., 2018). While projected climate change may negatively shift the distribution of *Olea europaea* subsp. *cuspidate,* due to increased precipitation and temperature, moisture availability, and low temperatures associated with higher latitudes, it may also facilitate its distribution under future climate conditions. Since the majority of *Olea europaea* subsp. *cuspidata* habitat loss is predicted in the mid-latitudes of both hemispheres; the region's surface temperature changes (Tamarin-Brodsky et al., 2020) explain the warming patterns and climatic-dependent factors.

A considerable reduction of the suitable habitats for *Olea europaea* subsp. *cuspidata* will occur under future climatic conditions. As a global trend, the lower the latitude, the more areas will be lost (Sheldon, 2019); the majority of the lost areas are on the American, African, and Australian subcontinents, indicating that many mainland areas will be subjected to more severe climatic changes than coastal areas. The areas predicted for future distribution suitability currently receive less precipitation than those with current distribution. Future climatic projections foresee the emergence of new suitable areas, mostly found at higher latitudes in both the northern and southern hemispheres (Figure 4). Under the model output, such projected latitudinal migration, with *Olea europaea* subsp. *cuspidata* shifting poleward, follows one of the most common and well-documented consequences of climate change on species distribution (VanDerWal et al., 2012; Telwala et al., 2013; Rathore et al., 2018). Considering the species diverse distribution patterns and relatively wide temperature and precipitation habitat ranges (Figure 3), future estimates suggest that the plant will be severely affected by the ongoing global climate change. Other widespread plant species have exhibited probable future range contractions (Kelly and Goulden, 2008; Parmesan and Hanley, 2015; Madani et al., 2018) due to increased temperatures leading to severe heat stress (Tollefson, 2020).

Conclusion

The present work is the first attempt to assess global range shifts not only for a wild olive species but also for a Lamiales species in a climate change scenario. Ecophysiological features of *Olea europaea* subsp. *cuspidata* may be linked to the shrinkage of potential areas in the year 2070 compared to the present. The extraction and comparison of climatic values of gained and lost areas in relation to present and future distribution ranges revealed that *Olea europaea* subsp. *cuspidata* would tend to be displaced to locations with currently low precipitation values. As previously stated, the species appears to be unable to endure significant temperature fluctuations (Bio-1, Bio-3, and Bio-5). As a result, climatically appropriate areas for *Olea europaea* subsp. *cuspidata* are predicted to be drastically reduced by 2070, as a portion of the current potential ranges will become unsuitable due to excessive temperature changes. This is in line with worldwide trend changes, which have been anticipated to include a large increase in extreme periods of lengthy dry cycles (IPCC, 2013; Tollefson, 2020). Finally, we investigated where most suitable habitats will be lost or gained in the future due to climate change. With this ensemble modeling approach, firstly, we can predict the main current locations of *Olea europaea* subsp. *cuspidata* will still appear as suitable. Secondly, it is estimated that several diverse geographical locations where the species has not been documented will be potential colonization sites for the species in the future. Considering the ecological and economical importance, the areas predicted to be suitable for the *O. europaea* subsp. *cuspidata* may be used for the plantation of this species, while the deforested land should be restored for human welfare.

Data availability statement

The raw data supporting the conclusions of this article will be made available by the authors, without undue reservation.

Author contributions

SK wrote and analyzed the manuscript. SV supervised, visualized, reviewed, and edited the manuscript. Both authors contributed to the article and approved the submitted version.

Funding

The authors appreciate the financial support from the National Mission on Himalayan Studies (NMHS) under Fellowship Grant No. GBPNI/NMHS-2018-19/HSF-24-02/153.

Acknowledgments

The authors are grateful to the Head Department of Botany, BGSB University, Rajouri, for providing necessary facilities.

Conflict of interest

The authors declare that the research was conducted in the absence of any commercial or financial relationships that could be construed as a potential conflict of interest.

Publisher's note

References

Ahmad, R., Khuroo, A. A., Charles, B., Hamid, M., Rashid, I., and Aravind, N. A. (2019a). Global distribution modelling, invasion risk assessment and niche dynamics of *Leucanthemum vulgare* (Ox-eye Daisy) under climate change. *Sci. Rep.* 9, 476–485. doi: 10.1038/s41598-019-47859-1

Ahmad, R., Khuroo, A. A., Hamid, M., Charles, B., and Rashid, I. (2019b). Predicting invasion potential and niche dynamics of *Parthenium hysterophorus* (Congress grass) in India under projected climate change. *Biod. Conser.* 28, 2319–2344. doi: 10.1007/s10531-019-01775-y

Albuquerque, D., Macías-Rodríguez, F. S., Búrquez, M. A., and Astudillo-Scalia, Y. (2019). Climate change and the potential expansion of buffelgrass (*Cenchrus ciliaris* L., *Poaceae*) in biotic communities of Southwest United States and northern Mexico. *Biol. Invas.* 21, 3335–3347. doi: 10.1007/s10530-019-02050-5

Allouche, O., Tsoar, A., and Kadmon, R. (2006). Assessing the accuracy of species distribution models: prevalence, kappa and the true skill statistic (TSS). *J. Appl. Ecol.* 43, 1223–1232. doi: 10.1111/j.1365-2664.2006.01214.x

Almeida, A. M., Martins, M. J., Campagnolo, M. L., Fernandez, P., Albuquerque, T., Gerassis, S., et al. (2022). Prediction scenarios of past, present, and future environmental suitability for the Mediterranean species *Arbutus unedo* L. *Sci. Rep.* 12, 84. doi: 10.1038/s41598-021-03996-0

Alvarado-Serrano, D. F., and Knowles, L. L. (2014). Ecological niche models in phylogeographic studies: applications, advances and precautions. *Mol. Ecol. Resour.* 14, 233–248. doi: 10.1111/1755-0998.12184

Amiri, M., Tarkeshi, M., Jafari, R., and Jetschke, G. (2020). Bioclimatic variables from precipitation and temperature records vs. remote sensing-based bioclimatic variables: which side can perform better in species distribution modeling. *Ecol. Inform.* 57, 1–16. doi: 10.1016/j.ecoinf.2020.101060

Araujo, M. B., and Rahbek, C. (2006). How does climate change affect biodiversity? *Science* 313, 1396–1397. doi: 10.1126/science.1131758

Ashraf, U., H., Ali, M. N., Chaudry, I., Ashraf, A., Batool, and Saqib, Z. (2016). Predicting the potential distribution of *Olea ferruginea* subsp. cuspidata in Pakistan incorporating climate change by using Maxent model. *Sustainability* 8, 722. doi: 10.3390/su8080722

Ashraf, U., Peterson, A. T., Chaudhry, M. N., Ashraf, I., Saqib, Z., Rashid Ahmad, S., et al. (2017). Ecological niche model comparison under different climate scenarios: a case study of Olea spp. in Asia. *Ecosphere* 8, e01825. doi: 10.1002/ecs2.1825

Barbet-Massin, M., Jiguet, F., Albert, C. H., and Thuiller, W. (2012). Selecting pseudo-absences for species distribution models: how, where and how many? *Meth. Ecol. Evol.* 3, 327–338. doi: 10.1111/j.2041-210X.2011.00172.x

Beaumont, L. J., Pitman, A. J., Poulsen, M., and Hughes, L. (2007). Where will species go? Incorporating new advances in climate modelling into projections of species distributions. *Glob. Chang. Biol.* 13,1368-1385. doi: 10.1111/j.1365-2486.2007.01357.x

Becerra-López, J., Ramírez-Bautista, A., Romero-Méndez, U., Pavón, N., and Sánchez-Rojas, G. (2017). Effect of climate change on halophytic grasslands loss and its impact in the viability of *Gopherus flavomarginatus*. *Nat. Conserv*. 21, 39–55. doi: 10.3897/natureconservation.21.13614

Bellard, C., Bertelsmeier, C., Leadley, P., Thuiller, W., and Courchamp, F. (2012). Impacts of climate change on the future of biodiversity. *Ecol. Lett.* 15, 365–377. doi: 10.1111/j.1461-0248.2011.01736.x

Besnard, G., Dupuy, J., Larter, M., Cuneo, P., Cooke, D., and Chikhi, L. (2014). History of the invasive African olive tree in Australia and Hawaii: evidence for sequential bottlenecks and hybridization with the Mediterranean olive. *Evol. App.* 7, 195–211. doi: 10.1111/eva.12110

Bezeng, B. S., Morales-Castilla, I., Van der Bank, M., Yessoufou, K., Daru, B. H., and Davies, T. J. (2017). Climate change may reduce the spread of non-native species. *Ecosphere* 8, e01694. doi: 10.1002/ecs2.1694

Bradley, B. A., and Mustard, J. F. (2006). Characterizing the landscape dynamics of an invasive plant and risk of invasion using remote sensing. *Ecol. Appl.* 16, 1132–1147. doi: 10.1890/1051-0761(2006)016[1132:CTLDOA]2.0.CO;2

Bradley, B. A., Oppenheimer, M., and Wilcove, D. S. (2009). Climate change and plant invasions: restoration opportunities ahead? *Glob. Chang. Biol.* 15, 1511–1521. doi: 10.1111/j.1365-2486.2008.01824.x

Bradstock, R., Penman, T., Boer, M., Price, O., and Clarke, H. (2014). Divergent responses of fire to recent warming and drying across south-eastern Australia. *Glob. Chang. Biol.* 20, 1412–1428. doi: 10.1111/gcb.12449

Breiman, L. (2001). Random forests. *Mach. Learn.* 45, 5–32. doi: 10.1023/A:1010933404324

Breiman, L., Friedman, J. H., Olshean, R. A., and Stone, C. J. (1984). *Classification and Regression Trees*. Belmont, CA: Wadsworth.

Brito, C., Dinis, L. T., Moutinho-Pereira, J., and Correia, C. M. (2019). Drought stress effects and olive tree acclimation under a changing climate. *Plants* 8, 232. doi: 10.3390/plants8070232

Busby, J. R. (1991). "BIOCLIM—a bioclimate analysis and prediction system," in *Nature Conservation: Cost Effective Biological Surveys and Data Analysis*, eds Margules, C. R., and Austin, M. P. (Canberra: CSIRO), 64–68.

Butchart, S. H. M., Walpole, M., Collen, B., van Strien, A., Scharlemann, J. P. W., Almond, R. E. A., et al. (2010). Global biodiversity: indicators of recent declines. *Science* 328, 1164–1168. doi: 10.1126/science.1187512

Chen, I.-C., Hill, J. K., Ohlemuller, R., Roy, D. B., and Thomas, C. D. (2011). Rapid range shifts of species associated with high levels of climate warming. *Science* 333, 1024–1026. doi: 10.1126/science.1206432

Convention on Biological Diversity (2020). *Convention on Biological Diversity Zero Draft of the Post-2020 Global Biodiversity Framework.* Convention on Biological Diversity.

Cook, B. I., Wolkovich, E. M., Davies, T. J., Ault, T. R., Betancourt, J. L., Allen, J. M., et al. (2012). Sensitivity of spring phenology to warming across temporal and spatial climate gradients in two independent databases. *Ecosystems* 15, 1283–1294. doi: 10.1007/s10021-012-9584-5

Dad, J. M., Muslim, M., Rashid, I., Rashid, I., and Reshi, Z. A. (2021). Time series analysis of climate variability and trends in Kashmir Himalaya. *Ecol. Indicat.* 126, 107690. doi: 10.1016/j.ecolind.2021.107690

Davis-Reddy, C. L., and Vincent, K. (2017). *Climate Risk and Vulnerability: A Handbook for Southern Africa,* Second Edn. Pretoria: CSIR.

De Candolle, A. (1882). *Origine des plantescultivées.* Geneva: FAO.

De Ollas, C., Morillón, R., Fotopoulos, V., Puértolas, J., Ollitrault, P., Gómez-Cadenas, A., et al. (2019). Facing climate change: biotechnology of iconic Mediterranean woody crops. *Front. Plant Sci.* 10. doi: 10.3389/fpls.2019.00427

Deblauwe, V., Droissart, V., Bose, R., Sonké, B., Blach-Overgaard, A., Svenning, J. C., et al. (2016). Remotely sensed temperature and precipitation data improve species distribution modeling in the tropics. *Glob. Ecol Biogeogr*. 25, 443–454. doi: 10.1111/geb.12426

Duursma, D. E., Gallagher, R. V., Roger, E., Hughes, L., Downey, P. O., and Leishman, M. R. (2013). Next-generation invaders? Hotspots for naturalised sleeper weeds in Australia under future climates. *PLoS ONE* 8, e84222. doi: 10.1371/journal.pone.0084222

Elith, J., Ferrier, S., Huettmann, F., and Leathwick, J. (2005). The evaluation strip: a new and robust method for plotting predicted responses from species distribution models. *Ecol. Model*. 186: 280–289. doi: 10.1016/j.ecolmodel.2004.12.007

Elith, J., Kearney, M., and Phillips, S. (2010). The art of modelling range-shifting species. *Methods Ecol. Evol*. 1, 330–342. doi: 10.1111/j.2041-210X.2010.00036.x

Fei, S., Desprez, J. M., Potter, K. M., Jo, I., Knott, J. A., and Oswalt, C. M. (2017). Divergence of species responses to climate change. *Sci. Adv*. 3, e1603055. doi: 10.1126/sciadv.1603055

GBIF (2021). Available online at: http://www.gbif.org (accessed July 15, 2021).

Ghafoor, G. Z., Sharif, F., Khan, M. U. H., Shahid, M. G., Siddiq, Z., and Shahzad, L. (2021). Effect of climate warming on seedling growth and biomass accumulation of *Acacia modesta* and *Olea europaea* Subsp. cuspidata in a subtropical scrub forest of Pakistan. *Ecoscience*. 29, 133–146. doi: 10.1080/11956860.2021.1958536

Gillard, M., Thiébaut, G., Deleu, C., and Leroy, B. (2017). Present and future distribution of three aquatic plants taxa across the world: decrease in native and increase in invasive ranges. *Biol. Invas*. 19, 59–2170. doi: 10.1007/s10530-017-1428-y

Green, P. S. (2002). A revision of Olea L. (Oleaceae). *Kew Bull*. 57, 91–140. doi: 10.2307/4110824

Guisan, A., Thuiller, W., and Zimmermann, N. E. (2017). *Habitat Suitability and Distribution Models With Applications in R*. Cambridge: Cambridge University Press. doi: 10.1017/9781139028271

Hastie, T., Tibshirani, R., and Buja, A. (1994). Flexible discriminant analysis by optimal scoring. *J. Am. Stat. Assoc*. 89, 1255–1270. doi: 10.1080/01621459.1994.10476866

Hastie, T. J., and Tibshirani, R. (1990). *Generalized Additive Models*. London: Chapman and Hall.

Hijmans, R. J., Cameron, S. E., Parra, J. L., Jones, P. G., and Jarvis, A. (2005). Very high resolution interpolated climate surfaces for global land areas. *Int. J. Clim*. 25, 1965–1978. doi: 10.1002/joc.1276

Hijmans, R. J., Phillips, S., Leathwick, J., and Elith, J. (2020). *dismo: Species Distribution Modeling*. R package version 1.3-3. Available online at: https://CRAN.R-project.org/package=dismo (accessed August 01, 2021).

Hoffmann, A. A., Rymer, P. D., Byrne, M., Ruthrof, K. X., Whinam, J., McGeoch, M., et al. (2018). Impacts of recent climate change on terrestrial flora and fauna: some emerging Australian examples. *Aust. Ecol*. 44, 3–27. doi: 10.1111/aec.12674

IPCC (2013). *Climate Change 2013: The Physical Science Basis*. Cambridge: Cambridge University Press.

IPCC (2014). "Summary for policymakers," in *Climate Change 2014: Impacts, Adaptation, and Vulnerability. Part A: global and sectoral aspects. Contribution of Working Group II to the Fifth Assessment Report of the Intergovernmental Panel on Climate Change*, eds Field et al. (Cambridge and New York: Cambridge University Press).

IPCC (2019). *Climate Change and Land: An IPCC Special Report on Climate Change, Desertification, Land Degradation, Sustainable Land Management, Food Security, and Greenhouse Gas Fluxes in Terrestrial Ecosystems*, eds Shukla, P. R., Skea, J., Calvo Buendia, E., Masson-Delmotte, V., Pörtner, H.-O., Roberts, D. C., et al. (Cambridge: Cambridge University Press).

IPCC (2021). "Summary for policymakers," in *Climate Change 2021: The Physical Science Basis. Contribution of Working Group I to the Sixth Assessment Report of the Intergovernmental Panel on Climate Change*, eds Masson-Delmotte, V., Zhai, P., Pirani, A., Connors, S. L., Péan, C., Berger, S., Caud, N., et al. (Cambridge: Cambridge University Press).

IPCC. (2012). "Managing the risks of extreme events and disasters to advance climate change adaptation," in *A Special Report of Working Groups I and II of the Intergovernmental Panel on Climate Change*, eds C. B. Field, V. Barros, T. F. Stocker, D. Qin, D. J. Dokken, K. L. Ebi, M. D. Mastrandrea, K. J. Mach, G. -K. Plattner, S. K. Allen, M. Tignor, and P. M. Midgley (Cambridge; New York, NY: Cambridge University Press), p. 582.

Kassout, J., Terral, J. F., Ouahrani, A. E., Houssni, M., Ivorra, S., et al. (2022). "Species distribution based-modelling under climate change: the case of two native wild *Olea europaea* subspecies in Morocco, O. e. subsp. europaea var. sylvestris and O. e. subsp. Maroccana," in *Climate Change in the Mediterranean and Middle Eastern Region. Climate Change Management,* eds Leal Filho, W., Manolas, E. (Cham: Springer). doi: 10.1007/978-3-030-78566-6_2

Kelly, A. E., and Goulden, M. L. (2008). Rapid shifts in plant distribution with recent climate change. *Proc. Nat. Acad. Sci. USA* 105, 11823–11826. doi: 10.1073/pnas.0802891105

Kumari, P., Wani, I. A., Khan, S., Verma, S., Mushtaq, S., Gulnaz, A., et al. (2022). Modeling of *Valeriana wallichii* habitat suitability and niche dynamics in the Himalayan Region under anticipated climate change. *Biology* 11, 498. doi: 10.3390/biology11040498

Long, H. S., Tilney, P. M., and Van Wyk, B. E. (2010). The ethnobotany and pharmacognosy of *Olea europaea* subsp. *africana (Oleaceae). S. Afri. J. Bot*. 76, 324–331. doi: 10.1016/j.sajb.2009.12.005

Madani, N., Kimball, J. S., Ballantyne, A. P., Affleck, D. L. R., van Bodegom, P. M., Reich, P. B., et al. (2018). Future global productivity will be affected by plant trait response to climate. *Sci. Rep*. 8, 2870. doi: 10.1038/s41598-018-21172-9

Maitner, B. S., Boyle, B., Casler, N., Condit, R., Donoghue, J., Durán, S. M., et al. (2018). The BIEN R package: a tool to access the botanical information and ecology network (BIEN) database. *Meth. Ecol. Evol*. 9, 373–379. doi: 10.1111/2041-210X.12861

Malhi, Y., Franklin, J., Seddon, N., Solan, M., Turner, M. G., Field, C. B., et al. (2020). Climate change and ecosystems: threats, opportunities and solutions. *Philos. Trans. R. Soc. B Biol. Sci*. 375, 20190104. doi: 10.1098/rstb.2019.0104

Manzoor, S. A., Griffiths, G., and Lukac, M. (2018). Species distribution model transferability and model grain size—finer may not always be better. *Sci. Rep*. 8, 1–9. doi: 10.1038/s41598-018-25437-1

Masoko, P., and Makgapeetja, D. M. (2015). Antibacterial, antifungal and antioxidant activity of Olea africana against pathogenic yeast and nosocomial pathogens. *BMC Comp. Altern. Med*. 15. doi: 10.1186/s12906-015-0941-8

McCullagh, P., and Nelder, J. A. (1989). *Generalized Linear Models*, 2nd edn. London: Chapman and Hall. doi: 10.1007/978-1-4899-3242-6

Moraira, H. S., Vitales, D., Nualart, N., et al. (2020). Global distribution patterns and niche modelling of the invasive *Kalanchoe houghtonii* (Crassulaceae). *Sci. Rep*. 10, 3143. doi: 10.1038/s41598-020-60079-2

Morris, W. F., Ehrlén, J., Dahlgren, J. P., Loomis, A. K., and Louthan, A. M. (2019). Biotic and anthropogenic forces rival climatic/abiotic factors in determining global plant population growth and fitness. *Proc. Nat. Acad. Sci. USA* 2019, 18363. doi: 10.1073/pnas.1918363117

Moss, R. H. (2010). The next generation of scenarios for climate change research and assessment. *Nature* 463, 747–756. doi: 10.1038/nature08823

Mudelsee, M. (2018). Trend analysis of climate time series: a review of methods. *Earth-Sci. Rev*. doi: 10.1016/j.earscirev.2018.12.005

Naimi, B. (2015). *On uncertainty in Species Distribution Modelling (PhD Dissertation)*. Twente: University of Twente, ITC.

Negash, L. (2010). *A Selection of Ethiopia's Indigenous Trees: Biology, Uses and Propagation Techniques*. Addis Ababa: Addis Ababa University Press.

Negi, G. C. S., Singh, P., and Singh, S. P. (2021). Atmospheric warming-associated phenological earliness does not increase the length of growing season in Himalayan Trees. *Forest Sci*. 67, 694–700. doi: 10.1093/forsci/fxab040

Norberg, A., Abrego, N., Blanchet, F. G., Adler, F. R., Anderson, B. J., Anttila, J., et al. (2019). Comprehensive evaluation of predictive performance of 33 species distribution models at species and community levels. *Ecol. Monogr*. 89, e01370. doi: 10.1002/ecm.1370

Pacifici, M., Foden, W. B., Visconti, P., Watson, J. E. M., Butchart, S. H. M., Kovacs, K. M., et al. (2015). Assessing species vulnerability to climate change. *Nat. Clim Chang*. 5, 215–224. doi: 10.1038/nclimate2448

Pacifici, M., Visconti, P., Butchart, S. H. M., Watson, J. E. M., Cassola, F. M., and Rondinini, C. (2017). Species' traits influenced their response to recent climate change. *Nat. Clim. Chang*. 7, 205–208. doi: 10.1038/nclimate3223

Palmer, G., Hill, J. K., Brereton, T. M., Brooks, D. R., Chapman, J. W., Fox, R., et al. (2015). Individualistic sensitivities and exposure to climate change explain variation in species' distribution and abundance changes. *Sci. Adv*. 1, e1400220. doi: 10.1126/sciadv.1400220

Panda, R. M., and Behera, M. D. (2018). Assessing harmony in distribution patterns of plant invasions: a case study of two invasive alien species in India. *Biodivers. Conserv*. 28,2245–2258. doi: 10.1007/s10531-018-1640-9

Parey, S. (2019). Generating a set of temperature time series representative of recent past and near future climate. *Front. Envir. Sci*. 7, 99. doi: 10.3389/fenvs.2019.00099

Parmesan, C. (2006). Ecological and evolutionary responses to recent climate change. *Ecol. Evol*. 37, 637–669. doi: 10.1146/annurev.ecolsys.37.091305.110100

Parmesan, C., Duarte, C., Poloczanska, E., Richardson, A. J., and Singer, M. C. (2011). Overstretching attribution. *Nat. Clim. Change*. 1, 2–4. doi: 10.1038/nclimate1056

Parmesan, C., and Hanley, M. E. (2015). Plants and climate change: complexities and surprises. *Ann. Bot*. 116, 849–864. doi: 10.1093/aob/mcv169

Pecl, G. T., Araújo, M. B., Bell, J. D., Blanchard, J., Bonebrake, T. C., Chen, I.-C., et al. (2017). Biodiversity redistribution under climate change: impacts on ecosystems and human well-being. *Science* 355, eaai9214. doi: 10.1126/science.aai9214

Phillips, S. J., Anderson, R. P., and Schapire, R. E. (2006). Maximum entropy modelling of species geographic distributions. *Ecol. Model*. 190, 231–259. doi: 10.1016/j.ecolmodel.2005.03.026

Porfirio, L. L., Harris, R. M. B., Lefroy, E. C., Hugh, S., Gould, S. F., Lee, G., et al. (2014). Improving the use of species distribution models in conservation planning and management under climate change. *PLoS ONE* 9, e113749. doi: 10.1371/journal.pone.0113749

Priyanka, N., and Joshi, P. K. (2013). Effects of climate change on invasion potential distribution of Lantana camara. *J. Earth Sci. Clim. Chang*. 4, 164. doi: 10.4172/2157-7617.1000164

Pyke, C. R., and Fischer, D. T. (2005). Selection of bioclimatically representative biological reserve systems under climate change. *Biol. Conserv*. 121, 429–441. doi: 10.1016/j.biocon,.2004.05.019

Rabasa, S. G., Granda, E., Benavides, R., Kunstler, G., Espelta, J. M., Ogaya, R., et al. (2013). Disparity in elevational shifts of European trees in response to recent climate warming. *Glob. Chang. Biol*. 19, 2490–2499. doi: 10.1111/gcb.12220

Rather, Z. A., Ahmad, R., Dar, T. U. H., and Khuroo, A. A. (2022). Ensemble modelling enables identification of suitable sites for habitat restoration of threatened biodiversity under climate change: a case study of Himalayan Trillium. *Eco. Engin*. 176, 106534. doi: 10.1016/j.ecoleng.2021.106534

Rathore, P., Roy, A., and Karnatak, H. (2018). Assessing the vulnerability of Oak (*Quercus*) forest ecosystems under projected climate and land use land cover changes in Western Himalaya. *Biodiver. Conser*. 28, 2275–2294. doi: 10.1007/s10531-018-1679-7

Ridgeway, G. (1999). The state of boosting. *Comput. Sci. Stat*. 31, 172–181.

Ripley, B. (1996). *Pattern Recognition and Neural Networks*. New York, NY: Cambridge University Press. doi: 10.1017/CBO9780511812651

Román-Palacios, C., and Wiens, J. J. (2020). Recent responses to climate change reveal the drivers of species extinction and survival. *Proc. Nat. Acad. Sci. USA* 117, 4211–4217. doi: 10.1073/pnas.1913007117

Schorr, G., Holstein, N., Pearman, P. B., Guisan, A., and Kadereit, J. W. (2012). Integrating species distribution models (SDM) and phylogeography for two species of Alpine Primula. *Ecol. Evol*. 2, 1260–1277. doi: 10.1002/ece3.100

Sharma, G. P., and Raghubanshi, A. S. (2006). Tree population structure, regeneration and expected future composition at different levels of *Lantana camara* L. invasion in the Vindhyan tropical dry deciduous forest of India. *Lyonia* 11, 25–37.

Sheldon, K. S. (2019). Climate change in the tropics: ecological and evolutionary responses at low latitudes. *Annu. Rev. Ecolsys*. 50, 110218. doi: 10.1146/annurev-ecolsys-110218-025005

Solman, S. A., and Orlanski, I. (2016). Climate change over the extratropical southern hemisphere: The tale from an ensemble of reanalysis datasets. *J. Clim*. 29, 1673–1687. doi: 10.1175/JCLI-D-15-0588.1

Srivastava, V., Lafond, V., and Griess, V. C. (2019). Species distribution models (SDM): applications, benefits and challenges in invasive species management. *CAB Rev. Perspect. Agric. Vet. Sci. Nutr. Nat. Resour*. 2019, 1–13. doi: 10.1079/PAVSNNR201914020

Tamarin-Brodsky, T., Hodges, K., Hoskins, B. J., and Shepherd, T. G. (2020). Changes in Northern Hemisphere temperature variability shaped by regional warming patterns. *Nat. Geo*. doi: 10.1038/s41561-020-0576-3

Taylor, S., Kumar, L., Reid, N., and And Kriticos, D. J. (2012). Climate change and the potential distribution of an invasive shrub, *Lantana camara* L. *PLoS ONE* 7, e35565. doi: 10.1371/journal.pone.0035565

Telwala, Y., Brook, B. W., Manish, K., and Pandit, M. K. (2013). Climate-induced elevational range shifts and increase in plant species richness in a himalayan biodiversity epicentre. *PLoS ONE* 8, e57103. doi: 10.1371/journal.pone.0057103

Thapa, S., Chitale, V., Rijal, S. J., Bisht, N., and Shrestha, B. B. (2018). Understanding the dynamics in distribution of invasive alien plant species under predicted climate change in Western Himalaya. *PLoS ONE* 13, e0195752. doi: 10.1371/journal.pone.0195752

Thomas, C. D., Cameron, A., Green, R. E., Bakkenes, M., Beaumont, L. J., Collingham, Y. C., et al. (2004). Extinction risk from climate change. *Nature* 427, 145–148. doi: 10.1038/nature02121

Thuiller, W., Cade, B., Engler, R., and Araújo, M. B. (2009). BIOMOD a platform for ensemble forecasting of species distributions. *Ecography*. 32, 369–373. doi: 10.1111/j.1600-0587.2008.05742.x

Thuiller, W., Georges, D., Engler, R., and Breiner, F. (2020). *biomod2:Ensemble Platform for Species Distribution Modeling. R package version 3.4.6. (Version R package version 3.4.6)*. Available online at: https://CRAN.R-project.org/package=biomod2

Thuiller, W., Guéguen, M., Renaud, J., Karger, D. N., and Zimmermann, N. E. (2019). Uncertainty in ensembles of global biodiversity scenarios. *Nat. Commun*. 10, 1–9. doi: 10.1038/s41467-019-09519-w

Tollefson, J. (2020). Why deforestation and extinctions make pandemics more likely. *Nature* 584, 175–176. doi: 10.1038/d41586-020-02341-1

VanDerWal, J., Murphy, H. T., Kutt, A. S., Perkins, G. C., Bateman, B. L., Perry, J. J., et al. (2012). Focus on poleward shifts in species' distribution underestimates the fingerprint of climate change. *Nat. Clim. Chang*. 3, 239–243. doi: 10.1038/nclimate1688

Vuuren, D. P., Van Edmonds, J., Kainuma, M., Riahi, K., Nakicenovic, N., Smith, S. J., et al. (2011). The representative concentration pathways: an overview. *Clim. Chang*. 109, 5–31. doi: 10.1007/s10584-011-0148-z

Waltari, E., Schroeder, R., McDonald, K., Anderson, R. P., and Carnaval, A. (2014). Bioclimatic variables derived from remote sensing: assessment and application for species distribution modelling. *Meth. Ecol. Evol*. 5, 1033–1042. doi: 10.1111/2041-210X.12264

Wan, J. Z., Wang, C. J., and Yu, F. H. (2016). Risk hotspots for terrestrial plant invaders under climate change at the global scale. *Environ. Earth Sci*. 75, 1–8. doi: 10.1007/s12665-016-5826-8

Wani, I. A., Khan, S., Verma, S., Al-Misned, F. A., Shafik, H. M., and El-Serehy, H. A., et al. (2022a). Predicting habitat suitability and niche dynamics of *Dactylorhiza hatagirea* and *Rheum webbianum* in the Himalaya under projected climate change. *Sci. Rep*. 12, 13205. doi: 10.1038/s41598-022-16837-5

Wani, Z. A., Ridwan, Q., Khan, S., Pant, S., Siddiqui, S., Moustafa, M., et al. (2022b). Changing climatic scenarios anticipate dwindling of suitable habitats for endemic species of himalaya-predictions of ensemble modelling using *Aconitum heterophyllum* as a model plant. *Sustainability*. 14, 8491. doi: 10.3390/su14148491

Weiskopf, S. R., Rubenstein, M. A., Crozier, L. G., Gaichas, S., Griffis, R., Halofsky, J. E., et al. (2020). Climate change effects on biodiversity, ecosystems, ecosystem services, and natural resource management in the United States. *Sci. Tot. Env*. 773, 137782. doi: 10.1016/j.scitotenv.2020.137782

Woodward, F. I., Lomas, M. R., and Kelly, C. K. (2004). Global climate and the distribution of plant biomes. *Phil. Trans. R. Soc. B Biol. Sci*. 359, 1465–1476. doi: 10.1098/rstb.2004.1525

Xu, Y., Huang, Y., Zhao, H., Yang, M., Zhuang, Y., and Ye, X. (2021). Modelling the effects of climate change on the distribution of endangered *Cypripedium japonicum* in China. *Forests* 12, 429. doi: 10.3390/f12040429

Zu, K., Wang, Z., Zhu, X., Lenoir, J., Shrestha, N., Lyu, T., et al. (2021). Upward shift and elevational range contractions of subtropical mountain plants in response to climate change. *Sci. Tot. Env*. 783, 146896. doi: 10.1016/j.scitotenv.2021.146896

frontiers | Frontiers in Forests and Global Change

TYPE Original Research
PUBLISHED 10 November 2022
DOI 10.3389/ffgc.2022.1022082

OPEN ACCESS

EDITED BY
Yashwant Singh Rawat,
Federal Technical and Vocational Education and Training Institute (FTVETI), Ethiopia

REVIEWED BY
Mohd Tariq,
Parul University, India
Rajendra Mohan Panda,
Indian Institute of Technology Kharagpur, India
Om Prakash Tiwari,
Hemwati Nandan Bahuguna Garhwal University, India

*CORRESPONDENCE
Indra D. Bhatt
id_bhatt@yahoo.com

SPECIALTY SECTION
This article was submitted to Forest Management,
a section of the journal
Frontiers in Forests and Global Change

RECEIVED 18 August 2022
ACCEPTED 10 October 2022
PUBLISHED 10 November 2022

CITATION
Thakur S, Dhyani R, Negi VS and Bhatt ID (2022) Water–energy, climate, and habitat heterogeneity mutually drives spatial pattern of tree species richness in the Indian Western Himalaya.
Front. For. Glob. Change 5:1022082.
doi: 10.3389/ffgc.2022.1022082

Water–energy, climate, and habitat heterogeneity mutually drives spatial pattern of tree species richness in the Indian Western Himalaya

Shinny Thakur, Rupesh Dhyani, Vikram S. Negi and Indra D. Bhatt*

G.B. Pant National Institute of Himalayan Environment (NIHE), Almora, Uttarakhand, India

Analyzing plant species richness across a broad geographic gradient is critical for understanding the patterns and processes of biodiversity. In view of this, a species richness map was developed by stacking the ranges of 51 tree species along an elevational gradient in the Western Himalaya using stacked species distribution models (SSDMs). Among modeling algorithms available in SSDMs, random forest and artificial neural networks exhibited the best performance ($r = 0.81$, $p < 0.001$). The predicted tree species richness distribution pattern revealed a mid-elevation peak at around 2,000 m asl, which is in concordance with the observed richness pattern ($R^2 = 0.94$, $p < 0.001$). Additionally, structural equation models (SEMs) were used to confirm the key factors that influence tree richness. The results based on SEMs confirm that the elevational pattern of predicted tree species richness is explained by mutual effects of water–energy availability, climate, and habitat heterogeneity. This study also validates that the impact of moisture on tree species richness coincides geographically with climate factors. The results have revealed that water–energy-related variables are likely to impact the species richness directly at higher elevations, whereas the effect is more likely to be tied to moisture at lower elevations. SSDMs provide a good tool to predict a species richness pattern and could help in the conservation and management of high biodiverse areas at different spatial scales. However, more investigation is needed to validate the SSDMs in other parts of the Himalayan region to provide a comprehensive synoptic perspective of Himalayan biodiversity at a larger scale.

KEYWORDS

elevational gradient, environmental variables, species richness, species distribution modelling, Western Himalaya

Introduction

Species distribution modeling (SDM) is a tool that offers robust estimates of biodiversity mapping using field-based observations of species localities. In recent years, SDM has become a useful approach for predicting species distribution ranges, based on the relationships between species records and environmental variables (Pineda and Lobo, 2009). Mapping of species richness using SDM has increased significantly and gaining the attention of policy planners in forest management and conservation (Fitzpatrick et al., 2008; Colombo and Joly, 2010; Schmidt-Lebuhn et al., 2012; Benito et al., 2013; Brown et al., 2015; D'Amen et al., 2015; Pouteau et al., 2018). It is well known that the assessment of plant species richness in any ecosystem is critical for long-term management and conservation initiatives (Gutiérrez and Huth, 2012; Rawal et al., 2018; Negi et al., 2019). A hump-shaped pattern or a higher number of species at mid-elevation has been reported as a prominent pattern across the mountain regions (Stevens, 1992; Rahbek, 1995; Grytnes and McCain, 2013; Guo et al., 2013; Negi et al., 2021). Several hypotheses, e.g., energy and water availability, energy–water balance, seasonality, and habitat heterogeneity, have been proposed to explain the elevational pattern of species richness. The habitat heterogeneity hypothesis states that an increase in heterogeneity leads to an increase in species richness (MacArthur and MacArthur, 1961). Similarly, the energy hypothesis states that greater availability of energy is an optimum condition for enhancing species richness and climate stability (Turner et al., 1987; Hawkins et al., 2003; Panda et al., 2017).

The Himalaya, a global biodiversity hotspot (Myers, 1988) and a climatically sensitive region, supports more than 10,500 species of flowering plants, which are distributed across the subtropical foothills to high alpine climatic zones. These regions are important to study species richness patterns across a wider geographical coverage (Rana and Rawat, 2017). Studies based on field observations and overlapping elevational ranges along an elevational gradient in the Himalaya show a common pattern of a mid-elevation peak in the species richness (Vetaas and Grytnes, 2002; Bhattarai and Vetaas, 2003, 2006; Oommen and Shanker, 2005; Acharya et al., 2011; Kluge et al., 2017; Manish et al., 2017; Thakur et al., 2021). Field observation-based studies along the elevational gradients in the Himalaya report the highest number of species at the mid-elevations (Kharkwal et al., 2005; Sharma et al., 2018; Rana et al., 2019a; Bhat et al., 2020). The causes of such variations include a primary role of water–energy dynamics (Acharya et al., 2011), evolutionary history (Rana et al., 2019b), and disturbances (Negi et al., 2018a,b; Thakur et al., 2021; Rana et al., 2022). However, spatial and climatic patterns are postulated to explain these patterns of variation in species richness over elevational gradients (Connell and Orias, 1964). Panda et al. (2017) suggested that energy variables (i.e., potential evapotranspiration and temperature seasonality) provide a better explanation than water variables (i.e., aridity index and precipitation of the driest quarter) in explaining plant species richness in the Western Himalaya. Similarly, a combination of ambient energy (i.e., air temperature, solar radiation, and potential evapotranspiration) and water availability (i.e., soil water content and precipitation) was found to be the main drivers of the elevational pattern of species richness in the Eastern Himalaya (Manish et al., 2017). Recent studies from the Himalayan region indicate that the freezing line and disturbance also play important roles in driving the species turnover along the elevational gradient (Rana et al., 2022). However, the specific causes for the hump structure of association between plant species richness and elevation are difficult to decipher due to the intricate linkages among these processes (Acharya et al., 2011). Thus, currently, many hypotheses still remain to be tested for habitat heterogeneity and climate stability, which can provide important insights into explaining species richness patterns (Pan et al., 2016).

Many assessments of biodiversity patterns along elevational gradients rely on field data gathered in transects or plots. Species richness maps based on field observations have been proven to be the best alternative for identifying biodiversity-rich areas with complete geographical coverage (Murray-Smith et al., 2009; Oliveira et al., 2019; Testolin et al., 2021). Identification of degraded regions, sensitive and species-specific habitats (Negi et al., 2018a), and hotspots of invasive species (Gallardo-Cruz et al., 2009; Bellard et al., 2013; Pouteau et al., 2018) through spatially explicit methods is useful for climate change adaptation, restoration of degraded lands, and conservation of specific habitat or region (Bellard et al., 2013).

Modeling species richness using SDMs is frequently used to anticipate how potential plant species richness in mountains may alter due to climate change. Although only a few research studies focus on the use of SDMs to predict richness patterns along elevational gradients (Syfert et al., 2018), no attempts have been made to predict a spatial pattern of species richness using SDM approach in the Indian Himalayan region (IHR). The true ranges of most plant species are unknown due to a limited number of their recorded locations. This has prompted for using a valid species distribution model for mapping, using field-based data on species locale. In such cases, the use of SDM without knowing the true species ranges of plant species can add ambiguity in predictions for research and policy issues, such as conservation priority. Thus, this study is an attempt to prove that SDM algorithms are a useful approach for predicting true species richness patterns at a spatial scale. This was followed by testing the ecological hypotheses related to water, energy, climate, and habitat heterogeneity to identify determinants of tree species richness in the Western Himalaya.

Materials and methods

Study area and species data

The study area located in Pithoragarh district (Uttarakhand) in the Western Himalaya (**Figure 1**) has a unique importance in terms of diverse and unique flora and fauna (Oli and Zomer, 2011). It is situated at the confluence of the Western, Central, and Trans-Himalayan bioregions, forming an intersection of flora, fauna, and human cultures. The study area has a wide elevational gradient ranging from 412 to 7,132 m asl constituting the vegetation types covering subtropical to alpine regions. It is also an important ecological barrier depending on varying topographies from the outer Siwalik to the inner high Himalaya and consists of a variety of plant diversity covering subtropical to alpine vegetation (Saxena et al., 1985). The region is attitudinally divisible into subtropical (300 to 1,500 m), temperate (1,500 to 3,500 m), and alpine (>3,500 m) zones (Saxena et al., 1985). The mean annual temperature of the area ranges from 30 to 12°C lower to higher altitudinal ranges (Thakur et al., 2020). Vegetation sampling was carried out during 2016–2019 along an elevational gradient ranging from 800 to 4,000 m asl at 33 sites of an approximate interval of 100 m in the Pithoragarh district. We have used the phytosociological method (Misra, 1968, Muller Dombois and Ellenberg, 1974; Negi et al., 2018a; Rawal et al., 2018) to sample trees species. The sample plots were randomly laid at the interval of 100 m elevation along the altitude. Within 100 m elevation, we have randomly placed three plots of 2500 m^2 each, and within one random plot (2,500 m^2), five quadrats of 10 × 10 m (100 m^2 size each) were placed for tree sampling. Thus, a total of 99 plots (2,500 m^2 size) were laid along 33 elevations or sites (800–4,000 m asl) along the elevational gradient in the studied area. Trees with a circumference at breast height (cbh) > 30 cm were considered for sampling. A total of 2,193 geocoordinates for 51 tree species were recorded using a global positioning system (**Supplementary Table 1**).

Environmental data

A comprehensive set of environmental variables that were considered to be the main factors influencing the distribution of plant species (Dirnböck et al., 2003; Körner, 2012) were used in this study. We have used 23 environmental variables to understand the relative importance of climate, water, energy, and habitat heterogeneity for explaining spatial variation in tree species richness at the regional scale (**Supplementary Table 2**). We extracted 19 bioclimatic variables from Worldclim2[1] at the resolution ~1 km^2 (Fick and Hijmans, 2017) and elevation from USGS GTOPO-30[2] with a resolution of 30 arc seconds. The slope and aspect were extracted from an elevation layer using the "slope" and "aspect" tools in the spatial analyst tools of ArcGIS 10.1. In addition, the normalized difference vegetation index (NDVI), which has been suggested to be useful in predicting plant species distribution and richness (Williams et al., 2009; Cramer and Verboom, 2017), was also derived from the public domain Sentinel-2B of 10-m-resolution images for pre-monsoon and post-monsoon seasons. The data were extracted on March 10, 2019, and October 19, 2019, from the open-source Earth Resources Observation and Science (EROS) Data Center of the US Geological Survey (USGS) archive.[3] All the environmental layers were resampled to 1 km^2 using bilinear transformation to maintain the uniformity. To deal with collinearity, we have performed the multicollinearity test among the predictor variables using the "usdm" package in R (Naimi, 2015) and retained only variables with a variance inflation factor (VIF) less than 8 or correlation coefficient $r \geq 0.8$ (**Supplementary Figure 1**). Based on the multicollinearity test, we used a non-collinear set of predictor variables, i.e., precipitation seasonality (PS), mean diurnal range (MDR), mean temperature of driest quarter (MTDQ), precipitation of warmest quarter (PWQ), slope, aspect, and normalized difference vegetation index (NDVI) in the final ensemble model (**Supplementary Figure 2**). These variables were categorized into water, energy, climate stability, and habitat heterogeneity based on the potential importance of factors to plant species richness. The MTDQ surrogates as energy availability (Panda et al., 2017; Gao and Liu, 2018), PWQ as water availability (Panda et al., 2017; Gao and Liu, 2018), MDR and PS as climate stability (Gao and Liu, 2018), and NDVI, slope, and aspect as habitat heterogeneity (Mouchet et al., 2015; Nieto et al., 2015).

Stack species distribution modeling

As uncertainty in distribution predictions can skew policymaking and planning, fitting a number of alternative statistical approaches finds an agreement among SSDM projections (Marmion et al., 2009; Gritti et al., 2013). The SSDM is ideal for extrapolation of predicted species richness, even with a small number of presence locations with a narrow environmental range (Cayuela et al., 2009; Williams et al., 2009; Mateo et al., 2010). We used the SSDM approach and implemented the R package "SSDM" which integrates multiple individual SDMs to produce a community-level model (Ferrier and Guisan, 2006). The SSDM package provides eight different methods, namely, the generalized linear model (GLM), generalized additive model (GAM), multivariate adaptive regression splines (MARS), generalized boosted regression model (GBM), classification tree analysis (CTA), random forest (RF), support vector machines (SVM), and artificial neural

---

[1] www.worldclim.org

[2] https://lta.cr.usgs.gov/GTOPO30

[3] http://earthexplorer.usgs.gov/

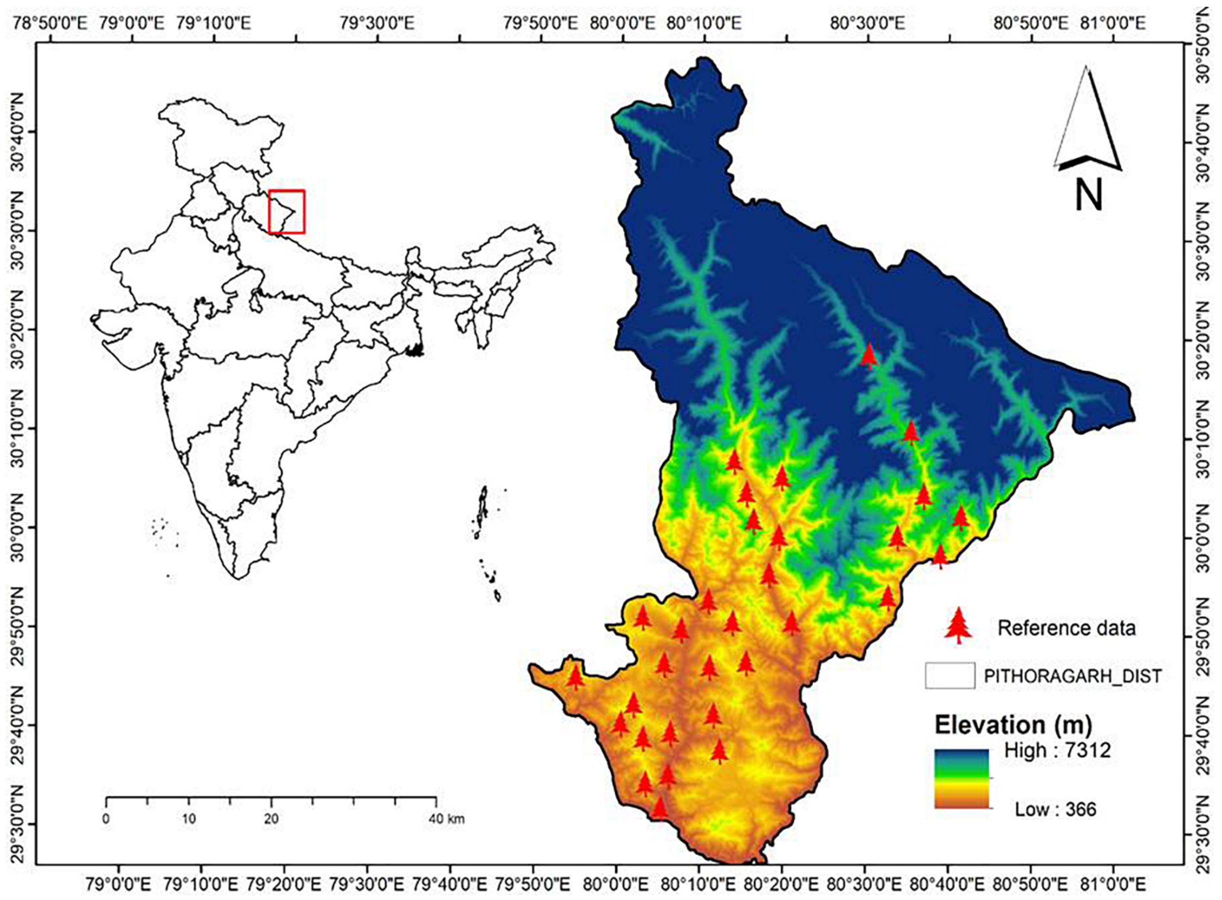

FIGURE 1
Study area map with sites locations. Scale in the map represents the study site.

networks (ANN), to generate a distribution model for a given species. To get the binary map, we used the sensitivity–specificity equality (SES) to compute the binary map threshold (Schmitt et al., 2017). We first produced individual binary maps for each species using these modeling algorithms. We have then checked values of area under the curve (AUC) and kappa metrics that evaluate the accuracy of the individual model for each species. The AUC metric is a widely used statistic for assessing the discriminatory capacity of species distribution models (Barbet-Massin et al., 2012; Leroy et al., 2018). This metric assesses the balance between a true-positive rate (sensitivity) and a false-positive rate (100 − specificity), which is a threshold-independent metric that varies from 0 to 1, where values near or equal to 1 represent that the models reached excellent discriminatory power and values around 0.5 represent species predictions no better than a random distribution. The model needs the presence and absence data of the occurrence data. Many studies proved that the presence–absence of biotic data in species distribution models tended to perform better than the presence-only models (Barbet-Massin et al., 2012; Schmitt et al., 2017; Leroy et al., 2018). It is believed that presence–absence models will yield more reliable results if the presence data that are available seem insufficient or uncertain. To reduce over-prediction and extrapolation into unknown areas can be minimized by absence and/or pseudo-absence points (Barbet-Massin et al., 2012). We randomly created pseudo-absence data of each species with an equal number of its presence data randomly within the study. We summed individual binary maps generated using the SSDM approach for all species, and the final model was selected for AUC > 0.90 to produce an ensemble species richness map. The accuracy (disagreements between the prediction and reality) of the species richness maps across the sets of spatial grains was assessed using the observed occurrence data of the species. We analyzed the proportion of accurate richness predictions and true negatives, true positives, and similarities in species richness using the species richness error, prediction success, and Cohen's kappa coefficient (Schmitt et al., 2017). The work flow of modeling approach is shown in **Figure 2**. Subsequently, we developed the partial dependency plots to better explain the relationship between tree species richness and predictor variables. The partial dependency plots represent the influence

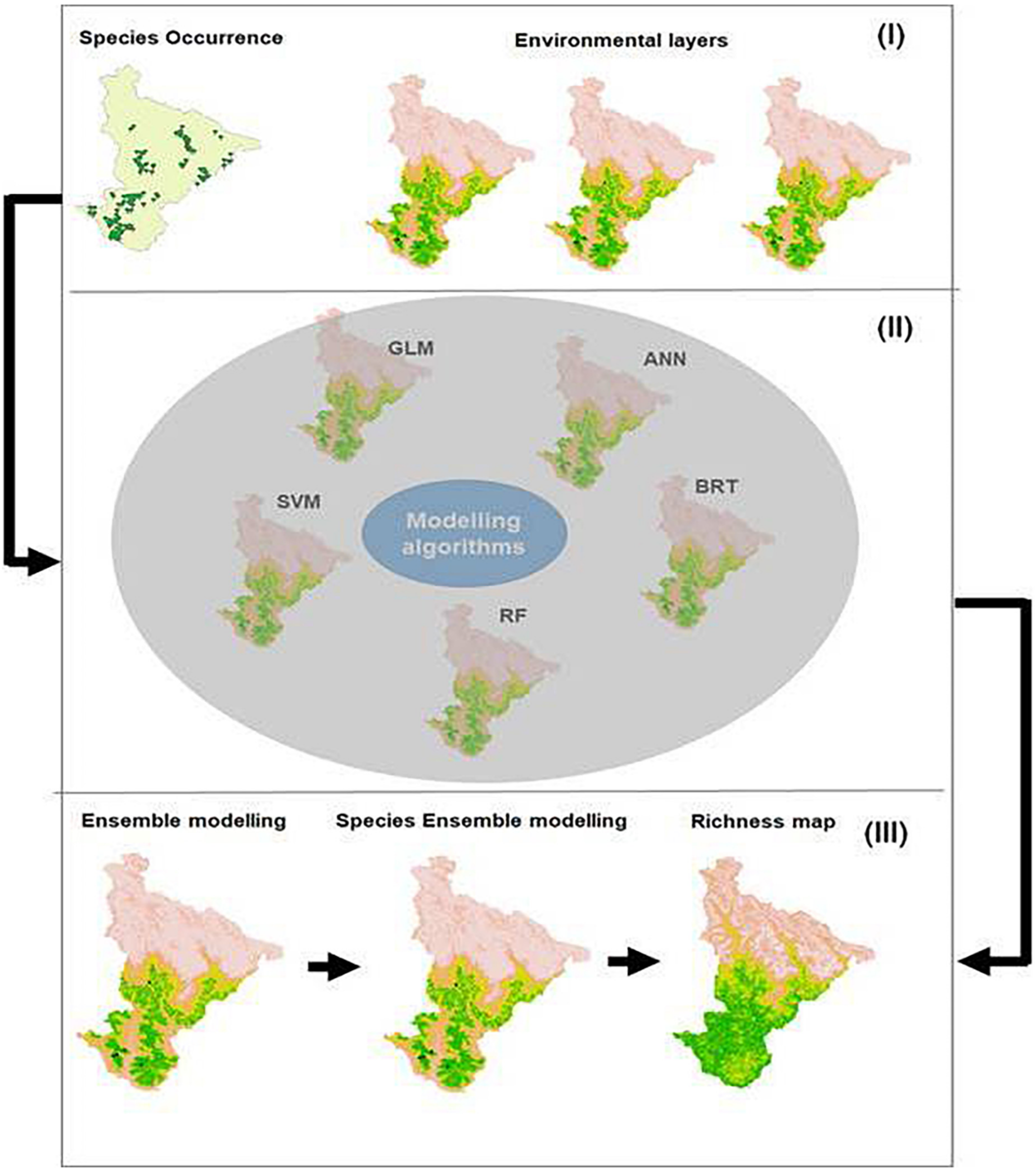

FIGURE 2
Methodological flow diagram of SSDM approach. **(I)** Input species occurrences and environmental layers; **(II)** modeling algorithms for deriving binary maps; and **(III)** ensembling binary maps to produce community-level richness.

of predictor variable on target variable (richness in our case) while controlling the average effects of other predictor variables (Mouchet et al., 2015). For interpretation, we have smoothed the response variables with a spline fit (Mouchet et al., 2015).

Species richness–environment relationship

To validate the relative importance of environmental factors for determining tree species richness generated from SSDM, we have used the structural equation model (SEM) approach. SEM is a sophisticated and reliable regression model commonly employed in ecological research (Panda et al., 2017; Rana et al., 2019b). SEM general methodology entails the creation of a multivariate dependence model that can be statistically validated using field data. This multivariate technique not only aids in a model selection among alternatives, but also presents a quick and efficient solution to a succession of overlapping regression associations. The analysis was carried out in R using the packages "lavaan," "semPlot," and "lavaan" from the CRAN repository (Rosseel, 2012). We compared tree species richness to each group of ecological determinants. Then, for each ecological driver, we investigated the combination of

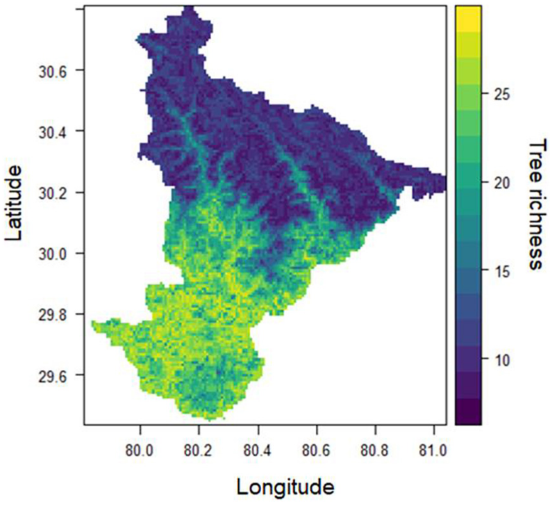

FIGURE 3
Tree species richness map, derived from adding all individual species distribution maps.

environmental variables with tree species richness. The beta coefficient, R^2 value, and root mean square error were used to assess the model's performance.

Results

Pattern of species richness

The SSDM approach successfully predicted a tree species richness map with a spatial resolution of 1 km^2 under the present climatic environments (**Figure 3**). We extracted pixel values of predicted richness with an elevation to derive the elevational pattern of tree species. The observed pattern shows higher synchronicity ($R^2 = 0.94$, $p < 0.001$) with an expected richness pattern (**Supplementary Figure 3**). The elevational pattern of predicted species richness showed a positively skewed hump-shaped pattern with a richness of 20–27 species peaked at approximately 2000 m asl. The predicted richness was about 10–15 species between 2,000 and 3,000 m asl elevation. However, above 3,000 m asl, the tree richness recorded was far less, ranging from 2 to 6 species (**Figure 4**). Consequently, the predicted richness shows a sharp decline in the occurrence of species above 2,000 m asl.

Variables determining tree species richness

Interestingly, all variables explained marginal variance (about 11–16%) to explain tree species richness in the region (**Supplementary Figure 4**). Habitat heterogeneity variables, i.e., NDVI, aspect, and slope, explained 16.46, 15.18, and 11.90% of the variance, respectively, in explaining tree species richness. Water (PWQ) and energy (MTDQ) variables contributed 14.28 and 12.96% of the variance, respectively, to explain tree species richness. Climate stability variables, i.e., MDR and PS, have explained 15.90 and 13.32% of the variance, respectively, to explain tree species richness. These results indicate that the predicated richness patterns are explained differently by various factors, but their relative importance varies. The SEMs adequately fitted the output of key predictor variables for the water–energy, habitat heterogeneity, and climate stability models. The SEM of habitat heterogeneity, water–energy, and climate stability explained 36, 23, and 32% of the variance, respectively, in explaining tree species richness. The habitat heterogeneity model shows a strong significant positive correlation ($r = 0.76$, $p < 0.001$) between NDVI and tree species richness and aspect ($r = -0.23$, $p < 0.05$) and a weak negative correlation with slope ($r = -0.05$, $p > 0.05$) (**Figure 5A**). Similarly, a water–energy model based on MTDQ shows a positive relationship ($r = 0.52$, $p < 0.05$) between tree species richness (**Figure 5B**). In a climate stability model, a strong positive relationship ($r = 0.80$, $p < 0.001$) between PS and tree species richness was found (**Figure 5C**). The partial dependency plots show a sharp increase in richness values with an increase in NDVI values above 0.25, indicating higher values of NDVI sustain higher tree species (**Figure 6A**). These plots also reflect a relationship between MDR and predicted tree species richness that generates a hump-shaped curve with the maximum predicted species richness at an approximate increase in MDR between 10 and 12°C (**Figure 6B**). The richness varies between 10 and 12 species with an increase in MDR from 8 to 13°C (**Figure 6B**). For MTDQ, a tree species richness pattern increased with an increase in MTDQ (**Figure 6C**). The relationship between tree species richness and PS shows a

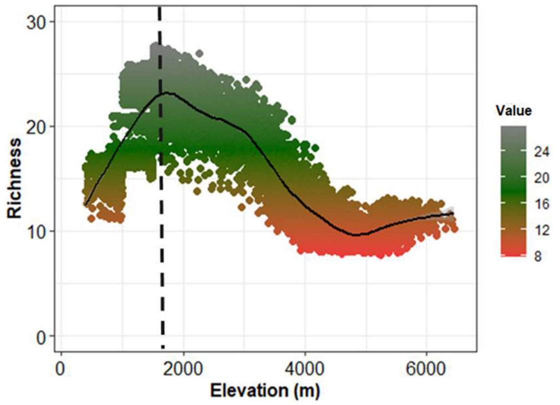

FIGURE 4
Elevational pattern of predicted tree species richness showing positively skewed humped. Dotted black line indicates the richness peak.

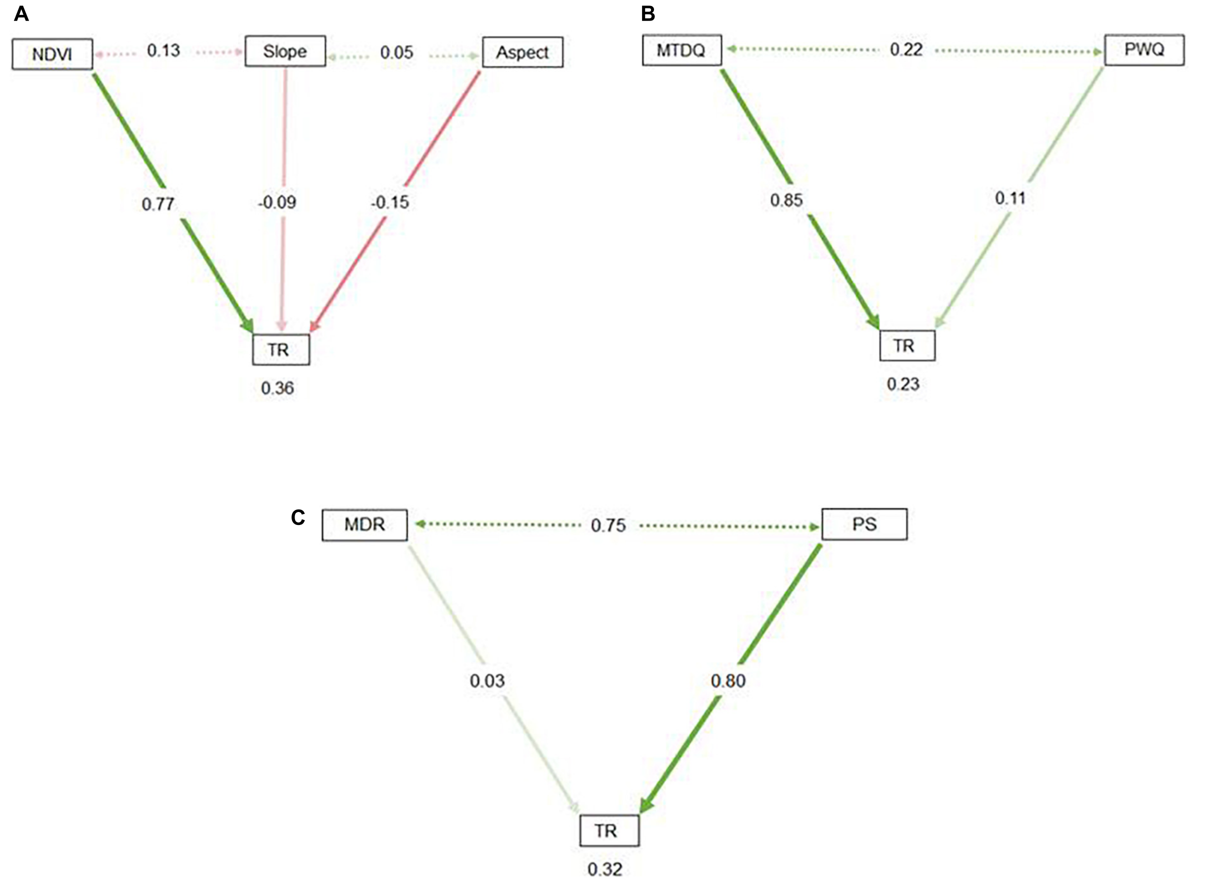

FIGURE 5
SEM output to evaluate the significance of environmental determinants: **(A)** Habitat heterogeneity, **(B)** water–energy, and **(C)** climate stability on tree richness (TR).

parabolic response and increased with an increase in PS ranging from 80 to 120 mm (**Figure 6D**); it reflected an inverse response for species richness values up to 15 species (**Figure 6D**). The predicted richness and PWQ relationship has revealed an accelerating unimodal pattern peaked at a PWQ value of 750 mm (**Figure 6E**). Overall, this research contribution reveales a combined effect of water, energy, and habitat heterogeneity and climate stability, which have a greater role in explaining tree species richness in the mountain region.

Model evaluation and validation

The relative success of all the models was evaluated in predicting tree species richness by comparing mean AUC values and kappa statistics. Among all the models, RF and ANN generated results with the maximum mean AUC and kappa values >0.90. The cross-model correlations showed a high correlation between RF and ANN models (r = 0.81; **Supplementary Table 3**); thus, we used an ensemble model of these two variables to obtain a reliable predicted richness map. It was also reflected in the investigation of maps and correlation statistics that RF and ANN generated similar results, in terms of both AUC scores and the physical locations where species occurrences were projected. The final model exhibiting a high kappa value (0.99) signifies that the model performance was excellent (**Supplementary Table 4**). The mean richness error, i.e., the difference between actual and predicted richness, is quite low (4.95), revealing a superior utility of the map (**Supplementary Table 4**).

Discussion

Pattern of species richness

Mapping spatial pattern of species richness using ground observations is important for biodiversity monitoring, and conservation, as well as developing management and adaptation strategies (Rodríguez et al., 2007). The predicted pattern of tree species richness using SSDM showed a positive skewed

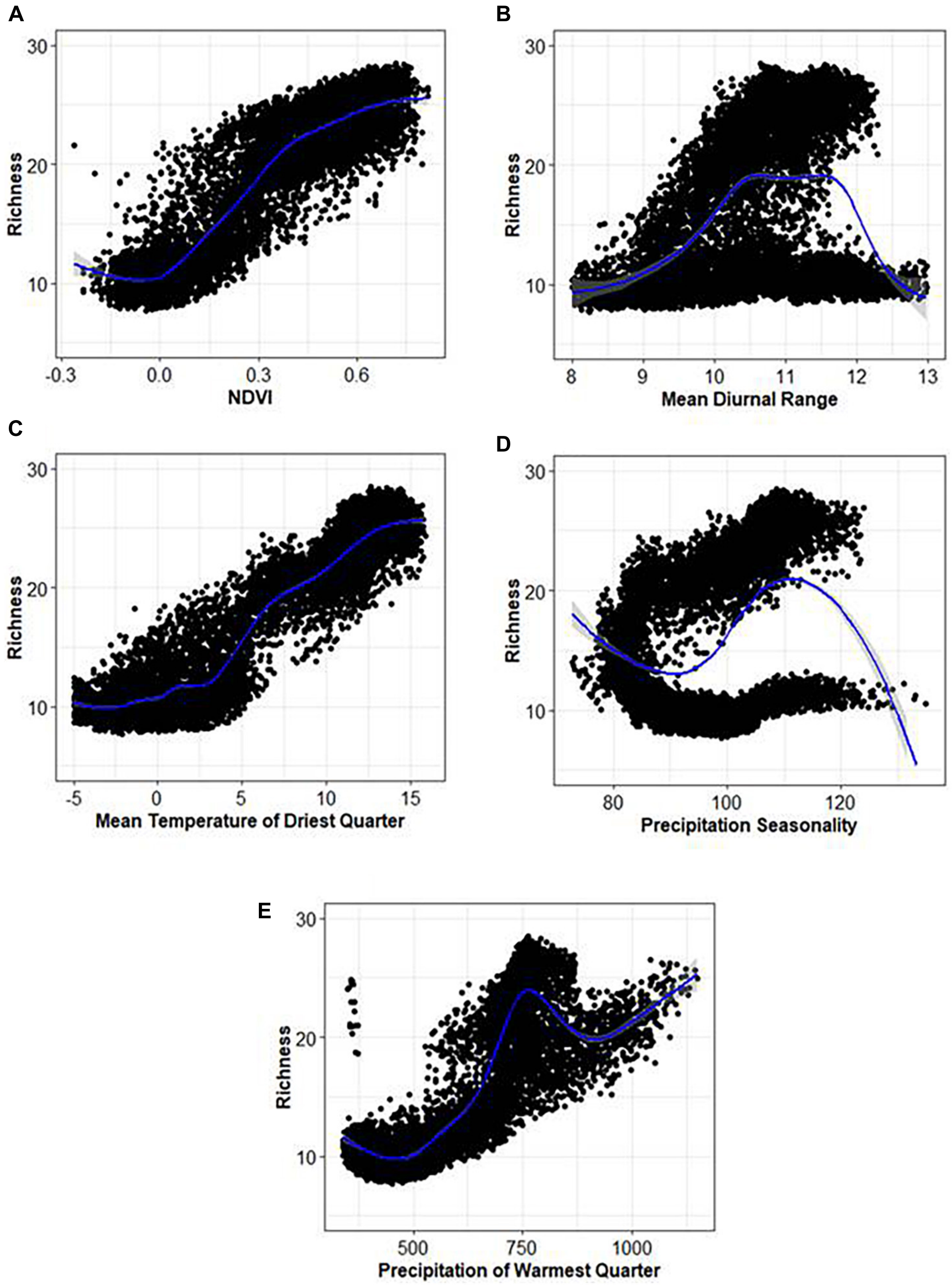

FIGURE 6

(A–E) Examples of partial dependency plot showing the relationships between the predicted tree species richness with important predictor variables.

hump-shaped pattern. The hump-shaped association predicted by SSDM between species richness and elevation is consistent with various earlier investigations (Krömer et al., 2013; Syfert et al., 2018). The results of this study reveal that tree species richness peaks at around 2,000 m containing 20–27 taxa; however, most other Himalayan studies show that a richness peaks at much lower elevations: (i) 1,000 m (Bhattarai and Vetaas, 2006), (ii) 600–1,000 m (Behera and Kushwaha, 2006), (iii) 1,500 m (Acharya et al., 2011), and (iv) 500–1,000 m (Rana et al., 2019a). In the study region, a mid-elevation zone is dominated by various tree genera such as *Quercus, Rhododendron, Pinus,* and *Alnus* with a sharp decline in species richness toward higher elevations. The uppermost limits in our sampling at around 4,000 m in the region were dominated by *Abies pindrow*, *Betula utilis*, and *Pinus wallichiana*. This indicates that subalpine trees are primarily sink populations in the region and are unable to cope with the harsh and stressful open subalpine environment. Findings from other parts of the Himalayan region have revealed that the elevation ranging between 1,500 and 2,000 m is an essential transition zone between subtropical and temperate flora (Rana et al., 2019a). If we examine the species–area relationships of the region, the lower half of the region is anticipated to have more species due to the larger area available for species (**Supplementary Figure 5**). The present results have reflected that the richness was high at 2,000 m and in consonance with the previous field-based studies from the Himalaya (Vetaas and Grytnes, 2002; Bhattarai et al., 2004). The higher peak of tree species richness in our study can thus be attributed to the habitat specificity of tree species and a low level of anthropogenic pressure. Generally, mountain regions with a wider elevational gradient exhibited a unimodal pattern of diversity, and this kind of pattern is globally well-recognized for the respective transects (Rahbek, 1995; Gaston, 2000; Arya et al., 2017; Rana et al., 2019a). Previous studies have suggested that elevational patterns of plant richness may be influenced by biotic processes, environmental heterogeneity, climate, and evolutionary history (McCain and Grytnes, 2010; Rana et al., 2019a).

In a study from Nepal, Bhattarai and Vetaas (2006) observed a decreasing trend of trees above 1500 m asl with narrow elevational ranges at the transition zone of the gradient with a wider elevational range in the middle. This is due to boundary effects, i.e., a change in environmental or climatic conditions at lower and higher elevational zones (Feng et al., 2016). In addition, optimum water (precipitation seasonality in our study) and temperature (mean diurnal range in our study) create more favorable conditions, which results in more plant species at mid-elevation (McCain, 2007). Even at high elevations, the decline in species richness may be due to the decreasing temperature, precipitation, and humidity (Sinha et al., 2018). Furthermore, we observed that a declining pattern of predicted tree species richness after 2000 m is also supported by observed tree species richness over the Himalayan region (Stevens, 1992; Kharkwal et al., 2005; Rodríguez et al., 2007; Malik, 2014; Malik and Nautiyal, 2016; Sharma et al., 2018; Sinha et al., 2018; Rana et al., 2019a; Bhat et al., 2020). This suggests that the SSDM has the potential utility to predict the observed richness pattern using field-based plant species data.

Role of habitat heterogeneity

Habitat heterogeneity is widely recognized as a key driver of high species richness in mountain environments, as it promotes diversification, reduces extinction, and provides niche space for species cohabitation (Stein et al., 2014). Environmental variables related to habitat heterogeneity (slope, aspect, and especially NDVI) are critical in explaining the overall tree species richness patterns. In a study, Pouteau et al. (2018) reported that the inclusion of remotely sensed derived NDVI provides a better prediction of plant species richness because of its multispectral nature. Interestingly, high NDVI values were observed around 2,000 m asl elevation in our study region strongly explaining a mid-elevation peak in tree species richness (**Supplementary Figure 6A**). The wider elevational gradient in our study site shows variations in NDVI values and climatic conditions which depicted a different zonation of vegetation types. Feilhauer et al. (2012) have also emphasized that a wider elevational gradient and a clear floristic and climatic gradient have a clear association between NDVI and plant species richness. Forests may have a diverse range of vegetation types with significant internal heterogeneity, which is likely to support a greater number of ecological groupings, such as species associated with clear-cuts, broadleaf or coniferous, forest floors (Ellenberg and Leuschner, 2010). We found evidence for habitat heterogeneity, implying that a greater variety of vegetation types should support a greater number of species. Slope and elevation have an important role in the species composition of the region due to a change in the incoming solar radiation (Gallardo-Cruz et al., 2009; Scherrer and Körner, 2011), which changes over short horizontal distances. The small change in the distribution of solar radiation and water moisture with a change in the slope may contribute to a difference in the micro-climate of the area. This will directly or indirectly change the plant composition and species richness (Vetaas, 2000; Gallardo-Cruz et al., 2009; Moeslund et al., 2013). In those places where rainfall does not exceed 400 mm per year, species richness is comparatively high on damp north-facing slopes compared with sun-exposed south-facing slopes (Vetaas, 1992; Sternberg and Shoshany, 2001). However, at higher elevations, energy inputs may be an important limiting factor. Our findings are consistent with these facts that changes in land-use patterns between contrasting slopes may reflect varied vegetation structures and plant diversity (Burnett et al., 1998). The land-use patterns, microclimatic conditions, and their interactions potentially regulate vegetation structure and abiotic factors (Shrestha and Vetaas, 2009). Our findings, as well as prior research on other plant groups (Shrestha and Vetaas, 2009; Shrestha et al., 2018), found support for the role of habitat heterogeneity in maintaining high richness in the mountain region.

Role of water and energy

The energy (MTDQ) and water variables (PWQ) have explained much variance to define the distribution of tree species richness in this study. The MTDQ and PWQ explained 14.28 and 12.96% of the variance, respectively, in tree species richness. Both MTDQ and PWQ values show a declining trend with a more pronounced decline after 2,000 m asl along the elevational gradient in the region (**Supplementary Figures 6B,C**). These findings suggest that richness patterns around 2,000 m asl are the best-suited environments for the growth of tree species, and they are confined under exceptionally severe conditions (such as extremely cold temperatures) at high elevations and warmer climates at low elevations (i.e., subtropical climate). Despite the availability of sufficient energy, water stress has a negative impact on species richness, and with optimal water availability, plants would use the maximal photon flux required for their physiological processes (Panda et al., 2017). This can be explained by the area's cold and dry climates, which may have resulted in a high biotic reliance on energy (Panda et al., 2017). Interaction between water and energy, either directly or indirectly (via plant productivity), provides a strong explanation for globally extensive plant diversity along the gradients (Hawkins et al., 2003). Thus, energy and water can better explain the hump-shaped pattern of tree species richness as reflected in **Figures 6C,E**. Sufficient energy and moisture stimulate photosynthesis in plants, which increases plant species richness through physiological processes (Bhattarai and Vetaas, 2003; Hawkins et al., 2003; Currie et al., 2004). Similar observations have been reported from other mountain regions of the world (O'Brien, 1998; Hawkins et al., 2003; Marini et al., 2008; Gao and Liu, 2018; Lu et al., 2018; Pandey et al., 2020a,b) and from the Himalaya (Panda et al., 2017; Vetaas et al., 2019; Pandey et al., 2020b). However, if we had also evaluated the lowest portion of the gradient, our general positive association between species richness and temperature along the elevational gradient might have assumed a different shape (Bhattarai et al., 2004). Despite the fact that the energy (MTDQ) and water variables (PWQ) may underlie such cumulative species–energy connections, knowledge of their relative contributions is limited so far, and further investigation is necessary to gain insight into these mechanisms. Thus, integrating water–energy variables is critical for future biodiversity research.

Role of climate stability

Climatic stability is an important driving force in shaping the geographical distribution of plant species in mountain regions. Our results have shown that MDR and PS (representing climate stability) influenced the tree species richness pattern in the Himalayan region. In the study region, we observed that areas with a moderate mean MDR are more favorable for the survival of tree species around 2,000 m asl (**Supplementary Figure 6D**). The high and low values of MDR are an indication of high and low moisture, respectively. Vetaas (1993) has suggested that ideal moisture conditions at mid-elevation may be associated with the existence of the cloud zone, where a significant amount of water is deposited directly onto plants from clouds and light mist consequently decreases sunlight and evapotranspiration, resulting in a higher atmospheric humidity that may promote high species richness. Contrary to this, high moisture at higher elevations and substantial diurnal temperature during growing seasons (as depicted in **Figure 6B**) could trigger physical harm to the plants and their reproductive success. This suggests that stable climates enhance species richness as has previously been reported in other mountain regions (Gao and Liu, 2018; Zhao et al., 2018).

Conclusion, limitations, and implications of the study

The current SSDM analysis demonstrates the relevance of water, energy, climate, and habitat heterogeneity in determining the mid-elevation peak in species richness, paving the way for the next step of extending the model inference regarding diversity patterns to a larger range of the Himalaya. The water–energy, climate stability, and habitat heterogeneity variables had significant effects in explaining plant species richness. This is implying that climate and land cover should be incorporated as explanatory factors in models of species richness along elevational gradients. The mapped richness is baseline data for the region and can be updated with more robust field observations. Investigation of the relationship between elevation and plant distribution ranges by putting hypotheses related to habitat heterogeneity and climate stability will improve the understanding of ecological drivers of plants in the Himalayan region. Furthermore, the SSDM approach has shown the potential utility to predict the observed richness pattern which would be useful for biodiversity management and conservation planning in the region. Due to the lack of accurate absence information in the data used for SSDMs, it is expected that some plant absence records that appear to be accurately predicted are actually incorrect, thereby increase the predictive success of performance metrics. In addition, it is obvious that additional surveys would improve the dataset.

The mapped species richness can also be used to identify biodiversity-rich areas for conservation and decision-making. Further, the areas with low species richness can be identified for restoration and management planning. The plantation of habitat-specific tree species in degraded areas would be useful for the mitigation of climate change. These maps can be utilized as a potential input for assessing the vulnerability of forests under current and contrasting future climate change scenarios. Therefore, mapping areas of biological importance along with their respective degrees of knowledge is the first step toward effective conservation planning.

Data availability statement

The original contributions presented in this study are included in the article/**Supplementary material**, further inquiries can be directed to the corresponding author.

Author contributions

ST: conceptualization, field study, data curation, validation, analysis, and writing – original draft. RD: data analysis, software, and writing and editing in first draft. VSN: writing – review and editing. IDB: writing – review and editing, and supervising.

Acknowledgments

We thank Sunil Nautiyal, Director, G.B. Pant National Institute of Himalayan Environment (NIHE), Kosi-Katarmal, Almora, for encouragement and facilities. We also thank late R. S. Rawal for the conceptualization of the study and guidance. Partial funding from the Department of Science and Technology (DST), Government of India, under NMSHE—Task Force 3 "Forest Resources and Plant Biodiversity" Phase II, and ICIMOD under KSLCDI-II is gratefully acknowledged.

Conflict of interest

The authors declare that the research was conducted in the absence of any commercial or financial relationships that could be construed as a potential conflict of interest.

Publisher's note

Supplementary material

The Supplementary Material for this article can be found online at: https://www.frontiersin.org/articles/10.3389/ffgc.2022.1022082/full#supplementary-material

References

Acharya, B. K., Chettri, B., and Vijayan, L. (2011). Distribution pattern of trees along an elevation gradient of Eastern Himalaya, India. *Acta Oecol.* 37, 329–336. doi: 10.1016/j.actao.2011.03.005

Arya, V., Kumar, B., and Rawat, J. S. (2017). Tree species diversity, community composition and distribution across six forest stands of Uttarakhand, Central Himalaya, India. *Ind. J. Ecol.* 44, 722–728.

Barbet-Massin, M., Jiguet, F., Albert, C. H., and Thuiller, W. (2012). Selecting pseudo-absences for species distribution models: how, where and how many? *Methods Ecol. Evol.* 3, 327–338. doi: 10.1111/j.2041-210X.2011.00172.x

Behera, M. D., and Kushwaha, S. P. S. (2006). "An analysis of altitudinal behavior of tree species in Subansiri district, Eastern Himalaya," in *Plant conservation and biodiversity*, eds D. L. Hawksworth, and A. T. Bull (Dordrecht: Springer), 277–291.

Bellard, C., Thuiller, W., Leroy, B., Genovesi, P., Bakkenes, M., and Courchamp, F. (2013). Will climate change promote future invasions? *Glob. Chang. Biol.* 19, 3740–3748. doi: 10.1111/gcb.12344

Benito, B. M., Cayuela, L., and Albuquerque, F. S. (2013). The impact of modelling choices in the predictive performance of richness maps derived from species-distribution models: guidelines to build better diversity models. *Methods Ecol. Evol.* 4, 327–335. doi: 10.1111/2041-210x.12022

Bhat, J. A., Kumar, M., Negi, A. K., Todaria, N. P., Malik, Z. A., Pala, N. A., et al. (2020). Altitudinal gradient of species diversity and community of woody vegetation in the Western Himalayas. *Glob. Ecol. Conserv.* 24:e01302. doi: 10.1016/j.gecco.2020.e01302

Bhattarai, K. R., and Vetaas, O. R. (2003). Variation in plant species richness of different life forms along a subtropical elevation gradient in the Himalayas, east Nepal. *Glob. Ecol. Biogeogr.* 12, 327–340. doi: 10.1046/j.1466-822X.2003.00044.x

Bhattarai, K. R., and Vetaas, O. R. (2006). Can Rapoport's rule explain tree species richness along the Himalayan elevation gradient, Nepal? *Divers. Distrib.* 12, 373–378. doi: 10.1111/j.1366-9516.2006.00244.x

Bhattarai, K. R., Vetaas, O. R., and Grytnes, J. A. (2004). Fern species richness along a central Himalayan elevational gradient, Nepal. *J. Biogeogr.* 31, 389–400. doi: 10.1046/j.0305-0270.2003.01013.x

Brown, K. A., Parks, K. E., Bethell, C. A., Johnson, S. E., and Mulligan, M. (2015). Predicting plant diversity patterns in Madagascar: understanding the effects of climate and land cover change in a biodiversity hotspot. *PLoS One* 10:e0122721. doi: 10.1371/journal.pone.0122721

Burnett, M. R., August, P. V., Brown, J. H., and Killingbeck, K. T. (1998). The influence of geomorphological heterogeneity on biodiversity I. A patch-scale perspective. *Conserv. Biol.* 12, 363–370. doi: 10.1046/j.1523-1739.1998.96238.x

Cayuela, L., Golicher, D. J., Newton, A. C., Kolb, M., de Alburquerque, F. S., Arets, E. J. M. M., et al. (2009). Species distribution modeling in the tropics: problems, potentialities, and the role of biological data for effective species conservation. *Trop. Conserv. Sci.* 2, 319–352. doi: 10.1177/194008290900200304

Colombo, A. F., and Joly, C. A. (2010). Brazilian Atlantic Forest lato sensu: the most ancient Brazilian forest, and a biodiversity hotspot, is highly threatened by climate change. *Braz. J. Biol.* 70, 697–708. doi: 10.1590/S1519-69842010000400002

Connell, J. H., and Orias, E. (1964). The ecological regulation of species diversity. *Am. Nat.* 98, 399–414. doi: 10.1086/282335

Cramer, M. D., and Verboom, G. A. (2017). Measures of biologically relevant environmental heterogeneity improve prediction of regional plant species richness. *J. Biogeogr.* 44, 579–591. doi: 10.1111/jbi.12911

Currie, D. J., Mittelbach, G. G., Cornell, H. V., Field, R., Guégan, J.-F., Hawkins, B. A., et al. (2004). Predictions and tests of climate-based hypotheses of broad-scale variation in taxonomic richness. *Ecol. Lett.* 7, 1121–1134. doi: 10.1111/j.1461-0248.2004.00671.x

D'Amen, M., Dubuis, A., Fernandes, R. F., Pottier, J., Pellissier, L., and Guisan, A. (2015). Using species richness and functional traits predictions to constrain assemblage predictions from stacked species distribution models. *J. Biogeogr.* 42, 1255–1266. doi: 10.1111/jbi.12485

Dirnböck, T., Dullinger, S., and Grabherr, G. (2003). A regional impact assessment of climate and land-use change on alpine vegetation. *J. Biogeogr.* 30, 401–417. doi: 10.1046/j.1365-2699.2003.00839.x

Ellenberg, H., and Leuschner, C. (2010). *Vegetation mitteleuropas mit den alpen: in ökologischer, dynamischer und historischer sicht*. Stuttgart: Utb.

Feilhauer, H., He, K. S., and Rocchini, D. (2012). Modeling species distribution using niche-based proxies derived from composite bioclimatic variables and MODIS NDVI. *Remote Sens.* 4, 2057–2075. doi: 10.3390/rs4072057

Feng, J., Hu, X., Wang, J., and Wang, Y. (2016). Support for the elevational Rapoport's rule among seed plants in Nepal depends on biogeographical affinities and boundary effects. *Ecol. Evol.* 6, 7246–7252. doi: 10.1002/ece3.2473

Ferrier, S., and Guisan, A. (2006). Spatial modelling of biodiversity at the community level. *J. Appl. Ecol.* 43, 393–404. doi: 10.1111/j.1365-2664.2006.01149.x

Fick, S. E., and Hijmans, R. J. (2017). WorldClim 2: new 1-km spatial resolution climate surfaces for global land areas. *Int. J. Climatol.* 37, 4302–4315. doi: 10.1002/joc.5086

Fitzpatrick, M. C., Gove, A. D., Sanders, N. J., and Dunn, R. R. (2008). Climate change, plant migration, and range collapse in a global biodiversity hotspot: the Banksia (Proteaceae) of Western Australia. *Glob. Chang. Biol.* 14, 1337–1352. doi: 10.1111/j.1365-2486.2008.01559.x

Gallardo-Cruz, J. A., Pérez-García, E. A., and Meave, J. A. (2009). β-diversity and vegetation structure as influenced by slope aspect and altitude in a seasonally dry tropical landscape. *Landsc. Ecol.* 24, 473–482. doi: 10.1007/s10980-009-9332-1

Gao, J., and Liu, Y. (2018). Climate stability is more important than water–energy variables in shaping the elevational variation in species richness. *Ecol. Evol.* 8, 6872–6879. doi: 10.1002/ece3.4202

Gaston, K. J. (2000). Global patterns in biodiversity. *Nature* 405, 220–227. doi: 10.1038/35012228

Gritti, E. S., Duputie, A., Massol, F., and Chuine, I. (2013). Estimating consensus and associated uncertainty between inherently different species distribution models. *Methods Ecol. Evol.* 4, 442–452. doi: 10.1111/2041-210X.12032

Grytnes, J. A., and McCain, C. M. (2013). "Elevational trends in biodiversity," in *Encyclopedia of biodiversity*, 2nd Edn, Vol. 3, ed. S. A. Levin (Amsterdam: Elsevier), 149–154. doi: 10.1016/B978-0-12-384719-5.00227-6

Guo, Q., Kelt, D. A., Sun, Z., Liu, H., Hu, L., Ren, H., et al. (2013). Global variation in elevational diversity patterns. *Sci. Rep.* 3:3007. doi: 10.1038/srep03007

Gutiérrez, A. G., and Huth, A. (2012). Successional stages of primary temperate rainforests of Chiloé Island, Chile. *Perspect. Plant Ecol. Evol. Syst.* 14, 243–256. doi: 10.1016/j.ppees.2012.01.004

Hawkins, B. A., Field, R., Cornell, H. V., Currie, D. J., Guégan, J.-F., Kaufman, D. M., et al. (2003). Energy, water, and broad-scale geographic patterns of species richness. *Ecology* 84, 3105–3117. doi: 10.1890/03-8006

Kharkwal, G., Mehrotra, P., Rawat, Y. S., and Pangtey, Y. P. S. (2005). Phytodiversity and growth form in relation to altitudinal gradient in the Central Himalayan (Kumaun) region of India. *Curr. Sci.* 89, 873–878.

Kluge, J., Worm, S., Lange, S., Long, D., Boehner, J., Yangzom, R., et al. (2017). Elevational seed plants richness patterns in Bhutan, Eastern Himalaya. *J. Biogeogr.* 44, 1711–1722. doi: 10.1111/jbi.12955

Körner, C. (2012). Treelines will be understood once the functional difference between a tree and a shrub is. *Ambio* 41, 197–206. doi: 10.1007/s13280-012-0313-2

Krömer, T., Acebey, A., Kluge, J., and Kessler, M. (2013). Effects of altitude and climate in determining elevational plant species richness patterns: a case study from Los Tuxtlas, Mexico. *Flora Morphol. Distrib. Funct. Ecol. Plants* 208, 197–210. doi: 10.1016/j.flora.2013.03.003

Leroy, B., Delsol, R., Hugueny, B., Meynard, C. N., Barhoumi, C., Barbet-Massin, M., et al. (2018). Without quality presence–absence data, discrimination metrics such as TSS can be misleading measures of model performance. *J. Biogeogr.* 45, 1994–2002. doi: 10.1111/jbi.13402

Lu, L., Cai, H., Yang, Y., Wang, Z., and Zeng, H. (2018). Geographic patterns and environmental determinants of gymnosperm species diversity in China. *Biodivers. Sci.* 26:1133. doi: 10.17520/biods.2018098

MacArthur, R. H., and MacArthur, J. W. (1961). On bird species diversity. *Ecology* 42, 594–598. doi: 10.2307/1932254

Malik, Z. A. (2014). *Phytosociological behaviour, anthropogenic disturbances and regeneration status along an altitudinal gradient in Kedarnath Wildlife Sanctuary (KWLS) and its adjoining areas*. PhD thesis. Uttarakhand: HNB Garhwal University Srinagar.

Malik, Z. A., and Nautiyal, M. C. (2016). Species richness and diversity along the altitudinal gradient in Tungnath, the Himalayan benchmark site of HIMADRI. *Trop. Plant Res.* 3, 396–407.

Manish, K., Pandit, M. K., Telwala, Y., Nautiyal, D. C., Koh, L. P., and Tiwari, S. (2017). Elevational plant species richness patterns and their drivers across non-endemics, endemics and growth forms in the Eastern Himalaya. *J. Plant Res.* 130, 829–844. doi: 10.1007/s10265-017-0946-0

Marini, L., Prosser, F., Klimek, S., and Marrs, R. H. (2008). Water-energy, land-cover and heterogeneity drivers of the distribution of plant species richness in a mountain region of the European Alps. *J. Biogeogr.* 35, 1826–1839. doi: 10.1111/j.1365-2699.2008.01924.x

Marmion, M., Parviainen, M., Luoto, M., Heikkinen, R. K., and Thuiller, W. (2009). Evaluation of consensus methods in predictive species distribution modelling. *Divers. Distrib.* 15, 59–69. doi: 10.1111/j.1472-4642.2008.00491.x

Mateo, R. G., Croat, T. B., Felicísimo, Á. M., and Munoz, J. (2010). Profile or group discriminative techniques? Generating reliable species distribution models using pseudo-absences and target-group absences from natural history collections. *Divers. Distrib.* 16, 84–94.

McCain, C. M. (2007). Could temperature and water availability drive elevational species richness patterns? A global case study for bats. *Glob. Ecol. Biogeogr.* 16, 1–13. doi: 10.1111/j.1466-8238.2006.00263.x

McCain, C. M., and Grytnes, J. A. (2010). "Elevational gradients in species richness," in *Encyclopedia of life sciences (ELS)*. (Chichester: John Wiley & Sons, Ltd), 1–10. doi: 10.1002/9780470015902.a0022548

Misra, R. (1968). *Ecology work book*. Calcutta: Oxford and IBH Publishing Co.

Moeslund, J. E., Arge, L., Bøcher, P. K., Dalgaard, T., and Svenning, J.-C. (2013). Topography as a driver of local terrestrial vascular plant diversity patterns. *Nord. J. Bot.* 31, 129–144. doi: 10.1111/j.1756-1051.2013.00082.x

Mouchet, M., Levers, C., Zupan, L., Kuemmerle, T., Plutzar, C., Erb, K., et al. (2015). Testing the effectiveness of environmental variables to explain european terrestrial vertebrate species richness across biogeographical scales. *PLoS One* 10:e0131924. doi: 10.1371/journal.pone.0131924

Muller Dombois, D., and Ellenberg, H. (1974). *Aims and methods of vegetation ecology*. Hoboken, NJ: John Wiley & Sons Inc.

Murray-Smith, C., Brummitt, N. A., Oliveira-Filho, A. T., Bachman, S., Moat, J., Lughadha, E. M. N., et al. (2009). Plant diversity hotspots in the Atlantic coastal forests of Brazil. *Conserv. Biol.* 23, 151–163. doi: 10.1111/j.1523-1739.2008.01075.x

Myers, N. (1988). Threatened biotas:" hot spots" in tropical forests. *Environmentalist* 8, 187–208. doi: 10.1007/BF02240252

Naimi, B. (2015). *USDM: uncertainty analysis for species distribution models. R package version 1.1–15.*

Negi, V. S., Giri, L., and Sekar, K. C. (2018a). Floristic diversity, community composition and structure in Nanda Devi National Park after prohibition of human activities, Western Himalaya, India. *Curr. Sci.* 115, 1056–1064. doi: 10.18520/cs/v115/i6/1056-1064

Negi, V. S., Joshi, B. C., Pathak, R., Rawal, R. S., and Sekar, K. C. (2018b). Assessment of fuelwood diversity and consumption patterns in cold desert part of Indian Himalaya: implication for conservation and quality of life. *J. Clean. Prod.* 196, 23–31. doi: 10.1016/j.jclepro.2018.05.237

Negi, V. S., Maletha, A., Pathak, R., and Maikhuri, R. K. (2021). Expansion of a native species and its impacts on alpine ecosystems, Indian Himalaya. *Biologia* 76, 889–899. doi: 10.1007/s11756-021-00693-1

Negi, V. S., Pathak, R., Rawal, R. S., Bhatt, I. D., and Sharma, S. (2019). Long-term ecological monitoring on forest ecosystems in Indian Himalayan region: criteria and indicator approach. *Ecol. Indic.* 102, 374–381. doi: 10.1016/j.ecolind.2019.02.035

Nieto, S., Flombaum, P., and Garbulsky, M. F. (2015). Can temporal and spatial NDVI predict regional bird-species richness? *Glob. Ecol. Conserv.* 3, 729–735. doi: 10.1016/j.gecco.2015.03.005

O'Brien, E. (1998). Water-energy dynamics, climate, and prediction of woody plant species richness: an interim general model. *J. Biogeogr.* 25, 379–398. doi: 10.1046/j.1365-2699.1998.252166.x

Oli, K. P., and Zomer, R. (2011). *Kailash sacred landscape conservation initiative: feasibility assessment report*. Lalitpur: International Centre for Integrated Mountain Development (ICIMOD). doi: 10.53055/ICIMOD.545

Oliveira, U., Soares-Filho, B. S., Santos, A. J., Paglia, A. P., Brescovit, A. D., de Carvalho, C. J. B., et al. (2019). Modelling highly biodiverse areas in Brazil. *Sci. Rep.* 9:6355. doi: 10.1038/s41598-019-42881-9

Oommen, M. A., and Shanker, K. (2005). Elevational species richness patterns emerge from multiple local mechanisms in Himalayan woody plants. *Ecology* 86, 3039–3047. doi: 10.1890/04-1837

Pan, X., Ding, Z., Hu, Y., Liang, J., Wu, Y., Si, X., et al. (2016). Elevational pattern of bird species richness and its causes along a central Himalaya gradient, China. *PeerJ* 4:e2636. doi: 10.7717/peerj.2636

Panda, R. M., Behera, M. D., Roy, P. S., and Biradar, C. (2017). Energy determines broad pattern of plant distribution in Western Himalaya. *Ecol. Evol.* 7, 10850–10860. doi: 10.1002/ece3.3569

Pandey, B., Khatiwada, J. R., Zhang, L., Pan, K., Dakhil, M. A., Xiong, Q., et al. (2020a). Energy–water and seasonal variations in climate underlie the spatial distribution patterns of gymnosperm species richness in China. *Ecol. Evol.* 10, 9474–9485. doi: 10.1002/ece3.6639

Pandey, B., Nepal, N., Tripathi, S., Pan, K., Dakhil, M. A., Timilsina, A., et al. (2020b). Distribution pattern of gymnosperms' richness in nepal: effect of environmental constrains along elevational gradients. *Plants* 9:625. doi: 10.3390/plants9050625

Pineda, E., and Lobo, J. M. (2009). Assessing the accuracy of species distribution models to predict amphibian species richness patterns. *J. Anim. Ecol.* 78, 182–190. doi: 10.1111/j.1365-2656.2008.01471.x

Pouteau, R., Gillespie, T. W., and Birnbaum, P. (2018). Predicting tropical tree species richness from Normalized Difference Vegetation Index time series: the devil is perhaps not in the detail. *Remote Sens.* 10:698. doi: 10.3390/rs10050698

Rahbek, C. (1995). The elevational gradient of species richness: a uniform pattern? *Ecography* 18, 200–205. doi: 10.1111/j.1600-0587.1995.tb00341.x

Rana, S. K., and Rawat, G. S. (2017). Database of himalayan plants based on published floras during a century. *Data* 2:36. doi: 10.3390/data2040036

Rana, S. K., Gross, K., and Price, T. D. (2019a). Drivers of elevational richness peaks, evaluated for trees in the east Himalaya. *Ecology* 100:e02548. doi: 10.1002/ecy.2548

Rana, S. K., Price, T. D., and Qian, H. (2019b). Plant species richness across the Himalaya driven by evolutionary history and current climate. *Ecosphere* 10:e02945. doi: 10.1002/ecs2.2945

Rana, S. K., White, A. E., and Price, T. D. (2022). Key roles for the freezing line and disturbance in driving the low plant species richness of temperate regions. *Glob. Ecol. Biogeogr.* 31, 280–293. doi: 10.1111/geb.13427

Rawal, R. S., Rawal, R., Rawat, B., Negi, V. S., and Pathak, R. (2018). Plant species diversity and rarity patterns along altitude range covering treeline ecotone in Uttarakhand: conservation implications. *Trop. Ecol.* 59, 225–239.

Rodríguez, J. P., Brotons, L., Bustamante, J., and Seoane, J. (2007). The application of predictive modelling of species distribution to biodiversity conservation. *Divers. Distrib.* 13, 243–251. doi: 10.1111/j.1472-4642.2007.00356.x

Rosseel, Y. (2012). lavaan: an R package for structural equation modeling. *J. Stat. Softw.* 48, 1–36. doi: 10.18637/jss.v048.i02

Saxena, A. K., Pandey, T., and Singh, J. S. (1985). "Altitudinal variation in the vegetation of Kumaon Himalayas," in *Perspectives in environ-mental botany*, eds D. N. Rao, K. J. Ahmed, M. Yunus, and S. N. Singh (Lucknow: Print House), 43–66.

Scherrer, D., and Körner, C. (2011). Topographically controlled thermal-habitat differentiation buffers alpine plant diversity against climate warming. *J. Biogeogr.* 38, 406–416. doi: 10.1111/j.1365-2699.2010.02407.x

Schmidt-Lebuhn, A. N., Knerr, N. J., and González-Orozco, C. E. (2012). Distorted perception of the spatial distribution of plant diversity through uneven collecting efforts: the example of Asteraceae in Australia. *J. Biogeogr.* 39, 2072–2080. doi: 10.1111/j.1365-2699.2012.02756.x

Schmitt, S., Pouteau, R., Justeau, D., de Boissieu, F., and Birnbaum, P. (2017). ssdm: an r package to predict distribution of species richness and composition based on stacked species distribution models. *Methods Ecol. Evol.* 8, 1795–1803. doi: 10.1111/2041-210X.12841

Sharma, C. M., Mishra, A. K., Tiwari, O. P., Krishan, R., and Rana, Y. S. (2018). Regeneration patterns of tree species along an Elevational gradient in the Garhwal Himalaya. *Mt. Res. Dev.* 38, 211–219. doi: 10.1659/MRD-JOURNAL-D-15-00076.1

Shrestha, K. B., and Vetaas, O. R. (2009). The forest ecotone effect on species richness in an arid Trans-Himalayan landscape of Nepal. *Folia Geobot.* 44, 247–262. doi: 10.1007/s12224-009-9046-9

Shrestha, N., Su, X., Xu, X., and Wang, Z. (2018). The drivers of high Rhododendron diversity in south-west China: does seasonality matter? *J. Biogeogr.* 45, 438–447. doi: 10.1111/jbi.13136

Sinha, S., Badola, H. K., Chhetri, B., Gaira, K. S., Lepcha, J., and Dhyani, P. P. (2018). Effect of altitude and climate in shaping the forest compositions of Singalila National Park in Khangchendzonga Landscape, Eastern Himalaya, India. *J. Asia Pac. Biodivers.* 11, 267–275. doi: 10.1016/j.japb.2018.01.012

Stein, A., Gerstner, K., and Kreft, H. (2014). Environmental heterogeneity as a universal driver of species richness across taxa, biomes and spatial scales. *Ecol. Lett.* 17, 866–880. doi: 10.1111/ele.12277

Sternberg, M., and Shoshany, M. (2001). Influence of slope aspect on Mediterranean woody formations: comparison of a semiarid and an arid site in Israel. *Ecol. Res.* 16, 335–345. doi: 10.1046/j.1440-1703.2001.00393.x

Stevens, G. C. (1992). The elevational gradient in altitudinal range: an extension of Rapoport's latitudinal rule to altitude. *Am. Nat.* 140, 893–911. doi: 10.1086/285447

Syfert, M. M., Brummitt, N. A., Coomes, D. A., Bystriakova, N., and Smith, M. J. (2018). Inferring diversity patterns along an elevation gradient from stacked SDMs: a case study on Mesoamerican ferns. *Glob. Ecol. Conserv.* 16:e00433. doi: 10.1016/j.gecco.2018.e00433

Testolin, R., Attorre, F., Borchardt, P., Brand, R. F., Bruelheide, H., Chytrý, M., et al. (2021). Global patterns and drivers of alpine plant species richness. *Glob. Ecol. Biogeogr.* 30, 1218–1231. doi: 10.1111/geb.13297

Thakur, S., Negi, V. S., Dhyani, R., Bhatt, I. D., and Yadava, A. K. (2021). Influence of environmental factors on tree species diversity and composition in the Indian western Himalaya. *For. Ecol. Manage.* 503:119746. doi: 10.1016/j.foreco.2021.119746

Thakur, S., Negi, V. S., Pathak, R., Dhyani, R., Durgapal, K., and Rawal, R. S. (2020). Indicator based integrated vulnerability assessment of community forests in Indian west Himalaya. *For. Ecol. Manage.* 457:117674. doi: 10.1016/j.foreco.2019.117674

Turner, J. R. G., Gatehouse, C. M., and Corey, C. A. (1987). Does solar energy control organic diversity? Butterflies, moths and the British climate. *Oikos* 48, 195–205. doi: 10.2307/3565855

Vetaas, O. R. (1992). Micro-site effects of trees and shrubs in dry Savannas. *J. Veg. Sci.* 3, 337–344. doi: 10.2307/3235758

Vetaas, O. R. (1993). Spatial and temporal vegetation changes along a moisture gradient in Northeastern Sudan. *Biotropica* 25, 164–175. doi: 10.2307/2389180

Vetaas, O. R. (2000). Comparing species temperature response curves: population density versus second-hand data. *J. Veg. Sci.* 11, 659–666.

Vetaas, O. R., and Grytnes, J.-A. (2002). Distribution of vascular plant species richness and endemic richness along the Himalayan elevation gradient in Nepal. *Glob. Ecol. Biogeogr.* 11, 291–301. doi: 10.1046/j.1466-822X.2002.00297.x

Vetaas, O. R., Paudel, K. P., and Christensen, M. (2019). Principal factors controlling biodiversity along an elevation gradient: water, energy and their interaction. *J. Biogeogr.* 46, 1652–1663. doi: 10.1111/jbi.13564

Williams, J. N., Seo, C., Thorne, J., Nelson, J. K., Erwin, S., O'Brien, J. M., et al. (2009). Using species distribution models to predict new occurrences for rare plants. *Divers. Distrib.* 15, 565–576. doi: 10.1111/j.1472-4642.2009.00567.x

Zhao, Y., Cao, H., Xu, W., Chen, G., Lian, J., Du, Y., et al. (2018). Contributions of precipitation and temperature to the large-scale geographic distribution of fleshy-fruited plant species: growth form matters. *Sci. Rep.* 8:17017. doi: 10.1038/s41598-018-35436-x

Frontiers in Forests and Global Change

TYPE Original Research
PUBLISHED 16 November 2022
DOI 10.3389/ffgc.2022.1019139

Floristic composition, biological spectrum, and phytogeographic distribution of the Bin Dara Dir, in the western boundary of Pakistan

Fazal Manan[1], Shujaul Mulk Khan[1]*, Zahir Muhammad[2], Zeeshan Ahmad[1], Abdullah Abdullah[1], Amjad ur Rahman[1], Heesup Han[3]*, Antonio Ariza-Montes[4], Nicolás Contreras-Barraza[5] and António Raposo[6]

[1]Department of Plant Sciences, Quaid-i-Azam University Islamabad, Islamabad, Pakistan, [2]Department of Botany, University of Peshawar, Peshawar, Pakistan, [3]College of Hospitality and Tourism Management, Sejong University, Seoul, South Korea, [4]Social Matters Research Group, Universidad Loyola Andalucía, Córdoba, Spain, [5]Facultad de Economía y Negocios, Universidad Andres Bello, Santiago, Chile, [6]CBIOS (Research Center for Biosciences and Health Technologies), Universidade Lusófona de Humanidades e Tecnologias, Lisboa, Portugal

OPEN ACCESS

EDITED BY
Jahangeer A. Bhat,
Fiji National University, Fiji

REVIEWED BY
Zahid Ullah,
China University of Geosciences Wuhan, China
Ishfaq Ahmad Wani,
Central University of Jammu, India
Tajamul Islam,
University of Kashmir, India
Rupesh Dhyani,
Govind Ballabh Pant National Institute of Himalayan Environment and Sustainable Development, India

*CORRESPONDENCE
Shujaul Mulk Khan
shuja60@gmail.com
Heesup Han
heesup.han@gmail.com

SPECIALTY SECTION
This article was submitted to Forest Management, a section of the journal Frontiers in Forests and Global Change

RECEIVED 14 August 2022
ACCEPTED 17 October 2022
PUBLISHED 16 November 2022

CITATION
Manan F, Khan SM, Muhammad Z, Ahmad Z, Abdullah A, Rahman Au, Han H, Ariza-Montes A, Contreras-Barraza N and Raposo A (2022) Floristic composition, biological spectrum, and phytogeographic distribution of the Bin Dara Dir, in the western boundary of Pakistan. *Front. For. Glob. Change* 5:1019139. doi: 10.3389/ffgc.2022.1019139

This study assessed the floristic composition, biological spectrum, and phytogeographical elements of the Bin Dara western boundary of Pakistan. The flora consisted of 140 plant species belonging to 47 families. The most dominant family was Poaceae (with 14 species), followed by Asteraceae (11 species). The biological spectrum showed the therophytes (71 species, 50.71%) as the dominant life form class, followed by mega -phanerophytes (27 species, 19.28%), nano-phanerophytes (15 species, 10.71%), geophytes (10 species, 7.14%), chamaephytes (9 species, 6.42%), and hemi-cryptophytes (8 species, 5.71%). Leaf size classes comprised of nanophylls (48 species, 34.28%), microphylls (32 species, 22.85%), mesophylls (22 species, 15.71%), macrophylls (17 species, 12.14%), leptophylls (12 species, 8.57), megaphylls (8 species, 5.75%), and aphyllous (1 species, 0.71%). Cosmopolitan was the most prominent form of phytogeographic elements (with 17 species, 12.14%), followed by pantropical and Euro-Siberian Mediterranean Irano-Turanian (14 species, 10%) each. The pluriregional represented (13 species, 9.28%), Holarctic and Mediterranean Irano-Turanian (10 species, 7.14%), Irano-Turanian and Western Himalayan (9 species, 6.42%) each. It is recommended that further study is needed to map the vegetation, its indicators, and rare species that face a huge threat of endangerment.

KEYWORDS

life form, leaf size, floristic elements, western Himalayan, plants distribution

Introduction

The floristic composition of any area gives us essential information about different plant species diversity and their distribution (Ali et al., 2018; Bano et al., 2018; Gul et al., 2018). It leads to the proper identification of plant species and thereby conservation in a scientific and systematic way. The distribution of plant species is a valuable source of information for environmental factors and ecosystem services in a particular habitat (Angyalossy et al., 2022; Flores-Argüelles et al., 2022; Magray et al., 2022; Shannon et al., 2022; Wani et al., 2022b; Watts et al., 2022). Floristic diversity is used to interpret plant species of any geographical area, whether cultivated or wild in their nature (Farooq et al., 2019; Khan and Badshah, 2019; Ca et al., 2020; Wani and Pant, 2021; Wani et al., 2022a). The presence of all plant species found in a particular area is termed flora while vegetation is related to the relative importance of plant species, their life and leaf form, population, and distribution in relation to space and time. Floristic inventory can help us to understand the features of vegetation characteristics (Mehmood et al., 2015, 2017; Rahman et al., 2016; Li et al., 2021; Zhao et al., 2021) and it is important for human existence, economic health, ecosystem function, and stability (Khan et al., 2016; Wani et al., 2021; Su et al., 2022; Wani and Pant, 2022).

The biological spectrum of an area also gives the climate picture of that region. It tells about weather patterns, especially the rainfall and temperature phenomena, and their distribution over the year. Climatic conditions over a longer period give rise to phytogeographic consistency among the floristic elements. According to Takhtajan (1969a) and Ali and Qaiser (1986), there are three phytogeographical regions in Pakistan i.e., Irano-Turanian, Saharo-Sindian, and the Indian regions (Khan et al., 2020). But Kitamura (1960) and Hara (1966) also recognized the Sino-Japanese region. Thus, four phytogeographical regions are recognized in Pakistan. Each region is delimited based on certain criteria, apart from others, by Zohary (1950), and characterized by the presence of a component of the flora or phytogeographical elements.

In the Irano-Turanian Region, there are both diurnal and annual plant species characterized by extreme temperature and low precipitation. There is a considerable difference of opinion so far as the subdivision of the region is concerned. Two sub-regions, i.e. Western and Eastern Irano-Turanian sub-regions were recognized because of the climatic and physiognomic factors (Zohary, 1950). The Eastern Irano-Turanian sub-region occurs at 35°-36° north latitude and the Western Irano-Turanian sub-region is at 29°-30° north latitude. The western Himalayas are situated in the Western Irano-Turanian subregion, which has many endemic plant species. The western boundaries of the Sino-Japanese region in the Himalayas touch western Nepal (Takhtajan, 1969b) and according to the findings of Zohary (1950), Kitamura (1960), and Hara (1966) it further spreads through Pakistan into Afghanistan to their western limit. This is supported by the interruption of the maximum rainfall (180 cm) areas (Haq et al., 2020). Before glaciation, the present Sino-Japanese flora had changed relatively little from the vegetation of the north-temperate regions that surrounded the whole northern hemisphere (Axelrod and Raven, 1978). While the name "Saharo-Sindian" was given by Eig (1931), the area spreads from the Atlantic coast of north Africa through the Sinai Peninsula, the entire Sahara, most of Arabia, more than half of Palestine, part of Syria, south Iran, south Iraq, southern Baluchistan, Sindh, most parts of Punjab in Pakistan and the Rajasthan desert in India (Eig, 1931).

The Indian region comprises the flanks of the Himalayas, the Gangetic plain, the Indian peninsula proper, and Sri Lanka. The territory of this region is not continuous in Pakistan. It lies between 27° and 28° north latitude in the southeastern part and between 29° and 32° north latitude in the eastern Punjab province. Distribution of phytogeographic elements helps in tracing plant migration, origination, evaluation, plant speciation, distribution range, conservation plans, perception of ecological nature, diversification, and plant wealth.

However, very little attention has been given to the assessment of phytogeographic elemental distribution patterns in these areas. Therefore, the present study was conducted to find out the floristic composition, biological spectrum, and phytogeographic distribution of the Bin Dara, in the western boundary of Pakistan. The results might be helpful to ecologists, plant geographers, conservationists, and ethnobotanists in understanding the vegetation structure, conservation status, and characteristics in the region. The procedure adopted in the current study can be followed for the assessment of phytogeographic elements of any ecosystem of the world.

Materials and methods

Study area

The Bin Dara lies at $35^\circ 5' 23.82''$ to $35^\circ 6' 1.41''$ N latitude and $71^\circ 40' 48.28''$ to $71^\circ 41' 52.66''$ E longitude with an elevation range of 1,553–2,764 m in the western Himalaya floristic region in Pakistan (Figure 1). It has rigid topography, dominated by hills with hard rocks. Its temperature remains moderate and warm in the summer season. June and July are the hot months of the year (Manan et al., 2020). The area's mean annual minimum and maximum temperatures are 10 and 27°C, respectively.

The current study was conducted through the detailed methodology as follows.

Field survey

Regular field surveys were conducted throughout Bin Dara, Dir, using standard ecological techniques (Ahmad et al., 2016;

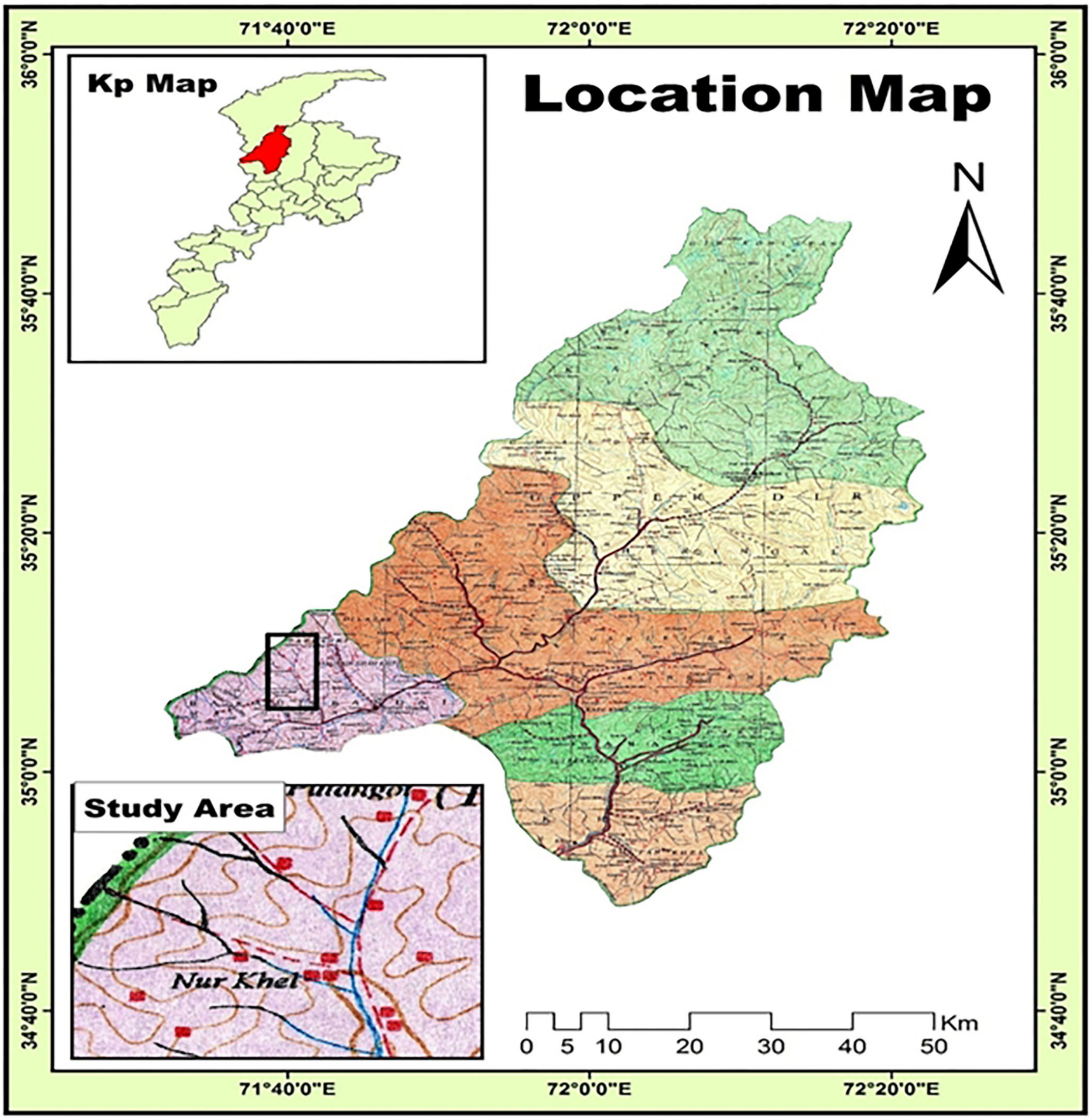

FIGURE 1
Map showing Bin Dara, western boundary of Pakistan.

Amri et al., 2019; Mumshad et al., 2021; Ur Rahman et al., 2021; Ali et al., 2022). We followed the standard taxonomic procedures for collecting, drying, and further processing the herbarium specimens (Bridson and Forman, 1998). Plant specimens were collected, labeled, placed in blotting papers, pressed with a plant presser, and poisoned using mercuric chloride plus ethyl alcohol solution. Specimens were then fixed on the standard herbarium sheets, having a size of $17.5'' \times 11.5''$. All the plant species were identified with the help of "Flora of Pakistan" and other available literature (Nasir and Ali, 1972). Complete floristic lists of species along with ecological descriptions were prepared for further analyses.

Life form classification

All recorded plant species were classified into different life form classes using the Raunkiaer (1934) method. Its detailed descriptions are as follows:

Phanerophytes (Ph)

Plants with perennating buds emerging at least 25 cm above the ground surface are called Phanerophytes. Based on height, Phanerophytes are further divided into the following subclasses.

Megaphanerophytes: (Mg). > 30 m.
Mesophanerophytes: (Ms). 7.6–30 m.
Microphanerophytes: (Mp). 2–7.5 m.
Nanophanerophytes: (N). 0.25–2 m.

Chamaephytes (Ch)

These are perennial plants in which their shoots or buds lie up to 25 cm on an upright stem from the ground. Chamaephytes are also called surface plants. They are characteristically found in cool and dry climates.

Hemicryptophytes (He)

These are plants whose perennial buds lie near the ground where they are covered by soil and litter. Such plants are found in cold and moist climates. They include a multitude of grasses and forbs.

Geophytes/cryptophytes (G/Cr)

The plant's perennial buds lie beneath the ground level or underwater (hydrophytes). The underground reproductive parts (rhizome, corn, bulb, and tuber) are drying and freezing.

Therophytes (Th)

These plants survive unfavorable conditions in the form of seeds. They are annual herbs and usually grow in the rainy season only from seeds. Therophytes are typically found in desert grasslands.

Climbers and Liana

These plants use rocks, manmade structures, and other plants for their support and growth. Liana is a woody climber that is generally rooted in soil, but its leaves are often in full sun. They are often many meters from the ground.

$$\text{Raunkiar Biological Spectrum} = \frac{\text{No. of individual of a species of a particular life form class}}{\text{Total No. of all species in a single strand}} \times 100$$

Leaf size spectra

The leaf size spectrum gives the idea of the adaptations and physiology of plant leaves. Plants are classified into different leaf size spectra using Raunkiaer (1934) method. Detailed leaf size classes descriptions are as follows:

Leptophyll (L): 25 sq. mm
Nanophyll (N): 9 × 25 sq. mm
Microphyll (Mic): $9^2 \times 25$ sq. mm
Mesophyll (Mes): $9^3 \times 25$ sq. mm
Macrophyll (Mac): $9^4 \times 25$ sq. mm
Megaphyll (Ma): Larger than class Macrophyll.

$$\text{Raunkiar leaf size spectrum} = \textit{nonumber} \\ \frac{\text{No. of individual of a species of a particular leaf size class}}{\text{Total No. of all species for that strand}} \times 100$$

Floristic elements classification

Vegetation of the study area is described and classified into various floristic elements based on Brummitt et al. (2001) as defined in Table 1.

Results

Plant species composition

A total of 140 plant species were recorded belonging to 50 families. Out of which 46 families were Dicotyledons, two families Monocotyledons, and one family of Gymnosperm and Pteridophyte each. The most dominant family was Poaceae (with 14 species) followed by Asteraceae (11 species) and Lamiaceae (10 species). Regarding the habitat of the plant species, 101 were herbs, 12 were shrubs and 27 were trees (Figure 2).

Raunkiaer life form classification

Based on the Raunkiaer life form system of classification, Therophytes were the dominant plant species along with 71 members (50.71% of the total vegetation), followed by Megaphanerophytes (27 species, 19.28%), Nanophanerophytes (15 species, 10.71%), Geophytes (10 species, 7.14%), Chamaephytes (9 species, 6.42%) and Hemicryptophytes (8 species and 5.71%) (Table 2).

Raunkiaer life size classification

The leaf size of the region was dominated by Nanophylls containing a total of 48 species (34.28%), followed by Microphyllous with 32 species (22.85%), Mesophylls with 22 species (15.71%), Macrophylls with 17 species (12.14%), and Leptophylls with 12 species (8.57%). Furthermore, Megaphylls

TABLE 1 A description of the floristic elements in Bin Dara, Pakistan.

Floristic elements	Description
Central Asian	Central Asian elements are distributed in temperate central Asia, western Asia, Caucasus, Siberia and Tien-Shan; the distribution centers are mainly in temperate Asia
Cosmopolitan	These species are distributed on almost all continents (Having worldwide distribution)
Eurasian	These species are widely distributed through the temperate zone of Europe and Asia. Some of the species may range into the northernmost part of Africa
Holarctic	These species are primarily distributed in the cold temperate regions of Europe, Asia and North America
Irano-Turanian	These elements have a center of diversity in western Asia: Anatolia, Mesopotamia, Irano-Armenia and extend up to Tien-Shan
Neotropical	These elements occur in and nearby the tropical and subtropical regions of the world; some taxa may extend to temperate regions
Mediterranean	These elements are distributed across the Mediterranean region in southern Europe, North Africa and western Asia
Palaeotropical	Taxa are distributed in the tropics of Asia, Australia and Africa, also called the old World's tropics
Circumboreal	Many of these species extend their ranges southward in the mountains, Arizona, Mexico and some species may also found in Arctic flora
Pantropical	Taxa are distributed in the tropical and subtropical regions of the world, some may extend to temperate region
Western Himalayan	Species with a center of diversity in northwest Himalayas, however, occasionally may extend eastward to eastern Himalayas or northwards to central Asia and Afghanistan

with 8 species (5.75%), and Aphyllous with 1 species (0.71%) were the least concentrated in the area (Table 3, Figure 3).

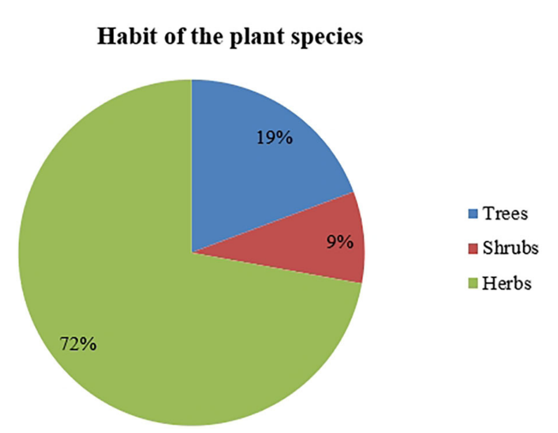

FIGURE 2
Percentage-wise representation of the plant's habitat in Bin Dara, the western boundary of Pakistan.

TABLE 2 Life form spectra of the Bin Dara vegetation.

Life form	No. of species	Percentage (%)
Megaphanerophytes	27	19.28
Nannophanerophytes	15	10.71
Chamaephytes	09	6.42
Hemicrytophyte	08	5.71
Geophytes	10	7.14
Therophytes	71	50.71

TABLE 3 Life form spectra of the Bin Dara, Dir, vegetation.

Life size	No. of species	Percentage (%)
Megaphylls	8	5.71
Macrophylls	17	12.14
Mesophylls	22	15.71
Microphylls	32	22.85
Nanophylls	48	34.28
Leptophylls	12	8.57
Aphyllous	1	0.71

Phytogeographic/floristic elements

The vegetation of the present study recognized 27 different floristic elements. Cosmopolitan (12.14%) was the highest percentage of elements, followed by Pantropical and Euro Siberian-Mediterranean-Irano-Turanian (ES-M-IT) with 10% each. The Pluriregional (PL) represents 9.28%, holarctic and Mediterranean- Irano-Turanian (7.14%), IT and WH 6.42% each (Figure 4). The other elements were less represented in the study area. Six species (4.28%) were endemic or nearly endemic to the western Himalayan region. These endemic species were *Parrotiopsis jacquemontiana, Cedrus deodra, Pinus wallichiana, Quercus baloot, Viburnum cotinifolium,* and *Bistorta amplexicaulis* (Table 4).

Discussion

Ecological sampling and analyses are of prime importance for the vegetation of any geographic zone. Its precise interpretation can help in successfully achieving this aim. Many such sampling-based studies frequently interpret the vegetation

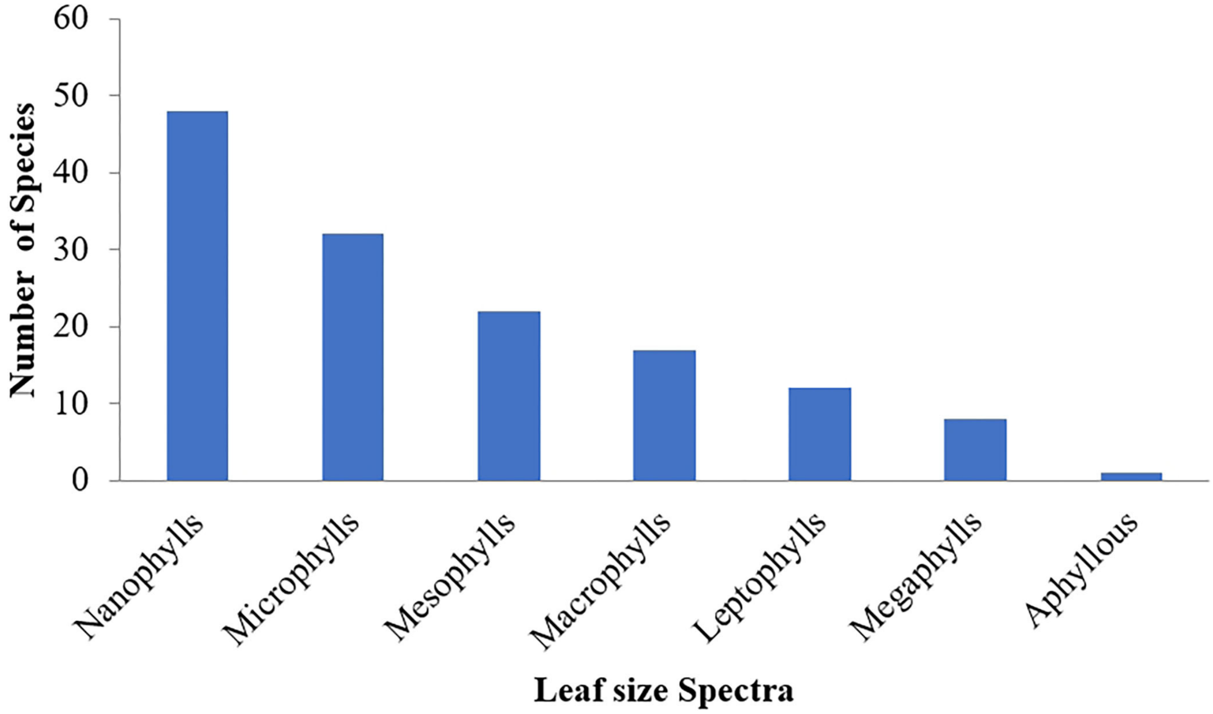

FIGURE 3
Leaf size spectrum in Bin Dara, western boundary of Pakistan.

at habitats, ecosystems, and regional and global levels (Khan et al., 2011; Longo et al., 2019; Abbas et al., 2021; Ahmad et al., 2022b; Anwar et al., 2022; Haq et al., 2022; Munyasya et al., 2022; Rasheed et al., 2022; Yang et al., 2022). Such studies interpret the intricate vegetation structure more meaningfully in relation to the abiotic environment (Khan et al., 2017; Miao et al., 2018; Ahmad et al., 2021, 2022a; Iqbal et al., 2021; Ali et al., 2022a,b; Hussain et al., 2022; Khan S. A. et al., 2022). The present study revealed that the dried condition of the Bin Dara, Dir, is reflected in its vegetation in the form of stunted growth, small leaf size, sparse distribution, dwarf height, and isolated individuals of plant species that in turn are characteristics of the xerophytic flora. Our findings are also supported by some of the studies from adjacent areas (Abbas et al., 2019; Ahmad et al., 2019; Ahmed et al., 2019; Anwar et al., 2019; Hussain et al., 2019; Kamran et al., 2020; Khan, 2022). Furthermore, biological spectra are used to assess the life form and leaf sizes for better interpretations of the climatic conditions of an ecosystem. These physiognomic characteristics are considered indicators of biotic interaction, and climatic and habitat deterioration. A similar biological spectrum of different areas shows similar climatic conditions. According to Raunkiaer (1934), the climate and habitat of an area are characterized by the life form and biological spectrum of an area, though, the proportion of life forms can be altered due to biological disturbances.

The overall vegetation of the study region is dominated by therophytes with 71 species (50.71%) followed by megaphanerophytes with 27 species (19.28%). The dominance of therophytes shows that the study area is under huge anthropogenic and biotic pressure like grazing pressure and human disturbance (Ullah and Badshah, 2017; Manan et al., 2020; Bedair et al., 2021). Hence, as a result, hemicryptophytes cannot survive in such type of environment. Our results are similar to the finding of Al-Yemeni and Sher (Al-Yemeni and Sher, 2010), who reported that therophytes are a dominant life form spectra due to different environmental gradients in the Asir Mountain, Saudi Arabia. In addition, similar studies being carried out in the adjacent area like Sher and Khan (2007), Khan et al. (2013), Sharma et al. (2014), and Hussain et al. (2015) reported that therophytes, along with hemicryptophytes and megaphanerophytes, are the dominant vegetation in their respective regions.

The leaf size spectrum identified nanophyll and microphyll as the dominant leaf size spectra in the current project area. Similarly, Nasir and Sultan (2002) reported Nanophylls as the dominant life form from the Botanical Garden at Azakhel, District Nowshera, Pakistan. Whereas Hussain et al. (2014) studied the flora of Sarsawa Hills, District Kotli in Azad Kashmir. They stated that Leptophylls, Nanophylls, and Microphylls were the dominant classes. Microphylls are characteristic of steppes,

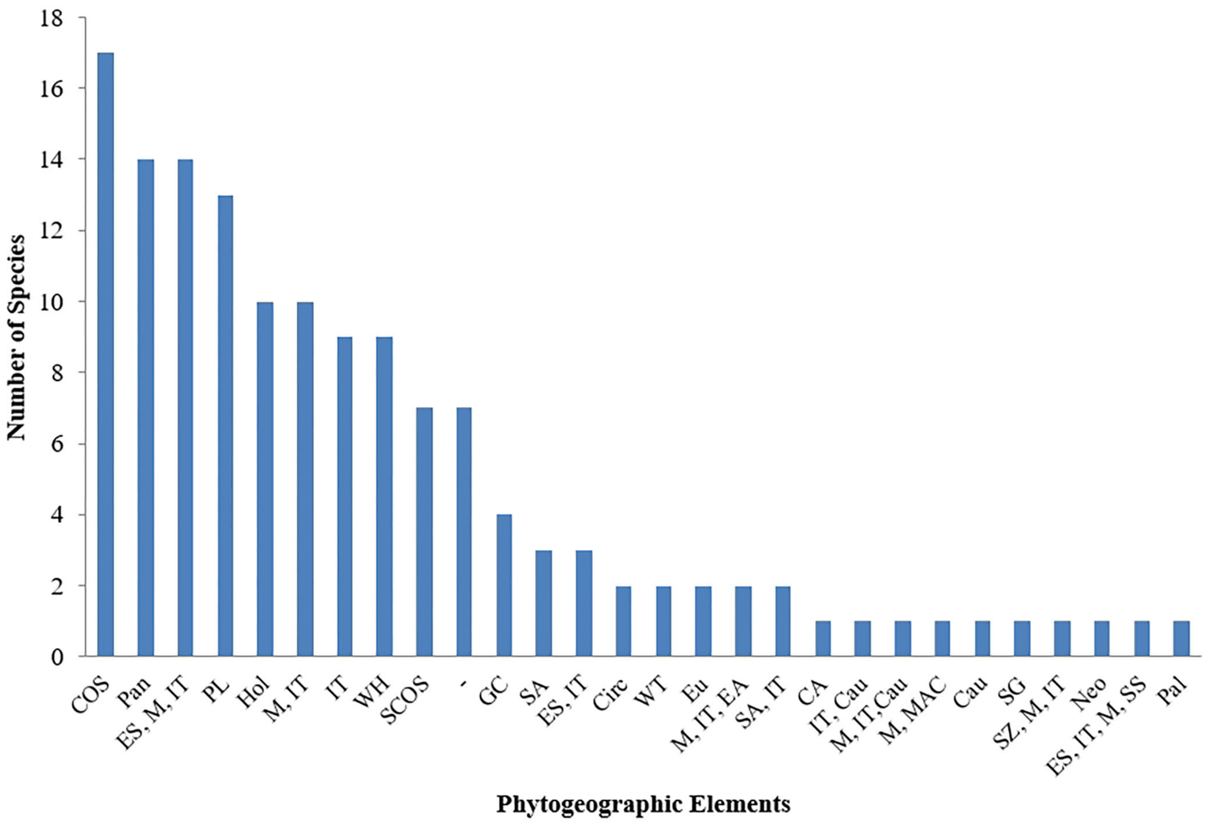

FIGURE 4
Floristic elements in Bin Dara, western boundary of Pakistan.

while Nanophylls are characteristic of hot deserts (Tareen and Qadir, 1993; Badshah et al., 2013). Large leaf species occur in warm moist climates while smaller leaves are characteristic of dry and cold climates and degraded habitats.

In the present study, the dominance of cosmopolitan elements can be attributed to dispersal mechanisms and geological activities in the past. These species are distributed on almost all continents (having worldwide distribution). The flora of the western Himalayan province is transitional between the eastern Asiatic and ancient Mediterranean (Takhtajan, 1986; Khan et al., 2020; Zeb et al., 2021; Khan S. M. et al., 2022). Bin Dara, being part of the western Himalayas, receives the monsoon rains during summer and heavy snowfall in winter; the plants renew growth at the approach of spring in the months of March–April (Manan et al., 2020). Ullah et al. (2015) also reported the dominance of Cosmopolitan, Pantropical, Euro-Siberian, Mediterranean, Irano-Turanian, and Pluriregion elements in Myankaleh Wildlife Refuge, Mazandaran Province, Iran. Siadati et al. (2010) also found the dominance of Euro-Siberian and Pluriregion elements in Hyrcanian forests in northern Iran. Some of the unique floristic elements in the study region might be due to the collision of Eurasian and Indian tectonic plates. Further studies are recommended to study the edapho-physiological pattern of the area to understand the underlying mechanisms of the present-day vegetation for its future management and conservation purposes. This study also covers the three sustainable development goals including life on land, climate action, good and wellbeing (Ejaz et al., 2022; Shehzadi et al., 2022).

Conclusion

Therophytes and nanophylls are the dominant life form and leaf form spectra of the Bin Dara, Dir, in the western boundary of Pakistan. Cosmopolitan, pantropical, Euro-Siberian, Mediterranean, Irano-Turanian, and pluriregion were the dominating phytogeographic elements in the studied region. The dominance of therophytes indicates that the study area is under immense anthropogenic pressure and an accelerated rate of deforestation. It is therefore recommended that the eastern and western Himalayan regions should be given more focus on the proper management and conservation of vegetation in the current scenario of climate change in the studied mountainous regions. It is also recommended that the methodology adopted in the current study can be

TABLE 4 Life form, geographical distribution, leaf size, and floristic elements of the Bin Dara, in the western boundary of Pakistan.

S. No	Family	Plant species	Life form	Leaf size	Habit	Geographical distribution	Floristic elements
1	Amaranthaceae	*Amaranthus lividus* L.	Th	N	Herb	Throughout the warmer regions of the world	Pan
		Amaranthus tricolor L.	Th	N	Herb	Asia, India, China, Japan and Indonesia	M, IT
		Amaranthus viridis L.	Th	N	Herb	Widely distributed in tropical and subtropical regions of the world	COS
		Chenopodium album L.	Th	N	Herb	Cosmopolitan	COS
2	Amaryllidaceae	*Allium cepa* L.	G	N	Herb	Cosmopolitan	SCOS
		Allium sativum L.	G	N	Herb	Cultivated widely in Europe, Asia and North America	IT
3	Apiaceae	*Coriandrum sativum* L.	Th	L	Herb	Cosmopolitan	COS
		Cuminum cyminum L.	Th	N	Herb	North Africa, Central Asia, Mediterranean region, Middle East and Western Pakistan	–
		Daucus carota L.	Th	N	Herb	Cosmopolitan	COS
		Foeniculum vulgare Mill.	Th	N	Herb	Cosmopolitan	COS
		Torilis leptophylla (L.) Rchb.f.	Th	N	Herb	Europe, Africa, United State America and Central Asia	ES, IT
4	Araliaceae	*Hedera nepalensis* K.Koch	Mp	Mes	Shrub	West Asia, Japan, Afghanistan and Himalaya	WH
5	Asparagaceae	*Polygonatum verticillatum* (L.) All.	Th	N	Herb	Europe, Russia, Afghanistan, Pakistan (Chitral, Dir, Swat, Hazara, Gilgit), Kashmir, India, Nepal, Sikkim, Bhutan and China	M, IT
6	Asteraceae	*Conyza canadensis* (L.) Cronquist	Th	Mic	Herb	North America, South America, Europe, Asia, and Africa	SCOS
		Helianthus annuus L.	Th	Mac	Shrub	Widely cultivated in China (native to North America).	M, IT
		Lactuca sativa L.	Th	Mac	Herb	Cultivated throughout China (probably originating from Mediterranean to South West Asia).	ES, M, IT
		Matricaria chamomilla L.	Th	N	Herb	Europe, North America, Mongolia, Russia and Uzbekistan	–
		Parthenium hysterophorus L.	Th	Mic	Herb	Native to tropical America, a widely introduced weed in the tropics and China (Guangdong, Guangxi, Guizhou, Yunnan).	Pan
		Setaria pumilla (Poir.) Roem. & Schult.	Th	Mic	Herb	Tropical and warm temperate regions of the World, Pakistan and introduced to North America	PL
		Sonchus asper (L.) Hill	Th	Mic	Herb	Madagascar and Africa	M, IT
		Sonchus oleraceus L.	Th	N	Herb	Europe and Mediterranean region	PL
		Taraxacum officinale F. H Wigg.	Th	Mic	Herb	Cosmopolitan weed of temperate areas	COS
7	Brassicaceae	*Brassica rapa* L.	Th	N	Herb	Europe and Central Asia	PL
		Brassica napus L.	Th	N	Herb	Europe, China and Pakistan	PL
		Capsella bursa-Pastoris (L.) Medik.	Th	Mic	Herb	Widely distributed in temperate regions	COS
		Cardaria chalepensis L.	Th	Mic	Herb	Europe, Central and Western Asia	CA
		Cardaria draba (L.) Desv.	Ch	Mic	Herb	Europe, Central and Western Asia	COS
		Coronopus didymus (L.) Smith	Th	L	Herb	South America, but widely introduced in the world	SCOS
		Neslia apiculata Fisch.	Th	L	Herb	South Europe, Southern and Central Asia,	ES, M, IT

(Continued)

TABLE 4 (Continued)

S. No	Family	Plant species	Life form	Leaf size	Habit	Geographical distribution	Floristic elements
						Northern Africa, North West Himalaya and Pakistan	
		Raphanus sativus L.	Th	Mac	Herb	China and Mediterranean region	Circ
		Sisymbrium irio L.	Th	N	Herb	Europe, Asia and North Africa	ES, M, IT
8	Cannabaceae	*Cannabis sativa* L.	Th	Mic	Herb	Russia, China, India, Pakistan and Iran	IT
9	Caryophyllaceae	*Silene vulgaris* (Moench) Garcke	Th	N	Herb	Europe, North Africa, temperate Asia and Arabia	M, IT
		Stellaria media (L.) Vill.	Th	N	Herb	Cosmopolitan	COS
10	Compositae	*Artemisia absinthium* L.	Th	N	Herb	Eurasia, North Africa, United State America and Canada	M, IT
		Artemisia maritima L.	Th	Mic	Herb	United Kingdom, Native to France, Italy, Belgium, Germany, Denmark, Sweden and Russia	ES, M, IT
		Artemisia scoparia Waldest.	Ch	N	Herb	Central and Eastern Europe, Iraq, Turkey, Iran, Afghanistan, Pakistan (Baluchistan, Khyber Pakhtunkhwa and Punjab), India, China, Mongolia and Russia	ES, M, IT
11	Convolvulaceae	*Convolvulus arvensis* L.	Th	N	Herb	Temperate and tropical regions of the world, except Australia	COS
12	Cucurbitaceae	*Citrullus colocynthis* (L.) Schrad.	Th	Mic	Herb	North Africa, Atlantic Islands, North West India, Pakistan and Australia	SA
		Cucumis sativus L.	Th	Mg	Herb	Throughout the tropical and subtropical countries of the world	IT
		Cucurbita maxima Duchesne	Th	Mg	Herb	South American, India, Pakistan and elsewhere	Pan
		Cucurbita moschata Duchesne	Th	Mg	Herb	Tropical and subtropical countries	Pan
		Cucurbita pepo L.	Th	Mg	Herb	North America, China and Pakistan	–
		Lagenaria siceraria (Molina.) Standl.	Th	Mg	Herb	Asia, Africa and Pakistan	SG
		Momordica charantia L.	Th	Mg	Herb	South Africa, South East and Far East Asia to Australia	Pan
13	Cyperaceae	*Cyperus esculentus* L.	Ch	N	Herb	Tropical and Sub tropical Africa, Mediterranean region	Pan
		Cyperus rotundus L.	Ch	N	Herb	Tropical and subtropical areas of all continents	COS
14	Ebenaceae	*Diospyros kaki* L.	Mp	Mg	Tree	Eastern Asia, Japan and China	GC
		Diospyros lotus L.	Mp	Mes	Tree	Iran, Afghanistan, Pakistan, India, China and Japan	Cau
		Diospyros virginiana L.	Mp	Mg	Tree	South Atlantic and Gulf states	GC
15	Equisetaceae	*Equisetum arvense* L.	G	Ap	Herb	Central and South West Asia, Japan, Korea, Mongolia, Europe, Nepal, Russia, North India	Circ
16	Euphorbiaceae	*Euphorbia helioscopia* L.	Th	N	Herb	Europe, North Africa and Asia; introduced into North America	ES, M, IT
17	Fabaceae	*Medicago polymorpha* L.	Th	N	Herb	Cosmopolitan	M, IT
		Medicago sativa L.	Th	N	Herb	Europe, North Africa, Central Asia, Pakistan and, India	ES, M, IT

(Continued)

TABLE 4 (Continued)

S. No	Family	Plant species	Life form	Leaf size	Habit	Geographical distribution	Floristic elements
		Mimosa pudica L.	Np	L	Herb	South America and Pakistan	Pan
		Robinia pseudoacacia L.	Mp	N	Tree	North America, China except Hainan and Xizang regions	Hol
		Trifolium repens L.	Th	N	Herb	Central Asia, Pakistan, India, Russia, Afghanistan, Siberia and Kashmir	ES, M, IT
		Vicia sativa L.	Th	N	Herb	Pakistan, Kashmir, India, Orient, Europe, Russia and Far East	ES, M, IT
18	Fagaceae	*Quercus baloot* Griff.	Mp	Mes	Tree	Pakistan, Afghanistan and Kashmir	WH
		Quercus incana Bartram	Mp	Mes	Tree	North West Himalayas to Nepal and Upper Burma	Hol
19	Geraniaceae	*Geranium rotundifolium* L.	Th	N	Herb	Africa, Western and Central Europe, Siberia, Turkey, Iran and Afghanistan	ES, M, IT
20	Hamamelidaceae	*Parrotiopsis jacquemontiana* (Decne.) Rehder	Np	Mes	Shrub	Pakistan (Murree, Hazara division, Swat, Dir and Kurram) and Kashmir	WH
21	Hypericaceae	*Hypericum perforatum* L.	Th	N	Herb	Europe, Africa, East Asia, West China, north west India, America and Australia	PL
22	Juglandaceae	*Juglans regia* L.	Mp	Mac	Tree	Central America, Southern Europe, Caucasus, Syria, Northern Iran, Afghanistan, West Pakistan, Tibet, Nepal, West China and Upper Burma	PL
23	Lamiaceae	*Ajuga integrifolia* Buch.-Ham.	H	Mic	Herb	Afghanistan, Pakistan, Kashmir, China, Bhutan, Burma, China and Malaysia	Hol
		Lallemantia royleana (Benth.) Benth.	Th	Mic	Herb	South Russia, South West and Central Asia, West China	IT
		Marrubium vulgare L.	H	Mic	Herb	Europe, Asia, North America, South Africa and Australia	SZ, M, IT
		Mentha arvensis L.	H	Mic	Herb	Eurasia and tropical Asia	Eu
		Mentha longifolia L.	G	Mic	Herb	Europe, Asia and South Africa	PL
		Ocimum basilicum L.	Ch	N	Herb	Subtropical and tropical Asia, Africa and South East Asia	Pan
		Origanum vulgare L.	Ch	Mi	Herb	South Europe, Southern and Central Asia, Mediterranean countries, Macaronesia, Himalaya, China and Taiwan	ES, IT
		Phlomis cashmeriana Benth.	G	N	Herb	Central Asia, Afghanistan, Pakistan and Kashmir	IT
		Prunella vulgaris L.	Th	L	Herb	Europe, North and South Africa, North America, Asia and Australia	PL
		Salvia nubicola Wall. ex Sweet	Ch	Mes	Herb	Eastern Afghanistan, Pakistan, Kashmir, North India, Nepal, Tibet, Sikkim and Bhutan	WT
24	Leguminosae	*Astragalus lentiginosus* Hook.	Ch	L	Herb	North America, California Coast Ranges, south to Mexico and north to British Columbia	SA
		Bauhinia tomentosa L.	Mp	Mes	Tree	Tropical Africa, India, China, Western Pakistan and in tropics	PL
25	Moraceae	*Ficus carica* L.	Np	Mes	Tree	North Africa, Europe, Middle East, India, Pakistan, Afghanistan, Russia and Iran	M, IT, Cau

(Continued)

TABLE 4 (Continued)

S. No	Family	Plant species	Life form	Leaf size	Habit	Geographical distribution	Floristic elements
		Morus alba L.	Mp	Mes	Tree	North Africa, South and Central Europe, China, Malaya, Burma, India and Pakistan	IT
		Morus nigra L.	Mp	Mes	Tree	North Africa, Central Asia, Central and Southern Europe, Northern Pakistan,	Pan
26	Onagraceae	*Oenothera macrocarpa* Nutt.	Th	N	Herb	Southern and central United States	–
		Oenothera rosea L'Hér. ex Aiton.	Th	N	Herb	Central and Southern Texas United State America, throughout Mexico, Central and South America	Neo
27	Orchidaceae	*Dactylorhiza hatagirea* D.Don.	Th	N	Herb	Bhutan, Himalaya region from Chitral to Nepal and Tibet	IT, Cau
28	Oxalidaceae	*Oxalis corniculata* L.	G	Mic	Herb	Cosmopolitan	COS
29	Papaveraceae	*Fumaria indica* Hausskn, Pugsley	Th	N	Herb	Central Asia, India, Pakistan and Afghanistan	M, IT
		Papaver hybridum L.	Th	Mic	Herb	Europe, North Africa, South West and Central Asia, Afghanistan and West Pakistan	M, IT, EA
		Papaver somniferum L.	Th	Mac	Herb	Asia and Europe	M, IT, EA
30	Pinaceae	*Cedrus deodara* Roxb.	Mp	L	Tree	Afghanistan, Pakistan (Kurram eastward) to Kashmir and Western Nepal	WH
		Pinus roxburghii Sarg.	Mp	L	Tree	Afghanistan, Himalaya from Chitral eastward to Bhutan, Sikkim.	WH
		Pinus wallichiana A. B. Jacks.	Mp	L	Tree	Afghanistan, Chitral eastward to West Nepal	WH
31	Plantaginaceae	*Plantago lanceolata* L.	Th	N	Herb	Europe, North Africa, South Asia to the mountains of Tien Shan and introduced all over the world	ES, IT, M, SS
		Plantago major L.	Th	Mic	Herb	Throughout Europe, northern and central Asia, introduced all over the world	SCOS
32	Platanaceae	*Platanus mexicana* Moric.	Mp	Mac	Tree	United State America (Arizona, New Mexico)	M, IT
		Platanus orientalis L.	Mp	Mac	Tree	Central and West Asia, Southern Europe to Turkey, North Iran, Afghanistan, India and Pakistan	SCOS
33	Poaceae	*Arundo donax* L.	Np	Mes	Shrub	Pakistan (Baluchistan, Punjab, Khyber Pakhtunkhwa and Kashmir), Mediterranean region eastwards to Burma and North Africa	ES, M, IT
		Avena sativa L.	Th	N	Herb	Cultivated in non-tropical regions of both hemispheres	PL
		Cynodon dactylon (L.) Pers.	H	L	Herb	Tropical and warm temperate regions throughout the world	COS
		Dichanthium annulatum (Forssk.) Stapf	Ch	N	Herb	Pakistan, Kenya, Tanzania and Senegal	SA
		Hemarthria compressa (L.f) R. Br.	Th	L	Herb	Pakistan, Iraq, Afghanistan India, China, Taiwan and Thailand	WH
		Heteropogon contortus (L.) P.Beauv.	H	Mic	Herb	Tropical and warm temperate regions generally	Pan
		Hordeum vulgare L.	Th	Mic	Herb	Cultivated worldwide in all non-tropical countries and in montane areas of tropics	ES, M, IT
		Oryza sativa L.	Th	Mic	Herb	Africa, Asia, South Europe, South America and Australia	–

(Continued)

TABLE 4 (Continued)

S. No	Family	Plant species	Life form	Leaf size	Habit	Geographical distribution	Floristic elements
		Poa annua L.	Th	L	Herb	Cosmopolitan	SCOS
		Secale cereale L.	Th	Mic	Herb	Largely cultivated in Europe as a cereal forming a staple food	SCOS
		Sorghum halepense (L.) Pers.	H	Mic	Herb	Mediterranean region and Pakistan	PL
		Triticum aestivum L.	Th	Mes	Herb	Pakistan, India, Nilgiri and Palini	COS
		Zea mays L.	Th	Mac	Herb	Tropical America and cold regions of Pakistan	–
34	Polygonaceae	*Bistorta amplexicaulis* (D.Don) Greene	Th	Mes	Herb	Afghanistan, Northern Pakistan and Kashmir	WH
		Persicaria glabra (Willed.) M.Gomez	H	N	Herb	Africa, Tropical Asia, Pakistan, India extending up to Malaysia and Philippine	Pan
		Persicaria hydropiper (L.) Delarbre	H	N	Herb	North America, Widely distributed in North West Africa, Temperate Asia, Pakistan, India and extending to far east up to Japan	Pan
		Rumex dentatus L.	G	Mes	Herb	East Asia, Afghanistan, Pakistan and India	SA, IT
		Rumex hastatus D. Don	G	Mes	Herb	Northern Pakistan, North Eastern Afghanistan and South West China	SA, IT
35	Primulaceae	*Myrsine africana* L.	Np	N	Shrub	Asia and Africa	Eu
36	Ranunculaceae	*Clematis graveolens* Lindl.	Np	N	Herb	Afghanistan, Pakistan, Kashmir eastward to Nepal	COS
37	Rhamnaceae	*Ziziphus jujuba* Mill.	Mp	N	Tree	South Europe, South and East Asia, Mediterranean region, Afghanistan, Iran, Pakistan, India, Mongolia, Japan, China and Tibet	Pal
38	Rosaceae	*Cydonia oblonga* Mill.	Np	Mac	Shrub	South America, Mediterranean regions of Europe, China and elsewhere	M, IT
		Malus pumila Mill.	Mp	Mac	Tree	North West and South West China (Bhutan, Native to South West Asia and Europe).	Hol
		Prunus armeniaca L.	Mp	Mes	Tree	North America in the western United States, mostly in the San Joaquin Valley of California	Hol
		Prunus domestica L.	Mp	Mac	Tree	Widely cultivated in China (native to South West Asia and Europe).	Hol
		Rosa brunonii Lindl.	Np	N	Shrub	Nepal, India, Afghanistan, Bhutan South West China and Northern Pakistan	IT
		Rosa indica L.	Np	Mic	Shrub	West China, Nepal, India and Pakistan	IT
39	Rubiaceae	*Galium tricornutum* Dandy	Th	N	Herb	Europe, North Africa, Western Asia, Pakistan, Iran, Afghanistan and Caucasia	WT
40	Salicaceae	*Populus afghanica* Aitch.	Mp	Mac	Tree	Pakistan (Kurram, South Waziristan, Quetta, Kalat); Afghanistan, Tajikistan, Uzbekistan, Kirgyzstan, Kazakistan, North Africa and east Mediterranean region	IT
		Populus alba L.	Mp	Mes	Tree	Europe, North Africa, South West and West Central Asia including Kashmir and Pakistan (Khyber Pakhtunkhwa, Murree, Baluchistan).	ES, IT
		Populus ciliata Wall. ex Royle	Mp	Mac	Tree	Pakistan (Chitral) eastwards to Kashmir, along with Himalayas through India, Nepal, Sikkim, Bhutan and Myanmar	Hol

(Continued)

TABLE 4 (Continued)

S. No	Family	Plant species	Life form	Leaf size	Habit	Geographical distribution	Floristic elements
		Populus nigra L.	Mp	Mac	Tree	West and Central Asia, Europe and North Africa, Native to China (Xinjiang), widely cultivated in Pakistan, Kashmir and China	Hol
		Salix alba L.	Mp	Mes	Tree	Europe, Western and Central Asia, Siberia, Mediterranean region	ES, M, IT
		Salix tetrasperma Roxb.	Mp	Mes	Tree	Pakistan (Khyber Pakhtunkhwa, Punjab, Baluchistan), India, Myanmar, China, Thailand, Indonesia, Malaysia, Philippines and Vietnam	ES, M, IT
41	Simaroubaceae	*Ailanthus altissima* (Mill.) Swingle	Np	Mic	Tree	Native to China and cultivated in temperate and subtropical regions of the world. It is cultivated as a roadside tree in Pakistan	Pan
42	Solanaceae	*Capsicum frutescens* L.	Th	Mic	Herb	Tropical America	Pan
		Datura stramonium L.	Th	Mac	Herb	Mostly in temperate and subtropical regions of both the hemispheres	COS
		Lycopersicum esculentum Mill.	Th	Mic	Herb	Native to Central and South America	–
		Solanum melongena L.	Np	Mes	Herb	Asia, Africa and America (Native to India)	GC
		Solanum nigrum L.	Th	Mic	Herb	Cosmopolitan but absent from the arctic and subarctic regions	COS
		Solanum tuberosum L.	G	Mes	Herb	Native to the mountainous areas of Mexico, Chile and Peru (South America), cultivated throughout the world	GC
43	Thymelaeaceae	*Daphne mucronata* Royle	Np	Mic	Shrub	North Africa, South Europe, Afghanistan, west Pakistan and Iran	M, MAC
44	Urticaceae	*Urtica dioica* L.	G	Mic	Herb	Widespread in the temperate regions of both hemispheres	PL
45	Verbenaceae	*Verbena officinalis* L.	Np	N	Herb	Europe and Asia, North Africa; introduced in North America and South Africa	PL
46	Viburnaceae	*Viburnum cotinifolium* D. Don	Np	Mes	Shrub	Afghanistan and Pakistan Himalaya	WH
		Viburnum grandiflorum Wall. ex DC.	Mp	Mac	Shrub	Himalaya from Swat eastward to Bhutan and South Tibet	Hol
47	Vitaceae	*Vitis vinifera* L.	Np	Mac	Shrub	South Asia, North and South Africa, cultivated extensively in Central Europe, Mediterranean region, Iran, China, Japan, Australia, India, Afghanistan and Pakistan	Hol

Pal, Palaeotropical; M, Mediterranean; SA, South Arabian; CA, Central Asian; GC, Guineo-Congolian; Hol, Holarctic; MAC, Macaronesian; SG, Sudano/Guinean transition; SCOS, Sub Cosmopolitan; Cau, Caucasian; WT, wide temperate; PL, Pluriregional; SZ, Sudano-Zambezian; Eu, Eurasian; ES, Euro-Siberian; SS, Saharo-Sindian; TR, Tropical; WH, Western Himalayan; Pan, Pantropical; Neo, Neotropical; Circ, Circumboreal; IT, Irano-Turanian.

followed to assess the phytogeographic elements of any habitat in the world.

Data availability statement

The original contributions presented in the study are included in the article/supplementary material, further inquiries can be directed to the corresponding author.

Author contributions

This work was conducted and written jointly by FM, SK, ZM, ZA, AA, AuR, and AR. Funding acquisition: HH, AA-M, and NC-B. Project administration: HH. Writing—review and

editing: AA-M and NC-B. All authors have read and agreed to the published version of the manuscript.

Conflict of interest

The authors declare that the research was conducted in the absence of any commercial or financial relationships that could be construed as a potential conflict of interest.

Publisher's note

References

Abbas, Z., Alam, J., Khan, S. M., Hussain, M., and Abbasi, A. M. (2019). Diversity, ecological feature and conservation of a high montane flora of the Shigar valley (Karakorum Range) Baltistan region, northern Pakistan. *Pak. J. Bot.* 51, 985–1000. doi: 10.30848/PJB2019-3(23)

Abbas, Z., Khan, S. M., Alam, J., Peer, T., Abideen, Z., Bussmann, R. W., et al. (2021). Vegetation dynamics along altitudinal gradients in the Shigar Valley (Central Karakorum) Pakistan: zonation, physiognomy, ecosystem services and environmental impacts. *Pak. J. Bot.* 53, 1865–1874. doi: 10.30848/PJB2021-5(43)

Ahmad, Z., Hussain, M., Iqbal, M., Khalid, S., Ahmad, H., Khan, S. M., et al. (2022a). "Weed vegetation in maize crop of the Shahbaz Garhi, District Mardan: gradient of diversity and species composition," in *Biodiversity, Conservation and Sustainability in Asia*, eds M. Öztürk, S. M. Khan, V. Altay, R. Efe, D. Egamberdieva, and F. O. Khassanov (Berlin: Springer), 657–679. doi: 10.1007/978-3-030-73943-0_36

Ahmad, Z., Khan, S. M., Abd_Allah, E. F., Alqarawi, A. A., and Hashem, A. (2016). Weed species composition and distribution pattern in the maize crop under the influence of edaphic factors and farming practices: a case study from Mardan, Pakistan. *Saudi J. Biol. Sci.* 23, 741–748. doi: 10.1016/j.sjbs.2016.07.001

Ahmad, Z., Khan, S. M., Ali, M. I., Fatima, N., and Ali, S. (2019). Pollution indicandum and marble waste polluted ecosystem; role of selected indicator plants in phytoremediation and determination of pollution zones. *J. Clean. Prod.* 236, 117709. doi: 10.1016/j.jclepro.2019.117709

Ahmad, Z., Khan, S. M., and Page, S. (2021). Politics of the natural vegetation to balance the hazardous level of elements in marble polluted ecosystem through phytoremediation and physiological responses. *J. Hazard. Mater.* 414, 125451. doi: 10.1016/j.jhazmat.2021.125451

Ahmad, Z., Khan, S. M., Page, S., Alamri, S., and Hashem, M. (2022b). Plants predict the mineral mines—a methodological approach to use indicator plant species for the discovery of mining sites. *J. Adv. Res.* 39, 119–133. doi: 10.1016/j.jare.2021.10.005

Ahmed, J., Rahman, I. U., AbdAllah, E. F., Ali, N., Shah, A. H., Ijaz, F., et al. (2019). Multivariate approaches evaluated in the ethnoecological investigation of Tehsil Oghi, Mansehra, Pakistan. *Acta Ecol. Sin.* 39, 443–450. doi: 10.1016/j.chnaes.2018.11.006

Ali, H., Muhammad, Z., Ahmad, Z., and Khan, S. (2022). Environmental determinants of vegetation in District Malakand, a sub-tropical zone of the outer Hindu Kush mountain range. *Appl. Ecol. Environ. Res.* 20, 339–361. doi: 10.15666/aeer/2001_339361

Ali, S., Khan, S. M., Ahmad, Z., Ejaz, U., and Khalid, N. (2022a). Indicator species analysis and assessment of ornamental plants using multivariate statistical techniques in the home gardens of Rustam Valley, Pakistan. *Int. J. Appl. Exp. Biol.* 1, 87–95. doi: 10.56612/ijaeb.v1i2.16

Ali, S., Khan, S. M., Siddiq, Z., Ahmad, Z., Ahmad, K. S., Abdullah, A., et al. (2022b). Carbon sequestration potential of reserve forests present in the protected Margalla Hills National Park. *J. King Saud Univ. Sci.* 34, 101978. doi: 10.1016/j.jksus.2022.101978

Ali, S., Zeb, U., Lei, W., Khan, H., Shehzad, K., Khan, H., et al. (2018). Floristic inventory and ecological characterization the village Sherpao, District Charsadda, Khyber Pakhtunkhwa-Pakistan. *Acta Ecol. Sin.* 38, 329–333. doi: 10.1016/j.chnaes.2017.12.004

Ali, S. I., and Qaiser, M. A. (1986). phytogeographical analysis of the phanerogams of Pakistan and Kashmir. *Proc. R. Soc. Edinburgh Section B Biol. Sci.* 89, 89–101. doi: 10.1017/S0269727000008939

Al-Yemeni, M., and Sher, H. (2010). Biological spectrum with some other ecological attributes of the flora and vegetation of the Asir Mountain of South West, Saudi Arabia. *African J. Biotechnol.* 9:34. Available online at: http://www.academicjournals.org/AJB

Amri, C. N. A. B. C., Mokhtar, N. A. B. M., and Shahari, R. (2019). Leaf anatomy and micromorphology of selected plant species in coastal area of Kuantan, Pahang, Malaysia. *Sci. Heritage J.* 3, 22–25. doi: 10.26480/gws.02.2019.22.25

Angyalossy, V., Nogueira, A., Rocha, E. X., Schietti, J., Lohmann, L. G., Vicentini, A., et al. (2022). Hydro-edaphic gradient and phylogenetic history explain the landscape distribution of a highly diverse clade of lianas in the Brazilian Amazon. *Front. For. Global Change* 5, 809904. doi: 10.3389/ffgc.2022.809904

Anwar, S., Khan, S. M., Ahmad, Z., Ullah, Z., Afza, R., Abbas, Z., et al. (2022). Plant diversity and communities pattern with special emphasis on the indicator species of a dry temperate forest: a case study from Liakot area of the Hindu Kush mountains, Pakistan. *Trop. Ecol.* 2022, 1–16. doi: 10.1007/s42965-022-00238-w

Anwar, S., Khan, S. M., Ahmad, Z., Ullah, Z., and Iqbal, M. (2019). Floristic composition and ecological gradient analyses of the Liakot Forests in the Kalam region of District Swat, Pakistan. *J. For. Res.* 30, 1407–1416. doi: 10.1007/s11676-019-00919-8

Axelrod, D., and Raven, P. (1978). *Late Cretaceous and Tertiary vegetation history of Africa. Biogeography and Ecology of Southern Africa*. Dordrecht: Springer, 77–130. doi: 10.1007/978-94-009-9951-0_5

Badshah, L., Hussain, F., and Sher, Z. (2013). Floristic inventory, ecological characteristics and biological spectrum of rangeland, District Tank, Pakistan. *Pak. J. Bot.* 45, 1159–1168. Available online at: http://www.pakbs.org/.../04.pdf

Bano, S., Khan, S. M., Alam, J., Alqarawi, A. A., Abd_Allah, E. F., et al. (2018). Eco-floristic studies of native plants of the Beer Hills along the Indus River in the districts Haripur and Abbottabad, Pakistan. *Saudi J. Biol. Sci.* 25, 801–810. doi: 10.1016/j.sjbs.2017.02.009

Bedair, R., Ibrahim, A. A., Alyamani, A. A., Aloufi, S., and Ramadan, S. (2021). Impacts of anthropogenic disturbance on vegetation dynamics: a case study of Wadi Hagul, Eastern Desert, Egypt. *Plants*. 10, 1906. doi: 10.3390/plants10091906

Bridson, D. M., and Forman, L. (1998). *Herbarium Handbook*. Kew: Royal Botanic Gardens.

Brummitt, R. K., Pando, F., Hollis, S., and Brummitt, N. (2001). "World geographical scheme for recording plant distributions," in *International Working Group on Taxonomic Databases for Plant Sciences (TDWG)*.

Ca, P., Cc, P., Sb, C., and Na, D. (2020). Evaluation of vermiculite application rates on growth and yield of brassica napus (RAPE). *Science*. 4, 27–31. doi: 10.26480/gws.02.2020.27.31

Eig, A. (1931). Les elements et les groupes phytogeographiques *Quxiliaires dans* la flore palestinienne. *Verlag des Repertoriums;* 1931.

Ejaz, U., Khan, S. M., Aqeel, M., Khalid, N., Sarfraz, W., Naeem, N., et al. (2022). Use of Parthenium hysterophorus with synthetic chelator for enhanced uptake of cadmium and lead from contaminated soils—a step toward better public health. *Front. Public Health* 10:1009479. doi: 10.3389/fpubh.2022.1009479

Farooq, M., Hussain, M., Saqib, Z., Khan, K. R., Shah, A. H., Shah, G. M., et al. (2019). Spatial distribution and correlation of important edaphic and climatic gradients in Tanawal area of Himalayas, Pakistan. *Acta Ecol. Sinica*. 39, 267–272. doi: 10.1016/j.chnaes.2018.09.014

Flores-Argüelles, A., Espejo-Serna, A., López-Ferrari, A. R., and Krömer, T. (2022). Diversity and vertical distribution of epiphytic angiosperms, in natural and disturbed forest on the northern coast of Jalisco, Mexico. *Front. For. Global Change*. 76, 828851. doi: 10.3389/ffgc.2022.828851

Gul, B., Ahmad, I., Khan, H., Zeb, U., and Ullah, H. (2018). Floristic inventory of wild plants of Peshawar university campus. *Acta Ecol. Sin*. 38, 375–380. doi: 10.1016/j.chnaes.2018.04.005

Haq, Z., Khan, S., Ahmad, Z., Shah, S., Mustafa, G., Razzaq, A., et al. (2020). An evaluation of conservation status and ecological zonation of Alnus nitida; a monophyletic species of the sino-Japanese region. *JAPS*. 30, 1224–1235. doi: 10.36899/JAPS.2020.5.0140

Haq, Z., Khan, S. M., Abdullah, Z. A., Iqbal, M., Khan, R., Rasheed, S., et al. (2022). Macro and Micro Anatomical diversity in the *Alnus nitida* (Spach) Endl. growing in varying Climatic conditions of Sino Japanese Region of Pakistan. *Pak J Bot*. 54, 1055–1064. doi: 10.30848/PJB2022-1(36)

Hara, H. (1966). *Flora of Eastern Himalaya Results of the Botanical Expedition to Eastern Himalaya Organized by the University of Tokyo 1960 and 1963. Botanical Expedition to Eastern Himalaya (1960-1963).* Tokyo: University of Tokyo Press.

Hussain, F., Shah, S. M., Badshah, L., and Durrani, M. J. (2015). Diversity and ecological characteristics of flora of Mastuj valley, district Chitral, Hindukush range, Pakistan. *Pak. J. Bot*. 47, 495–510.

Hussain, M., Ahmad, Z., Iqbal, M., Zuhra, B., Rasheed, S., Khan, S., et al. (2022). *Plants and Plant Communities of the Kurram Valley, Pakistan. Biodiversity, Conservation and Sustainability in Asia.* Cham; New York, NY: Springer, 241–265. doi: 10.1007/978-3-030-73943-0_14

Hussain, M., Khan, S. M., Abd_Allah, E. F., Ul Haq, Z., Alshahrani, T. S., Alqarawi, A. A., et al. (2019). Assessment of Plant communities and identification of indicator species of an ecotonal forest zone at durand line, district Kurram, Pakistan. *Appl. Ecol. Environ. Res*. 17, 6375–6396. doi: 10.15666/aeer/1703_63756396

Hussain, S., Malik, Z. H., Malik, N. Z., and Ajaib, M. (2014). Life form and leaf spectra reported from India Morr District Kotli, Azad Jammu & Kashmir. *Biologia (Pakistan)*. 60, 129–133.

Iqbal, M., Khan, S. M., Ahmad, Z., Hussain, M., Shah, S. N., Kamran, S., et al. (2021). Vegetation Classification of the Margalla Foothills, Islamabad under the influence of edaphic factors and anthropogenic activities using modern ecological tools. *Pak. J. Bot*. 53, 1831–1843. doi: 10.30848/PJB2021-5(22)

Kamran, S., Khan, S. M., Ahmad, Z., Ur Rahman, A., Iqbal, M., Manan, F., et al. (2020). The role of graveyards in species conservation and beta diversity: a vegetation appraisal of sacred habitats from Bannu, Pakistan. *J. For. Res*. 31, 1147–1158. doi: 10.1007/s11676-019-00893-1

Khan, M., Hussain, F., and Musharaf, S. (2013). Floristic composition and biological characteristics of the vegetation of Sheikh Maltoon Town, District Mardan, Pakistan. *Annu. Rev. Res. Biol.* 3, 31–41. Available online at: https://journalarrb.com/index.php/ARRB/article/view/24612

Khan, M., Khan, S. M., Ilyas, M., Alqarawi, A. A., Ahmad, Z., and Abd_Allah, E. F. (2017). Plant species and communities assessment in interaction with edaphic and topographic factors; an ecological study of the mount Eelum District Swat, Pakistan. *Saudi J. Biol. Sci*. 24, 778–786. doi: 10.1016/j.sjbs.2016.11.018

Khan, M. N., and Badshah, L. (2019). Floristic diversity and utility of flora of district charsadda, Khyber Pakhtunkhwa. *Acta Ecol. Sinica*. 39, 306–320. doi: 10.1016/j.chnaes.2018.10.003

Khan, S. A., Khan, S. M., Ullah, Z., Ahmad, Z., Alam, N., Shah, S. N., et al. (2020). Phytogeographic classification using multivariate approach; a case study from the Jambil Valley Swat, Pakistan. *Pak. J. Bot*. 52, 279–290. doi: 10.30848/PJB2020-1(11)

Khan, S. A., Khan, S. M., Ullah, Z., Zada, M., Ejaz, U., Alam, N., et al. (2022). *Phytogeography of Plants Distributed in the Jambil Valley, Swat District, Pakistan; A Revisit for Evaluating Vegetation of the Region. Biodiversity, Conservation and Sustainability in Asia.* Cham; New York, NY: Springer, 121–147. doi: 10.1007/978-3-030-73943-0_8

Khan, S. M. (2022). *Plant Communities and Vegetation Ecosystem Services in the Naran Valley, Western Himalaya.* Leicester: University of Leicester.

Khan, S. M., Haq, Z. U., and Ahmad, Z. (2022). "Muslim graveyard groves: plant diversity, ecosystem services, and species conservation in Northwest Pakistan," in *Sacred Forests of Asia*, eds C. Coggins and B. Chen (Oxfordshire: Routledge), 77–87. doi: 10.4324/9781003143680-8

Khan, S. M., Harper, D., Page, S., and Ahmad, H. (2011). Species and community diversity of vascular flora along environmental gradient in Naran Valley: a multivariate approach through indicator species analysis. *Pak. J. Bot*. 43, 2337–2346.

Khan, W., Khan, S. M., Ahmad, H., Ahmad, Z., and Page, S. (2016). Vegetation mapping and multivariate approach to indicator species of a forest ecosystem: a case study from the Thandiani sub Forests Division (TsFD) in the Western Himalayas. *Ecol. Indic*. 71, 336–351. doi: 10.1016/j.ecolind.2016.06.059

Kitamura, S. (1960). *Flora of Afghanistan. Results of the Kyoto University Scientific Expedition to the Karakoram and Hindu-kush, 1955, Vol. II.*

Li, W., Shi, Y., Zhu, D., Wang, W., Liu, H., Li, J., et al. (2021). Fine root biomass and morphology in a temperate forest are influenced more by the nitrogen treatment approach than the rate. *Ecol. Indicators*. 130, 108031. doi: 10.1016/j.ecolind.2021.108031

Longo, M., Knox, R. G., Medvigy, D. M., Levine, N. M., Dietze, M. C., Kim, Y., et al. (2019). The biophysics, ecology, and biogeochemistry of functionally diverse, vertically and horizontally heterogeneous ecosystems: the Ecosystem Demography model, version 2.2-Part 1: Model description. *Geosci. Model Dev*. 12, 4309–4346. doi: 10.5194/gmd-12-4309-2019

Magray, J. A., Wani, B. A., Islam, T., Ganie, A. H., and Nawchoo, I. A. (2022). Phyto-ecological analysis of *Phytolacca acinosa* Roxb. assemblages in Kashmir Himalaya, India. *Front. For. Global Change*. 155, 976902. doi: 10.3389/ffgc.2022.976902

Manan, F., Khan, S. M., Ahmad, Z., Kamran, S., Haq, Z. U., Abid, F., et al. (2020). Environmental determinants of plant associations and evaluation of the conservation status of *Parrotiopsis jacquemontiana* in Dir, the Hindu Kush Range of Mountains. *Trop. Ecol* 61, 509–526. doi: 10.1007/s42965-020-00109-2

Mehmood, A., Khan, S. M., Shah, A. H., Shah, A. H., and Ahmad, H. (2015). First floristic exploration of the district Torghar, Khyber Pakhtunkhwa, Pakistan. *Pak J Bot*. 47, 57–70.

Mehmood, A., Shah, A. H., Shah, A. H., Khan, S. M., Rahman, I. U., Ahmad, H., et al. (2017). Floristic list and indigenous uses of poaceae family in district Tor Ghar, Khyber Pakhtunkhwa, Pakistan. *J. Appl. Environ. Biol. Sci*. 7, 169–177.

Miao, R., Qiu, X., Guo, M., Musa, A., and Jiang, D. (2018). Accuracy of space-for-time substitution for vegetation state prediction following shrub restoration. *J. Plant Ecol*. 11, 208–217. doi: 10.1093/jpe/rtw133

Mumshad, M., Ahmad, I., Khan, S. M., Rehman, K., Islam, M., Sakhi, S., et al. (2021). Phyto-ecological studies and distribution pattern of plant species and communities of Dhirkot, Azad Jammu and Kashmir, Pakistan. *PLoS ONE*. 16, e0257493. doi: 10.1371/journal.pone.0257493

Munyasya, A. N., Koskei, K., Zhou, R., Liu, S.-T., Indoshi, S. N., Wang, W., et al. (2022). Integrated on-site & off-site rainwater-harvesting system boosts rainfed maize production for better adaptation to climate change. *Agric. Water Manag*. 269, 107672. doi: 10.1016/j.agwat.2022.107672

Nasir, E., and Ali, S. (1972). *Flora of West Pakistan*. Pakistan Agricultural Research Council. Actual publisher not stated.

Nasir, Z. A., and Sultan, S. (2002). Floristic, biological and leaf size spectra of weeds in gram, lentil. *Pak. J. Biol. Sci*. 5, 758–762. doi: 10.3923/pjbs.2002.758.762

Rahman, A. U., Khan, S. M., Khan, S., Hussain, A., Rahman, I. U., Iqbal, Z., et al. (2016). Ecological assessment of plant communities and associated edaphic and topographic variables in the Peochar Valley of the Hindu Kush mountains. *Mountain Res. Dev*. 36, 332–341. doi: 10.1659/MRD-JOURNAL-D-14-00100.1

Rasheed, S., Khan, S. M., Ahmad, Z., Mustafa, G., Haq, Z., Shah, H., et al. (2022). Ecological assessment and indicator species analyses of the Cholistan desert using multivariate statistical tools. *Pak. J. Bot*. 54, 683–694. doi: 10.30848/PJB2022-2(24)

Raunkiaer, C. (1934). *The Life Forms of Plants and Statistical Plant Geography; Being the collected Papers of C. Raunkiaer.*

Shannon, J., Kolka, R., Van Grinsven, M., and Liu, F. (2022). Joint impacts of future climate conditions and invasive species on black ash forested wetlands. *Front. For. Global Change*. 148, 957526. doi: 10.3389/ffgc.2022.957526

Sharma, J., Raina, A. K., and Sharma, S. (2014). Life form classification and biological spectrum of Lamberi Forest Range, Rajouri, J&K, India. *Int. J. Curr. Microbiol. App. Sci.* 3, 234–239. Available online at: http://www.ijcmas.com/vol-3-11/Jyoti%

Shehzadi, S., Khan, S. M., Mustafa, G., Abdullah, A., Khan, I., Ahmad, Z., et al. (2022). Antiviral COVID-19 protein and molecular docking: *In silico* characterization of various antiviral compounds extracted from *Arisaema jacquemontii* Blume. *Front. Public Health* 10:964741. doi: 10.3389/fpubh.2022.964741

Sher, Z., and Khan, Z. (2007). Floristic composition, life form and leaf spectra of the vegetation of Chagharzai Valley, District Buner. *Pak. J. Plant Sci.* 13, 55–64.

Siadati, S., Moradi, H., Attar, F., Etemad, V., Hamzeh'ee, B., and Naqinezhad, A. (2010). Botanical diversity of Hyrcanian forests; a case study of a transect in the

Kheyrud protected lowland mountain forests in northern Iran. *Phytotaxa*. 7, 1–18. doi: 10.11646/phytotaxa.7.1.1

Su, N., Jarvie, S., Yan, Y., Gong, X., Li, F., Han, P., et al. (2022). Landscape context determines soil fungal diversity in a fragmented habitat. *Catena*. 213, 106163. doi: 10.1016/j.catena.2022.106163

Takhtajan, A. (1969a). *Flowering Plants: Origin and Dispersal.* Edinbur: Oliver and Boyd.

Takhtajan, A. (1969b). *Flowering Plants: Origin and Dispersal* (transl. from Russian by C. Edinburgh.: Jeffrey). Gen_monocots, Gen_dicots, Evolution, Phylogeny (Edinbur: Oliver & Boyd).

Takhtajan, A. (1986). *Floristic Regions of the World* (translated by TJ. Crovello, edited by A. Cronquist). Berkeley, California: University of California Press.

Tareen, R. B., and Qadir, S. (1993). Harnai, Sinjawi to Duki regions of Pakistan. *Pak. J. Bot*. 25, 83–92.

Ullah, S., and Badshah, L. (2017). Floristic structure and ecological attributes of Jelar valley flora, district Upper Dir, Pakistan. *JBES*. 10, 89–105.

Ullah, Z., Ahmad, M., Sher, H., Shaheen, H., and Khan, S. M. (2015). Phytogeographic analysis and diversity of the grasses and sedges (Poales) of northern Pakistan. *Pak. J. Bot*. 47, 93–104.

Ur Rahman, A., Khan, S. M., Ahmad, Z., Alamri, S., Hashem, M., Ilyas, M., et al. (2021). Impact of multiple environmental factors on species abundance in various forest layers using an integrative modeling approach. *Global Ecol. Conserv*. 29, e01712. doi: 10.1016/j.gecco.2021.e01712

Wani, Z. A., Khan, S., Bhat, J. A., Malik, A. H., Alyas, T., Pant, S., et al. (2022a). Pattern of β-diversity and plant species richness along vertical gradient in Northwest Himalaya, India. *Biology*. 11, 1064. doi: 10.3390/biology11071064

Wani, Z. A., and Pant, S. (2021). *Aconitum heterophyllum* Wall. ex Royle: an endemic, highly medicinal and critically endangered plant species of Northwestern Himalaya in Peril. *Curr. Trad. Med*. 7, 2–7. doi: 10.2174/2215083807666210924162204

Wani, Z. A., and Pant, S. (2022). Tree diversity and regeneration dynamics in Gulmarg Wildlife Sanctuary, Kashmir Himalaya. *Acta Ecol. Sinica*. doi: 10.1016/j.chnaes.2022.05.003

Wani, Z. A., Samant, S. S., and Pant, S. (2021). Diversity, utilization pattern and representativeness of dye yielding plants in North Western and Western Himalaya, India: an untapped source for Bioprospection. *Environ. Dev. Sustain.* 2021, 1–18. doi: 10.1007/s10668-021-01664-x

Wani, Z. A., Satish, K., Islam, T., Dhyani, S., and Pant, S. (2022b). Habitat suitability modelling of Buxus wallichiana Bail.: an endemic tree species of Himalaya. *Vegetos*. 2022, 1–8. doi: 10.1007/s42535-022-00428-w

Watts, M., Hutton, C., Mata Guel, E., Suckall, N., and Peh, K. S.-H. (2022). Impacts of climate change on tropical agroforestry systems: a systematic review for identifying future research priorities. *Front. For. Global Change*. 175, 880621. doi: 10.3389/ffgc.2022.880621

Yang, Y., Chen, X., Liu, L., Li, T., Dou, Y., Qiao, J., et al. (2022). Nitrogen fertilization weakens the linkage between soil carbon and microbial diversity: a global meta-analysis. *Global Change Biol.* doi: 10.1111/gcb.16361

Zeb, S. A., Khan, S. M., and Ahmad, Z. (2021). Phytogeographic elements and vegetation along the river Panjkora-Classification and ordination studies from the Hindu Kush Mountains range. *Bot. Rev*. 2021, 1–25. doi: 10.1007/s12229-021-09247-1

Zhao, T., Shi, J., Entekhabi, D., Jackson, T. J., Hu, L., Peng, Z., et al. (2021). Retrievals of soil moisture and vegetation optical depth using a multi-channel collaborative algorithm. *Remote Sens. Environ*. 257, 112321. doi: 10.1016/j.rse.2021.112321

Zohary, M. (1950). The Flora of Iraq and its phytogeographical divisions. *Bull. Direct. General Agric. Iraq*. 31, 103–111.

frontiers | Frontiers in Forests and Global Change

TYPE Original Research
PUBLISHED 06 January 2023
DOI 10.3389/ffgc.2022.1044182

EDITED BY
Jahangeer A. Bhat,
Fiji National University, Fiji

REVIEWED BY
Sourav Mukhopadhyay,
Deccan College Post-Graduate and
Research Institute, Pune, India
Animesh Ghose,
McGill University, Canada

*CORRESPONDENCE
Amalava Bhattacharyya
✉ amalava@yahoo.com

†These authors have contributed equally to this work

SPECIALTY SECTION
This article was submitted to
Forest Management,
a section of the journal
Frontiers in Forests and Global Change

RECEIVED 14 September 2022
ACCEPTED 28 November 2022
PUBLISHED 06 January 2023

CITATION
Dhyani R, Bhattacharyya A, Joshi R, Shekhar M, Chandra Kuniyal J and Singh Ranhotra P (2023) Tree rings of *Rhododendron arboreum* portray signal of monsoon precipitation in the Himalayan region.
Front. For. Glob. Change 5:1044182.
doi: 10.3389/ffgc.2022.1044182

Tree rings of *Rhododendron arboreum* portray signal of monsoon precipitation in the Himalayan region

Rupesh Dhyani[1]†, Amalava Bhattacharyya[2]*†, Rajesh Joshi[3]†, Mayank Shekhar[2]†, Jagdish Chandra Kuniyal[1] and Parminder Singh Ranhotra[2]

[1]G.B. Pant National Institute of Himalayan Environment, Almora, Uttarakhand, India, [2]Birbal Sahni Institute of Palaeosciences, Lucknow, India, [3]G.B. Pant National Institute of Himalayan Environment, Sikkim Regional Centre, Pangthang, Sikkim, India

The Himalayas has a significant impact not just on the Indian subcontinent's monsoon patterns but also on the global climate. Monsoon failure causing drought has become more common in recent years. As a result, it poses a major threat to ecosystem sustainability. We reported for the first time, a climatic-sensitive tree ring chronology of a broadleaf tree, *Rhododendron arboreum,* spanning 1732–2017 CE from the Himalayan region. We discovered that the climate during the monsoon season limits the growth of this tree in this region. The correlation analysis between tree ring chronology and climate revealed a significant positive relationship with precipitation ($r = 0.63$, $p < 0.001$) and a negative relationship with temperature ($r = -0.48$, $p < 0.01$) during the months of June–August (JJA). This strong relationship allowed us to reconstruct monsoon precipitation spanning 1780 to 2017 CE which explained 40% of the variance of the observed climate data for the calibration period. The reconstructed data are validated by the existence of a significant association with the gridded JJA precipitation data of the Climate Research Unit (CRU) of this region. The monsoon rainfall record captured extremely wet years during 1793, 1950, 2011, 2013, and 2017 and extremely dry years during 1812, 1833, 1996, 2002, 2004, and 2005. The extremely dry and wet years well coincided with major catastrophic historical and instrumental droughts and floods in the region. Furthermore, the reconstructed data are also validated by the significant positive correlation ($r = 0.36$, $p < 0.001$, $n = 163$) with the all Indian summer monsoon rainfall series. Such data will be useful to predict the incidence of future droughts, which can help to assess the vulnerability of the forest ecosystem to extreme events.

KEYWORDS

summer monsoon, El-Nino Southern Oscillation (ENSO), tree rings, *Rhododendron arboreum*, Himalaya

1. Introduction

Comprehending the long-term frequency and severity of drought occurrences caused by monsoon failure is critical for understanding the negative impacts on natural ecosystems, food security, the economy, society, and civilization (IPCC, 2014). The Himalayas, which have the largest snow cover outside of the South and North Poles, act as a third pole. It has a significant impact on the monsoon climate dynamics of the Indian subcontinent and other regions of the world. The major shifts in climate causing floods and droughts are linked with the rise and fall of civilizations (Kathayat et al., 2017). The potential effect of hydroclimate alterations as a result of a changing global climate creates significant issues in mountainous regions, which are a source of public concern (Tiwari et al., 2018; Valdiya, 2020; Shekhar et al., 2022). The Indian summer monsoon is connected to numerous large-scale ocean/atmospheric circulation patterns and is exacerbated under global warming scenarios (Lal, 2003; Kripalani et al., 2007; Lucas-Picher et al., 2011; Menon et al., 2013; Roxy et al., 2015; Huang et al., 2020; Sabin et al., 2020). Studies have shown that monsoon dynamics are complicated and that spatiotemporal coverage of paleoclimatic data has to be enhanced to better understand long-term changes in atmospheric circulation patterns in monsoon Asia (Kale et al., 2003; Gupta et al., 2019). To enhance knowledge of the dynamics and causes of monsoon variability in Southeast Asia, several proxies, such as tree rings, ice cores, and speleothems, have been investigated to extend climatic records (Singhvi and Kale, 2010). Tree ring width is a commonly used proxy in the Himalayan regions to reconstruct precipitation and temperature (Bhattacharyya and Yadav, 1999; Singh et al., 2006; Yadav et al., 2011; Shekhar, 2014; Shekhar et al., 2022), relative humidity (Dhyani et al., 2021b), and droughts (Cook et al., 2010; Yadav et al., 2017; Shekhar et al., 2018; Dhyani et al., 2022a). In addition, a gridded spatial reconstruction of the Palmer Drought Severity Index (PDSI) throughout Asia included building the Himalayan drought history (Cook et al., 2010). There is a lack of tree ring width data from trees sensitive to monsoon precipitation in these studies, which were largely based on tree ring analysis of conifer trees, and are suited for the study of mostly pre-monsoon temperature and precipitation (Yadav et al., 1999, 2011; Singh et al., 2006; Dhyani et al., 2022b). The ability to reconstruct monsoon precipitation from the core monsoon area is limited, owing to a lack of lengthy meteorological data to calibrate and the assumption that trees associated with generally humid or copious rainfall have weak climate-sensitive tree ring sequences (Bhattacharyya et al., 1992; Bhattacharyya and Yadav, 1999). In the Himalayan region, there are various broad-leafed tree species with unique growth rings (Gamble, 1922; Bhattacharyya and Yadav, 1999; Dhyani et al., 2021a), and their responses to climate change may vary from conifers.

However, no effort has been made to reconstruct climate using tree ring data from this broad-leafed tree from the Himalayan region. In order to fill this gap, we examined the tree rings of *Rhododendron arboreum* which is an essential component of subtropical to temperate forests in the Himalayas. The *Rhododendron* genus, as a whole, confines in a vast variety of forests from lower subtropical to alpine and extending from east to west Himalayas (Wester et al., 2019). In the Himalayas, this genus has 87 species, six of which have been identified from the Western Himalayan region (Sekar and Srivastava, 2010). It may grow in a variety of conditions, including steep zones with a lot of rain (Cox, 1990; Gibbs et al., 2011). Despite its vast range of niches from subtropical to alpine, tree ring research has been limited mostly to its shrub form in the Hindu Kush Himalaya (HKH) mountain's tree line zone (Liang and Eckstein, 2009; Kong et al., 2012; Li et al., 2013; Bi et al., 2017). The tree ring sequence of *Rhododendron* spp. extends up to 400 years (Lu et al., 2015).

The objective of the present study was to develop the tree ring chronology of a broad-leafed tree *Rhododendron arboreum*, from the Western Himalayan region and assess its potential for hydroclimatic reconstruction and its linkages to rising temperatures and erratic monsoon precipitation as a result of global warming.

2. Materials and methods

2.1. Study area and sample collection

For the present study, the target area of Darma valley falls in an area under Pithoragarh District in Kumaun Province (29^0 59′ to 30^0 04′ N and 80^0 28′ to 80^0 57′ E). This site is located in the eastern part of the Western Himalayas (**Figure 1**). In this area, *R. arboreum* is an under-canopy medium-sized evergreen tree growing between 1,200 m and 3,000 m altitude, mostly in oak-dominated forests. We collected 84 increment cores from 45 *R. arboreum* trees growing at the upper approximately limit of the forest around 2,700 m in a south-facing moderate gently slope, using the dendrochronological concept that trees from the ecotone zone of forests along altitudinal range have comparatively more climatic sensitive tree rings. Considering this view, we have selected trees growing in the ecotone of temperate and subalpine forests at the study site. We have collected a minimum of two cores from each tree at a height of approximately 1.37 m, using an increment borer, preferably in the opposite direction except in some trees where other sides are rotten.

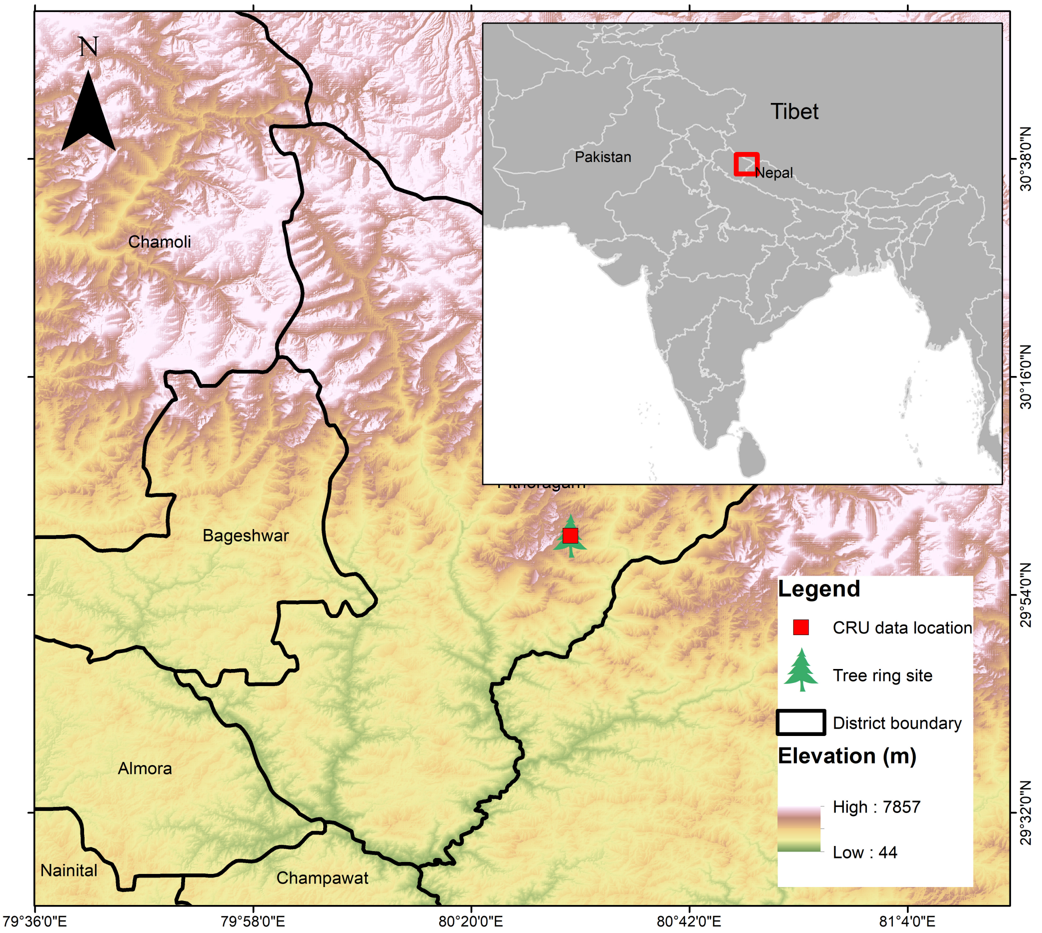

FIGURE 1
Map of the study sites showing tree ring sampling locations (green trees) and nearest Climate Research Unit (CRU) grid locations (red squares).

2.2. Climate data

In order to establish relationships between tree growth and climatic parameters, climate data from surrounding tree ring sites are often preferable. However, there are few meteorological stations with long records in the Himalayan region, and most of them are located distant from tree ring sampling locations. In the absence of a meteorological station at the close of the sampling site, we used g data for tree growth climate relationships that would reflect the natural habitat of *Rhododendron*. Monthly temperature and precipitation data from the gridded data set CRU TS version 4.01 (Harris et al., 2020) with a spatial resolution of 0.5° × 0.5° were used as a predictor for tree growth–climate response analyses for the period of 1901–2017 CE. The area receives most of its rainfall during the summer monsoon season (June–September) which contributes 70.45% of the total. The rainfall during the winter season (December–February) is quite low (**Figure 2A**). The annual mean temperature in the study area is 11.7°C, varying from 9–16°C in spring (MAM) to 17–17.95°C in summer (JJAS) and in winter from 3 to 5°C (**Figure 2B**). The higher temperature is observed during June (17.95°C) and July (17.81°C).

2.3. Tree ring chronology

Samples were mounted and processed using standard procedures of tree-ring analysis. Boundaries of tree rings in *R. arboreum* are faint, delineated by a light line of terminal parenchyma. Thus, counting rings under a stereo-zoom microscope required careful examination. Each ring of these cores was dated to the calendar year of its formation using the cross-dating technique (Fritts, 2012). The ring widths of each dated core were measured using an increment measuring stage with 0.001 mm precision coupled with a microcomputer. Later, these measurements and dates were checked using the computer program COFECHA (Holmes, 1983; Grissino-Mayer, 2001). Cores having errors were reexamined to evaluate the

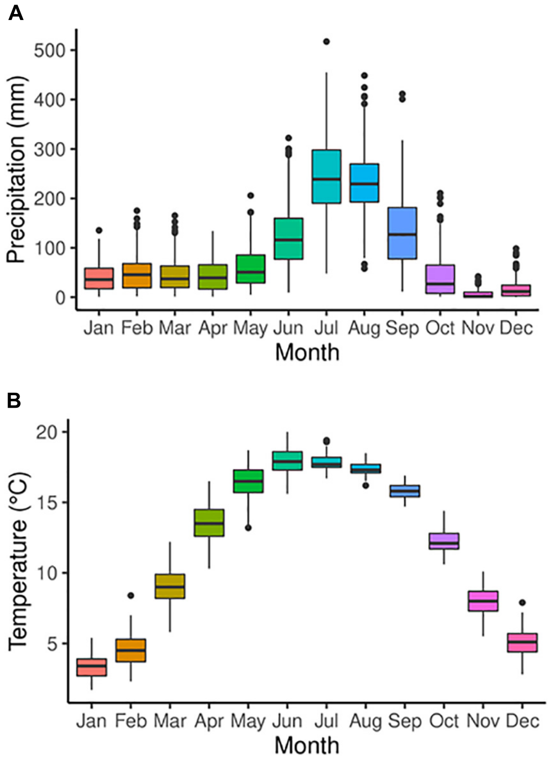

FIGURE 2

Boxplot showing monthly mean climate data for the region. **(A)** Monthly mean precipitation; **(B)** monthly mean temperature over the period 1902–2017.

source of the errors, and corrections were made. Ring-width data were standardized using the program ARSTAN (Holmes, 1983), which removes growth trends related to age and stand dynamics while retaining the maximum common signal to form tree-ring indices. For standardization, we used the cubic spline method using a cutoff of 2/3 of the time series to enhance the common climate signal in the chronology (Cook and Holmes, 1996). The variance of individual tree ring width data was stabilized using power transformation method by minimizing the heteroscedasticity before the standardization (Cook and Peters, 1997). We used residual chronology (**Figure 3**) that was developed using an autoregressive model by removing persistence from the raw tree ring chronology (Cook and Peters, 1997). The chronology was evaluated by several statistical parameters including mean sensitivity (MS), signal-to-noise ratio (SNR), common variance (Rbar), and low first-order autocorrelation (AC1) which are commonly used in tree ring analysis (Fritts, 2012). We also employed the Durbin-Watson statistic test in order to confirm that the residuals from the observed and reconstructed data are independent and have no autocorrelation (Fritts, 2012). The expressed population signal (EPS $\geq$ 0.85) was taken as an indicator of the threshold for dendroclimatic reconstruction (Wigley et al., 1984).

2.4. Statistical analysis

The climate-tree growth relationship was analyzed using Pearson's correlation coefficients on a monthly basis for the identification of significant months or seasons limiting the growth of *Rhododendron* from the common period of tree ring chronology and climate record (1902–2017 CE). Both the stability and reliability of the regression equations were assessed using the split sample method (Fritts, 1991). These validation trials were performed by calibrating climate data from a sub-period 1902–1957 CE and verifying the reconstruction using the remaining data from 1958 to 2017 CE. The results were evaluated by the correlation coefficient (r), sign test (ST), reduction of error test (RE), product mean test (t), and coefficient of efficiency (CE) during the verification period (Fritts, 2012). The values of RE and CE greater than zero specify well model skill (Cook et al., 1999). Moreover, the values of CE are more rigorous and are typically lower than those of RE, but it is more difficult for CE values to pass the test (Cook et al., 1999). We quantified high and low precipitation here based on values greater or lesser than mean ± standard deviation ($m \pm 1$ SD). The extreme high and low precipitation was designated based on values greater or lesser than $m \pm 2$ SD. To analyze the cyclic behavior of reconstructed data, we performed spectrally and wavelet analysis (Grinsted et al., 2004). We also assessed the regional behavior of reconstructed data, by spatial correlation of reconstructed data with gridded Climate Research Unit (CRU TS4.02) precipitation (Harris et al., 2020) using KNMI climate explorer (Van Oldenborgh and Burgers, 2005). We also analyzed the effect of the El-Nino Southern Oscillation (ENSO) on our tree ring chronology using correlation with NINO3.4 sea surface temperatures (SSTs) and Pacific Decadal Oscillation (PDO). Moreover, we performed a 21-year moving correlation analysis with the time series of the reconstructed monsoon and NINO3.4 and PDO, respectively, to understand their long-term teleconnections. Furthermore, we made correlation analysis between the reconstructed data with all Indian summer monsoon rainfall (ISMR) to validate whether the monsoon precipitation of this site is a part of the Indian summer monsoon regime. We have also performed a regime shift analysis method to determine the timing and magnitude of regime shifts in the reconstructed data (Room et al., 2022).

3. Results

3.1. Tree ring chronology statistics

Tree ring width index (RWI) chronology of 286 years (spanning 1732–2017 CE, **Figure 3**) revealed a moderate MS, high SD, and high SNR and Rbar (**Table 1**). The value of MS (0.29) indicated low inter-annual variations. The Rbar (0.34) and EPS (0.88) values were also indicators of the reliability of

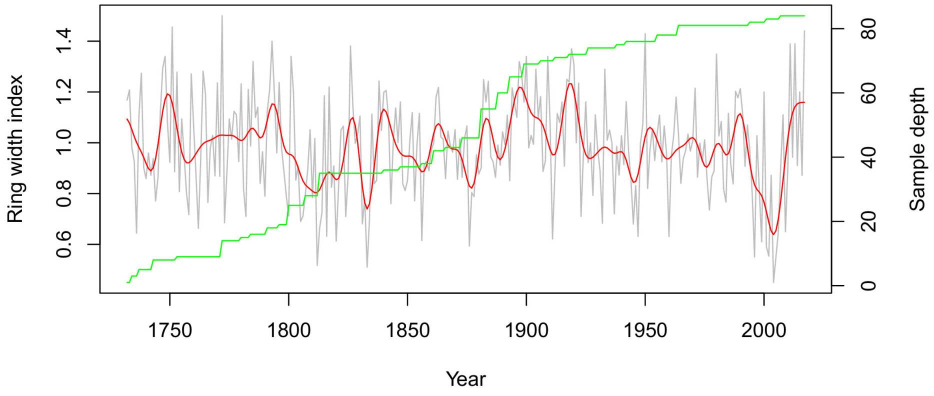

FIGURE 3
Ring-width index (RWI) chronology of *Rhododendron arboreum* from Darma valley; green line indicates sample depth, and red line plot indicates 10-year low-pass filter.

this chronology for climate reconstruction. The EPS value > 0.85 for the period 1780–2017 CE was considered reliable for climate reconstruction. We have not used chronology beyond 1780 CE because EPS is low due less number of samples in early part of the tree growth. By observing chronology, we noted distinct changes in tree growth patterns in recent decades. There is a declining trend during 1990–2004 CE followed by an increasing trend in recent years (**Figure 3**).

3.2. Tree growth and climate relationship

The growth of *R. arboreum* has a significant negative correlation with temperature for the months of June ($r = -0.31$, $n = 115$, $p < 0.001$), July ($r = -0.32$, $n = 115$, $p < 0.001$), and August ($r = -0.34$, $n = 115$, $p < 0.001$) (**Figure 4A**) and positive correlation with precipitation of the current year's monsoon months June ($r = 0.46$, $n = 115$, $p < 0.001$), July ($r = 0.39$, $n = 115$, $p < 0.001$), and August ($r = 0.41$, $n = 115$, $p < 0.001$) (**Figure 4B**). The overall high correlation with precipitation during the monsoon season for the months June–August (JJA) ($r = 0.63$, $p < 0.001$) indicates its suitability for the reconstruction of precipitation.

TABLE 1 Statistics of developed tree ring chronology of *Rhododendron arboreum*.

Time period	1732–2017
Number of cores (Tree)	84 (45)
Mean sensitivity	0.29
Standard deviation	0.25
Rbar	0.34
Signal to noise ratio	11.24
Expressed population signal	0.88
EPS > 0.85	1780

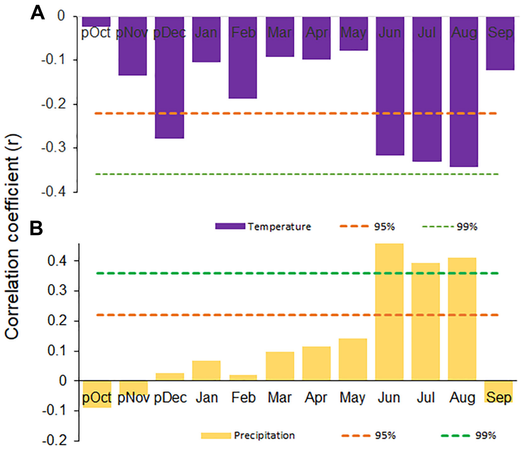

FIGURE 4
Pearson correlation between tree ring width chronology and climate data; **(A)** mean temperature (purple bar) and **(B)** mean precipitation (yellow bar). The red and green dotted lines indicate 95 and 99% significant confidence levels.

3.3. Extended records of monsoon precipitation

A linear model $PPT_{JJA} = 60.99 + 246.18*RWI$, where PPT_{JJA} represents reconstructed June–August precipitation, was developed and used for the reconstruction of precipitation during JJA of monsoon season since 1780 AD based on the residual tree ring chronology (**Figure 5A**). The regression model accounts for 40% of the variance over the calibration period from 1902 to 2017 (**Figure 5B**). The statistics of

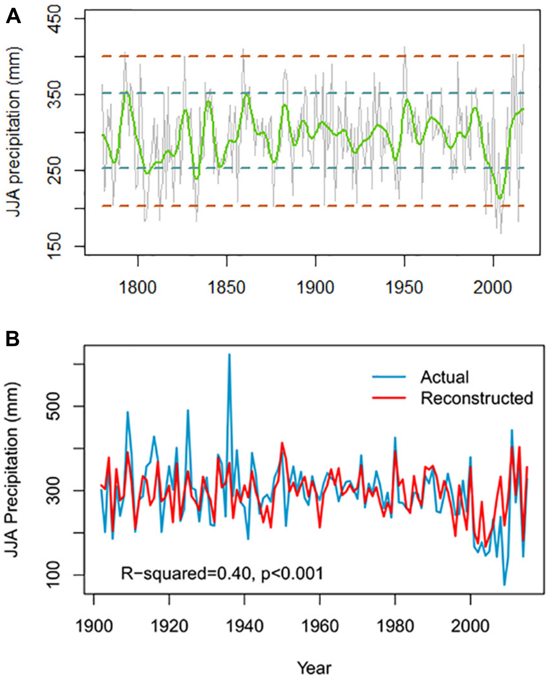

FIGURE 5
Reconstruction of PPT_{JJA} in Darma, valley, Western Himalaya; **(A)** the reconstructed June–August (JJA) precipitation (Grey line plot) for the period 1780–2017. Dotted blue and orange line plots indicate $m \pm$ SD and $m \pm 2$ SD of the reconstructed data. The green smoothed line indicates a 10-year low-pass filter and **(B)** time series of observed (blue line plot) and reconstructed (red line plot) JJA.

calibration and verification showed that model performance is reliable (Table 2). Importantly, the positive values of rigorous tests CE and RE during the verification period indicated good skills in our reconstructed data. The value of Durbin-Watson statistics shows that autocorrelation in regression model residuals is negligible. The synchronicity between actual and reconstructed data confirmed the reliability of the regression model (**Figure 5B**). We recorded 43 wet and 34 dry years which accounted for 18.06 and 14.28% of the total years since 1780 (**Supplementary Table 1**). Also, we recorded 6 (2.10%) extreme wet and 6 (2.10%) extreme dry years in the reconstructed data (**Supplementary Table 1**). Regime shift analysis indicated that the region experienced significant ($p < 0.05$) phases depicting prolonged wet conditions during the period 1780–2004 and 2011–2017 and prolonged dry conditions during 1805–1837 and 1995–2010 (**Supplementary Figure 1**).

3.4. Spatial characteristics and teleconnections

Reconstructed precipitation shows a strong positive correlation with the ISMR data, 1900–2017 CE ($r = 0.36$, $p < 0.001$, **Supplementary Figure 2A**), which indicates that the site is under the regional impact of the Indian summer monsoon. The spatial correlation analysis between reconstructed PPT_{JJA} with gridded JJA precipitation over the western and central parts of the Indian Himalayas exhibited a significant positive correlation ($p < 0.05$) during the period 1902–2017 (**Figure 6**). Such coherence in records represents a regional behavior of monsoon precipitation covering a wider area in the Himalayan region. Moreover, wavelet analysis identified significant high-frequency cycles ranging from 2–8 years to 16–32 years (**Figure 7**). Furthermore, a significant negative correlation ($r = -0.16$, $p < 0.05$, **Supplementary Figure 2B**) with June–August NINO3.4 SSTs for the period 1900–2017 CE and June–August PDO ($r = -0.19$, $p < 0.05$, **Supplementary Figure 2C**) during 1850–2017 indicate a long-term effect of ENSO and PDO over the monsoon variability at this region. The 21-year moving correlation analysis between NINO3.4 and PDO each with the reconstructed JJA precipitation shows a distinct pattern of correlation at some intervals (**Supplementary Figure 3**). For NINO3.4, a significant negative correlation was observed during 1900–1943 ($r = -0.47$, $p < 0.05$, **Supplementary Figure 3**) and 1946–1971 ($r = -0.42$, $p < 0.05$, **Supplementary Figure 3**). For other time intervals, we did not find any significant correlations. In the case of PDO, a significant negative correlation was observed for the periods 1940–1971 ($r = -0.43$, $p < 0.05$, **Supplementary Figure 3**) and 1957–1981 ($r = -0.48$, $p < 0.05$, **Supplementary Figure 3**).

4. Discussion

4.1. Growth/climate response of *R. arboreum*

Through dendroclimatic analysis of the *R. arboreum tree*, growing in Drama valley, Western Himalaya, we established the potentiality of this broad-leaved tree in the reconstruction of the monsoon precipitation. It is so far, the longest tree ring record of *Rhododendron* that showed evidence of sensitivity to summer monsoon season. This is evident with the existence of significant positive correlations with precipitation (JJA) and an inverse relationship with the temperature of the same months. The earlier tree ring analyses of *Rhododendron* species were on its shrub form growing in the Tibetan plateau and central Himalayas (Liang and Eckstein, 2009; Lu et al., 2015; Bi et al., 2017; Panthi et al., 2017). Regarding the response to climate, the mean temperature of July, irrespective of slope aspects, and elevations play a key role in controlling wood formation in the Tibetan plateau (Frank et al., 2005; Leal et al., 2007; Hallinger et al., 2010; Blok et al., 2011; Weijers et al., 2012; Lu et al., 2015). In the central Himalayas, increased minimum winter temperatures have a significant role in the growth of this taxon (Panthi et al., 2021). However, our results are not consistent

TABLE 2 Calibration and verification statistics of reconstructed PPT_{JJA}.

Calibration period					Verification period						
	r	R^2	Adj. R^2	F		Sign test (+/−)	PMT	RMSE	RE	CE	DW
1902–1957	0.59	0.35	0.34	29.28**	1958–2017	40+/16−*	2.91	49.05	0.52	0.22	1.21
1958–2017	0.71	0.51	0.50	61.02	1902–1957	41+/15−*	1.72	67.55	0.32	0.31	1.81
1902–2017	0.63	0.40	0.39	98.99**							

r: correlation coefficient; R^2: explained variance; F: F-test. Sign-test sign of paired observed and estimated departures from their mean on the basis of the number of agreements/disagreements. Pmt, product mean test; RMSE, Root mean squared error, RE, reduction of error; CE, coefficient of efficiency; DW, Durbin–Watson test; $^*p < 0.05$, $^{**}p < 0.01$.

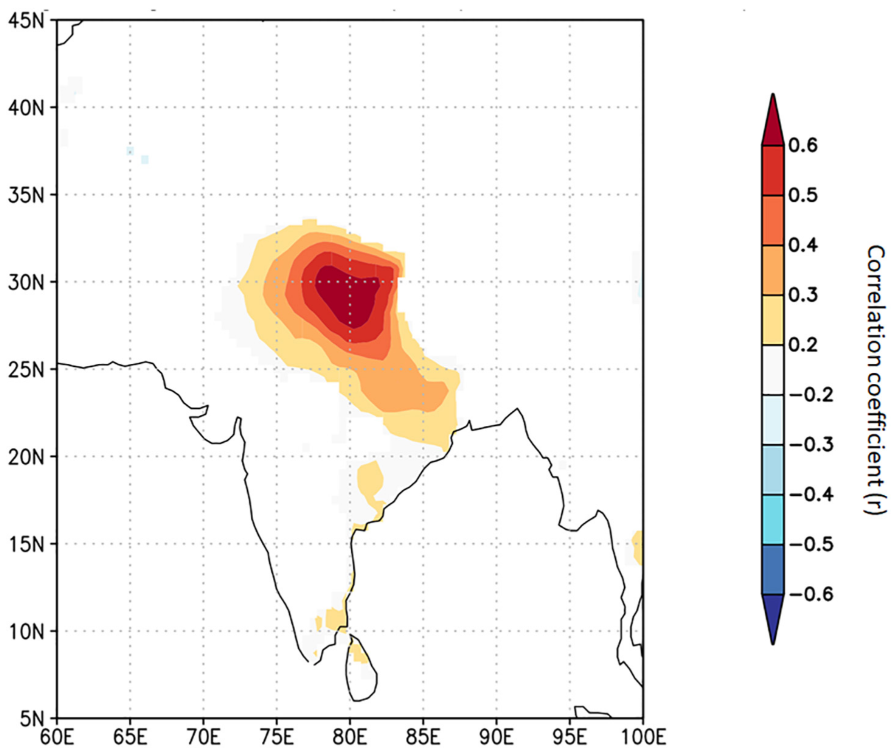

FIGURE 6

Spatial correlation of the reconstructed PPT_{JJA} with gridded CRU JJA precipitation during the period 1902–2017.

with these findings. Tree growth response to climate changes is differing from site to site due to differences in life forms (tree/shrub), species, geographical locations, and elevation differences. Tree growth climate relationship recorded in the present study, however, showed some consistency in climatic response with *Rhododendron aganniphum* shrub growing at the 4,000–4,500 m of the Tibetan plateau where it also shows a similar favorable response to July month's precipitation though it is not statistically significant (Lu et al., 2015). We recorded in *R. arboreum* that the increased temperature during the monsoon season is detrimental to its growth in the temperate belt of the western Indian Himalayan region. During the JJA months, both temperature and precipitation are at their highest in this region. Thus, a rise in temperature during these months might limit photosynthesis by increasing evapotranspiration. It appears that the increased summer precipitation and low temperature in the Himalayan region promote the growth of *Rhododendron*. This also supports the current spatial distribution of 127 species in the Indian Himalayan region. A greater concentration (98%) of species is confined to the cool moist part of the North-East in comparison to the drier western part (Mao, 2010), indicating a preference for cool-moist environments.

4.2. Salient features of reconstructed PPT_{JJA}

The present study is a maiden attempt to derive a reliable 238-year (1780–2017) summer monsoon precipitation record from the Western Himalayan region. This reconstruction

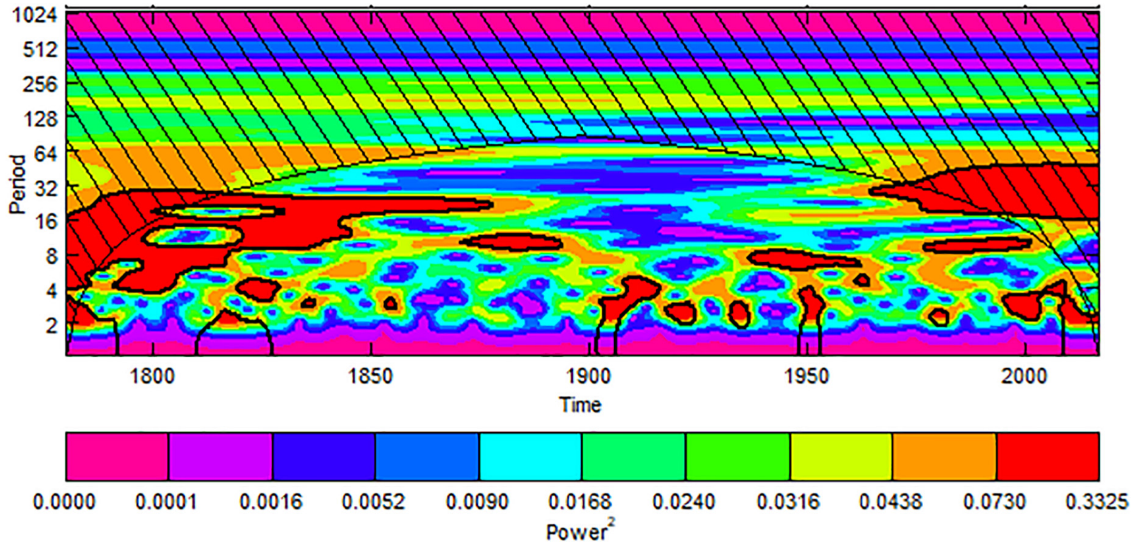

FIGURE 7
Morlet wavelet spectrum with a high edge effect and a red-noise background at 95% confidence level (black lines/contours) for reconstructed PPT_{JJA}.

provides a long-term drought variability and captured extreme events that are also witnessed in the historical records. In the recent past, the region exhibited a rapid and extended dry period from 1995 to 2010, which is consistent with the recent decadal decrease in tree ring-based rainfall reconstruction in the Western Himalayan region (Sano et al., 2012, 2017; Xu et al., 2018) and even in climatic assessment based on meteorological data (Roxy et al., 2015). However, in recent decades, we observed an increase in rainfall patterns that was not captured by earlier studies. This inconsistency may be due to the Himalayan region's distinct sources and seasonal distribution of precipitation. The decreased monsoon locations seem to be more influenced by the increased snow cover than the present study sites. During the monsoon season, years with high snowfall in the preceding winter and spring are followed by summer with less monsoon rain (Blanford, 1884; Bamzai and Kinter, 1997). This is further reinforced by the idea that greater wetness in the northwestern Himalayas has influenced anomalous glacier progress in recent years and that increasing snowfall may contribute to dry conditions in summer (Yadav et al., 2017; Ahmad et al., 2020). Interestingly, since 2010, an increase in Indian summer rainfall has been reported in several gridded and observed datasets throughout the Indian subcontinent (Jin and Wang, 2017). This increase in summer monsoon precipitation has been linked to greater thermal contrast between land and ocean, as seen by a faster warming rate across the Indian subcontinent compared with a slower warming rate over the Indian Ocean (Jin and Wang, 2017). On the contrary, due to the rapid warming of the Indian Ocean, the land-sea thermal contrast weaken, and a significant reducing trend of summer monsoon during 1995–2010 was caused. The extreme droughts of the Indian summer monsoon years 2002 and 2004[1] are consistent with our reconstructed data. Singh et al. (2019) also from the central Himalayan region reported the severe droughts of 2002 and 2004. The major extreme wet years in 2013 and 2017 are also consistent with regional floods that happened in Kumaun which caused catastrophic damage and devastation in the region. We have noticed that several key prolonged dry and wet conditions in the reconstructed monsoon records are correlated with the other tree ring proxy-based reconstructions from the Himalayan region. A significant positive correlation of our reconstructed PPT_{JJA} with reconstructed JJA PDSI ($r = 0.20$, $p < 0.001$) from monsoon Asia during the period 1780–2005 (Cook et al., 2010) and May–September precipitation ($r = 0.14$, $p < 0.05$) from Bhutan Himalaya (Sano et al., 2013) during the period 1780–2011 further indicates regional linkages. The late 18th century droughts from 1785 to 1794s in JJA PDSI (Cook et al., 2010), March–September precipitation (Sano et al., 2013), March–September PDSI (Ahmad et al., 2020), and March–July precipitation (Singh et al., 2009), as well as historical East India Drought (1790–1796), are also common in our reconstructed precipitation data (**Figure 8**). Similarly, the dry episodes of 1830–1836 synchronize with May–September precipitation reconstruction (Sano et al., 2013). The other common dry phase of 1865–1875 in March–September PDSI (Ahmad et al., 2020), MS precipitation (Sano et al., 2013), May–June PDSI (He et al., 2018), and the previous year October to current year September precipitation reconstruction (Singh et al., 2021)

---

[1] https://www.tropmet.res.in/~kolli/MOL/Monsoon/Historical/air.html

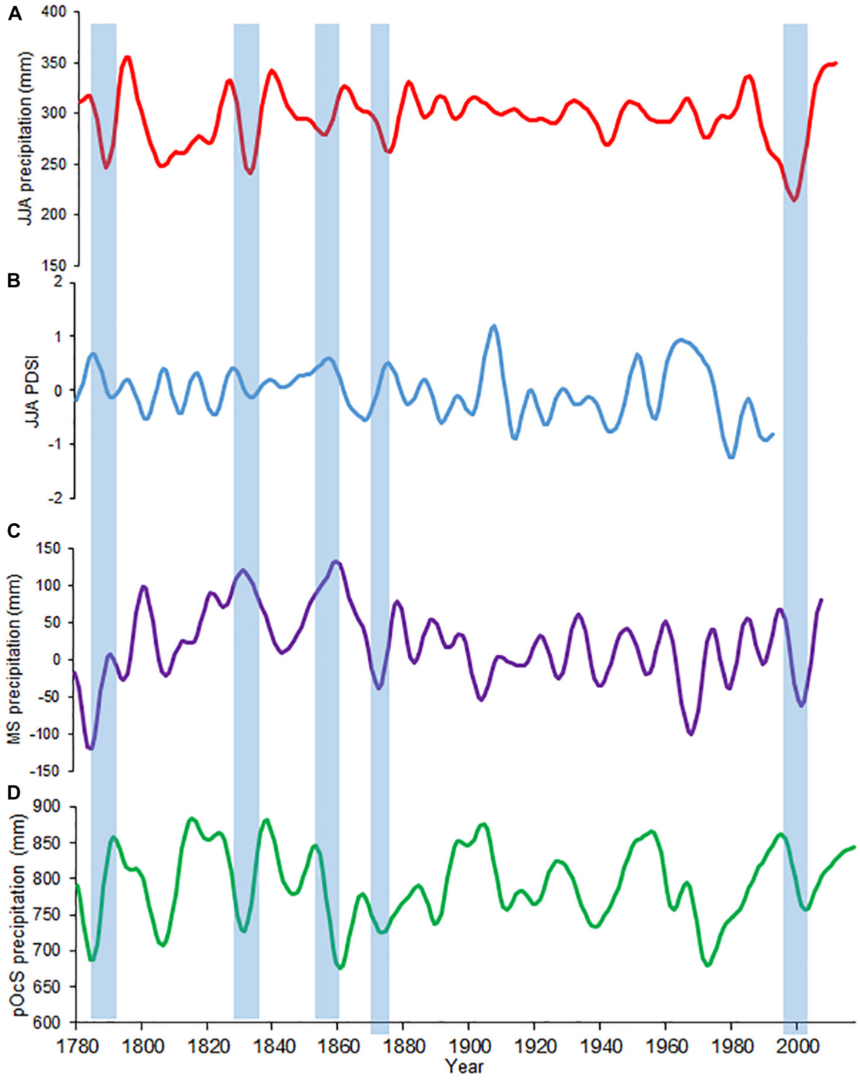

FIGURE 8
Comparison of **(A)** reconstructed PPT_{JJA} with **(B)** JJA PDSI reconstruction from Asia (Cook et al., 2010), **(C)** May–September (MS) precipitation reconstruction from Bhutan Himalaya (Sano et al., 2013), and **(D)** previous October–Current September (pOcS) precipitation reconstruction from Indian Western Himalaya (Singh et al., 2021). All the line plots are smoothed by a 10-year low-pass smoothing filter.

are also more or less synchronized with our reconstruction. Since last three decades, late 1995–2004s drought phase (Sano et al., 2013; Singh et al., 2021) and drought records (Cook et al., 2010) are also congruent with our study. The wet phase after 2010 was well coincide with May–September precipitation records from Bhutan Himalaya (Sano et al., 2013). The historical East India Drought (1790–1796) is also common with the reconstructed low monsoon precipitation data (Cook et al., 2010). Such coherence in drought events are observed at some intervals in these studies, even when sites are not from under similar climatic zones and use of different climatic proxies. Such coherence may be a role of upper atmospheric circulation affecting both monsoon and western disturbance. We observed that the calibration period (1905–1957) was unable to capture extreme event years. These extreme values were underestimated in tree ring calibrations, because of precipitation beyond a threshold value are not always possible to retrieve from tree rings (Singh et al., 2009; Yadav, 2011). Moreover, according to wavelet analysis, the cyclicity of 2–4 and 16–32 years is likely to be associated with ENSO and PDO which is also found in moving correlation analysis between reconstructed PPT_{JJA} with ENSO and PDO (**Figure 6**). It indicates that PPT_{JJA} changes in our study area have teleconnections with large-scale atmospheric circulation systems. Interestingly, the severe drought occurrences of 2009 coincided with the same El-Nino year; nevertheless, other extreme drought years, such as 2005 and 2006, correspond to the preceding El-Nino event years of 2004 and 2005, respectively. This might be due to the lag effect of tree growth in relation to climate. Extreme wet/dry growth years are often recorded to follow with years of wide/narrow tree rings due to role of stored food in trees. Stored food effect subsidized the impact of El-Nino in the same year but its role of deficient rainfall in reducing photosynthesis felt in the following year. To increase our knowledge of Asian monsoon dynamics, we need a better understanding of the spatial and temporal variability of precipitation in the Himalayas.

5. Conclusion

Tree ring width data of the broad-leaved *R. arboreum* tree (spanning 1780–2017 CE) was analyzed first time from the core monsoon region of the Himalayas. We recorded that the chronology of this tree is the potential for the reconstruction of monsoon (JJA) precipitation. The extended precipitation data not only provided information on long-term drought variability but also captured extreme events. With the absence of a sufficient long monsoon record in the Himalayan region, the present database would help improving in the understanding of regional climate models, especially variability in monsoon precipitation. Moreover, the biogeographical point of view of this study has great relevance, providing insight into the growth behavior of the temperate tree, *Rhododendron* in relation to monsoon precipitation. This information would be helpful to policymakers in taking adaptation measures in forest management to protect the marginal communities of the Himalayan region from the anticipated adverse impacts of future droughts. We observed that the great altitudinal distributional range of *Rhododendron* spp. would be ideal for dendroclimatic analyses for the understanding of diversified aspects of seasonal climate changes in the Himalayan region. The presence of shrub form, *Rhododendron Campanulatum*, above 3,500 m altitude at the present study site would be useful to analyze climatic factors governing its growth at its upper limit close to the snow line. Thus, a detailed study using multiple tree-ring chronologies of *Rhododendron* species from a wider altitudinal range, as well as combined with geomorphological, glacial mass balance records, and other evidence, would provide a better database to quantify tree growth/monsoon climate/glacial relationships over a longer timescale from the Himalayan region.

Data availability statement

The raw data supporting the conclusions of this article will be made available by the authors, without undue reservation.

Author contributions

RD: data creation, visualization, and writing—original draft. RD and MS: formal analysis. RD, RJ, MS, and AB: investigation. JC, PS, RD, and AB: methodology. RJ, RD, AB, MS, JC, and PS: writing—review and editing. All authors contributed to investigation, writing—review and editing, read, and agreed to the published version of the manuscript.

Funding

The financial support provided by the Department of Science and Technology, Government of India under NMSHETF3 (Phase-II) is highly acknowledged.

Acknowledgments

We are thankful to the Director, NIHE for providing facilities in the institute which could make the present study possible. We also thank the Forest Department, Government of Uttarakhand for providing necessary permission during the collection of tree–ring samples. AB and MS express gratitude to the Director BSIP, Lucknow for providing laboratory facilities and permission to carry out this collaborative research study.

Conflict of interest

The authors declare that the research was conducted in the absence of any commercial or financial relationships that could be construed as a potential conflict of interest.

Publisher's note

Supplementary material

The Supplementary Material for this article can be found online at: https://www.frontiersin.org/articles/10.3389/ffgc.2022.1044182/full#supplementary-material

References

Ahmad, S., Zhu, L., Yasmeen, S., Zhang, Y., Li, Z., Ullah, S., et al. (2020). A 424-year tree-ring-based palmer drought severity index reconstruction of *Cedrus deodara* D. don from the hindu kush range of Pakistan: Linkages to ocean oscillations. *Clim. Past* 16, 783–798. doi: 10.5194/cp-16-783-2020

Bamzai, A., and Kinter, J. (1997). *Climatology and interannual variability of Northern Hemisphere snow cover and depth based on satellite observations*. Kanagawa: Institute of Global Environment.

Bhattacharyya, A., LaMarche, V. Jr., and Hughes, M. (1992). Tree-ring chronologies from Nepal. *Tree Ring Bull.* 52, 59–66.

Bhattacharyya, A., and Yadav, R. (1999). Climatic reconstructions using tree-ring data from tropical and temperate regions of India-a review. *IAWA J. Brill* 20, 311–316. doi: 10.1163/22941932-90000693

Bi, Y., Xu, J., Yang, J., Li, Z., Gebrekirstos, A., Liang, E., et al. (2017). Ring-widths of the above tree-line shrub *Rhododendron* reveal the change of minimum winter temperature over the past 211 years in Southwestern China. *Clim. Dyn.* 48, 3919–3933. doi: 10.1007/s00382-016-3311-4

Blanford, H. II (1884). On the connexion of the Himalaya snowfall with dry winds and seasons of drought in India. *Proc. R. Soc. Lond.* 37, 3–22. doi: 10.1098/rspl.1884.0003

Blok, D., Sass-Klaassen, U., Schaepman-Strub, G., Heijmans, M., Sauren, P., and Berendse, F. (2011). What are the main climate drivers for shrub growth in Northeastern Siberian tundra? *Biogeosciences* 8, 1169–1179. doi: 10.5194/bg-8-1169-2011

Cook, E., Anchukaitis, K., Buckley, B., D'Arrigo, R., Jacoby, G., and Wright, W. (2010). Asian monsoon failure and megadrought during the last millennium. *Science* 328, 486–489. doi: 10.1126/science.1185188

Cook, E., and Holmes, R. (1996). Guide for computer program arstan. *Int. Tree Ring Data Bank Prog. Lib. Vers.* 2, 75–87.

Cook, E., Meko, D., Stahle, D., and Cleaveland, M. (1999). Drought reconstructions for the continental United States. *J. Clim.* 12, 1145–1162. doi: 10.1175/1520-0442(1999)012<1145:DRFTCU>2.0.CO;2

Cook, E., and Peters, K. (1997). Calculating unbiased tree-ring indices for the study of climatic and environmental change. *Holocene* 7, 361–370. doi: 10.1177/095968369700700314

Cox, P. (1990). *The larger rhododendron species*. London: Batsford.

Dhyani, R., Shekhar, M., Joshi, R., Bhattacharyya, A., Ranhotra, P., Pal, A., et al. (2021b). Reconstruction of pre-monsoon relative humidity since 1800 C.E. based on tree-ring data of *Pinus roxburghii sarg.* (chir–pine) from Pithoragarh, Western Himalaya. *Q. Int.* 629, 4–15. doi: 10.1016/j.quaint.2021.04.026

Dhyani, R., Bhattacharyya, A., and Rawal, R. (2021a). The oldest Birch tree in the Western Himalaya depicting signature of major climatic events of the recent era in its tree rings. *Curr. Sci.* 121, 350–353.

Dhyani, R., Bhattacharyya, A., Singh Rawal, R., Joshi, R., Shekhar, M., and Singh Ranhotra, P. (2022a). Is tree ring chronology of blue pine (*Pinus wallichiana* A. B. Jackson) prospective for summer drought reconstruction in the Western Himalaya? *J. Asian Earth Sci.* 229:105142. doi: 10.1016/j.jseaes.2022.105142

Dhyani, R., Joshi, R., Ranhotra, P., Shekhar, M., and Bhattacharyya, A. (2022b). Age dependent growth response of *Cedrus deodara* to climate change in temperate zone of western himalaya. *Trees For. People* 8:100221. doi: 10.1016/j.tfp.2022.100221

Frank, D., Wilson, R., and Esper, J. (2005). Synchronous variability changes in alpine temperature and tree-ring data over the past two centuries. *Boreas* 34, 498–505. doi: 10.1080/03009480500231443

Fritts, H. (1991). *Reconstructing large-scale climatic patterns from tree-ring data: T diagnostic analysis*. Arizona: University of Arizona Press.

Fritts, H. (2012). *Tree rings and climate*. Amsterdam: Elsevier.

Gamble, J. (1922). *A manual of Indian timbers: An account of the growth, distribution, and uses of the trees and shrubs of India and Ceylon, with descriptions of their wood-structure*. London: S. Low, Marston & Company Limited.

Gibbs, D., Chamberlain, D., and Argent, G. (2011). *The red list of Rhododendrons*. Richmond, UK: Botanic Gardens Conservation International.

Grinsted, A., Moore, J., and Jevrejeva, S. (2004). Application of the cross wavelet transform and wavelet coherence to geophysical time series. *Nonlinear Process. Geophys.* 11, 561–566. doi: 10.5194/npg-11-561-2004

Grissino-Mayer, H. (2001). . Evaluating crossdating accuracy: A manual and tutorial for the computer program cofecha. *Tree Ring Soc.* 57, 205–221.

Gupta, A., Negi, M., Nandy, S., Alatalo, J., Singh, V., and Pandey, R. (2019). Assessing the vulnerability of socio-environmental systems to climate change along an altitude gradient in the Indian Himalayas. *Ecol. Indicat.* 106:105512. doi: 10.1016/j.ecolind.2019.105512

Hallinger, M., Manthey, M., and Wilmking, M. (2010). Establishing a missing link: Warm summers and winter snow cover promote shrub expansion into alpine tundra in Scandinavia. *New Phytol.* 186, 890–899. doi: 10.1111/j.1469-8137.2010.03223.x

Harris, I., Osborn, T., Jones, P., and Lister, D. (2020). Version 4 of the CRU TS monthly high-resolution gridded multivariate climate dataset. *Sci. Data* 7, 1–18. doi: 10.1038/s41597-020-0453-3

He, M., Bräuning, A., Grießinger, J., Hochreuther, P., and Wernicke, J. (2018). May–June drought reconstruction over the past 821 years on the south-central Tibetan Plateau derived from tree-ring width series. *Dendrochronologia* 47, 48–57. doi: 10.1016/j.dendro.2017.12.006

Holmes, R. (1983). Computer-assisted quality control in tree-ring dating and measurement. *Tree Ring Bull.* 43, 69–78.

Huang, X., Zhou, T., Turner, A., Dai, A., Chen, X., Clark, R., et al. (2020). The recent decline and recovery of indian summer monsoon rainfall: Relative roles of external forcing and internal variability. *J. Clim.* 33, 5035–5060. doi: 10.1175/JCLI-D-19-0833.1

IPCC (2014). "Mitigation of climate change," in *Contribution of working group III to the fifth assessment report of the intergovernmental panel on climate change*, eds O. Edenhofer, R. Pichs-Madruga, Y. Sokona, E. Farahani, S. Kadner, K. Seyboth, et al. (Cambridge, MA: Cambridge University Press), 1454.

Jin, Q., and Wang, C. (2017). A revival of Indian summer monsoon rainfall since 2002. *Nat. Clim. Change* 7, 587–594. doi: 10.1038/nclimate3348

Kale, V., Gupta, A., and Singhvi, A. (2003). "Late Pleistocene–Holocene Palaeohydrology of Monsoon Asia," in *Palaeohydrology: Understanding global change*, eds K. J. Gregory and G. Benito (Hoboken, NJ: Wiley), 213.

Kathayat, G., Cheng, H., Sinha, A., Yi, L., Li, X., Zhang, H., et al. (2017). The indian monsoon variability and civilization changes in the indian subcontinent. *Sci. Adv.* 3:e1701296. doi: 10.1126/sciadv.1701296

Kong, G., Luo, T., Liu, X., Zhang, L., and Liang, E. (2012). Annual ring widths are good predictors of changes in net primary productivity of alpine *Rhododendron* shrubs in the Sergyemla Mountains, southeast Tibet. *Plant Ecol.* 213, 1843–1855. doi: 10.1007/s11258-012-0140-3

Kripalani, R., Oh, J., Kulkarni, A., Sabade, S., and Chaudhari, H. (2007). South Asian summer monsoon precipitation variability: Coupled climate model simulations and projections under IPCC AR4. *Theor. Appl. Climatol.* 90, 133–159. doi: 10.1007/s00704-006-0282-0

Lal, M. (2003). Global climate change: India's monsoon and its variability. *J. Environ. Stud. Policy* 6, 1–34.

Leal, S., Melvin, T., Grabner, M., Wimmer, R., and Briffa, K. (2007). Tree-ring growth variability in the Austrian Alps: The influence of site, altitude, tree species and climate. *Boreas* 36, 426–440. doi: 10.1080/03009480701267063

Li, Z., Liu, G., Fu, B., Zhang, Q., Ma, K., and Pederson, N. (2013). The growth-ring variations of alpine shrub *Rhododendron przewalskii* reflect regional climate signals in the alpine environment of Miyaluo Town in Western Sichuan Province, China. *Acta Ecol. Sin.* 33, 23–31. doi: 10.1016/j.chnaes.2012.12.004

Liang, E., and Eckstein, D. (2009). Dendrochronological potential of the alpine shrub *Rhododendron* nivale on the south-eastern Tibetan Plateau. *Ann. Bot.* 104, 665–670. doi: 10.1093/aob/mcp158

Lu, X., Camarero, J., Wang, Y., Liang, E., and Eckstein, D. (2015). Up to 400-year-old *Rhododendron* shrubs on the southeastern tibetan plateau: Prospects for shrub-based dendrochronology. *Boreas* 44, 760–768. doi: 10.1111/bor.12122

Lucas-Picher, P., Christensen, J., Saeed, F., Kumar, P., Asharaf, S., Ahrens, B., et al. (2011). Can regional climate models represent the Indian monsoon? *J. Hydrometeorol.* 12, 849–868. doi: 10.1175/2011JHM1327.1

Mao, A. (2010). The genus *Rhododendron* in north-east India. *Bot. Orient.* 7, 26–34. doi: 10.3126/botor.v7i0.4370

Menon, A., Levermann, A., Schewe, J., Lehmann, J., and Frieler, K. (2013). Consistent increase in Indian monsoon rainfall and its variability across CMIP-5 models. *Earth Syst. Dyn.* 4, 287–300. doi: 10.5194/esd-4-287-2013

Panthi, S., Bräuning, A., Zhou, Z., and Fan, Z. (2017). Tree rings reveal recent intensified spring drought in the central Himalaya. Nepal. *Glob. Planet. Change* 157, 26–34. doi: 10.1016/j.gloplacha.2017.08.012

Panthi, S., Fan, Z., and Bräuning, A. (2021). Ring widths of *Rhododendron* shrubs reveal a persistent winter warming in the central Himalaya. *Dendrochronologia* 65:125799. doi: 10.1016/j.dendro.2020.125799

Room, A., Franco-Gaviria, F., and Urrego, D. (2022). . *rshift STARS manual-regime shift analysis for paleoecological data v2. 1.1*.

Roxy, M., Ritika, K., Terray, P., Murtugudde, R., Ashok, K., and Goswami, B. (2015). Drying of Indian subcontinent by rapid Indian Ocean warming and a weakening land-sea thermal gradient. *Nat. Commun.* 6:7423. doi: 10.1038/ncomms8423

Sabin, T., Krishnan, R., Vellore, R., Priya, P., Borgaonkar, H., Singh, B., et al. (2020). "Climate Change Over the Himalayas," in *Assessment of climate change over the indian region: A report of the ministry of earth sciences (MoES), Government of India*, eds R. Krishnan, J. Sanjay, C. Gnanaseelan, M. Mujumdar, A. Kulkarni, and S. Chakraborty (Singapore: Springer), 207–222. doi: 10.1007/978-981-15-432break7-2_11

Sano, M., Dimri, A., Ramesh, R., Xu, C., Li, Z., and Nakatsuka, T. (2017). Moisture source signals preserved in a 242-year tree-ring δ18O chronology in the western Himalaya. *Glob. Planet. Change* 157, 73–82. doi: 10.1016/j.gloplacha.2017.08.009

Sano, M., Ramesh, R., Sheshshayee, M., and Sukumar, R. (2012). Increasing aridity over the past 223 years in the Nepal Himalaya inferred from a tree-ring δ18O chronology. *Holocene* 22, 809–817. doi: 10.1177/0959683611430338

Sano, M., Tshering, P., Komori, J., Fujita, K., Xu, C., and Nakatsuka, T. (2013). May–September precipitation in the Bhutan Himalaya since 1743 as reconstructed from tree ring cellulose δ18O. *J. Geophys. Res.* 118, 8399–8410. doi: 10.1002/jgrd.50664

Sekar, K., and Srivastava, S. (2010). *Rhododendrons* in Indian Himalayan region: Diversity and conservation. *Am. J. Plant Sci.* 1:131. doi: 10.4236/ajps.2010.12017

Shekhar, M. (2014). *Application of multi-proxy tree-ring parameters in the reconstruction of climate vis-a-vis 'glacial fluctuation from the eastern Himalaya*. Ph.D thesis. Lucknow: Department of Botnay, University of Lucknow.

Shekhar, M., Pal, A., Bhattacharyya, A., Ranhotra, P., and Roy, I. (2018). Tree-ring based reconstruction of winter drought since 1767 CE from Uttarkashi, Western Himalaya. *Q. Int.* 479, 58–69. doi: 10.1016/j.quaint.2017.08.029

Shekhar, M., Ranhotra, P., Bhattacharyya, A., Singh, A., Dhyani, R., and Singh, S. (2022). "Tree-Ring-Based Hydrological Records Reconstructions of the Himalayan Rivers: Challenges and Opportunities," in *Climate change: Impacts, responses and sustainability in the Indian Himalaya*, eds S. Rani and R. Kumar (Cham: Springer International Publishing), 47–72. doi: 10.1007/978-3-030-92782-0_3

Singh, J., Park, W., and Yadav, R. (2006). Tree-ring-based hydrological records for western Himalaya, India, since AD 1560. *Clim. Dyn.* 26, 295–303. doi: 10.1007/s00382-005-0089-1

Singh, J., Singh, N., Chauhan, P., Yadav, R., Bräuning, A., Mayr, C., et al. (2019). Tree-ring δ18O records of abating June–July monsoon rainfall over the Himalayan region in the last 273 years. *Q. Int.* 532, 48–56. doi: 10.1016/j.quaint.2019.09.030

Singh, J., Yadav, R., and Wilmking, M. (2009). A 694-year tree-ring based rainfall reconstruction from Himachal Pradesh. India. *Clim. Dyn.* 33, 1149–1158. doi: 10.1007/s00382-009-0528-5

Singh, V., Misra, K., Singh, A., Yadav, R., and Yadava, A. (2021). Little ice age revealed in tree-ring-based precipitation record from the Northwest Himalaya, India. *Geophys. Res. Lett.* 48:e2020GL091298. doi: 10.1029/2020GL091298

Singhvi, A., and Kale, V. (2010). *Paleoclimate studies in India: Last ice age to the present*. New Delhi: Indian National Science Acad.

Tiwari, S., Kar, S., and Bhatla, R. (2018). Mid-21st century projections of hydroclimate in Western Himalayas and Satluj River basin. *Glob. Planet. Change* 161, 10–27. doi: 10.1016/j.gloplacha.2017.10.013

Valdiya, K. (2020). Anomalous weather events in central Himalaya: Real-world observations and some questions. *Curr. Sci.* 119, 19–25. doi: 10.18520/cs/v119/i1/19-25

Van Oldenborgh, G., and Burgers, G. (2005). Searching for decadal variations in ENSO precipitation teleconnections. *Geophys. Res. Lett.* 32, 1–2. doi: 10.1029/2005GL023110

Weijers, S., Greve Alsos, I., Bronken Eidesen, P., Broekman, R., Loonen, M., and Rozema, J. (2012). No divergence in *Cassiope tetragona*: Persistence of growth response along a latitudinal temperature gradient and under multi-year experimental warming. *Ann. Bot.* 110, 653–665. doi: 10.1093/aob/mcs123

Wester, P., Mishra, A., Mukherji, A., and Shrestha, A. (2019). *The Hindu Kush Himalaya assessment: Mountains, climate change, sustainability and people*. Berlin: Springer. doi: 10.1007/978-3-319-92288-1

Wigley, T., Briffa, K., and Jones, P. (1984). On the average value of correlated time series, with applications in dendroclimatology and hydrometeorology. *J. Appl. Meteorol. Climatol.* 23, 201–213. doi: 10.1175/1520-0450(1984)023<0201:OTAVOC>2.0.CO;2

Xu, C., Sano, M., Dimri, A., Ramesh, R., Nakatsuka, T., Shi, F., et al. (2018). Decreasing Indian summer monsoon on the northern Indian sub-continent during the last 180 years: Evidence from five tree-ring cellulose oxygen isotope chronologies. *Clim. Past* 14, 653–664. doi: 10.5194/cp-14-653-2018

Yadav, R. (2011). Tree ring evidence of a 20th century precipitation surge in the monsoon shadow zone of the western Himalaya, India. *J. Geophys. Res.* 116:D02112. doi: 10.1029/2010JD014647

Yadav, R., Braeuning, A., and Singh, J. (2011). Tree ring inferred summer temperature variations over the last millennium in western Himalaya. India. *Clim. Dyn.* 36, 1545–1554. doi: 10.1007/s00382-009-0719-0

Yadav, R., Gupta, A., Kotlia, B., Singh, V., Misra, K., Yadava, A., et al. (2017). Recent wetting and glacier expansion in the northwest Himalaya and Karakoram. *Sci. Rep.* 7:6139. doi: 10.1038/s41598-017-06388-5

Yadav, R., Park, W., and Bhattacharyya, A. (1999). Spring-temperature variations in western Himalaya, India, as reconstructed from tree-rings: AD 1390-1987. *Holocene* 9, 85–90. doi: 10.1191/095968399667529322

frontiers | Frontiers in Forests and Global Change

TYPE Original Research
PUBLISHED 06 February 2023
DOI 10.3389/ffgc.2023.1124677

OPEN ACCESS

EDITED BY
Shreekar Pant,
Baba Ghulam Shah Badshah University, India

REVIEWED BY
Madhusudhana Reddy,
Dr. B.R. Ambedkar Open University, India
Kiranmay Sarma,
Guru Gobind Singh Indraprastha University, India

*CORRESPONDENCE
Manthena Prashanth
✉ mprashanth@ignou.ac.in
Arun Kumar
✉ arundhawan92@yahoo.com

SPECIALTY SECTION
This article was submitted to
Forest Management,
a section of the journal
Frontiers in Forests and Global Change

RECEIVED 15 December 2022
ACCEPTED 09 January 2023
PUBLISHED 06 February 2023

CITATION
Prashanth M, Kumar A, Dhar S, Verma O, Rai SK and Kouser B (2023) Land use/land cover change and its implication on soil erosion in an ecologically sensitive Himachal Himalayan watershed, Northern India.
Front. For. Glob. Change 6:1124677.
doi: 10.3389/ffgc.2023.1124677

Land use/land cover change and its implication on soil erosion in an ecologically sensitive Himachal Himalayan watershed, Northern India

Manthena Prashanth[1]*, Arun Kumar[1]*, Sunil Dhar[2], Omkar Verma[1], Shashi Kant Rai[2] and Beena Kouser[1]

[1]Geology Discipline Group, School of Sciences, Indira Gandhi National Open University, New Delhi, India, [2]Department of Environmental Sciences, Central University of Jammu, Samba, India

Soil erosion is a major environmental problem that affects land and water resources. It has many negative implications that lead to deforestation, poor agricultural practices, loss of soil fertility, and siltation that hinder socio-economic development. In view of this, the present study was conducted with the aim of estimating soil loss in relation to long-term land use/land cover change (LULC) in the Dehar watershed, Himachal Himalaya, North India. The study was carried out using Landsat and Sentinel imageries for the years 1999, 2010, and 2020. A GIS-based Revised Universal Soil Loss Equation (RUSLE) model was applied to assess the potential soil risk. The parameters used as input for computing the spatiotemporal changes of soil loss were rainfall erosivity, soil erodibility, topographic, crop management, and conservation support practice factors. The results showed a mean soil loss of 63.71, 60.99, and 66.71 t/ha/yr for the years 1999, 2010, and 2020, respectively. In the LULC class defined as Built-up Land, the mean soil loss decreased from 32.19 t/ha/yr in 1999 to 18.77 t/ha/yr in 2010, and in the year 2020 the mean soil loss slightly increased to 20.15 t/ha/yr. Moreover, the LULC class Barren Land registered a decrease in mean soil loss for the years 1999, 2010, and 2020 of 86.43, 74.60, and 73.19 t/ha/yr, respectively. Regarding the Agriculture Land class, the rate of mean soil loss slightly increased from 32.55 t/ha/yr in 1999 to 33.35 t/ha/yr in 2010, and the mean soil loss decreased to 25.43 t/ha/yr in the year 2020. Areas covered under Forest Land experienced an increase in mean soil loss from 65.30 t/ha/yr in 1999 to 65.87 in 2010 and 74.72 t/ha/yr in 2020. The study demonstrated that LULC changes apparently influenced the soil loss in the Dehar watershed. Therefore, urgent interventions are required with the involvement of scientists, policymakers, and the general public for conservation and management of soil resources.

KEYWORDS

soil erosion, land use/land cover, GIS, RUSLE, Himachal Himalaya, North India

Introduction

Land use/land cover change (LULC) change is one of the leading global environmental problems and poses an alarming threat to humankind. LULC change is a decisive factor in most of the initiatives carried out by the public, as can be evidenced by various development activities taken up in almost all parts of the globe (Steffen et al., 2001; Glaeser and Kahn, 2004; Lambin et al., 2010; Ayele et al., 2014; Haregeweyn et al., 2015). Land use change is a key factor that contributes to soil erosion and is of prime concern in environmental studies (Senanayake et al., 2020). Moreover, LULC changes are considered to affect the hydrological characteristics of a watershed and enhance land degradation problems like soil erosion and sedimentation if they are not addressed scientifically (Abdulkareem et al., 2019; Mohammadi et al., 2021). Hence, knowing LULC dynamics and their implications on soil erosion can help policymakers in decision-making processes (Waltner et al., 2020). Extensive soil erosion results in soil erosion hazards, which influence landscape processes including land productivity, hydrological activity, and eventual human wellbeing. Therefore, soil erosion assessment is important for understanding the dynamics of landscape processes.

Soil erosion plays a pivotal role in land degradation and is considered a serious environmental hazard (Eswaran et al., 2001; Panagos et al., 2017; Poesen, 2018; Steinmetz et al., 2018). In recent times, land degradation has become a major environmental concern in many regions of the world, particularly in developing countries where agriculture is a main occupation (Krishna Bahadur, 2009; Xu et al., 2013; Rawat et al., 2016; Samanta et al., 2016; Saha et al., 2018). Further, it has many negative impacts including the loss of soil fertility that hinders socio-economic development on a global scale (Kouli et al., 2009).

At a global level, nearly 85% of land degradation is mainly caused by soil erosion (Tang et al., 2015). Soil erosion has become a serious issue in almost all parts of the globe (Pimentel and Burgess, 2013; Prashanth et al., 2021, 2022). Moreover, LULC change is affecting the availability of natural resources mainly soil resources in most regions of the world (Abdulkareem et al., 2019; Mohammadi et al., 2021; Zhu et al., 2022; Moisa et al., 2023). Generally, soil erosion is a natural process but has become a significant environmental issue in the last century due to anthropogenic interventions (Alkharabsheh et al., 2013). The problem is expected to exacerbate in the 21st century (Hurni et al., 2005). Out of the different types of soil erosion, the effects caused by water erosion are of more concern, as this disturbs soil texture, structure, and quality, as well as endangers other natural resources, such as land and water, which mankind depend upon for survival (Pimentel et al., 1993; Hrissanthou et al., 2010; Yang et al., 2013; Keno and Suryabhagavan, 2014; Srinivasan et al., 2019; Kolli et al., 2021). The immediate on-the-spot effect is a decrease in soil productivity, and *ex-situ* impacts include sediment deposition that triggers floods (Meshesha et al., 2012; Negash et al., 2021). Further, anthropogenic interference often intensifies the process of soil erosion on the steep slopes of highly elevated areas particularly in a mountainous ecosystem, because of various unsustainable activities such as deforestation, forest fires, intensive farming, and improper land management practices (Mandal and Sharda, 2013; Jayasekara et al., 2018).

Stocking (1993) depicted land degradation as a global environmental problem and found it to be a major environmental crisis in the developing world. Land degradation is one of the ecologically sensitive issues in India, and increasing populations, increasing urbanization, and over-exploitation of natural resources are the main drivers of land degradation. Moreover, Singh and Panda (2017) observed that out of the total geographical area of India, nearly 47.7% of the area suffers from land degradation. Further, the National Bureau of Soil Survey and Land Use Planning (NBSS and LUP, 2005) estimated that almost 146.8 Mha of land in India is degraded. Ravi et al. (2010) viewed soil erosion as one of the major processes of land degradation spreading in arid and semi-arid regions of India.

In India, soil erosion due to water is considered to be the most severe land degradation aspect that affects the topsoil and landscape of an area in general and Himalaya in particular (Mandal and Sharda, 2011; Bhattacharyya et al., 2015; Mahapatra et al., 2018). Himalaya is considered a highly land-degraded region due to various factors including soil erosion, which poses a major challenge to mountain ecosystems (Stoddart, 1969; Chalise et al., 2019). Most of the climatic regions of the world, including mountain areas such as Himalaya, are prone to soil erosion (e.g., Garcia-Ruiz et al., 2015). The main drivers of soil erosion in Himalaya are thought to be associated with both natural and anthropogenic activities (Hamilton, 1987; Jain et al., 2001; Prashanth et al., 2021, 2022). Thus, soil erosion assessment in highly ecologically sensitive Himalayan watersheds will be supportive to land degradation evaluation and to minimize the stress on sustainable agricultural practices (Singh and Singh, 2018).

Oliveira et al. (2019) observed that runoff from mountain regions toward regions of lower elevations increases the rate of erosion of an area. Further, regular land-use changes stimulate runoff and soil productivity loss, thus resulting in land degradation (Ang and Oeurng, 2018). Sharma (2008) assessed that out of the total degraded land in the Himalaya region, 79% is related to water erosion and is mostly confined to the river catchments. Significantly, lower Himalaya is more prone to soil erosion resulting in land degradation and making the land unproductive (Kaiser, 2004). About 54% of the state of Himachal Pradesh, Himachal Himalaya (North India) is prone to soil erosion, out of which, 98% is mainly because of water erosion (Kumar et al., 2014). The uneven complex dissected terrain, tectonic pressure, and diverse climatological influences supported by anthropogenic interventions have increased stress on natural resources, mainly land resources in lower Himalaya (Prashanth et al., 2021). Hence, under these circumstances, the estimation of soil loss with emphasis on land-degraded areas is quite necessary for sustainable planning and effective conservation of natural resources in Himalaya (Yadav and Sidhu, 2010).

Several models have been developed to predict soil erosion, including: empirical models such as the Universal Soil Loss Equation (USLE) developed by Wischmeier and Smith (1978); a revised model of the USLE known as the Revised Universal Soil Loss Equation (RUSLE) (Renard et al., 1997); and process-based models like the USDA-Water Erosion Prediction Project (WEPP) (Nearing et al., 1989), European Soil Erosion Model (EUROSEM) (Morgan et al., 1998), and Large Scale Catchment Model LASCAM (Viney and Sivapalan, 1999). Though many models are used for predicting soil erosion, the most widely used model for soil erosion estimation studies is the RUSLE (Shrestha, 1997; Angima et al., 2003; Prasannakumar et al., 2011, 2012; Mandal and Sharda, 2013; Wang et al., 2013; Pan and Wen, 2014; Erol et al., 2015; Uddin et al., 2016; Panditharathne et al., 2019). For assessing soil erosion, the combined application of geospatial technologies such as geographical information systems (GIS), remote sensing, and RUSLE techniques are quite economical, time-saving, and more precise than most other models (Wang et al., 2003; Prasannakumar et al., 2011; Galdino et al., 2016; Gelagay and Minale, 2016; Zerihun et al., 2018; Adongo et al., 2019; Kumar et al., 2020; Kumar and Hole, 2021; Sandeep et al., 2021). Integrating soil erosion models with GIS acts as a potential tool in land degradation assessment practices. RUSLE is one of the soil erosion models applied for calculating and predicting the spatial and temporal differences in soil erosion in a GIS environment (Islam et al., 2020). It is used to estimate long-term annual average soil loss in certain areas with specific ground slope characters (Boggs et al., 2001). It is found to be a simple and pertinent model with limited data requirements and is widely used all over the globe because of its suitability and easy computational approaches (Jha and Paudel, 2010). Further, it is mostly an applied model for hilly terrains (Ganasri and Ramesh, 2016; Dissanayake et al., 2019) to assess erosion risk with potential application capabilities (Boggs et al., 2001). The primary objectives of

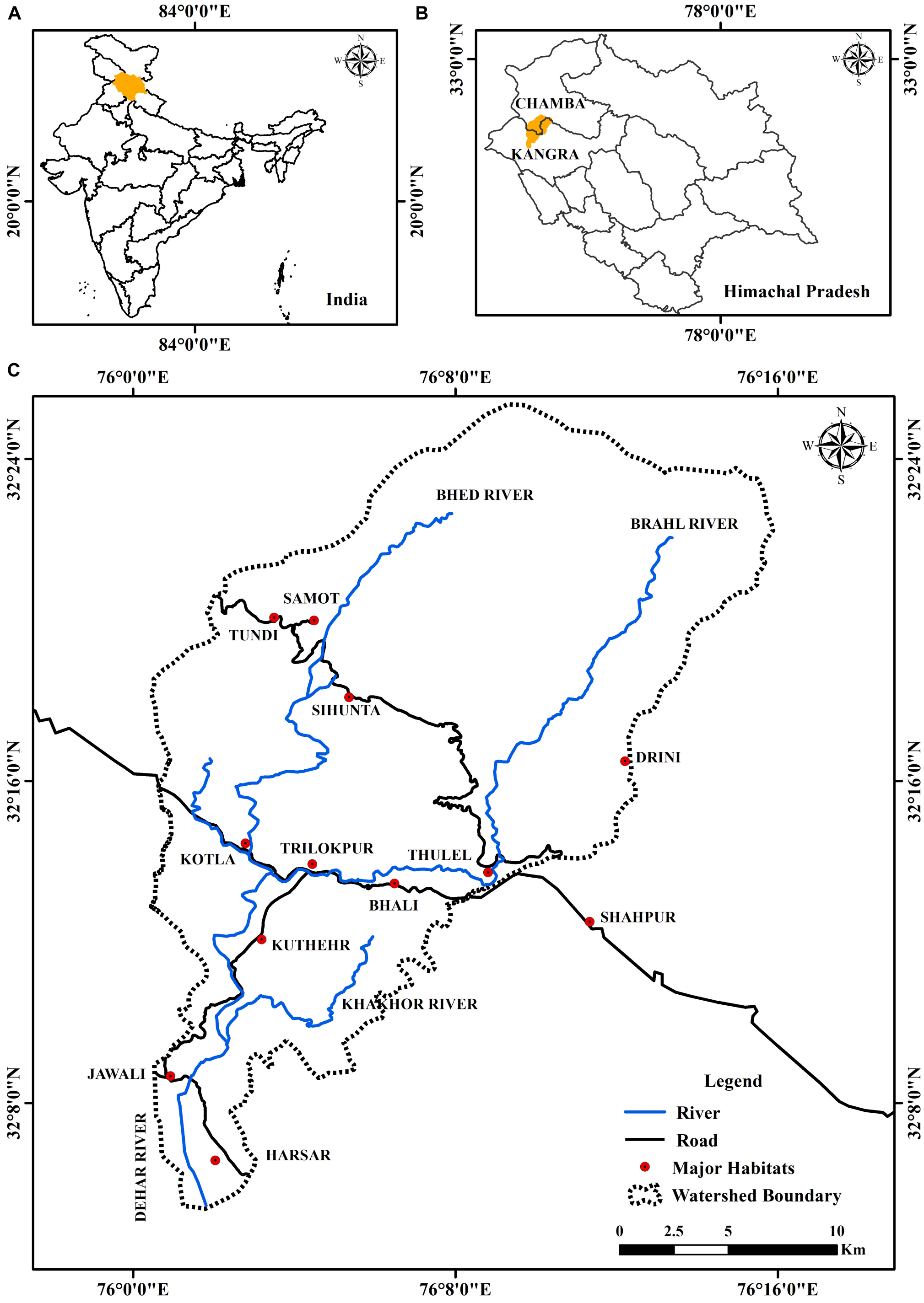

FIGURE 1

Location maps. **(A)** Map of India showing the location of the Himachal Pradesh state (shaded by yellow color). **(B)** Map of the Himachal Pradesh state showing area (shaded by yellow color) covered by the Dehar watershed. **(C)** Enlarged map showing the Dehar watershed.

the present study are to: (1) evaluate the long-term LULC changes of a Himalayan watershed; (2) assess the soil erosion due to LULC changes in the watershed using remote sensing, GIS, and RUSLE techniques; and (3) understand the potential risks of soil erosion caused by changing land-use patterns. The study will help to suggest suitable measures required for the conservation, planning, and sustainable management of soil resources in the study area and watersheds of similar settings.

Materials and methods

Study area

The Dehar river is a tributary of the Beas River system. The Dehar watershed is located between the boundaries of the Kangra and Chamba districts of the state of Himachal Pradesh between latitudes 32°5′21″ N to 32°23′47″ N and longitudes 76°0′25′’ E to 76°12′29″ E. In the course of its journey, the Dehar river traverses several places, such as Trilokpur, Kotla, Kuther, Sihunta, Thulel, and Jawali, before joining the Pong Reservoir also known as Maharana Pratap Sagar (**Figure 1**). The Dehar watershed is covered by the Survey of India (SOI) top-sheet maps nos. 52D/3, 52D/4, and 52D/7 with 1:50000 scales. It covers an area of 450 km^2 and with a minimum and maximum elevation of 395 and 4080 m above mean sea level, respectively. Geographically, the area is located in Himachal Himalaya and consists of almost parallel hills disconnected by longitudinal valleys. The area experiences a varied climate, sub-tropical at lower elevations and temperate at higher altitudes. The area experiences a maximum temperature of 38°C and a minimum temperature of 0°C with an average temperature of 22°C. It has a normal annual rainfall of 2500 mm. The dominant soil varieties that cover the watershed are sandy-skeletal, coarse-loamy, fine-loamy and mesic-loamy soils (Sidhu et al., 1997). Geologically, the watershed is covered by rocks of the Lower Himalaya in the North and Siwaliks (Outer Himalaya) in the South (Srikantia and Bhargava, 1998). From north to south, it is covered by various geological formations, such as Dhauladhar Granites, Mandi Darla Volcanics, Shali Formation, Dharamshala Formation, Siwalik Group, and fluvio-glacial deposits. The Lesser Himalayan zone is represented by major rock types: Precambrian gneissic and granitic rocks (the Dhauladhar Group); slate, schist, phyllite, and limestone (Salooni Formation); older rocks include slate, quartzite, schist, basic lava flows, marl, salt, and dolomites (Sundernagar, Jutogh, and Shali Formations). The lesser Himalaya is represented by the Subathu Group which includes rocks of Cenozoic age (green shales and fossiliferous limestones), and the Siwalik Group, with sedimentary rocks consisting of shale, conglomerate, clay, and sandstone (Srikantia and Bhargava, 1998). The area is tectonically active and traversed by several northeast-southwest trending major tectonic faults/lineaments, the Chail Thrust, the MBT, the Drini Thrust, and the Jwalamukhi Thrust, which separate different geological units by bordering them

TABLE 1 Different data sets used in the study.

S. no	Data type	Source	Description
I	Rainfall data	Indian meteorological department (IMD), (https://dsp.imdpune.gov.in)	Rainfall data for a period of 30 years (1999–2020) from 11 nearby stations
II	Soil data	NBSS and LUP, 2005	Soil map of Himachal Pradesh (1: 500,000 scale)
III	Digital elevation model	https://earthexplorer.usgs.gov/	SRTM digital elevation model (DEM) of 30 m spatial resolution
IV	Satellite data	https://earthexplorer.usgs.gov/	(i) LANDSAT 7 ETM$^+$ image (Path/row: 148/038) of 20-09-1999 (30 m resolution) (ii) LANDSAT 5TM$^+$ image (Path/row: 148/038) of 11-11-2010 (30 m resolution (iii) Sentinel 2 images (L1C_T43SFR_A028173) (L1C_T43SFR_AD18621) of 13-11-2020 and 29-09-2020 (10 m resolution)

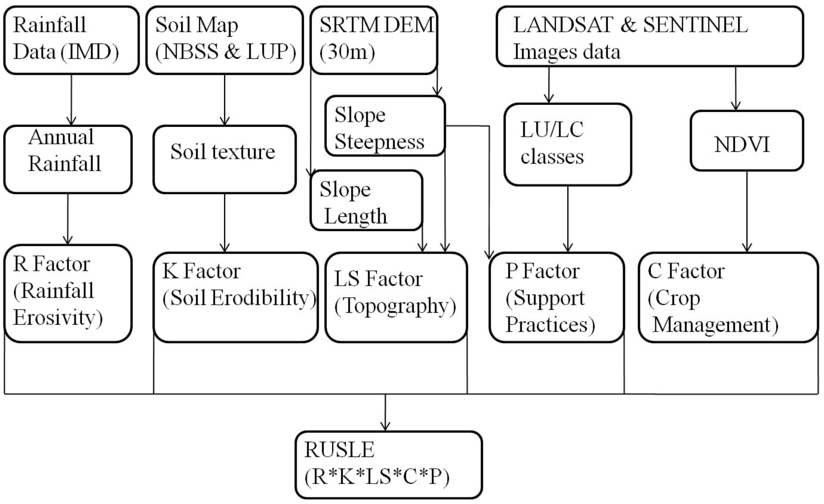

FIGURE 2
Flow chart demonstrating the methodology adopted for RUSLE model.

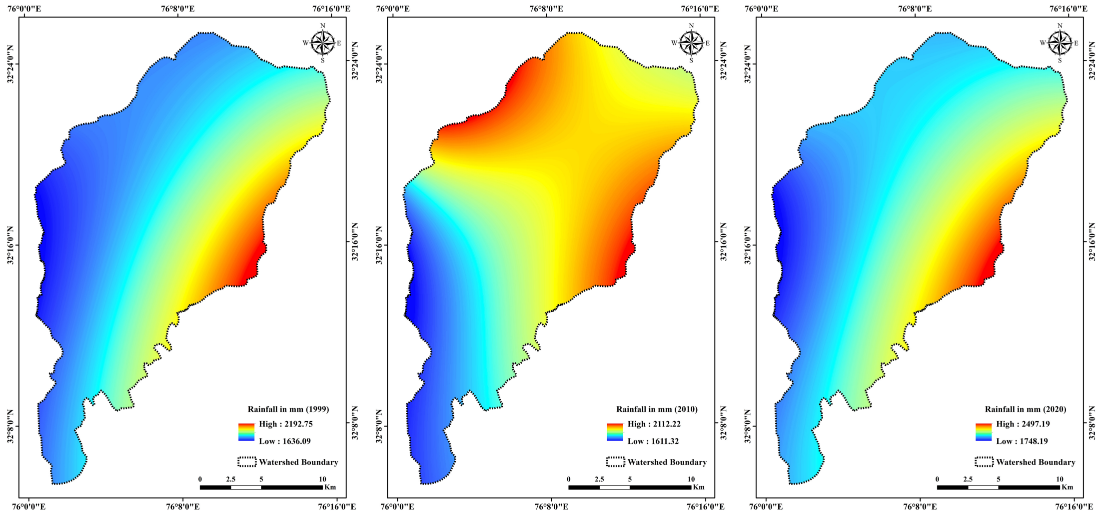

FIGURE 3
Maps of the Dehar watershed showing the average annual rainfall for the years 1999, 2010, and 2020.

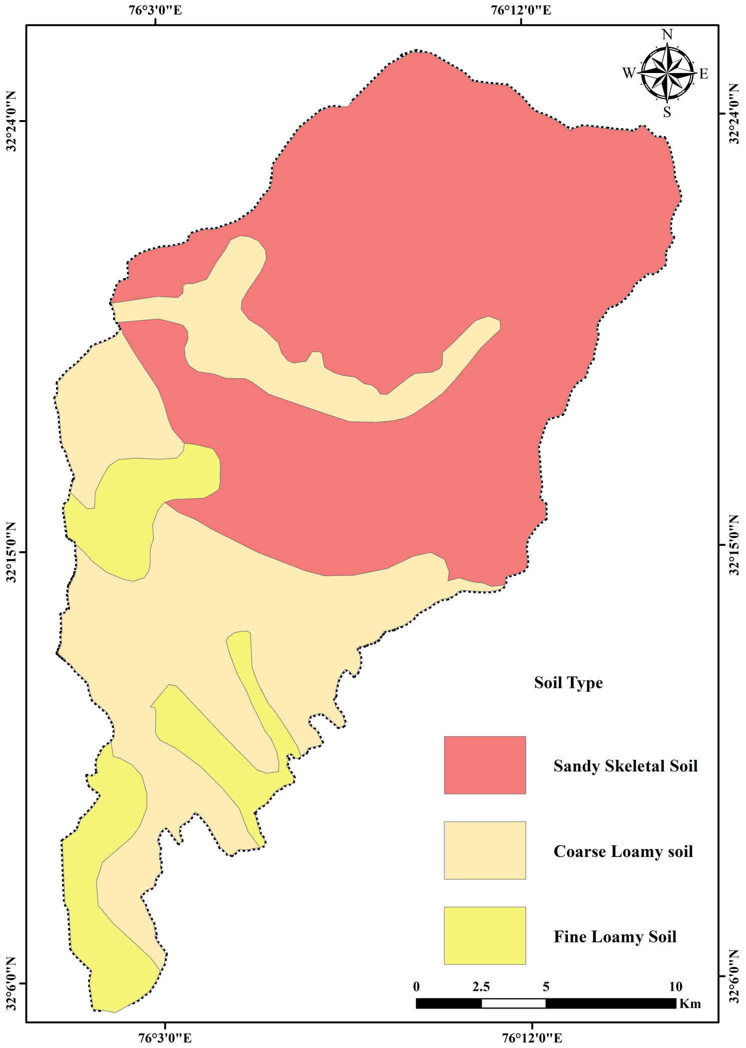

FIGURE 4
Map showing different soil types in the Dehar watershed.

TABLE 2 *K*-values for different soil types (after Jain et al., 2010).

Soil type	*K*-value (Mg h/MJ/mm)
Sandy soil	0.042
Loamy soil	0.020
Coarse loamy soil	0.032

(Kumar and Nanda, 1989; Srikantia and Bhargava, 1998; Kumar and Mahajan, 2001).

Data sets used

Shuttle Radar Topographic Mission (SRTM) digital elevation model data of 30 m resolution was used in the extraction of basin boundaries and for determining topographic factors (LS factors) for RUSLE modeling using ArcGIS 10.8 software (Table 1). Time series data of LANDSAT-7, LANDSAT-5, and SENTINAL-2 for the years 1999, 2010, and 2020, respectively, were used for preparing LULC maps and determining crop management (C) and conservation practice (P) factors used in RUSLE modeling (Table 1). The soil maps required to determine soil classes and soil erodibility (K factor) for the study were obtained from the database of NBSS and LUP (2005). Rainfall data procured from the India Meteorological Department (IMD) of 11 nearby rain gauge stations for the duration of 1999–2020 was used in determining the rainfall erosivity (R) factor (Table 1). All factors used in RUSLE modeling for determining soil loss were derived independently.

RUSLE model

To estimate soil erosion, various parameters such as precipitation, soil categories, terrain characters, and land cover changes are required (Kouli et al., 2009; Vijith et al., 2018). The annual average soil loss per unit area per year was estimated as per the following equation (Eq. 1) given by Renard et al. (1997) using the required parameters generated through DEM, rainfall data, soil types, and satellite images (Figure 2):

$$A = R \times K \times LS \times C \times P \tag{1}$$

Where A denotes the average annual soil loss (t/ha/year), R represents the rainfall erosivity factor (MJ mm/ha/hr/year), K refers

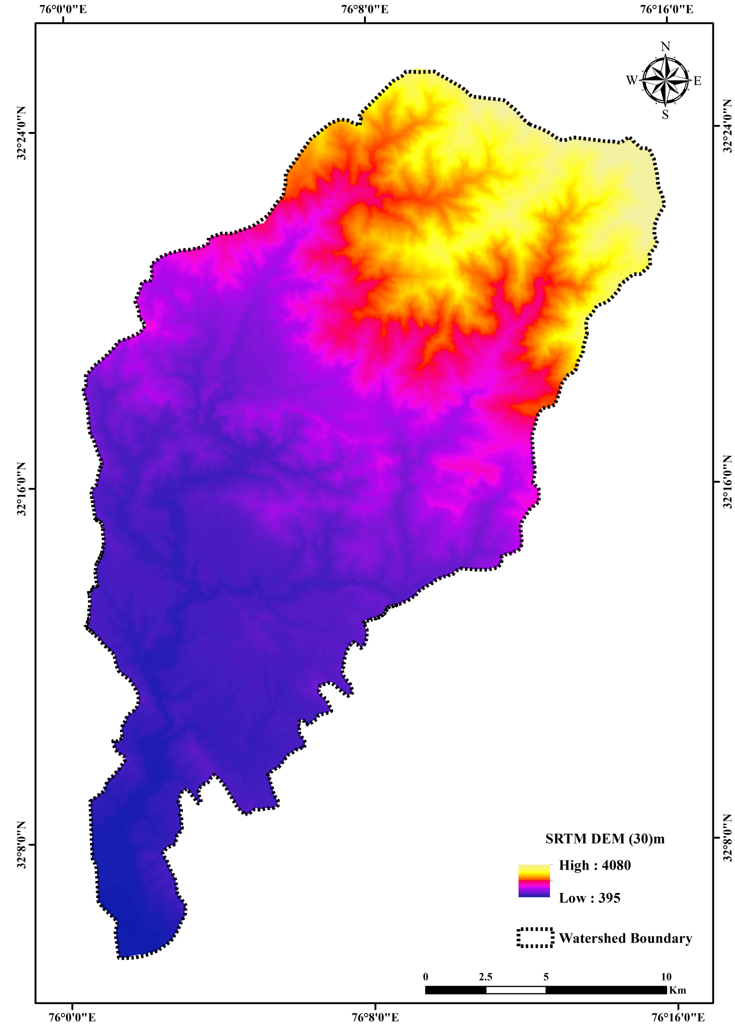

FIGURE 5
Digital elevation model (DEM) of the Dehar watershed.

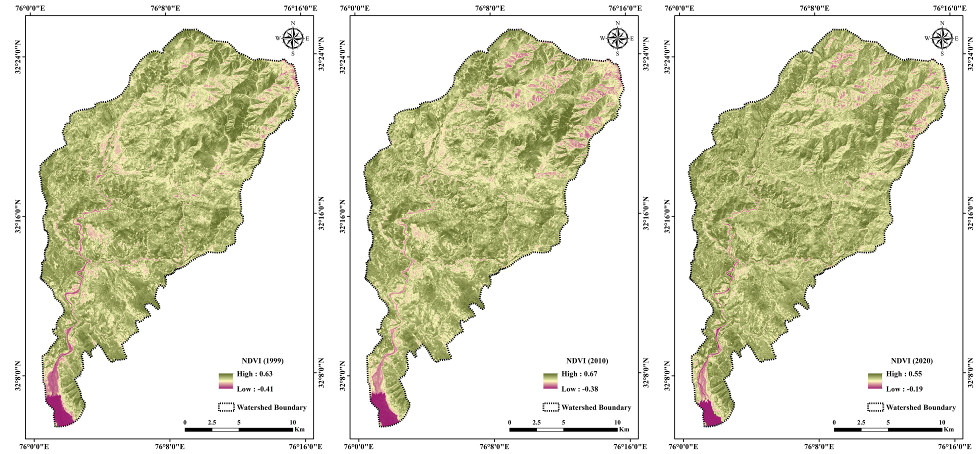

FIGURE 6
Maps of the Dehar watershed showing NDVI for the years 1999, 2010, and 2020.

TABLE 3 *P*-values for different LULC classes (complied after Wischmeier and Smith, 1978; Wanielista and Yousef, 1993; Londhe et al., 2010).

LULC class	*P*-value
Forest	1
Barren land	1
Agricultural land (3–8% slope)	0.5
Agricultural land (8–12% slope)	0.6
Agricultural land (12–16% slope)	0.7
Agricultural land (16–20% slope)	0.8
Agricultural land (20–25% slope)	0.9
Agricultural land (<3% and > 25% slope)	1
Built-up	1
Water body	0

to the soil erodibility factor (Mg h/MJ/mm), LS indicates the topological factor expressed as slope length and steepness factor, C is crop management, and P signifies the conservation support practice factor (**Figure 2**). Of all these factors, LS, C, and P factors are dimensionless.

Land use/land cover dynamics

To determine the LULC changes in the study area, the satellite imageries of LANDSAT-7, LANDSAT-5, and SENTINAL-2 for the years 1999, 2010, and 2020, respectively, were used. Image enhancement techniques were adopted to categorize the LULC features. All the downloaded images were in TIFF format and therefore exported to .img format *via* application of a layer stack function using ERDAS Imagine 2020. These stacked images were georeferenced into the same map projection of the World Geodetic System 1984 Zone 43N (WGS 1984-43N). All images were subset (sub-mapped) with reference to the boundaries of the watershed for marking the whole study area. Red, Green, Blue (RGB) band composition was used for all the images to interpret and classify the surface features with more precision (Teng et al., 2016). False color composite (FCC) of satellite images were generated for the years 1999, 2010, and 2020 by displaying different band combinations such as band 4 (NIR), band 3 (red), and band 2 (green). Various LULC classes were identified in the study area, specifically, Built-Up, Agricultural Land, Forest, Barren, and Water Bodies. With the aim to check the level of accuracy of the generated LULC layers, nearly 200 randomly collected sample points were selected from each of the created LULC layers. These layers were again opened and overlaid in Google Earth Pro software to validate the generated LULC layers for accuracy. Further, a confusion matrix was computed with the validated data.

Rainfall erosivity factor (R factor)

R factor is the measure of the intensity of rainfall in a certain place based on the quantum of soil erosion (Koirala et al., 2019). Incessant rainfall data is required to compute the R factor, as it is valuable in knowing the influence of rainfall intensity on soil erosion triggered by water erosion (Wischmeier and Smith, 1978). From the literature, it was noticed that a multitude of equations have been developed to quantify the R factor (Kouli et al., 2009; Khosrokhani and Pradhan, 2014). Nevertheless, the formula (Eq. 2) given by Singh et al. (1981) was used for discerning the rainfall erosivity factor. In addition, the equation illustrates the relationship between the rainfall erosivity factor and the average annual precipitation, which has been found to be more reliable for soil erosion studies in India (Saha et al., 2018; Sandeep et al., 2021; Sangeetha and Ambujam, 2021). Monthly rainfall data was procured from the IMD for the 11 rain gauge stations located in and around the Dehar watershed for the duration of 1999 to 2020. Further, the mean annual rainfall data (for the duration of 1999 to 2020) of the rain gauge stations, which is essential for the computation of the R factor, was drawn from the collected rainfall data sets (**Figure 3**). The R factor was computed by inverse distance weighting (IDW) interpolation method and converted to a raster data set of 30 m cell grid size (**Figure 9**).

$$R = 79 + 0.363 \times R_n \tag{2}$$

Where R_n denotes the average annual rainfall expressed in mm.

Soil erodibility factor (K factor)

The soil erodibility factor (K) describes the characteristic eroding capacity of soils. It measures the susceptibility of soils to detach and be transported predominantly caused by rainfall and overland flow. The K factor refers to the impact of the physical and chemical properties of soils on erodibility during precipitation events in an elevated region (Wischmeier and Smith, 1978). The K factor is affected by various soil properties that comprise soil texture, structure, organic matter, permeability, porosity, and soil profile (Prasannakumar et al., 2011). For the present study, the soil map was procured from the NBSS and LUP (2005). The three different soil classes, sandy-skeletal, coarse-loamy, and fine-loamy soils, were recognized in the watershed (**Figure 4**; Sidhu et al., 1997). The *K*-values for these three soil classes were assigned considering the *K*-values proposed by Jain et al. (2010) (**Table 2**). The soil map was initially generated in vector format to decipher the soil classes considering *K*-values and later converted into raster format with a 30 m × 30 m grid (**Figure 10**).

TABLE 4 Area under different LULC classes for the years 1999, 2010, and 2020.

Year	LULC classes (area in km^2 and percentage)									
	Built-up		Agricultural land		Forest		Barren land		Water body	
	km^2	Percentage	km^2	Percentage	km^2	Percentage	km^2	Percentage	km^2	Percentage
1999	2.3	0.51	48.16	10.74	342.1	76.26	50.15	11.18	5.89	1.31
2010	3.96	0.88	61.09	13.62	343.2	76.50	34.75	7.75	5.6	1.25
2020	5.36	1.19	64.28	14.33	346.2	77.17	26.85	5.99	5.91	1.32

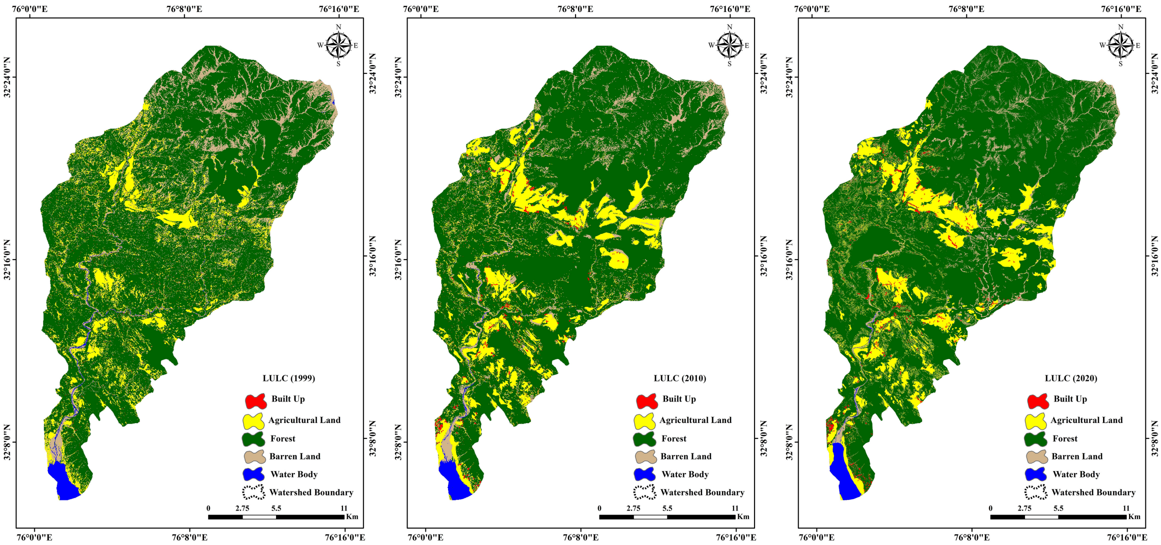

FIGURE 7
Showing LULC maps for the years 1999, 2010, and 2020 of the Dehar watershed.

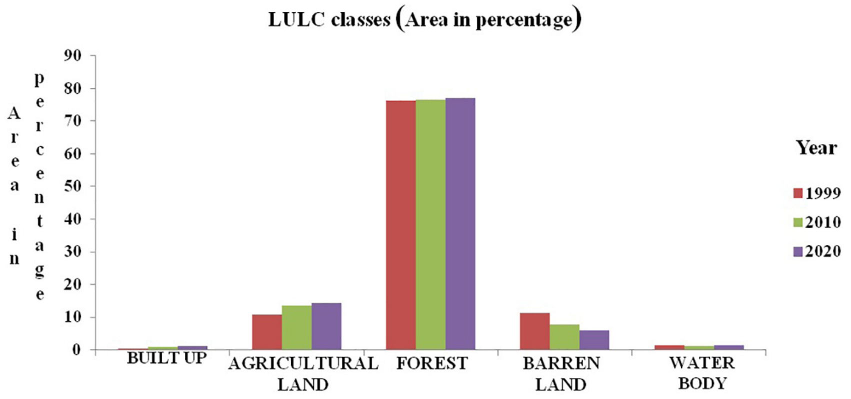

FIGURE 8
Bar graph showing the change in different LULC classes for the years 1999, 2010, and 2020 of the Dehar watershed.

Topographic factor (LS factor)

The topographic factor (LS) is generated from the two significant aspects of slope-length factor (L) and slope-gradient factor (S), and these factors are primarily created from the Digital Elevation Method (DEM). Zhang et al. (2013) determined that the LS factor is an essential component of the RUSLE model soil erosion estimation as gravitational forces play a major role in overland flow. The LS factor revealed that the landscape setting of terrain with steep slopes and heavy precipitations is more vulnerable to soil erosion. Paul et al. (2021) viewed that if the length and steepness of an area are higher, the velocity and runoff volume escalates, leading to soil erosion. The DEM is considered to be the best option for the calculation of the LS factor in a particular area (Panagos et al., 2015). The LS factor was calculated from SRTM DEM of 30 m spatial (**Figure 5**). The LS factor map was generated by adopting equation (Eq. 3) (Wischmeier and Smith, 1978) and using a tool developed in Arc Macro Language by Hickey (2001). The tool takes DEM in ASCII format as input to calculate the LS factor (**Figure 11**).

$$LS = (l/72.6)^{m}(65.41\ \mathrm{Sin}^{2}\beta + 4.56\ \mathrm{Sin}\beta + 0.065) \tag{3}$$

Where, LS represents the slope length and steepness factor, l is cumulative slope length in meters, and β *is* the downhill slope angle.

TABLE 5 Confusion matrix for LULC classification for the years 1999, 2010, and 2020.

Assigned classes	Water body	Forest	Agricultural land	Barren land	Built-up	Sum	User's accuracy (%)
Referenced classes (1999)							
Water body	6	0	3	1	0	10	60
Forest	0	43	2	5	0	50	86
Agricultural land	0	3	46	3	0	52	88.46
Barren land	0	2	2	37	0	41	90.24
Built-up	0	0	3	1	33	37	89.19
Sum	6	48	56	47	33	190	
Producer's accuracy (%)	100	89.58	82.14	78.72	0	Overall accuracy 86.84	
Referenced classes (2010)							
Water body	7	3	0	0	0	10	70
Forest	0	44	2	4	0	50	88
Agricultural land	0	1	46	4	0	51	90.19
Barren land	0	3	2	34	1	40	85
Built-up	0	0	4	0	36	40	90
Sum	7	51	54	42	37	191	
Producer's accuracy (%)	100	86.27	85.18	80.95	97.29	Overall accuracy 87.43	
Referenced classes (2020)							
Water body	7	3	0	0	0	10	70
Forest	0	42	6	3	0	51	82.35
Agricultural land	0	1	55	4	0	60	91.66
Barren land	0	0	4	26	0	30	86.66
Built-up	0	3	0	0	47	50	94
Sum	7	49	65	33	47	201	
Producer's accuracy (%)	100	85.71	84.61	78.78	100	Overall accuracy 88.05	

TABLE 6 Area under different soil loss potential classes and mean soil loss for the year 1999, 2010, and 2020.

Soil loss potential class	Area (in percentage)						Mean soil loss (t/ha/year)
	Very low (0–1)	Low (1–5)	Moderate (5–10)	High (10–20)	Very high (20–50)	Extreme (> 50)	
1999	46.42	0.45	2.53	5.05	10.81	34.74	63.71
2010	46.52	1.32	3.31	5.91	11.69	31.25	60.99
2020	46.1	0.56	2.71	4.68	10.03	35.92	66.71

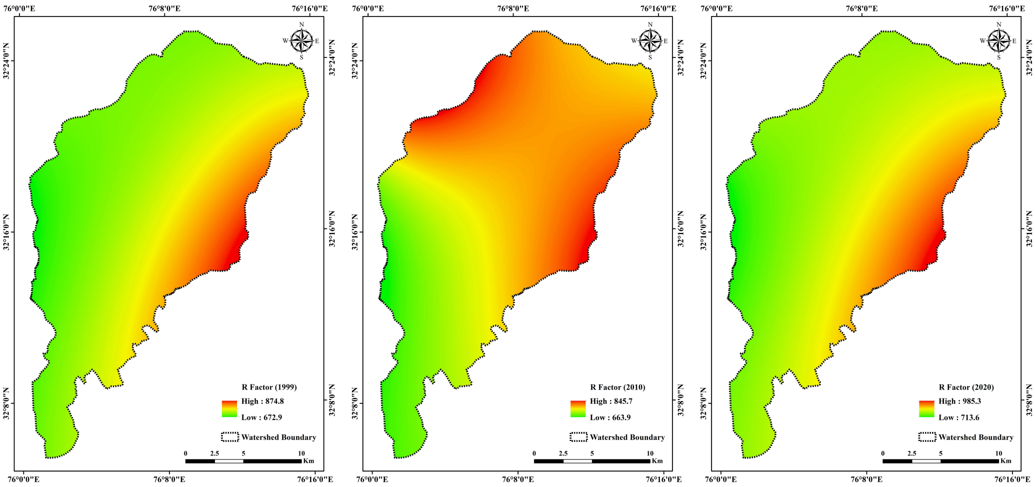

FIGURE 9
Maps showing R factor for the years 1999, 2010, and 2020 of the Dehar watershed.

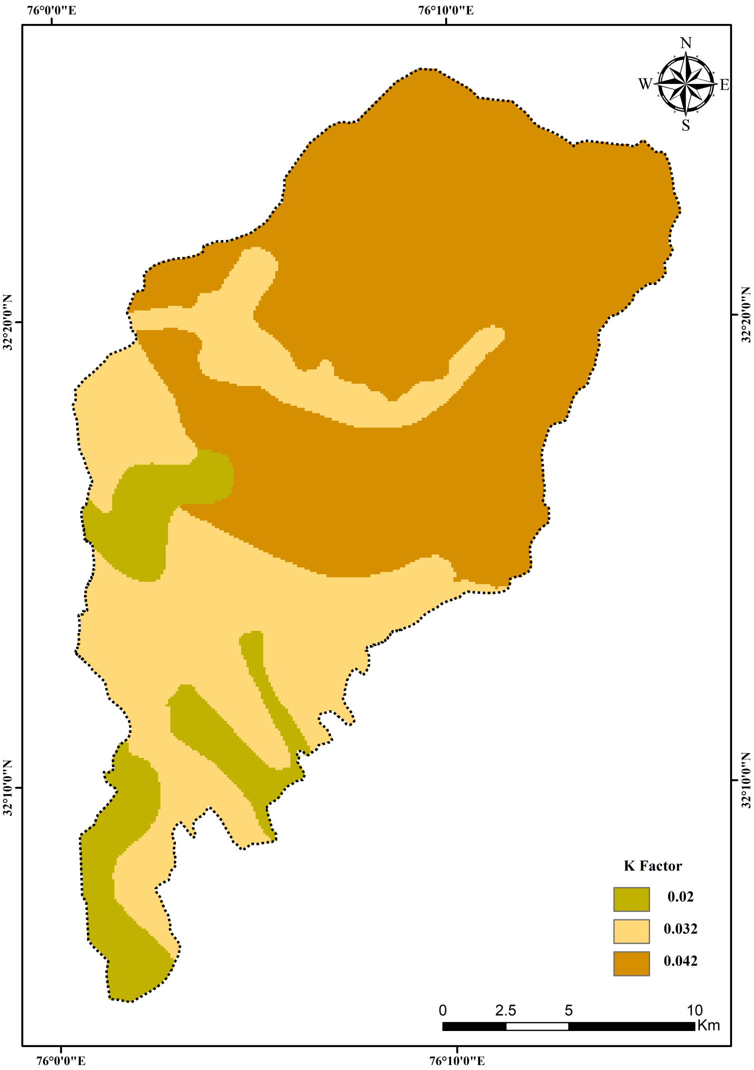

FIGURE 10
Map showing K factor of the Dehar watershed.

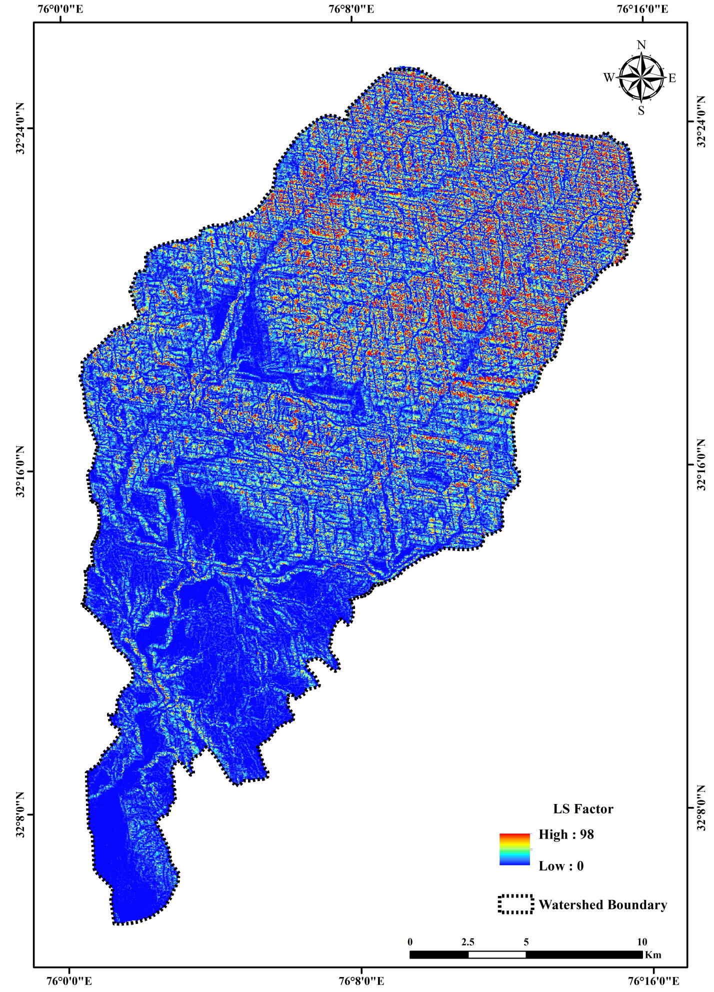

FIGURE 11
Map showing LS factor of the Dehar watershed.

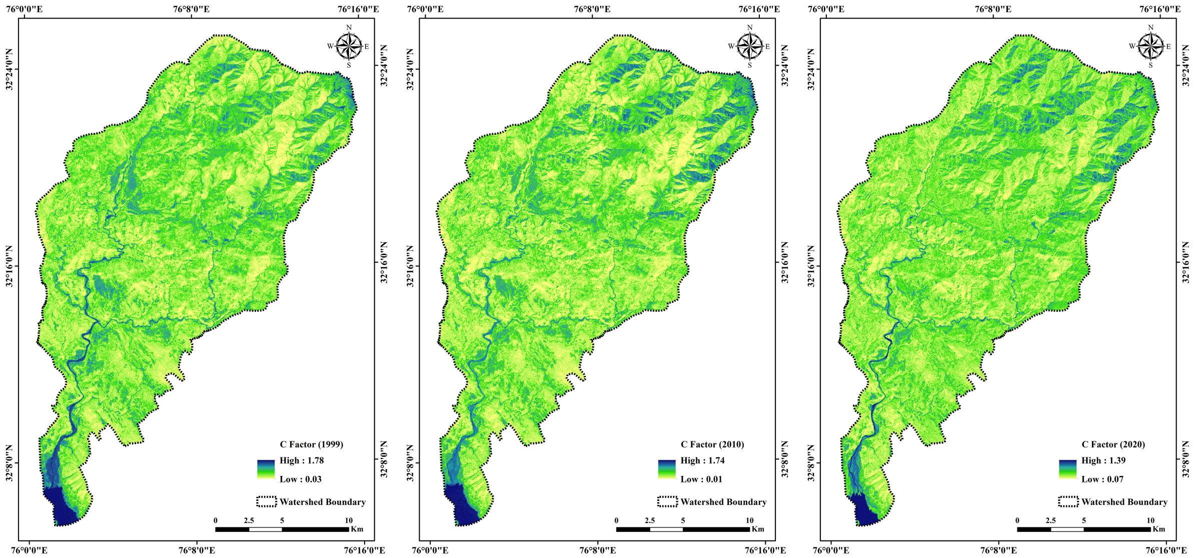

FIGURE 12
Maps showing C factor of the Dehar watershed for the years 1999, 2010, and 2020.

Crop management factor (C factor)

The crop management factor (C factor), also known as the cover management factor, shows the influence of cropping and other allied practices on soil erosion (Chalise et al., 2019; Sandeep et al., 2021). It also expresses the response of vegetative cover to water erosion. Areas with unprotected vegetative cover are commonly prone to high water erosion. On the other hand, soil erosion is low in the areas where the land is protected by vegetative cover. Nearing et al. (2004) viewed the C factor as sensitive to spatiotemporal variations, as it depends on vegetative growth and rainfall conditions. The C factor is represented as the erosion-weighted ratio of soil loss from crop/cover land to the corresponding loss from bare fallow or unprotected soil cover (Wischmeier and Smith, 1978). This factor holds a dimensionless number and the values range between 0 and 1, where 0 signifies the area has vegetative cover and is erosion-protected, whereas 1 represents the area is bare, uncovered, and prone to soil erosion. Significantly, thick vegetation protects from soil erosion by reducing runoff intensity and raindrop influence on the soil-covered ground surface (Ranzi et al., 2012). Therefore, vegetative cover is known to be a crucial factor along with the topographic factor in controlling the rate of soil loss (Zhou et al., 2008; Li et al., 2019).

In this study, an LU/LC-related method was adopted for calculating C factor values of the area. The C factor values for the respective years were generated from Normalized Differential Vegetative Index (NDVI) derived from LANDSAT-07, LANDSAT-05, and SENTINAL-2 images for the years 1999, 2010, and 2020, respectively (**Figure 6**). For calculating the C factor, the equation (Eq. 4) proposed by van der Knijff et al. (2000) was adopted.

$$C = \exp\left[-\alpha\left((\mathrm{NDVI}/(\beta - \mathrm{NDVI})\right)\right] \quad (4)$$

Where α and β are unitless parameters that fix the shape of the NDVI and the C factor curve. This equation has been widely used for Indian mountainous terrains (Kumar et al., 2014).

Conservation practice factor (P factor)

The conservation practice factor reveals the positive outcome of soil and water conservation processes of soil erosion in relation to agricultural practices. Wischmeier and Smith (1978) viewed the P factor as the percentage of erosion during the period of conservation and protective conditions compared to the usual circumstances of erosion occurrence.

The P factor values range between 0 and 1, where the values falling near to 0 signify the area is under healthy soil and water conservation practices, whereas the values close to 1 represent that the area lacks appropriate conservation practices (**Table 3**). In this study, the P factor map was developed by adopting the existing P factor values of the related land-cover classes collected from published sources (Wischmeier and Smith, 1978; Wanielista and Yousef, 1993; Londhe et al., 2010).

Results

Land use/land cover change

It was inferred from the analysis of the LULC classes that Built-Up areas increased from 2.3 km^2 in the year 1999 to 3.96 km^2 in 2010 and 5.36 km^2 in 2020. Agricultural Land increased from 48.16 km^2 in the year 1999 to 61.09 km^2 in 2010 and 64.28 km^2 in 2020. Conversely, Barren Land decreased from 50.15 km^2 in the year 1999 to 34.75 km^2 in 2010 and 26.85 km^2 in 2020. Forest Land increased from 342.1 km^2 in 1999 to 343.2 km^2 in 2010 and 346.2 km^2 in 2020. However, in the case of Water Bodies, there was a decrease from 5.89 km^2 in the year 1999 to 5.6 km^2 in 2010, and an increase 5.91 km^2 in 2020 (**Table 4** and **Figures 7**, **8**). The results of the area under very low, low, moderate, high, very high, and extremely severe erosion classes during the years 1999, 2010, and 2020 with respect to different LULC classes such as Built-Up area, Agriculture Land, Forest Land, and Barren Land are presented in **Table 7**. The confusion matrix resulted

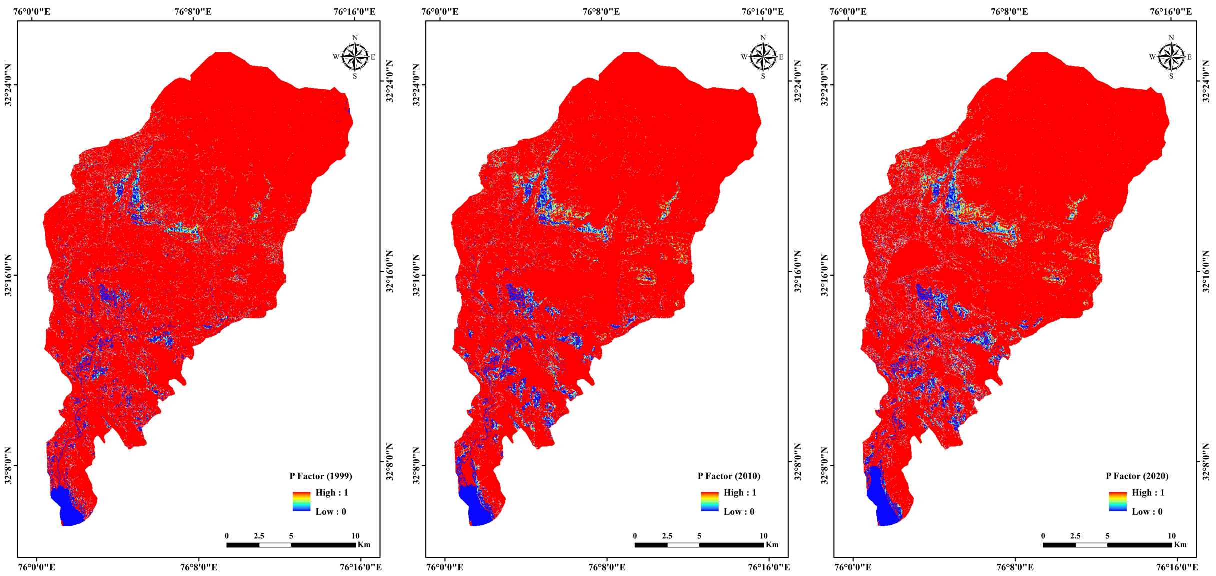

FIGURE 13
Maps showing P factor of the Dehar watershed for the years 1999, 2010, and 2020.

TABLE 7 LULC class-wise area in percentage under different soil loss potential classes for the years 1999, 2010, and 2020.

LULC Classes	Area (in percentage) of different soil loss potential classes																	
	Very low (0–1)			Low (1–5)			Moderate (5–10)			High (10–20)			Very high (20–50)			Extreme (> 50)		
Year	1999	2010	2020	1999	2010	2020	1999	2010	2020	1999	2010	2020	1999	2010	2020	1999	2010	2020
Built-up	48.39%	61.38%	63.05%	0.1%	1.13%	0.74%	2.1%	5.27%	4.67%	6.76%	9.44%	8.37%	13%	11.38%	10.12%	29.65%	11.40%	13.05%
Agricultural land	63.91%	60.58%	60.87%	0.4%	1.39%	1.84%	3.59%	3.97%	5.48%	6.36%	5.91%	5.65%	8.05%	8.41%	8.74%	17.69%	19.74%	17.42%
Forest	43.21%	42.52%	42.15%	0.55%	1.49%	0.42%	2.88%	3.53%	2.52%	5.47%	6.31%	4.68%	12.16%	13.01%	10.65%	35.73%	33.14%	39.58%
Barren land	45.14%	50%	47.69%	0.01%	0.18%	0.08%	0.57%	1.15%	1.13%	2.75%	3.59%	4.04%	7.18%	7.66%	8.39%	44.35%	37.42%	38.67%
Water body	100%	100%	100%															

in an overall accuracy of 86.84% for 1999, 87.43% for 2010, and 88.05% for 2020 with a Kappa coefficient value of 0.827, 0.835, and 0.842 for the years 1999, 2010, and 2020, respectively (Table 5). It was inferred from the obtained results that the image classification was performed with accuracy.

R factor

The erosivity rate is directly related to the total amount of precipitation that occurred in a particular area (Sandeep et al., 2021). The *R*-values of the study area varied between 713 and 985 MJ mm/ha/hr/year in 2020, 663 to 845 MJ mm/ha/hr/year in 2010, and 672 to 874 MJ mm/ha/hr/year in 1999 (**Figure 9**). The watershed receives high rainfall from July to September during the southwest monsoon season. The eastern part of the watershed has a high *R*-value in comparison to the western part (**Figure 9**). Thus, this indicated that high R factor values influence the rate of soil erosion in the watershed.

K factor

The prominent soil types of the area are sandy-skeletal, coarse-loamy, and fine-loamy soils. Almost 57% of the total geographical area is covered by sandy-skeletal soil followed by coarse-loamy soil (32%), then fine-loamy soil (11%) (**Figure 4**). The soil erodibility (K factor) values of the study area vary from 0.020 to 0.042 (**Table 2**). The northern part of the watershed is covered by sandy-skeletal soil signifying the highest K factor value (**Figure 10**), while the central and southern parts of the watershed are covered by coarse- and fine-loamy soils with lower K factor values.

LS factor

The elevation of the Dehar watershed ranges from 395 to 4080 m with a relief of 3,695 m. The LS factor was calculated using DEM and equation (Eq. 3), by considering the interface between flow accumulation and topographic features (**Figure 5**). The LS factor of the watershed ranged from 0 to 98 with a mean value of 5.38 (**Figure 11**).

C factor

The vegetative cover factor (C) was determined using the equation (Eq. 4) for the years 1999, 2010, and 2020 (**Figure 12**). The NDVI values for the years 1999, 2010, and 2020 ranged from−0.41 to 0.63, −0.38 to 0.67, and −0.19 to 0.55, respectively (**Figure 6**). The C factor values generated from the NDVI ranged from 0.03 to 1.78 for 1999, 0.01 to 1.74 for 2010, and 0.07 to 1.39 for 2020 (**Figure 12**). The derived C factor values revealed that higher values were found in barren land and lower values were reported in vegetative cover areas.

P factor

The P factor value of the study area varied from 0 to 1 (**Figure 13** and **Table 3**). The lowest value (0) was assigned to a water body where conservation measures were undertaken, while a P factor value (1) was given to vegetation, barren land, built-up area, and agriculture land (less than 3% and more than 25% slope) where appropriate soil-water conservation strategies were not adopted. The different agricultural land use classes (with slopes varying from 3–8, 8–12, 12–16, 16–20, and 20–25%) were assigned *P*-values ranging from 0.5 to 0.9.

Effect of LULC changes on soil erosion

The different RUSLE parameters were multiplied in an ArcGIS 10.8 environment by applying a raster calculator tool to find the geoenvironmental conditions in the Dehar watershed by knowing the spatiotemporal changes and the rate of soil erosion during the years 1999, 2010, and 2020. The assessed rate of soil erosion was grouped into five classes: very low (0–1 t/ha/y), low (1–5 t/ha/y), moderate (5–10 t/ha/y), high (10–20 t/ha/y), very high (20–50 t/ha/y), and extreme (>50 t/ha/y), as shown in **Table 6** (Dabral et al., 2008). The very low class (0–1 t/ha/yr) showed a higher area in percentage with respect to soil loss followed by the extremely severe class (>50 t/ha/yr) for all three years (1999, 2010, and 2020) of the LULC settings (**Figure 14**).

In 1999, the percentages of areas that experienced very low, low, moderate, high, very high, and extremely severe erosion were 46.42, 0.45, 2.53, 5.05, 10.81, and 34.74%, respectively (**Table 6**). Whereas in 2010, the percentages of areas that experienced very low, low, moderate, high, very high, and extremely severe erosion were 46.52, 1.32, 3.31, 5.91, 11.69, and 31.25%, respectively. Similarly, in 2020, the areas prone to very low, low, moderate, high, very high, and extremely severe erosion were 46.1, 0.56, 2.71, 4.68, 10.03, and 35.92%, respectively. The results representing areas under very low, low, moderate, high, very high, and extremely severe erosion classes and mean soil loss within different land use classes are presented in **Tables 6–8**.

Discussion

In the present study, the influence of LULC changes on soil loss dynamics in the Dehar watershed was estimated using the empirical model RUSLE in the GIS environment. RUSLE is widely applied in mountain terrains and very suitable for the Himalayan mountains system (Cevik and Topal, 2003; Dissanayake et al., 2019; Thapa, 2020; George et al., 2021; Kumar and Hole, 2021). It was inferred from the study that a subsequent rise in Built-Up and Agricultural Land was observed in the years 2010 and 2020 and, conversely, Barren Land decreased in the years 2010 and 2020 due to the rise in the population and expansion of habitats and agricultural fields in the lesser and Sub-Himalayan zone in recent years, leading to the conversion of Barren Land to Built-Up and Agricultural fields. The class Forest also showed a minor rise in the years 2010 and 2020 due to sustainable forest conservation and management practices (**Table 4**). In the Built-Up class of land use, the mean soil loss decreased from 32.19 in 1999 to 18.77 t/ha/yr in 2010, but in the year 2020 the mean soil loss slightly increased to 20.15 t/ha/yr (**Table 8**). Further, Barren Land registered a decrease in the mean soil loss from 86.43 t/ha/yr in the year 1999 to 74.60 t/ha/yr in 2010 and 73.19 t/ha/yr in the year 2020. Regarding the Agriculture class, the rate of mean soil loss slightly increased from 32.55 t/ha/yr in 1999 to 33.35 t/ha/yr in 2010, but then

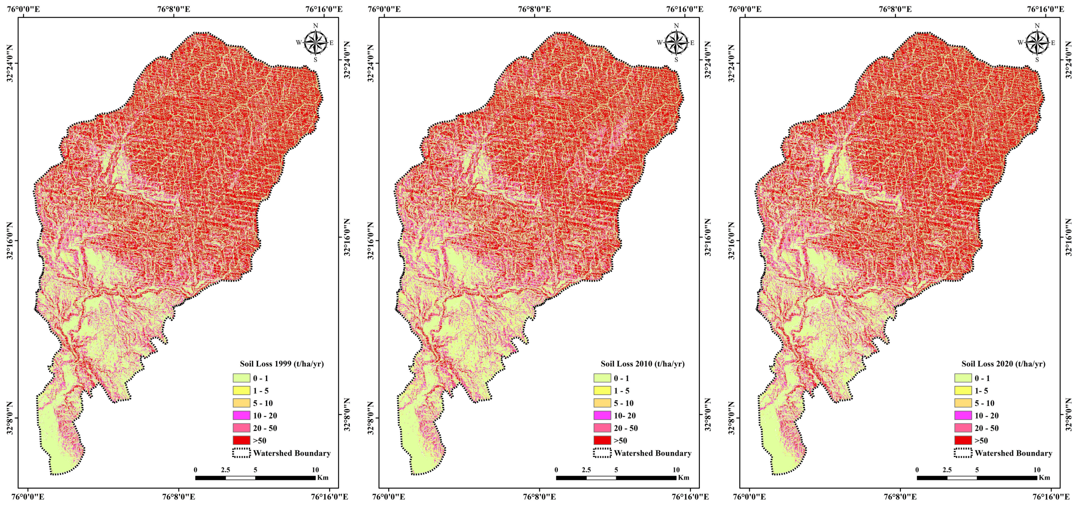

FIGURE 14
Maps showing soil erosion trends of the Dehar watershed for the years 1999, 2010, and 2020.

TABLE 8 Mean soil loss in different LULC classes for the years 1999, 2010, and 2020.

LULC classes	Mean soil loss (t/ha/year)			
	Built-up	Barren land	Agricultural land	Forest
1999	32.19	86.43	32.55	65.30
2010	18.77	74.60	33.35	65.87
2020	20.15	73.19	25.43	74.72

decreased to 25.43 t/ha/yr in 2020. The area covered under Forest experienced an increase in mean soil loss, from 65.30 t/ha/yr in 1999 to 65.87 in 2010 and 74.72 t/ha/yr in 2020. From the current study, it is inferred that the Barren Land and Forest classes experienced a higher rate of soil erosion in comparison to other classes because the Dehar watershed is prone to high precipitation and its presence in a high altitudinal area with hilly terrain, steep to very steep slopes, incidents of forest fires, and unsustainable forest management practices. In the Sub-Himalayas, the Barren and Forest areas experience a high rate of soil erosion due to their spread on high elevations and steep slopes (Kumar et al., 2014; Fayas et al., 2019; Uddin et al., 2019).

Rainfall erosivity (R factor) indicated a rise in the mean soil loss between the years 2010 and 2020. Further, the R factor clearly illustrated the importance of rainfall erosivity in soil loss estimation, as its values increased between the years 2010 and 2020. Interestingly, the area experienced a decrease in total mean soil loss between the years 1999 and 2010 and an increase in the total mean soil loss between the years 2010 and 2020 (**Table 6**).

Conclusion

This study evaluated the influence of LULC changes on soil erosion in a hilly watershed in the northern western Himalaya region in the state of Himachal Pradesh, India, for the years 1999, 2010, and 2020. The methodology adopted was to apply the RUSLE method for soil loss estimation in a GIS environment to create and compare soil loss estimation maps of 1999, 2010, and 2020. Moreover, the main aim was to identify soil loss changes that occurred due to LULC change. The RUSLE model in combination with the GIS technique was applied to estimate the rate of soil erosion in different LULC classes. The RUSLE model was successfully employed by giving due importance to different factors (R, K, LS, P, and C). The results yielded mean soil loss of 63.71, 60.99, and 66.71 t/ha/yr for the year 1999, 2010, and 2020, respectively, indicating that the LULC changes considerably influenced the rate of soil loss in the Dehar watershed. Overall, the present study clearly shows that soil erosion is a serious geoenvironmental issue and it needs the urgent attention of scientists, policymakers, and the general public for sustainable management of soil resources. Additionally, the data used in the present study was of coarser resolution and of a larger scale. There is wider scope for further studies at micro-watershed levels using high-resolution satellite imageries and more accurate rainfall data sets derived from different sources and validated with field-based models. More precise soil-loss estimations would help various stakeholders in taking suitable measures for the prevention of soil erosion.

Data availability statement

The raw data supporting the conclusions of this article will be made available by the author, without undue reservation.

Author contributions

MP: investigation, visualization, supervision and formal analysis, writing – original draft, and reviewing and editing. AK: conceptualization, methodology, investigation, data collection and data generation, writing, and reviewing and editing. SD: conceptualization, methodology, investigation, writing, and reviewing and editing. OV, SR, and BK: writing and reviewing and editing. All authors contributed to the article and approved the submitted version.

Conflict of interest

The authors declare that the research was conducted in the absence of any commercial or financial relationships that could be construed as a potential conflict of interest.

Publisher's note

References

Abdulkareem, J. H., Pradhan, B., Sulaiman, W. N. A., and Jamil, N. R. (2019). Prediction of spatial soil loss impacted by long-term land-use/land-cover change in a tropical watershed. *Geosci. Front.* 10, 389–403. doi: 10.1016/j.gsf.2017.10.010

Adongo, T. A., Agyare, W. A., Abagale, F. K., and Buffour, N. K. (2019). Spatial soil loss estimation using an integrated GIS-based revised universal soil loss equation. *Int. J. Sci. Technol.* 11, 58–71. doi: 10.4314/ijest.v11i4.6

Alkharabsheh, M. M., Alexandridis, T. K., Bilas, G., Misopolinos, N., and Silleos, N. (2013). Impact of land cover change on soil erosion hazard in northern Jordan using remote sensing and GIS. *Procedia Environ. Sci.* 19, 912–921. doi: 10.1016/j.proenv.2013.06.101

Ang, R., and Oeurng, C. (2018). Simulating streamflow in an ungauged catchment of Tonlesap Lake basin in Cambodia using soil and water assessment tool (SWAT) model. *Water Sci.* 32, 89–101. doi: 10.1016/j.wsj.2017.12.002

Angima, S. D., Stott, D. E., O'neill, M. K., Ong, C. K., and Weesies, G. A. (2003). Soil erosion prediction using RUSLE for central Kenyan highland conditions. *Agric. Ecosyst. Environ.* 97, 295–308. doi: 10.1016/S0167-8809(03)00011-2

Ayele, K. F., Suryabhagavan, K. V., and Sathishkumar, B. (2014). Assessment of habitat changes in Holeta watershed, central Oromiya, Ethiopia. *Int. J. Earth Sci. Eng.* 7, 1370–1375.

Bhattacharyya, R., Ghosh, B. N., Mishra, P. K., Mandal, B., Rao, C. S., Sarkar, D., et al. (2015). Soil degradation in India: Challenges and potential solutions. *Sustainability* 7, 3528–3570. doi: 10.3390/su7043528

Boggs, G., Devonport, C., Evans, K., and Puig, P. (2001). GIS-based rapid assessment of erosion risk in a small catchment in the wet/dry tropics of Australia. *Land Degrad. Dev.* 12, 417–434. doi: 10.1002/ldr.457

Cevik, E., and Topal, T. (2003). GIS-based landslide susceptibility mapping for a problematic segment of the natural gas pipeline, Hendek (Turkey). *Environ. Geol.* 44, 949–962. doi: 10.1007/s00254-003-0838-6

Chalise, D., Kumar, L., and Kristiansen, P. (2019). Land degradation by soil erosion in Nepal: A review. *Soil Syst.* 3:12. doi: 10.3390/soilsystems3010012

Dabral, P. P., Baithuri, N., and Pandey, A. (2008). Soil erosion assessment in a hilly catchment of North Eastern India using USLE, GIS and remote sensing. *Water Resour. Manag.* 22, 1783–1798. doi: 10.1007/s11269-008-9253-9

Dissanayake, D. M. S. L. B., Morimoto, T., and Ranagalage, M. (2019). Accessing the soil erosion rate based on RUSLE model for sustainable land use management: A case study of the Kotmale watershed, Sri Lanka. *Model. Earth Syst. Environ.* 5, 291–306. doi: 10.1007/s40808-018-0534-x

Erol, A., Koşkan, Ö., and Başaran, M. A. (2015). Socioeconomic modifications of the universal soil loss equation. *Solid Earth* 6, 1025–1035. doi: 10.5194/se-6-1025-2015

Eswaran, H., Lal, R., and Reich, P. F. (2001). "Land degradation: An overview," in *Proceedings of the 2nd international conference on land degradation and desertification. Responses to land degradation*, eds E. Bridges, I. Hannam, L. Oldeman, F. Penning de Vries, S. Scherr, and S. Sompatpanit (Thailand: Oxford Press), 20–35. doi: 10.1201/9780429187957-4

Fayas, C. M., Abeysingha, N. S., Nirmanee, K. G. S., and Samaratunga, M. D. (2019). A Soil loss estimation using rusle model to prioritize erosion control in KELANI river basin in Sri Lanka. *Int. Soil Water Conserv. Res.* 7, 130–137. doi: 10.1016/j.iswcr.2019.01.003

Galdino, S., Sano, E. E., Andrade, R. G., Grego, C. R., Nogueira, S. F., Bragantini, C., et al. (2016). Large-scale modeling of soil erosion with RUSLE for conservationist planning of degraded cultivated Brazilian pastures. *Land Degrad. Dev.* 27, 773–784. doi: 10.1002/ldr.2414

Ganasri, B., and Ramesh, H. (2016). Assessment of soil erosion by RUSLE model using remote sensing and GIS-A case study of Nethravathi Basin. *Geosci. Front.* 7, 953–961. doi: 10.1016/j.gsf.2015.10.007

Garcia-Ruiz, J. M., Beguería, S., Nadal-Romero, E., Gonzalez-Hidalgo, J. C., Lana-Renault, N., and Sanjuán, Y. (2015). A meta-analysis of soil erosion rates across the world. *Geomorphology* 239, 160–173. doi: 10.1016/j.geomorph.2015.03.008

Gelagay, H. S., and Minale, A. S. (2016). Soil loss estimation using GIS and remote sensing techniques: A case of Koga watershed, Northwestern Ethiopia. *Int. Soil Water Conserv. Res.* 4, 126–136. doi: 10.1016/j.iswcr.2016.01.002

George, K. J., Kumar, S., and Hole, R. M. (2021). Geospatial modelling of soil erosion and risk assessment in Indian Himalayan region—A study of Uttarakhand state. *Environ. Adv.* 4:100039.

Glaeser, E. L., and Kahn, M. E. (2004). "Sprawl and urban growth," in *Handbook of regional and urban economics, cities and geography*, Vol. 4, eds J. V. Henderson and J. E. Thisse (Amsterdam: Elsevier), 2481–2527. doi: 10.1016/S1574-0080(04)80013-0

Hamilton, L. S. (1987). What are the impacts of Himalayan deforestation on the Ganges-Brahmaputra lowlands and delta? Assumptions and facts. *Mt. Res. Dev.* 7, 256–263. doi: 10.2307/3673202

Haregeweyn, N., Tsunekawa, A., Nyssen, J., Poesen, J., Tsubo, M., Meshesha, D., et al. (2015). Soil erosion and conservation in Ethiopia: A review. *Prog. Phys. Geogr.* 39, 750–774. doi: 10.1177/0309133315598725

Hickey, R. (2001). Slope angle and slope length solutions for GIS. *Cartography* 29, 1–8. doi: 10.1080/00690805.2000.9714334

Hrissanthou, V., Delimani, P., and Xeidakis, G. (2010). Estimate of sediment inflow into Vistonis Lake, Greece. *Int. J. Sediment Res.* 25, 161–174. doi: 10.1016/S1001-6279(10)60035-2

Hurni, H., Tato, K., and Zeleke, G. (2005). The implications of changes in population, land use, and land management for surface runoff in the upper Nile basin area of Ethiopia. *Mt. Res. Dev.* 25, 147–154. doi: 10.1659/0276-4741(2005)025[0147:TIOCIP]2.0.CO;2

Islam, M. R., Jaafar, W. Z. W., Hin, L. S., Osman, N., and Karim, M. R. (2020). Development of an erosion model for Langat River Basin, Malaysia, adapting GIS and RS in RUSLE. *Appl. Water Sci.* 10, 1–11. doi: 10.1007/s13201-020-01185-4

Jain, M. K., Mishra, S. K., and Shah, R. B. (2010). Estimation of sediment yield and areas vulnerable to soil erosion and deposition in a Himalayan watershed using GIS. *Curr. Sci.* 98, 213–221.

Jain, S. K., Kumar, S., and Varghese, J. (2001). Estimation of soil erosion for a Himalayan watershed using GIS technique. *Water Resour. Manag.* 15, 41–54. doi: 10.1023/A:1012246029263

Jayasekara, M. J. P. T. M., Kadupitiya, H. K., and Vitharana, U. W. A. (2018). Mapping of soil erosion hazard zones of Sri Lanka. *Trop. Agric. Res.* 29, 135–146. doi: 10.4038/tar.v29i2.8284

Jha, M. K., and Paudel, R. C. (2010). Erosion predictions by empirical models in a mountainous watershed in Nepal. *J. Spat. Hydrol.* 10, 89–102.

Kaiser, J. (2004). Wounding earth's fragile skin. *Science* 304, 1616–1618. doi: 10.1126/science.304.5677.1616

Keno, K., and Suryabhagavan, K. V. (2014). Multi-temporal remote sensing of landscape dynamics and pattern change in Dire district, Southern Ethiopia. *J. Geomorphol.* 8, 189–194. doi: 10.4172/2157-7617.1000226

Khosrokhani, M., and Pradhan, B. (2014). Spatio-temporal assessment of soil erosion at Kuala Lumpur metropolitan city using remote sensing data and GIS. *Geomat. Nat. Hazards Risk* 5, 252–270. doi: 10.1080/19475705.2013.794164

Koirala, P., Thakuri, S., Joshi, S., and Chauhan, R. (2019). Estimation of soil erosion in Nepal using a RUSLE modeling and geospatial tool. *Geosciences* 9:147. doi: 10.3390/geosciences9040147

Kolli, M. K., Opp, C., and Groll, M. (2021). Estimation of soil erosion and sediment yield concentration across the Kolleru Lake catchment using GIS. *Environ. Earth Sci.* 80:161. doi: 10.1007/s12665-021-09443-7

Kouli, M., Soupios, P., and Vallianatos, F. (2009). Soil erosion prediction using the revised universal soil loss equation (RUSLE) in a GIS framework, Chania, Northwestern Crete, Greece. *Environ. Geol.* 57, 483–497. doi: 10.1007/s00254-008-1318-9

Krishna Bahadur, K. C. (2009). Mapping soil erosion susceptibility using remote sensing and GIS: A case of the Upper Nam Wa Watershed, Nan Province, Thailand. *Environ. Geol.* 57, 695–705. doi: 10.1007/s00254-008-1348-3

Kumar, A., Devi, M., and Deshmukh, B. (2014). Integrated remote sensing and geographic information system based RUSLE modelling for estimation of soil loss in western Himalaya, India. *Water Resour. Manag.* 28, 3307–3317. doi: 10.1007/s11269-014-0680-5

Kumar, R., and Nanda, A. C. (1989). Sedimentology of the middle Siwalik subgroup of Mohand area, Dehra Dun valley, India. *J. Geol. Soc. India* 34, 597–616.

Kumar, S., and Hole, R. M. (2021). Geospatial modelling of soil erosion and risk assessment in Indian Himalayan region—A study of Uttarakhand state. *Environ. Adv.* 4:100039. doi: 10.1016/j.envadv.2021.100039

Kumar, S., and Mahajan, A. K. (2001). Seismotectonics of the Kangra region, northwest Himalaya. *Tectonophysics* 331, 359–371. doi: 10.1016/S0040-1951(00)00293-6

Kumar, T., Jhariya, D. C., and Pandey, H. K. (2020). Comparative study of different models for soil erosion and sediment yield in Pairi watershed, Chhattisgarh, India. *Geocarto Int.* 35, 1245–1266. doi: 10.1080/10106049.2019.1576779

Lambin, E. F., Turner, B. L., Geist, H. J., Agbola, S. B., Angelsen, A., Bruce, J. W., et al. (2010). Land degradation in dry lands: Interactions among hydrologic-aeolian erosion and vegetation dynamics. *Geomorphology* 116, 236–245. doi: 10.1016/j.geomorph.2009.11.023

Li, Y., Qi, S., Liang, B., Ma, J., Cheng, B., Ma, C., et al. (2019). Dangerous degree forecast of soil loss on highway slopes in mountainous areas of the Yunnan–Guizhou Plateau (China) using the Revised Universal Soil Loss Equation. *Nat. Hazards Earth Syst. Sci.* 19, 757–774. doi: 10.5194/nhess-19-757-2019

Londhe, S., Nathawat, M. S., and Subudhi, A. P. (2010). Erosion susceptibility zoning and prioritization of mini-watersheds using geomatics approach. *Int. J. Geomat. Geosci.* 1, 511–528.

Mahapatra, S. K., Reddy, G. O., Nagdev, R., Yadav, R. P., Singh, S. K., and Sharda, V. N. (2018). Assessment of soil erosion in the fragile Himalayan ecosystem of Uttarakhand, India using USLE and GIS for sustainable productivity. *Curr. Sci.* 115, 108–121. doi: 10.18520/cs/v115/i1/108-121

Mandal, D., and Sharda, V. N. (2011). Assessment of permissible soil loss in India employing a quantitative bio-physical model. *Curr. Sci.* 100, 383–390.

Mandal, D., and Sharda, V. N. (2013). Appraisal of soil erosion risk in the Eastern Himalayan region of India for soil conservation planning. *Land Degrad. Dev.* 24, 430–437.

Meshesha, D. T., Tsunekawa, A., Tsubo, M., and Haregeweyn, N. (2012). Dynamics and hotspots of soil erosion and management scenarios of the Central Rift Valley of Ethiopia. *Int. J. Sediment Res.* 27, 84–99. doi: 10.1016/S1001-6279(12)60018-3

Mohammadi, M., Khaledi Darvishan, A. K., Spalevic, V., Dudic, B., and Billi, P. (2021). Analysis of the impact of land use changes on soil erosion intensity and sediment yield using the intErO model in the Talar watershed of Iran. *Water* 13:881. doi: 10.3390/w13060881

Moisa, M. B., Babu, A., and Getahun, K. (2023). Integration of geospatial technologies with RUSLE model for analysis of soil erosion in response to land use/land cover dynamics. A case of Jere watershed, Western Ethiopia. *Sustain. Water Resour. Manag.* 9:13. doi: 10.1007/s40899-022-00805-y

Morgan, R. P. C., Quinton, J. N., Smith, R. E., Govers, G., Poesen, J. W. A., Auerswald, K., et al. (1998). The European soil erosion model (EUROSEM): A dynamic approach for predicting sediment transport from fields and small catchments. *Earth Surf. Process. Landf.* 23, 527–544. doi: 10.1002/(SICI)1096-9837(199806)23:6<527::AID-ESP868>3.0.CO;2-5

NBSS and LUP (2005). *Annual report 2005*. Nagpur: National Bureau of Soil Survey and Land Use Planning.

Nearing, M. A., Foster, G. R., Lane, L. J., and Finkner, S. C. (1989). A process-based soil erosion model for USDA-water erosion prediction project technology. *Trans. ASAE* 32, 1587–1593. doi: 10.13031/2013.31195

Nearing, M. A., Pruski, F. F., and O'neal, M. R. (2004). Expected climate change impacts on soil erosion rates: A review. *J. Soil Water Conserv.* 59, 43–50.

Negash, D. A., Moisa, M. B., Merga, B. B., Sedeta, F., and Gemeda, D. O. (2021). Soil erosion risk assessment for prioritization of sub-watershed: The case of Chogo Watershed, Horo Guduru Wollega, Ethiopia. *Environ. Earth Sci.* 80:589. doi: 10.1007/s12665-021-09901-2

Oliveira, M. L., Saikia, B. K., da Boit, K., Pinto, D., Tutikian, B. F., and Silva, L. F. (2019). River dynamics and nanopaticles formation: A comprehensive study on the nanoparticle geochemistry of suspended sediments in the Magdalena River, Caribbean Industrial Area. *J. Clean. Prod.* 213, 819–824. doi: 10.1016/j.jclepro.2018.12.230

Pan, J., and Wen, Y. (2014). Estimation of soil erosion using RUSLE in Caijiamiao watershed, China. *Nat. Hazards* 71, 2187–2205. doi: 10.1007/s11069-013-1006-2

Panagos, P., Borrelli, P., and Meusburger, K. (2015). A new European slope length and steepness factor (LS-Factor) for modeling soil erosion by water. *Geosciences* 5, 117–126. doi: 10.3390/geosciences5020117

Panagos, P., Borrelli, P., Meusburger, K., Yu, B., Klik, A., Jae, L. K., et al. (2017). Global rainfall erosivity assessment based on high-temporal resolution rainfall records. *Sci. Rep.* 7:4175. doi: 10.1038/s41598-017-04282-8

Panditharathne, D. L. D., Abeysingha, N. S., Nirmanee, K. G. S., and Mallawatantri, A. (2019). Application of revised universal soil loss equation (RUSLE) model to assess soil erosion in "Kalu Ganga" River Basin in Sri Lanka. *Appl. Environ. Soil Sci.* 2019:4037379. doi: 10.1155/2019/4037379

Paul, S. S., Li, J., Li, Y., and Shen, L. (2021). Assessing land use–land cover change and soil erosion potential using a combined approach through remote sensing, RUSLE and random forest algorithm. *Geocarta Int.* 36, 361–375. doi: 10.1080/10106049.2019.1614099

Pimentel, D., Allen, J., Beers, A., Guinand, L., Hawkins, A., Linder, R., et al. (1993). "Soil erosion and agricultural productivity," in *World soil erosion and conservation*, ed. D. Pimentel (Cambridge: Cambridge University Press), 277–292. doi: 10.1017/CBO9780511735394.014

Pimentel, D., and Burgess, M. (2013). Soil erosion threatens food production. *Agriculture* 3, 443–463. doi: 10.3390/agriculture3030443

Poesen, J. (2018). Soil erosion in the Anthropocene: Research needs. *Earth Surf. Process. Landf.* 43, 64–84. doi: 10.1002/esp.4250

Prasannakumar, V., Shiny, R., Geetha, N., and Vijith, H. J. E. E. S. (2011). Spatial prediction of soil erosion risk by remote sensing, GIS and RUSLE approach: A case study of Siruvani river watershed in Attapady valley, Kerala, India. *Environ. Earth Sci.* 64, 965–972. doi: 10.1007/s12665-011-0913-3

Prasannakumar, V., Vijith, H., Abinod, S., and Geetha, N. J. G. F. (2012). Estimation of soil erosion risk within a small mountainous sub-watershed in Kerala, India, using Revised Universal Soil Loss Equation (RUSLE) and geo-information technology. *Geosci. Front.* 3, 209–215. doi: 10.1016/j.gsf.2011.11.003

Prashanth, M., Kumar, A., Dhar, S., Verma, O., and Gogoi, K. (2022). Hypsometric analysis for determining erosion proneness of Dehar watershed, Himachal Himalaya, North India. *J. Geosci. Res.* 7, 86–94.

Prashanth, M., Kumar, A., Dhar, S., Verma, O., and Sharma, S. (2021). Morphometric characterization and prioritization of sub-watersheds for assessing soil erosion susceptibility in the Dehar watershed (Himachal Himalaya), Northern India. *Him. Geol.* 42, 345–358.

Ranzi, R., Le, T. H., and Rulli, M. C. (2012). A RUSLE approach to model suspended sediment load in the Lo River (Vietnam): Effects of reservoirs and land use changes. *J. Hydrol.* 422–423, 17–29. doi: 10.1016/j.jhydrol.2011.12.009

Ravi, S., Breshears, D. D., Huxman, T. E., and D'Odorico, P. (2010). Land degradation in dry lands: Interactions among hydrologic–aeolian erosion and vegetation dynamics. *Geomorphology* 116, 236–245.

Rawat, K. S., Mishra, A. K., and Bhattacharyya, R. (2016). Soil erosion risk assessment and spatial mapping using LANDSAT-7 ETM+, RUSLE, and GIS—a case study. *Arab. J. Geosci.* 9:288. doi: 10.1007/s12517-015-2157-0

Renard, K., Foster, G., Weesies, G., McCool, D., and Yoder, D. (1997). Predicting soil erosion by water: A guide to conservation planning with the Revised Universal Soil Loss Equation (RUSLE). *Agric. Handb.* 703, 65–100.

Saha, A., Ghosh, P., and Mitra, B. (2018). GIS based soil erosion estimation using Rusle model: A case study of upper Kangsabati watershed, West Bengal, India. *J. Environ. Sci. Nat. Resour.* 13, 119–126. doi: 10.19080/IJESNR.2018.13.555871

Samanta, S., Koloa, C., Pal, D. K., and Palsamanta, B. (2016). Estimation of potential soil erosion rate using RUSLE and E30 model. *Model. Earth Syst. Environ.* 2:149. doi: 10.1007/s40808-016-0206-7

Sandeep, P., Kumar, K. C., and Haritha, S. (2021). Risk modelling of soil erosion in semi-arid watershed of Tamil Nadu, India using RUSLE integrated with GIS and Remote Sensing. *Environ. Earth Sci.* 80:511. doi: 10.1007/s12665-021-09800-6

Sangeetha, R., and Ambujam, N. K. (2021). The over shadow of the human evolvement process in the dynamics of soil drift of an agricultural watershed in Nilgiri Hills, India. *Soil Water Res.* 16, 103–111. doi: 10.17221/105/2020-SWR

Senanayake, S., Pradhan, B., Huete, A., and Brennan, J. (2020). Assessing soil erosion hazards using land-use change and landslide frequency ratio method: A case study of Sabaragamuwa Province, Sri Lanka. *Remote Sens.* 12:1483. doi: 10.3390/rs12091483

Sharma, J. C. (2008). "Soil and water conservation in river catchments in Himalayan region," in *Land resources management in river valley and flood prone areas of Himalayan region*, eds J. C. Sharma, I. P. Sharma, and J. N. Raina (Dehradun: Bishen Singh Mahendra Pal Singh), 113–123.

Shrestha, D. P. (1997). Assessment of soil erosion in the Nepalese Himalaya: A case study in Likhu Khola Valley, Middle Mountain Region. *Land Husb.* 2, 59–80.

Sidhu, G. S., Rana, K. P. C., Larsem, L., Sehgal, J., and Velayutham, M. (1997). *Soils of Himachal Pradesh for optimizing land use, India, Bulletin* 57(b). Nagpur: National Bureau of Soil Survey and Land Use Planning, 20–25.

Singh, G., Babu, R., and Chandra, S. (1981). *Soil loss prediction research in India, Bulletin No. T-12/D9*. Dehradun: Central Soil and Water Conservation Research and Training Institute.

Singh, G., and Panda, R. K. (2017). Grid-cell based assessment of soil erosion potential for identification of critical erosion prone areas using USLE, GIS and remote sensing: A case study in the Kapgari watershed, India. *Int. Soil Water Conserv. Res.* 5, 202–211. doi: 10.1016/j.iswcr.2017.05.006

Singh, O., and Singh, J. (2018). Soil erosion susceptibility assessment of the lower Himachal Himalayan Watershed. *J. Geol. Soc. India* 92, 157–165. doi: 10.1007/s12594-018-0975-x

Srikantia, S. V., and Bhargava, O. N. (1998). *Geology of Himachal Pradesh*. Bangalore: Geological Society of India.

Srinivasan, R., Singh, S. K., Nayak, D. C., Hegde, R., and Ramesh, M. (2019). Eurasian journal of soil science. *Eurasian J. Soil Sci.* 8, 321–328. doi: 10.18393/ejss.598120

Steffen, W., Stone, G. D., Svedin, U., Veldkamp, T. A., Vogel, C., and Xu, J. (2001). The causes of land-use and land-cover change: Moving beyond the myths. *Glob. Environ. Change* 11, 261–269. doi: 10.1016/S0959-3780(01)00007-3

Steinmetz, A. A., Cassalho, F., Caldeira, T. L., Oliveira, V. A. D., Beskow, S., and Timm, L. C. (2018). Assessment of soil loss vulnerability in data-scarce watersheds in southern Brazil. *Ciênc. Agrotec.* 42, 575–587. doi: 10.1590/1413-70542018426022818

Stocking, M. (1993). *Soil erosion in developing countries: Where geomorphology fears to tread*. Norwich: School of Development Studies University of East Anglia, 241.

Stoddart, D. R. (1969). "World erosion and sedimentation in water," in *Water, earth and man*, ed. R. J. Chorley (London: Methuen), 43–64. doi: 10.4324/9781003170181-5

Tang, Q., Xu, Y., Bennett, S. J., and Li, Y. (2015). Assessment of soil erosion using RUSLE and GIS: A case study of the Yangou watershed in the Loess Plateau, China. *Environ. Earth Sci.* 73, 1715–1724. doi: 10.1007/s12665-014-3523-z

Teng, H., Rossel, R. A. V., Shi, Z., Behrens, T., Chappell, A., and Bui, E. (2016). Assimilating satellite imagery and visible–near infrared spectroscopy to model and map soil loss by water erosion in Australia. *Environ. Model. Softw.* 77, 156–167. doi: 10.1016/j.envsoft.2015.11.024

Thapa, P. (2020). Spatial estimation of soil erosion using RUSLE modeling: A case study of Dolakha district, Nepal. *Environ. Syst. Res.* 9:15. doi: 10.1186/s40068-020-00177-2

Uddin, K., Matin, M. A., and Maharjan, S. (2019). Assessment of land cover change and its impact on changes in soil erosion risk in Nepal. *Sustainability* 10:4715. doi: 10.3390/su10124715

Uddin, K., Murthy, M. S. R., Wahid, S. M., and Matin, M. A. (2016). Estimation of soil erosion dynamics in the Koshi basin using GIS and remote sensing to assess priority areas for conservation. *PLoS One* 11:e0150494. doi: 10.1371/journal.pone.0150494

van der Knijff, J. M., Jones, R. J. A., and Montanarella, L. (2000). *Soil erosion risk assessment in Europe, EUR 19044 EN*. Luxembourg: Office for official publications of the European Communities, 1–34.

Vijith, H., Seling, L. W., and Dodge-Wan, D. (2018). Estimation of soil loss and identification of erosion risk zones in a forested region in Sarawak, Malaysia, Northern Borneo. *Environ. Dev. Sustain.* 20, 1365–1384. doi: 10.1007/s10668-017-9946-4

Viney, N. R., and Sivapalan, M. (1999). A conceptual model of sediment transport: Application to the Avon River Basin in Western Australia. *Hydrol. Process.* 13, 727–743. doi: 10.1002/(SICI)1099-1085(19990415)13:5<727::AID-HYP776>3.0.CO;2-D

Waltner, I., Saeidi, S., Grósz, J., Centeri, C., Laborczi, A., and Pásztor, L. (2020). Spatial assessment of the effects of Land cover change on soil erosion in Hungary from 1990 to 2018. *ISPRS Int. J. Geo Inf.* 9:667. doi: 10.3390/ijgi9110667

Wang, G., Gertner, G., Fang, S., and Anderson, A. B. (2003). Mapping multiple variables for predicting soil loss by geostatistical methods with TM images and a slope map. *Photogramm. Eng. Remote Sens.* 69, 889–898. doi: 10.14358/PERS.69.8.889

Wang, L., Huang, J., Du, Y., Hu, Y., and Han, P. (2013). Dynamic assessment of soil erosion risk using Landsat TM and HJ satellite data in Danjiangkou Reservoir area, China. *Remote Sens.* 5, 3826–3848. doi: 10.3390/rs5083826

Wanielista, M. P., and Yousef, Y. A. (1993). *Stormwater management*. New York, NY: John Wiley & Sons, 399–410.

Wischmeier, W. H., and Smith, D. D. (1978). *Predicting rainfall erosion losses: A guide to conservation planning (No. 537). Department of agriculture, science and education administration, agriculture handbook*. Washington, DC: U.S. Department of Agriculture.

Xu, L., Xu, X., and Meng, X. (2013). Risk assessment of soil erosion in different rainfall scenarios by RUSLE model coupled with information diffusion model: A case study of Bohai Rim, China. *Catena* 100, 74–82. doi: 10.1016/j.catena.2012.08.012

Yadav, R. P., and Sidhu, G. S. (2010). Assessment of soil erosion in Himachal Pradesh. *J. Indian Soc. Soil Sci.* 58, 212–220.

Yang, X., Gao, W., Shi, Q., Chen, F., and Chu, Q. (2013). Impact of climate change on the water requirement of summer maize in the Huang-Huai-Hai farming region. *Agric. Water Manag.* 124, 20–27. doi: 10.1016/j.agwat.2013.03.017

Zerihun, M., Mohammedyasin, M. S., Sewnet, D., Adem, A. A., and Lakew, M. (2018). Assessment of soil erosion using RUSLE, GIS and remote sensing in NW Ethiopia. *Geoderma Reg.* 12, 83–90. doi: 10.1016/j.geodrs.2018.01.002

Zhang, H., Yang, Q., Li, R., Liu, Q., Moore, D., He, P., et al. (2013). Extension of a GIS procedure for calculating the RUSLE equation LS factor. *Comput. Geosci.* 52, 177–188. doi: 10.1016/j.cageo.2012.09.027

Zhou, P., Luukkanen, O., Tokola, T., and Nieminen, J. (2008). Effect of vegetation cover on soil erosion in a mountainous watershed. *Catena* 75, 319–325. doi: 10.1016/j.catena.2008.07.010

Zhu, Y., Li, W., Wang, D., Wu, Z., and Shang, P. (2022). Spatial pattern of soil erosion in relation to Land use change in a rolling hilly region of Northeast China. *Land* 11:1253. doi: 10.3390/land11081253

Frontiers in Forests and Global Change

TYPE Original Research
PUBLISHED 14 February 2023
DOI 10.3389/ffgc.2023.1019277

EDITED BY
Zafar Ahmad Reshi,
University of Kashmir, India

REVIEWED BY
Bognounou Fidèle,
Laurentian Forestry Centre, Canada
Alan Feest,
University of Bristol, United Kingdom

*CORRESPONDENCE
Shreekar Pant
✉ shreekarpant.2@gmail.com

SPECIALTY SECTION
This article was submitted to
Forest Management,
a section of the journal
Frontiers in Forests and Global Change

RECEIVED 14 August 2022
ACCEPTED 12 January 2023
PUBLISHED 14 February 2023

CITATION
Wani ZA, Negi VS, Bhat JA, Satish KV, Kumar A, Khan S, Dhyani R, Siddiqui S, Al-Qthanin RN and Pant S (2023) Elevation, aspect, and habitat heterogeneity determine plant diversity and compositional patterns in the Kashmir Himalaya. *Front. For. Glob. Change* 6:1019277. doi: 10.3389/ffgc.2023.1019277

Elevation, aspect, and habitat heterogeneity determine plant diversity and compositional patterns in the Kashmir Himalaya

Zishan A. Wani[1], Vikram S. Negi[2], Jahangeer A. Bhat[3], K. V. Satish[4], Ashish Kumar[5], Sajid Khan[1], Rupesh Dhyani[2], Sazada Siddiqui[6], Rahmah N. Al-Qthanin[6] and Shreekar Pant[1]*

[1]Department of Botany, Baba Ghulam Shah Badshah University, Rajouri, Jammu and Kashmir, India, [2]G. B. Pant, National Institute of Himalayan Environment, Kosi-Katarmal, Almora, Uttarakhand, India, [3]College of Horticulture and Forestry, Rani Lakshmi Bai Central Agricultural University, Jhansi, UP, India, [4]Remote Sensing Laboratory, Institute of Environment and Sustainable Development, Banaras Hindu University, Varanasi, India, [5]G. B. Pant National Institute of Himalayan Environment, Garhwal Regional Centre, Srinagar Garhwal, Srinagar, Uttarakhand, India, [6]Department of Biology, College of Science, King Khalid University, Abha, Saudi Arabia

Elevational gradient, slope, and aspect offer a unique opportunity to explore the response of plant species under changing environmental conditions. The present study aimed to analyze the species diversity and distribution patterns with respect to altitude, aspect, and habitat types in the Kashmir Himalayas. Considering major aspects and habitats, a total of 123 representative sites were selected along the elevational gradients for the present study. The plant species composition of each selected site was studied by organized sampling following the standard ecological methods. During the present study, a total of 361 vascular plant species belonging to 71 families and 214 genera were identified in the study area. At the lower altitudes, the southern aspect and drier habitats showed the highest diversity. Moreover, a significant amount of compositional dissimilarity was observed between the studied aspects, habitats, and elevation belts and was mainly due to species turnover rather than the nestedness component. Further, among the studied variables, altitude was the most important contributing variable, explaining the greatest variation in the species composition. The paired effects of altitude and habitat explained the maximum variation in plant species composition. It may be concluded that floristic diversity should be studied not only with reference to elevational gradients but should also include aspects and habitats. The current study will act as a reference in this direction. A similar study must be replicated in other parts of the Himalayan region in the future to improve our understanding of the distribution and preferences of plant species in mountainous zones. This, in turn, will be immensely helpful in the conservation and sustainable utilization of resources in these ecologically fragile regions.

KEYWORDS

Kashmir Himalaya, composition, β-diversity, variation partitioning, elevation

1. Introduction

In an ecosystem, the vegetational structure, composition, and function are among the significant attributes showing considerable variation with changing biotic and abiotic variables (Bisht and Bhat, 2013; Rawat et al., 2018; Wani et al., 2022a). Slope, aspect, elevation, and edaphic factors are some examples of the widely studied variables that shape the community structure and distribution of species, especially in mountainous ecosystems (Gairola et al., 2011;

Dar and Sundarapandian, 2016). Among these factors, the topographic factors significantly impact vegetation and plants' growth (Davies et al., 2007), especially when the research scale is narrow (Zhang et al., 2021). Therefore, it is imperative to undertake site-specific studies instead of regional and national ones to better understand the changing patterns of biodiversity and its key drivers, especially in mountainous regions. In mountainous regions, the topographic alterations are considerable, and local environmental conditions are complex. Topographic variations act as significant indicators because of their key role in influencing the temperature and moisture of the habitat (Raulings et al., 2010). The biotic and abiotic gradients on mountains have the enormous potential to improve our understanding of species distributions and richness patterns (McCain and Grytnes, 2010). The main biotic and abiotic factors under the local topographic influence are hydrology, incident solar radiation, wind exposure, geochemistry, and biotic conditions (Moeslund et al., 2013). Micro-climatic conditions may vary significantly over short spatial scales in mountainous areas due to the steep environmental gradients and thus substantially influence vegetation distribution and species richness patterns (McCain and Grytnes, 2010). Hamid et al. (2021) found significant differences in the edaphic properties along elevation gradients and changing aspects in their study. They also discovered that aspect play an important role, in addition to elevation, in determining the survival of plant populations in mountainous areas.

On a habitat scale, the presence of a species is limited by the vegetation structure, edaphic gradients, and management-related gradients of the habitat (Wamelink et al., 2014). These gradients within the habitats not only affect the overall vegetation composition but also substantially impact the distribution of native and alien plant species (Khuroo et al., 2011). According to previous studies (McCain and Colwell, 2011), altitudinal gradients in mountainous regions provide valuable natural settings for investigating the long-term ecological and evolutionary effects of environmental changes on different species. These gradients are characterized by several predictable changes in environmental factors, including a decline in temperature with increasing elevation and an average of 0.6°C per 100 m (Barry, 2008). Other abiotic factors that vary along the elevation gradients include decreasing air pressure and increasing solar radiation (Barry, 2008; McCain and Grytnes, 2010). However, precipitation does not change consistently with elevation on all mountains but varies greatly due to regional mountains and weather conditions (Barry, 2008). The gradients in these abiotic factors strongly influence the distribution of species along the elevation gradient. Owing to these changing abiotic factors with increasing elevations, it is believed that diversity decreases linearly with elevation (MacArther, 1972; Korner, 1998); however, recent studies (Trigas et al., 2013; Zhou et al., 2018; Rawat et al., 2021) showed that plant diversity often peaks at mid-elevations (reflecting hump-shaped patterns of species richness), which vary among taxa and mountainous ranges in different climatic conditions across the world (McCain, 2007; Sharma et al., 2019). Therefore, altitude is one of the foremost ecological factors influencing the distribution of species and composition of the ecosystem and is thus significant for understanding the patterns of biodiversity in an ecosystem (Rezende et al., 2015).

The Himalayan mountains are among the highest in the world and act as treasure troves of biodiversity. The higher level of endemism in the region suggests the presence of diverse critical habitats and ecoregions of global importance in the region. Owing to the rich biodiversity of the region, it is among the world's major biodiversity hotspots (Khoshoo, 1992; Myer et al., 2000). The Himalayan mountains provide an altitudinal range representing the world's longest bioclimatic gradient (Grytnes and Vetaas, 2002). All these features have made the Himalayas an interesting candidate for biodiversity studies along the altitudinal gradients. Many researchers have studied patterns of species diversity along altitudinal gradients in the Himalayan region (Rawat et al., 2018; Ahmad et al., 2020; Bhat et al., 2020; Sharma and Kala, 2022). However, due to the remote and difficult-to-reach terrains in high-altitude areas, only a few studies have been conducted on the species composition and diversity in these remote areas of the Himalayas. As a result, the available information about vegetation distribution and its core drivers in the Himalayan mountains is scarce (Wani et al., 2022b). To address this knowledge gap, the present study attempts to examine plant species diversity and distribution patterns with respect to changing elevations, aspects, and habitat types in the Kashmir Himalaya—an integral part of the Himalayan Biodiversity Hotspot. The present study hypothesizes that species diversity and composition change with changes in elevation, aspect, and habitat types and that species diversity and richness decrease with an increase in elevation, with elevation being the most important factor determining changes in species diversity and composition.

2. Materials and methods

2.1. Study area

The Gulmarg Wildlife Sanctuary (GWLS) is located between 74°17′-74°79′ N latitude and 34°55′-34°60′ E longitude (Figure 1). The sanctuary is situated 52 km southwest of the Baramulla district, on the western side of Kashmir Himalaya within the Pir Panjal range. This sanctuary encompasses two administrative units: the Ferozpora/Tangmarg Block and the Gulmarg Block, covering a total area of 180 km^2. Furthermore, the sanctuary is composed of two distinct altitudinal regions, with 120 km^2 of the area falling in the alpine zone and the remaining 60 km^2 lying in the lower altitudinal area (www. jkwildlife.com, assessed on 15 April 2021). The natural beauty of Gulmarg and its proximity to Srinagar make it a popular destination for tourists, both local and international, attracting a huge influx of visitors annually (Nanda et al., 2019). The forest area of the sanctuary is primarily dominated by *Abies pindrow, Pinus wallichiana*, *Cedrus deodara*, *Picea smithiana,* and *Betula utilis*, with the latter forming the tree line in the region (Naqshi et al., 1984).

2.2. Site selection and data collection

Sites were selected randomly to represent each accessible aspect and habitat type along the vertical gradient. Physical characters and dominance of the vegetation were analyzed for habitat identification. The study classified habitats according to canopy cover, humus content, and moisture levels. Habitats with closed canopies and high levels of humus and moisture were referred to as "shady, moist habitats," while habitats with low levels of humus and moisture were referred to as "dry habitats." Habitats with high moisture

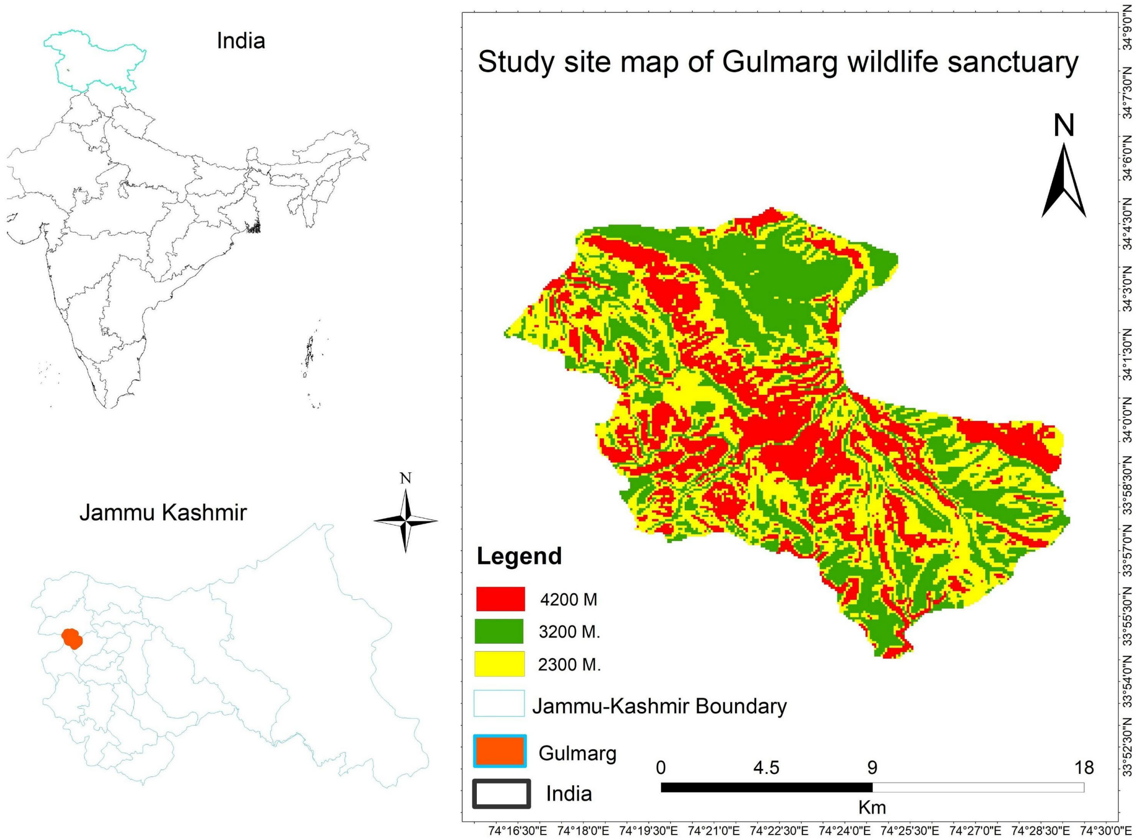

FIGURE 1
Location map of the study area.

concentrations but no canopy cover were designated as "moist habitats." Habitats with more than 50% of their area covered by boulders were classified as "boundary habitats," and habitats with more than 50 rocks were classified as "rocky habitats." Grassland patches within forests were considered "open habitats." Additionally, habitats facing high levels of human-induced degradation, such as deforestation, overgrazing, and trampling, were classified as "degraded habitats." To assess the pattern of plant diversity in these habitats, vegetational sampling was conducted throughout the study area, taking into consideration environmental variables such as altitude, aspect, and habitat type. The plant species composition of each selected site was studied using the quadrat method, which is a widely-used and unbiased method of sampling (Bhatta et al., 2012). Elevation and aspect measurements were recorded using a Garmin GPS 73. The study area was mapped using ArcGIS 10.3. To assess diversity, plots of 50 × 50 m in the forest zone and 20 × 20 m in the alpine zone were established at each site. Within each plot, 10 (10 × 10 m) quadrats for trees, 10 (5 × 5 m) quadrats for shrubs, and 20 (1 × 1 m) quadrats for herbs were laid out at each elevational belt, representing different aspects and habitat types, following previous studies (Samant et al., 2007a; Negi et al., 2018; Rawat et al., 2018). As the alpine zone is devoid of trees, only 10 (5 × 5 m) quadrats for shrubs and 20 (1 × 1 m) quadrats for herbs were laid in each plot. Vascular plant species encountered during field surveys were collected, tagged, and brought to the laboratory, where they were mounted on herbarium sheets using standard herbarium techniques (Smith, 1971; Jain and Rao, 1976; Smith and Chinnappa, 2015). All the collected specimens were identified to the species level using local floras (Bhat, 1984; Naqshi et al., 1984; Singh et al., 2002) and further authenticated at the Centre for Biodiversity and Taxonomy, University of Kashmir. The correct nomenclature and family were assigned to each identified plant species using the Plants of the World Online database[1].

2.3. Data analysis

Abundance data from all the sampling sites were analyzed in relation to aspect and habitat types. However, to study the diversity patterns along the altitudinal gradient, the total sampling sites were grouped into 20 100-m elevation belts, and the average species abundance at each 100-m elevational interval from 2,300 to 4,200 m above sea level was calculated. To estimate the total plant diversity at each site and each 100-m elevational belt, we used the Renyi diversity profiles within the vegan 2.5–7 package (Oksanen et al., 2020). The values of the Renyi diversity profiles ($H\alpha$) were calculated from the average abundance values of the quadrats laid out at each site and the elevational belt using a scaling parameter (α) ranging from zero to

---

[1] Powo (2022). Available online at: https://powo.science.kew.org.

infinity (Kindt and Coe, 2005) according to the following formula:

$$H_\alpha = 1\frac{1}{1-\alpha}\ln\sum_{i=1}^{S} pi^{\alpha},$$

where pi is the average abundance of a species at a site and α is the scaling parameter (Kindt and Coe, 2005; Oksanen et al., 2020). Diversity values were calculated for the default α scale of 0 to infinity following the study of Wani et al. (2022b). Further, a generalized additive model using the "mgcv" package was performed to analyze the impact of altitude on total species richness and the Shannon diversity index.

For analyzing the difference in the observed species composition among the selected sites and elevational belts, non-metric multidimensional scaling (NMDS) using abundance data was performed in a vegan 2.5-7 package (Oksanen et al., 2020). According to the NMDS, the studied sites are ordered in a multidimensional space so that the sites with comparable floristic compositions are assembled in the ordination diagram (Hochstedler et al., 2007; Rawat et al., 2021). Further, to evaluate its accuracy, the associated stress value was calculated. The value of associated stress ranges from 0 to 1; 0 represents no stress, whereas 1 represents a complete lack of fit (Legendre and Legendre, 2012; Rawat et al., 2021; Shahabuddin et al., 2021). The observed degree of compositional dissimilarities between the selected sites was statistically tested using the permutational analysis of variance (PERMANOVA), wherein both the Bray–Curtis and Jaccard indices were used to investigate whether species relative abundances or the presence and/or absence of species are responsible for the observed compositional differences (Shahabuddin et al., 2021). The associated statistical significance was calculated by setting alpha at 0.05 based on 999 permutations.

Moreover, the overall and pairwise β diversity between the studied sites and elevational belts was calculated using the beta version 1.5.4 package (Baselga et al., 2021). This method uses presence/absence data and separates the observed dissimilarity (β_{SOR}) into species turnover (β_{SIM}) and nestedness (β_{SNE}) (Baselga and Orme, 2012). It also clusters different aspects and habitat types along elevation belt-based dissimilarity resulting from both β_{SIM} and β_{SNE} components separately. Additionally, variation partitioning was performed to investigate the relative effects of altitude, aspect, and habitat type on plant species composition using the varpart function from the vegan package version 2.5-7 (Oksanen et al., 2020). This method partitions the total variation into seven fractions attributed to (i) the individual effect of altitude (A), (ii) the individual effect of aspect (AS), (iii) the individual effect of habitat (H), and the shared effect due to each possible pair (iv) altitude and aspect (A n AS), (v) altitude and habitat (A n H), (vi) aspect and habitat (AS n H) and the combined effect of all three underlying variables, and (vii) altitude, aspect, and habitat (A n AS n H). We evaluated the associated statistical significance based on the Monte Carlo permutation test using 999 permutations. As the shared effects were obtained simply by subtraction, they were not tested for statistical significance (Legendre and Legendre, 2012).

3. Results

In the present study, a total of 123 sites were sampled, representing all possible aspects and habitat types in the study area. Of these sites, the greatest number (25) were in the southern aspect, followed by the northern (20), northwest (19), eastern (17), southeast (13), northeast (11), southwest (10), and western (8) aspects. The habitats of the sites were primarily represented by shady moist at 27 sites, followed by rocky (24), bouldary (20), degraded (17), riverine (13), dry (12), open (6), and moist (4). A total of 361 plant species from 71 families and 214 genera were identified from the study area (Supplementary Table S1). The *Asteraceae* were the dominant family with 54 species, followed by the *Lamiaceae*, *Rosaceae*, and *Ranunculaceae* with 23, 20, and 19 species, respectively. The *Ranunculus* genus was the most prevalent with seven species, followed by *Anaphalis* and *Nepeta* with six and five species, respectively. The dominant growth form was represented by herbaceous forms (82.7%), followed by shrubs (10.5%), trees (5.7%), and climbers (1.1%).

3.1. Diversity patterns

The Renyi diversity profiles for the selected aspects are presented in Figure 2A. The diversity profile revealed that the highest plant species diversity was found in the southern aspect at the scaling parameter (α) values between 0 and 1, while the diversity was higher in the southeast aspect for the rest of the scaling parameter (α) values. In contrast, the lowest plant species diversity was observed at the northeast aspect at all scaling parameter (α) values (Figure 2A). Furthermore, the Renyi diversity profiles for the studied habitat types are presented in Figure 2B. The highest plant species diversity was observed in dry habitats at α values between 0 and 2 and in moist habitats for the remaining scaling parameters. In contrast, the lowest plant species diversity was found in open aspects at α values between 0 and 2 but in rocky and degraded habitats for the remaining α values (Figure 2B). Additionally, the Renyi diversity profiles for the selected elevation belts showed that the highest plant species diversity was found at an elevation of 2,400 m for α values between 0 and 1 but at a 2,700-m elevation belt for the remaining α values. In contrast, the lowest species diversity was found at an elevation of 4,200 m for α values between 0 and 1 but at 3,700 m for the remaining α values (Figure 2C). Furthermore, GAM analysis revealed that total species richness and diversity decreased with an increase in elevation and follow a unimodal pattern (Figure 3).

3.2. Plant species composition

The NMDS analysis revealed greater compositional dissimilarity among the selected aspects. More precisely, a varying degree of overlap was observed between the southwest (SW), northwest (NW), and south (S) aspects. The west (W) aspect was the most dissimilar in terms of plant species composition from the rest of the aspects. However, the partially overlapping ellipses indicate that the composition of the plant species in other aspects was not as significantly different (Figure 4). Moreover, the associated stress level for the NMDS plot was very low (0.10) for the first three dimensions. The PERMANOVA analysis indicated significant compositional differences among the studied aspects due to both changes in the number and relative abundance of species (Jaccard: $F = 31.88$, $p < 0.001$; Bray-Curtis: $F = 25.20$; $p < 0.001$).

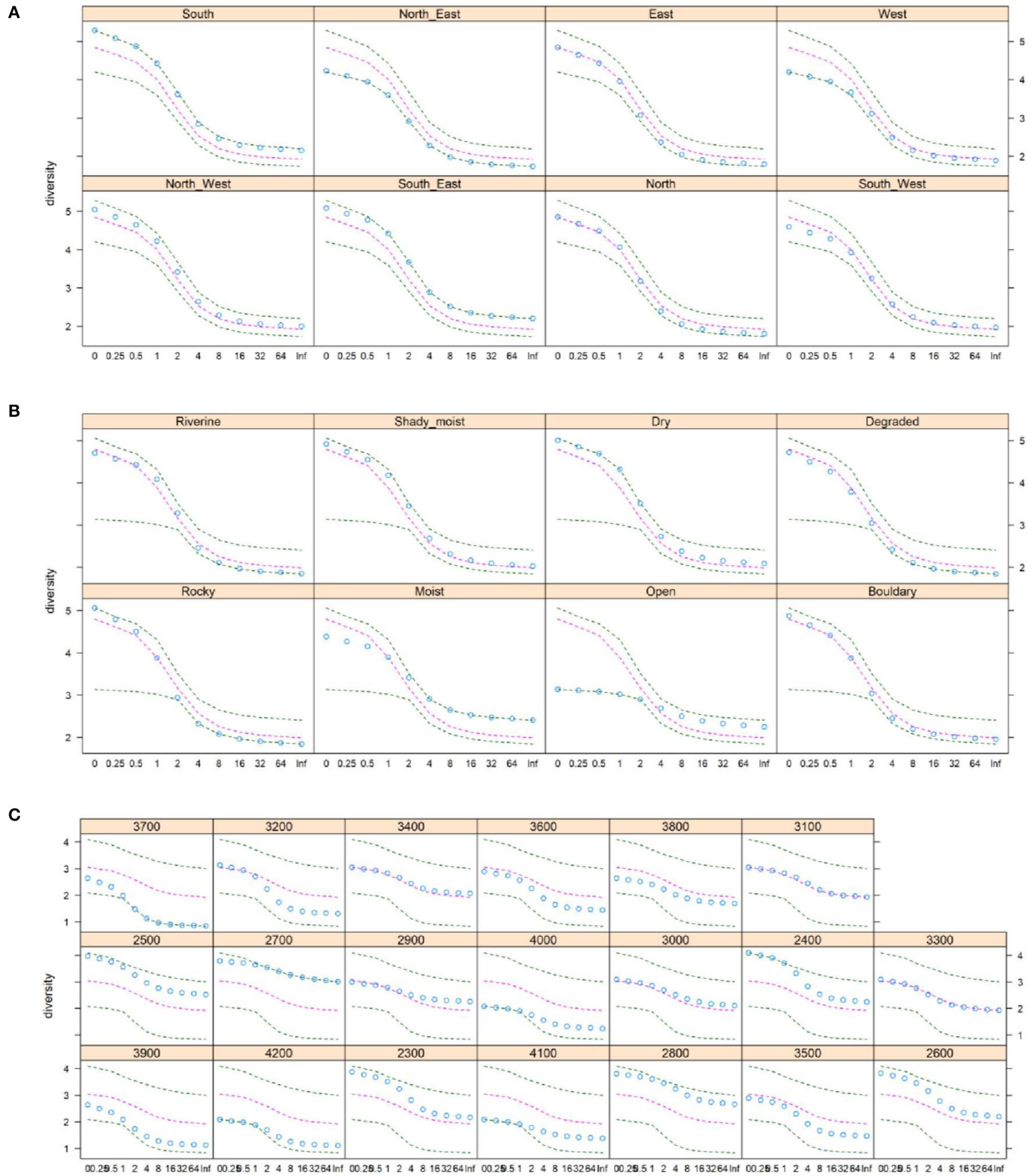

FIGURE 2
The Renyi diversity profiles, showing the total plant species diversity along the selected **(A)** aspects, **(B)** habitats, and **(C)** 100-m elevational belts. The dots represent the diversity value at different values of the scaling parameter (α). The outer two black dashed lines represent the extremes, and the inner pink lines represent the median in the data.

Based on the studied habitat types, the NMDS analysis revealed a significant extent of compositional differences among the studied habitats (Figure 5). The open habitats were the most dissimilar in terms of plant species composition from the rest of the studied habitats. Moreover, the associated stress level for the NMDS plot was very low (0.13) for the first three dimensions. The PERMANOVA analysis indicated significant compositional differences among the studied habitats due to both changes in the number and relative abundance of species (Jaccard: $F = 43.14$, $p < 0.001$; Bray–Curtis: $F = 36.01$; $p < 0.001$).

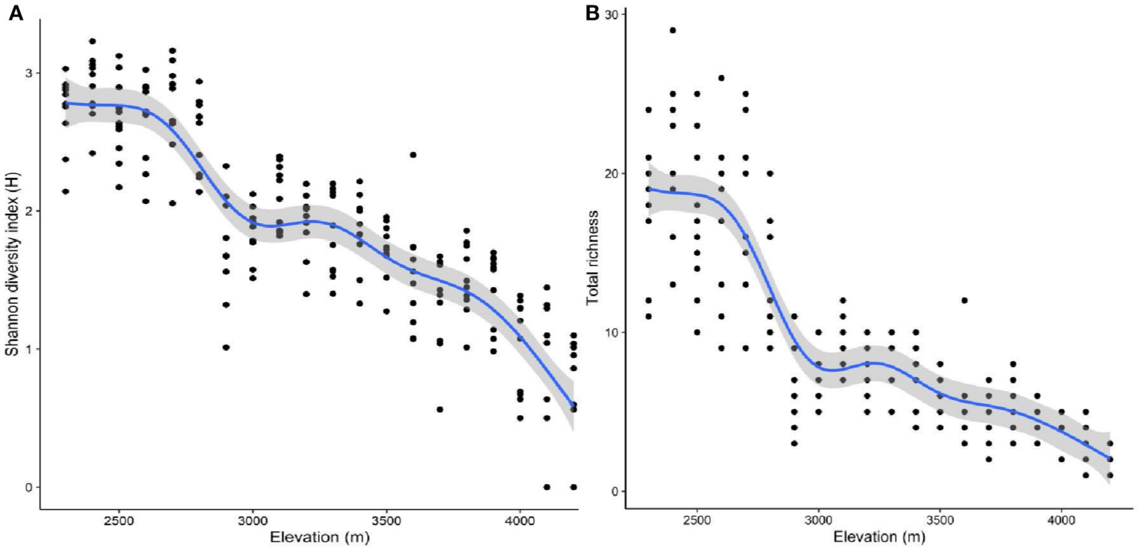

FIGURE 3
The relationship between elevation and **(A)** the Shannon diversity index and **(B)** total species richness. *The blue lines represent the best-fit regression splines from GAM; the gray shading represents the standard errors; and the black dots represent the observations.

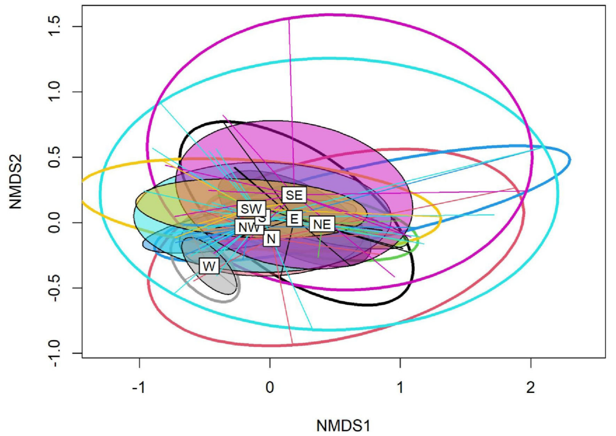

FIGURE 4
A non-metric multidimensional scaling (NMDS) plot showing compositional differences between the studied aspects.

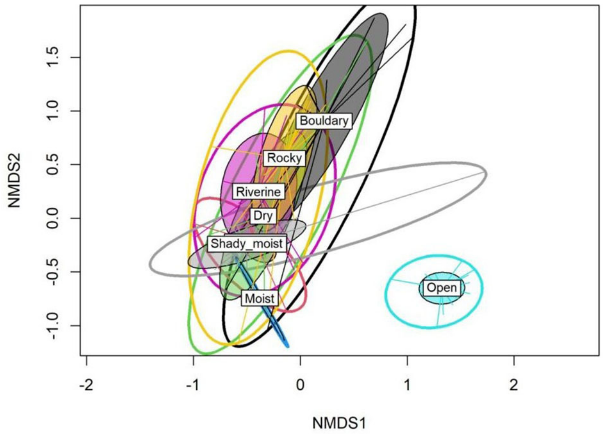

FIGURE 5
The non-metric multidimensional scaling (NMDS) plot showing a difference in total plant species composition between the studied habitats.

Based on altitude, the results of the NMDS analysis revealed a significant extent of dissimilarity in the total plant species composition between the studied elevation belts (Figure 6). A significant degree of overlap was observed between the sites at lower altitudes, except for those at 2,500-m above the sea level, and the sites at higher altitudes, representing the forest and alpine communities, respectively. Additionally, the cluster formed by the lower elevational belts is connected to the higher elevational cluster by four elevation belts, e.g., 3,100–3,400 m, representing the ecotone. Similar to aspect and habitat types, the associated stress level for the NMDS plot was very low (0.11) for the first three dimensions. The PERMANOVA analysis indicated a significant compositional difference among the altitudinal belts due to both changes in the number and relative abundance of species (Jaccard: $F = 17.63$, $p < 0.001$; Bray–Curtis: $F = 29.69$; $p < 0.001$).

3.3. Spatial β-diversity patterns

Overall, the observed multiple-site Sorensen dissimilarity index among the selected aspects was high ($\beta_{SOR} = 0.71$). The contribution of species turnover to the observed dissimilarity was relatively much higher ($\beta_{SIM} = 0.57$) than the nestedness component ($\beta_{SNE} = 0.13$). Furthermore, a significant variation was observed for the pairwise Sorensen dissimilarity index, with the highest β_{SOR} found between the west and southeast aspects ($\beta_{SOR} = 0.70$). The contribution of β_{SIM} to the resulting pairwise dissimilarity was greater than that of the βSNE component in most comparisons (Supplementary Table S2). This suggests that the observed dissimilarity was greater due to β_{SIM} than the β_{SNE} component (Figure 7A). A cluster analysis based on the β_{SIM} component revealed the southwest aspect was significantly

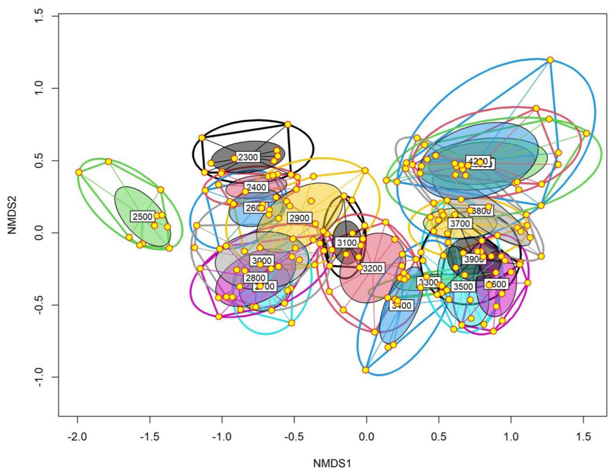

FIGURE 6
The non-metric multidimensional scaling (NMDS) plot showing the difference in total plant species composition between the studied 100-m elevational belts.

different from the rest of the selected aspects in terms of species composition, followed by the southeast and east aspects (Figure 7B). In contrast, a cluster analysis approach based on the β_{SNE} component indicated that the south aspect was highly dissimilar in terms of species composition from the rest of the selected aspects (Figure 7C).

An analysis of habitat types revealed a high multiple-site Sorensen dissimilarity index ($\beta_{\mathrm{SOR}} = 0.75$). The contribution of the turnover component to this dissimilarity was higher ($\beta_{\mathrm{SIM}} = 0.64$) than that of the nestedness component ($\beta_{\mathrm{SNE}} = 0.10$). Further, a significant difference was also observed for the pairwise Sorensen dissimilarity index, with the highest β_{SOR} found between the open and riverine habitats ($\beta_{\mathrm{SOR}} = 0.84$). The contribution of β_{SIM} to the resulting pairwise dissimilarity was greater than that of the β_{SNE} component (Supplementary Table S2). This suggests that the observed dissimilarity was primarily due to the β_{SIM} component rather than the β_{SNE} component (Figure 8A). A cluster analysis based on the β_{SIM} component identified the moist habitat as being highly different from the rest of the other selected habitats in terms of plant species composition, followed by bouldary and riverine habitats (Figure 8B). In contrast, a cluster analysis approach based on the β_{SNE} component indicated that open habitats have a highly distinct plant species composition compared to the other studied habitats (Figure 8C).

The analysis of the selected elevational belts revealed a much higher multiple-site Sorensen dissimilarity index ($\beta_{\mathrm{SOR}} = 0.92$), with a greater contribution from species turnover ($\beta_{\mathrm{SIM}} = 0.88$) than from nestedness ($\beta_{\mathrm{SNE}} = 0.04$). Further, a significant difference was observed for the pairwise Sorensen dissimilarity index, and once again, the contribution of β_{SIM} to this pairwise dissimilarity was greater than that of the β_{SNE} component (Supplementary Table S2). This indicates that the observed dissimilarity was primarily due to β_{SIM} than the β_{SNE} component (Figure 9A). A cluster analysis based on the β_{SIM} component resulted in four major clusters, representing lower, higher, sub-alpine elevational belts (ecotones), and a distinct cluster at 2,500-m altitude (Figure 9B). In contrast, a cluster analysis approach based on the β_{SNE} component resulted in three clusters representing lower, higher, and extreme higher elevation belts (Figure 9C).

3.4. Variation partitioning

In terms of variation partitioning, the results for plant species composition showed that the total variation explained by the three variables (altitude, aspect, and habitat) was 16.5% (Figure 10). Of the individual effects, altitude (A) turned out to be the most important contributing variable, explaining the greatest amount of variation (9.7%) in plant species composition (Table 1). In addition, the individual effects of aspect (AS) and habitat type (H) were relatively small at 3.4 and 9.4%, respectively (Figure 10; Table 1). Furthermore, the variation explained by each variable was statistically significant (Table 1). Notably, the paired effect of altitude and habitat (A n H) explained the maximum variation (14.2%) in plant species composition.

4. Discussions

Topographic and environmental conditions in the Himalayan region vary significantly, leading to variations in biodiversity patterns with respect to aspect, elevation, and habitat types (Rana et al., 2020; Ahmad et al., 2021). Many workers in the Himalayan region have studied the effects of topography on plant species diversity and composition (Vetaas and Grytnes, 2002; Carpenter, 2005; Kharkwal et al., 2005; Paudel and Vetaas, 2014; Subedi et al., 2020; Rawat and Negi, 2021; Wani S. A. et al., 2022). These studies have revealed that species diversity and composition vary significantly with changes in the topographic features of a region. The Gulmarg Wildlife Sanctuary (GWLS) embodies a broad elevation range with complex topography, providing a large variation in environmental variables to harbor higher species richness in a smaller area. The species richness reported in the present study was comparatively higher (361 species) than earlier reports from the Indian Himalayan region, i.e., Chawla et al., 2008 (313 species), Haq et al., 2018 (183 species), Ahmad et al., 2020 (255 species), and Haq et al., 2021 (181 species). The higher species richness recorded in the present study may be attributed to the fact that the present study was extensive and covered forest and alpine zones of the study area. *Asteraceae*, *Lamiaceae*, and *Ranunculaceae* were the most dominant families in the study area; these families have also been reported as being dominant in the Himalayan region (Dar and Khuroo, 2013; Ahmad et al., 2021; Altaf et al., 2021). These plant families have larger ecological amplitudes and wide distributions, increasing the possibility of encountering the members of these families (Mumshad et al., 2021). The dominance of herbaceous growth forms in the present study is in accordance with several other studies conducted in the Indian Himalayan region (Samant et al., 2007b; Malik et al., 2015; Sharma et al., 2019; Haq et al., 2021; Rawat et al., 2021). It may be due to the fact that herbs are considered common growth forms in most mountainous regions owing to their ability to acclimate to an extensive range of ecological settings (Wani S. A. et al., 2022).

In the present study, we calculated the plant species diversity more robustly than the randomly chosen single diversity index method, which led to biased generalizations and outcomes (Ahmad et al., 2019). The present study revealed that southern and southeast

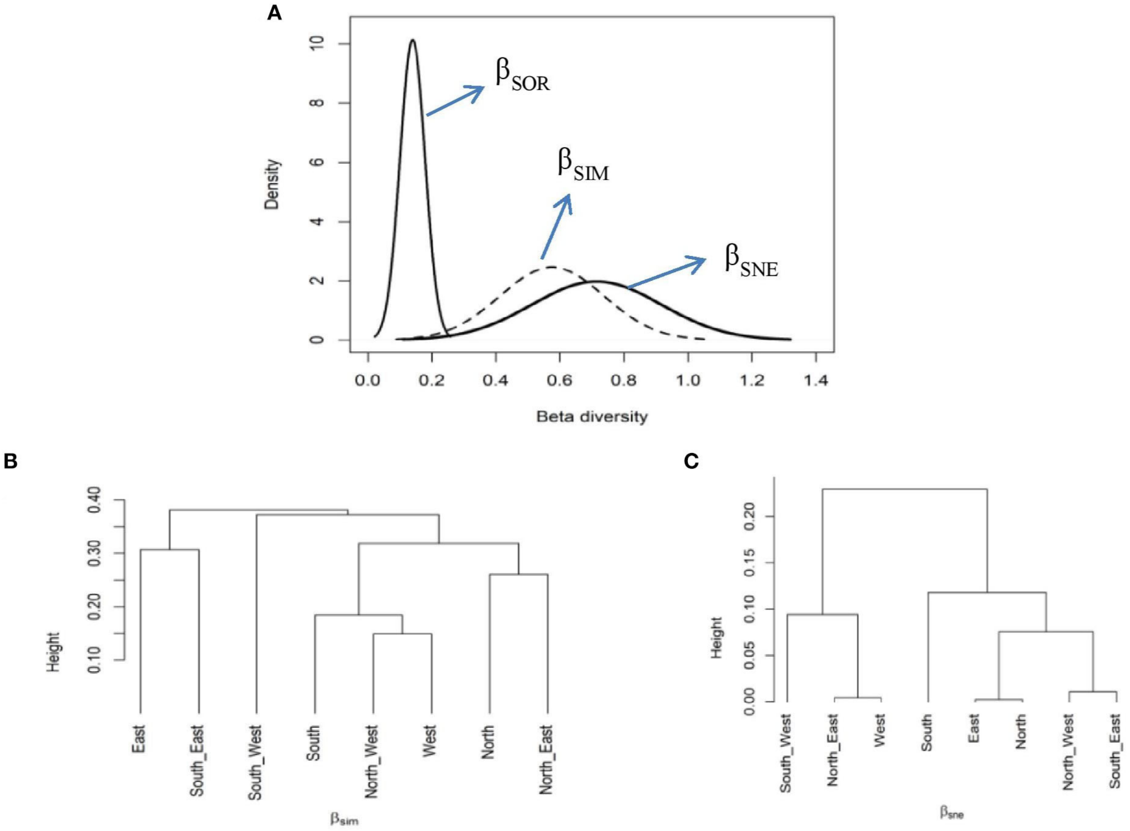

FIGURE 7
The multiple-site β dissimilarity patterns across the selected aspects using total plant species composition. The figure shows the partitioning of total dissimilarity (β_{SOR}−solid black line) into species turnover (β_{SIM}−dashed line) and nestedness (β_{SNE}−solid gray line) components **(A)** and average clustering based on β_{SIM} **(B)** and β_{SNE} **(C)** components of total plant species dissimilarity among the studied aspects.

aspects favor rich plant species diversity, which is in accordance with the findings of previous studies (Winkler et al., 2016). This pattern may be attributed to the differential degree of exposure to sunlight and, thus, temperature differences with respect to changing aspects (Korner and Hiltbrunner, 2018). Aspect causes prominent temperature alterations and therefore affects species richness and composition in the mountains indirectly by affecting the soil-plant-atmosphere continuum (SPAC) (Aalto et al., 2013). The south aspect receives higher inputs of solar radiation in comparison to the north and west-facing aspects (Nepali et al., 2021). Furthermore, in temperate mountain regions like the study area, convective cloud formation is a common phenomenon (Geiger, 1950). This results in reduced daily solar radiation on the western aspect compared to the southern aspect.

Temperature is the most significant abiotic factor affecting plant growth and physiology at higher elevations (Korner and Hiltbrunner, 2018). Aspect causes prominent alterations in the thermal input and thus considerably affects the biodiversity on a mountain slope (Hamid et al., 2020). Further, the heterogeneity in aspect and altitude within a landform shows an important correlation with habitat heterogeneity (Aguilar-Santelises and del Castillo, 2013). During the present study, it was found that certain species, such as *Oxyria digyna*, *Nasturtium officinale*, *Rorippa islandica*, *Caltha alba*, *Ranunculus trichophyllus,* and *Polygonum amphibia,* prefer riverine habitats, whereas species such as *Valeriana jatamansii, Viola odorata, Silene baccifera, Epimedium elatum,* and *Ainsliaea Aptera* prefer shady, moist habitats. These species, which have narrow habitat preferences and specialized ecological niches, are less tolerant and less resilient, making them more susceptible to extinction (Wani S. A. et al., 2022; Wani et al., 2022c) compared to those species with wider habitat preferences.

Further, open and degraded sites were populated with exotic species such as *Rumex* sp., *Digitalis grandiflora*, *Sambucus wightiana*, *Leucanthemum vulgare,* and *Achillea millifolium*. Thus, due to habitat destruction, plant species with specific habitat preferences may suffer, and the whole community structure may be altered due to the increasing invasion of alien species (Fletcher et al., 2018; Fahrig et al., 2019). Habitats not only play an imperative role in the growth and development of species but also maintain species diversity. Habitat fragmentation and degradation are considered the primary causes of biodiversity loss (Su et al., 2022). As such, the preservation of habitats is equally important to the conservation of particular species.

The plant species diversity and richness decreased with increasing altitude due to environmental filtering and the dominance of plant species tolerant of extreme environmental conditions at higher altitudes (Trigas et al., 2013; Rana et al., 2020). According to the climate hypotheses, if the temperature is the main determinant of elevational species richness, the pattern predicted is decreasing diversity with increasing elevation (Heaney, 2001; McCain, 2007). The disparity in species composition and richness with changing

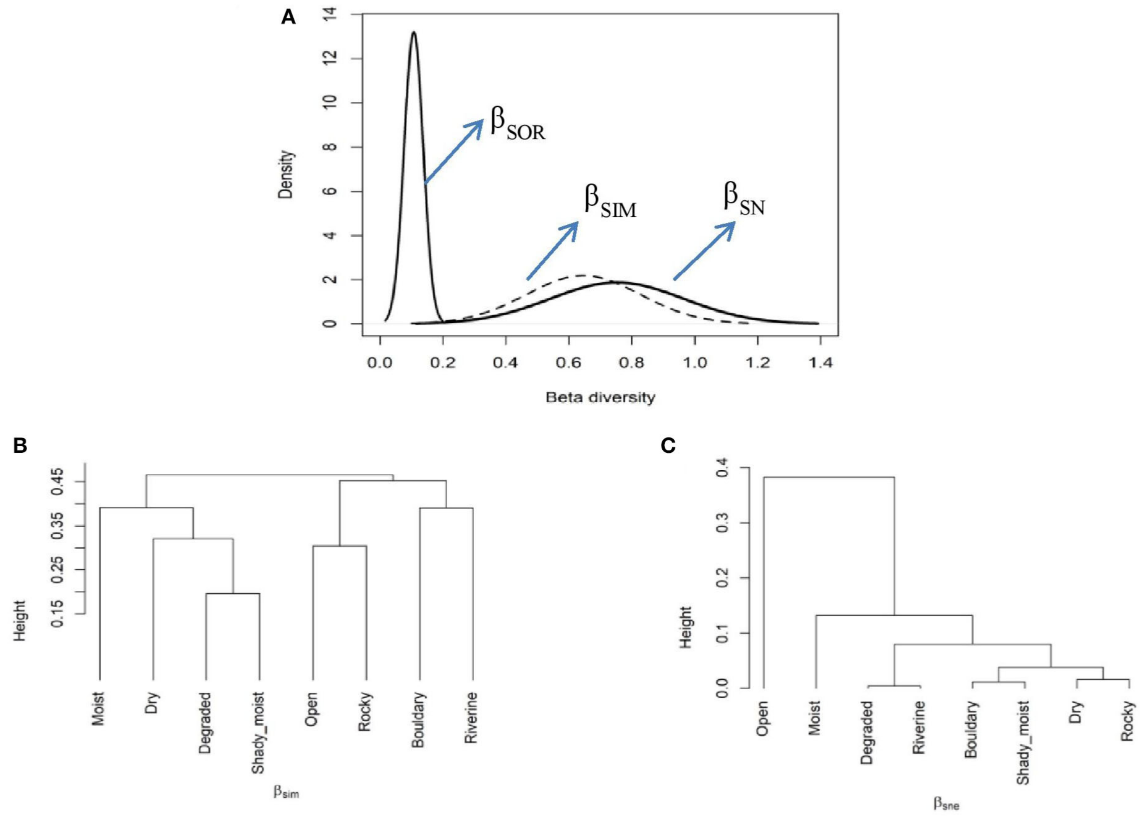

FIGURE 8
The multiple-site β dissimilarity patterns across the selected habitats using total plant species composition. The figure illustrates the partitioning of total dissimilarity (β_{SOR} −solid black line) into components of species turnover (β_{SIM} −dashed line) and nestedness (β_{SNE} −solid gray line) components **(A)** average clustering based on β_{SIM} **(B)** and β_{SNE} **(C)** components of total plant species dissimilarity among the studied habitats.

altitude is a common phenomenon in the Himalayan and other mountainous ecosystems across the globe (Khuroo et al., 2011; Rawat et al., 2018). In the present study, species composition at lower altitudes was different than at higher altitudes. Mid-altitudes (3,100 and 3,400m) representing the ecotone form a transition between the lower and higher altitudes and are occupied by species from both lower and higher altitudes, forming a distinct cluster in terms of species composition.

Further, the 2,500-m elevation belt was found to be dissimilar from the rest of the lower altitudinal belts. The possible reason for this can be the observed anthropogenic pressure owing to the nomadic (Gujjars and Bakerwals) settlements at particular elevational belts. In the present study, total plant species richness and diversity followed a unimodal pattern, which is considered a general pattern (Stevens, 1992). However, analysis of wide-ranging elevational gradients usually results in hump-shaped patterns, while the exclusion of elevations of the gradient at the higher or lower ends favors a monotonic upsurge or decline with elevation (Fontana et al., 2020). At higher altitudes, plant species are exposed to various eco-physiological limitations, which in turn reduce species richness and diversity (Ahmad et al., 2020). In contrast, the higher species richness and diversity at lower and mid-elevations are chiefly associated with favorable environmental settings (Manish, 2021).

β-diversity, a central element of species diversity, provides insights into the extent to which environmental heterogeneity is partitioned by different species (Rawat et al., 2003). Greater β-diversity values indicate a higher level of species variation in response to environmental gradients (Bisht and Bhat, 2013). In the present study, we found relatively higher plant species diversity in southern aspects and dry habitats, likely due to the prominence of heliophytes and early successional species in forest gaps (Li et al., 2019). The patterns of β-diversity may be associated with the degree of variation in habitats along altitudinal gradients and changing aspects (Tang and Fang, 2004). Comparing compositional dissimilarities among the studied sites, further partitioned into species replacement and nestedness as attempted in this study, allows a better understanding of how biodiversity is assembled across environmental variables. Both these components of β-diversity have been acknowledged to sufficiently perceive spatial diversity patterns due to the underlying dissimilarity measures which compare species composition between two sampling units. Species replacement is supposed to be driven by environmental influences, while nestedness may reflect extinction patterns (Fontana et al., 2020). The present study revealed that turnover was more prominent than nestedness for all the studied variables (aspect, habitat, and elevation), which is consistent with the idea that the environmental filtering effects on vegetation structure along environmental gradients primarily result in turnover (Anderson et al., 2011; Zellweger et al., 2017). Furthermore, we found that the values of turnover and total β-diversity were more prominent along the elevational gradient than variation in aspects and habitat types. Temperature and solar radiations are the most important variables that influence β-diversity

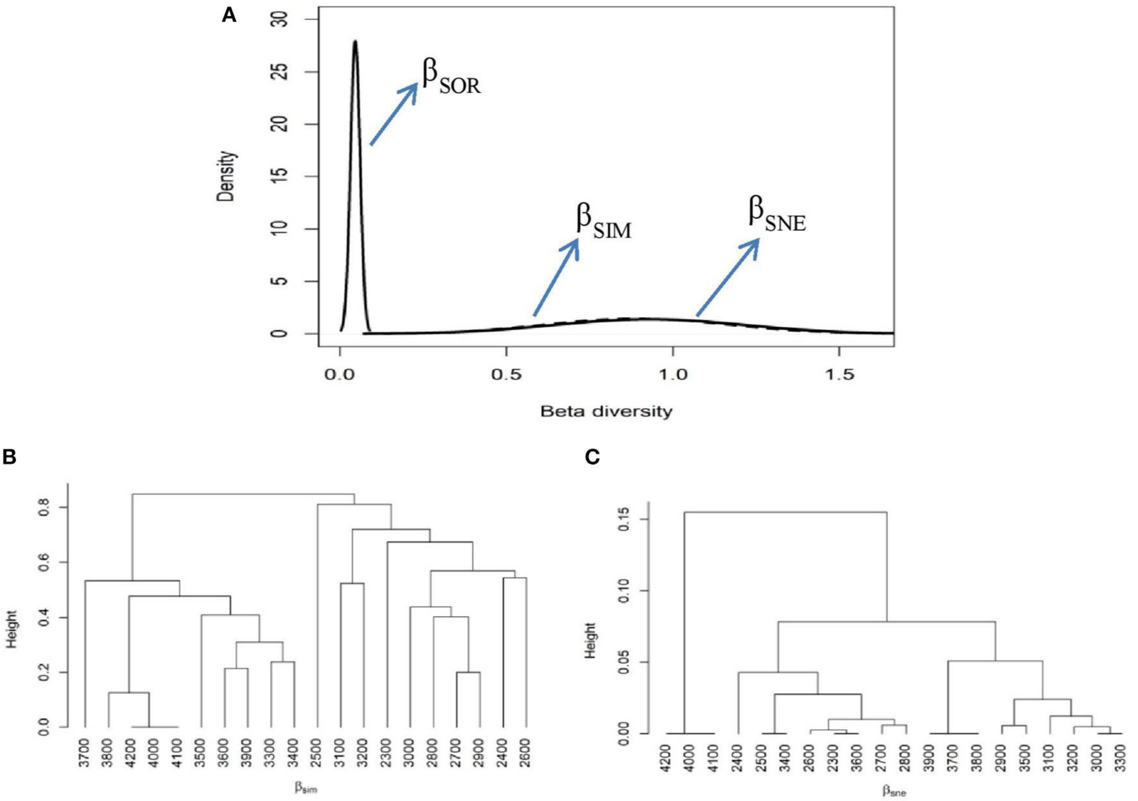

FIGURE 9
The multiple-site β dissimilarity patterns for the selected elevation belts using total plant species composition. The partitioning of total dissimilarity (β_{SOR}−solid black line) into components of species turnover or replacement (β_{SIM}−dashed line) and nestedness (β_{SNE}−solid gray line) components **(A)** is shown. This figure represents the average clustering based on β_{SIM} **(B)** and β_{SNE} **(C)** components of total plant species dissimilarity among the studied elevational belts.

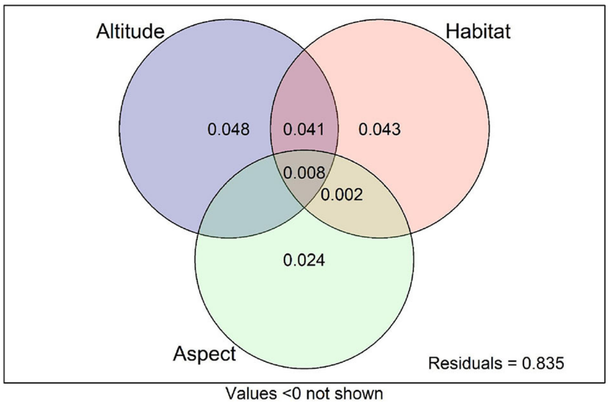

FIGURE 10
The variation in total plant species composition explained by altitude, aspect, and habitat types, as indicated by the adjusted R^2 values.

TABLE 1 A variation partitioning analysis, displaying the individual and combined effects of altitude (A), aspect (AS), and habitat type (H) on plant species composition.

	Individual effect			Combined effect			
	A	AS	H	A∩AS	A∩H	AS∩H	A∩AS∩H
Composition	9.7 (0.001)	3.4 (0.001)	9.4 (0.001)	12.3	14.2	11.8	16.5 (0.001)

The values presented are the adjusted R-squared values as a percentage, with corresponding p-values based on 999 permutations in brackets.
The values indicate the adjusted R^2 values in percentage along with the p-values based on 999 permutations in brackets.

along an elevational gradient. Additionally, a significant percentage of plant species (specialists) is restricted to certain ecological zones and does not colonize entire environmental gradients (Broennimann et al., 2006; Trigas et al., 2013).

Environmental and topographic variables are significant factors in the distribution of plant species within an ecosystem. In the present study, variation in altitude was found to be the main factor leading to variation among the studied sites. Rawat and Negi (2021) also found that elevation is the most influential variable influencing species distribution patterns. The combined effect of altitude and habitat on species composition and richness among the sites was also found to be significant. Environmental and resource parameters determine the growth and competitive interactions of species, while environmental heterogeneity parameters tend to enhance coexistence and favor higher species richness. It is crucial to consider both levels of environmental parameters and heterogeneity concurrently to distinguish between the two types of parameters. Environmental heterogeneity is scale dependent and may create high niche diversity, allowing species to coexist at a large spatial scale.

5. Conclusions

The present study revealed that elevation is the most important factor contributing to variations in plant species diversity and composition. However, the present study also highlighted the importance of aspect and habitat heterogeneity in determining plant species richness. The southern aspect was found to support higher plant diversity compared to other studied aspects due to its greater exposure to sunlight. Furthermore, the plant species found in the study region exhibit distinct ecological preferences. For example, *Betula utilis* is found along northern aspects.

Similarly, the recorded species have varying habitat preferences. Therefore, the present study suggests that floristic diversity should be studied not only in relation to elevational gradients but also in relation to aspects and habitats. This study serves as a model for future research in this direction. Similar studies should be conducted in other parts of the Himalayan region to expand our understanding of the distribution and preferences of plant species in mountainous areas. This, in turn, will greatly aid in the conservation and sustainable utilization of resources in these ecologically fragile regions.

Data availability statement

The original contributions presented in the study are included in the article/Supplementary material, further inquiries can be directed to the corresponding author.

Author contributions

ZW: conceptualization, methodology, data collection, curation and analysis, investigation, and writing an original draft. VN and JB: writing—review and validation. KS, SK, RD, and RA-Q: writing—review. AK: prepared the map of the study area and writing—review. SS: writing—review and funding acquisition. SP: conceptualization, methodology, supervision, validation, and writing—review. All authors contributed to the article and approved the submitted version.

Funding

The authors extend their appreciation to the Deanship of Scientific Research at King Khalid University for funding this work through a Large Group Research Project under grant number (RGP2/90/44).

Acknowledgments

The authors are thankful to Dr. Akhtar H. Malik of the University of Kashmir's Centre for Biodiversity and Taxonomy for his assistance in identifying plant specimens.

Conflict of interest

Publisher's note

Supplementary material

The Supplementary Material for this article can be found online at: https://www.frontiersin.org/articles/10.3389/ffgc.2023.1019277/full#supplementary-material

References

Aalto, J., le Roux, P. C., and Luoto, M. (2013). Vegetation mediates soil temperature and moisture in arctic-alpine environments. *Arc. Ant. Alpine. Res.* 45, 429–439. doi: 10.1657/1938-4246-45.4.429

Aguilar-Santelises, R., and del Castillo, R. F. (2013). Factors affecting woody plant species diversity of fragmented seasonally dry oak forests in the Mixteca Alta, Oaxaca, Mexico. *Rev. Mex. de. Biodiv.* 84, 575–590. doi: 10.7550/rmb.30458

Ahmad, M., Sharma, P., Rathee, S., Singh, H. P., Batish, D. R., Lone, G. R., et al. (2021). Niche width analyses facilitate identification of high-risk endemic species at high altitudes in western Himalayas. *Ecol. Eng.* 126. doi: 10.1016/j.ecolind.2021.107653

Ahmad, M., Uniyal, S. K., Batish, D. R., Singh, H. P., Jaryan, V., Rathee, S., et al. (2020). Patterns of plant communities along vertical gradient in Dhauladhar Mountains in Lesser Himalayas in North-Western India. *Sci. Tot. Env.* 716, 136919. doi: 10.1016/j.scitotenv.2020.136919

Ahmad, R., Khuroo, A. A., Hamid, M., Malik, A. H., and Rashid, I. (2019). Scale and season determine the magnitude of invasion impacts on plant communities. *Flora.* 260, 151481. doi: 10.1016/j.flora.2019.151481

Altaf, A., Haq, S. M., Shabnum, N., and Jan, H. A. (2021). Comparative assessment of Phyto diversity in Tangmarg Forest division in Kashmir Himalaya, India. *Acta. Ecol. Sin.* doi: 10.1016/j.chnaes.2021.04.009

Anderson, M. J., Crist, T. O., Chase, J. M., Vellend, M., Inouye, B. D., Freestone, A. L., et al. (2011). Navigating the multiple meanings of b diversity: A roadmap for the practicing ecologist. *Ecol. Lett.* 14, 19–28. doi: 10.1111/j.1461-0248.2010.01552.x

Barry, R. G. (2008). *Mountain Weather and Climate*. Cambridge, UK: Cambridge University Press.

Baselga, A., and Orme, C. D. L. (2012). The relationship between species replacement, dissimilarity derived from nestedness, and nestedness. *Glo. Eco. Biogeo.* 21, 1223–1232. doi: 10.1111/j.1466-8238.2011.00756.x

Baselga, A., Orme, D., Villeger, S., De Bortoli, J., Leprieur, F., Logez, M., et al. (2021). *Betapart: Partitioning beta diversity into turnover and nestedness components. R package version 1 5.4.* Available online at: https://CRAN.R-project.org/package=betapart (assessed May 28, 2022).

Bhat, J. A., Kumar, M., Pala, N. A., Shah, S., Dayal, S., Gunathilake, C., et al. (2020). Influence of altitude on the distribution pattern of flora in a protected area of Western Himalaya. *Acta. Ecol. Sin.* 40, 30–43. doi: 10.1016/j.chnaes.2018.10.006

Bhat, N. A. (1984). *Floristic Composition of Gulmarg (Baramulla)*. Ph. D. Thesis, University of Kashmir, Srinagar.

Bhatta, K. P., Chaudhary, R. P., and Vetaas, O. R. (2012). A comparison of systematic versus stratified-random sampling design for gradient analyses: a case study in sub-alpine Himalaya, Nepal. *Phytocoeno.* 42, 191–202. doi: 10.1127/0340-269X/2012/0042-0519

Bisht, A. S., and Bhat, A. B. (2013). Vegetation structure and plant diversity relation in a sub-alpine region of Garhwal Himalaya, Uttarakhand, India. *Afr. J. Plant. Sci.* 7, 401–406. doi: 10.5897/AJPS11.013

Broennimann, O., Thuiller, W., Hughes, G., Midgley, G. F., Alkemade, J. R., Guisan, A., et al. (2006). Do geographic distribution, niche property and life form explain plants' vulnerability to global change?. *Glo. Chan. Biol.* 12, 1079–1093. doi: 10.1111/j.1365-2486.2006.01157.x

Carpenter, C. (2005). The environmental control of plant species density on a Himalayan elevation gradient. *J. Biogeogr.* 32, 999–1018. doi: 10.1111/j.1365-2699.2005.01249.x

Chawla, A., Rajkumar, S., Singh, K. N., Lal, B., Singh, R. D., Thukral, A. K., et al. (2008). Plant species diversity along an altitudinal gradient of Bhabha Valley in western Himalaya. *J. Mount. Sci.* 5, 157–177. doi: 10.1007/s11629-008-0079-y

Dar, G. H., and Khuroo, A. A. (2013). Floristic diversity in the Kashmir Himalaya: progress, problems and prospects. *Sains. Malay*. 42, 1377–1386.

Dar, J. A., and Sundarapandian, S. (2016). Patterns of plant diversity in seven temperate forest types of Western Himalaya, India. *J. Asia-Pac. Biod.* 9, 280–292. doi: 10.1016/j.japb.2016.03.018

Davies, K. W., Bates, J. D., and Miller, R. F. (2007). Environmental and vegetation relationships of the *Artemisia. tridentata* spp. *wyomingensis* alliance. *J. Arid. Envir*. 70, 478–498. doi: 10.1016/j.jaridenv.2007.01.010

Fahrig, L., Arroyo-Rodriguez, V., Bennett, J. R., et al. (2019). Is habitat fragmentation bad for biodiversity? *Biol Conser.* 230, 179–186. doi: 10.1016/j.biocon.2018.12.026

Fletcher, R. J., Didham, R. K., Banks-Leite, C., et al. (2018). Is habitat fragmentation good for biodiversity? *Biol. Conser*. 226, 9–15. doi: 10.1016/j.biocon.2018.07.022

Fontana, V., Guariento, E., Hilpold, A., Niedrist, G., Steinwandter, M., Spitale, D., et al. (2020). Species richness and beta diversity patterns of multiple taxa along an elevational gradient in pastured grasslands in the European Alps. *Sci. Rep*. 10, 12516. doi: 10.1038/s41598-020-69569-9

Gairola, S., Sharma, C. M., Suyal, S., and Ghildiyal, S. K. (2011). Species composition and diversity in mid-altitudinal moist temperate forests of the western Himalaya. *J. For. Envir. Sci* 27, 1–15. doi: 10.7747/JFS.2011.27.1.1

Geiger, R. (1950). *The Climate Near the Ground*. Cambridge: Rowman and Littlefield.

Grytnes, J. A., and Vetaas, O. R. (2002). Species richness and altitude: a comparison between null models and interpolated plant species richness along the Himalayan altitudinal gradient, Nepal. *Am. Nat.* 159, 294–304. doi: 10.1086/338542

Hamid, M., Khuroo, A. A., Malik, A. H., Ahmad, R., and Singh, C. P. (2020). Assessment of alpine summit flora in Kashmir Himalaya and its implications for long-term monitoring of climate change impacts. *J. Moun. Sci* 17, 1974–1988. doi: 10.1007/s11629-019-5924-7

Hamid, M., Khuroo, A. A., Malik, A. H., Ahmad, R., and Singh, C. P. (2021). Elevation and aspect determine the differences in soil properties and plant species diversity on Himalayan mountain summits. *Ecol. Res.* 36, 340–352. doi: 10.1111/1440-1703.12202

Haq, S. M., Malik, A. H., Khuroo, A. A., and Rashid, A. (2018). Floristic composition and biological spectrum of Keran—a remote valley of northwest Himalaya. *Acta. Ecol. Sin.* 39, 372–379. doi: 10.1016/j.chnaes.2018.12.001

Haq, S. M., Singh, B., Bashir, B., Farooq, A. J., Singh, B., Calixtod, E. S., et al. (2021). Exploring and understanding the floristic richness, life-form, leaf-size spectra and phenology of plants in protected forests: A case study of Dachigam National Park in Himalaya, Asia. *Acta. Ecol. Sin.* 41, 479–790. doi: 10.1016/j.chnaes.2021.07.010

Heaney, L. R. (2001). Small mammal diversity along elevational gradients in the Philippines: an assessment of patterns and hypotheses. *Global. Ecol. Biogeogr.* 10, 15–39. doi: 10.1046/j.1466-822x.2001.00227.x

Hochstedler, W. W., Slaughter, B. S., Gorchov, D. L., Suander, L. P., and Stevens, M. H. (2007). Forest floor plant community response to experimental control of the invasive biennial, *Alliaria. petiolata* (garlic mustard). *J. Tor. Bot. Soc.* 134, 155–165. doi: 10.3159/1095-5674(2007)134155:FFPCRT2.0.CO;2

Jain, S. K., and Rao, R. R. (1976). *Handbook of Field and Herbarium Methods*. New Delhi: Today and Tomorrows Printers and Publishers.

Kharkwal, G., Mehrotra, P., Rawat, Y. S., and Pangtey, Y. P. S. (2005). Phytodiversity and growth form in relation to altitudinal gradient in the Central Himalayan (Kumaun) region of India. *Curr. Sci.* 873–878.

Khoshoo, T. N. (1992). *Plant Diversity in the Himalaya: Conservation and Utilization, II. Pl.* G.B. Pant memorial lecture Almora (India): G.B. Pant Institute of Himalayan Environment and Development. p. 120.

Khuroo, A. A., Weber, E., Malik, A. H., Reshi, Z. A., and Dar, G. H. (2011). Altitudinal distribution pattern of the native and alien woody flora in Kashmir Himalaya, India. *Envir. Res.* 111, 967–977. doi: 10.1016/j.envres.2011.05.006

Kindt, R., and Coe, R. (2005). *Tree Diversity Analysis. A manual and software for common statistical methods for ecological and biodiversity studies.* Nairobi, Kenya: World Agroforestry Centre (ICRAF).

Korner, C. (1998). A re-assessment of high elevation treeline positions and their explanation. *Oecologia.* 115, 445–459. doi: 10.1007/s004420050540

Korner, C., and Hiltbrunner, E. (2018). The 90 ways to describe plant temperature. *Persp. Plant. Ecol. Evol. Syst.* 30, 16–21. doi: 10.1016/j.ppees.2017.04.004

Legendre, P., and Legendre, L. (2012). "Developments in environmental modelling," in *Numerical Ecology, 3rd Edition.* Amsterdam: Elsevier.

Li, C., Wangya, H., Dan, L., and Guohua, L. (2019). How forest gaps shaped plant diversity along an elevational gradient in Wolong National Nature Reserve. *J. Geog. Sci.* 29, 1081–1097. doi: 10.1007/s11442-019-1646-6

MacArther, R. H. (1972). *Geographical Ecology*. Harper and Row, New York.

Malik, A. H., Rashid, I., Ganie, A. H., Khuroo, A. A., and Dar, G. H. (2015). Benefitting from geoinformatics: estimating floristic diversity of Warwan valley in Northwestern Himalaya, India. *J. Mount. Sci.* 12, 854–863. doi: 10.1007/s11629-015-3457-2

Manish, K. (2021). Species richness, phylogenetic diversity and phylogenetic structure patterns of exotic and native plants along an elevational gradient in the Himalaya. *Ecol. Proc.* 10, 64. doi: 10.1186/s13717-021-00335-z

McCain, C. M. (2007). Could temperature and water availability drive elevational species richness? A global case study for bats. *Global. Ecol. Biogeogr.* 16, 1–13. doi: 10.1111/j.1466-8238.2006.00263.x

McCain, C. M., and Colwell, R. K. (2011). Assessing the threat to montane biodiversity from discordant shifts in temperature and precipitation in a changing climate. *Ecol. Lett.* 14, 1236–1245. doi: 10.1111/j.1461-0248.2011.01695.x

McCain, C. M., and Grytnes, J. A. (2010). *Elevational Gradients Species Richness Encyclopidia Life Sciences*. Chichester: John Wiley and Sons.

Moeslund, J. E., Arge, L., Bøcher, P. K., Dalgaard, T., and Svenning, J. C. (2013). Topography as a driver of local terrestrial vascular plant diversity patterns. *Nordic. J. Bot.* 31, 129–144. doi: 10.1111/j.1756-1051.2013.00082.x

Mumshad, M., Ahmad, I., Khan, S. M., Rehman, K., Islam, M., Sakhi, S., et al. (2021). Phyto-ecological studies and distribution pattern of plant species and communities of Dhirkot, Azad Jammu and Kashmir, Pakistan. *PLoS ONE*. 16, e0257493. doi: 10.1371/journal.pone.0257493

Myer, N., Muttermeier, R. A., Muttermeier, C. A., da Fornseca, G. A. B., and Kent, J. (2000). Biodiversity hotspots for conservation priorities. *Nature*. 403, 853–858. doi: 10.1038/35002501

Nanda, A. B., Nelofar, and Lone, R. A. (2019). Study of phenology of woody flora of Gulmarg and its neighbourhood for landscape use. *J. Sci. Res. Rep*. 22, 1–7. doi: 10.9734/jsrr/2019/v22i430095

Naqshi, A. R., Malla, M. Y., and Dar, G. H. (1984). Plants of Gulmarg. *J. Eco. Tax. Bot.* 5, 709–741.

Negi, V. S., Giri, L., and Sekar, K. C. (2018). Floristic diversity, community composition and structure in Nanda Devi National Park after prohibition of human activities, Western Himalaya, India. *Curr. Sci.* 115, 1056–1064. doi: 10.18520/cs/v115/i6/1056-1064

Nepali, B. R., Skartveit, J., and Baniya, C. B. (2021). Impacts of slope aspects on altitudinal species richness and species composition of Narapani-Masina landscape, Arghakhanchi, West Nepal. *J. Asia. Pac. Biod.* 14, 415–424. doi: 10.1016/j.japb.2021.04.005

Oksanen, J., Blanchet, F. G., Friendly, M., Kindt, R., Legendre, P., McGlinn, D., et al. (2020). *vegan: Community Ecology Package. R package version 2*, 5–7. Available online at: https://CRAN.R-project.org/package=vegan (assessed May 28, 2022).

Paudel, S., and Vetaas, O. R. (2014). Effects of topography and land use on woody plant species composition and beta diversity in an arid Trans-Himalayan landscape, Nepal. *J. Mount. Sci.* 11, 1112–1122. doi: 10.1007/s11629-013-2858-3

Rana, D., Kapoor, K. S., Samant, S. S., and Bhatt, A. (2020). Plant species conservation priority index for preparing management strategies: A case study from western Himalayas of India. *Small. Scale. For*. 19, 461–481. doi: 10.1007/s11842-020-09447-4

Raulings, S., Morris, K., Roache, M., et al. (2010). The importance of water regimes operating at small spatial scales for the diversity and structure of wetland vegetation. *Freshwater. Biol.* 55, 701–715. doi: 10.1111/j.1365-2427.2009.02311.x

Rawat, A. S., Pharswan, A. S., and Nautiyal, M. C. (2003). Propagation of *Aconitum. atrox.* (Bruhl) Muk. (Ranunculaceae). A regionally threatened medicinal herb. *Eco. Bot.* 46, 337–338.

Rawat, B., Gaira, K. S., Gairola, S., Tewari, L. M., and Rawal, R. S. (2021). Spatial prediction of plant species richness and density in high-altitude forests of Indian west Himalaya. *Trees,. For. Peo.* 6, 100132. doi: 10.1016/j.tfp.2021.100132

Rawat, B., and Negi, A. S. (2021). Plant diversity patterns along environmental gradients in Nanda Devi Biosphere Reserve, West Himalaya. *Tropl. Ecol.* 62, 61–70. doi: 10.1007/s42965-020-00122-5

Rawat, R. S., Rawal, R., Rawat, B., Negi, V. S., and Pathak, R. (2018). Plant species diversity and rarity patterns along altitude range covering treeline ecotone in Uttarakhand: conservation implications. *Trop. Ecol.* 59, 225–239.

Rezende, V. L., de Miranda, P. L., Meyer, L., Moreira, C. V., Linhares, M. F., de Oliveira-Filho, P. V., et al. (2015). Tree species composition and richness along altitudinal gradients as a tool for conservation decisions: the case of Atlantic semideciduous forest. *Biod. Conser*. 24, 2149–2163. doi: 10.1007/s10531-015-0939-z

Samant, S. S., Butola, J. S., and Sharma, A. (2007a). Assessment of diversity, distribution, conservation status and preparation of management plan for medicinal plants in the catchment areas of Parbati Hydroelectric Power Project Stage–III in Northwestern Himalaya. *J. Mountain. Science* 4, 34–56. doi: 10.1007/s11629-007-0034-3

Samant, S. S., Pant, S., Singh, M., Lal, M., Singh, A., Sharma, A., et al. (2007b). Medicinal plants in Himachal Pradesh, north western Himalaya, India. *Inter. J. Biod. Sci. Managt*. 3, 234–251. doi: 10.1080/17451590709618177

Shahabuddin, G., Goswami, R., Krishnadas, M., and Menon, T. (2021). Decline in forest bird species and guilds due to land use change in the Western Himalaya. *Glob. Ecol. Conser*. 25, e01447. doi: 10.1016/j.gecco.2020.e01447

Sharma, N., Behera, M. D., Das, A. P., and Panda, R. M. (2019). Plant richness pattern in an elevation gradient in the Eastern Himalaya. *Biod. Conser*. 28, 2085–2104. doi: 10.1007/s10531-019-01699-7

Sharma, N., and Kala, C. P. (2022). Patterns in plant species diversity along the altitudinal gradient in Dhauladhar mountain range of the North-West Himalaya in India. *Trees. For. Peo*. 7, 100196. doi: 10.1016/j.tfp.2022.100196

Singh, N. P., Singh, D. K., and Uniyal, B. P. (2002). *Flora of Jammu and Kashmir*. Calcutta: Botanical Survey of India.

Smith, B., and Chinnappa, C. C. (2015). "Plant collection, identification, and herbarium procedures," in *Plant Microtechniques and Protocols* (Berlin, Germany: Springer, Cham), 541–572.

Smith, C. E. (1971). *Preparing Herbarium Specimens of Vascular Plants* (No. 348). US: Agricultural Research Service, US Department of Agriculture.

Stevens, G. C. (1992). The elevational gradient in altitudinal range: an extension of Rapoport's latitudinal rule to altitude. *Am. Nat.* 140, 893–911. doi: 10.1086/285447

Su, N., Jarvie, S., Yan, Y., Gong, X., Li, F., Han, P., et al. (2022). Landscape context determines soil fungal diversity in a fragmented habitat. *Catena*. 213, 106163. doi: 10.1016/j.catena.2022.106163

Subedi, C. K., Rokaya, M. B., Münzbergov,á, Z., Timsina, B., Gurung, J., Chettri, N., et al. (2020). Vascular plant diversity along an elevational gradient in the Central Himalayas, western Nepal. *Folia. Geobotanica* 55, 127–140. doi: 10.1007/s12224-020-09370-8

Tang, Z. Y., and Fang, J. Y. (2004). A review on the elevational patterns of plant species diversity. *Biod. Sci*. 12, 20–28. doi: 10.17520/biods.2004004

Trigas, P. M., Panitsa, M., and Tsiftsis, S. (2013). Elevational gradient of vascular plant species richness and endemism in Crete-The effect of post-isolation mountain uplift on a continental island system. *PLoS. ONE*. 8, e59425–e59425. doi: 10.1371/journal.pone.0059425

Vetaas, O. R., and Grytnes, J. A. (2002). Distribution of vascular plant species richness and endemic richness along the Himalayan elevation gradient in Nepal. *Glob. Ecol. Biogeogr*. 11, 291–301. doi: 10.1046/j.1466-822X.2002.00297.x

Wamelink, G. W. W., Goedhart, P. W., and Frissel, J. Y. (2014). Why some plants are rare. *PLoS ONE*. 9, e111293. doi: 10.1371/journal.pone.0102674

Wani, S. A., Ahmad, R., Gulzar, R., Rashid, I., Malik, A. H., Khuroo, A. A., et al. (2022). Diversity, Distribution and Drivers of Alien Flora in the Indian Himalayan Region. *Glob. Ecol. Conser. e*02246. doi: 10.1016/j.gecco.2022.e02246

Wani, Z. A., Islam, T., Satish, K. V., Ahmad, K., Dhyani, S., Pant, S., et al. (2022c). Cultural value and vegetation structure of *Buxus. wallichiana* Bail. in Rajouri-Poonch region of Indian Himalayan region (VSI: Mountainous regions). *Trees. For. Peo*. 7, 100182. doi: 10.1016/j.tfp.2021.100182

Wani, Z. A., Khan, S., Bhat, J. A., Malik, A. H., Alyas, T., Pant, S., et al. (2022b). Pattern of β-Diversity and Plant Species Richness along Vertical Gradient in Northwest Himalaya, India. *Biology*. 11, 1064.

Wani, Z. A., Akash, and Pant, S. (2022a). *Tree diversity and regeneration dynamics in Gulmarg Wildlife* Sanctuary, Kashmir Himalaya. *Acta Ecol Sin*. doi: 10.1016/j.chnaes.2022.05.003

Winkler, M., Lamprecht, A., Steinbauer, K., Hulber, K., Theurillat, J. P., Breiner, F., et al. (2016). The rich sides of mountain summits–a pan-European view on aspect preferences of alpine plants. *J. Biogeo*. 43, 2261–2273. doi: 10.1111/jbi.12835

Zellweger, F., Roth, T., Bugmann, H., and Bollmann, K. (2017). Beta diversity of plants, birds and butterflies is closely associated with climate and habitat structure. *Glob. Ecol. Biogeo*. 26, 898–906. doi: 10.1111/geb.12598

Zhang, Q., Wang, J., and Wang, Q. (2021). Effects of abiotic factors on plant diversity and species distribution of alpine meadow plants. *Ecol. Infor*. 61, 101210. doi: 10.1016/j.ecoinf.2021.101210

Zhou, Y., Chen, S., Hu, G., Mwachala, G., Yan, X., Wang, Q., et al. (2018). Species richness and phylogenetic diversity of seed plants across vegetation zones of Mount Kenya, East Africa. *Ecol. E*8, 8930. doi: 10.1002/ece3.4428

frontiers | Frontiers in Forests and Global Change

TYPE Original Research
PUBLISHED 23 March 2023
DOI 10.3389/ffgc.2023.1138317

OPEN ACCESS

EDITED BY
Zishan Ahmad Wani,
Baba Ghulam Shah Badshah University, India

REVIEWED BY
Zeeshan Ahmad,
Quaid-i-Azam University, Pakistan
Tajamul Islam,
University of Kashmir, India

*CORRESPONDENCE
Jie Xue
✉ xuejie11@ms.xjb.ac.cn
Zhiwei Zhang
✉ aiwoweige@163.com

SPECIALTY SECTION
This article was submitted to
Forest Management,
a section of the journal
Frontiers in Forests and Global Change

RECEIVED 05 January 2023
ACCEPTED 06 March 2023
PUBLISHED 23 March 2023

CITATION
Han J, Yin H, Xue J, Zhang Z, Xing Z, Wang S, Chang J, Chen X and Yu B (2023) Vertical distribution differences of the understory herbs and their driving factors on shady and sunny slopes in high altitude mountainous areas.
Front. For. Glob. Change 6:1138317.
doi: 10.3389/ffgc.2023.1138317

Vertical distribution differences of the understory herbs and their driving factors on shady and sunny slopes in high altitude mountainous areas

Jiahua Han[1], Huiyan Yin[1], Jie Xue[2,3,4]*, Zhiwei Zhang[1,5]*, Zhen Xing[1], Shunke Wang[2,3,4], Jingjing Chang[6], Xiaoqiang Chen[1,7] and Bo Yu[1]

[1]College of Resources and Environmental Sciences, Tibet Agricultural & Animal Husbandry University, Nyingchi, China, [2]State Key Laboratory of Desert and Oasis Ecology, Xinjiang Institute of Ecology and Geography, Chinese Academy of Sciences, Ürümqi, China, [3]Cele National Station of Observation and Research for Desert-Grassland Ecosystems, Hetian, China, [4]University of Chinese Academy of Sciences, Beijing, China, [5]Key Laboratory of Forest Ecology in Tibet Plateau, Tibet Agricultural & Animal Husbandry University, Nyingchi, China, [6]College of Ecology and Environment, Xinjiang University, Ürümqi, China, [7]College of Chemistry, Chemical Engineering and Resource Utilization, Northeast Forestry University, Harbin, China

The vertical distribution understanding of undergrowth herbaceous plants in high altitude mountain areas is of great significance to reveal the environmental gradient change law of plant diversity. However, the species composition of herbaceous plants at different altitude gradients and the relationship between diversity and environmental factors is still vague. This study takes the Sejila Mountain in southeast Tibet at an altitude of 2,000–3,300 m as the study area to analyze the vertical distribution differences of the understory herbs and their driving factors on shady and sunny slopes. The results showed that: (1) The number of families, genera and species of herbaceous plants on sunny slope is greater than that on shady slope. Asteraceae on shady and sunny slopes has the largest number of species; (2) The α diversity index of the herbs on shady slope shows a U-shaped trend. The Cody heterogeneity index (β_C) is negatively correlated with the β diversity index. The herb richness index (R) on sunny slope is unimodal. The β diversity index displays the same as that of shady slope; (3) Different environmental factors have different effects on herb diversity. The correlation between environmental factors and diversity indicators indicates that there is a certain degree of clustering among samples. The environmental factors of shady slope and sunny slope are separated; and (4) The difference of water and heat conditions caused by altitude and slope aspect is an important driving factor for the diversity of herbage species, followed by soil clay content, silt content and slope gradient. This study will help to understand the species diversity and ecosystem characteristics of the region, and provide a reference for the study of plant community structure and function and rational utilization of understory plant resources in high-altitude mountain areas.

KEYWORDS

herbs, species diversity, altitude gradient, driving factors, Qinghai-Tibet Plateau

1. Introduction

Species diversity is the basis for understanding the composition, structure and functional state of community species, and also the basis for studying biodiversity (Butchart et al., 2010; Cardinale et al., 2012; Chitale et al., 2014). As the largest terrestrial ecosystem, the forests are an important carrier of species diversity. In addition to trees and shrubs, the herbs are also an important part of the forests. Although the plants of herbaceous plants are small and their biomass proportion is low, they have the highest species diversity. The herbs play an important role in maintaining the material cycle and energy flow of the forest ecosystem, and play an important role in ensuring the function and stability of the ecosystem (Gilliam, 2007; Brockerhoff et al., 2017).

The alpine ecosystems are the most sensitive regions to environmental change, suitable for studying the response of ecosystem to climate change and predicting the response to future climate change (Ecology and Kessler, 2012). Altitude gradient in alpine ecosystems integrates changes in water, temperature, light, soil and other factors, and is considered to be one of the decisive factors affecting species diversity (Andra, 2016; Yılmaz et al., 2018). Many scholars have done some research on species diversity at different altitudes, but the differences are large. Species diversity has a variety of altitude gradient distribution patterns. There was significant positive, negative, unimodal, or u-type correlation between species diversity index and altitude (Sklenář and Jørgensen, 1999; Sklenár and Ramsay, 2001; Austrheim, 2002; Doležal and Šrůtek, 2002; da Silva et al., 2014; Ent et al., 2016; Gómez-Díaz et al., 2017; Dip et al., 2020; Walter et al., 2021).

The Qinghai-Tibet Plateau, known as the "third pole of the world," is one of the largest original forest regions in China and one of the provinces (regions) with the richest forest resources in China. It is of great significance for the study of undergrowth herbs in the study area. However, the research on herbaceous plants in the Qinghai-Tibet Plateau mainly focuses on the grassland degradation, plant diversity and biomass change of alpine meadow and alpine grassland in the source area of the Three Rivers, Gobi area in the north of the Qinghai-Tibet Plateau (Mu et al., 2018; Xue et al., 2018; Fayiah et al., 2019; Han et al., 2022; She et al., 2022). The research on plant diversity in southeast Tibet mainly focuses on woody plants, ferns and mosses (Li et al., 2013; Zu et al., 2019; Shi et al., 2021; Xian et al., 2021). The research on the diversity of undergrowth herbaceous plants mainly focuses on the composition of plant communities and species diversity in forest fire slash (Zhang et al., 2021, 2022; Yin et al., 2022; Zhou et al., 2022). There are relatively few studies on the diversity of undergrowth herbaceous plants.

Southeast Tibet is located in the southeast of the Qinghai-Tibet Plateau, the western line of Hengduan Mountains. As the Indian Ocean warm moisture flows northward, it brings a lot of rainfall every year, forming many forest vegetation types. The region has a variety of tropical, subtropical, temperate and cold climate zones. Influenced by the Indian Ocean warm and wet monsoon, it is cold and dry in winter, cold and rainy in summer with distinct dry and wet seasons. There are many types of primitive forests in this area, mainly dark coniferous forests (Wang et al., 2019; Xiangyang et al., 2022), and there are rich herbaceous plants under the forests. Studying the distribution characteristics of herbaceous plants at different altitudes and slope directions in Tongmai section of Sejila Mountain is helpful to understand the diversity and ecosystem characteristics of undergrowth herbaceous plants in southeast Tibet.

In this study, it is assumed that the distribution differences of the understory herbs is mainly affected by the alpine topography factors and soil conditions. Based on field investigation and relevant data, the diversity index of herbaceous plants was calculated and the difference analysis and principal component analysis were carried out. We studied the change pattern of herbage species composition and diversity index with altitude gradient in Tongmai section of Sejila Mountain, and the correlation between herbage diversity and environmental factors. The purpose is to provide reference for the study of plant community structure and function, rational utilization of understory plant resources, and ecological environment protection in the southeast of the high altitude Qinghai Tibet Plateau.

2. Materials and methods

2.1. Study area

Sejila Mountain is located in Bayi District, Linzhi City, at the junction of Nianqing Tanggula Mountain and Himalayas in the southeast of Tibet. It is mainly from Tongmai Town to Lulang Town. The geographical location is 29.79°–30.13°N, 94.75°–95.06 °E (**Figure 1**). It is located in the transition zone between semi humid and humid areas in southeast Tibet, with unique plateau ecological characteristics. The area is warm in winter and cool in summer, with distinct dry and wet seasons. The average annual temperature is 6–12°C, the average temperature of the warmest month is 10–18°C, the number of days ≥ 0°C is 210–350 days. The annual precipitation is 1,000–1,200 mm. The soil is mainly mountainous brown soil. The arbor layer is mainly composed of moist coniferous and broad-leaved mixed forest zone in the warm temperate zone of mountains and cool moist dark coniferous forest zone in the temperate zone of mountains. The main dominant species are *Alnus nepalensis, Populus szechuanica var.tibetica* and *Pinus densata*. The dominant species in shrub layer are *Viburnum kansuense, Rosa sericea* and *Elsholtzia fruticosa*. The herb layer is very rich in species in this area, mainly including *Pilea indolens*, *Duchesnea indica*, Fragaria moupinensis, *Eragrostis pilosa*, Synotis saluenensis, *Dryopteris redactopinnata*, and *Oplismus compositus*.

2.2. Methods

2.2.1. Sample plot setting and data collection

In October 2021, the herbaceous plants were investigated in the Tongmai section of Sejila Mountain. The survey area has an altitude range of 2,000–3,300 m. The specific altitude range (2,000–3,300 m) spans the warm temperate zone and temperate climate zone. The vegetation zone corresponds to the mountain warm temperate mixed coniferous forest and dark coniferous forest zone, The herbaceous plants are quite different between the two climate zones, so it is of great significance to study the replacement and

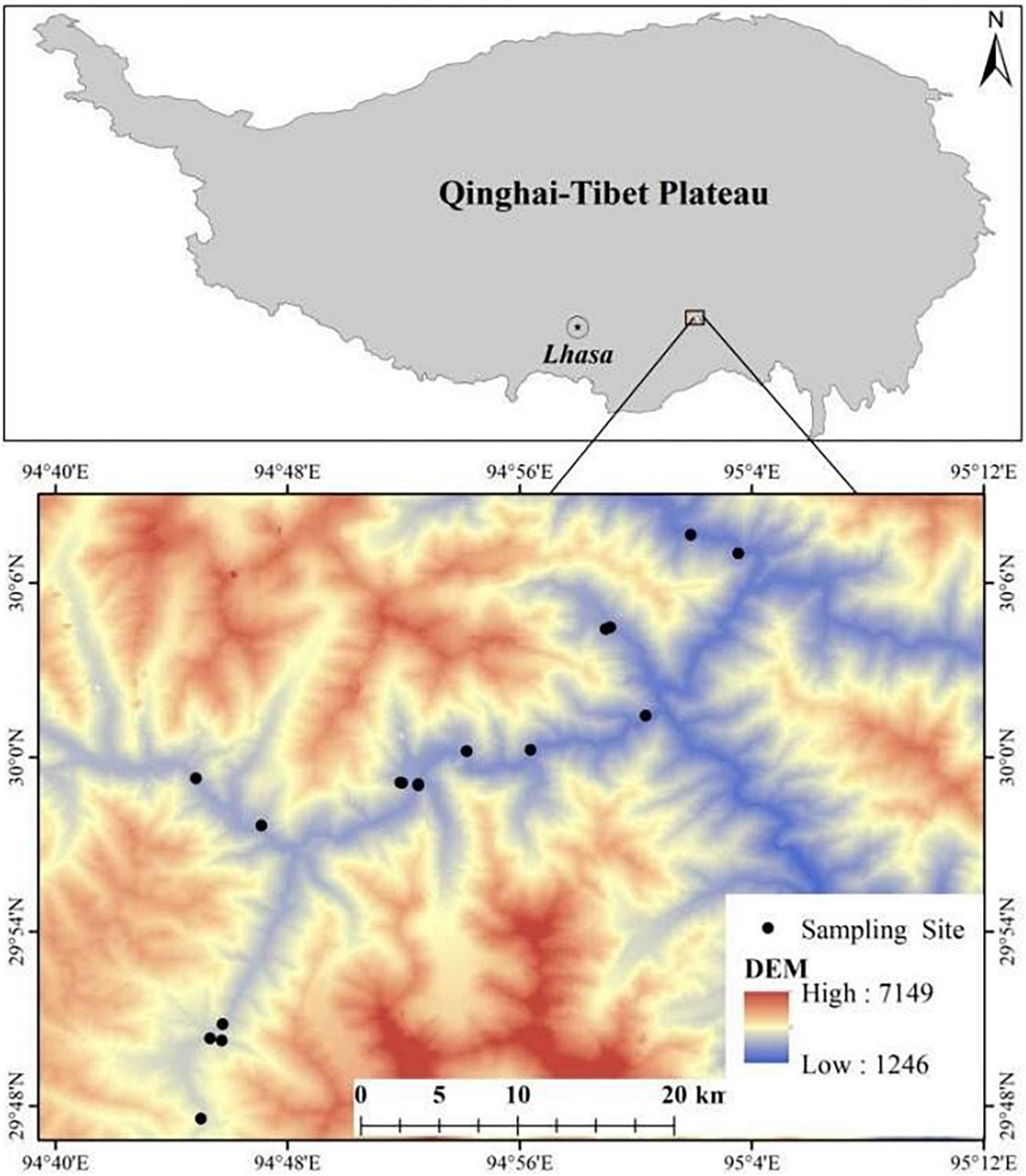

FIGURE 1
Location of the study area and distribution of soil sampling points.

continuation of herbaceous species in the altitude range of 2,000–3,300 m. Taking 200 m as an altitude gradient zone, there are 6 altitude gradient zones in total. Three 20 m × 30 m standard plots are set on the shady and sunny slopes of each elevation gradient. The 1 m × 1 m standard herbaceous investigation quadrat is set at the four corners and the center of the sample plot. 15 herbaceous investigation quadrats were set on the shady slope and sunny slope respectively for each elevation gradient. The basic contents of the survey include plant name, number of plants/clusters, coverage, height, base diameter, growth and distribution. We measured the longitude and latitude, elevation, slope, aspect and other factors of the quadrat with the real-time dynamic measuring instrument (RTK), and we collected all the herb species in the quadrat. We mark the sample number, collector, longitude and latitude, altitude, slope, aspect and associated plants, and take them back to make specimens for later species identification. Table 1 shows the basic information of the sample plot. Due to the influence of topographic factors, the cliff affected the sampling work in the elevation gradient of 2,800–3,000 m on the sunny slope.

2.2.2. Herb diversity index

(1) The important value is a comprehensive quantitative index to study the status and role of a species in the community, which can comprehensively evaluate the status and role of a species in the community (Torresani et al., 2020; Wang et al., 2021), reflecting the structure and functional characteristics of the plant community. The calculation formula of the important value of herbaceous plants is:

$$IV = \frac{RA + RC + RH}{3} \tag{1}$$

TABLE 1 Basic information of the research sites.

Aspect	Altitude gradient zone (m)	Latitude	Longitude	Altitude (m)	Slope	Vegetation coverage (%)	Forest type
Shady slope	2,000–2,200	30.12°N	95.06°E	2,033.3	44°	95	Alnus nepalensis forest
	2,200–2,400	30.07°N	94.99°E	2,330.7	17°	95	Evergreen mixed broad-leaved forest,understory no shrub
	2,400–2,600	29.99°N	94.87°E	2,579.3	31°	85	Evergreen mixed broad-leaved forest
	2,600–2,800	29.99°N	94.86°E	2,715.0	26°	87	Populus szechuanica forest
	2,800–3,000	29.85°N	94.76°E	2,933.3	7°	90	Evergreen mixed broad-leaved forest
	3,000–3,200	29.84°N	94.76°E	3,024.7	47°	95	Evergreen mixed broad-leaved forest
Sunny slope	2,000–2,200	30.02°N	95.01°E	2,002.3	30°	80	Deciduous broad-leaved forest
	2,200–2,400	30.00°N	94.94°E	2,207.6	12°	95	Evergreen mixed broad-leaved forest,understory no shrub
	2,400–2,600	29.98°N	94.88°E	2,495.4	33°	80	Mixed deciduous forest
	2,600–2,800	29.96°N	94.79°E	2,621.6	0°	78	High-mountain Pinus forest
	3,000–3,200	29.79°N	94.75°E	3,138.9	40°	80	Mixed conifer-broadleaf forest

where IV is the important value, RA is the relative abundance, RC is the relative coverage, and RH is the relative height.

(2) Species richness is an important indicator of plant diversity, and the calculation formula is:

$$R = S \tag{2}$$

where S is the number of quadrat species.

(3) α Diversity is used to describe the species diversity of local communities, which is generally affected by microenvironment and interactions between organisms (Ellum et al., 2010; Van Dam, 2019; Wang et al., 2021).

Shannon-Wiener diversity index:

$$H = -\sum N_i \ln N_i \tag{3}$$

Uniformity index Pielou:

$$J = \frac{H}{\ln S} \tag{4}$$

where S is the number of species in the community, and N_i is the important value of species i in the sample plot.

(4) β Diversity refers to the diversity of community species composition between different habitats along the environmental gradient or the rate of species replacement along the environmental gradient (Ellum et al., 2010; Van Dam, 2019; Wang et al., 2021).

Sorenson similarity index:

$$SI = \frac{2c}{a+b} \tag{5}$$

Cody anisotropy index:

$$\beta c = \frac{g(H) + l(H)}{2} \tag{6}$$

where a and b are the number of species in the 2 communities respectively, c is the number of common species in the 2 communities, $g\ (H)$ is the number of species increased along the environmental gradient H, and $l\ (H)$ is the number of species lost along the environmental gradient H.

2.2.3. Data processing

We summarize and sort out the herbaceous plant specimens we brought back, and identify the collected samples one by one based on relevant materials such as Flora of China, Flora of Tibet, Flora of Botany,[1] China Digital Herbarium (CVH)[2] and local plant experts in Tibet. Soil particle size was measured by laser particle size distribution instrument, and PH was measured by soil moisture temperature PH velocity meter. Based on the statistical analysis of the composition of families, genera and species of herbaceous plants at different altitudes in Sejila Mountain, the differences were analyzed with SPSS 23 software.ArcGIS 10.5 was used to draw regional overview maps, and Origin 2021 was used to make herb diversity index maps and principal component analysis maps.

3. Results

3.1. Species composition characteristics of herbaceous plants on shady and sunny slopes

It can be seen from Table 2 that 57 species of herbaceous plants belonging to 24 families and 49 genera have been investigated on the shady slope, among which Asteraceae has the most plants. There are 10 species of Asteraceae, accounting for 17.54% of the total herb species investigated on the shady slope of Sejila

---

[1] http://www.iplant.cn

[2] http://www.cvh.ac.cn

TABLE 2 Composition of herbaceous plants on shady slope.

Shady slope				
Plant family	Number of plant genera	Percentage of total genera (%)	Number of plant species	Percentage of total species (%)
Asteraceae	9	18.37	10	17.54
Apiaceae	4	8.16	4	7.02
Rosaceae	4	8.16	4	7.02
Dryopteridaceae	3	6.12	6	10.53
Urticaceae	3	6.12	3	5.26
Orchidaceae	3	6.12	3	5.26
Ranunculaceae	2	4.08	3	5.26
Araliaceae	2	4.08	3	5.26
Poaceae	2	4.08	2	3.51
Rubiaceae	2	4.08	2	3.51
Saxifragaceae	2	4.08	2	3.51
Polygonaceae	1	2.04	2	3.51
Balsaminaceae	1	2.04	2	3.51
Lamiaceae	1	2.04	1	1.75
Polypodiaceae	1	2.04	1	1.75
Oxalidaceae	1	2.04	1	1.75
Araceae	1	2.04	1	1.75
Athyriaceae	1	2.04	1	1.75
Pteridaceae	1	2.04	1	1.75
Geraniaceae	1	2.04	1	1.75
Adoxaceae	1	2.04	1	1.75
Plantaginaceae	1	2.04	1	1.75
Violaceae	1	2.04	1	1.75
Onagraceae	1	2.04	1	1.75
Total	49	100	57	100

Mountain. From the perspective of subordination, Asteraceae includes 9 genera, accounting for 18.37% of the total genera of herbs on the shady slope of Sejila Mountain. In the shady slope area, Asteraceae plants are dominant, Dryopteridaceae, Rosaceae and Apiaceae are important families in the shady slope of Sejila Mountain; Poaceae, Rubiaceae and Ranunculaceae enrich the vegetation composition of shady slopes.

In the sample plot on the sunny slope, according to Table 3, 73 species of herbaceous plants belonging to 35 families and 62 genera are found on the sunny slope, with the largest number of Asteraceae plants. There are 9 species of Asteraceae, accounting for 12.33% of the total herbaceous species investigated on the sunny slope of Sejila Mountain. From the perspective of subordinate species, Asteraceae includes 7 genera, accounting for 11.29% of the total genera of herbaceous plants on the sunny slope of Sejila Mountain. It can be seen that Asteraceae plants are dominant in the sunny slope of study area, and Lamiaceae and Rosaceae are important constituent families in the sunny slope of Sejila Mountain; Zingiberaceae, Geraniaceae and Rubiaceae enrich the vegetation composition of the sunny slope.

3.2. Analysis of important values of herbaceous plants in different altitude gradient zones on shady and sunny slopes

It can be seen from Figures 2, 3 that the species composition of herbaceous plants on shady and sunny slopes varies greatly at different altitudes. In the shady slope of the study area, the number of herbaceous species decreased first and then increased with the increase of altitude. Herbal species with higher important values in each altitude gradient zone include *Pilea insolens*, *Duchesnea indica* and *Fragaria moupinensis*; The most dominant is that the important value of *Pilea insolens* decreases with the increase of altitude. The important value of *Duchesnea indica* and *Fragaria moupinensis* increased with the elevation. In the sunny slope of the study area, the number of herbaceous species first increased and then decreased with the increase of altitude. In each elevation gradient zone, the importance value of herbaceous plants decreases with the increase of herbaceous species; On the whole, the

TABLE 3 Composition of herbaceous plants in sunny slope.

Sunny slope				
Plant family	Number of plant genera	Percentage of total genera (%)	Number of plant species	Percentage of total species (%)
Asteraceae	7	11.29	9	12.33
Lamiaceae	4	6.45	5	6.85
Rosaceae	4	6.45	4	5.48
Urticaceae	3	4.84	5	6.85
Ranunculaceae	3	4.84	4	5.48
Poaceae	3	4.84	3	4.11
Apiaceae	3	4.84	3	4.11
Polygonaceae	2	3.23	4	5.48
Araliaceae	2	3.23	2	2.74
Asparagaceae	2	3.23	2	2.74
Caprifoliaceae	2	3.23	2	2.74
Gentianaceae	2	3.23	2	2.74
Polypodiaceae	2	3.23	2	2.74
Orchidaceae	2	3.23	2	2.74
Balsaminaceae	1	1.61	3	4.11
Violaceae	1	1.61	2	2.74
Zingiberaceae	1	1.61	1	1.37
Rubiaceae	1	1.61	1	1.37
Verbenaceae	1	1.61	1	1.37
Piperaceae	1	1.61	1	1.37
Geraniaceae	1	1.61	1	1.37
Oxalidaceae	1	1.61	1	1.37
Onagraceae	1	1.61	1	1.37
Athyriaceae	1	1.61	1	1.37
Mazaceae	1	1.61	1	1.37
Plantaginaceae	1	1.61	1	1.37
Caryophyllaceae	1	1.61	1	1.37
Boraginaceae	1	1.61	1	1.37
Campanulaceae	1	1.61	1	1.37
Fabaceae	1	1.61	1	1.37
Dryopteridaceae	1	1.61	1	1.37
Ericaceae	1	1.61	1	1.37
Melanthiaceae	1	1.61	1	1.37
Apocynaceae	1	1.61	1	1.37
Pteridaceae	1	1.61	1	1.37
Total	62	100	73	100

higher herbaceous plant species on the sunny slope are *Fragaria moupinensis*, *Peperomia tetraphylla* and *Duchesnea indica*.

3.3. Herbaceous plants in different altitude gradient zones on shady and sunny slopes α diversity analysis

It can be seen from **Figures 4A, B** that the species richness index (R), Shannon-Wiener diversity index (H) and Pielou evenness index (J) of herbaceous plants on shady slopes show a trend of first decreasing and then increasing with the increase of altitude. Shannon-Wiener diversity index (H) and Pielou evenness index (J) showed no significant difference among different altitudes. It can be seen from **Figures 5A, B** that the species richness index (R) of herbaceous plants on the sunny slope increases first and then decreases with the increasing altitude. Shannon-Wiener diversity index (H) showed a trend of first decreasing and then increasing. Shannon-Wiener diversity index (H) was significantly higher than the altitude gradient of 2,400–2,600 m, 2,600–2,800 m and 3,000–3,200 m at 2,000–2,200 m and 2,200–2,400 m ($P < 0.05$). The Pielou evenness index (J) decreases first and then increases with the increase of altitude. The Pielou evenness index (J) at the altitude gradient of 2,000–2,200 m and 2,200–2,400 m was significantly higher than the altitude gradient of 2,400–2,600 m, 2,600–2,800 m and 3,000–3,200 m ($P < 0.05$), and there was no significant difference between 2,600–2,800 m and 3,000–3,200 m ($P > 0.05$).

3.4. Herbs in different altitude gradient zones on shady and sunny slopes β diversity analysis

According to **Figures 6A, C**, Sorenson similarity index (SI) of herbaceous plants in different altitude gradient zones on the shady slope is between 0.129 and 0.385. Cody anisotropy index(β_c) is between 8 and 13.5. Sorenson similarity index (SI) is the highest between 2,400–2,600 m and 2,600–2,800 m of the altitude gradient zone, indicating that there are many common species between the two altitude gradient zones. Cody anisotropy index(β_c) is the lowest, indicating that the replacement rate of herb species between the two altitude gradient zones is relatively slow. Sorenson Similarity Index (SI) is the lowest between 2,000–2,200 m and 2,200–2,400 m elevation gradient zones, indicating that there are fewer species in common between these two elevation gradient zones. Cody anisotropy index(β_c) is the highest, indicating that the area between the two altitude gradient zones is rich in herb species on the shady slope. It can be seen from **Figures 6B, D** that Sorenson similarity index (SI) of herbaceous plants in different altitude gradient zones on the sunny slope is between 0.269 and 0.690, and Cody dissimilarity index(β_c) is between 9.5 and 20. Sorenson similarity index (SI) is the highest between 2,000–2,200 m and 2,200–2,400 m in the altitude gradient zone, indicating that there are many common species between the two altitude gradient zones. Cody anisotropy index(β_c) is the lowest, indicating that the replacement rate of herb species between the two altitude gradient zones is relatively slow. Sorenson Similarity Index (SI) between 2,200–2,400 m and 2,400–2,600 m altitude gradient zones is the lowest, and there are few common species between the two altitude gradient zones.

3.5. Correlation between herb diversity and environmental factors

The results of principal component analysis (**Figure 7A**) show that different environmental factors have different loads in different principal components. Clay content, silt content, elevation, slope and other factors are positively correlated with the first principal component. Clay content, silt content, slope, PH value are positively correlated with the second principal component. Only the loadings of clay content, silt content and slope in the two principal components are positive, while the loadings of vegetation coverage and sand content in the two principal components are negative, indicating that different environmental factors have different effects on the herb diversity indicators. The grain size composition of soil determines its texture. Soil texture directly affects the maintenance and movement of soil moisture, soil fertility, soil aeration, soil temperature, and is closely related to crop growth and development. Vegetation coverage can reflect the quality of local habitats and is the result of the comprehensive effect of various environmental factors and plants. The correlation between environmental factors and diversity indicators (**Figure 7B**) shows that there is a certain degree of clustering among samples. The environmental factors of shady slope and sunny slope are separated. The sample plot on the shady slope has a higher altitude, with a higher content of clay and silt in the soil. The sunny slope sample plot has higher vegetation coverage and slope. The Shannon-Wiener diversity index (H) and evenness index (J) of herbaceous plant diversity showed significant positive correlation. Shannon-Wiener diversity index (H) and evenness index (J) were negatively correlated with species richness (R).

4. Discussion

4.1. Differences of herbaceous plants on the shady and sunny slopes

Herbs are an important part of the biodiversity of the forest ecosystem. Their species composition and structure are also important indicators of the natural recovery of forests and the healthy structure of the forest ecosystem (Chitale et al., 2014; Wani et al., 2022). Altitude has always been considered as the dominant factor affecting regional habitat differences. Different altitudinal gradients lead to different spatial distributions of hydrothermal conditions, thus forming different herbage community structures in different regions (Cuesta et al., 2016; Zhao et al., 2016; Borisade, 2020; Pérez-Postigo et al., 2021).

According to the survey results in the Sejila Mountain research area, there are relatively many single family (genus) plant species in the undergrowth herb diversity in southeast Tibet, and most families only include one genus and one species (Wang et al., 2021). The number of families, genera and species of herbaceous plants on sunny slope is greater than that on shady slope, which is caused by the difference of surface soil temperature between shady slope and sunny slope. Slope aspect plays a leading role in the distribution of herbaceous plants and the change of soil temperature, indicating that the distribution of mountain plants is greatly affected by the change of soil temperature. The soil temperature on the sunny slope is higher, which is more suitable for the growth of a variety of herbs (Zhao et al., 2016; Xue et al., 2018; Kwaku, 2021). Asteraceae species on shady slope and sunny slope are the largest, and the number of Asteraceae species on shady slope accounts for 17.54% of the total herbaceous species investigated on shady slope of Sejila Mountain. The number of Asteraceae species on the sunny slope accounts for 12.33% of the total herbaceous species investigated on the sunny slope of Sejila Mountain, which is related to the habitat heterogeneity under different altitude gradients in the study area. Habitat heterogeneity makes different herbs occupy different niches (Xu et al., 2011).

4.2. Driving factors for the vertical distribution of shady and sunny slopes

In the α diversity index, Shannon-Wiener diversity index (H) and Pielou evenness index (J) of shady slope and sunny slope decreased first and then increased with the increasing altitude (Zhang et al., 2016). The main reason is that due to the uplift of mountains, the precipitation will increase with the elevation and then decrease to a certain extent (Brien et al., 2000; Ent et al., 2016;

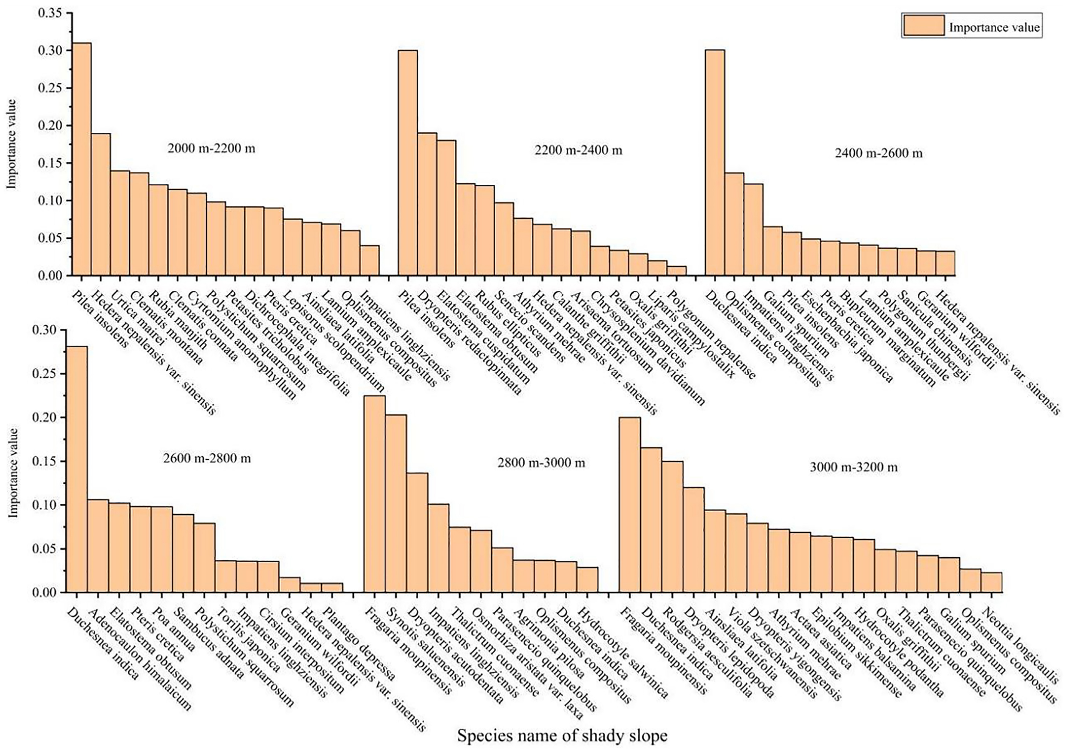

FIGURE 2
Important values of herbaceous plants in different altitude gradients of shady slope.

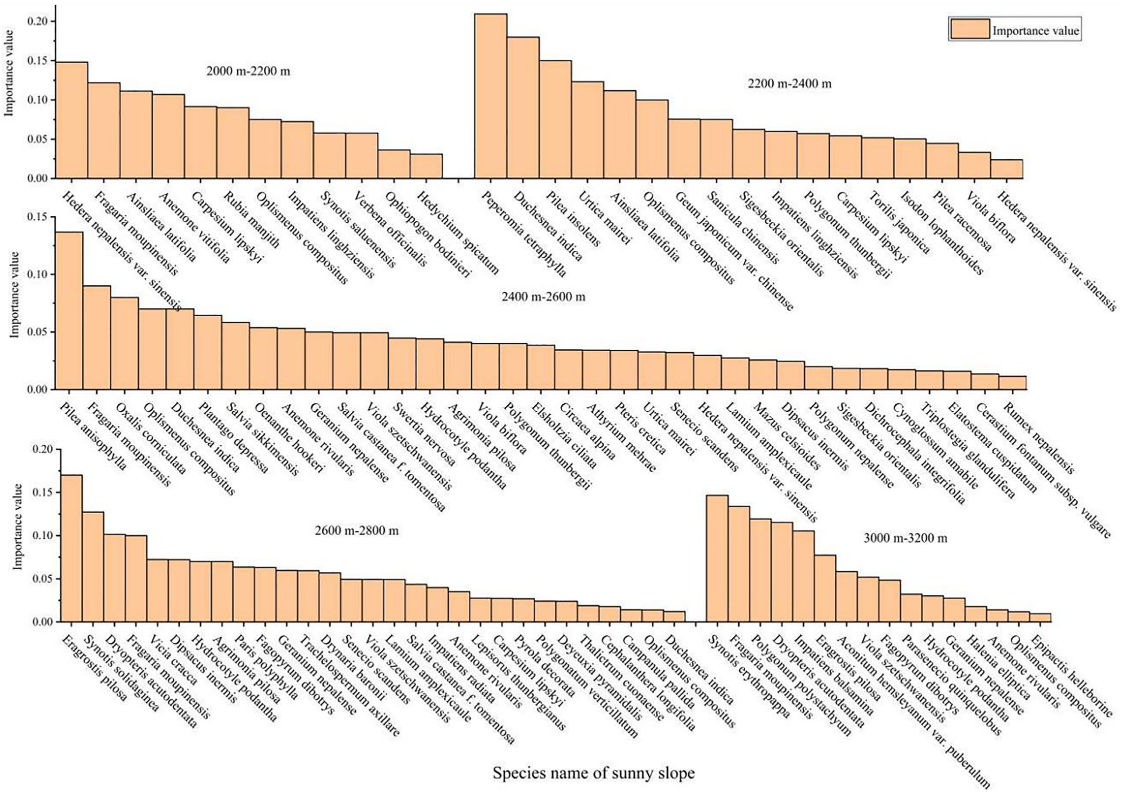

FIGURE 3
Important values of herbaceous plants in different altitude gradients of sunny slope.

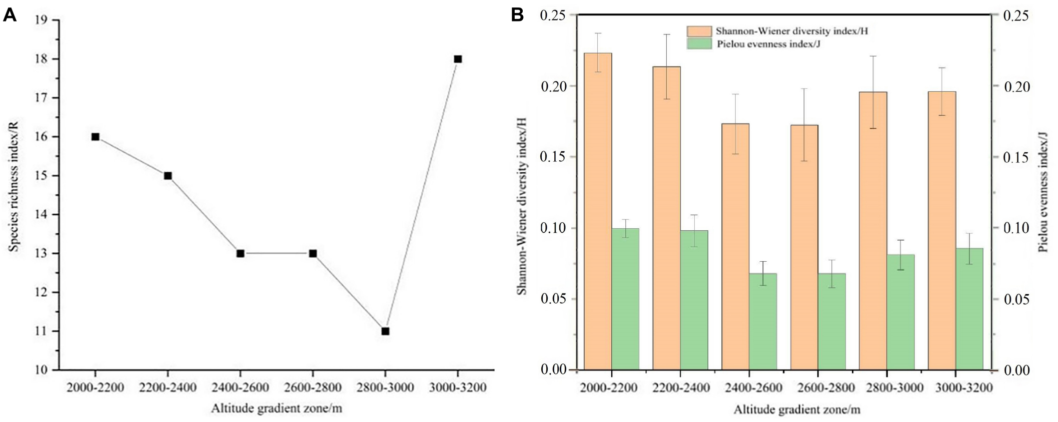

FIGURE 4

α diversity index of herbaceous plants in different altitude gradients of shady slope. **(A)** Species richness index, and **(B)** Shannon-Wiener diversity index and Pielou evenness index.

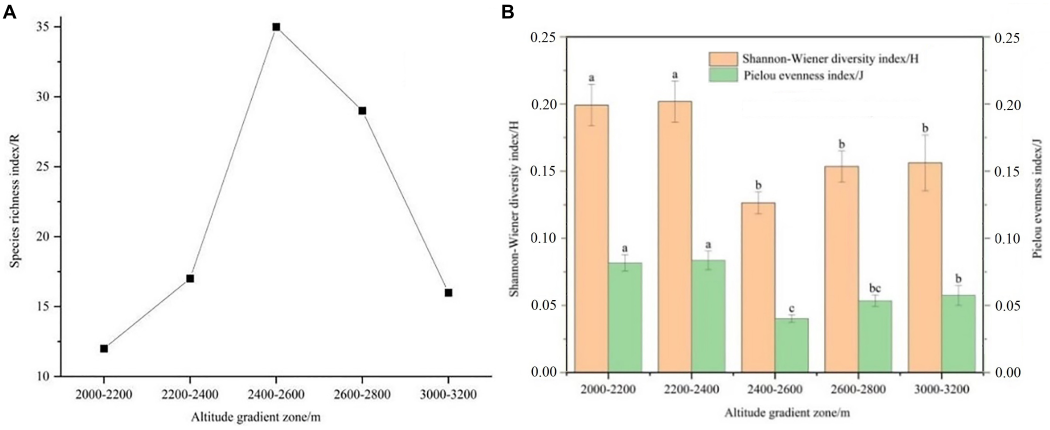

FIGURE 5

α diversity index of herbaceous plants in different altitude gradients of sunny slope. **(A)** Species richness index, and **(B)** Shannon-Wiener diversity index and Pielou evenness index. Different lower case letters in the figure indicate that there are significant differences between different altitude gradients ($P < 0.05$).

Tesfaye et al., 2016). The soil water content is high between 2,400–2,600 m above sea level, and the good habitat conditions meet the growth of trees and shrubs. This leads to the occupation of habitat conditions by trees and shrubs in this altitude gradient zone, squeezing the growth of herbaceous plants. Therefore, the Shannon Wiener diversity index (H) and Pielou evenness index (J) of herbaceous plants in this altitude gradient zone are the lowest. The number of herbaceous species is the largest in the area of 2,600–2,800 m above sea level on the sunny slope. This area has the lowest vegetation coverage, which is caused by more solar radiation reaching the ground through alpine pine forests (Kleinn et al., 2020). Therefore, in the same forest coverage area, the smaller the vegetation coverage, the more species of herbaceous plants. However, relevant scholars pointed out that the family and genus composition of undergrowth herbaceous vegetation species is complex, the community species diversity level is high, the evenness is large, and the habitat conditions are stable. The species diversity shows a different trend of increasing first and then decreasing with the increase of altitude gradient (Austrheim, 2002; Gómez-Díaz et al., 2017; Dip et al., 2020).

In the β diversity index, the Cody dissimilarity index(β_c) of shady slope and sunny slope generally shows a downward trend with the increase of altitude, while Sorenson similarity index (SI) is opposite. Cody anisotropy index(β_c) of shady slope and sunny slope generally shows a downward trend with the increase of altitude, and the substitution of herbaceous plants in different habitats is generally slow (Sánchez-gonzález and López-mata, 2005). This is related to the competition among species, resulting in the heterogeneity of habitats. Sorenson similarity index (SI) of herbaceous plants in different altitude gradient zones is generally higher on sunny slopes than on shady slopes, indicating that there are more common species on sunny slopes than on shady slopes among different altitude gradient zones. Cody anisotropy index(β_c) is generally higher on sunny slope than on shady slope, and the replacement rate of sunny slope is slower than that of shady slope.

The human disturbance, grazing pressure, and land use change is important in shaping and driving herbaceous plant communities.

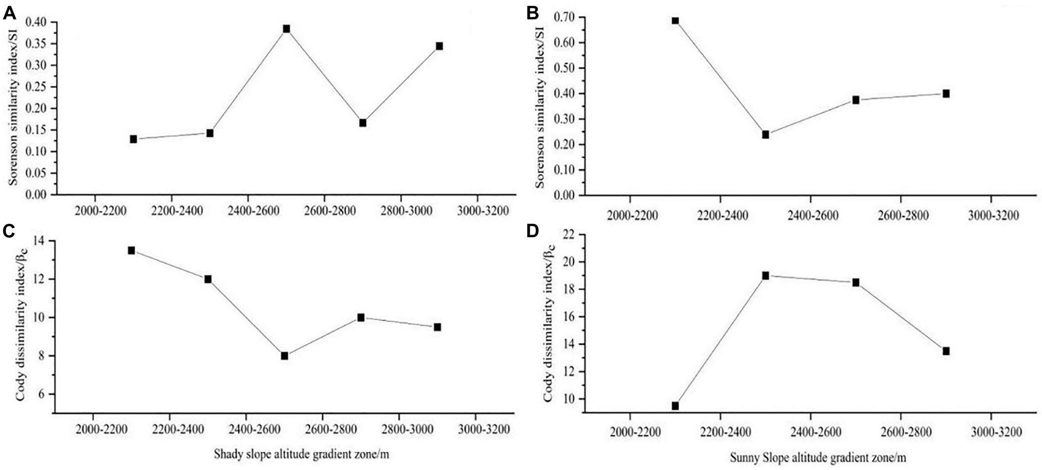

FIGURE 6

β diversity index of herbaceous plants in different altitude gradients. Panels **(A,C)** are Sorenson similarity index and Cody dissimilarity index on shady slope, and panels **(B,D)** are Sorenson similarity index and Cody dissimilarity index on sunny slope.

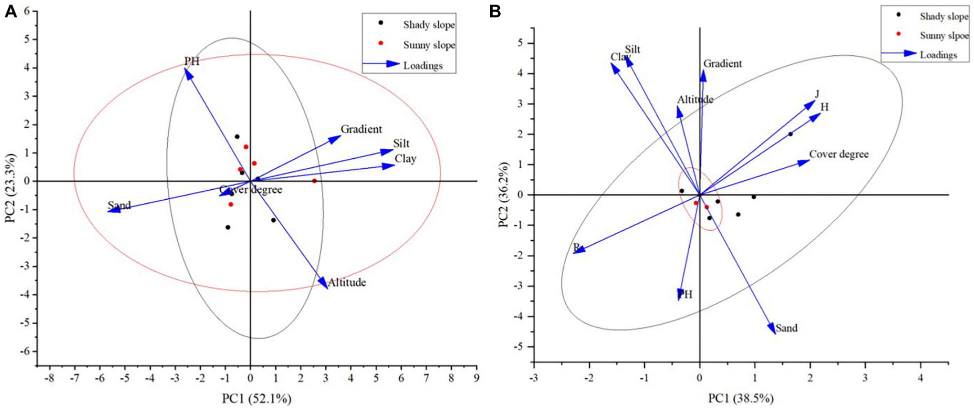

FIGURE 7

Principal component analysis of different environmental factors and herb diversity index. **(A)** Principal component analysis of environmental factors. **(B)** Correlation between environmental factors and diversity indices.

The Sejila Mountain on the Qinghai-Tibet Plateau is a region with dense original vegetation and steep mountain terrain. The human disturbance intensity and grazing pressure have little influence on the growth of herbaceous plants, and the change of land use under the original forest area is small (Xue et al., 2018; Zu et al., 2019; Han et al., 2022). Topography and local habitats are obviously different in the alpine environment. Among the driving factors affecting herb diversity, the topography factors including the slope, slope direction and altitude have a great impact on vegetation growth and spatial distribution (Davies et al., 2007). In this study, the elevation gradient and slope aspect have significant effects on the diversity index, which is consistent with the research findings of Korner (2001), Liao et al. (2008), and Sherman et al. (2008). Moreover, the physical and chemical properties of soil also have an important impact on the distribution of plant communities. The previous studies have shown that the soil factors strongly affect the species composition of alpine vegetation (Yan, 2007). This study also found that the soil clay content and silt content are key factors affecting the diversity of herbaceous plants. Under the influence of micro-climate and micro-topography in different regions, the soil texture also changes correspondingly. The influence of soil particle size on herb species diversity in Sejira Mountain shows a remarkable change.

In the future research on the vertical distribution pattern of herbaceous plants in high altitude mountain areas, we should expand to multiple biological groups, and deeply study the interaction between various groups (such as the influence of some microorganisms on herbaceous plant roots, the influence of insects on herbaceous plant pollination, etc.). This will greatly improve our understanding of the vertical distribution pattern of biodiversity and its driving factors. In addition, the study relies on a limited number of samples, which may not fully reflect the herbaceous plant communities in the alpine regions. Due to the influence of alpine geographical environment, it is difficult to reach the sufficient number of samples. This partly affects the reliability of conclusions. Further studies will provide a more accurate picture of the species composition and diversity of herbaceous plants using a larger number of samples and a more systematic sampling design in high-altitude mountain areas.

5. Conclusion

The types of herb communities in the study area are diverse, and the species diversity is high. A total of 57 species of herbs belonging to 49 genera and 24 families were found on the shady slope. A total of 73 species belonging to 62 genera and 35 families were found on the sunny slope. Asteraceae contains the most species; α Among the diversity indices, the richness index (R) of shady slope, Shannon-Wiener diversity index (H) and Pielou evenness index (J) all decreased first and then increased with the increasing altitude. The richness index (R) of the sunny slope increased first and then decreased with the elevation. Shannon-Wiener diversity index (H) and Pielou evenness index (J) both decreased first and then increased with the increasing altitude; In the β diversity index, Cody dissimilarity index (β_c) of shady slope and sunny slope generally showed a downward trend, while Sorenson similarity index (SI) was opposite; Altitude gradient and aspect have significant effects on diversity index. The diversity of herbaceous plants is affected by many factors. The difference of water and heat conditions caused by altitude and slope aspect is an important driving factor for the diversity of herbaceous plants. Moreover, the soil clay content, silt content and slope gradient are also important driving factors. The correlation between environmental factors and diversity index shows that there is a certain degree of clustering among samples. The driving environmental factors of shady and sunny slope are separated due to the different degrees of influence on alpine herbaceous plant diversity index. Therefore, the differential measure is necessary in the rational utilization of understory plant resources and ecological environment protection of the shady and sunny slopes in high-altitude mountain regions.

Data availability statement

The original contributions presented in this study are included in the article/supplementary material, further inquiries can be directed to the corresponding authors.

Author contributions

JH and HY: conceptualization. BY and SW: data curation. JX: formal analysis, supervision, and writing—review and editing. ZZ: methodology. XC: resources. JH and JC: validation. JH and ZZ: writing—original draft. All authors read and agreed to the published version of the manuscript.

Funding

This work was financially supported by Investigation on resource environment and biodiversity of typical mountainous areas in different climatic zones (2019FY101601-2), the original innovation project of the basic frontier scientific research program, Chinese Academy of Sciences (ZDBS-LY-DQC031), Ecological cultivation demonstration of Gentian at the Himalayan headwater of Chcedo, the National Natural Science Foundation of China (42071259), the Third Batch of Tianshan Talents Program of Xinjiang Uygur Autonomous Region (2021–2023), the Youth Innovation Promotion Association of the Chinese Academy of Sciences (2019430), the study on the support system of modern forestry technology in Tibet (2018xz503118002), and the study on the model of planting and breeding circular agriculture in Tibet.

Conflict of interest

The authors declare that the research was conducted in the absence of any commercial or financial relationships that could be construed as a potential conflict of interest.

Publisher's note

References

Andra, T. (2016). Environmental drivers of the composition and diversity of the herb layer in mixed temperate forests in hungary. *Plant Ecol.* 217, 549–556.

Austrheim, G. (2002). Plant diversity patterns in semi-natural grasslands along an elevational gradient in southern Norway. *Plant Ecol.* 161, 193–206. doi: 10.1023/A:1020315718720

Borisade, T. V. (2020). Nutrient status in herbaceous layer of riparian forests in Southwestern. *Trop. Ecol.* 61, 589–593.

Brien, E. M. O., Sciences, F., Wales, U., Road, D., Uw, L. L., Field, R., et al. (2000). Climatic gradients in woody plant (tree and shrub) diversity?: water-energy dynamics, residual variation, and topography. *Oikos* 89, 588–600.

Brockerhoff, E. G., Barbaro, L., Castagneyrol, B., Forrester, D. I., Gardiner, B., González-Olabarria, J. R., et al. (2017). Forest biodiversity, ecosystem functioning and the provision of ecosystem services. *Biodiversity Conserv.* 26, 3005–3035. doi: 10.1007/s10531-017-1453-2

Butchart, S. H., Walpole, M., Collen, B., van Strien, A., Scharlermann, J. P., and Almond, R. E. (2010). Global biodiversity: indicators of recent declines. *Science* 328, 1164–1168. doi: 10.1126/science.1187512

Cardinale, B. J., Duffy, J. E., Gonzalez, A., Hooper, D. U., Perrings, C., and Venail, P. (2012). Biodiversity loss and its impact on humanity. *Nature* 486, 59–67. doi: 10.1038/nature11148

Chitale, V. S., Behera, M. D., and Roy, P. S. (2014). Future of endemic flora of biodiversity hotspots in India. *PLoS One* 9:e115264. doi: 10.1371/journal.pone.0115264

Cuesta, F., Muriel, P., Llambí, L. D., Halloy, S., Aguirre, N., Beck, S., et al. (2016). Accepted article. *Ecography* 40, 1381–1394. doi: 10.1111/ecog.02567 da Silva, F. K. G., de Faria Lopes, S., Lopez, L. C. S., de Melo, J. I. M., de Brito Melo, and Trovão, D. M. (2014). Patterns of species richness and conservation in the Caatinga along elevational gradients in a semiarid ecosystem. *J. Arid Environ.* 110, 47–52. doi: 10.1016/j.jaridenv.2014.05.011

Davies, K. W., Bates, J. D., and Miller, R. F. (2007). Environmental and vegetation relationships of the Artemisia tridentata spp. wyomingensis alliance. *J. Arid Environ.* 70, 478–494. doi: 10.1016/j.jaridenv.2007.01.010

Dip, A. B., Sampietro-Vattuone, M. M., Garey, M. V., and Eleuterio, A. A. (2020). Altitudinal gradient of plant diversity patterns in the sierra de quilmes (monte desert – Argentina). *J. Arid Environmen.* 182:104274. doi: 10.1016/j.jaridenv.2020.104274

Doležal, J., and Šrůtek, M. (2002). Altitudinal changes in composition and structure of mountain-temperate vegetation: a case study from the Western Carpathians. *Plant Ecol.* 158, 201–221. doi: 10.1023/A:1015564303206

Ecology, S. P., and Kessler, M. (2012). Elevational gradients in species richness and endemism of selected plant groups in the central bolivian andes author (s): Michael Kessler reviewed work (s): elevational gradients in species richness and endemism groups in the central Bolivian Andes of. *Plant Ecol.* 149, 181–193.

Ellum, D. S., Ashton, M. S., and Siccama, T. G. (2010). Spatial pattern in herb diversity and abundance of second growth mixed deciduous-evergreen forest of southern New England. *U S A. For. Ecol. Manag.* 259, 1416–1426. doi: 10.1016/j.foreco.2010.01.011

Ent, A., Van Der Erskine, P., Mulligan, D., Repin, R., and Karim, R. (2016). Vegetation on ultramafic edaphic ' islands ' in Kinabalu park (Sabah, Malaysia) in relation to soil chemistry and elevation. *Plant Soil* 403, 77–101.

Fayiah, M., Dong, S., Li, Y., Xu, Y., Gao, X., Li, S., et al. (2019). The relationships between plant diversity, plant cover, plant biomass and soil fertility vary with grassland type on Qinghai-Tibetan Plateau. *Agric. Ecosyst. Environ.* 286:106659. doi: 10.1007/s11104-016-2831-3

Gilliam, F. S. (2007). The ecological significance of the herbaceous layer in temperate forest ecosystems. *BioScience* 57, 845–858. doi: 10.1890/12-1582.1

Gómez-Díaz, J. A., Krömer, T., Kreft, H., Gerold, G., Carvajal-Hernández, C. I., and Heitkamp, F. (2017). Diversity and composition of herbaceous angiosperms along gradients of elevation and forest-use intensity. *PLoS One* 12:e0182893. doi: 10.1371/journal.pone.0182893

Han, W., Chen, L., Su, X., Liu, D., Jin, T., Shi, S., et al. (2022). Effects of soil physico-chemical properties on plant species diversity along an elevation gradient over alpine grassland on the Qinghai-Tibetan Plateau, China. *Front. Plant Sci.* 13:822268. doi: 10.3389/fpls.2022.822268

Kleinn, C., Magnussen, S., Nölke, N., Magdon, P., and Álvarez-gonzález, J. G. (2020). Improving precision of field inventory estimation of aboveground biomass through an alternative view on plot biomass. *For. Ecosyst.* 7: 57. doi: 10.1186/s40663-020-00268-7

Korner, C. (2001). *Alpine Plant Life: Functional Plant Ecology of High Mountain Ecosystems*. Berlin: Springer.

Kwaku, E. A. (2021). Biomass and species diversity of different alpine plant. *Plants* 10, 1–11. doi: 10.3390/plants10122719

Li, X., Liang, E., Gričar, J., Prislan, P., Rossi, S., and Čufar, K. (2013). Age dependence of xylogenesis and its climatic sensitivity in Smith fir on the south-eastern Tibetan Plateau. *Tree Physiol.* 33, 48–56. doi: 10.1093/treephys/tps113

Liao, B. H., Nan, H. U., and Ding, S. Y. (2008). Dynamics of plant functional groups along altitudinal gradient on the northern slope of Funiu mountain. *J. Henan Univ.* 38, 618–632.

Mu, C., Li, L., Zhang, F., Li, Y., Xiao, X., Zhao, Q., et al. (2018). Impacts of permafrost on above- and belowground biomass on the northern Qinghai-Tibetan Plateau. *Arctic Antarctic Alpine Res.* 50:e1447192.doi: 10.1080/15230430.2018.1447192

Pérez-Postigo, I., Bendix, J., Vibrans, H., and Cuevas-Guzmán, R. (2021). Diversity of alien roadside herbs along an elevational gradient in western Mexico. *NeoBiota* 65, 71–91. doi: 10.3897/neobiota.65.67192

Sánchez-gonzález, A., and López-mata, L. (2005). Plant species richness and diversity along an altitudinal gradient in the Sierra. *Divers. Distrib.* 11, 567–575. doi: 10.1111/j.1366-9516.2005.00186.x

She, Y., Zhang, Z., Ma, L., Xu, W., Huang, X., and Zhou, H. (2022). Vegetation attributes and soil properties of alpine grassland in different degradation stages on the Qinghai-Tibet Plateau, China: a meta-analysis. *Arabian J. Geosci.* 15, 15–193. doi: 10.1007/s12517-021-09400-5

Sherman, R., Mullen, R., and Haomin, L. (2008). Spatial patterns of plant diversity and communities in alpine ecosystems of the Hengduan mountains, Northwest Yunnan, China. *J. Plant Ecol.* 1, 117–136. doi: 10.1016/j.pld.2021.09.001

Shi, S., Liu, G., Li, Z., and Ye, X. (2021). Elevation-dependent growth trends of forests as affected by climate warming in the southeastern Tibetan Plateau. *For. Ecol. Manag.* 498:119551. doi: 10.1016/j.foreco.2021.119551

Sklenář, P., and Jørgensen, P. M. (1999). Distribution patterns of paramo plants in ecuador. *J. Biogeogr.* 26, 681–691. doi: 10.3390/insects11010064

Sklenár, P., and Ramsay, P. M. (2001). Diversity of zonal páramo plant communities in ecuador. *Divers. Distrib.* 7, 113–124. doi: 10.1046/j.1472-4642.2001.00101.x

Tesfaye, M. A., Bravo, F., Ruiz-peinado, R., Pando, V., and Bravo-oviedo, A. (2016). Geoderma impact of changes in land use, species and elevation on soil organic carbon and total nitrogen in Ethiopian central highlands. *Geoderma* 261, 70–79. doi: 10.1016/j.geoderma.2015.06.022

Torresani, M., Rocchini, D., Sonnenschein, R., Zebisch, M., Hauffe, H. C., Heym, M., et al. (2020). Height variation hypothesis: a new approach for estimating forest species diversity with CHM LiDAR data. *Ecol. Indic.* 117:106520. doi: 10.1016/j.ecolind.2020.106520

Van Dam, A. (2019). Diversity and its decomposition into variety, balance and disparity. *R. Soc. Open Sci.* 6:190452. doi: 10.1098/rsos.190452

Walter, J. A., Stovall, A. E. L., and Atkins, J. W. (2021). Vegetation structural complexity and biodiversity in the Great Smoky mountains. *Ecosphere* 12:e03390. doi: 10.1002/ecs2.3390

Wang, G., Sun, Y., Zhou, M., Guan, N., Wang, Y., Jiang, R., et al. (2021). Effect of thinning intensity on understory herbaceous diversity and biomass in mixed coniferous and broad-leaved forests of Changbai mountain. *For. Ecosyst.* 8:53. doi: 10.1186/s40663-021-00331-x

Wang, J., Wang, G., Fu, Y., Chen, X., and Song, X. (2019). Short-term effects of nitrogen deposition on soil respiration components in two alpine coniferous forests, southeastern Tibetan Plateau. *J. For. Res.* 30, 1029–1041. doi: 10.1007/s11676-018-0678-6

Wani, S. A., Ahmad, R., Gulzar, R., Rashid, I., Malik, A. H., and Khuroo, A. A. (2022). Diversity, distribution and drivers of alien flora in the Indian Himalayan region. *Global Ecol. Conserv.* 38:e02246. doi: 10.1016/j.gecco.2022.e02246

Xian, H., Hao, Y., Lv, J., Wang, C., Zuo, P., Pei, Z., et al. (2021). Novel brominated flame retardants (NBFRs) in soil and moss in Mt. Shergyla, southeast Tibetan Plateau: occurrence, distribution and influencing factors. *Environ. Pollut.* 291:118252. doi: 10.1016/j.envpol.2021.118252

Xiangyang, S., Genxu, W., Juying, S., Shouqin, S., Zhaoyong, H., Chunlin, S., et al. (2022). Contrasting water sources used by a coniferous forest in the high-altitude, southeastern Tibetan Plateau. *Sci. Total Environ.* 849:157913. doi: 10.1016/j.scitotenv.2022.157913

Xu, X., Ouyang, H., Cao, G., Richter, A., Wanek, W., and Kuzyakov, Y. (2011). Dominant plant species shift their nitrogen uptake patterns in response to nutrient enrichment caused by a fungal fairy in an alpine meadow. *Plant Soil* 341, 495–504. doi: 10.1007/s11104-010-0662-1

Xue, R., Yang, Q., Miao, F., Wang, X., and Shen, Y. (2018). Slope aspect influences plant biomass, soil properties and microbial composition in alpine meadow on the Qinghai-Tibetan Plateau. *J. Soil Sci. Plant Nutr.* 18, 1–12. doi: 10.4067/S0718-95162018005000101

Yan, W. (2007). The impact of snow-cover on alpine vegetation type of different aspects in the west of Sichuan province. *Acta Ecol. Sin.* 27, 5120–5129.

Yılmaz, O. Y., Yılmaz, H., and Akyüz, Y. F. (2018). Effects of the overstory on the diversity of the herb and shrub layers of Anatolian black pine forests. *Eur. J. For. Res.* 137, 433–445. doi: 10.1007/s10342-018-1114-3

Yin, H., Yu, B., Zhang, Z., Jia, L., Xue, J., Chen, X., et al. (2022). Evaluating the impact of different afforestation time scales on the soil quality in a typical watershed valley using the criteria importance through intercriteria correlation method and gray target model. *Front. For. Glob. Change* 5:997949. doi: 10.3389/ffgc.2022.997949

Zhang, W., Huang, D., Wang, R., Liu, J., and Du, N. (2016). Altitudinal patterns of species diversity and phylogenetic diversity across temperate Mountain forests of Northern China. *PLoS One* 11:e159995. doi: 10.1371/journal.pone.0159995

Zhang, Z. W., Yin, H. Y., Chang, J. J., and Jie. X. (2022). Spatial variability of surface soil water content and its influencing factors on shady and sunny slopes of an alpine meadow on the Qinghai-Tibetan Plateau. *Glob. Ecol. Conserv*. 34:e02035. doi: 10.1016/j.gecco.2022.e02035

Zhang, Z. W., Yin, H. Y., Zhao, Y., Wang, S. P., Han, J. H., Yu, B., et al. (2021). Spatial heterogeneity and driving factors of soil moisture in alpine desert using the geographical detector method. *Water* 13:2652. doi: 10.3390/w13192652

Zhao, J., Li, X., Li, R., Tian, L., and Zhang, T. (2016). Effect of grazing exclusion on ecosystem respiration among three different alpine grasslands on the central Tibetan Plateau. *Ecol. Eng.* 94, 599–607. doi: 10.1016/j.ecoleng.2016.06.112

Zhou, X. L., Yan, Y. E., Zhang, J., Zhou, X. J., Yan, Y. Q., Yang, F. Q., et al. (2022). Vegetation community structure and diversity in a burned area of *Picea asperata-Abies fabri* forest on different aspects on the northeastern margin of the Qinghai-Tibetan Plateau. *Acta Prataculturae Sinica* 31, 144–155. doi: 10.11686/cyxb2021372

Zu, K., Luo, A., Shrestha, N., Liu, B., Wang, Z., and Zhu, X. (2019). Altitudinal biodiversity patterns of seed plants along Gongga mountain in the southeastern Qinghai–Tibetan Plateau. *Ecol. Evol.* 9, 9586–9596. doi: 10.1002/ece3.5483

Frontiers in Forests and Global Change

TYPE Original Research
PUBLISHED 04 April 2023
DOI 10.3389/ffgc.2023.1135219

EDITED BY
Vikram S. Negi,
Govind Ballabh Pant National Institute of Himalayan Environment and Sustainable Development, India

REVIEWED BY
Zeeshan Ahmad,
Quaid-i-Azam University, Pakistan
Balwant Rawat,
Graphic Era Hill University, India

*CORRESPONDENCE
Ali Asghar Shah
✉ aashah@bgsbu.ac.in

SPECIALTY SECTION
This article was submitted to Forest Management, a section of the journal Frontiers in Forests and Global Change

RECEIVED 31 December 2022
ACCEPTED 20 March 2023
PUBLISHED 04 April 2023

CITATION
Choudhary F, Bhardwaj A, Sayeed I, Rather SA, Khan MAH and Shah AA (2023) Elevational patterns of soil nematode diversity, community structure and metabolic footprint in the Trikuta mountains of Northwestern Himalaya.
Front. For. Glob. Change 6:1135219.
doi: 10.3389/ffgc.2023.1135219

Elevational patterns of soil nematode diversity, community structure and metabolic footprint in the Trikuta mountains of Northwestern Himalaya

Fozia Choudhary[1], Anil Bhardwaj[1], Iqra Sayeed[1], Shabir Ahmad Rather[2], Mohammad Abdul Hannan Khan[2] and Ali Asghar Shah[1]*

[1]Nematode Biodiversity and Genomics Research Lab, Department of Zoology, Baba Ghulam Shah Badshah University Rajouri, Jammu and Kashmir, India, [2]Biochemical and Molecular Parasitology Lab, Department of Zoology, Baba Ghulam Shah Badshah University Rajouri, Jammu and Kashmir, India

Nematodes are an integral part of soil biodiversity and play a vital role in soil nutrient cycling. The Himalayan mountainous ecosystems are amongst the extreme environments in the world. Still little is known about the diversity and distribution patterns of soil nematodes along the elevation gradient in the region, thus limiting our ability in understanding and comparing the structural patterns of nematode communities across different regions. To address this knowledge gap, we aim to disentangle the elevational patterns of soil nematode community structure and trophic diversity by studying the abundance, composition, diversity and functional indices, and metabolic footprint of soil nematodes at four elevation classes (Elev1, Elev2, Elev3, and Elev4 each being 400 m) along an altitudinal gradient (1,000–2,600 m) in the Trikuta mountain range of Pir-Panjal to Shivalik Himalaya. Overall, a total of 55 genera were found in the study region. The diversity and richness of soil nematodes varied significantly among the elevation classes, and exhibit a decreasing trend with elevation. Also, the nematode community composition varied significantly among the elevation classes along the elevational gradient. The bacterivores were the dominant trophic group at each elevation class. Further, the soil properties played a key role in explaining the changes in the nematode community composition across the elevation classes. Moreover, the total nematode, bacterivore and herbivore abundances showed an increasing trend, while as that of fungivores and predators exhibit a negative trend with elevation. In addition, a declining pattern in the overall maturity and metabolic footprint with elevation was observed, thus depicting the lower sustenance of k-strategic nematodes and their relatively lower contribution to belowground carbon cycling at higher elevations. The finding of our study could enhance our understanding of the overall community structure and diversity patterns of soil nematode along the elevation gradient, and the response of soil nematodes to ongoing climate change in the rapidly warming Himalayas.

KEYWORDS

soil nematode, composition, diversity, elevation, trophic group, Himalaya

Introduction

Soil nematodes (popularly called as roundworms) are one of the major components of belowground faunal diversity (Kergunteuil et al., 2016; Kouser et al., 2021). With more than 27,000 known species, soil nematodes constitute approximately 80% of the total belowground soil metazoan taxonomic and functional diversity (Hodda et al., 2009; Hodda, 2011; Kouser et al., 2021). The nematodes generally occupy all the major trophic guilds of the soil food web, including herbivores, fungivores, bacterivores, predators, parasites, and omnivores (Yeates et al., 1993; Kergunteuil et al., 2016; Zhang et al., 2021). Also, functionally the nematodes can be assigned to a wide degree of ecological adaptations ranging from being acting as "colonizers" (i.e., r strategists) to "persistents" (i.e., K strategists), as well as all the stages occuring in between, along the colonizer-persistents ("cp") continuum (Bongers, 1990; Kergunteuil et al., 2016; Kouser et al., 2021). Owing to vast trophic and functional diversity, nematodes play a key role in regulating several essential ecosystem processes including nutrient cycling, successional changes, and energy flow (Yeates, 2003; Bakonyi et al., 2007; Van Eekeren et al., 2010). As such, nematodes are considered to be the suitable indicators both for monitoring the ecosystem health and tracking environmental changes (Kitagami et al., 2017; Salamun et al., 2017; Zhang et al., 2021). Over decades, researchers have focused on studying the biogeographic distribution pattern of nematodes, however, such studied are mostly restricted to anthropogenic systems (Šalamún et al., 2014; Zhao et al., 2015; Kouser et al., 2021). Research focusing on the diversity and compositional patterns of soil nematodes in natural mountainous systems especially along elevational gradients is direly needed, as such studies can provide vital information on the casual relationship between belowground diversity, ecosystem functioning, soil properties, and local climate (van den Hoogen et al., 2019; Zhang et al., 2021).

Mountainous ecosystems provide an ideal and natural conditions for studying elevational variation in compositional structure of communities, and in unraveling the key environmental variables causing the variation, as both the climatic and edaphic variables change considerably with short distance along elevations (Körner, 2007; Kergunteuil et al., 2016; Wei et al., 2019; Yu et al., 2021; Wani et al., 2023). It has been reported that elevation has a strong filtering effect on soil nematode communities in terms of both climatic and edaphic factors (Thakur et al., 2017, 2019; Siebert et al., 2019; da Silva et al., 2020). For example, changes in the climatic variables (especially temperature and precipitation) directly affect the biotic environment and as such had a significant influence on the underlying community diversity and structure of soil nematodes (Nielsen et al., 2014; Song et al., 2017; Thakur et al., 2017; da Silva et al., 2020). Many studies have also reported the distinct elevational zonation of soil nematode communities due to varying climatic conditions along an elevational gradient (Kergunteuil et al., 2016; Dong et al., 2017). Also, the key role of changing soil physico-chemical properties including organic matter content, soil pH, and soil moisture, along elevational gradients in shaping the structure of soil nematode communities is well documented (Sun et al., 2013; Kitagami et al., 2017; Quist et al., 2019; Reid et al., 2019).

Recently, research efforts have been initiated to study the elevational patterns of nematode diversity and community structure, and draw diverse conclusions including a mid-elevation peak (Dong et al., 2017), increasing diversity with increase in elevation (Kergunteuil et al., 2016), decreasing diversity with elevation (Powers et al., 1998; Liu et al., 2019), irregular patterns to no change with elevation (Tong et al., 2010; Qing et al., 2015). Therefore, there is still a lack of consensus, which hampers our understanding of the overall biogeographical pattern of soil nematode across elevational gradients (Zhang et al., 2021). As such, additional studies in mountainous ecosystems need to be taken in order to arrive at general patterns about the effect of elevation on diversity and distributional patterns of soil nematodes (Dong et al., 2017; Afzal et al., 2021).

In the Himalayan biodiversity hotspot, few studies have been conducted to study the elevational patterns of soil nematodes (Devetter et al., 2017; Afzal et al., 2021). However, till date to the best of our knowledge, no study has attempted to study the elevational patterns of nematodes in conjugation with soil properties across the mountainous ecosystems of the Pir Panchal Himalaya. Toward bridging this knowledge gap, we aim to study the elevational pattern of nematodes along with the physico-chemical properties in soil system across the mountainous ecosystems. Specifically, our study aims to answer the following research questions: (1) whether the soil nematodes differ across elevational gradient? (2) Whether the different nematode trophic groups differ with elevation? (3) Whether the soil nematode diversity, abundance and derived functional indices (MI, PPI, CI, SI, and EI) change with increasing elevation? (4) Whether the soil nematode abundance and soil properties are correlated with each other (5) whether the soil properties change with elevation? Hopefully, the findings of our study can be immensely fruitful in assessing soil health and environmental change effects in the eco-fragile Himalayan mountainous ecosystem.

Materials and methods

Study area

The present study was carried out along the Trikuta mountain range located in the Reasi district of North Western Himalaya. The average elevation of the region ranges from 1,000 to 4,500 m above sea level (a.s.l.). The region experiences mean annual temperature of 14°C and precipitation of 1,360 mm, respectively. The higher altitudes of the region receive a significant amount of precipitation in the form of snowfall. Distinct vegetation classes are found with changing elevation in the region. The vegetation at an elevation range of 1,000–1,800 masl comprise of mixed forest with *Pinus roxburghii*, *Quercus leucotrichophora*, *Rhododendron arboreum,* and *Pyrus pashia* as the dominant species. The elevational zone between 1,800 and 2 600 masl comprise of moist temperate deciduous forests with predominance of *Pinus wallichiana*, *Abies pindrow*, *Quercus dilatata*, and *Picea smithiana*. However, above the elevation of 3,000 masl, the vegetation mainly comprises of alpine tundra and meadows (Afzal et al., 2021).

Soil sampling

We randomly carried soil sampling along a stratified altitudinal gradient in the month of September, 2020. In total, 48 soil samples were collected from four elevation classes (i.e., Elev1: 1,000–1,400 m; Elev2: 1,401–1,800 m; Elev3: 1,801–2,200 m; Elev4: 2,201–2,600 m) along elevation gradient. At each elevation class, four sites were selected which were separated from one another by an elevational distance of 100 m. From each of the selected site three samples and a total of 12 samples from each elevation class were collected (3 samples × 4 sites × 4 elevation classes). Each sample was taken by randomly laying 5 × 5 m quadrant and taking five sub-samples (four from the corners and one from the center) at a depth of 0–15 cm using a soil corer and mixing them together to form a composite sample of 500 g (Kouser et al., 2021; Kashyap et al., 2022) These soil samples were then packed in airtight polythene bags and carried to the laboratory for further analysis.

Soil physiochemical analysis

The soil physiochemical analysis was carried out at Sher-e-Kashmir University of Agricultural Sciences and Technology of Jammu. About 300 g of the bulk soil was used for measuring soil properties including pH, electrical conductivity, moisture, organic matter, total nitrogen, temperature, and soil texture). Soil pH and electrical conductivity were measured using a digital pH and conductivity meter fitted with glass electrodes, after shaking a soil water (1:2 w/v i.e., 50/100) suspension for 30 min on a rotator. The soil moisture was measured by gravimetric method (i.e., drying at 70°C till constant weight). The soil organic matter was estimated using loss on ignition method (Dar et al., 2015). The soil total nitrogen was estimated following the Kjeldahl method (Kjeldahl, 1883). The soil temperature was measured in the field using soil thermometer. Lastly, the soil texture was calculated as the relative proportion of sand and silt content expressed as percentage.

Nematode extraction and identification

The nematodes were extracted from 100 g of soil samples following the sieving and decantation procedure as proposed by Baermann funnel method (Barker, 1985). According to this method, each soil sample was first taken into a 1 L beaker and mixed with tap water. Second, the water suspension was then stirred thoroughly and decanted into another 1 L beaker using a sieve of 2 mm mesh size to remove the stones and large debris. Third, the water suspension was then mixed further and decanted through 53 μm mesh sized sieve, and the material that was left on the sieve was collected in another 250 mL beaker and the extraction was repeated by following Baermann funnel method. The extracted nematodes were removed for 2 days, stored at 4°C, fixed in triethanolamine-glycerol fixative (TAF) and counted using an Olympus stereo -zoom microscope (model: SZX16), and simultaneously mounted on slides for identification to the genus level using various texts (Goodey, 1963; Jairajpuri and Ahmad, 1992; Andrássy, 2005). Also, the identified genera were assigned to different functional guilds based on their trophic groups and life history strategies (Yeates et al., 1993; Bongers and Bongers, 1998).

Data analysis

Using the NINJA online application (Sieriebriennikov et al., 2014),[1] we calculated six nematode functional indices including maturity index (MI), sigma maturity index (ΣMI), plant parasitic index (PPI), enrichment index (EI), structure index (SI) and channel index (CI), based on c–p scale assigned to various genera of nematodes ranging from r-colonizers to k-persisters (cp1–cp5) (Sikora et al., 2018; Maina et al., 2022). The maturity index (MI), sigma maturity index (ΣMI), and plant parasitic index (PPI) were calculated following Bongers (1990), while as the enrichment index (EI) = (e/e + b) × 100, structure index (SI) = (s/s + b) × 100 and channel index (CI) = [0.8 Fu2/(3.2 Ba1 + 0.8 Fu2) × 100] which provide essential information on the soil food web dynamics and stability (Kashyap et al., 2022) were calculated following (Ferris et al., 2001). The structure index is an indicator of the maturity or stability of a system, with higher values reflecting structured and lower values representing a disturbed ecosystem (Afzal et al., 2021; Kashyap et al., 2022). Similarly, the channel index [CI = 0.8 Fu2/(3.2 Ba1 + 0.8 Fu2) × 100] provides information on the relative contribution of bacterial and fungal feeders in the decomposition pathway (Kashyap et al., 2022). In the above-mentioned enrichment and structure indices, the b component was calculated as $\Sigma \mathrm{k}_b \mathrm{n}_b$with k_b indicating the weightage assigned to basal characteristic guilds of the soil food web [0.8 (Ba2 + Fu2)] and n_b representing the nematode abundance of the corresponding guilds. Similarly, the enrichment and structure components were calculated based on the guilds representing enrichment [(3.2 Ba1) + (0.8 Fu2)] and structure (Ba3–Ba5, Fu3–Fu5, Ca2–Ca5), respectively, where Ba1-5 denote bacterivores of C–P group 1–5, Fu2-5 denotes fungivores of C–P group 2–5 and Ca2-5 denotes predators of C–P group 1–5 (Ferris et al., 2001). In addition, the metabolic footprints which acts as proxies to quantify the magnitude of ecosystem services and functions provided by nematode communities to soil food web (Afzal et al., 2021; Kashyap et al., 2022) were calculated following Andrassy (1956) [$W = (D^2 \times \mathrm{L})/(1.6 \times 10^6)$ and Ferris (2010)] [$F = \Sigma(\mathrm{N}_t$ $(0.1\ (\mathrm{W}_t/\mathrm{m}_t) + 0.273\ (\mathrm{W}_t 0.75)]$ using NINJA, where W represents the nematode biomass (μg), D and L denotes the maximum body diameter (μm) and body length (μm), respectively, N_t represents the number of nematodes in genus t, $\mathrm{W}_t$represents the estimated body weight of genus t, and m_t represents the c-p group of the genus t. We also calculated the Shannonfy the magnitude of ’); Pielou’s evenness (J’); and generic richness (GR) indices for estimation of nematode diversity using the “vegan” package (Oksanen et al., 2020) in R statistical software (R Core Team, 2020).

To check whether our data meets the assumption of normality, we performed the Shapiro–Wilk test. The Shapiro–Wilk test showed that the data was non-normally distributed (*p-value* < 0.05). We therefore performed Kruskal–Wallis test to study whether the soil nematode abundance, diversity, functional and metabolic indices, and physicochemical properties differed significantly among the studied elevational classes. In cases where statistically significant differences were found, multiple *post hoc* comparisons among studied elevational classes were performed using the Dunn test. Also, owing to the non-normality of data,

---

[1] https://shiny.wur.nl/ninja/

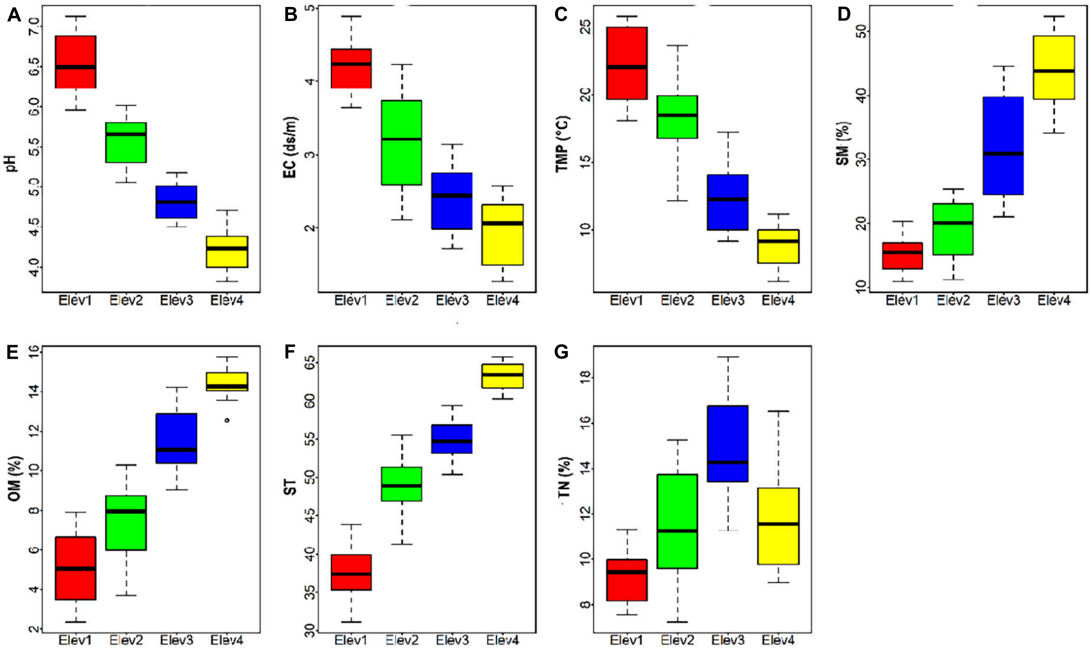

FIGURE 1
Soil physico-chemical properties across elevation classes **(A)** pH, **(B)** EC, electrical conductivity, **(C)** TMP, temperature, **(D)** SM, soil moisture, **(E)** OM, organic matter, **(F)** ST, soil texture, and **(G)** TN, total nitrogen. Elev, Elevation; where Elev1: 1,000–1,400 m, Elev2: 1,401–1,800 m, Elev3: 1,801–2,200 m, and Elev4: 2,201–2,600 m.

TABLE 1 Soil physico-chemical properties along the elevational gradient in the Trikuta mountains.

Variable	Elev1 (1,000–1,400)	Elev2 (1,401–1,800)	Elev3 (1,801–2,200)	Elev4 (2,201–2,600)
pH	6.54 ± 0.11^{a}	5.58 ± 0.09^{b}	4.82 ± 0.07^{c}	4.22 ± 0.08^{c}
EC (ds/m)	4.20 ± 0.10^{a}	3.17 ± 0.20^{b}	2.42 ± 0.14^{bc}	1.95 ± 0.13^{c}
TMP (°C)	22.08 ± 0.83^{a}	18.23 ± 0.86^{a}	12.37 ± 0.74^{b}	8.88 ± 0.45^{b}
SM (%)	15.27 ± 0.88^{a}	19.13 ± 1.37^{a}	32.07 ± 2.47^{b}	43.74 ± 1.78^{b}
OM (%)	5.08 ± 0.56^{a}	7.44 ± 0.58^{a}	11.44 ± 0.48^{b}	14.39 ± 0.25^{b}
ST	37.63 ± 1.07^{a}	49.05 ± 1.08^{b}	54.96 ± 0.81^{b}	63.26 ± 0.54^{c}
TN (%)	9.24 ± 0.33^{a}	11.49 ± 0.76^{b}	15.00 ± 0.66^{c}	11.75 ± 0.67^{b}

Shown are the means ± SE. Data with different small case superscript letters are significantly different at 5% level ($P < 0.05$). EC, electrical conductivity; TMP, temperature; SM, soil moisture; OM, organic matter; ST, soil texture; TN, total nitrogen.

we performed Spearman's multiple correlation among the studied soil physicochemical parameters and nematode trophic groups to study the relationship between them. The statistical significance of the resultant correlation was calculated at $p < 0.05$. Moreover, to investigate the relationship between soil physicochemical properties, nematode trophic groups and genera, we conducted the principal component analysis (PCA) using the "factoextra" package (Kassambara and Mundt, 2020) in R software.

Non-metric multidimensional scaling (NMDS) ordination based on Bray–Curtis distance was conducted using the "vegan" package (Oksanen et al., 2020) in R to investigate the differences in nematode communities along elevation gradient. Furthermore, the Permutational Multivariate Analysis of Variance (PERMANOVA) was used to quantify the compositional differences among the studied elevation classes, In PERMANOVA, we used both the abundance-based Bray-Curtis and incidence-based Jaccard indices to evaluate whether the observed compositional dissimilarity was due to species relative abundances or simply by the presence and/or absence of species (Shahabuddin et al., 2021). Furthermore, if significant differences were found, we also performed the pairwise multi-level comparisons using the vegan" package to assess differences between each pair of elevational classes. The associated statistical significance was assessed at $p < 0.05$ based on 999 permutations.

Results

Soil physicochemical properties along an elevational gradient

Along the elevational gradient, the studied soil physico-chemical parameters varied significantly between the elevational classes. More specifically, soil pH, electrical conductivity and

TABLE 2 Relative abundance of soil nematode genera at the studied elevation classes (mean ± standard error).

Genus	Elev1 (1,000–1,400)	Elev2 (1,401–1,800)	Elev3 (1,801–2,200)	Elev4 (2,201–2,600)
Bacterivores				
Acrobeles	4 ± 1.35	1.82 ± 1.03	3.74 ± 2.11	4.84 ± 2.11
Acrobeloides	1.65 ± 0.98	5.42 ± 1.90	1.85 ± 1.25	3.98 ± 2.27
Alaimus	1.59 ± 1.59	2.75 ± 1.23	2.65 ± 1.47	5.86 ± 2.78
Anaplectus	1.72 ± 1.08	1.68 ± 1.16	4.04 ± 2.15	7.21 ± 2.60
Bunonema	1.35 ± 0.67^{a}	1.03 ± 0.57^{ab}	3.74 ± 2.11^{b}	0.00 ± 0.00^{b}
Cephalobus	2.28 ± 1.26	2.10 ± 1.23	0.00 ± 0.00	4.66 ± 2.70
Cervidellus	2.66 ± 1.24	2.98 ± 1.11	4.25 ± 1.93	4.39 ± 2.36
Chiloplacus	3.90 ± 1.73	2.35 ± 1.29	1.28 ± 0.90	0.00 ± 0.00
Cuticularia	1.24 ± 0.84^{ab}	1.57 ± 0.75^{a}	0.00 ± 0.00^{b}	0.00 ± 0.00^{b}
Diplogastrid	2.55 ± 1.45	0.00 ± 0.00	5.14 ± 2.21	3.31 ± 2.28
Diploscapter	2.96 ± 1.17^{a}	4.75 ± 1.91^{a}	0.00 ± 0.00^{b}	0.00 ± 0.00^{b}
Eucephalobus	2.22 ± 0.98	2.90 ± 1.19	3.56 ± 1.73	2.15 ± 1.45
Mesorhabditis	4.29 ± 1.52	7.70 ± 2.51	5.12 ± 1.61	4.66 ± 2.07
Monhystera	1.30 ± 0.58	1.58 ± 0.76	3.11 ± 1.31	3.15 ± 1.90
Panagrolaimus	1.31 ± 0.70	0.00 ± 0.00	2.78 ± 1.60	2.94 ± 2.01
Pelodera	1.78 ± 0.96	0.77 ± 0.55	5.19 ± 2.39	0.00 ± 0.00
Plectus	2.29 ± 1.60	3.60 ± 1.68	1.08 ± 0.75	4.18 ± 2.34
Protorhabditis	2.11 ± 1.23^{a}	7.27 ± 2.14^{b}	2.12 ± 1.44^{a}	2.55 ± 1.75^{a}
Rhabditis	4.72 ± 1.64^{a}	2.02 ± 1.20^{ab}	7.74 ± 2.71^{a}	0.00 ± 0.00^{b}
Teratocephalus	2.41 ± 1.69	0.41 ± 0.29	1.23 ± 0.87	3.38 ± 1.91
Wilsonema	2.23 ± 1.31	1.72 ± 0.96	0.00 ± 0.00	2.89 ± 1.53
Fungivores				
Aphelenchoides	1.59 ± 0.74	1.38 ± 1.23	0.73 ± 0.73	1.47 ± 0.97
Aphelenchus	2.74 ± 1.32	1.17 ± 0.80	3.03 ± 2.01	0.61 ± 0.53
Diptherophora	1.46 ± 1.06	0.00 ± 0.00	1.33 ± 0.72	1.62 ± 0.93
Ditylenchus	1.13 ± 0.90	0.27 ± 0.27	0.00 ± 0.00	0.00 ± 0.00
Filenchus	1.76 ± 0.68	0.00 ± 0.00	0.96 ± 0.75	1.80 ± 1.03
Oxydirus	0.00 ± 0.00	1.15 ± 0.79	0.00 ± 0.00	0.00 ± 0.00
Tylencholaimulus	4.02 ± 1.83	1.17 ± 1.00	1.64 ± 1.14	0.42 ± 0.28
Tylencholaimus	0.00 ± 0.00	1.42 ± 0.98	0.00 ± 0.00	0.00 ± 0.00
Herbivores				
Helicotylenchus	0.89 ± 0.50	0.44 ± 0.34	3.55 ± 1.54	3.67 ± 1.71
Hemicriconemoides	2.33 ± 1.21^{a}	1.48 ± 0.78^{ab}	0.00 ± 0.00^{b}	0.00 ± 0.00^{b}
Hopolaimus	0.26 ± 0.19^{ab}	1.09 ± 0.48^{a}	0.00 ± 0.00^{b}	0.00 ± 0.00^{b}
Longidorus	0.77 ± 0.52	0.00 ± 0.00	0.00 ± 0.00	0.00 ± 0.00
Mesocriconema	0.64 ± 0.37	0.00 ± 0.00	3.51 ± 1.68	4.83 ± 2.23
Paralongidorus	0.82 ± 0.37	2.17 ± 0.75	2.96 ± 1.67	0.00 ± 0.00
Pratylenchus	0.57 ± 0.31	0.00 ± 0.00	2.53 ± 1.09	2.39 ± 1.69
Psilenchus	1.33 ± 0.63^{a}	2.26 ± 0.85^{a}	0.00 ± 0.00^{b}	0.00 ± 0.00^{b}
Tylenchorhynchus	0.22 ± 0.15	2.19 ± 0.95	1.83 ± 1.39	7.90 ± 2.82
Xiphinema	0.00 ± 0.00^{a}	3.27 ± 1.35^{b}	1.95 ± 1.03^{ab}	0.00 ± 0.00^{a}

(Continued)

TABLE 2 (Continued)

Genus	Elev1 (1,000–1,400)	Elev2 (1,401–1,800)	Elev3 (1,801–2,200)	Elev4 (2,201–2,600)
Omnivores				
Crassolabium	0.89 ± 0.61	3.72 ± 1.63	0.64 ± 0.64	2.50 ± 1.31
Eudorylaimus	1.72 ± 1.21	2.16 ± 0.95	1.51 ± 0.82	0.00 ± 0.00
Mesodorylaimus	3.60 ± 1.45	0.00 ± 0.00	3.35 ± 1.87	3.71 ± 1.78
Nygolamoides	0.00 ± 0.00^{a}	0.00 ± 0.00^{a}	2.86 ± 1.58^{b}	0.00 ± 0.00^{a}
Thornenema	3.77 ± 1.37^{a}	1.46 ± 0.97^{ab}	0.50 ± 0.50^{b}	0.35 ± 0.35^{b}
Tornaria	1.19 ± 0.84	3.35 ± 1.92	0.00 ± 0.00	1.16 ± 0.63
Predators				
Clarkus	4.48 ± 1.21	1.26 ± 0.85	2.30 ± 1.21	1.29 ± 0.79
Coomansus	0.00 ± 0.00	1.17 ± 0.86	1.91 ± 1.11	1.37 ± 0.88
Discolaimoides	2.84 ± 1.16^{a}	0.71 ± 0.61^{ab}	0.37 ± 0.37^{b}	0.00 ± 0.00^{b}
Discolaimus	0.54 ± 0.54	0.00 ± 0.00	1.32 ± 0.98	0.61 ± 0.43
Iotonchus	1.59 ± 0.65^{a}	0.78 ± 0.47^{ab}	0.00 ± 0.00^{b}	0.00 ± 0.00^{b}
Labronema	0.90 ± 0.48	0.00 ± 0.00	1.53 ± 0.81	0.38 ± 0.30
Mononchus	1.83 ± 0.79	1.22 ± 0.96	2.32 ± 1.57	0.82 ± 0.50
Mylonchulus	1.68 ± 0.90^{ab}	2.42 ± 0.99^{a}	0.00 ± 0.00^{b}	0.00 ± 0.00^{b}
Prionchulus	2.21 ± 0.94	2.74 ± 1.54	2.46 ± 1.10	1.80 ± 1.13
Tripyla	1.65 ± 0.89	4.87 ± 1.85	0.00 ± 0.00	1.18 ± 0.98

The means with different small case superscript letters are significantly different by means of *post-hoc* Dunn test ($p < 0.05$). Elev, elevation.

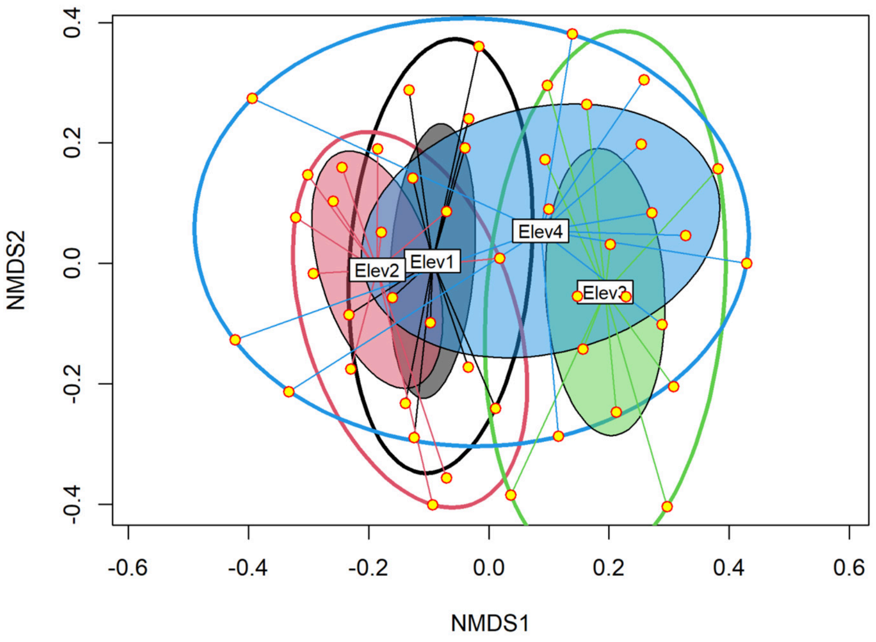

FIGURE 2
Non-metric multidimensional scaling (NMDS) plot of nematode communities based on Bray–Curtis dissimilarity metric. Each point represents the position of the nematode community in ordination space based on each individual sample. The size of each ellipse is proportional to within class dissimilarity, while as the degree of overlap between the two ellipses represents similarity in nematode composition between their respective elevational classes. Elev, Elevation; where Elev1: 1,000–1,400 m, Elev2: 1,401–1,800 m, Elev3: 1,801–2,200 m, and Elev4: 2,201–2,600 m.

temperature were significantly higher at the lower elevation class (i.e., Elev1) and lower at the highest elevation class (i.e., Elev4) (Figures 1A–C and Table 1). Contrary, the soil moisture, organic matter and texture were significantly lower at the lower elevation class (i.e., Elev1) and higher at the highest elevation class (i.e., Elev4) (Figures 1D–F and Table 1). Also, the soil pH at all the studied elevational classes was acidic in nature. Furthermore, the soil total nitrogen content was lower at the lowest elevation

TABLE 3 Pairwise nematode compositional dissimilarity between the studied elevational classes using Bray–Curtis dissimilarity metric.

Paired class	*F*-value	*P*-value
Elev1 vs. Elev2	1.72	0.031
Elev1 vs. Elev3	1.64	0.035
Elev1 vs. Elev4	2.50	0.002
Elev2 vs. Elev3	2.84	0.001
Elev2 vs. Elev4	2.77	0.001
Elev3 vs. Elev4	1.34	0.180

Elev, Elevation; where Elev1: 1,000–1,400 m, Elev2: 1,401–1,800 m, Elev3: 1,801–2,200 m and Elev4: 2,201–2,600 m.

class and higher at the third elevation class (i.e., 1,801–2,200 m) (Figure 1G and Table 1).

Soil nematode community composition along an elevation gradient

During the present study, we collected a total of 19,699 nematodes belonging to 55 genera and five trophic groups including bacterivores (21 genera), fungivores (8 genera), herbivores (10 genera), omnivores (6 genera), and predators (10 genera) (Table 2). The NMDS analysis using Bray-Curtis distance revealed that the soil nematode community composition differed considerably along the elevation gradient (Figure 2). Also, the PERMANOVA analysis showed that the nematode community composition differed significantly among the studied elevational classes both in terms of their relative abundances (Bray–Curtis: $F = 2.13$; $p < 0.001$) and number of species (Jaccard: $F = 1.68$; $p < 0.001$). Furthermore, the pairwise analysis showed a statistically significant difference in the nematode composition between all the elevation classes except between elevation 3 and elevation 4 (Table 3). Of the total 55 nematode genera identified, 14 genera differed significantly ($p < 0.05$) among the studied elevation classes (Table 2). More specifically, the nematode genera that differed significantly ($p < 0.05$) in their relative abundance among the studied elevation classes include bacterivores (*Bunonema*, *Cuticularia*, *Diploscapter*, *Protorhabditis*, *Rhabditis*), herbivores (*Hemicriconemoides*, *Hoplolaimus*, *Psilenchus*, *Xiphinema*), omnivores (*Nygolamoides*, *Thornenema*), and predators (*Discolaimoides, Iotonchus*, *Mylonchulus*) (Table 2). Moreover, 50, 44, 40, and 35 genera were reported from the first (1,000–1,400 m), second (1,401–1,800 m), third (1,801–2,200 m), and fourth (2,201–2,600 m) elevational class, respectively, (Table 2). Overall, the mean abundance of soil nematodes ranged from 203 to 886 (mean ± standard error: 410.40 ± 18.46) per 100 g of soil (Figure 3).

Trophic groups along an elevation gradient

We found statistically significant differences in the bacterivores and herbivores only among the studied elevation classes (Figure 3 and Table 4). Bacterivores were found to be the most abundant trophic group across all the studied elevational classes, whereas, fungivores were least abundant nematode group except for lowest elevation class where in herbivores was the least abundant taxonomic group (Table 4). Also, the abundances of total nematodes, bacterivores and herbivores was found to increase with increasing elevation, while as that of fungivores and predators

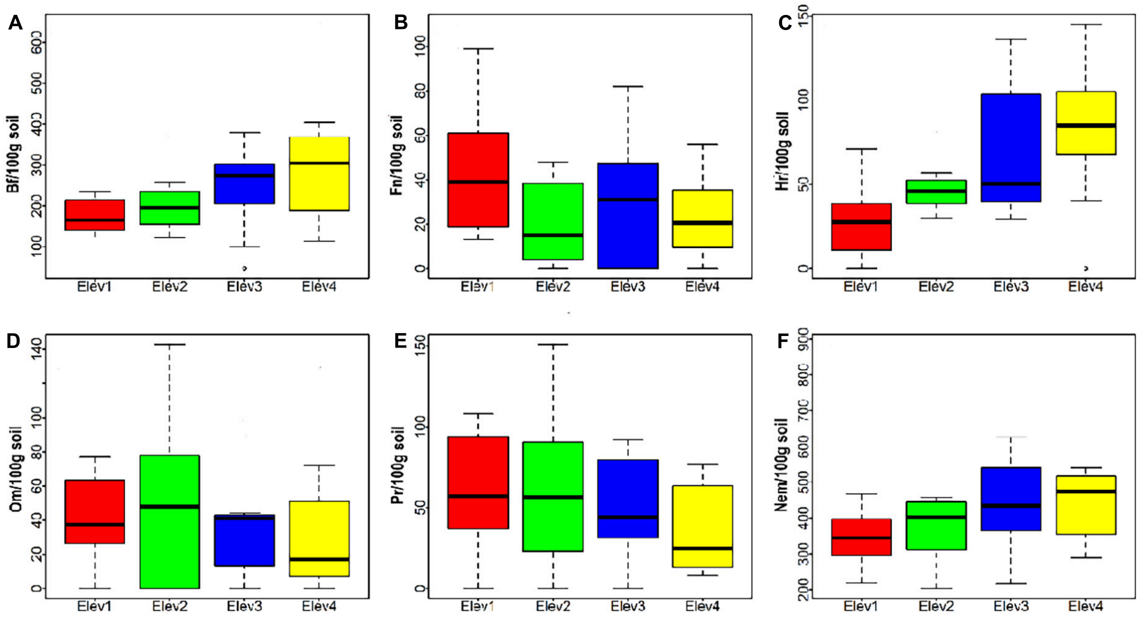

FIGURE 3
Nematode abundance of various trophic groups across studied elevational classes **(A)** Bf, bacterivores; **(B)** Fn, fungivores; **(C)** Hr, herbivores; **(D)** Om, omnivores; **(E)** Pr, predators; and **(F)** nem, total nematodes. Elev, elevation; where Elev1: 1,000–1,400 m, Elev2: 1,401–1,800 m, Elev3: 1,801–2,200 m, and Elev4: 2,201–2,600 m.

decreased with increasing elevation. However, the omnivore abundance was maximum at second elevational class (1,401–1,800 m) (Table 4).

Nematode functional, diversity and metabolic indices along an elevational gradient

Our study showed that among the nematode maturity indices, only the MI25 differed significantly across studied elevational classes, with highest value found at lowest elevation class (Elev1) and lowest value at highest elevation class (Elev4) (Table 5). Also, the other maturity indices showed decreasing effect from lowest to the highest elevational class, however, the effect was not statistically significant (Table 5). Similarly, the PPI and EI showed decreasing effect from lowest to the highest elevational class, but the effect was once again non-significant (Table 5). In contrast, the SI different significantly across the elevational classes, with highest value observed at lowest elevational class (Elev1) and lowest at highest elevational class (Elev4) (Table 5). Likewise, the CI exhibited significant differences across the elevational classes, with highest value observed at highest elevational class (Elev4) (Table 5). Furthermore, the Shannon Weiner (H'), Pielou's evenness (J'), and generic indices showed statistically significant difference among the elevational classes, with Shannon Weiner (H'), and Pielou's evenness (J') indices showing a decrease with increasing elevation (Table 5).

In addition, the soil nematode faunal profile using enrichment and structural indices (EI-SI) for all the studied elevational classes falls mainly under the quadrant B (indicating maturing, N-enriched, low C:, bacterial dominated and regulated system) except for some of the points from elevational classes third and four (Elev3 and Elev4) that fall under the quadrant C (indicating matured, fertile, moderate C: N, bacterial/fungal dominated and suppressive system) (Figure 4). Our study also showed that among the various nematode composite structure and trophic metabolic footprints, only the composite, enrichment and bacterivore footprints differed significantly among the elevational classes, with all of them showing higher values at third elevation (Elev3) (Table 5), while as the remaining footprints varied non-significantly among elevational classes (Table 5).

Relationship between soil nematode communities and physicochemical properties along an elevational gradient

The multiple correlation revealed that the soil properties and nematode communities were related to each other to a greater extent (Figure 5). More specifically, total nematode and bacterivore abundances showed a significant positive correlation with soil moisture, organic matter and texture and a significant negative correlation with soil electrical conductivity, pH and temperature (Figure 5). Similarly, herbivore abundance was significantly positively correlated with soil moisture, organic matter, total nitrogen and texture, but significantly negatively correlated with soil electrical conductivity, pH and temperature (Figure 5). In contrast, the fungivore, omnivore and predator abundances did not show statistically significant correlation with any of the soil variable (Figure 5). Moreover, the total nematode, bacterivore and herbivore abundances were significantly positively related with each other (Figure 5).

The principal component analysis (PCA) explained 19.5% of the total variation in the data, with first component (Dim1) accounting for 13.6% and the second component (Dim2) explaining 5.9% of this variation (Figure 6). Once again, the PCA showed that the majority of genera belonging to bacterivores and herbivores were positively related with soil moisture, organic matter, total nitrogen and texture (i.e., most of the genera from bacterivores and herbivores are widely distributed across those sites having higher content soil moisture, organic matter and total nitrogen and richer soil texture), but showed negative relation with soil electrical conductivity, pH and temperature (Figure 6). In contrast, the genera from other trophic groups were distributed uniformly throughout regardless of the position of soil variables (Figure 6).

Discussion

In the mountainous ecosystems, elevation gradients along which environmental variables change considerably within shortest distances, remain one of the mainstays for contemporary research in the field of ecology and evolution, and thus play a key role in understanding the large-scale patterns in biodiversity, global change and conservation (Wei et al., 2019; Afzal et al., 2021).

The present study showed that both the soil nematode diversity and generic richness decreased significantly among the elevational classes with increasing elevation. Our result is in line with the findings of several published studies conducted in the forest ecosystems both in the Himalaya (Afzal et al., 2021) and elsewhere (Yeates, 2007; Liu et al., 2019; Yu et al., 2021; Zhang et al., 2021). This pattern of soil nematode richness and diversity can be attributed to a number of reasons: (1) the occurrence of adverse climatic conditions at the higher elevations in the region alter abiotic and biotic factors, which ultimately result in decreasing nematode diversity and richness at higher elevations (Afzal et al., 2021; Kashyap et al., 2022). (2) In our study region, the temperature remains below optimum during the winter months. The availability of lower temperatures at higher elevations decreases the soil microbial activity and associated decomposition process, leading to lower nutrient levels and negatively affecting soil nematode diversity and richness (Margesin et al., 2016; Albright et al., 2020; Afzal et al., 2021). (3) The mean annual precipitation also plays a key role in affecting the diversity and richness patterns of soil nematodes by changing the above ground vegetation composition and below ground microbial activities and soil nutrients (Bai et al., 2008; Kardol et al., 2011). Also, the higher amount of precipitation at higher elevation greatly reduces the diversity of soil nematodes by causing oxygen deprivation due to reduced oxygen levels (Afzal et al., 2021; Yu et al., 2021) and (4) The higher diversity and generic richness at lower elevations in the forest ecosystems as evidenced in our study can also be due to the more resilient, balanced and sustainable ecosystem occuring at lower elevations (Yeates, 2007; Kashyap et al., 2022).

TABLE 4 Nematode abundance of various trophic groups across the studied elevation classes (mean ± standard error).

Trophic group	Elev1 (1,000–1,400)	Elev2 (1,401–1,800)	Elev3 (1,801–2,200)	Elev4 (2,201–2,600)
Bacterivores	171.67 ± 11.40^{a}	205.75 ± 19.33^{ab}	250.25 ± 28.97^{b}	294.42 ± 41.94^{b}
Fungivores	44.33 ± 8.19	30.08 ± 10.93	28.50 ± 8.38	23.25 ± 4.87
Herbivores	27.75 ± 5.96^{a}	46.83 ± 3.92^{ab}	71.25 ± 11.38^{bc}	84.58 ± 11.54^{c}
Omnivores	39.33 ± 7.32	47.17 ± 13.80	37.67 ± 9.11	32.92 ± 11.05
Predators	61.58 ± 9.47	58.25 ± 13.00	50.58 ± 8.55	35.42 ± 7.49
Total nematodes	344.67 ± 20.56	388.08 ± 35.66	438.25 ± 35.95	470.58 ± 44.73

The means with different small case superscript letters are significantly different by means of *post-hoc* Dunn test ($p < 0.05$). Elev, elevation.

TABLE 5 Soil nematode functional diversity and metabolic indices across the studied elevation classes (mean ± standard error).

Index	Elev1	Elev2	Elev3	Elev4
MI	2.57 ± 0.08	2.43 ± 0.17	2.34 ± 0.10	2.42 ± 0.12
ΣMI	2.64 ± 0.08	2.60 ± 0.14	2.55 ± 0.10	2.52 ± 0.10
MI25	3.09 ± 0.11^{a}	2.94 ± 0.12^{ab}	3.04 ± 0.09^{a}	2.69 ± 0.08^{b}
PPI	3.39 ± 0.22	3.60 ± 0.25	3.55 ± 0.24	3.00 ± 0.00
EI	73.92 ± 3.87	70.84 ± 5.58	77.57 ± 3.47	44.90 ± 9.66
SI	80.59 ± 4.10^{a}	73.39 ± 7.23^{ab}	80 12 ± 2.49^{ab}	67.21 ± 4.09^{b}
CI	7.31 ± 1.60^{a}	2.98 ± 1.36^{b}	5.18 ± 3.28^{b}	38.37 ± 14.75^{a}
H’	2.54 ± 0.06^{a}	2.42 ± 0.07^{a}	2.15 ± 0.07^{b}	1.99 ± 0.06^{b}
J’	0.94 ± 0.01^{a}	0.94 ± 0.01^{a}	0.97 ± 0.00^{b}	0.92 ± 0.01^{c}
Generic richness	15.00 ± 0.83^{a}	13.58 ± 0.94^{a}	9.50 ± 0.67^{b}	8.92 ± 0.62^{b}
Composite footprint	52.20 ± 4.42^{a}	50.56 ± 3.22^{a}	68.76 ± 9.40^{a}	29.53 ± 2.63^{b}
Enrichment footprint	18.44 ± 3.79^{ab}	11.69 ± 3.33^{a}	30.66 ± 7.17^{b}	3.87 ± 1.12^{c}
Structure footprint	23.53 ± 2.56	22.66 ± 3.88	19.73 ± 2.29	14.40 ± 1.69
Herbivore footprint	5.57 ± 1.43	11.48 ± 2.49	12.94 ± 5.35	2.83 ± 0.52
Fungivore footprint	2.61 ± 0.58	1.03 ± 0.29	1.68 ± 0.57	0.99 ± 0.40
Bacterivore footprint	22.77 ± 3.44^{ab}	16.74 ± 2.87^{a}	36.13 ± 7.01^{b}	14.05 ± 1.66^{a}
Predator footprint	14.05 ± 1.77	16.24 ± 3.87	12.09 ± 2.77	7.82 ± 2.20
Omnivore footprint	7.25 ± 1.24	5.08 ± 1.20	5.93 ± 1.53	3.84 ± 1.11

The means with different small case superscript letters are significantly different by means of *post-hoc* Dunn test ($p < 0.05$). Elev, elevation, where Elev1: 1,000–1,400 m, Elev2: 1,401–1,800 m, Elev3: 1,801–2,200 m and Elev4: 2,201–2,600 m.

The present study revealed that the soil nematode composition differed significantly among studied elevation classes along the elevation gradient. This result is in agreement with the findings of several other published studies especially from the mountainous ecosystems (Kergunteuil et al., 2016; Dong et al., 2017; Liu et al., 2019; Afzal et al., 2021; Yu et al., 2021). The plausible explanation for this can be that the vegetation composition, soil nutrients and bioclimatic variables vary considerably with elevation (Liu et al., 2019; Yu et al., 2021; Kashyap et al., 2022). All these abiotic and biotic factors shape soil nematode communities possibly due to net environmental filtering, varying environmental conditions and resource heterogeneity (Dong et al., 2017; Afzal et al., 2021). Another possible reason can be that the variation in the local floristic composition might cause changing nematode community structure along elevation gradients (Kergunteuil et al., 2016). For example, among the total nematode taxa characterizing the lowland communities, *Tripyla*is mainly found associated with the tree species, while as *Cervidellus*is generally found to occur with the sub alpine cushions like *Juniperus* (Kergunteuil et al., 2016). More interestingly, our study showed one exception that soil nematode composition of the two highest elevation classes (Elev3 and Elev4) was comparatively similar. The result in in accordance with the study conducted by Kashyap et al. (2022) which reported similar nematode composition between the two higher elevation classes in Gangotri National Park. The possible reason for this effect can be that the micro-environmental condition between these two elevation classes may not vary to the extent that causes differences in the nematode composition.

Our study found that the response of nematode abundance to increasing elevation varied with trophic groups, with total nematode, bacterivore and herbivore abundances showing increasing effect with increasing elevation, while as fungivore and predator abundances exhibiting the opposite trend. The increasing effect of elevation on total nematode, bacterivore and herbivore abundances is contradictory with the studies from Afzal et al. (2021). However, our results are in agreement with several

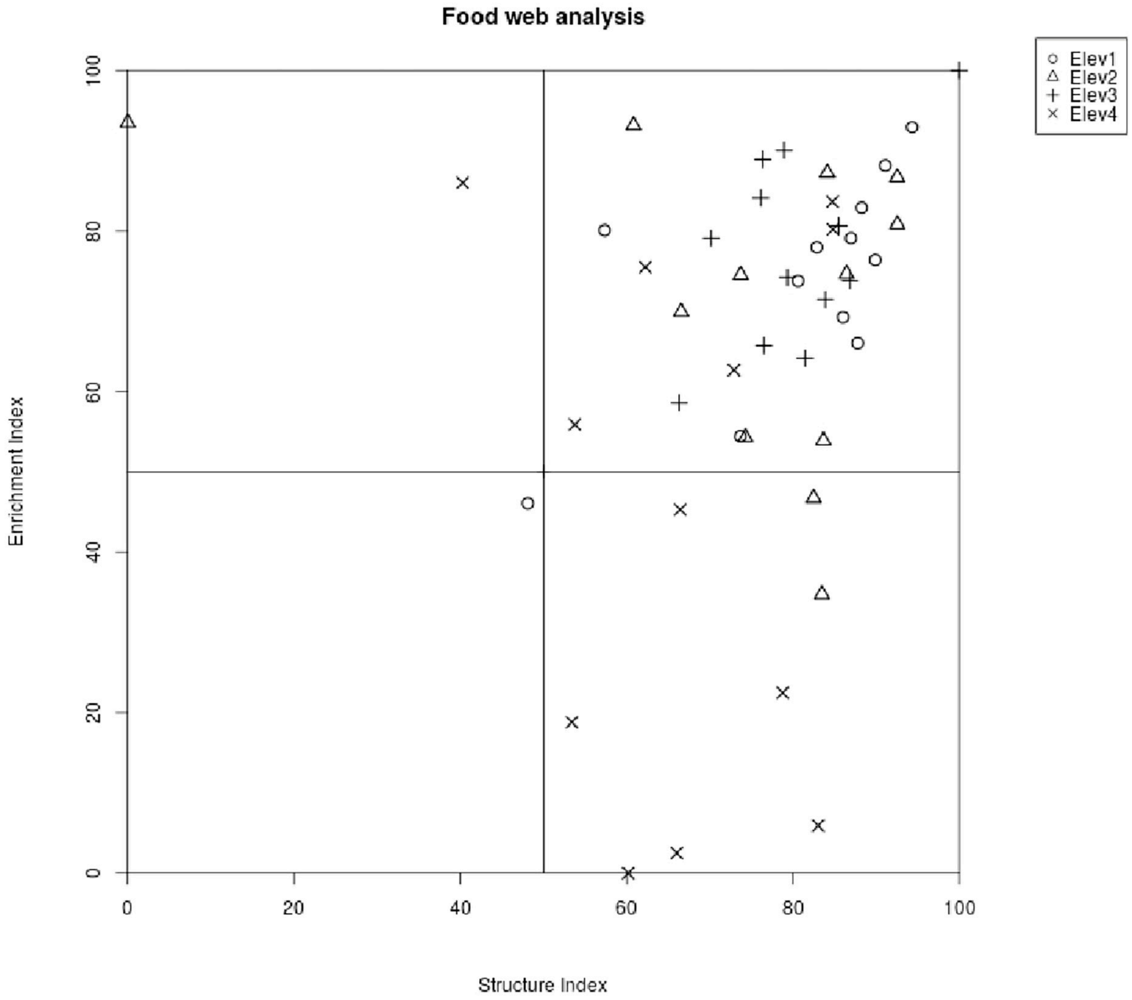

FIGURE 4
Food web diagnostic profile across the studied elevational classes. Elev, elevation; where Elev1: 1,000–1,400 m, Elev2: 1,401–1,800 m, Elev3: 1,801–2,200 m, and Elev4: 2,201–2,600 m.

other studies that reported increasing bacterivore (Kergunteuil et al., 2016; Veen et al., 2017) and herbivore (Kouser et al., 2021) abundances and decreasing fungivore (Veen et al., 2017; Afzal et al., 2021) and predator (Afzal et al., 2021; Kashyap et al., 2022) abundances with elevation. Our findings are also in line with the study carried out by Veen et al. (2017) which reported that the soil nematode trophic groups can exhibit differential response to elevation under different vegetation types. Generally, the declining effect of elevation on nematode abundance is based on the notion that climate becomes adverse and harsher at high elevations (Afzal et al., 2021; Kashyap et al., 2022). In contrast, nematodes have been reported to withstand harshest environments in case of extreme polar regions (Yeates, 2010), thereby indicating that nematodes can survive more at higher elevations (Kouser et al., 2021). Therefore, the elevational patterns exhibited by different nematode trophic groups in different environmental settings is still debated and a matter of further investigation. One plausible explanation for the increasing herbivore nematode abundance with elevation can be the presence of well-developed dense root systems which provide shelter from various types of abiotic and biotic stress (Kergunteuil et al., 2016). Similarly, the declining effect of predatory nematode abundance with elevation can be possibly due to their key role in the soil food web, wherein they can flexibly switch on to a different prey species depending on the host availability (Afzal et al., 2021). Likewise, the declining effect fungivore nematode abundance with elevation can be possibly due to increasing pH along elevational gradient. Since it has been reported that fungi prefer acidic soils to develop mycelia, therefore the abundance of fungivore nematodes can decrease with increasing soil pH (Frostegård and Bååth, 1996; Kitagami et al., 2017). Our study also showed that among all trophic groups, bacterivores were the most abundant across the studied elevational classes, whereas fungivores were least abundant group. This result is in agreement with the finding of other studies (Dong et al., 2017; Kashyap et al., 2022). This in turn indicates that a relatively faster bacterial energy channel-based decomposition model predominates in the study region.

Consistent with several previous studies (Zhao et al., 2015; Song et al., 2016; Dong et al., 2017), we found that the soil physico-chemical properties were key environmental variables influencing nematode community structure. More specifically, our study showed that total nematode, bacterivore and herbivore abundances

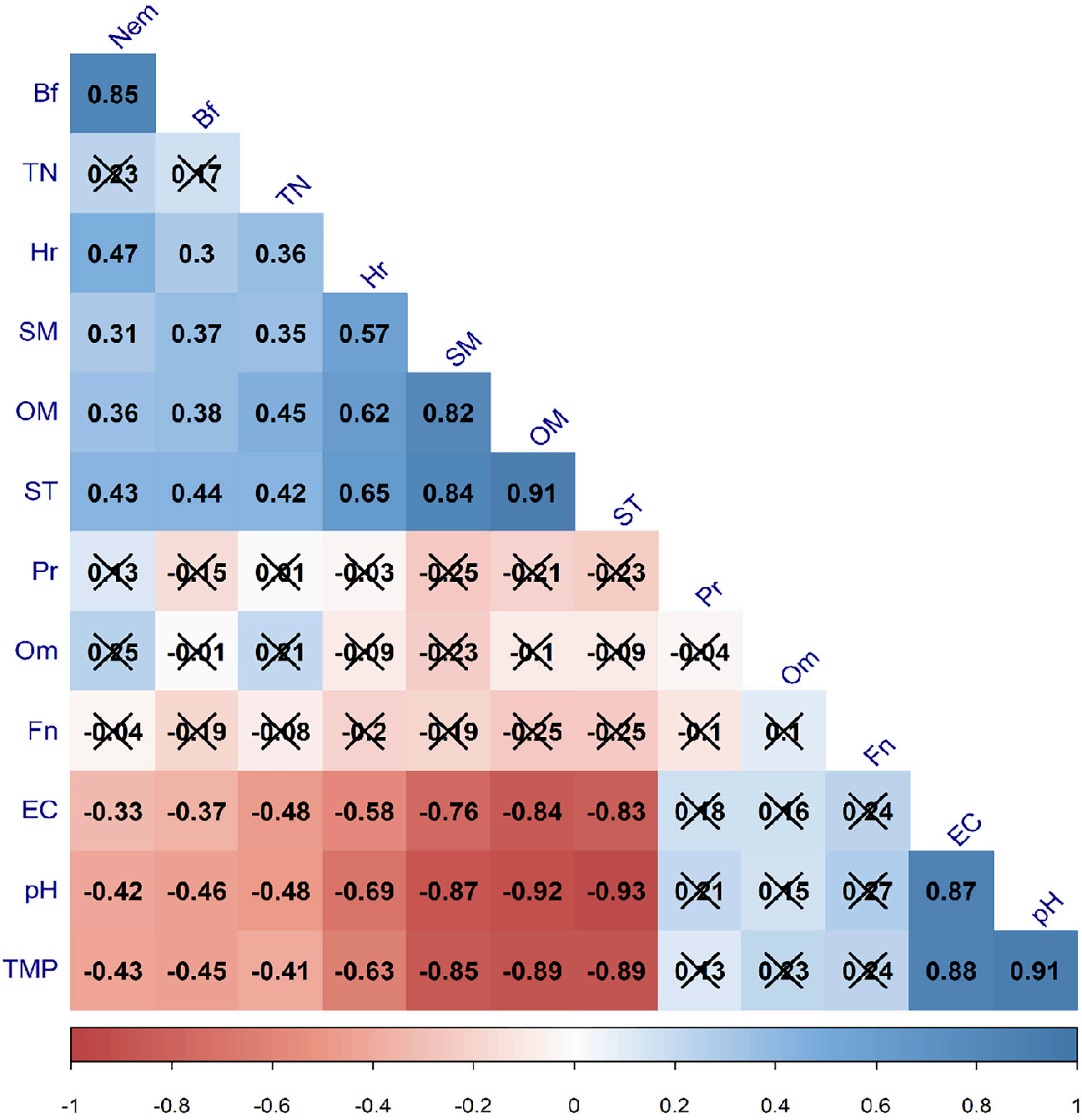

FIGURE 5
Correlation between soil nematode trophic groups and soil physico-chemical properties. The cross marked correlation coefficients denote non-significance at $p = 0.05$. BF, bacterivores; Fn, fungivores; Hr, herbivores; Om, omnivores; Pr, predators; nem, total nematode abundance; EC, electrical conductivity; OM, organic matter; SM, soil moisture; ST, soil texture; TMP, temperature; TN, total nitrogen.

were associated with higher pH, soil organic matter, soil moisture and total nitrogen levels, which agrees with the findings of other studies as well (Savin et al., 2001; Postma-Blaauw et al., 2005; Wall et al., 2010; Song et al., 2016; Liu et al., 2019). As evidenced in the present study, the key role of soil pH in governing nematode community composition especially that of bacterivores can be best explained by the direct feeding relationships between bacterivore nematodes and bacteria, whose abundance are greatly influenced by soil pH (Shen et al., 2015, 2020; Wang et al., 2015; Nottingham et al., 2018). The possible explanation for significant influence of soil moisture on certain trophic groups as evidenced from our study can be due to its enhanced effects on decomposition rates (Dong et al., 2017). Similarly, the positive effect of total nitrogen on certain nematode group can be due to its key role in regulating the content of soluble nutrients in an ecosystem (Liang et al., 2007).

In recent times, a number of studies have advocated the usage of functional and metabolic indices, along with taxonomic indices for understanding the mechanisms of ecosystem functioning (Montoya et al., 2015; Kergunteuil et al., 2016; Kouser et al., 2021). The present study evaluated several key functional and community indices to better understand both the relative contribution of nematode trophic groups to soil food web structure and changes in soil ecosystem functioning along elevation gradients. Our study showed that the maturity indices decreased with elevation, however, the effect was significant for MI25 index only. This decrease in the maturity indices with elevation is in line with

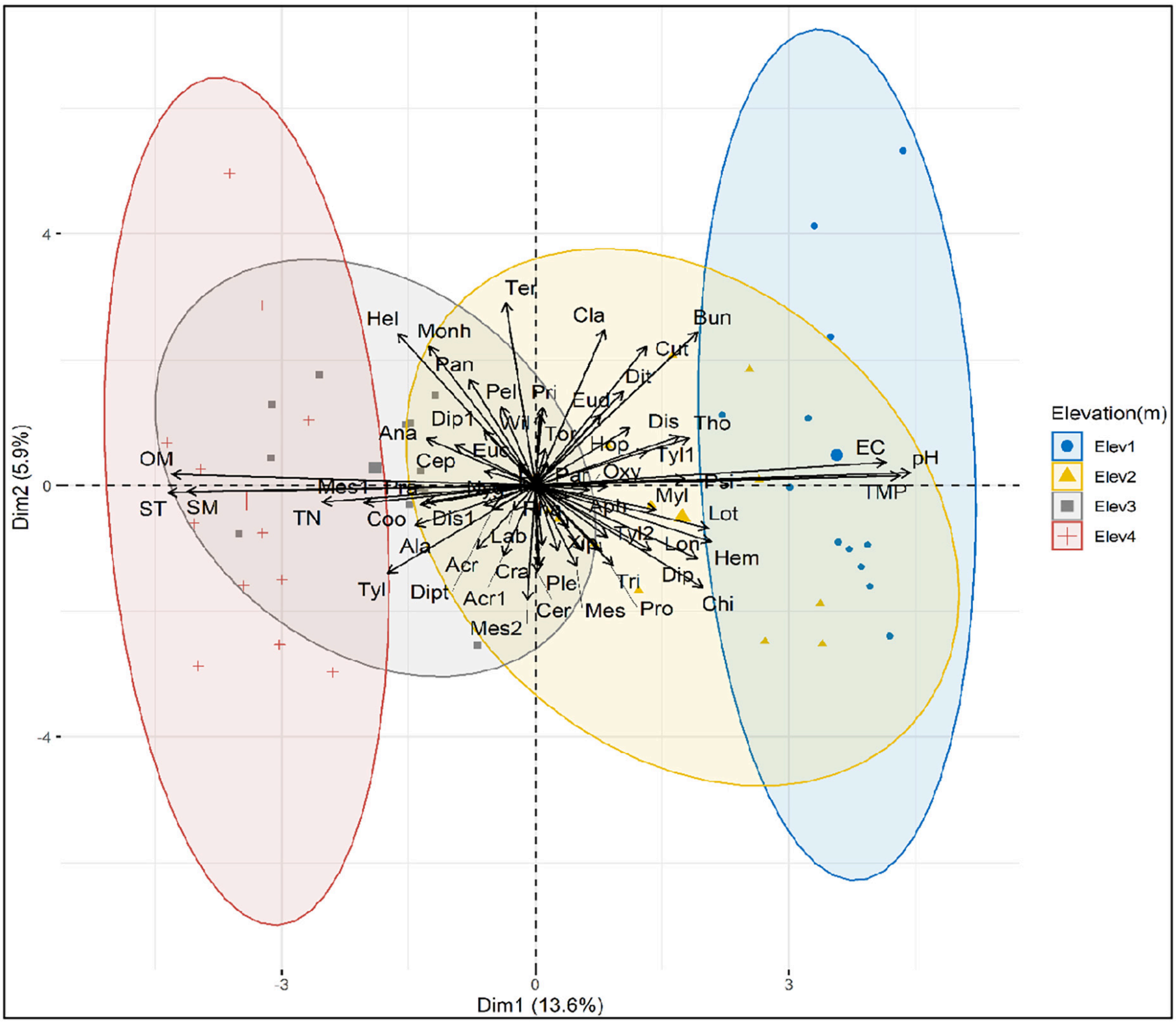

FIGURE 6
Principal component analysis (PCA) showing the relationship between soil nematode genera and soil properties across elevation classes.

the findings of several the studies (Afzal et al., 2021; Kashyap et al., 2022). Since the maturity indices are indicative of degree of disturbance associated with the soil ecosystem with lower values representing more disturbances (Bongers and Ferris, 1999; Afzal et al., 2021), this in turn reflect a comparatively higher degree of disturbance among the highest elevation classes as compared to lowest elevation classes in our study region. Also, the evidence of decreasing maturity indices with elevation in our study suggests lesser tolerance of K-selected free living and plant parasitic nematodes toward stressful conditions typically encountered at higher elevations (Afzal et al., 2021). Our study also found a decrease in structure index (SI) and plant parasitic index (PPI) with elevation, although the effect was significant for SI only. These results of elevation wise decrease in SI and PPI are in accordance with the finding of Afzal et al. (2021) and highlight the existence of relatively simpler, loosely structured soil food webs having fewer connections at higher elevation classes as compared to those found in lower elevations. Moreover, our study also showed significant difference in the channel index (CI), among the elevation classes, with highest CI value found at the top elevation class (Elev4). As the CI index is simply the ratio of fungivore to bacterivore nematodes, our results indicate that in the study region the fungal decomposition pathways support greater nematode biomass than bacterial decomposition at higher elevation classes (Afzal et al., 2021). The possible reason for this effect can be that at higher elevations some of the plant traits including slow growing and longer leaf life span cause slow mineralization rates, and lesser fertile soils which generally enhance the fungal-based energy flows within ecosystems as compared to lowlands with more bacterial-dominated pathways (Zhao and Neher, 2014; Kergunteuil et al., 2016). Our study also revealed a significant difference both in the composite and enrichment footprints among the elevation classes, with lowest values observed at the highest elevation class (Elev4). Since, these metabolic footprints are indicators of the magnitude of carbon and energy flow in soil food webs (Ferris, 2010; Afzal et al., 2021), our results indicate that the degree of carbon and other resource assimilation in soil food web from autotrophic organisms is relatively lower at highest elevation class than the lower elevation classes in the study region, owing to slower decomposition rates in the former as compared to latter ones.

Our study also showed that soil physico-chemical parameters varied significantly between the elevation classes, with soil pH, electrical conductivity and temperature showing a decrease with elevation, the soil moisture, organic matter and texture showing an increase with elevation, while as the total nitrogen content showing maximum at middle elevation class (Elev3). Our finding of decreasing soil pH along elevation gradients is in line with other studies (Afzal et al., 2021; Kouser et al., 2021; Zhang et al., 2021). The possible explanation for this effect could be the accumulation of litter at higher altitudes due to slow rates of decomposition that negatively effects the soil biota (Kappes et al., 2007). Similarly, our result of decreasing soil EC along elevation gradient is in line with other studies conducted by Kouser et al. (2021) and Kashyap et al. (2022), and can possibly be a result of reduced mobility of ions due to leaching and washing out of the solutes at higher elevations. Likewise, our finding of increasing soil moisture with elevation is in accordance with several other studies (Kouser et al., 2021; Zhang et al., 2021), and can be attributed to an elevation wise increase in mean annual precipitation and a decrease in precipitation seasonality (Kouser et al., 2021). Lastly, our finding of mid elevational peak in total nitrogen content is in line with the study conducted by Dong et al. (2017) in Norikura mountains, and can be explained be the relatively slower decay of plant products at moderately cool temperatures of the middle elevations, thereby resulting in the accumulation of nitrogen in the upper layer of soil (Sarathchandra et al., 2001; Dong et al., 2017).

Conclusion and future directions

The present study provides a novel understanding of the diversity and compositional patterns of soil nematodes in the mountainous ecosystems of Pir-Panjal Himalaya. Overall, our study showed that soil nematodes exhibit distinct elevational patterns, which are consistent with the trends observed for other groups of organisms, thereby indicating how evident these patterns exit in nature. Taken together, we conclude that the variation in soil nematode diversity and community composition along the elevation gradient could be due to the shared effects of soil and climatic factors, thus highlighting the crucial role of interaction among multiple environmental factors in shaping soil biodiversity. Looking ahead, a better understating of relative importance of various ecological correlates in governing nematode diversity and distributional patterns can provide vital information on the response of soil nematode communities to climate and land-use change in the current era of anthropogenic global environmental change.

Data availability statement

The original contributions presented in this study are included in the article/supplementary material, further inquiries can be directed to the corresponding author.

Author contributions

FC: conceptualization, methodology, data collection, curation and analysis, investigation, and writing—original draft. AB, IS, and SR: writing—review. MK: supervision and writing—review. AS: conceptualization, supervision, validation, and writing—review. All authors contributed to the article and approved the submitted version.

Conflict of interest

The authors declare that the research was conducted in the absence of any commercial or financial relationships that could be construed as a potential conflict of interest.

Publisher's note

References

Afzal, S., Nesar, H., Imran, Z., and Ahmad, W. (2021). Altitudinal gradient affect abundance, diversity and metabolic footprint of soil nematodes in Banihal-Pass of Pir-Panjal mountain range. *Sci. Rep.* 11:16214. doi: 10.1038/s41598-021-95651-x

Albright, M. B., Johansen, R., Thompson, J., Lopez, D., Gallegos-Graves, L. V., Kroeger, M. E., et al. (2020). Soil bacterial and fungal richness forecast patterns of early pine litter decomposition. *Front. Microbiol.* 11:542220. doi: 10.3389/fmicb.2020.542220

Andrássy, I. (2005). "Free-living nematodes of Hungary (*Nematoda errantia*), I," in *Pedozoologica hungarica No. 3*, eds C. Csuzdi and S. Mahunka (Budapest: Hungarian Natural History Museum).

Andrassy, I. T. (1956). Determination of volume and weight of nematodes. *Acta Zool. Acad. Sci. Hungaricae* 2, 1–15.

Bai, Y., Wu, J., Xing, Q., Pan, Q., Huang, J., Yang, D., et al. (2008). Primary production and rain use efficiency across a precipitation gradient on the Mongolia plateau. *Ecology* 89, 2140–2153. doi: 10.1890/07-0992.1

Bakonyi, G., Nagy, P., Kovacs-Lang, E., Kovacs, E., Barabás, S., Répási, V., et al. (2007). Soil Nematode community structure as affected by temperature and moisture in a temperate semiarid shrubland. *Appl. Soil Ecol.* 37, 31–40. doi: 10.1016/j.apsoil.2007.03.008

Barker, K. R. (1985). "Nematode extraction and bioassays," in *An advanced treatise on meloidogyne, methodology*, Vol. 2, eds K. R. Barker, C. C. Carter, and J. N. Sasser (Raleigh, NC: North Carolina State University Graphics), 19–35.

Bongers, T. (1990). The maturity index as an ecological measure of environmental disturbance based on nematode species composition. *Oecologia* 83, 14–19. doi: 10.1007/BF00324627

Bongers, T., and Bongers, M. (1998). Functional diversity of nematodes. *Appl. Soil Ecol.* 10, 239–251. doi: 10.1016/S0929-1393(98)00123-1

Bongers, T., and Ferris, H. (1999). Nematode community structure as a bioindicator in environmental monitoring. *Trends Ecol. Evol.* 14, 224–228. doi: 10.1016/S0169-5347(98)01583-3 da Silva, J. V. C. D. L., Hirschfeld, M. N. C., Cares, J. E., and Esteves, A. M. (2020). Land use, soil properties and climate variables influence the nematode communities in the Caatinga dry forest. *Appl. Soil Ecol.* 150:103474. doi: 10.1016/j.apsoil.2019.103474

Dar, T. A., Uddin, M., Khan, M. M. A., Hakeem, K. R., and Jaleel, H. (2015). Jasmonates counter plant stress: A review. *Environ. Exp. Bot.* 115, 49–57. doi: 10.1016/j.envexpbot.2015.02.010

Devetter, M., Hanel, L., Rehakova, K., and Anddolezal, J. (2017). Diversity and feeding strategies of soil microfauna along elevation gradients in Himalayan cold deserts. *PLoS One* 12:e0187646. doi: 10.1371/journal.pone.0187646

Dong, K., Moroenyane, I., Tripathi, B., Kerfahi, D., Takahashi, K., Yamamoto, N., et al. (2017). Soil nematodes show a mid-elevation diversity maximum and elevational zonation on Mt. Norikura, Japan. *Sci. Rep.* 7, 1–11. doi: 10.1038/s41598-017-03655-3

Ferris, H. (2010). Form and function: Metabolic footprints of nematodes in the soil food web. *Eur. J. Soil Biol.* 46, 97–104. doi: 10.1016/j.ejsobi.2010.01.003

Ferris, H., Bongers, T., and De Goede, R. G. M. A. (2001). Framework for soil food web diagnostics extension of the nematode faunal analysis concept. *Appl. Soil Ecol.* 18, 13–29. doi: 10.1016/S0929-1393(01)00152-4

Frostegård, Å, and Bååth, E. (1996). The use of phospholipid fatty acid analysis to estimate bacterial and fungal biomass in soil. *Biol. Fertility Soils* 22, 59–65. doi: 10.1007/BF00384433

Goodey, T. (1963). *Soil and freshwater nematodes*. Methuen, MA: Methuen and Cooperation Limited. doi: 10.1097/00010694-196404000-00018

Hodda, M. (2011). "Phylum Nematoda Cobb 1932," in *Animal biodiversity: An outline of higher-level classification and survey of taxonomic richness*, Vol. 3148, ed. Z.-Q. Zhang (Zootaxa), 63–95. doi: 10.11646/zootaxa.3148.1.11

Hodda, M. E., Peters, L., and Traunspurger, W. (2009). "Nematode diversity in terrestrial, freshwater aquatic and marine systems," in *Nematodes as environmental indicators*, 1st Edn, eds M. Wilson and T. Kakouli-Duarte (Oxfordshire: CABI Publishing), 45–93. doi: 10.1079/9781845933852.0045

Jairajpuri, M. S., and Ahmad, W. (1992). *Dorylaimida: Free-living, predaceous and plant-parasitic nematodes*. Leiden: Brill.

Kappes, H., Lay, R., and Topp, W. (2007). Changes in different trophic levels of litter-dwelling macrofauna associated with giant knotweed invasion. *Ecosystems* 10, 734–744. doi: 10.1007/s10021-007-9052-9

Kardol, P., Reynolds, W. N., Norby, R. J., and Classen, A. T. (2011). Climate change effects on soil microarthropod abundance and community structure. *Appl. Soil Ecol.* 47, 37–44. doi: 10.1016/j.apsoil.2010.11.001

Kashyap, P., Afzal, S., Rizvi, A. N., Ahmad, W., Uniyal, V. P., and Banerjee, D. (2022). Nematode community structure along elevation gradient in high altitude vegetation cover of Gangotri National Park (Uttarakhand), India. *Sci. Rep.* 12, 1–13. doi: 10.1038/s41598-022-05472-9

Kassambara, A., and Mundt, F. (2020). *Factoextra: Extract and visualize the results of multivariate data analyses.* R package version 1.0.7. Available online at: https://CRAN.R-project.org/package=factoextra (accessed November 5, 2022).

Kergunteuil, A., Campos-Herrera, R., Sánchez-Moreno, S., Vittoz, P., and Rasmann, S. (2016). The abundance, diversity, and metabolic footprint of soil nematodes is highest in high elevation alpine grasslands. *Front. Ecol. Evol.* 4:84. doi: 10.3389/fevo.2016.00084

Kitagami, Y., Kanzaki, N., and Matsuda, Y. (2017). Distribution and community structure of soil nematodes in coastal Japanese pine forests were shaped by harsh environmental conditions. *Appl. Soil Ecol.* 119, 91–98. doi: 10.1016/j.apsoil.2017.05.030

Kjeldahl, J. (1883). New method for the determination of nitrogen. *Chem. News* 48, 101–102. doi: 10.1038/scientificamerican10061883-6470bsupp

Körner, C. (2007). The use of 'altitude' in ecological research. *Trends Ecol. Evol.* 22, 569–574. doi: 10.1016/j.tree.2007.09.006

Kouser, Y., Shah, A. A., and Rasmann, S. (2021). The functional role and diversity of soil nematodes are stronger at high elevation in the lesser Himalayan Mountain ranges. *Ecol. Evol.* 11, 13793–13804. doi: 10.1002/ece3.8061

Liang, W. J., Zhong, S., Hua, J. F., Cao, C. Y., and Jiang, Y. (2007). Nematode faunal response to grassland degradation in horqin sandy land. *Pedosphere* 17, 611–618. doi: 10.1016/S1002-0160(07)60072-1

Liu, J., Yang, Q., Siemann, E., Huang, W., and Ding, J. (2019). Latitudinal and altitudinal patterns of soil nematode communities under tallow tree (Triadicasebifera) in China. *Plant Ecol.* 220, 965–976. doi: 10.1007/s11258-019-00966-5

Maina, S., Karuri, H., and Mugweru, J. (2022). Nematode diversity and its association with soil properties in monocrop pigeon pea. *J. Agric. Food Res.* 9:100336. doi: 10.1016/j.jafr.2022.100336

Margesin, R., Minerbi, S., and Schinner, F. (2016). Litter decomposition at two forest sites in the Italian Alps: A field study. *Arctic Antarctic Alpine Res.* 48, 127–138. doi: 10.1657/AAAR0015-012

Montoya, D., Yallop, M., and Memmott, J. (2015). Functional group diversity increases with modularity in complex food webs. *Nat. Commun.* 6:7379. doi: 10.1038/ncomms8379

Nielsen, U. N., Ayres, E., Wall, D. H., Li, G., Bardgett, R. D., Wu, T., et al. (2014). Global-scale patterns of assemblage structure of soil nematodes in relation to climate and ecosystem properties. *Glob. Ecol. Biogeogr.* 23, 968–978. doi: 10.1111/geb.12177

Nottingham, A. T., Fierer, N., Turner, B. L., Whitaker, J., Ostle, N. J., McNamara, N. P., et al. (2018). Microbes follow Humboldt: Temperature drives plant and soil microbial diversity patterns from the Amazon to the Andes. *Ecology* 99, 2455–2466. doi: 10.1002/ecy.2482

Oksanen, J., Blanchet, F. G., Friendly, M., Kindt, R., Legendre, P., McGlinn, D., et al. (2020). *vegan: Community Ecology Package.* R package version 2.5-7. Available online at: https://CRAN.R-project.org/package=vegan (accessed November 5, 2022).

Postma-Blaauw, M. B., de Vries, F. T., De Goede, R. G. M., Bloem, J., Faber, J. H., and Brussaard, L. (2005). Within-trophic group interactions of bacterivorous nematode species and their effects on the bacterial community and nitrogen mineralization. *Oecologia* 142, 428–439. doi: 10.1007/s00442-004-1741-x

Powers, L. E., Ho, M. C., Freckman, D. W., and Virginia, R. A. (1998). Distribution, community structure and microhabitats of soil invertebrates along an elevational gradient in Taylor Valley Antarctica. *Arct. Alp. Res.* 30, 133–141. doi: 10.2307/1552128

Qing, X., Bert, W., Steel, H., Quisado, J., and de Ley, I. T. (2015). Soil and litter nematode diversity of Mount Hamiguitan, the Philippines, with description of *Bicirronemahamiguitanense* n. sp (Rhabditida: Bicirronematidae). *Nematology* 17, 325–344. doi: 10.1163/15685411-00002870

Quist, C. W., Gort, G., Mooijman, P., Brus, D. J., van den Elsen, S., Kostenko, O., et al. (2019). Spatial distribution of soil nematodes relates to soil organic matter and life strategy. *Soil Biol. Biochem.* 136:107542. doi: 10.1016/j.soilbio.2019.107542

R Core Team (2020). *R: A language and environment for statistical computing.* Vienna, Austria: R Foundation for Statistical Computing.

Reid, M. L., Howes, A. S., and Emery, S. M. (2019). Dune soil communities primarily associated with climate factors, not exotic plant presence. *Plant Soil* 436, 503–515. doi: 10.1007/s11104-019-03944-y

Salamun, P., Hanzelová, V., Miklisová, D., Šestinová, O., Findoráková, L., and Kováčik, P. (2017). The effects of vegetation cover on soil Nematode communities in various biotopes disturbed by industrial emissions. *Sci. Total Environ.* 592, 106–114. doi: 10.1016/j.scitotenv.2017.02.238

Šalamún, P., Kucanová, E., Brázová, T., Miklisová, D., Renčo, M., and Hanzelová, V. (2014). Diversity and food web structure of nematode communities under high soil salinity and alkaline pH. *Ecotoxicology* 23, 1367–1376. doi: 10.1007/s10646-014-1278-7

Sarathchandra, S. U., Ghani, A., Yeates, G. W., Burch, G., and Cox, N. R. (2001). Effect of nitrogen and phosphate fertilisers on microbial and nematode diversity in pasture soils. *Soil Biol. Biochem.* 33, 953–964. doi: 10.1016/S0038-0717(00)00245-5

Savin, M. C., Gorres, J. H., Neher, D. A., and Amador, J. A. (2001). Biogeophysical factors influencing soil respiration and mineral nitrogen content in an old field soil. *Soil Biol. Biochem.* 33, 429–438. doi: 10.1016/S0038-0717(00)00182-6

Shahabuddin, G., Goswami, R., Krishnadas, M., and Menon, T. (2021). Decline in forest bird species and guilds due to land use change in the Western Himalaya. *Glob. Ecol. Conserv.* 25, e01447. doi: 10.1016/j.gecco.2020.e01447

Shen, C., Gunina, A., Luo, Y., Wang, J., He, J. Z., Kuzyakov, Y., et al. (2020). Contrasting patterns and drivers of soil bacterial and fungal diversity across a mountain gradient. *Environ. Microbiol.* 22, 3287–3301. doi: 10.1111/1462-2920.15090

Shen, C., Ni, Y., Liang, W., Wang, J., and Chu, H. (2015). Distinct soil bacterial communities along a small-scale elevational gradient in alpine tundra. *Front. Microbiol.* 6:582. doi: 10.3389/fmicb.2015.00582

Siebert, J., Sünnemann, M., Auge, H., Berger, S., Cesarz, S., Ciobanu, M., et al. (2019). The effects of drought and nutrient addition on soil organisms vary across taxonomic groups, but are constant across seasons. *Sci. Rep.* 9, 1–12. doi: 10.1038/s41598-018-36777-3

Sieriebriennikov, B., Ferris, H., and de Goede, R. G. (2014). NINJA: An automated calculation system for nematode-based biological monitoring. *Eur. J. Soil Biol.* 61, 90–93. doi: 10.1016/j.ejsobi.2014.02.004

Sikora, R. A., Coyne, D., Hallmann, J., and Timper, P. (Eds.) (2018). *Plant parasitic nematodes in subtropical and tropical agriculture*. Wallingford: CAB International, 62–83. doi: 10.1079/9781786391247.0000

Song, D., Pan, K., Tariq, A., Sun, F., Li, Z., Sun, X., et al. (2017). Large-scale patterns of distribution and diversity of terrestrial nematodes. *Appl. Soil Ecol.* 114, 161–169. doi: 10.1016/j.apsoil.2017.02.013

Song, M., Li, X., Jing, S., Lei, L., Wang, J., and Wan, S. (2016). Responses of soil nematodes to water and nitrogen additions in an old-field grassland. *Appl. Soil Ecol.* 102, 53–60. doi: 10.1016/j.apsoil.2016.02.011

Sun, X., Zhang, X., Zhang, S., Dai, G., Han, S., and Liang, W. (2013). Soil nematode responses to increases in nitrogen deposition and precipitation in a temperate forest. *PLoS One* 8:e82468. doi: 10.1371/journal.pone.0082468

Thakur, M. P., del Real, I. M., Cesarz, S., Steinauer, K., Reich, P. B., Hobbie, S., et al. (2019). Soil microbial, nematode, and enzymatic responses to elevated CO2, N fertilization, warming, and reduced precipitation. *Soil Biol. Biochem.* 135, 184–193. doi: 10.1016/j.soilbio.2019.04.020

Thakur, M. P., Tilman, D., Purschke, O., Ciobanu, M., Cowles, J., Isbell, F., et al. (2017). Climate warming promotes species diversity, but with greater taxonomic redundancy, in complex environments. *Sci. Adv.* 3:e1700866. doi: 10.1126/sciadv.1700866

Tong, F. C., Xiao, Y., and Wang, Q. L. (2010). Soil Nematode community structure on the northern slope of Changbai Mountain Northeast China. *J. For. Res.* 21, 93–98. doi: 10.1007/s11676-010-0016-0

van den Hoogen, J., Geisen, S., Routh, D., Ferris, H., Traunspurger, W., Wardle, D. A., et al. (2019). Soil nematode abundance and functional group composition at a global scale. *Nature* 572, 194–198. doi: 10.1038/s41586-019-1418-6

Van Eekeren, N., De Boer, H., Hanegraaf, M., Bokhorst, J., Nierop, D., Bloem, J., et al. (2010). Ecosystem services in grassland associated with biotic and abiotic soil parameters. *Soil Biol. Biochem.* 42, 1491–1504. doi: 10.1016/j.soilbio.2010.05.016

Veen, G. F., De Long, J. R., Kardol, P., Sundqvist, M. K., Snoek, L. B., and Wardle, D. A. (2017). Coordinated responses of soil communities to elevation in three subarctic vegetation types. *Oikos* 126, 1586–1599. doi: 10.1111/oik.04158

Wall, D. H., Bardgett, R. D., and Kelly, E. (2010). Biodiversity in the dark. *Nat. Geoence* 3, 297–298. doi: 10.1038/ngeo860

Wang, J.-T., Cao, P., Hu, H.-W., Li, J., Han, L.-L., Zhang, L.-M., et al. (2015). Altitudinal distribution patterns of soil bacterial and archaeal communities along Mt. Shegyla on the Tibetan Plateau. *Microb. Ecol.* 69, 135–145. doi: 10.1007/s00248-014-0465-7

Wani, Z. A., Negi, V. S., Bhat, J. A., Satish, K. V., Kumar, A., Khan, S., et al. (2023). Elevation, aspect, and habitat heterogeneity determine plant diversity and compositional patterns in the Kashmir Himalaya. *Front. For. Glob. Change* 6:11. doi: 10.3389/ffgc.2023.1019277

Wei, D., Jia-Liang, W., Scott, M., Yi-Hao, F., Shuo-Ran, L., Xiao-Yan, Y., et al. (2019). Effects of sampling on the elevational distribution of nematode-trapping fungi. *Res. Sq. BMC Microbiol.* doi: 10.21203/rs.2.14154/v1

Yeates, G. W. (2003). Nematodes as soil indicators: Functional and biodiversity aspects. *Biol. Fertility Soils* 37, 199–210. doi: 10.1007/s00374-003-0586-5

Yeates, G. W. (2007). Abundance diversity and resilience of Nematode assemblage in forest soils. *Can. J. For. Res.* 37, 216–225. doi: 10.1139/x06-172

Yeates, G. W. (2010). "Nematodes in ecological webs," in *Encyclopedia of life science*, (Chichester: John Wiley & Sons, Ltd), 1–10. doi: 10.1002/9780470015902.a0021913

Yeates, G. W., Bongers, T., De Goede, R. G., Freckman, D. W., and Georgieva, S. S. (1993). Feeding habits in soil nematode families and genera-an outline for soil ecologists. *J. Nematol.* 25, 315–331.

Yu, Z., Zou, S., Li, N., Kerfahi, D., Lee, C., Adams, J., et al. (2021). Elevation-related climatic factors dominate soil free-living nematode communities and their co-occurrence patterns on Mt. Halla, South Korea. *Ecol. Evol.* 11, 18540–18551. doi: 10.1002/ece3.8454

Zhang, Y., Ji, L., and Yang, L. (2021). Abundance and diversity of soil nematode community at different altitudes in cold-temperate montane forests in northeast China. *Glob. Ecol.d Conserv.* 29:e01717. doi: 10.1016/j.gecco.2021.e01717

Zhao, J., and Neher, D. A. (2014). Soil energy pathways of different ecosystems using nematode trophic group analysis: A meta-analysis. *Nematology* 16, 379–385. doi: 10.1163/15685411-00002771

Zhao, J., Zhao, C., Wan, S., Wang, X., Zhou, L., and Fu, S. (2015). Soil nematode assemblages in an acid soil as affected by lime application. *Nematology* 17, 179–191. doi: 10.1163/15685411-00002860

frontiers | Frontiers in Forests and Global Change

TYPE Original Research
PUBLISHED 28 April 2023
DOI 10.3389/ffgc.2023.1181299

Check for updates

OPEN ACCESS

EDITED BY
Jahangeer A. Bhat,
Fiji National University, Fiji

REVIEWED BY
Muhammad Majeed Majeed,
University of Gujrat, Pakistan
Rupesh Dhyani,
Govind Ballabh Pant National Institute of Himalayan Environment and Sustainable Development, India

*CORRESPONDENCE
Tanvir Ul Hassan Dar
✉ tanvirulhasan@gmail.com

RECEIVED 07 March 2023
ACCEPTED 10 April 2023
PUBLISHED 28 April 2023

CITATION
Mangral ZA, Islam SU, Tariq L, Kaur S, Ahmad R, Malik AH, Goel S, Baishya R, Barik SK and Dar TUH (2023) Altitudinal gradient drives significant changes in soil physico-chemical and eco-physiological properties of *Rhododendron anthopogon*: a case study from Himalaya.
Front. For. Glob. Change 6:1181299.
doi: 10.3389/ffgc.2023.1181299

Altitudinal gradient drives significant changes in soil physico-chemical and eco-physiological properties of *Rhododendron anthopogon*: a case study from Himalaya

Zahid Ahmed Mangral[1], Shahid Ul Islam[1], Lubna Tariq[1], Sharanjeet Kaur[2], Rameez Ahmad[3], Akhtar H. Malik[3], Shailendra Goel[2], Ratul Baishya[2], Saroj Kanta Barik[4] and Tanvir Ul Hassan Dar[1]*

[1]Department of Biotechnology, School of Biosciences and Biotechnology, Baba Ghulam Shah Badshah University, Rajouri, Jammu and Kashmir, India, [2]Department of Botany, University of Delhi, New Delhi, India, [3]Centre for Biodiversity and Taxonomy, Department of Botany, University of Kashmir, Srinagar, Jammu and Kashmir, India, [4]Pharmacology Division, Council of Scientific and Industrial Research-National Botanical Research Institute, Lucknow, India

The best natural laboratories for studying the ecological responses of plants are high-altitude areas like the Himalaya, where many gradients coexist on a relatively small spatial scale. Here, we investigate the effect of soil physico-chemical and eco-physiological properties on the broadleaf evergreen woody shrub *Rhododendron anthopogon* D.Don along an altitudinal gradient in the Kashmir Himalaya. We collected leaf and soil samples for eco-physiological and soil physico-chemical analysis, respectively, at five different sites along an altitudinal gradient (3,220–3,908 m). Our results demonstrate a significant difference between soil physico-chemical and eco-physiological parameters along the altitudinal gradient. A significant correlation was observed between different studied parameters and altitude. Principal component analysis of studied soil physico-chemical and eco-physiological parameters revealed that all the sites were grouped into four clusters according to altitude, suggesting a more pronounced effect of altitude. Our findings showed that soil infiltration capacity increased with altitude, which would be helpful for the growth and development of *R. anthopogon*. We also observed significant variations in eco-physiological parameters, demonstrating their critical involvement in adapting *R. anthopogon* to the harsh environment of the alpine regions of Kashmir Himalaya. Therefore, the present study adds to our understanding that *R. anthopogon* has sufficient soil physico-chemical and eco-physiological plasticity, which should be favorable for its survival in future climates, offering an adaptive advantage and expanding its range shortly.

KEYWORDS

***Rhododendron anthopogon*, eco-physiology, soil property, temperature, Kashmir Himalaya**

1. Introduction

Mountainous ecosystems support unique biodiversity with distinct vegetation zones along an altitudinal gradient. They exhibit considerable variation in microclimate even with a slight elevation difference, which affects the distribution and structure of plant communities (Maclean et al., 2017; Antonelli et al., 2018; Fatima et al., 2022). Distributional ranges for plant species are anticipated to move to higher elevations with rise in temperature (Alberto et al., 2013; Freeman et al., 2018; Wani and Pant, 2021). Substantial differences in environments can occur over short distances; hence, altitude gradients in alpines are studied to understand the consequences of climate change on plant distribution and soil properties (Adamczyk et al., 2019).

Variation in elevation gradients significantly impacts biotic and abiotic components, which are closely related to ongoing human progressive processes (Gupta et al., 2019). The change in vegetation along altitude reveals that temperature, wind, UV radiation, nutrient availability and precipitation are the main drivers (Piao et al., 2011; Wani et al., 2023). Due to different climatic conditions, soil physico-chemical properties and vegetation also vary significantly, which are related to lower levels of nitrification, pH, and organic carbon (Decker and Boerner, 2003; Kewlani et al., 2021). A major factor that decreases with increasing elevation is temperature; altitudinal gradients act as thermoclines to trigger long-term environmental conditions (Mayor et al., 2017). Plants with more phenotypic flexibility have been observed at higher elevations more frequently (Stöcklin et al., 2009; Pluess et al., 2016), allowing them to adapt to the changing environment. In several alpine and subalpine species, phenotypic plasticity compensates for the short growing season by permitting fast reproduction (Wani et al., 2022). In reaction to climate fluctuations, plants adjust critical physiological, reproductive, and physical features (Körner, 2007; Wani et al., 2022). The flexibility of plants allows them to inhabit various habitats across altitudinal gradients. Therefore, understanding the restrictions imposed by altitudinal gradients on plant distribution can be aided by studying these adaptive features and relating them to environmental factors (Fatima et al., 2022).

Altitudinal changes in soil characteristics significantly impact the composition of plant communities. Soil qualities can be affected by changes in vegetation along an elevational gradient, and the reverse is also true (Ahmad et al., 2018; Hou et al., 2019). Plant communities in alpine habitats can be better understood by examining the interaction between soil conditions and vegetation along an altitudinal gradient (Anic et al., 2010). Alpine mountains have a significant topographic role in soil physicochemical characteristics, such as slope aspects (Bardelli et al., 2017). Differences in air temperature with elevation are assumed to be the common cause driving changes in nutritional status across diverse locales (Sundqvist et al., 2013). Other variables, including soil temperature, slope exposure, vegetation, and altitude, can also impact soil qualities (Mården et al., 2015; Bardelli et al., 2017). Many studies have established the differential influence of variations in climate along an elevational gradient on soil attributes (Adamczyk et al., 2019; Hou et al., 2019; Hamid et al., 2020a; Zhang et al., 2021; Trujillo-González et al., 2022). Total organic carbon and nitrogen have been found to increase with altitude and were found to be positively correlated with annual mean temperature and precipitation (Zhang et al., 2021). Accordingly, soil temperature, pH, electrical conductivity and C:N ratio were found to show increased trend toward altitudinal gradient (Hamid et al., 2020a). A temperature reduction and precipitation increase is generally noticed with the rise in altitude (Körner, 2007; Hassan and Nile, 2021). Simon et al. (2018) reported linear correlation between soil organic carbon stock and pH with altitude. Climate change impacts the composition and biomass of plants, which is reflected in differences in soil characteristics and taxa (Zhu et al., 2019; Hamid et al., 2020a).

The eco-physiological characteristics of a plant species determine how it reacts to environmental changes (Rathore et al., 2018; Li H. et al., 2022; Visakorpi et al., 2022). The ability to forecast species mortality, distributions of species, and ecosystem-level processes can be improved with the knowledge of a species physiology (Fyllas et al., 2014; Anderegg et al., 2016; Visakorpi et al., 2022). However, due to their time-consuming testing requirements and frequent absences from trait databases, plant eco-physiological traits are rarely used to predict changes in the composition of plant communities. Instead, most research forecasting how plant communities will respond to climate change relies on morphological characteristics, such as height and leaf mass per area, which are thought to characterize species physiology implicitly and nutrient uptake (Shipley et al., 2016; Visakorpi et al., 2022). The primary goal of plant ecophysiology is to explain or comprehend ecological patterns through studies on the physiological mechanisms behind these ecological patterns. For instance, understanding the climatic effects of elevation on physiological processes is necessary to learn why plants in alpine ecosystems have distinct morphological and anatomical features from equivalent species in lowland habitats. Many authors have reported the effects of rising elevation on the eco-physiology of plants (Takahashi and Matsuki, 2017; Wang et al., 2017; Zhou et al., 2017; Rathore et al., 2018). In a study conducted by Rathore et al. (2018), a significant variation in leaf size, relative water content (RWC), chlorophyll and proline content (PR) were observed along an altitudinal gradient. Molina-Montenegro et al. (2012) studied the adaptability of *Taraxacum officinale's* invasive photoprotective approaches and performance along altitudinal gradient. They observed greater plasticity in individuals from higher altitudes compared to those from lower altitudes. Similar to this, individuals exposed to high light levels produced more photoprotective pigments, biomass, and flowers (Molina-Montenegro et al., 2012).

Due to the restructuring of populations or species as a result of climatic change along the altitudinal gradient, plants have evolved numerous resistance traits (Lenoir et al., 2008; Bellard et al., 2012). According to Rapp et al. (2012), plant species with comparatively more genotypic or phenotypic variety may be better able to tolerate these changes. Studying these characteristics and connecting them to environmental gradients might provide insightful data on the ability of plants to adapt to changing conditions or explain how they are distributed within a specific geographic range (Ahrens et al., 2020). At higher altitudes, lower resource availability and harsh environmental conditions encourage stress-tolerant species that establish xeric characteristics such as diminished leaf area (LA) and heavily pubescent leaf surface, more prostrate habit, water conservation-related increases in lignin deposition or possibly succulence (Körner, 2012; Fatima et al., 2022).

One of the best natural laboratories for studying how plants respond ecologically is high-altitude areas like the Himalaya, where numerous gradients are present on a very small spatial scale (Enquist et al., 2017; Rathore et al., 2018). The primary elements affecting plant functioning along these gradients include temperature, pH, UV radiation, atmospheric humidity, and wind speed (Rathore et al., 2018). Several studies have been conducted on the effect of eco-physiological and soil parameters on an altitudinal gradient (Rathore et al., 2018; Qi et al., 2019; Hamid et al., 2020a; Han et al., 2020; Fatima et al., 2022). However, most of these studies focused on herbaceous plants. In the present study, we focused on *Rhododendron anthopogon* D.Don, a broadleaf evergreen woody plant that belongs to the family Ericaceae. It is endemic to Himalaya to S. Tibet, and can be found at elevations ranging from treeline to 4,800 m.a.s.l. The plant is in high demand as herbal medicines. Leaf decoction is used to treat cough, cold, asthma, chronic bronchitis, and mucus in the nose or throat (Kumar and Srivastava, 2002; Popescu and Kopp, 2013). In post-delivery problems, dried and powdered flowers mixed with oil are used as a body massage (Bhattacharjee, 1998). *Rhododendron* species are great examples of investigating the functional significance of adaptive characteristics having a long history of research on trait variation among species and its importance to physiology and ecology (Nilsen, 1992). Drought tolerance, cold adaptation, nutrient use efficiency, and habitat selection of *Rhododendron* species have been shown to represent a condition that implies vascular system adaptive changes (Taneda and Noshiro, 2019). Plants in high-light environments have a shorter leaf survival span than plants growing in low-light conditions.

In light of this, the current study was conducted in the Kashmir Himalaya. Global warming has considerably impacted this Himalayan region during the last few decades (Murtaza and Romshoo, 2017). The climate of the area has experienced significant change, particularly in the irregular behavior of precipitation patterns and seasonal temperature (Hamid et al., 2020b; Dad et al., 2021). In this study, we hypothesized that (a) soil physico-chemical and eco-physiological parameters change along an altitudinal gradient, (b) there exist a strong correlation between soil physico-chemical, eco-physiological properties and altitude, (c) the overall variation of soil physico-chemical and eco-physiological properties affect *R. anthopogon* along an altitudinal gradient.

2. Materials and methods

2.1. Study area and sampling sites

The present study was conducted at Apharwat mountain in the Gulmarg region of Jammu and Kashmir, located in India's North-Western Himalaya. The study area is located in the Kashmir Himalaya between 34° 05′ N latitude and 74° 38′ E longitude. The altitude varies between 2,800 m (at Gulmarg) and 4,200 m (at Apharwat) above sea level. With 1,049 mm of annual precipitation on average, this area has a continental temperate climate. The hottest month of the year is July, with an average temperature of 20°C; the coldest month is January, with a decline in temperature up to −6°C (Hamid et al., 2020b). The sampling locations were built along an altitudinal gradient at five different sites: Site-1 is at 3,220 m, followed by Site-2 (3,351), Site-3 (3,500), Site-4 (3,716), and Site-5 (3,908 m) (**Figure 1**).

2.2. Soil and plant sampling

The soil samples were collected from randomly located three populations at each site. From each population, soil samples were collected from the surface (0–10 cm) and subsurface (10–20 cm) layers per site (Hamid et al., 2020a). The soil samples collected from 0 to 10 cm and 10 to 20 cm depths from each population were homogenized (appropriately mixed). At the same time, the soil samples were also air-dried, stored at room temperature, and sieved through a 2 mm sieve before the physicochemical examination. Fresh soil samples from each site were used to analyze soil pH, soil moisture content (MC) and temperature.

For the eco-physiological analysis, a total of 10 different parameters were measured as: RWC, LA, leaf dry mass content (LDMC), specific leaf area (SLA), proline content (PR), total chlorophyll (TCH), carotenoid content (CRT), total phenolics content (TPC), total flavonoids (TFV), and total soluble sugars (TSS).

2.3. Soil physico-chemical analysis

Soil temperature was measured using a field soil thermometer (TP 3001 Digital Thermometer). To determine soil moisture, we dried 5 g of fresh soil by keeping it overnight at 105°C. The percentage of soil MC was estimated as per Allen et al. (1974). Soil pH, electrical conductivity (CD), bulk density (BD), and particle density (PD) were measured by taking a soil: solution in distilled water at a ratio 1:2.5 at 24°C (Allen and Hajek, 1989). For the estimation of soil sodium (Na), magnesium (Mg), calcium (Ca) and sulfur (S), standard procedure of Allen et al. (1974) was followed. Total soil nitrogen (N) content was analyzed using the standard method of Kjeldahl (Bremner et al., 1965). The soil available phosphorous (P) was estimated by Olsen's sodium bicarbonate method (Olsen et al., 1954). Available potassium (K) was estimated using the ammonium acetate and flame photometric detection method (Hanway and Heidel, 1952). Total soil organic carbon (TOC) was analyzed using chromic acid titration (Walkley and Black, 1934). In contrast, soil organic matter (SOM) was estimated by following the method of Hoogsteen et al. (2015).

2.4. Eco-physiological analysis

2.4.1. Functional traits

The functional traits (RWC, LDMC, LA, and SLA) that reflect plant ecological strategies were measured. Thirty mature, sun-exposed, healthy, fresh leaves were randomly selected from different plants at each sampling site to measure RWC, LA, LDMC, and SLA. The traits were estimated using the method followed by Rathore et al. (2018).

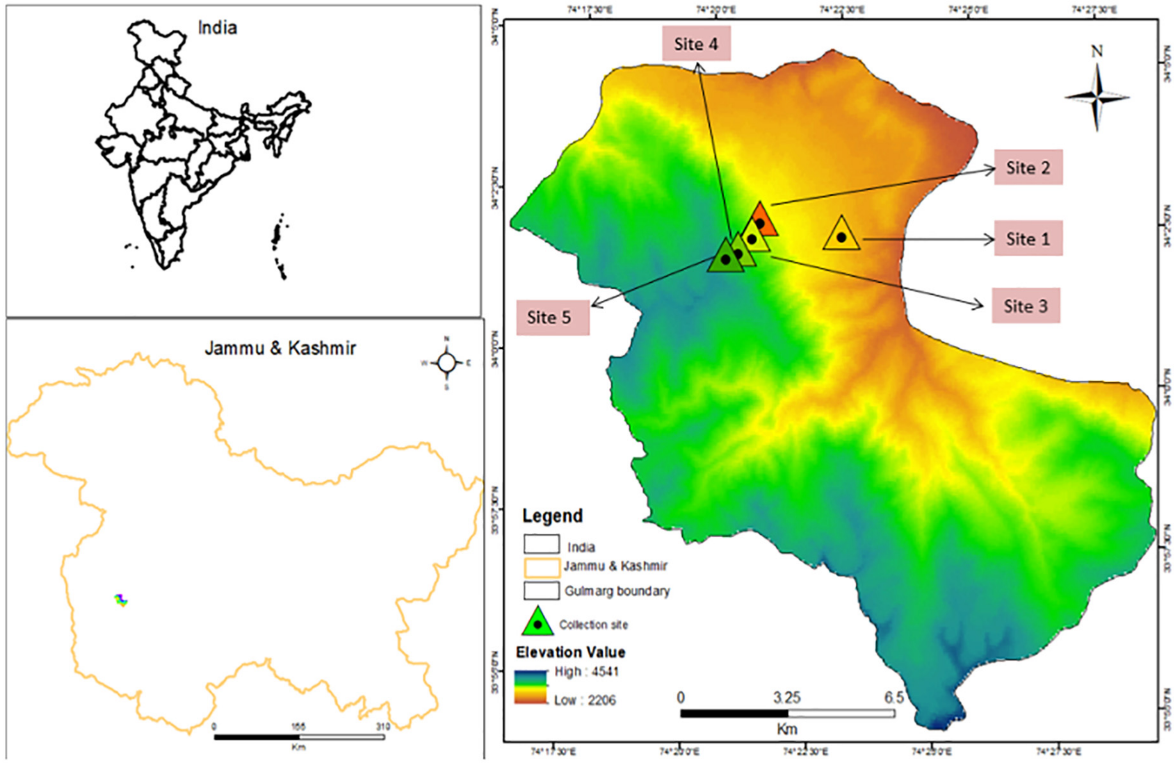

FIGURE 1
Map of the study area shows selected sampling sites in Kashmir Himalaya.

2.4.2. Determination of total phenolic and flavonoid content

The Folin–Ciocalteu's test was used to determine the total phenolic content using gallic acid as a reference (Idris et al., 2017). The results were expressed as milligram gallic acid equivalent (mg GAE) per gram of dry sample using the equation based on the calibration curve of gallic acid: $y = 0.0111x + 0.0456$, $R^2 = 0.9965$. The TFV content was measured using the aluminum chloride colorimetric technique with quercetin as a reference (Olajire and Azeez, 2011). The equation based on the quercetin calibration curve was used to translate the results into milligrams of quercetin equivalent (mg QE) per gram of dry sample: $y = 0.0209x + 0.0503$, $R^2 = 0.9984$.

2.4.3. Determination of total chlorophyll and carotenoid content

We used the Arnon (1949) method to estimate the TCH and CRT. The following methods were used to calculate the chlorophyll concentrations: TCH (a + b) (mg.g^{-1}) was calculated as $(8.02 \times A663 + 20.20 \times A645) \times A663 \times V/1{,}000 \times W$, where V is the volume of the extract (ml) and W is the weight of the leaf tissue (g). The following calculation was used to calculate the amount of carotenoid present: $A480 + (0.114 \times A663 – 0.638 \times A645)$.

2.4.4. Determination of total soluble sugars and proline assay

With minor changes, the anthrone method proposed by Yemm and Willis (1954) was used to estimate TSSs. The TSSs were estimated as mg.g^{-1} fresh weight using a calibration curve for a standard glucose solution. According to Bates et al. (1973), the calorimetric approach was utilized to quantify proline by generating a proline-acid ninhydrin complex. L-proline was employed as a control. The PR was determined and expressed using a standard curve as mol g^{-1} DW.

2.5. Data analysis

Data generated had three replicates per variable. A Two-way analysis of variance (ANOVA) was employed to evaluate the effects of altitude and soil depth (fixed effects) on soil physico-chemical parameters (response variable) by performing multiple pairwise-comparison between the means of sites and to identify the values with significant differences ($p \leq 0.05$). Also, One-way ANOVA was performed to evaluate the effects of altitude on the eco-physiological parameters as a response variable to identify the values with significant differences ($p \leq 0.05$). Principal component analysis (PCA) was performed to illustrate the commonalities between the different soil physico-chemical parameters, eco-physiological parameters and altitude using the *FactoMineR* (Husson et al., 2020) and *factoextra* (Kassambara and Mundt, 2020) packages. We employed Pearson's pairwise multiple correlation analysis between soil and eco-physiological parameters, using the *Performance Analytics* package (Peterson and Carl, 2020) to visualize the relationship between different parameters. To study the effect of altitude on the soil's physicochemical properties and eco-physiological parameters, we also used a linear regression model with the *basicTrendline* R package

(Weiping and Guangchuang, 2020). R statistical software version 4.0.2 was used for all analyses (R Core Team, 2020).

3. Results

3.1. Variation in soil physico-chemical parameters of *Rhododendron anthopogon* along an altitudinal gradient

We observed a significant difference between soil physico-chemical properties and soil depth among five sites along the altitudinal gradient. The results of ANOVA pertaining to altitude and soil depth are given in **Table 1** and **Supplementary Table 1**. The soil at all altitudes was slightly acidic 0–10 cm (5.54–4.52) and 10–20 cm (5.67–4.64). Soil pH varied significantly, decreasing with increasing altitude at 0–10 cm and 10–20 cm depths ($p < 0.001$). In addition, with 10–20 cm depth increase in soil pH was recorded ($p < 0.001$). We also observed a slight rise in Mg, C, Na ($p < 0.001$) and S ($p < 0.01$) with the increasing altitude at both 0–10 cm and 10–20 cm depths, while a decline in Mg and C was observed at 10–20 cm depth. Similarly, Na and S increase with altitude at 10–20 cm depth. BD was slightly decreased with the increase in altitude at both 0–10 cm and 10–20 cm depths ($p < 0.001$), and a rise in 10–20 cm depth was also recorded ($p < 0.001$). Soil MC, OM, SL, CD, N, K, and Ca show an increase with altitude at 0–10 cm and 10–20 cm depths ($p < 0.001$). Interestingly, all these parameters were significantly reduced with soil at 10–20 cm depth (**Table 1** and **Supplementary Table 1**).

The linear regression analysis of soil physico-chemical parameters along the altitude gradient reveals a significant decreasing trend in pH and temp ($p < 0.0001$) with increasing altitude (**Figure 2**). With increasing altitude, the data also shows a significant increasing trend in MC, OM, K ($p = 0.0001$), SL ($p = 0.00778$), CD ($p = 0.00806$), N ($p = 0.000442$), and Ca ($p = 0.00586$). In contrast, BD ($p = 0.747$), C ($p = 0.408$), Na ($p = 0.475$), Mg ($p = 0.768$) and S ($p = 0.343$) do not show any trend with the altitude.

3.2. Relationship between soil physico-chemical parameters of *Rhododendron anthopogon* along an altitudinal gradient

The PCA analysis is shown in **Figure 3** wherein the first two principal components (PCs) show about 71.7% of the total variation. The plot grouped sites into four classes based on soil parameters. Site 1 and Site 2 (RGS1 and RGS2) were not differentiated from each other and made a clear group, whereas the other three sites differed well from this group by pH and temperature. The Site 3 (RGS3) was found to be dominated by BD, Mg and C. Site 4 (RGS4) revealed dominance of Na, Ca, MC, SL, N and S. Site 5 (RGS5) was dominated by OM, K, ALT and CD, which significantly separated Site 5 (RGS5) from the rest of the four sites (**Figure 3**).

Pearson's correlation analysis indicated a relationship among studied soil parameters. Soil pH showed a significant negative

TABLE 1 Physico-chemical properties of soil at five sites along the altitudinal gradient in Gulmarg area of Kashmir Himalaya.

Site	Altitude m.a.s.l	Depth (cm)	pH	Temp (°C)	MC (%)	BD (g/cm^3)	OM (%)	CD (µs/cm)	SL (ppm)	N (g/cm^2)	C (%)	Mg (%)	K (%)	Ca (%)	Na (%)	S (%)
RGS1	3,220	0–10	5.54 ± 0.015	9.1	34.9 ± 0.21	1.26 ± 0.0055	1.23 ± 0.0141	485 ± 15.52	287.33 ± 13.61	0.0071 ± 0.00021	3.7 ± 0.10	0.225 ± 0.001	0.01 ± 0.0005	0.17 ± 0.002	0.026 ± 0.003	0.00176 ± 0.00001
		10–20	5.67 ± 0.020	7.5	32.76 ± 0.17	1.35 ± 0.019	1.131 ± 0.121	193.86 ± 8.02	185.67 ± 12.06	0.0080 ± 0.00012	3.8 ± 0.01	0.186 ± 0.004	0.014 ± 0.0005	0.14 ± 0.004	0.03 ± 0.0003	0.0018 ± 0.00014
RGS2	3,351	0–10	5.2 ± 0.020	8.9	37.9 ± 0.2	1.20 ± 0.012	1.1694 ± 0.01	606.67 ± 60.91	227.33 ± 8.02	0.0077 ± 0.00015	3.6 ± 0.02	0.228 ± 0.0004	0.01 ± 0.001	0.12 ± 0.001	0.02 ± 0.001	0.00157 ± 0.0001
		10–20	5.41 ± 0.005	7.2	35.96 ± 0.11	1.30 ± 0.010	1.102 ± 0.098	337 ± 9.54	91.26 ± 4.38	0.0124 ± 0.0001	3.2 ± 0.043	0.201 ± 0.002	0.01 ± 0.0005	0.11 ± 0.0058	0.01 ± 0.0002	0.00185 ± 0.00006
RGS3	3,500	0–10	4.96 ± 0.015	7.3	38.93 ± 0.24	1.18 ± 0.0099	1.297 ± 0.012	621 ± 37.16	292.67 ± 8.02	0.0095 ± 0.00026	3.8 ± 0.05	0.232 ± 0.002	0.019 ± 0.0008	0.12 ± 0.001	0.02 ± 0.00002	0.00157 ± 0.00
		10–20	5.17 ± 0.056	5.1	36.73 ± 0.11	1.28 ± 0.022	1.227 ± 0.104	404.33 ± 30.27	153.66 ± 5.03	0.0142 ± 0.00011	3.5 ± 0.036	0.203 ± 0.008	0.01 ± 0.0003	0.108 ± 0.0052	0.02 ± 0.0002	0.0018 ± 0.00003
RGS4	3,700	0–10	4.73 ± 0.005	6.1	41.96 ± 0.115	1.117 ± 0.0129	1.365 ± 0.0015	626.33 ± 23.03	281.33 ± 26.73	0.0099 ± 0.00015	3.8 ± 0.02	0.250 ± 0.007	0.018 ± 0.0002	0.16 ± 0.0026	0.020 ± 0.0002	0.0016 ± 0.00001
		10–20	4.91 ± 0.02	3.9	39.2 ± 0.25	1.26 ± 0.011	1.261 ± 0.058	473.33 ± 21.22	218 ± 7.21	0.0174 ± 0.00045	3.8 ± 0.036	0.206 ± 0.009	0.013 ± 0.0003	0.15 ± 0.0036	0.023 ± 0.0001	0.0018 ± 0.00003
RGS5	3,900	0–10	4.52 ± 0.01	5.4	43.57 ± 0.50	1.11 ± 0.0015	1.434 ± 0.007	664.33 ± 27.30	298.33 ± 26.95	0.0111 ± 0.00047	3.8 ± 0.06	0.252 ± 0.001	0.025 ± 0.0008	0.18 ± 0.002	0.025 ± 0.0002	0.0018 ± 0.00001
		10–20	4.64 ± 0.0057	3.1	39.71 ± 0.14	1.25 ± 0.0064	1.408 ± 0.119	641.47 ± 49.72	310 ± 11.27	0.0184 ± 0.00035	3.5 ± 0.208	0.210 ± 0.0036	0.019 ± 0.0005	0.17 ± 0.0043	0.028 ± 0.00017	0.0019 ± 0.00001

Data were shown as mean ± standard deviation, $n = 3$. pH, soil pH; Temp, soil temperature; MC, moisture content; BD, bulk density; OM, organic matter; CD, soil electrical conductivity; SL, salinity; N, total soil nitrogen content; C, total soil organic carbon; Mg, magnesium; K, potassium; Ca, calcium; Na, sodium; S, sulfur.

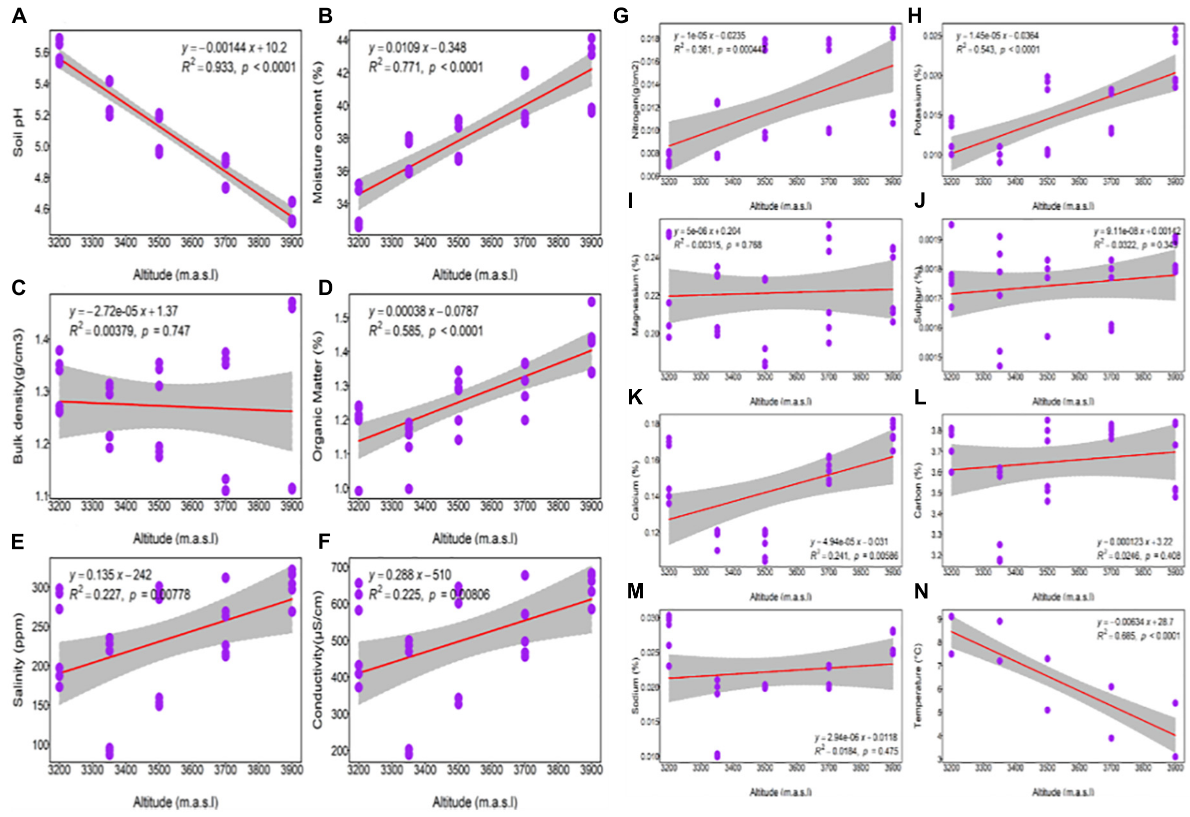

FIGURE 2
Linear regression representing a change in soil physico-chemical parameters of *Rhododendron anthopogon* along the altitude gradient. Relationship between altitude and **(A)** soil pH; **(B)** moisture content; **(C)** bulk density; **(D)** organic matter; **(E)** salinity; **(F)** soil electrical conductivity; **(G)** nitrogen; **(H)** potassium; **(I)** magnesium; **(J)** sulfur; **(K)** calcium; **(L)** total soil organic carbon; **(M)** sodium; **(N)** soil temperature. Each purple dot in the plot represents the mean value of the soil physico-chemical parameters, and the gray areas represent a 95% confidence interval.

correlation with ALT, MC, OM, K, SL, and CD, whereas there was a positive correlation with temp ($p < 0.001$). Soil K, MC, OM ($p < 0.001$), SL, CD, Ca and ($p < 0.01$) show a significant positive correlation with altitude. Temperature showed a negative correlation with N, ALT ($p < 0.001$), MC, OM and S ($p < 0.01$), whereas positive with Mg $p < 0.05$. C showed only a positive correlation with SL, CD, Na ($p < 0.001$), and Mg ($p < 0.01$), while CD ($p < 0.001$) shows a significant negative correlation with the pH and a positive correlation with the soil SL, K, OM, C, Mg, Ca ($p < 0.001$), ALT, MC and Na ($p < 0.01$) (Figure 4).

3.3. Variation in eco-physiological parameters of *Rhododendron anthopogon* along an altitudinal gradient

Eco-physiological parameters in the current study reveal a significant variation among different sites along altitude (Table 2 and Supplementary Table 2). One-way ANOVA shows a significant effect of altitude on eco-physiological parameters (Supplementary Table 2). We observed that RWC varied significantly, showing an increasing trend with the increasing altitude ($p < 0.001$). In contrast, LA and SLA significantly show a decreasing trend with the rising altitude ($p < 0.001$), and LDMC does not show any significant trend with the altitude. Similarly, PR, CRT, TPC, TFV and TSS varied significantly, showing an increasing trend with the increase in altitude ($p < 0.001$). On the other hand, TCH significantly decreased with the increase in altitude ($p < 0.001$) (Table 2 and Supplementary Table 2).

The linear regression analysis of eco-physiological parameters concerning altitude shows a positive increasing trend of RWC, PR CRT, TSS, TPC ($p < 0.0001$) and TFV ($p = 0.000194$). Similarly, we also found a negative trend in LA, SLA and TCH ($p < 0.0001$) along altitude, while LDMC ($p = 0.167$) does not show any significant trend with increasing altitude (Figure 5).

3.4. Relationship between eco-physiological traits of *Rhododendron anthopogon* along an altitudinal gradient

In the PCA analysis, the first two PCs show about 93.9% of total variation (Figure 6). Site 1 and Site 2 (RGS1 and RGS2) formed a separate group based on TCH, and LA from the rest of the sites. Similarly, Site 4 (RGS4) and Site 5 (RGS5) were separated by the most significant variables ALT, PR, RWC, TPC, CRT, TSS and LDMC, while Site 3 (RGS3) was different by SLA and TFV from other sites.

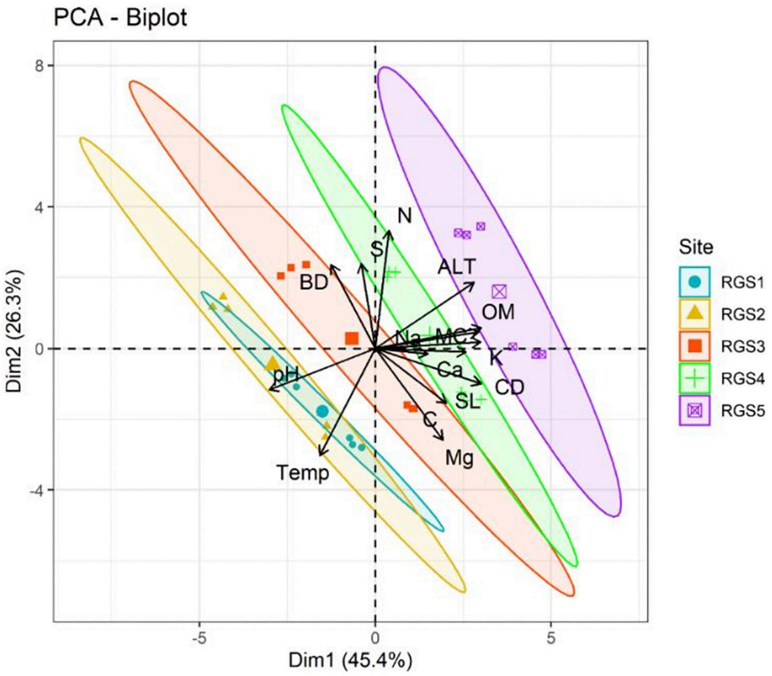

FIGURE 3
Principal component analysis (PCA) biplot of *Rhododendron anthopogon* soil physico-chemical parameters across the five sampling sites: Site-1 (RGS1), Site-2 (RGS2), Site-3 (RGS3), Site-4 (RGS4), and Site-5 (RGS5) along an altitudinal gradient in the Gulmarg area of Kashmir Himalaya. N, total soil nitrogen content; pH, soil pH; Temp, soil temperature; MC, moisture content; BD, bulk density; OM, organic matter; CD, soil electrical conductivity; SL, salinity; C, total soil organic carbon; Mg, magnesium; K, potassium; Ca, calcium; Na, sodium; S, sulfur; ALT, altitude.

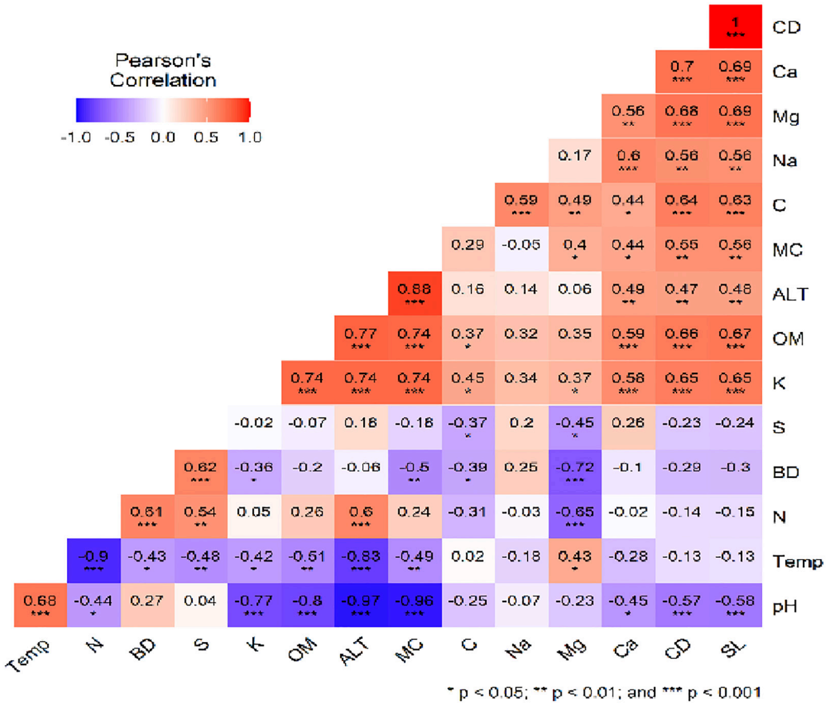

	Temp	N	BD	S	K	OM	ALT	MC	C	Na	Mg	Ca	CD	SL
CD														1***
Ca													0.7***	0.69***
Mg												0.56**	0.68***	0.69***
Na											0.17	0.6***	0.56**	0.56**
C										0.59***	0.49**	0.44*	0.64***	0.63***
MC									0.29	-0.05	0.4*	0.44*	0.55**	0.56**
ALT								0.88***	0.16	0.14	0.06	0.49**	0.47**	0.48**
OM							0.77***	0.74***	0.37*	0.32	0.35	0.59***	0.66***	0.67***
K						0.74***	0.74***	0.74***	0.45*	0.34	0.37*	0.58***	0.65***	0.65***
S					-0.02	-0.07	0.18	-0.16	-0.37*	0.2	-0.45*	0.26	-0.23	-0.24
BD				0.62***	-0.36*	-0.2	-0.06	-0.5**	-0.39*	0.25	-0.72***	-0.1	-0.29	-0.3
N			0.61***	0.54**	0.05	0.26	0.6***	0.24	-0.31	-0.03	-0.65***	-0.02	-0.14	-0.15
Temp		-0.9***	-0.43*	-0.48**	-0.42*	-0.51**	-0.83***	-0.49**	0.02	-0.18	0.43*	-0.28	-0.13	-0.13
pH	0.68***	-0.44*	0.27	0.04	-0.77***	-0.8***	-0.97***	-0.96***	-0.25	-0.07	-0.23	-0.45*	-0.57***	-0.58***

* p < 0.05; ** p < 0.01; and *** p < 0.001

FIGURE 4
Pearson's correlation plot among studied soil physico-chemical parameters. The distribution of each variable and correlation coefficient plus the significance level is given in the figure. Full forms of abbreviations are presented in Figure 2.

TABLE 2 Altitudinal variations in eco-physiological traits of *Rhododendron anthopogon* at five sites along the altitudinal gradient in Gulmarg area of Kashmir Himalaya.

Site	Altitude m.a.s.l.	RWC (%)	LDMC (gg^{-1})	LA (cm^2)	SLA (cm^2 g^1)	PR (μ-moles^{-1})	TCH ($mg.g^{-1}$)	CRT ($mg.g^{-1}$)	TPC ($mg.g^{-1}$)	TFV ($mg.g^{-1}$)	TSS ($mg.g^{-1}$)
RGS1	3,200	70.5 ± 0.954	0.424 ± 0.0292	3.12 ± 0.104	73.1 ± 1.86	2.94 ± 0.0539	2.30 ± 0.00666	0.559 ± 0.00632	41.9 ± 0.138	26.6 ± 0.259	26.0 ± 0.299
RGS2	3,351	71.9 ± 1.19	0.42 ± 0.0100	2.97 ± 0.0416	70.5 ± 2.23	3.06 ± 0.0666	2.18 ± 0.00321	0.598 ± 0.00429	42.9 ± 0.104	25.7 ± 0.215	26.6 ± 0.538
RGS3	3,500	74.5 ± 0.999	0.407 ± 0.0115	2.83 ± 0.0577	69.7 ± 2.93	3.49 ± 0.0513	1.98 ± 0.00586	0.738 ± 0.00381	42.7 ± 0.316	28.6 ± 0.206	28.4 ± 0.376
RGS4	3,700	76.1 ± 0.899	0.441 ± 0.0406	2.75 ± 0.127	62.5 ± 4.51	4.08 ± 0.0426	1.93 ± 0.00153	0.758 ± 0.00261	43.7 ± 0.180	27.9 ± 0.157	29.4 ± 0.456
RGS5	3,900	80.6 ± 1.98	0.445 ± 0.0278	2.56 ± 0.0529	57.7 ± 4.30	4.57 ± 0.0610	1.78 ± 0.00510	0.839 ± 0.00351	44.5 ± 0.275	29.4 ± 0.309	33.5 ± 0.228

Data were shown as mean ± standard deviation, $n = 3$. RWC, relative water content; LDMC, leaf dry mass content; LA, leaf area; SLA, specific leaf area; PR, proline content; TCH, total chlorophyll; CRT, carotenoid content; TPC, total phenolics content; TFV, total flavonoids; TSS, total soluble sugars.

Pearson's correlation analysis shows the relationship among different studied eco-physiological parameters (**Figure 7**). The result reveals that the SLA, LA and TCH show a significant negative correlation with the PR, ALT, CRT, TSS, RWC, TPC, and TFV. In contrast, SLA positively correlates with LA and TCH with $p < 0.001$. In comparison, TFV shows a significant positive correlation with PR, ALT, CRT, TSS and RWC with $p < 0.001$. Similarly, TPC, RWC, TSS, CRT and PR show a significant positive correlation with the ALT ($p < 0.001$).

4. Discussion

4.1. Variation in soil physico-chemical parameters of *Rhododendron anthopogon* along an altitudinal gradient

A significant difference was observed between the soil physico-chemical properties of *Rhododendron anthopogon* among all the sites along the altitudinal gradient (**Table 1** and **Figure 2**). Soil pH varied significantly, showing decreasing trend with increasing altitude. This can be attributed to the differences in soil temperature along the altitudinal gradient, as we also observed a decline in temperature with an increase in altitude. Variations in species composition and SOM along altitudinal gradients can also influence soil acidity by accumulating various organic acids (Egli et al., 2009). Furthermore, environmental factors such as slope and aspect substantially influence pH in alpine regions. A fall in pH at higher elevations may be attributable to the leaching of base cations caused by increased precipitation and a steeper slope (Tsui et al., 2004). The acidic nature of soil found in all altitudes confirms that *R. anthopogon* flourishes in acidic soil. The lower temperature at higher altitudes results in a slower decomposition rate and accumulates more organic matter (Northcott et al., 2009; Liang et al., 2016; Kumar et al., 2019). This is consistent with our findings as organic matter (OM) shows an increasing trend with an increase in altitude. Soil bulk density (BD) is an important parameter influencing root development, soil aeration, and water infiltration (Basso et al., 2013). The results of our study revealed that the average soil bulk density slightly decreased with the increase in altitude at both 0–10 cm and 10–20 cm depths, and a rise in 10–20 cm depth was also recorded. The observed pattern is consistent with findings from other research (Griffiths et al., 2009; Yang et al., 2018). The decrease in bulk density with increasing altitude might be due to soil porosity (Li et al., 2017), increased soil organic carbon content (Haynes and Naidu, 1998), increased ratio of silt and clay content in the soil (Wen et al., 2005) and freezing and thawing process (Chen et al., 1998). The present findings revealed that with an increase in altitude in the study area, soil infiltration capacity increased, which would be helpful for the growth and development of *R. anthopogon*.

Soil MC significantly affects the growth and distribution of vegetation (Porporato et al., 2004; Paschalis et al., 2015). In the present study, we observed a significant increase in MC with altitude. The presence of high precipitation and low temperature at higher altitudes could explain this trend. Optimum MC in the soil increases the decomposition of organic matter and microbial movement, which controls nutrient availability (Zhou et al., 2002).

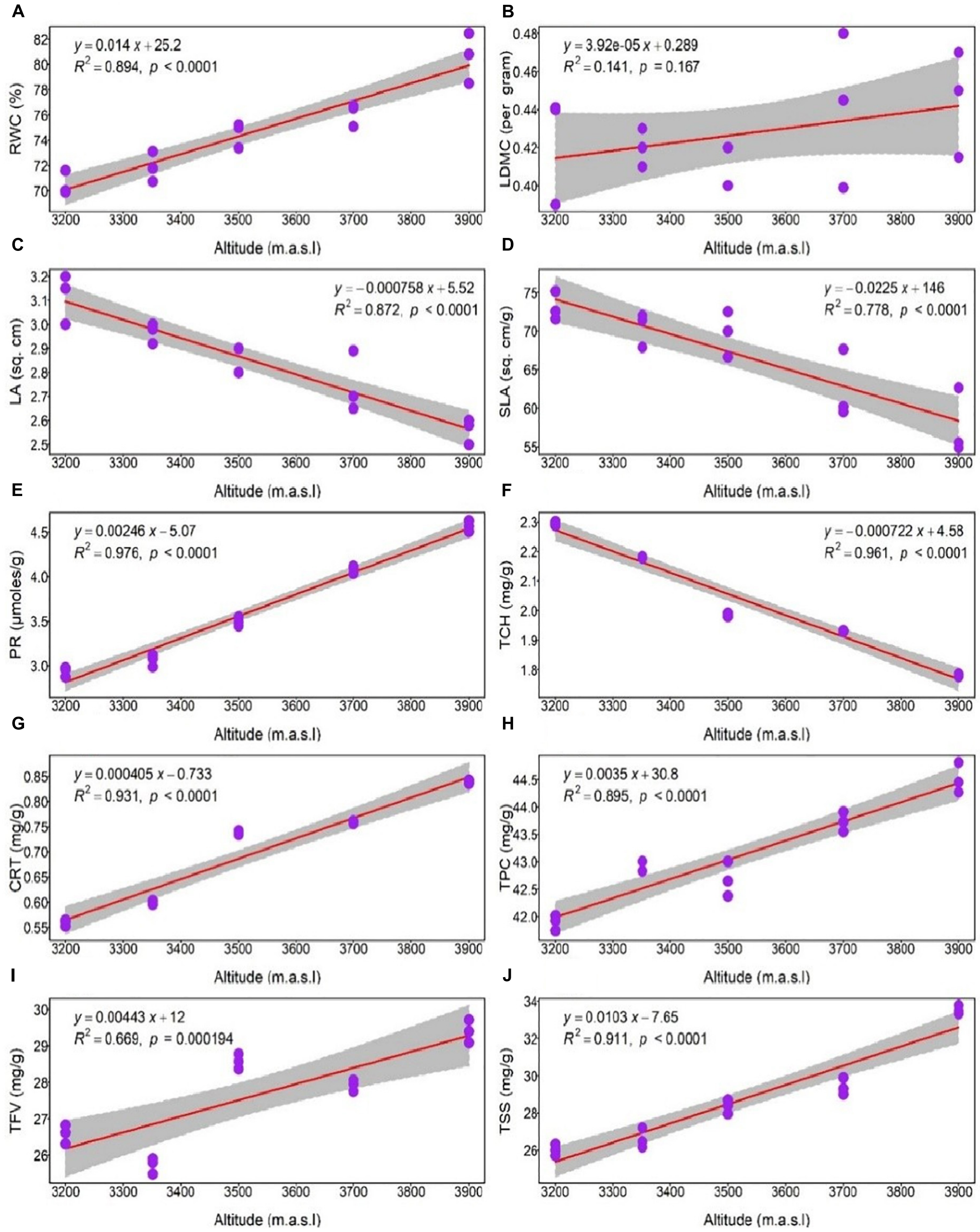

FIGURE 5
Linear regression representing a change in eco-physiological parameters of *Rhododendron anthopogon* along the altitude gradient. Relationship between altitude and **(A)** RWC, relative water content; **(B)** LDMC, leaf dry mass content; **(C)** LA, leaf area; **(D)** SLA, specific leaf area; **(E)** PR, proline content; **(F)** TCH, total chlorophyll; **(G)** CRT, carotenoid content; **(H)** TPC, total phenolics content; **(I)** TFV, total flavonoids; **(J)** TSS, total soluble sugars. Each purple dot in the plot represents the mean value of the eco-physiological parameters, and the gray areas represent a 95% confidence interval.

This might have an impact on *R. anthopogon's* ecophysiology. Like soil MC, the CD also showed an increased trend with altitude. Low temperature at higher altitudes is responsible for the slow decomposition of organic matter, leading to higher soil cation exchange capacity and increasing CD values (Bardelli et al., 2017). Similarly, we observed a slight rise in Mg, C, Na and S with the increasing altitude; thus, they are not limiting factors of alpine regions. A similar trend in micronutrient dynamics with respect to altitudinal variation was found (Wang et al., 2011; Kidanemariam et al., 2012; Charan et al., 2013; Du et al., 2014; Yang et al., 2018; Mishra and Francaviglia, 2021).

In the case of N and K, increasing trends along the altitudinal gradient were observed (**Figure 2**). These results align with several other studies (Göransson et al., 2014; Bardelli et al., 2017; Zhu et al., 2019). Differences in soil temperature along the altitudinal gradient in our study area could be attributed to the availability of different levels of soil N. Furthermore, an increased K concentration with altitude could be related to better rock and mineral dissolution in slightly higher acidic conditions at higher altitudes. Usually, the

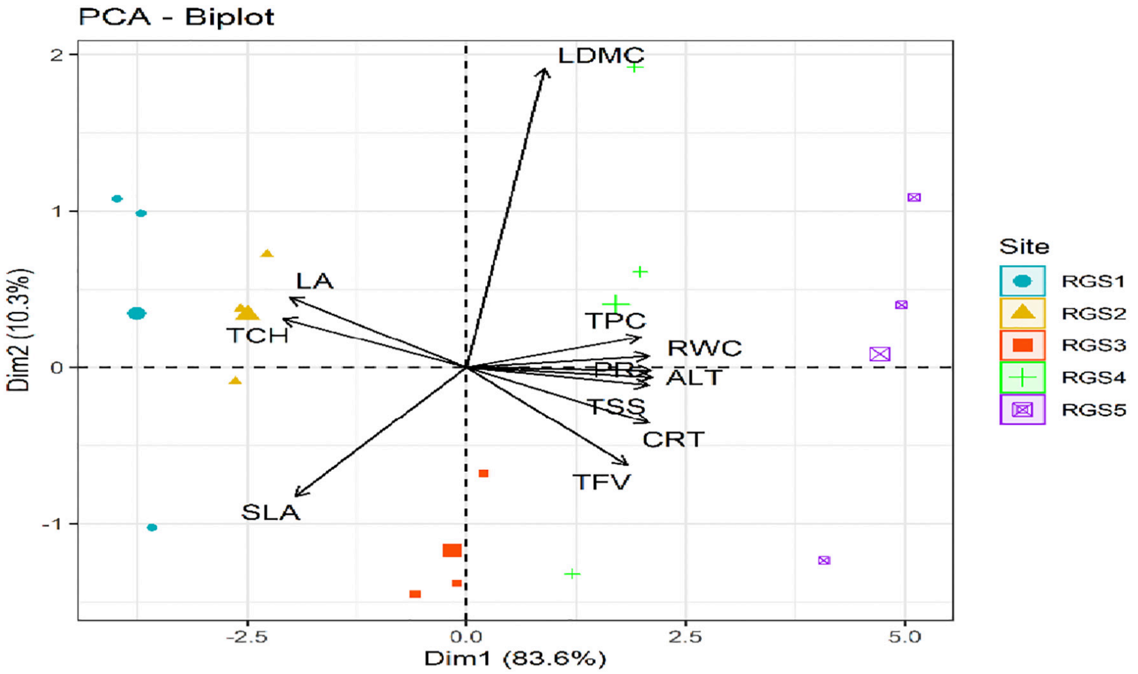

FIGURE 6
Principal component analysis (PCA) biplot of *Rhododendron anthopogon* eco-physiological traits across the five sampling sites: Site-1 (RGS1), Site-2 (RGS2), Site-3 (RGS3), Site-4 (RGS4), and Site-5 (RGS5) along an altitudinal gradient in the Gulmarg area of Kashmir Himalaya. RWC, relative water content; LDMC, leaf dry mass content; LA, leaf area; SLA, specific leaf area; PR, proline content; TCH, total chlorophyll; CRT, carotenoid content; TPC, total phenolics content; TFV, total flavonoids; TSS, total soluble sugars; ALT, altitude.

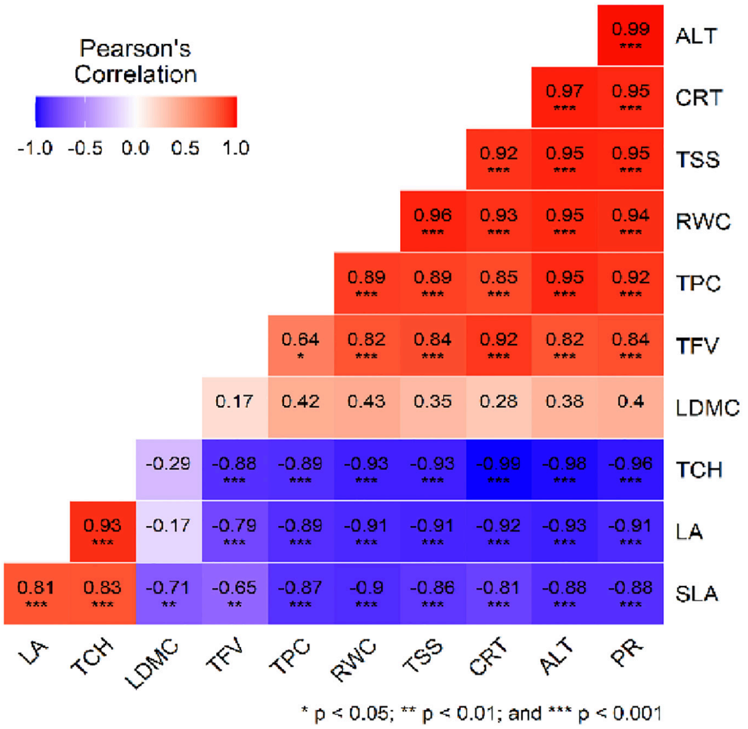

	LA	TCH	LDMC	TFV	TPC	RWC	TSS	CRT	ALT	PR
ALT										0.99 ***
CRT									0.97 ***	0.95 ***
TSS								0.92 ***	0.95 ***	0.95 ***
RWC							0.96 ***	0.93 ***	0.95 ***	0.94 ***
TPC						0.89 ***	0.89 ***	0.85 ***	0.95 ***	0.92 ***
TFV					0.64 *	0.82 ***	0.84 ***	0.92 ***	0.82 ***	0.84 ***
LDMC				0.17	0.42	0.43	0.35	0.28	0.38	0.4
TCH			-0.29	-0.88 ***	-0.89 ***	-0.93 ***	-0.93 ***	-0.99 ***	-0.98 ***	-0.96 ***
LA		0.93 ***	-0.17	-0.79 ***	-0.89 ***	-0.91 ***	-0.91 ***	-0.92 ***	-0.93 ***	-0.91 ***
SLA	0.81 ***	0.83 ***	-0.71 **	-0.65 **	-0.87 ***	-0.9 ***	-0.86 ***	-0.81 ***	-0.88 ***	-0.88 ***

* $p < 0.05$; ** $p < 0.01$; and *** $p < 0.001$

FIGURE 7
Pearson's correlation plot of the eco-physiological parameters and altitude. The distribution of each variable and correlation coefficient plus the significance level is given in the figure. Full forms of abbreviations are presented in Figure 6.

topsoil layer is more vulnerable to changing environments, such as changes in temperature, precipitation, and organic matter input (Hamid et al., 2020a). In all elevations of the study area, topsoil (0–10 cm) revealed a significantly higher concentration of soil parameters than the subsoil (10–20 cm). These results also conform to other studies (Huang et al., 2011; Liu et al., 2013; He et al., 2016; Qasba et al., 2017; Yang et al., 2018). The present study also indicates that leaching, commonly associated with alpines, did not occur in the study area, which plays an essential role in transporting the subsurface's extractable nutrients away from the surface layer (Hamid et al., 2020a).

4.2. Variation in eco-physiological parameters of *Rhododendron anthopogon* along an altitudinal gradient

We found a significant variation in eco-physiological parameters of *R. anthopogon* along altitude (**Table 2** and **Figure 5**). An increasing trend of RWC observed in the present study could be explained by high precipitation and low temperature at higher altitudes. However, Rathore et al. (2018) reported a negative relationship between RWC with altitude, while Schob et al. (2013) reported a positive correlation with altitude. Photosynthetic pigments which absorb and transform light directly impact plant photosynthetic capability and are susceptible to environmental challenges. Water stress, intense sunlight, and high temperature can diminish chlorophyll concentration by slowing chlorophyll synthesis, hastening decomposition, or causing damage to chloroplast structures (Ashraf and Harris, 2013; Hazrati et al., 2016; Cui et al., 2018). In the present study, TCH, LA and SLA decreased with increasing elevation, which could be an adaptive response of *R. anthopogon* to avoid oxidative damage by limiting light absorption and preventing reactive oxygen species (ROS) generation (Cui et al., 2018). Thus, plants have developed efficient ways to eliminate surplus energy to avoid damage to the photosynthetic mechanism at high altitudes where radiation is more potent (Li H. et al., 2022). This indicates that the efficient defense mechanism against damage from high radiation in *R. anthopogon* was primarily implemented through heat dissipation at higher altitudes. There was no discernible variation in LDMC throughout the altitudinal gradient; therefore, it is likely not a limiting factor in alpine areas.

Carotenoids are versatile compounds that play an essential role in photosynthesis and the construction of light-harvesting complexes, as well as can remove accumulated ROS efficiently to prevent photooxidation-related damage to chloroplasts (Armstrong and Hearst, 1996; Li T. X. et al., 2022). High altitudes are known to cause a decrease in carotenoid concentration, while the contrary has also been reported (Ahmad et al., 2016). Our study showed an increasing trend of CRT along the altitudinal gradient, indicating the possibility that environmental elements at a higher altitude may have encouraged the biosynthesis of CRT. These findings are consistent with other studies (Cui et al., 2018; Rathore et al., 2018). The significant decrease in TCH and the increase in CRT in high-altitude zones could be attributed to a reduction in photosynthesis and photoinhibition (Demmig-Adams and Adams, 1992).

Phenolic compounds protect plants from structural damage by shielding harmful UV-B radiations. Because of more intense UV-B radiation stress, plants in alpine regions are likely to include more phenolics than in low altitudes (Bernal et al., 2013). Similarly, we observe an increasing trend of TPC and TFV in *R. anthopogon* along an altitudinal gradient (**Figure 5**). These phenolic and flavonoid chemicals significantly improve the adaptation to abiotic oxidative stress (Hashim et al., 2020). Increasing phenolic concentrations have been reported as a herbivore defense system for plant attacks (Chadwick et al., 2013; Rathore et al., 2018). Herbivore attacks decrease with increasing altitude, which may account for the higher TPC at higher altitudes (Carey and Wink, 1994; Hodkinson, 2005; Rathore et al., 2018).

Proline and TSS are the two most significant osmotic regulators under abiotic stress conditions, allowing plants to tolerate harsh environments, such as cold temperatures (Bartels and Sunkar, 2005; Zhang et al., 2012; Adnan et al., 2016). Accumulation of proline with increasing altitude observed in the present study could effectively lower the freezing temperature and shield *R. anthopogon* from frozen injury, highlighting the significance of proline accumulation in plant adaptation. This concurs with previous related studies showing an increasing trend in proline (Ma et al., 2015; Cui et al., 2018; Rathore et al., 2018; Li T. X. et al., 2022). A significant increase in the TSS observed in the present study could be the ability of carbohydrates to withstand low temperatures and boost the supercooling capability of long-lasting *R. anthopogon* leaves (Rada et al., 2001). As described in earlier studies, the ability to accumulate soluble sugars on high mountains may also be the primary reason for the persistence of *R. anthopogon* in future (Rathore et al., 2018).

Overall, we observed significant variations in eco-physiological parameters, demonstrating their critical involvement in adapting *R. anthopogon* to the harsh environment of the alpine regions of Kashmir Himalaya. The observed patterns revealed how important trait flexibility is for the survival and function of this species. Additionally, it is believed that variation in traits brought on by plasticity in functional features will impact the expansion of this species' niche breadth, leading to more comprehensive ranges (Bolnick et al., 2011). The Himalayan region is warming considerably more quickly than the rest of the world; hence the projected climate change scenario will not face limitations imposed by low temperatures (Salinger et al., 2014). In alpine regions, this will cause shrubs to move upward. A prolonged growing season brought on by climate change will help *R. anthopogon* to spread to higher elevations (He et al., 2016; Rathore et al., 2018).

4.3. Relationship between soil physico-chemical parameters of *Rhododendron anthopogon* along an altitudinal gradient

Various environmental variables, such as temperature, moisture, oxygen, photoperiod, UV intensity, and light intensity, fluctuate along the altitudinal gradient (Chen et al., 2014). As the altitude rises, precipitation, light, oxygen pressure, and radiation intensity all rise while gravity and temperature decrease concurrently. Soil nutrients also significantly influence species distribution along an altitudinal gradient. Consequently, the impact of altitude on plant growth and development results from several elements functioning in concert (Ahmad et al., 2016). In the present study, the PCA analysis of studied soil physico-chemical parameters of *R. anthopogon* revealed that all the sites were grouped into four clusters according to altitude, suggesting a more pronounced effect of altitude (**Figure 3**). The most significant variables differentiating Site 1 and Site 2 from the rest were pH and temperature. Soil pH and Temperature are important factors affecting plant diversity in alpine regions. As soil pH directly affects nutrient availability, microbial activity, immobilization and mineralization (Curtin et al., 1998; Evans et al., 2012). At the same time, soil temperature affects alpine plants by providing a fundamental niche and is essential to withstand extreme climatic conditions (Hamid et al., 2020a). Accordingly, Site 5 was dominated by OM, K, ALT, and CD variables, significantly separating Site 5 from the rest of the four sites. These variables can be considered helpful for the growth and development of *R. anthopogon* at higher altitudes. This is consistent with the notion that changes in soil variables account for variation in vegetation in higher altitudes and the species-specific diversity of alpine plants (Arnesen et al., 2007; Hamid et al., 2020a).

The current investigation results showed that most soil variables had strong correlations with one another (**Figure 4**). This also conforms with results from other studies (Ahmad et al., 2016; Yang et al., 2018; Yuan et al., 2019; Hamid et al., 2020a). Litter decomposition and pH variations in the soil impact the overall availability of nutrients in the soil (Curtin et al., 1998). Soil pH is an essential factor regulating nutrient availability by favoring conditions that accelerate oxidation, mineralization, and immobilization (Mathew et al., 2016). In the present study, we noticed a substantial negative correlation of soil pH with ALT, MC, OM, K, SL and CD. This is in line with the fact that acidic solid conditions and decomposition rates at higher altitudes favored the availability of these soil variables. The present study also observed a significant positive correlation between soil pH with temperature. The increased temperature significantly increases soil pH. Guoju et al. (2012) reported that 0.5°C–2.0°C increases in winter temperature increased soil pH by 0.42–0.67 compared to no temperature increase. Similarly, soil K, MC, OM, SL, CD, and Ca show a significant positive correlation with altitude, suggesting their relationship enhances their availability. Therefore, the present study adds to our understanding that *R. anthopogon* have effective metabolic separation and resource preferences, even over short distances, due to their variable reactions to soil physico-chemical parameters, which may aid the conservation of this endemic species.

4.4. Relationship between eco-physiological traits of *Rhododendron anthopogon* along an altitudinal gradient

Efficient physiological modifications are essential for developing and growing high-altitude plants, as their seasonal changes are caused by environmental variables (Magaña Ugarte et al., 2019). In the present study, PCA analysis of studied eco-physiological traits of *R. anthopogon* revealed that Site 1 and Site 2 formed a separate group based on TCH and LA from the rest of the sites (**Figure 6**). TCH and LA are considered critical factors in promoting photosynthesis and growth (Takashima et al., 2004; Han et al., 2020). A higher concentration of these traits in Site 1 and Site 2 suggests an apparent disparity among altitudes. Similarly, Site 4 and Site 5 were separated by the most significant variables ALT, PR, RWC TPC, CRT, TSS and LDMC. Therefore, these variables might have a more dramatic impact on the eco-physiology of *R. anthopogon*. In a related study on *R. anthopogon* by Rathore et al. (2018), the PCA biplot showed distinct clusters based on the season compared to altitude. In another study, the eco-physiological traits of four *Rhododendrons* had similar adaptive features to warm and cold seasonal adversity in subalpine regions (Li H. et al., 2022). The present study's correlation analysis revealed a significant relationship among eco-physiological parameters (**Figure 7**). Our results indicated that the SLA, LA and TCH showed a significant negative correlation with the PR, ALT, CRT, TSS, RWC, TPC and TFV. This suggests that higher altitude with a low concentration of SLA, LA, and TCH favors the availability of PR, ALT, CRT, TSS, RWC, TPC, and TFV parameters. Galiba (1994) found a positive correlation between proline synthesis and plant adaptability. Other researchers have unambiguously stated that, in addition to other solutes, the proline level increase substantially during cold hardening (Galiba, 1994; Mahajan and Tuteja, 2005).

Furthermore, proline, which has been demonstrated to be an excellent cryoprotectant, is one of the critical variables associated with freezing tolerance (Mahajan and Tuteja, 2005). According to Kandler and Hopf (1982), cold stress caused TSS to accumulate in various plant species. For example, Bano and Fatima (2009) noted that higher-altitude alpine herbs in Pakistan's Hunza Valley had the highest level of TSS. To protect plant components such as cell membranes from cold stress, TSS buildup along the altitudinal gradient is an excellent method. The present study also observed a significant positive correlation of TPC, RWC, TSS, CRT and PR with the ALT. This indicates that these parameters play an important role in adapting *R. anthopogon* in the alpine regions of Kashmir Himalaya.

5. Conclusions

Understanding the variation in soil physico-chemical and eco-physiological attributes along altitudinal gradient is essential to predict indirectly how climate change will affect *R. anthopogon*. The present study revealed that soil physico-chemical and eco-physiological parameters along an altitudinal gradient significantly affect *R. anthopogon* in Kashmir Himalaya. We observed that with an increase in altitude in the study area, soil in filtration capacity increased, which would be helpful for the growth and development of *R. anthopogon*. A significant variation observed in eco-physiological parameters, demonstrating their critical involvement in adapting *R. anthopogon* to the harsh environment of the alpine regions of Kashmir Himalaya. Our results indicate how soil physico-chemical and eco-physiological properties help *R. anthopogon* spread widely and withstand various stresses. Additionally, by repeatedly observing the plasticity of soil physico-chemical and eco-physiological characteristics across different altitudes, we will be able to extrapolate the effects of climate change on these geographical gradients. The results generated during the present study also revealed that *R. anthopogon* has a significant potential for conducting studies on cold tolerance in the Himalaya's fragile ecology. Therefore, from the present work, we deduce that *R. anthopogon* has sufficient soil physico-chemical and eco-physiological plasticity, which should be favorable for its survival in future climates, offering an adaptive advantage and expanding its range shortly.

Data availability statement

The original contributions presented in this study are included in the article/**Supplementary material**, further inquiries can be directed to the corresponding author.

Author contributions

TD conceptualized, designed, and supervised the study. ZM carried out the field and laboratory work. SI, LT, SK, and AM, supported in field and laboratory work. RA, SG, RB, and SB analyzed the data. TD and ZM wrote the manuscript. All authors reviewed the manuscript and approved it for publication.

Funding

This work was supported by funding from Department of Biotechnology, Ministry of Science and Technology, Government of India, New Delhi, under grant no.: BT/PR29259/FCB/125/2/2018.

Acknowledgments

We are thankful to Dr. A. A. Shah, Associate Dean, School of Biosciences and Biotechnology, Baba Ghulam Shah Badshah University, Rajouri, for facilitating this work. During this work, financial support received from the Department of Biotechnology, Government of India, New Delhi to TD under grant no.: BT/PR29259/FCB/125/2/2018 is highly acknowledged.

Conflict of interest

The authors declare that the research was conducted in the absence of any commercial or financial relationships that could be construed as a potential conflict of interest.

Publisher's note

Supplementary material

The Supplementary Material for this article can be found online at: https://www.frontiersin.org/articles/10.3389/ffgc.2023.1181299/full#supplementary-material

References

Adamczyk, M., Hagedorn, F., Wipf, S., Donhauser, J., Vittoz, P., Rixen, C., et al. (2019). The soil microbiome of Gloria Mountain summits in the Swiss Alps. *Front. Microbiol.* 10:1080. doi: 10.3389/fmicb.2019.01080

Adnan, M. Y., Hussain, T., Asrar, H., Hameed, A., Gul, B., Nielsen, B. L., et al. (2016). *Desmostachya bipinnata* manages photosynthesis and oxidative stress at moderatesalinity. *Flora Morphol. Dist. Func. Ecol. Plants* 225, 1–9. doi: 10.1016/j.flora.2016.09.006

Ahmad, K. S., Hameed, M., Fatima, S., Ashraf, M., Ahmad, F., and Naseer, M. (2016). Morpho-anatomical and physiological adaptations to high altitude in some Aveneae grasses from NeelumValley, Western Himalayan Kashmir. *Acta Physiol. Plantar.* 38:93. doi: 10.1007/s11738-016-2114-x

Ahmad, K. S., Hameed, M., Hamid, A., Nawaz, F., Kiani, B. H., Ahmad, M. S. A., et al. (2018). Beating cold by being tough: impact of elevationon leaf characteristics in *Phleum himalaicum* Mez. endemic to Himalaya. *Acta Physiol. Plantar.* 40, 1–17. doi: 10.1007/s11738-018-2637-4

Ahrens, C. W., Andrew, M. E., Mazanec, R. A., Ruthrof, K. X., Challis, A., Hardy, G., et al. (2020). Plant functional traits differ in adaptability and arepredicted to be differentially affected by climate change. *Ecol. Evol.* 10, 232–248. doi: 10.1002/ece3.5890

Alberto, F. J., Aitken, S. N., Alía, R., González-Martínez, S. C., Hänninen, H., Kremer, A., et al. (2013). Potential forevolutionary responses to climate change–evidence from tree populations. *Glob. Change Biol.* 19, 1645–1661. doi: 10.1111/gcb.12181

Allen, B. L., and Hajek, B. F. (1989). Mineral occurrence in soil environments. *Min. Soil. Environ.* 1, 199–278. 2ed.c5 doi: 10.2136/sssabookser1

Allen, S. E., Grimshaw, H. M., Parkinson, J. A., Quarmby, C., and Roberts, J. D. (1974). *Chemical analysis of ecological materials*. London: Blackwell Scientific Publications.

Anderegg, W. R., Klein, T., Bartlett, M., Sack, L., Pellegrini, A. F., Choat, B., et al. (2016). Meta-analysis reveals that hydraulic traits explain cross-species patterns of drought-induced tree mortality across the globe. *Proc. Natl. Acad. Sci. U.S.A.* 113, 5024–5029. doi: 10.1073/pnas.1525678113

Anic, V., Hinojosa, L. F., Díaz-Forester, J., Bustamante, E., de la Fuente, L. M., Casale, J. F., et al. (2010). Influence of soil chemical variables and altitude on the distribution ofhigh-alpine plants: the case of the Andes of Central Chile. *Arctic Antarctic Alpine Res.* 42, 152–163. doi: 10.1657/1938-4246-42.2.152

Antonelli, A., Kissling, W. D., Flantua, S. G. A., Bermúdez, M. A., Mulch, A., MuellnerRiehl, A. N., et al. (2018). Geological and climatic influences onmountain biodiversity. *Nat. Geosci.* 11, 718–725. doi: 10.1038/s41561-018-0236-z

Armstrong, G. A., and Hearst, J. E. (1996). Carotenoids 2: genetics and molecular biology ofcarotenoid pigment biosynthesis. *FASEB J.* 10, 228–237. doi: 10.1096/fasebj.10.2.8641556

Arnesen, G., Beck, P. S., and Engelskjøn, T. (2007). Soil acidity, content of carbonates, and available phosphorus are the soil factors best correlated with alpine vegetation: evidence from Troms, North Norway. *Arctic Antarctic Alpine Res.* 39, 189–199. doi: 10.1657/1523-0430200739[189:sacoca]2.0.co;2

Arnon, D. I. (1949). Copper enzymes in isolated chloroplasts. Polyphenol oxidase in *Beta vulgaris*. *Plant Physiol.* 24, 1–15. doi: 10.1104/pp.24.1.1

Ashraf, M., and Harris, P. J. C. (2013). Photosynthesis under stressful environments: an overview. *Photosynthetica* 51, 163–190. doi: 10.1007/s11099-013-0021-6

Bano, A., and Fatima, M. (2009). Salt tolerance in *Zea mays* (L.) following inoculation withRhizobium and *Pseudomonas*. *Biol. Fertil. Soils* 45, 405–413. doi: 10.1007/s00374-008-0344-9

Bardelli, T., Gómez-Brandón, M., Ascher-Jenull, J., Fornasier, F., Arfaioli, P., and Francioli, D. (2017). Effects of slope exposure on soil physico-chemical and microbiological properties along an altitudinal climosequence in the Italian Alps. *Sci. Total Environ.* 575, 1041–1055. doi: 10.1016/j.scitotenv.2016.09.176

Bartels, D., and Sunkar, R. (2005). Drought and salt tolerance in plants. *Crit. Rev. Plant Sci.* 24, 23–58. doi: 10.1080/07352680590910410

Basso, A. S., Miguez, F. E., Laird, D. A., Horton, R., and Westgate, M. (2013). Assessing potential of biochar for increasing water-holding capacity of sandy soils. *Glob. Change Biol. Bioenergy* 5, 132–143. doi: 10.1111/gcbb.12026

Bates, L. S., Waldren, R. P., and Teare, I. D. (1973). Rapid determination of free proline for water-stress studies. *Plant Soil* 39, 205–207.

Bellard, C., Bertelsmeier, C., Leadley, P., Thuiller, W., and Courchamp, F. (2012). Impacts of climate change on the future of biodiversity. *Ecol. Lett.* 15, 365–377. 01736.x doi: 10.1111/j.1461-0248.2011

Bernal, M., Llorens, L., Julkunen-Tiitto, R., Badosa, J., and Verdaguer, D. (2013). Altitudinaland seasonal changes of phenolic compounds in *Buxus sempervirens* leaves and cuticles. *Plant Physiol. Biochem.* 70, 471–482. doi: 10.1016/j.plaphy.2013.06.012

Bhattacharjee, S. K. (1998). *Handbook of medical plants*. Jaipur: Pointer Publishers.

Bolnick, D. I, Amarasekare, P., Araújo, M. S., Bürger, R., Levine, J. M., Novak, M., et al. (2011). Why intraspecific trait variation matters in community ecology. *Trends Ecol. Evol.* 26, 183–192. doi: 10.1016/j.tree.2011.01.009

Bremner, J. M. (1965). "Total nitrogen," in *Methods of soil analysis: Part 2 chemical and microbiological properties*, Vol. 9, ed. A. G. Norman (Madison, WI: American Society of Agronomy), 1149–1178.

Carey, D., and Wink, M. (1994). Elevational variation of quinolizidine alkaloid contents in alupine (Lupinus argentus) of the rocky mountains. *J. Chem. Ecol.* 20, 849–857. doi: 10.1007/BF02059582

Chadwick, M., Trewin, H., Gawthrop, F., and Wagstaff, C. (2013). Sesquiterpenoids Lactones: benefits to plants and people. *Int. J. Mol. Sci.* 14, 12780–12805. doi: 10.3390/ijms140612780

Charan, G., Bharti, V. K., Jadhav, S. E., Kumar, S., Acharya, S., Kumar, P., et al. (2013). Altitudinal variations in soil physico-chemical properties at cold deserthigh altitude. *J. Soil Sci. Plant Nutr.* 13, 267–277. doi: 10.4067/S0718-95162013005000023

Chen, B. X., Zhang, X. Z., Tao, J., Wu, J. S., Wang, J. S., Shi, P. L., et al. (2014). The impact of climate change and anthropogenic activities on alpine grassland over the Qinghai-Tibet Plateau. *Agr. For. Meteorol.* 189, 11–18. doi: 10.1016/j.agrformet.2014.01.002

Chen, Y., Tessier, S., and Rouffignat, J. (1998). Soil bulk density estimation for soil tillagesystem and soil texture. *Trans. ASAE.* 41, 1601–1610. doi: 10.13031/2013.17328

Cui, G., Li, B., He, W., Yin, X., Liu, S., Lian, L., et al. (2018). Physiological analysis ofthe effect of altitudinal gradients on *Leymus secalinus* on the Qinghai-Tibetan Plateau. *PLoS One* 13:e0202881. doi: 10.1371/journal.pone.0202881

Curtin, D., Campbell, C. A., and Jalil, A. (1998). Effects of acidity on mineralization: dependence of organic matter mineralization in weakly acidic soils. *Soil Biol. Biochem.* 30:5764. doi: 10.1016/S0038-0717(97)00094-1

Dad, J. M., Muslim, M., Rashid, I., and Reshi, Z. A. (2021). Time series analysis of climatevariability and trends in Kashmir Himalaya. *Ecol. Indicat.* 126:107690. doi: 10.1016/j.ecolind.2021.107690

Decker, K. L., and Boerner, R. E. J. (2003). Elevation and vegetation influences on soil properties in Chilean Nothofagus forests. *Rev. Chil. Hist. Nat.* 76, 371–381.

Demmig-Adams, B., and Adams, W. W. (1992). Carotenoid composition in sun and shade leaves of plants with different life forms. *Plant Cell Environ.* 15, 411–419. doi: 10.1111/j.1365-3040.1992.tb00991.x

Du, B., Kang, H., Pumpanen, J., Zhu, P., Yin, S., Zou, Q., et al. (2014). Soil organiccarbon stock and chemical composition along an altitude gradient in the Lushan Mountain, subtropical China. *Ecol. Res.* 29, 433–439. doi: 10.1007/s11284-014-1135-4

Egli, M., Sartori, G., Mirabella, A., Favilli, F., Giaccai, D., and Delbos, E. (2009). Effect of northand south exposure on organic matter in high alpine soils. *Geoderma* 149, 124–136. doi: 10.1016/j.geoderma.2008.11.027

Enquist, B. J., Bentley, L. P., Shenkin, A., Maitner, B., Savage, V., Michaletz, S., et al. (2017). Assessingtrait-based scaling theory in tropical forests spanning a broad temperature gradient. *Glob. Ecol. Biogeogr.* 26, 1357–1373. doi: 10.1111/geb.12645

Evans, C. D., Jones, T. G., Burden, A., Ostle, N., Zielinski, P., Cooper, M. D., et al. (2012). Acidity controls on dissolved organic carbon mobility in organic soils. *Glob. Change Biol.* 18, 3317–3331. doi: 10.1111/j.1365-2486.2012.02794.x

Fatima, S., Hameed, M., Ahmad, F., Ahmad, M. S. A., Khalil, S., Munir, M., et al. (2022). Structural and functional responses in widespread distribution of some dominant grasses along climatic elevation gradients. *Flora* 289:152034. doi: 10.1016/j.flora.2022.152034

Freeman, B. G., Scholer, M. N., Ruiz-Gutierrez, V., and Fitzpatrick, J. W. (2018). Climatechange causes upslope shifts and mountaintop extirpations in a tropical bird community. *Proc. Natl. Acad. Sci. U.S.A* 115, 11982–11987. pnas.1804224115 doi: 10.1073/

Fyllas, N. M., Gloor, E., Mercado, L. M., Sitch, S., Quesada, C. A., Domingues, T. F., et al. (2014). Analysing Amazonian Forest productivity using a new individual and trait-based model (TFS v. 1). *Geosci. Model Dev.* 7, 1251–1269. doi: 10.5194/gmd-7-1251-2014

Galiba, G. (1994). In-vitro adaptation for drought and cold hardiness in wheat. *Plant Breeding Rev.* 12, 115–162. doi: 10.1002/9780470650493.ch5

Göransson, H., Edwards, P. J., Perreijn, K., Smittenberg, R. H., and Venterink, H. O. (2014). Rocks create nitrogen hotspots and N: P heterogeneity by funnelling rain. *Biogeochemistry* 121, 329–338. doi: 10.1007/s11104-016-2821-5

Griffiths, R. P., Madritch, M. D., and Swanson, A. K. (2009). The effects of topography on forestsoil characteristics in the Oregon Cascade Mountains (USA): implications for the effects ofclimate change on soil properties. *Forest Ecol. Manage.* 257, 1–7. doi: 10.1016/j.foreco.2008.08.010

Guoju, X., Qiang, Z., Jiangtao, B., Fengju, Z., and Chengke, L. (2012). The relationship between winter temperature rise and soil fertility properties. *Air Soil Water Res.* 5:8599. doi: 10.4137/ASWR.S8599

Gupta, A. K., Negi, M., Nandy, S., Alatalo, J. M., Singh, V., and Pandey, R. (2019). Assessing thevulnerability of socio-environmental systems to climate change along an altitude gradient in theIndian Himalayas. *Ecol. Indic.* 106:105512. doi: 10.1016/j.ecolind.2019.105512

Hamid, M., Khuroo, A. A., Malik, A. H., Ahmad, R., and Singh, C. P. (2020a). Elevation and aspect determine the differences in soil properties and plant species diversity on Himalayan Mountain summits. *Ecol. Res.* 36, 340–352. doi: 10.1111/1440-1703.12202

Hamid, M., Khuroo, A. A., Malik, A. H., Ahmad, R., Singh, C. P., Dolezal, J., et al. (2020b). Early evidence of shifts in alpine summit vegetation: a case study from KashmirHimalaya. *Front. Plant Sci.* 11:421. doi: 103389/fpls.2020.00421

Han, Y. J., Gharibeshghi, A., Mewis, I., Foerster, N., Beck, W., and Ulrichs, C. (2020). Plant responses to ozone: effects of different ozone exposure durations on plant growth and biochemical quality of Brassica campestris L. spp. chinensis. *Sci. Horticul.* 262:108921. doi: 10.1016/j.scienta.2019.108921

Hanway, J. J., and Heidel, H. (1952). Soil analysis methods as used in Iowa State College Soil Testing Laboratory. *Iowa Agric.* 57, 187–193.

Hashim, A. M., Alharbi, B. M., Abdul Majeed, A. M., Awatif, M., Elkelish, A., Hozzein, W. N., et al. (2020). Oxidative stress responses of some endemic plants to high altitudes byintensifying antioxidants and secondary metabolites content. *Plants* 9:869. doi: 10.3390/plants9070869

Hassan, W. H., and Nile, B. K. (2021). Climate change and predicting future temperature in Iraqusing CanESM2 and HadCM3 modeling. Model. *Earth Syst. Environ.* 7, 737–748. doi: 10.1007/s40808-020-01034-y

Haynes, R. J., and Naidu, R. (1998). Influence of lime, fertilizer and manure applications on soilorganic matter content and soil physical conditions: a review. *Nutr. Cycling Agroecosyst.* 51, 123–137. doi: 10.1023/A:1009738307837

Hazrati, S., Tahmasebi-Sarvestani, Z., Modarres-Sanavy, S. A. M., Mokhtassi-Bidgoli, A., and Nicola, S. (2016). Effects of water stress and light intensity on chlorophyll fluorescence parameters and pigments of Aloe vera L. *Plant Physiol. Biochem.* 106, 141–148. doi: 10.1016/j.plaphy.2016.04.046

He, X., Hou, E., Liu, Y., and Wen, D. (2016). Altitudinal patterns and controls of plant and soilnutrient concentrations and stoichiometry in subtropical China. *Sci. Rep.* 6:24261. doi: 10.1038/srep24261

Hodkinson, I. D. (2005). Terrestrial insects along elevation gradients: species and community responses to altitude. *Biol. Rev. Camb. Philos. Soc.* 80, 489–513. doi: 10.1017/s1464793105006767

Hoogsteen, M. J., Lantinga, E. A., Bakker, E. J., Groot, J. C., and Tittonell, P. A. (2015). Estimatingsoil organic carbon through loss on ignition: effects of ignition conditions and structural waterloss. *Eur. J. Soil Sci.* 66, 320–328. doi: 10.1111/ejss.12224

Hou, X., Han, H., Tigabu, M., Cai, L., Meng, F., Liu, A., et al. (2019). Changes in soilphysicochemical properties following vegetation restoration mediate bacterial community composition and diversity in Changting. *China. Ecol. Eng.* 138, 171–179. doi: 10.1016/j.ecoleng.2019.07.031

Huang, D., Yu, L., Zhang, Y., and Zhao, X. (2011). Belowground biomass and its relationship toenvironmental factors of natural grassland on the northern slopes of the Qilian mountains. *Acta Prataculturae Sinica.* 20, 1–10.

Husson, F., Josse, J., Le, S., Mazet, J., and Husson, M. F. (2020). *Package "FactoMineR"*. Available online at: https://github.com/husson/FactoMineR

Idris, O. A., Wintola, O. A., and Afolayan, A. J. (2017). Phytochemical and antioxidant activitiesof Rumex crispus L. in treatment of gastrointestinal helminths in Eastern Cape Province, SouthAfrica. *Asian Pac. J. Trop. Biomed.* 7, 1071–1078. doi: 10.1016/j.apjtb.2017.10.008

Kandler, O., and Hopf, H. (1982). Oligo saccharides based on sucrose. *Encycl. Plant Physiol. N. Ser.* 13, 348–382.

Kassambara, A., and Mundt, F. (2020). *Factoextra: Extract and visualize the results of multivariate data analyses (R package version 1.0.7).*

Kewlani, P., Negi, V. S., Bhatt, I. D., Rawal, R. S., and Nandi, S. K. (2021). Soil nutrients concentration along altitudinal gradients in Indian Western Himalaya. *Scand. J. For. Res.* 36, 98–104. doi: 10.1080/02827581.2020.1871065

Kidanemariam, A., Gebrekidan, H., Mamo, T., and Kibret, K. (2012). Impact of altitude and land use type on some physical and chemical properties of acidic soils in Tsegede Highlands, Northern Ethiopia. *Open J. Soil Sci.* 2, 223–233. doi: 10.4236/ojss.2012.23027

Körner, C. (2007). The use of 'altitude' in ecological research. *Trends Ecol. Evol.* 22, 569–574. doi: 10.1016/j.tree.2007.09.006

Körner, C. (2012). Treelines will be understood once the functional difference between a tree and a shrub is. *Ambio.* 41, 197–206. doi: 10.1007/s13280-012-0313-2

Kumar, S., and Srivastava, N. (2002). Herbal research in Garhwal Himalayas: Retrospects & amp. *Prospect. Ann. For.* 10, 99–118.

Kumar, S., Suyal, D. C., Yadav, A., Shouche, Y., and Goel, R. (2019). Microbial diversity andsoil physicochemical characteristic of higher altitude. *PLoS One.* 14:e0213844. doi: 10.1371/journal.pone.0213844

Lenoir, J., Gégout, J. C., Marquet, P. A., de Ruffray, P., and Brisse, H. (2008). A significant upward shift in plant species optimum elevation during the 20th century. *Science* 320, 1768–1771. doi: 10.1126/science.1156831

Li, H., Guo, Q., Yang, L., Quan, H., and Wang, S. (2022). Seasonal eco-physiologycharacteristics of four evergreen rhododendron species to the subalpine habitats. *Forests* 13:653. doi: 10.3390/f13050653

Li, Q., Liu, G. B., Zhang, Z., Tuo, D. F., Bai, R. R., and Qiao, F. F. (2017). Relative contribution of root physical enlacing and biochemistrical exudates to soil erosion resistance in the Loesssoil. *Catena* 153, 61–65. doi: 10.1016/j.catena.2017.01.037

Li, T. X., Shen-Tu, X. L., Xu, L., Zhang, W. J., Duan, J. P., Song, Y. B., et al. (2022). Intraspecific and sex-dependent variation of leaf traits along altitude gradient in the endangered dioecious tree Taxus fuana Nan Li & RR Mill. *Front. Plant Sci.* 13:996750. doi: 10.3389/fpls.2022.996750

Liang, J., Reynolds, T., Wassie, A., Collins, C., and Wubalem, A. (2016). Effects of exotic*Eucalyptus* spp. plantations on soil properties in and around sacred natural sites in the northernEthiopian highlands. *AIMS Agric. Food* 1, 175–193. doi: 10.3934/agrfood.2016.2.175

Liu, X. D., Zhao, W. J., Zhang, X. L., Jing, W. M., and Fan, L. M. (2013). Variation of soilnutrient content and pH value under *Picea crassifolia* forest in the Pailugou drainage basin in the Qilian mountains. *Arid Zone Res.* 30, 1013–1020.

Ma, L., Sun, X., Kong, X., Galvan, J. V., Li, X., Yang, S., et al. (2015). Physiological, biochemical and proteomics analysis reveals the adaptation strategies of the alpine plant *Potentilla saundersiana* at altitude gradient of the Northwestern Tibetan Plateau. *J. Prot.* 112, 63–82. doi: 10.1016/j.jprot.2014.08.009

Maclean, J. E., Mitchell, R. J., Burslem, D. F., Genney, D., Hall, J., and Pakeman, R. J. (2017). Understorey plant community composition reflects invasion history decades after invasive *Rhododendron* has been removed. *J. Appl. Ecol.* 55, 874–884. doi: 10.1111/1365-2664.12973

Magaña Ugarte, R., Escudero, A., and Gavilán, R. G. (2019). Metabolic and physiological responsesof Mediterranean high-mountain and alpine plants to combined abiotic stresses. *Physiol. Plant* 165, 403–412. doi: 10.1111/ppl.12898

Mahajan, S., and Tuteja, N. (2005). Cold, salinity, and drought Stresses: an overview. *Arch. Biochem. Biophys.* 444, 139–158. doi: 10.1002/9783527628964.ch7

Måren, I. E., Karki, S., Prajapati, C., Yadav, R. K., and Shrestha, B. B. (2015). Facing north orsouth: does slope aspect impact forest stand characteristics and soil properties in semiarid trans Himalayan valley? *J. Arid Environ.* 121, 112–123. doi: 10.1016/j.jaridenv.2015.06.004

Mathew, M. M., Majule, A. E., Marchant, R., and Sinclair, F. (2016). Variability of Soilmicronutrients concentration along the slopes of Mount Kilimanjaro, Tanzania. *Appl. Environ. Soil Sci.* 2016:9814316. doi: 10.1155/2016/9814316

Mayor, J. R., Sanders, N. J., Classen, A. T., Bardgett, R. D., Clement, J. C., Fajardo, A., et al. (2017). Elevation alters ecosystem properties across temperate treelinesglobally. *Nature* 542, 91–95. doi: 10.1038/nature21027

Mishra, G., and Francaviglia, R. (2021). Land uses, altitude and texture effects on soilparameters. A comparative study in two districts of Nagaland, northeast India. *Agriculture* 11:171. doi: 10.3390/agriculture11020171

Molina-Montenegro, M. A., Peñuelas, J., Munné-Bosch, S., and Sardans, J. S. (2012). Higher plasticity in ecophysiological traits enhances the performance and invasion success of *Taraxacum officinale* (dandelion) in alpine environments. *Biol. Invasions* 14, 21–33. doi: 10.1007/s10530-011-0055-2

Murtaza, K. O., and Romshoo, S. A. (2017). Recent glacier changes in the Kashmir alpine Himalayas, India. *Geocarto Int.* 32, 188–205. doi: 10.1080/10106049.2015.1132482

Nilsen, E. T. (1992). Thermonastic leaf movements: a synthesis of research with *Rhododendron. Bot. J. Linn. Soc.* 110, 205–233. 1992.tb00291.x doi: 10.1111/j.1095-8339

Northcott, M. L., Gooseff, M. N., Barrett, J. E., Zeglin, L. H., Takacs-Vesbach, C. D., and Humphrey, J. (2009). Hydrologic characteristics of lake and stream-side riparian margins in theMcMurdo Dry Valleys, Antarctica. *Hydrol. Process.* 23, 1255–1267. doi: 10.1002/hyp.7262

Olajire, A. A., and Azeez, L. (2011). Total antioxidant activity, phenolic, flavonoid and ascorbicacid contents of Nigerian vegetables. *Afr. J. Food Sci. Technol.* 2, 22–29.

Olsen, S. R., Cole, C. V., Watanabe, F. S., and Dean, L. A. (1954). *Estimation of availablephosphorus in soils by extraction with sodium bicarbonate circular No. 939.* Washington, DC: U.S.Department of Agriculture.

Paschalis, A., Fatichi, S., Katul, G. G., and Ivanov, V. Y. (2015). Cross-scale impact of climatetemporal variability on ecosystem water and carbon fluxes. *J. Geophy. Res. Biogeosci.* 120, 1716–1740. doi: 10.1002/2015JG003002

Peterson, B. G., and Carl, P. (2020). *Performance analytics: econometric tools for performance and risk analysis. R package version 2.0.4.*

Piao, S., Wang, X., Ciais, P., Zhu, B., Wang, T. A. O., and Liu, J. I. E. (2011). Changes insatellite-derived vegetation growth trend in temperate and boreal Eurasia from 1982 to 2006. *Glob. Change Biol.* 17, 3228–3239. 02419.x doi: 10.1111/j.1365-2486.2011

Pluess, A. R., Frank, A., Heiri, C., Lalagüe, H., Vendramin, G. G., and Oddou-Muratorio, S. (2016). Genome–environment association study suggests local adaptation to climate at the regional scale in Fagus sylvatica. *N. Phytol.* 210, 589–601. doi: 10.1111/nph.13809

Popescu, R., and Kopp, B. (2013). The genus Rhododendron: an ethnopharmacological and toxicological review. *J. Ethnopharmacol.* 147, 42–62. doi: 10.1016/j.jep.2013.02.022

Porporato, A., Daly, E., and Rodriguez-Iturbe, I. (2004). Soil water balance and ecosystem response to climate change. *The Amer. Nat.* 164, 625–632. doi: 10.1086/424970

Qasba, S., Masoodi, T. H., Bhat, S. J. A., Paray, P. A., Bhat, A., and Khanday, M. U. D. (2017). Effect of altitude and aspect on soil physicochemical characteristics in Shankaracharya Reserved Forest. *Int. J. Pure Appl. Biosci.* 5, 585–596.

Qi, X., Jia, J., Liu, H., and Lin, Z. (2019). Relative importance of climate change and humanactivities for vegetation changes on China & 39;s silk road economic belt over multipletimescales. *Catena* 180, 224–237. doi: 10.1016/j.catena.2019.04.027

R Core Team. (2020). *R: a language and environment for statistical computing.* Vienna: R Foundation for Statistical Computing.

Rada, F., García-Núñez, C., Boero, C., Gallardo, M., Hilal, M., González, J., et al. (2001). Low-temperature resistance in *Polylepis tarapacana*, a tree growing at the highest altitudes in the world. *Plant Cell Environ.* 24, 377–381. 00685.x doi: 10.1046/j.1365-3040.2001

Rapp, J. M., Silman, M. R., Clark, J. S., Girardin, C. A., Galiano, D., and Tito, R. (2012). Intra-and interspecific tree growth across a long altitudinal gradient in the Peruvian Andes. *Ecology* 93, 2061–2072. doi: 10.1890/11-1725.1

Rathore, N., Thakur, D., and Chawla, A. (2018). Seasonal variations coupled with elevationgradient drives significant changes in eco-physiological and biogeochemical traits of a high-altitude evergreen broadleaf shrub, Rhododendron anthopogon. *Plant Physiol. Biochem.* 132, 708–719. doi: 10.1016/j.plaphy.2018.08.009

Salinger, M. J., Shrestha, M. L., Ailikun, Dong, W., McGregor, J. L., and Wang, S. (2014). "Climate in Asia and the Pacific: climate variability and change," in *Climate in Asia and the Pacific*, Vol. 56, eds M. Manton and L. Stevenson (Dordrecht: Springer), doi: 10.1007/978-94-007-7338-7_2

Schob, C., Armas, C., Guler, M., Prieto, I., and Pugnaire, F. I. (2013). Variability in functional traits mediates plant interactions along stress gradients. *J. Ecol.* 101, 753–762. doi: 10.1111/1365-2745.12062

Shipley, B., De Bello, F., Cornelissen, J. H. C., Laliberté, E., Laughlin, D. C., and Reich, P. B. (2016). Reinforcing loose foundation stones in trait-based plant ecology. *Oecologia* 180, 923–931. doi: 10.1007/s00442-016-3549-x

Simon, A., Dhendup, K., Rai, P. B., and Gratzer, G. (2018). Soil carbon stocks along elevational gradients in Eastern Himalayan Mountain forests. *Geoder. Reg.* 12, 28–38. doi: 10.1016/j.geodrs.2017.11.004

Stöcklin, J., Kuss, P., and Pluess, A. R. (2009). Genetic diversity, phenotypic variation and local adaptation in the alpine landscape: case studies with alpine plant species. *Bot. Helv.* 119, 125–133. doi: 10.1007/s00035-009-0065-1

Sundqvist, M. K., Sanders, N. J., and Wardle, D. A. (2013). Community and ecosystem response to elevational gradients: processes, mechanisms, and insights for global change. *Annu. Rev. Ecol. Evol. Syst.* 44, 261–280. doi: 10.1146/annurev-ecolsys-110512-135750

Takahashi, K., and Matsuki, S. (2017). Morphological variations of the *Solidago virgaurea* L. complex along an elevational gradient on Mt Norikura, Central Japan. *Plant Species Biol.* 32, 238–246. doi: 10.1111/1442-1984.12148

Takashima, T., Hikosaka, K., and Hirose, T. (2004). Photosynthesis or persistence: nitrogen allocation in leaves of evergreen and deciduous Quercus species. *Plant Cell Environ.* 27, 1047–1054. 01209.x doi: 10.1111/j.1365-3040.2004

Taneda, H., and Noshiro, S. (2019). Altitudinal trends of efficiency and stability of water transport in the stems and leaves of Nepalese Rhododendron species, based on morphological traits. *Rhododendr. Int.* 3, 43–65.

Trujillo-González, J. M., Torres-Mora, M. A., Ballesta, R. J., and Brevik, E. C. (2022). Spatial variability of the physicochemical properties of acidic soils along an altitudinal gradient in Colombia. *Environ. Earth Sci.* 81:108. doi: 10.1007/s12665-022-10235-w

Tsui, C. C., Chen, Z. S., and Hsieh, C. F. (2004). Relationships between soil properties and slopeposition in a lowland rain forest of southern Taiwan. *Geoderma* 123, 131–142. doi: 10.1016/j.geoderma.2004.01.031

Visakorpi, K., Block, S., Pellissier, L., Levine, J. M., and Alexander, J. (2022). Eco-physiological and morphological traits explain alpine plant species' response to warming. *Funct. Ecol.* 37, 287–301. doi: 10.1111/1365-2435.14228

Walkley, A., and Black, I. A. (1934). An examination of the Degtjareff method for determining soil organic matter, and a proposed modification of the chromic acid titration method. *Soil Sci.* 37, 29–38. doi: 10.1097/00010694-193401000-00003

Wang, H., Prentice, I. C., Davis, T. W., Keenan, T. F., Wright, I. J., and Peng, C. (2017). Photosynthetic responses to altitude: an explanation based on optimality principles. *N. Phytol.* 213, 976–982. doi: 10.1111/nph.14332

Wang, W. J., Qiu, L., Zu, Y. G., Dong-Xue, S., Jing, A., Hong-Yan, W., et al. (2011). Changes in soil organic carbon, nitrogen, pH and bulk density with the development of larch (*Larix gmelinii*) plantations in China. *Glob. Change Biol.* 17, 2657–2676. doi: 10.1111/j.1365-2486.201102447.x

Wani, I. A., Khan, S., Verma, S., Al-Misned, F. A., Shafik, H. M., and El-Serehy, H. A. (2022). Predicting habitat suitability and niche dynamics of *Dactylorhiza hatagirea* and *Rheum webbianum* in the Himalaya under projected climate change. *Sci. Rep.* 12:13205. doi: 10.1038/s41598-022-16837-5

Wani, Z. A., and Pant, S. (2021). *Betula utilis* D. Don: an ecologically and economically important timberline species of himalayan region in jeopardy. *Bot. Rev.* 87, 377–391.

Wani, Z. A., Negi, V. S., Bhat, J. A., Satish, K. V., Kumar, A., Khan, S., et al. (2023). Elevation, aspect, and habitat heterogeneity determine plant diversity and compositional patterns in the Kashmir Himalaya. *Front. For. Glob. Change* 6:1019277. doi: 10.3389/ffgc.2023.1019277

Weiping, M., and Guangchuang, Y. (2020). *Basic trendline: add trendline and confidence interval of basic regression models to plot. R package version 2.0.5.*

Wen, H. Y., Zhao, H. L., and Fu, H. (2005). Effects of years for reclamation and enclosure yearson soil properties of degraded sandy grassland. *Acta Pratacul. Sin.* 14, 31–37.

Yang, Y., Wu, J., Zhao, S., Han, X., He, F., and Chen, C. (2018). Assessment of the responses of soil pore properties to combined soil structure amendments using X-ray computed tomography. *Sci. Rep.* 8:695. 18997-1 doi: 10.1038/s41598-017-

Yemm, E. W., and Willis, A. J. (1954). The estimation of carbohydrates in plant extracts by anthrone. *Biochem. J.* 57, 508–514. doi: 10.1042/bj0570508

Yuan, Z. Q., Jiang, X. J., Liu, G. J., Jin, H. J., Chen, J., and Wu, Q. B. (2019). Responses of soilorganic carbon and nutrient stocks to human-induced grassland degradation in a Tibetan alpinemeadow. *Catena* 178, 40–48. doi: 10.1016/j.catena2019.03.001

Zhang, S. B., Zhang, J. L., Slik, J. W. F., and Cao, K. F. (2012). Leaf element concentrations of terrestrial plants across China are influenced by taxonomy and the environment. *Glob. Ecol. Biogeogr.* 21, 809–818. doi: 10.1111/j.1466-8238.2011.00729.x

Zhang, Y., Ai, J., Sun, Q., Li, Z., Hou, L., Song, L., et al. (2021). Soil organic carbon and total nitrogen stocks as affected by vegetation types and altitude across the mountainous regions in the Yunnan Province, south-western China. *Catena* 196:104872. doi: 10.1016/j.catena.2020.104872

Zhou, J., Xia, B., Treves, D. S., Wu, L. Y., Marsh, T. L., O'Neill, R. V., et al. (2002). Spatial and resource factors influencing high microbial diversity insoil. *Appl. Environ. Microbiol.* 68, 326–334. doi: 10.1128/AEM.68.1.326-334.2002

Zhou, X., Chen, S., Wu, H., Yang, Y., and Xu, H. (2017). Biochemical and proteomics analyses of antioxidant enzymes reveal the potential stress tolerance in *Rhododendron chrysanthum. Pall. Biol. Direct* 12, 1–9. doi: 10.1186/s13062-017-0181-6

Zhu, M., Feng, Q., Qin, Y., Cao, J., Zhang, M., Liu, W., et al. (2019). The role of topography in shaping the spatial patterns of soil organic carbon. *Catena* 176, 296–305. doi: 10.1016/j.catena.2019.01.029

frontiers | Frontiers in Forests and Global Change

TYPE Original Research
PUBLISHED 15 June 2023
DOI 10.3389/ffgc.2023.1199304

OPEN ACCESS

EDITED BY
Shreekar Pant,
Baba Ghulam Shah Badshah University, India

REVIEWED BY
Marifatul Haq,
University of Kashmir, India
Yashwant Singh Rawat,
Federal Technical and Vocational Education and Training Institute (FTVETI), Ethiopia

*CORRESPONDENCE
Chunnan Fan
✉ fanchunnanbh@163.com

RECEIVED 03 April 2023
ACCEPTED 30 May 2023
PUBLISHED 15 June 2023

CITATION
Liu Q, Cheng Y, Yu F and Fan C (2023) The effects of forest types and age groups on forest provisioning and supporting service value in Sanhu Nature Reserve, Northeast China.
Front. For. Glob. Change 6:1199304.
doi: 10.3389/ffgc.2023.1199304

The effects of forest types and age groups on forest provisioning and supporting service value in Sanhu Nature Reserve, Northeast China

Qiang Liu[1], Yan Cheng[2], Fang Yu[1] and Chunnan Fan[1]*

[1]Forestry College, Beihua University, Jilin City, Jilin, China, [2]Jilin Songhuajiang Sanhu National Nature Reserve Administration, Jilin City, Jilin, China

The promotion of forest resource protection and sustainable development relies greatly on the value of forest ecosystem services. In Jilin Songhuajiang Sanhu National Nature Reserve in Northeast China, a total of 169 sample plots were examined and analyzed to evaluate the provisioning and supporting services provided by the forest ecosystem. The study revealed that the near-mature and over-mature *Fraxinus mandshurica* forest have relatively high timber supply and species resources conservation values per unit area, respectively. Furthermore, the mature *Betula platyphylla* forest has the highest forest nutrient retention value, while the near-mature *Juglans mandshurica* forest has the highest soil conservation value, with the nitrogen fixation value accounting for the highest proportion. The forest ecosystem services in the reserve have a total value of 659.07 million $\$\cdot y^{-1}$. The main contributors to the value are the services of soil fertilizer conservation, timber supply, and species resources conservation, with the mixed broad-leaved forest and *Quercus mongolica* forest being the main contributors, accounting for 63.1 and 18.8% of the total value, respectively. Nonetheless, the service value of per unit area in *J. mandshurica* forest is the highest. Near-mature and mature forests are the main contributors to the total value, accounting for 42.3 and 34.9%, respectively. Forest lands exhibit significant variations in the values of provisioning and supporting services across different stand types and age groups.

KEYWORDS

nature reserve, forest ecosystem, forest type, age group, supporting service value, provisioning service value

1. Introduction

The forest ecosystem is a crucial component of the global natural ecosystem and plays an integral role in ensuring sustainable human development (Ma et al., 2021). Unfortunately, people's understanding of the forest ecosystem has been limited to its economic uses, particularly the provision of timber and forest by-products for economic development, with a lack of comprehensive understanding of its service values (Hettiarachchi and Ranasinghe, 2013). Despite the high economic value of forest wood, it is not adequately accounted for in political and economic policies resulting in insufficient investments in its protection and management. The one-sided pursuit of rapid economic development has led to significant damage to the ecosystem (Smith et al., 2019). Therefore, raising awareness regarding the importance of the ecosystem has become a pressing issue. A scientific and comprehensive evaluation of forest ecosystem service value has become a global focus and hot issue (Niu et al., 2012; Ninan and Inoue, 2013b).

Ecosystem services are essential for human survival as they provide nutritious food, and clean water, regulate disease and climate, support crop pollination and soil formation, and offer recreational, cultural, and spiritual benefits. Ecosystems provide four main types of services to the world, namely provisioning services, regulating services, supporting services, and cultural services (Food and Agriculture Organization, 2020). However, quantifying the aesthetic appreciation of nature and the inspiration it provides for culture and innovation remains challenging. To quantitatively estimate service values, scholars have employed various methods, including the conditional value method, market value method, emergy evaluation method, and income conversion method, to assess ecosystem service values (Costanza et al., 1997; Odum and Odum, 2000; Zhang, 2010; Hidemichi et al., 2017). Some researchers have evaluated the ecosystem service values based on ecology alone (Daily and Ehrlich, 1999), while others investigate the impact of biodiversity on ecosystem services to characterize their value (Fromm, 2000; Farnsworth et al., 2012). Given the structural complexity and peculiarities of different ecosystems, evaluation techniques, and methods have garnered significant attention to ensure accurate service value assessment (Villa et al., 2014; Cheng et al., 2019).

Since the 1950s, various methods such as the travel cost, replacement cost, and contingent valuation method have been utilized internationally to assess the direct use value of forest ecosystems (Tobias and Mendelsohn, 1991; Hanley, 1993; Beaumont et al., 2014). It has been estimated that the per unit area value of forest ecosystem services in Mexico is US$80 per year, totaling to US$4 billion (Adger and Weiguang, 1995). Some scholars have calculated the overall value of forest ecosystems in national nature reserves (Tobias and Mendelsohn, 1991; Hanley, 1993; Ninan and Inoue, 2013a; Beaumont et al., 2014; Jin et al., 2016; Chang et al., 2019; Liu et al., 2022). Moreover, utilizing NOAA-AVHRR and Landsat imagery, the ecosystem service value of land under various use methods was calculated (Konarska et al., 2002). By considering tourists' preferences for landscapes in the protected areas and utilizing the travel cost method, recreational value of the protected area can be inferred. The recreational value of the conservation area can be estimated by analyzing the tourists' demand for the landscape (Font, 2000), and other values such as timber supply value, soil conservation value, forest nutrient retention, and species conservation value can be evaluated based on stock volume, soil erosion, tree nutrients, and species composition (Villa et al., 2014; Cheng et al., 2019).

In recent years, there has been an increase in studies on the service values of different forest ecosystems based on small-scale areas, particularly forest nature reserves. These reserves can be classified into various value areas based on plant and animal species, environmental categories, species richness, and other factors, and the conservation priority can be ranked based on the evaluation value (Goodfellow and Peterken, 1981). By considering tourists' preferences for landscapes in the protected areas and utilizing the travel cost method, recreational value of the protected area can be inferred. The recreational value of the conservation area can be estimated by analyzing the tourists' demand for the landscape (Font, 2000), and other values such as timber supply value, soil conservation value, forest nutrient retention, and species conservation value can be evaluated based on stock volume, soil erosion, tree nutrient, and species composition (Villa et al., 2014; Cheng et al., 2019). The study on the value of forest nature reserves has garnered the attention of scholars worldwide, and the evaluation system of nature reserves has been scientifically divided into different types such as conservation value, resource value, and economic value (Zhang et al., 2011). However, there are still issues such as the lack of standardization and uniformity in evaluation methods, and incomplete evaluation metrics.

Forest type and forest have a significant impact on forest structure, plant growth, and vegetation biomass accumulation (Shengjun et al., 2009; Grytnes, 2010; Gamfeldt et al., 2013), so they are fundamental factors that strongly influence the ecosystem services provided by forests. As time passes, the biomass, biodiversity, and soil quality of forest ecosystems change, and different tree species exhibit significant differences in their biomass and nutrient content (Gamfeldt et al., 2013; Musavi et al., 2017; Kuuluvainen and Gauthier, 2018), compared with other service functions, the change of forest type and forest age has a more direct relationship with the function of support and provision service. Therefore, studying the support and provision of ecosystem services from the perspective of forest age and type can accurately quantify the value of these services, and the assessment results of the ecosystem service value in different forest types and ages are highly practical and scientific to provide evidence and guidance for the rational management, protection, and sustainable utilization of forests. Therefore, the primary aim of this study is to analyze the forest provision and support service values in Jilin Songhuajiang Sanhu National Nature Reserve under various forest types and age groups. Additionally, the study intends to perform a comprehensive evaluation of the forest supply value, species resource conservation value, forest nutrient retention value, and soil conservation value in forests with different types and ages. The results of this study can be used by policymakers to identify target forests for enhancing forest service values through operational strategies.

2. Materials and methods

2.1. Study area

The Jilin Songhuajiang Sanhu National Nature Reserve is located in the central and eastern part of Jilin Province (42°20′10″∼43°33′06″N, 126°51′40″∼127°45′21″E) (**Figure 1**), which undertakes the functions of soil and water conservation and groundwater recharge in the Songhua River Basin, and it is an important hydropower base in Northeast China. The climate belongs to the continental monsoon climate of northern temperate zone. The annual average temperature is between 3.9 and 4.9°C. The average temperature in January and July is about −18 and 20°C, respectively. The average annual precipitation is about 644.8∼825.1 mm, and the rainfall is concentrated in June to August. The annual sunshine hours is 2,350∼2,450 h, and the frost-free period is 92∼134 days. The soil type is mainly dark brown soil. The reserve is dominated by mountain forest ecosystems, with abundant plant resources, which can be divided into seven types: coniferous forest, mixed coniferous and broad-leaved forest, deciduous broad-leaved forest, shrub, meadow, swamp, and aquatic vegetation. The forestland area is 122,800 ha, accounting for 78.4% of the total area of the reserve, and which is mainly closed forest land, with an area of 111,500 ha. The forest community types are mainly broad-leaved mixed forest and oak forest, and the main dominant tree species include *Pinus koraiensis*, *Fraxinus mandshurica*, *Phellodendron amurense*, *Chosenia arbutifolia*, *Tilia amurensis*, *Juglans mandshurica*, *Quercus mongolica*, and so on. However, affected by many factors such as man-made destruction, historical unreasonable development, natural disasters, and global climate change, the Sanhu Reserve is faced with a variety of ecological environmental problems and protection pressure (Lei, 2006), and clarifying the service value of the forest ecosystem in this region is an important basis for determining the protection object and strength. Maintaining the quality of air and soil, providing flood and disease control, or pollinating crops are some of the regulating services provided by ecosystems, and the non-material benefits of aesthetic inspiration, cultural identity, sense of home, and spiritual experience related to the natural environment are called cultural services, but it is still difficult to accurately and quantitatively evaluate the value of regulating services and cultural services from a large regional scale, especially considering the conditions of different forest types and ages.

2.2. Field investigation and sample analysis

According to the historical forest resource inventory data of study area, it is known that the main forest community types in the reserve include *Betula platyphylla* forest, *F. mandshurica* forest, *J. mandshurica* forest, *Q. mongolica* forest, mixed broad-leaved forest, and mixed coniferous broad-leaved forest. In order to obtain the values of the provisioning and supporting services provided by different forest types and age groups in the reserve, the sample plots in each forest type were selected based on the reserve's forest types, age groups, distribution area, and proportion of each forest type. A total of 169 plots were set up and investigated in different forest stand types in the reserve (**Figure 1**), the stand types, age groups, and number of plots in each forest type are shown in **Table 1**. The sample plots for the investigation of the basic characteristics of the community were selected from the representative sections of the typical community. The forest compass was used to enclose the rectangular basic survey plots of the community with an area of 20 m × 30 m (Song et al., 2002), and then measured the tree height and DBH (diameter at breast height) of each tree in the plot, and record the basic information of the tree species, and only record the tree species and tree height for the individuals whose tree height is <1.3 m. Five small quadrats with an area of 2 m × 2 m were set up at the corners and center of the plot to survey shrubs (Song et al., 2002; Yuan et al., 2015; see **Figure 2**), and we recorded the species, average height, and number of shrubs within these plots. Within each shrub plot, one small plot with an area of 1 m × 1 m was designated to survey herbaceous plants (Song et al., 2002; Yuan et al., 2015), and the species, height, number, and coverage of herbaceous plants were surveyed and recorded, and then the average plant height was obtained by calculating the average plant height of different species of herbaceous plants.

To clarify the age group and annual volume growth of forests, about five standard trees of dominant tree species in each survey plot were selected for the collection of annual ring strips, and the annual ring sample core was collected at 1.3 m above the ground of the sample tree with a growth cone to drill from south to north, and then put it into a straw, and record the tree species, DBH, skin thickness, and collection time. Then, the age group of forest was determined based on the average age of the group specie, and the criteria for age group classification are shown in **Table 1**, which mainly includes young forests, half-mature forests, near-mature forests, mature forests, and over-mature forests for each forest type. A total of 10 tree species (*B. platyphylla* Sukaczev, *Populus davidiana* Dode, *F. mandshurica* Rupr., *J. mandshurica* Maxim., *P. amurense* Rupr., *T. amurensis* Rupr., *Q. mongolica* Fisch. ex Ledeb., *Ulmus davidiana* Planch. var. *Japonica* (Rehd.) Nakai, *Acer pictum* Thunb., and *P. koraiensis* Sieb et Zucc.) sample cores were obtained, with 20∼25 ring sample cores for each tree species, and after processing the sample cores, the Lintab tree ring analyzer was used to accurately measure the annual ring width of the tree ring samples.

To determine the nutrient content and bulk density of the soil in each plot, we collected five surface soil samples, the sampling sites are shown in **Figure 2**. After being brought back to the laboratory, the samples are naturally air-dried, and then the dried particles, fine roots, and other impurities are removed from the air-dried soil with tweezers. The samples are then ground and screened through a 0.25 mm steel sieve for subsequent chemical property analysis. At the same time, a 100 cm^3 soil core sampler is used to collect undisturbed soil from each sampling point, which are then used for soil density determination (NY/T 1,121.4). The main analysis indicators include soil organic matter (LY/T 1,237–1,999), total nitrogen (LY/T 1,228–1,999), total phosphorus (LY/T 1,232–1,999), and total potassium (LY/T 1,232–1,999), etc. In addition, the leaf, branch, stem, and root organ samples from 55 trees of the 10 dominant tree species in the plots were collected, and a total of 220 mixed samples of each organ were obtained, and the total nitrogen, total phosphorus and total potassium in each sample were determined (LY/T 1,271–1,999).

2.3. Statistical analysis

Statistical analysis of the data was carried out using software such as SPSS16.0 and SAS9.1. The current study mainly evaluates the provisioning and supporting service functions according to the "Specifications for assessment of forest ecosystem services" (GB/T 38582-2020) (NFGA, 2020), and the main value indicators for evaluation include the forest supply value, species resource conservation value, soil conservation value, and forest nutrition retention value.

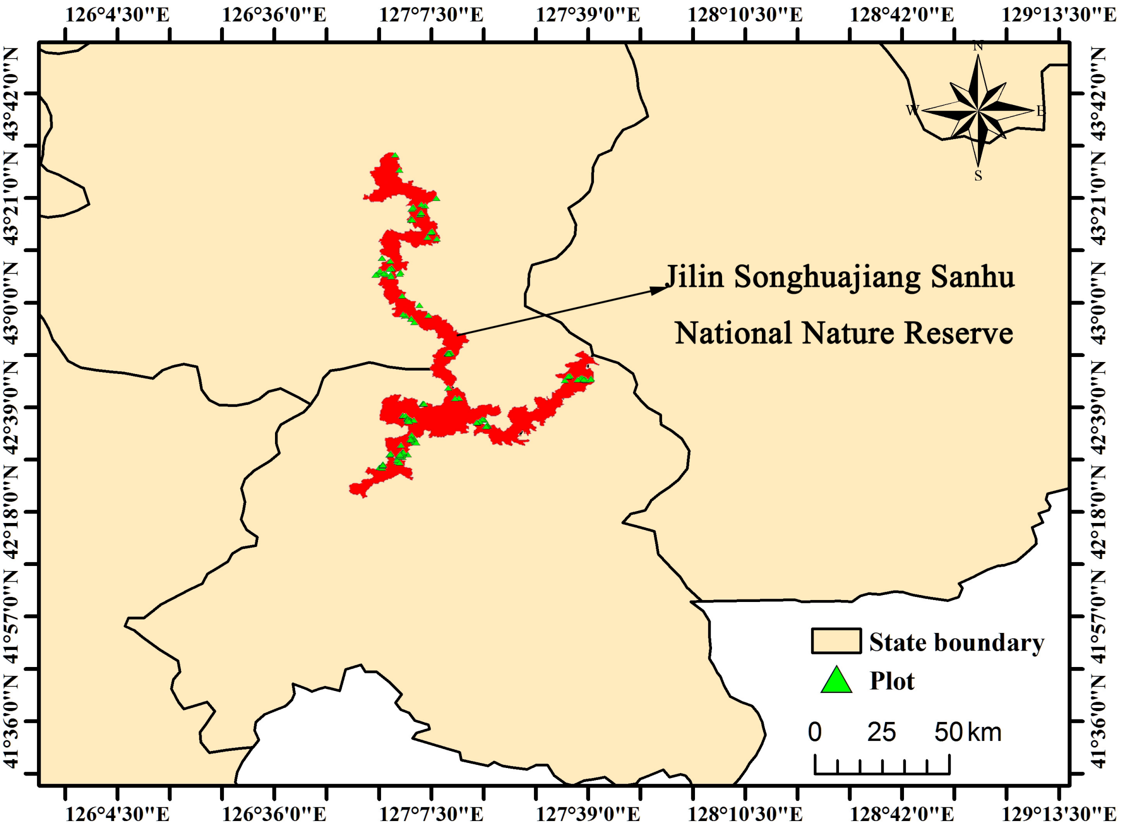

FIGURE 1
Study area and the plots of sites.

TABLE 1 Sample plots and forest distribution status.

Age group		Stand type					
		Betula platyphylla forest	*Fraxinus mandshurica* forest	*Juglans mandshurica* forest	*Quercus mongolica* forest	Mixed broad-leaved forest	Mixed coniferous broad-leaved forest
Young	Number of plots	6	1	1	3	11	2
	Area (ha)	297	179	44	393	836	2,000
	Age (years)	Below 30	Below 40	Below 40	Below 40	Below 40	Below 60
Half-mature	Number of plots	5	2	3	3	13	4
	Area (ha)	926	178	549	8,625	8,837	1,349
	Age (years)	31–50	41–60	41–60	41–60	41–60	61–100
Near-mature	Number of plots	4	1	4	3	33	4
	Area (ha)	2,028	691	2,682	1,415	25,645	1,512
	Age (years)	51–60	61–80	61–80	61–80	61–80	101–120
Mature	Number of plots	5	2	2	3	39	4
	Area (ha)	1,867	884	27,054	7,602	26,295	822
	Age (years)	61–80	81–120	81–120	81–120	81–120	121–160
Over-mature	Number of plots	1	1	1	1	5	2
	Area (ha)	147	232	177	1,188	2,983	416
	Age (years)	Above 81	Above 121	Above 121	Above 121	Above 121	Above 161

Age group classification is derived from "Technical regulations for inventory for forest management planning and design" (GB/T 26424-2010) (NFGA, 2010).

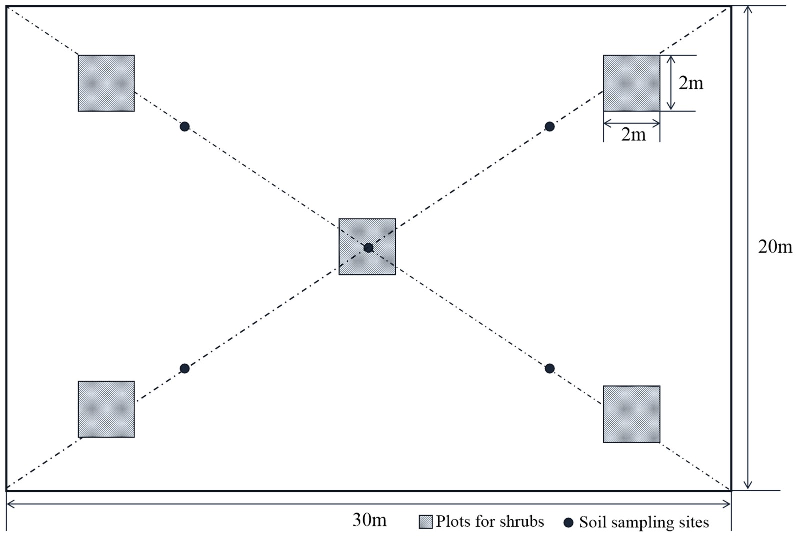

FIGURE 2
Distribution of quadrats and soil sample points.

2.3.1. Forest supply value

The supply values of different individual timber are calculated based on the annual volume growth of the main tree species in different stand types, and then sum up to obtain the forest supply value ($\$\cdot ha^{-1}\cdot y^{-1}$) of per unit area for different stand types and age groups, which mainly refers to the value of living trees in the study area, the calculation formula is as follow:

$$U_{\text{wood product}} = \sum_{i}^{n} (S_i U_i A_i) \tag{1}$$

where, $U_{\text{woodproduct}}$ is the annual timber supply product value in the study area ($\$\cdot y^{-1}$); A_i is the distribution area of the i-th wood product (ha); S_i is the annual volume growth per unit area of the i-th wood product ($m^3\ ha^{-1}\cdot y^{-1}$); U_i is the price of the i-th wood product ($\$\cdot m^{-3}$); $i = 1,2,3\ldots n$.

This study conducted statistical analysis on the annual ring samples of 10 major tree species in the study area, and plotted their diameter growth curves. By using the fitting equation of the diameter growth curve of each tree species and the stand volume table for single trees in Jilin Province (JPFD, 2003), this study calculated and analyzed the 2-year volume and stand volume per unit area for each tree species. Furthermore, the study obtained the unit area increment of stand volume (Si) for different forest types. The arithmetic average of the measured annual ring width data of different tree species was used to eliminate differences in different growth processes and growth environments. And because there is an error in drilling the annual ring samples, there will be a difference between the DBH calculated from the annual ring sample and the actual measurement value. Therefore, it is necessary to correct the annual ring width and the values measured by the girth to improve the accuracy of the DBH, the correction formula is as follows (Eq. 1):

$$\theta = \frac{D_{bh} - D_{ic}}{2t} \tag{2}$$

where θ is the corrected value (cm); D_{bh} is the DBH measured by a tape (cm); D_{ic} is the product of the accumulation of complete growth core growth ring sequence and complete DBH (cm); t is the tree age from tree core determination. The corrected tree-ring sequence is obtained by adding the θ value to each tree-ring sequence, which takes the existing bark thickness as part of the xylem (Zhang et al., 2012).

2.3.2. Species resource conservation value

According to the calculation formula of species resource conservation value in the assessment standard of "Specifications for assessment of forest ecosystem services" (NFGA, 2020), endangered species and ancient trees are included in the species conservation value evaluation. In the current study, the classification and statistics of plant species in various plots are based on the "China Species Red List" and its index system and ancient tree age index system.

The formula for calculating species conservation value is as follows:

$$Ui_{\text{biata}} = \left(1 + \sum_{m=1}^{x} E_m \times 0.1 + \sum_{n=1}^{y} B_n \times 0.1 + \sum_{r=1}^{z} O_r \times 0.1\right) A_i S_{\text{biota}} \tag{3}$$

where, Ui_{biota} is the value of the forest to protect biodiversity every year ($\$\cdot y^{-1}$); E_m is the rare and endangered index assessing species m within a stand (or area); x is the counted number of rare and endangered species; B_n is the endemic index for assessing species n within a stand (or area); O_r is the ancient tree age index for evaluating species r in the stand (or area); z is the number of species for calculating ancient tree species; S_{biota} is the opportunity cost of annual species loss per unit area ($\$\cdot ha^{-1}\cdot y^{-1}$), and the corresponding Shannon-Wiener index classes and values are shown in **Table 2** (GB/T 38582-2020); A_i is the forest area (ha); $i = 1,2,3\ldots n$.

The formula for the Shannon-Wiener index calculation is as follows:

$$H' = -\sum_{i=1}^{S} P_i \ln P_i \tag{4}$$

where, H' is Shannon-Wiener index; P_i represents the importance value of the i-th species; S represents the number of species in the community, and i = 1,2,3. . .n.

The formula for the calculation of the overall diversity of the community is as follows:

$$D_{\text{total}} = W_1 D_1 + W_2 D_2 + W_3 D_3 \tag{5}$$

$$W_i = (C_i/C + h_i/h)/2 \tag{6}$$

where, D_1, D_2, and D_3 represent the diversity index of the tree layer, shrub layer, and herb layer, respectively;,W_1, W_2, and W_3 represent the weighting coefficients of the tree layer, shrub layer, and herb layer, respectively; C_i represents the coverage of different layers; C represents the total coverage of the community in different layers; h_i represents the average height of vegetation in different community layers; h represents the sum of the average heights of the community in different layers; i = 1,2,3. . .n.

2.3.3. Soil conservation value

In the current study, the shadow engineering method and the market value method (Li et al., 2011; Villa et al., 2014) were used to calculate the value of soil stabilization and soil fertility conservation, respectively, and the calculation formulas are as follows:

$$\mathrm{G_i} = \sum_{\mathrm{i}=1}^{\mathrm{n}} \mathrm{A_i}\,(\mathrm{X_2}-\mathrm{X_1}) \tag{7}$$

$$\mathrm{U_{i\text{-}soil}} = \mathrm{G_i} \times \mathrm{C_{soil}}/\rho \tag{8}$$

$$\mathrm{U_{i\text{-}fertility}} = \mathrm{A_i}\,(\mathrm{X_2}-\mathrm{X_1})\,\left(\frac{\mathrm{N_{nutrition}C_1}}{\mathrm{R_1}} + \frac{\mathrm{P_{nutrition}C_1}}{\mathrm{R_2}} + \frac{\mathrm{K_{nutrition}C_2}}{\mathrm{R_3}} + \mathrm{MC_3}\right) \tag{9}$$

where, G_i is the amount of soil retained by the forest (t y^{-1}); A_i is the forest area (ha); X_1 and X_2 are the soil erosion modulus of forested land and unforested land in Northeast China, respectively (t·ha^{-1}·y^{-1}). $U_{\text{i-soil}}$ is the market value of soil retained by the forest ($·y^{-1}); C_{soil} is the cost of excavating and transporting a unit volume of earthwork in the market ($·m^{-3}); ρ is the soil bulk density of forest woodland (g·cm^{-3}); $U_{\text{i-fertility}}$ is the annual value of each stand to conserve soil fertility ($·y^{-1}); $N_{\text{nutrition}}$, $P_{\text{nutrition}}$, $K_{\text{nutrition}}$, and M are the measured N content (%), P content (%), K content (%), and organic matter content (%) of soil, respectively; R_1 and R_2 are the N content (%) and P content (%) of the phosphoric acid fertilizer, respectively; C_1, C_2, and C_3 are the price of phosphoric acid fertilizer, potassium chloride fertilizer, and organic matter ($·t^{-1}), respectively; i = 1,2,3. . .n.

TABLE 2 Value and classification of Shannon-Wiener index.

Class	Shannon-Wiener index	S_{biota} ($·ha^{-1}· y^{-1})
I	$S \geq 6$	7,345
II	$6 \geq S \geq 5$	5,876
III	$5 \geq S \geq 4$	4,407
IV	$4 \geq S \geq 3$	2,938
V	$3 \geq S \geq 2$	1,469
VI	$2 \geq S \geq 1$	735
VII	$1 \geq S$	441

Value and classification of Shannon-Wiener index are derived from the "Specifications for assessment of forest ecosystem services" (GB/T 38582-2020) (NFGA, 2020).

2.3.4. Forest nutrition retention value

In order to obtain the value of the nutrients retained by the trees, the substitution value method is used to convert the large amount of N, P, K, and other nutrients that the trees absorb from the soil or air each year into the market value of chemical fertilizers, and the forest nutrition retention value is calculated as follows:

$$\mathrm{G_N} = \mathrm{N_{nutrition}B_{year}} \tag{10}$$

$$\mathrm{G_P} = \mathrm{P_{nutrition}B_{year}} \tag{11}$$

$$\mathrm{G_K} = \mathrm{K_{nutrition}B_{year}} \tag{12}$$

$$\mathrm{U_{i\text{-}nutrition}} = \mathrm{B_{year}}\left(\frac{\mathrm{N_{nutrition}C_1}}{\mathrm{R_1}} + \frac{\mathrm{P_{nutrition}C_1}}{\mathrm{R_2}} + \frac{\mathrm{K_{nutrition}C_2}}{\mathrm{R_3}}\right) \tag{13}$$

where, G_N, G_P, and G_K are the amounts of nitrogen, phosphorus, and potassium accumulated by trees each year (t·y^{-1}), respectively; $U_{\text{i}-\text{nutrition}}$ is the accumulated value of nutrients in the tree year ($·y^{-1}); $N_{\text{nutrition}}$, $P_{nutrition}$, and $K_{\text{nutrition}}$ are the ratios (%) of N, P, and K contained in forest trees, respectively; B_{year} is the annual growth of forest biomass (kg); R_1 and R_2 are the N content and P content (%) of the phosphoric acid fertilizer, respectively; R_3 is the K content (%) of potassium chloride fertilizer; C_1 and C_2 are the prices of diammonium phosphate fertilizers and potassium chloride fertilizers, respectively ($·t^{-1}); i = 1,2,3. . .n.

Using the tree species DBH growth curve fitting results and the biomass allometric growth equation (Wang, 2006), the biomass growth of each tree species was obtained, and then the N, P, and K contents of different tree species were used to obtain the annual tree nutrient retention of each survey plot. Finally, the prices of different fertilizers and the contents of fertilizer nutrients are converted into market values to obtain the nutrient retention value per unit area of forest trees in different stand types and age groups ($·y^{-1}). While the annual net productivity and nutrient content of different forest vegetation types are different, and the nutrient content of different organs of the same plant is also different, so the average nutrient content of plant branches, stems, leaves, and roots cannot truly represent the overall nutrient content of plants, and it is necessary to comprehensively consider the nutrient content and biomass weight. The calculation formulas are as follows:

$$\mathrm{G_{nutrition}} = \frac{\sum \mathrm{C_i W_j}}{\mathrm{W_t}} \tag{14}$$

where, G_{nutrient} is the weighted average nutrient ratio of the arbor; C_i is the percentage of nutrients in an organ of the tree; W_j is the biomass of a certain organ of the tree; W_t is the total biomass of tree; $i = 1,2,3...n$.

The related parameter values are listed in **Table 3**. The DBH growth fitting equations, volume growth, biodiversity index, soil nutrition contents and soil bulk density of different stand types, and weighted nutrient contents of different organs and individuals for each tree specie are showed in supplementary material.

3. Results

3.1. The value of provisioning services function of different stand types

3.1.1. Supply value of forest trees

The highest supply value of forest trees per unit area among different stand types is in near-mature *F. mandshurica* forest, which is 2,190 $\$\cdot ha^{-1}\cdot y^{-1}$ (**Figure 3**), and the young *B. platyphylla* forest is the lowest, only 388 $\$\cdot ha^{-1}\cdot y^{-1}$, moreover, the difference in supply value of mixed coniferous broad-leaved forest among different age groups can reach 1410 $\$\cdot ha^{-1}\cdot y^{-1}$.

3.1.2. Conservation value of species resources

The survey results showed that the vegetation types of the near threatened (LU) level in the study area were *F. mandshurica*, *P. amurense*, and *P. koraiensis*, which were mostly found in mixed broad-leaved forest and mixed coniferous and broad-leaved forest. And the ancient trees (100∼299a) included and other tree species totaling 94, mainly in the mature and over-mature forest stage. And a total of 94 ancient trees (100∼299a), including *P. koraiensis*, *Q. mongolica*, *F. mandshurica*, *T. amurensis*, and *J. mandshurica*, were found, mainly in the mature and over-mature forest stages. Based on the distribution of endangered species, precious ancient trees and endemic species in the study area and the Shannon-Wiener index classes and values, the species conservation value ($\$\cdot y^{-1}$) of per unit area of different stand types and age groups was calculated (**Figure 3**).

With the increase of the age, the species conservation value per unit area of *B. platyphylla* forest, *J. mandshurica* forest, and *B. platyphylla* forest showed a unimodal change (**Figure 3**), and the peaks appeared in mature forest, near-mature forest and near-mature forest, respectively. The species conservation value of *Q. mongolica* forest showed a continuous increasing trend as a whole, and reached the maximum value in over-mature forest, and the value for *F. mandshurica* forest was relatively high in near-mature forest and over-mature forest, while those in mixed coniferous broad-leaved forest were higher in mature and half-mature forests. Among the six stand types, the conservation value of over-mature *F. mandshurica* forest is the highest, which is 1,777 $\$\cdot ha^{-1}\cdot y^{-1}$, and the value of half-mature *Q. mongolica* forest is the lowest, which is only 539 $\$\cdot ha^{-1}\cdot y^{-1}$.

3.2. The value of supporting services function of different stand types

3.2.1. Soil conservation value

The soil reinforcement value per unit area of different stand types is as follows: *J. mandshurica* forest (231 $\$\cdot ha^{-1}\cdot y^{-1}$) > mixed broad-leaved forest (200 $\$\cdot ha^{-1}\cdot y^{-1}$) > *F. mandshurica* forest (199 $\$\cdot ha^{-1}\cdot y^{-1}$) > *B. platyphylla* forest (195 $\$\cdot ha^{-1}\cdot y^{-1}$) > mixed coniferous broad-leaved forest (194 $\$\cdot ha^{-1}\cdot y^{-1}$) > *Q. mongolica* forest (176 $\$\cdot ha^{-1}\cdot y^{-1}$) (see **Figure 4**). The soil fertilizer retention value per unit area of different stand types and age groups ranges from 1,073 to 6,414 $\$\cdot ha^{-1}\cdot y^{-1}$, the highest value is in the near-mature *J. mandshurica* forest, and the lowest is in the young *F. mandshurica* forest. Among them, the retention value of N element is relatively high, ranging from 301 to 4,501 $\$\cdot ha^{-1}\cdot y^{-1}$, and the highest and lowest values are in young *F. mandshurica* forest and near-mature *J. mandshurica* forest, respectively. The retention values for K and P are 344∼1,165 and 6∼1,485 $\$\cdot ha^{-1}\cdot y^{-1}$, respectively, and the lowest values both appear in the young *F. mandshurica* forest, and the highest values are in the near-mature *Q. mongolica* forest and half-mature *F. mandshurica* forest, respectively. The soil fertilizer retention value of organic matter is between 49 and 825 $\$\cdot ha^{-1}\cdot y^{-1}$ with the highest value in over-mature *F. mandshurica* forest.

3.2.2. Forest nutrient retention value

The tree nutrient values of N, P, and K elements per unit area of different stand types and age groups were ranked as follows: N > P > K (**Figure 5**). The forest nutrient retention values of per unit area of N and P are 43∼177 and 9∼61 $\$\cdot ha^{-1}\cdot y^{-1}$, respectively, and the highest value is in mature *B. platyphylla* forest. The retention value of K is between 2 and 16 $\$\cdot ha^{-1}\cdot y^{-1}$, and the near-mature forest of *F. mandshurica* forest is relatively high. The lowest retention values of N, P, and K are the over-mature mixed coniferous broad-leaved forest. Based on N, P, and K, the retention value of different stand types is between 53 and 252 $\$\cdot ha^{-1}\cdot y^{-1}$, and the value of mature *B. platyphylla* forest is relatively high, while the mixed coniferous broad-leaved forest is the lowest. The nutrient retention values of near-mature forest and mature forest are relatively high among different age groups, for example, the values of mature *B. platyphylla* forest and near-mature *F. mandshurica* forest are more than 235 $\$\cdot ha^{-1}\cdot y^{-1}$. The values of young and over-mature forests are relatively low, such as the retention values of young and over-mature mixed coniferous broad-leaved forest are only 63 and 53 $\$\cdot ha^{-1}\cdot y^{-1}$, respectively.

3.3. The value of supporting services function of different stand types

The total forest area of the reserve is 116,234 ha, and the forest composition is mainly mixed broad-leaved forest and *Q. mongolica* forest, accounting for 83.1% of the forest area. The forest areas of *B. platyphylla* forest, *J. mandshurica* forest, and mixed coniferous broad-leaved forest are similar, which are between 4 and 6%, while the *F. mandshurica* forest has the smallest area (1.9%). Based on the calculation results of the services function value per unit area of different forest types and age groups, combined with the survey data, the value of forest community provision and support service function in Sanhu Nature Reserve ($\$\cdot y^{-1}$) was obtained (**Figure 6**). The total value of forest ecosystem provision and support services in the reserve is 659.07 million $\$\cdot y^{-1}$, and the average value per unit area is 5,670 $\$\cdot ha^{-1}\cdot y^{-1}$. The value of different service functions are as follows: soil fertilizer retention value (319.30 million $\$\cdot y^{-1}$) > forest trees supply value

TABLE 3 Related parameter value.

Parameter	Value	Unit	Data sources
Price of standing forest stock	191 for *Betula platyphylla*, 118 for *Populus davidiana*, 391 for *Fraxinus mandshurica*, *Juglans mandshurica*, *Phellodendron amurense*, *Tilia amurensis*, and *Acer pictum*, 257 for *Quercus mongolica*, 206 for *Ulmus davidiana* var. *Japonica*, and 494 for *Pinus koraiensis*	$\$\cdot\text{m}^{-3}$	http://www.chinatimber.org/
Soil erosion modulus for unforested land	12.5	$\text{t}\cdot(\text{ha}^{-1}\cdot\text{y}^{-1})$	Classification standard for soil erosion (SL190-2007)
Soil erosion modulus for forested land	75	$\text{t}\cdot(\text{ha}^{-1}\cdot\text{y}^{-1})$	Classification standard for soil erosion (SL190-2007)
Soil excavation cost	2.5	$\$\cdot\text{m}^{-3}$	http://www.jooxoo.com/
Nitrogen content of diamine phosphate fertilizer	14	%	Fertilizer use guide (Wu, 2001)
Phosphorus content of diamine phosphate fertilizer	15		
Potassium content of potassium chloride fertilizer	50		
Price of organic matter	47	$\$\cdot\text{t}^{-1}$	http://www.jgjcndrc.org.cn/
Price of diamine phosphate	353	$\$\cdot\text{t}^{-1}$	http://www.jgjcndrc.org.cn/
Price of potassium chloride fertilizer	323	$\$\cdot\text{t}^{-1}$	http://www.jgjcndrc.org.cn/

The exchange rate used in the calculation is 1 RMB yuan = 0.1469 $.

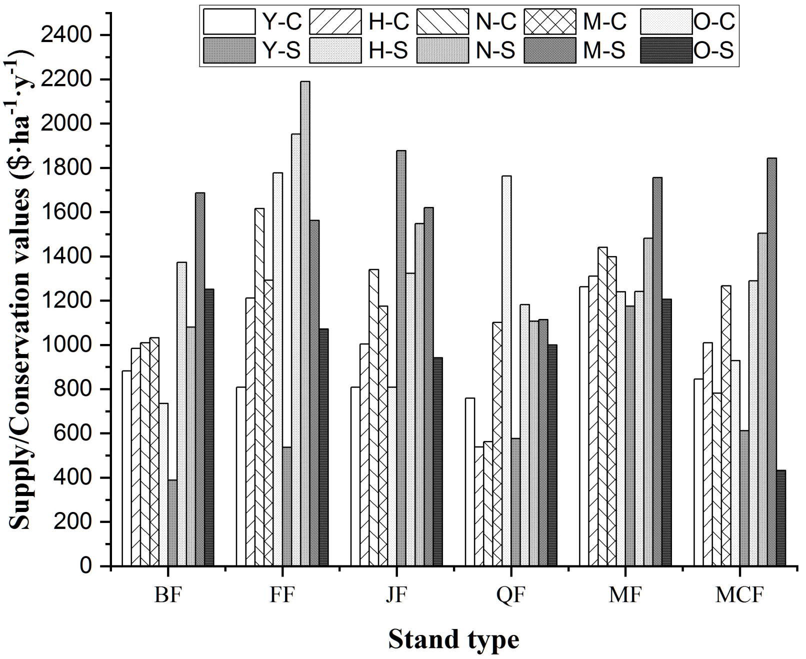

FIGURE 3
Supply value and species resources conservation value of per unit area of different stand types and age groups. Y-C, H-C, N-C, M-C, and O-C are the conservation values of species resources of young forest, half-mature forest, near-mature forest, mature forest and over-mature forest, respectively; Y-S, H-S, N-S, M-S, and O-S are the supply values of young forest, half-mature forest, near-mature forest, mature forest and over-mature forest, respectively. Stand types include *Betula platyphylla* forest (BF), *Fraxinus mandshurica* forest (FF), *Juglans mandshurica* forest (JF), *Quercus mongolica* forest (QF), mixed broad-leaved forest (MF), and mixed coniferous broad-leaved forest (MCF).

(61.96 million $\$\cdot\text{y}^{-1}$) > species resources conservation value (134.48 million $\$\cdot\text{y}^{-1}$) > soil reinforcement value (22.63 million $\$\cdot\text{y}^{-1}$) > forest nutrient retention value (19.02 million $\$\cdot\text{y}^{-1}$), and soil fertilizer retention value accounts for the highest proportion, followed by forest trees supply value (24.6%) and species resources conservation value (20.5%) (Figure 7). The proportion of provision and service function value of different stand types is mainly affected by the size of the stand area. The mixed broad-leaved forest has the highest proportion, accounting for 62.9%, followed by the *Q. mongolica* forest with 19.0%, accounting for 81.9% in total, which are the main body of the reserve's service function value. The value proportion of *J. mandshurica* forest was 7.1%, while the values of *F. mandshurica* forest, *B. platyphylla* forest, and mixed coniferous broad-leaved forest all accounted for less

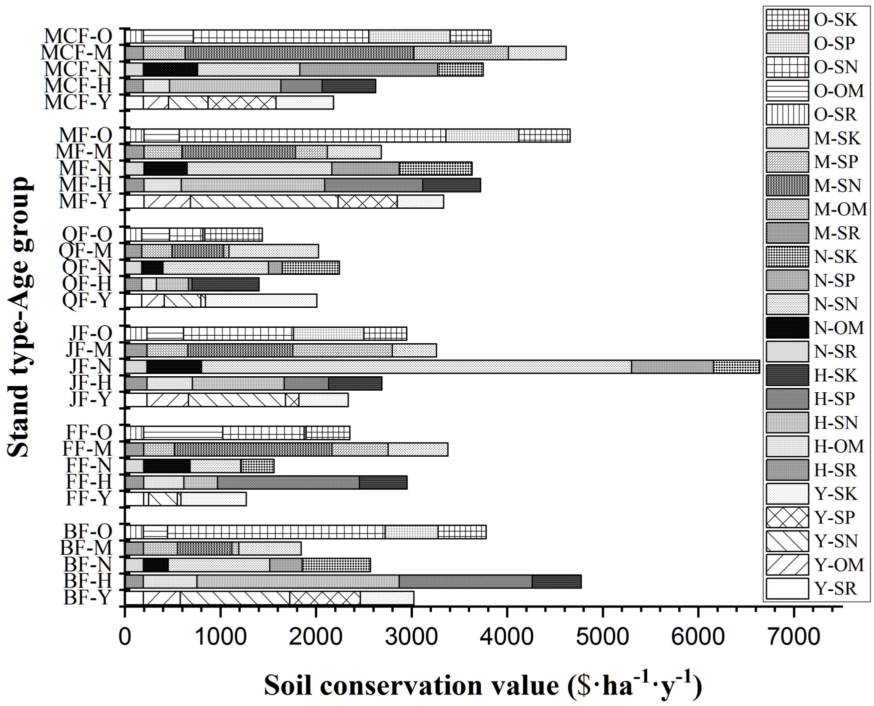

FIGURE 4

Soil conservation value of per unit area of different stand types and age groups. Y-(SN, SP, SK, OM, SR), H-(SN, SP, SK, OM, SR), M-(SN, SP, SK, OM, SR), and O-(SN, SP, SK, OM, SR) are the soil conservation value for N, P, K, organic matter and soil retention of young forest, half-mature forest, near-mature forest, mature forest, and over-mature forest, respectively; *Betula platyphylla* forest (BF)-Y, H, N, M, O, *Fraxinus mandshurica* forest (FF)-Y, H, N, M, O, *Juglans mandshurica* forest (JF)-Y, H, N, M, O, *Quercus mongolica* forest (QF)-Y, H, N, M, O, mixed broad-leaved forest (MF)-Y, H, N, M, O, and mixed coniferous broad-leaved forest (MCF)-Y, H, N, M, O are the young forest, half-mature forest, near-mature forest, mature forest, and over-mature forest of different stand types, respectively.

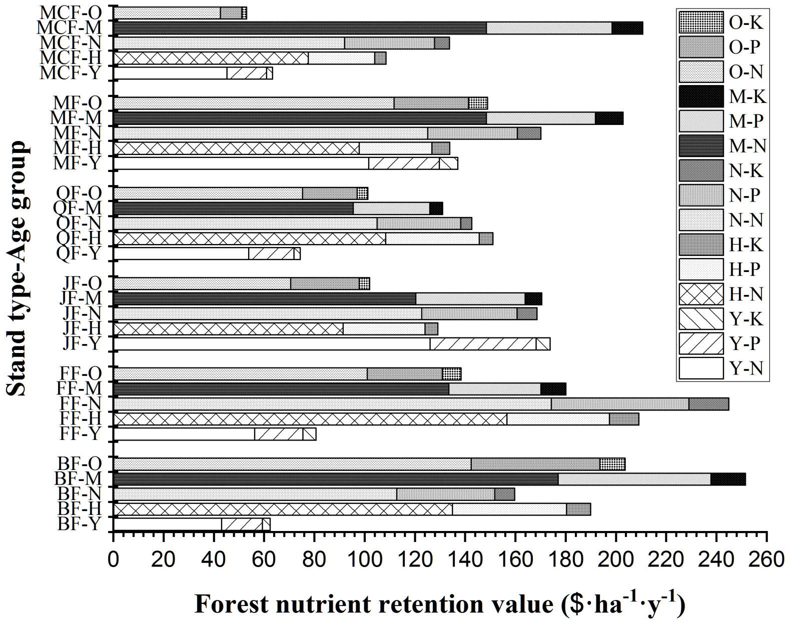

FIGURE 5

Forest nutrient retention value of per unit area of different stand types and age groups. Y-(N, P, K), H-(N, P, K), M-(N, P, K), and O-(N, P, K) are the forest nutrient retention values of young forest, half-mature forest, near-mature forest, mature forest, and over-mature forest, respectively; *Betula platyphylla* forest (BF)-Y, H, N, M, O, *Fraxinus mandshurica* forest (FF)-Y, H, N, M, O, *Juglans mandshurica* forest (JF)-Y, H, N, M, O, *Quercus mongolica* forest (QF)-Y, H, N, M, O, mixed broad-leaved forest (MF)-Y, H, N, M, O, and mixed coniferous broad-leaved forest (MCF)-Y, H, N, M, O are the young forest, half-mature forest, near-mature forest, mature forest, and over-mature forest of different stand types, respectively.

than 5% with a total of 11.0% (**Figure 7**). The service value per unit area is between 7,595 and 5,259 $\$\cdot ha^{-1}\cdot y^{-1}$, which is represented by *J. mandshurica* forest > mixed broad-leaved forest > *F. mandshurica* forest > mixed coniferous broad-leaved forest > *B. platyphylla* forest.

Among all age groups, the value of provision and supply of near-mature forest is the highest, reaching 272.50 million $\$\cdot y^{-1}$, accounting for 42.3% of the total value, followed by mature forest (34.9%). The proportion of half-mature forest is 15.5%, and the proportions of over-mature forest (4.8%) and young forest (2.4%) are relatively small. The service value of the near-mature *J. mandshurica* forest is the highest (9,607 $\$\cdot ha^{-1}\cdot y^{-1}$), and the young *F. mandshurica* forest is the lowest (2,703 $\$\cdot ha^{-1}\cdot y^{-1}$). Near-mature forest not only occupies the largest area of forest land in the reserve, but also has high supply value and soil fertilizer retention value, which is crucial for the sustainable and stable performance of ecological functions and value growth of nature reserve, followed by mature forest (**Figures 6**, **7**).

4. Discussion

There are noticeable variations in economic utilization, species conservation, nutrient retention, soil stabilization, and fertilizer conservation among different types of trees, shrubs, and herbs. As critical biological resources, forest plants, and their products are now an essential aspect of human life and production. They serve various purposes such as production of wood products, provision of food and medicine, and industrial production (Weckwerth, 2011). The varying vegetation compositions of forest ecosystems in different stand types cause differences in the value of their service functions (Blattert et al., 2017; Uhde et al., 2017). The increase in population and domestic economy has significantly heightened the demand for timber products in recent years (Wenda et al., 1999), Evaluating the provision value of forests across different stands and age groups is crucial for achieving sustainable and efficient usage of trees. In this study, *F. mandshurica* forest has the highest provision value of forest products per unit area, attributed to a higher volume growth and wood price. Meanwhile, young *B. platyphylla* forest has the lowest value, primarily due to its low volume growth, and comprising mostly low-priced tree species such as *B. platyphylla* and *P. davidiana*. Forest products' provision values are primarily affected by stock volume, as the *B. platyphylla* forest, *F. mandshurica* forest, *J. mandshurica* forest, and *Q. mongolica* forest have relatively single species. While the values of mixed broad-leaved forest and mixed coniferous broad-leaved forest are affected not only by the difference in volume growth of age groups, but also by the proportion of tree species due to their complex compositions. Therefore, the forest type is closely linked to the ecological service value (Guan et al., 2022). The growth rate of each tree species at different age stages determined the growth of the forest, and although the DBH growth curves of the 10 primary tree species studied demonstrated that the growth rate gradually declined with an increase in DBH, it remains affected by species-specific factors (Lee et al., 2004; Chen et al., 2020). In this study, all forest types except for *J. mandshurica* forest showed low annual supply value during the young forest stage, and a significant decline in supply value during the over-mature forest stage. This is mainly because growth volume was relatively high during the half-mature, near-mature, and mature stages, and relatively small in the young stage, with a significant decrease in the over-mature stage (Wang, 2006), which is why half-mature, near-mature, and mature forests have higher supply value. Furthermore, significant differences in the annual volume growth of different stand types were the main reason for the variation in the annual supply value among forest types (Faccoli and Bernardinelli, 2014). Therefore, the growth potential of forest provision values should be comprehensively considered before logging. Overall, to enhance the supply value of forest ecosystems in the study area, decision-makers should focus on the management and operation of *F. mandshurica* forest during the half-mature to mature stages, followed by the mixed coniferous broad-leaved forest.

Maintaining biodiversity is the basis for ensuring the stability of forest ecosystem functions, and how to quantify the values of these functions is an important issue at home and abroad (Chazdon et al., 2009). Among the species conservation values of different stand types, the value of *F. mandshurica* forest is the highest, mainly because of its large diversity index, and there are many endangered tree species and precious ancient trees in this stand type. The conservation value of the half-mature *Q. mongolica* forest was the lowest, which should be attributed to the absolute dominance of *Q. mongolica* in the community, and the low diversity index (Sang and Bai, 2009). Moreover, with the development of the forest, the species conservation value of *B. platyphylla* forest, *J. mandshurica* forest, and mixed broad-leaved forest shows an increasing trend up to the mature and over-mature forest stages, while the *Q. mongolica* forest maintains continuous growth (He et al., 2016). Overall, to enhance the conservation value of species diversity in the reserve, it is recommended to strengthen the management and operation of *F. mandshurica* forest and *Q. mongolica* forest during the over-mature forest stage.

Soil is a crucial component and environmental factor in the forest ecosystem that maintains energy flow and dynamic balance. The forest ecosystem plays a key role in soil reinforcement and fertilizer protection to ensure soil quality (Guo et al., 2001). Among the six main stand types examined in this study, the *Q. mongolica* forest demonstrated the largest soil bulk density (0.75), with *B. platyphylla* forest and mixed coniferous broad-leaved forest following closely behind, followed by *F. mandshurica* forest and mixed broad-leaved forest. *J. mandshurica* forest had the smallest bulk density. Soil with a small bulk density is looser and conducive to intercepting seepage, storing water, and slowing down runoff scouring. In contrast, soil with higher density is typically more susceptible to erosion (Qian, 1999). Therefore, the *Q. mongolica* forest has relatively low soil reinforcement value. Moreover, the soil organic matter and nutrient contents of different stand types varied significantly (Gan et al., 2020). The mixed coniferous broad-leaved forest had relatively high organic matter, N and P contents, whereas the *Q. mongolica* forest had low contents for these parameters. However, the *Q. mongolica* forest had relatively high K content in the soil (Li et al., 2017). Using the market value method to estimate soil fertility retention value, the results showed that N element had the highest fertility retention value, followed by K and P, while the organic matter had the lowest value. Additionally, the soil fertilizer retention value was higher in *J. mandshurica* forest and mixed broad-leaved forest, followed by *B. platyphylla* forest and mixed coniferous broad-leaved forest, and was lower in *F. mandshurica*

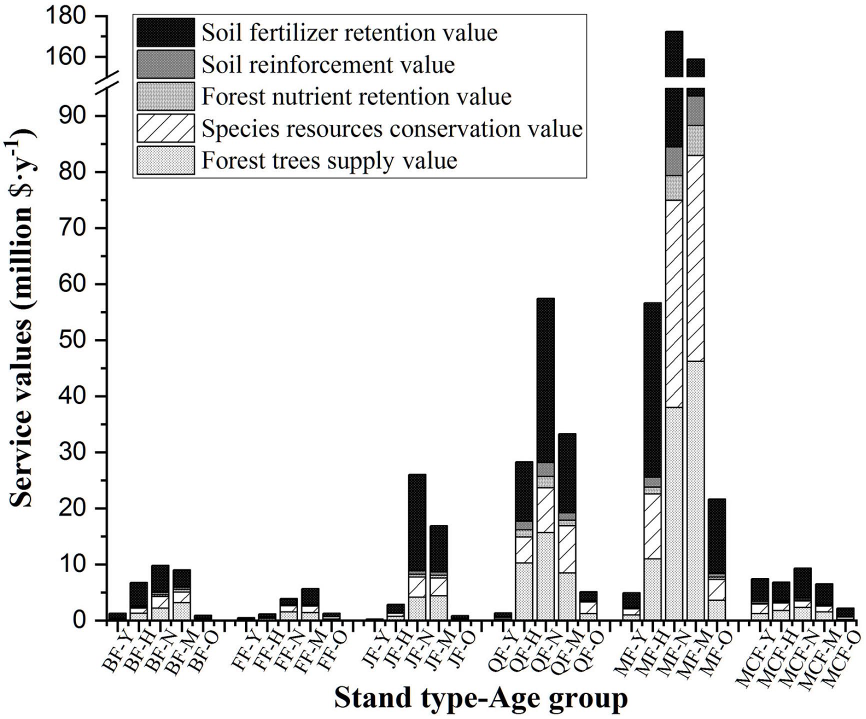

FIGURE 6
The values of provision and support service functions in Sanhu Reserve. *Betula platyphylla* forest (BF)-Y, H, N, M, O, *Fraxinus mandshurica* forest (FF)-Y, H, N, M, O, *Juglans mandshurica* forest (JF)-Y, H, N, M, O, *Quercus mongolica* forest (QF)-Y, H, N, M, O, mixed broad-leaved forest (MF)-Y, H, N, M, O, and mixed coniferous broad-leaved forest (MCF)-Y, H, N, M, O are the young forest, half-mature forest, near-mature forest, mature forest, and over-mature forest of different stand types, respectively.

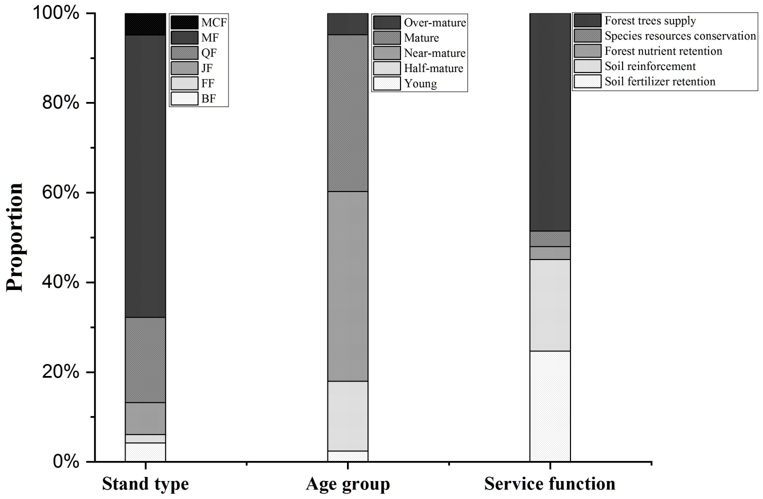

FIGURE 7
Proportion of the values of different service functions, stand types, and age groups. Stand types include *Betula platyphylla* forest (BF), *Fraxinus mandshurica* forest (FF), *Juglans mandshurica* forest (JF), *Quercus mongolica* forest (QF), mixed broad-leaved forest (MF), and mixed coniferous broad-leaved forest (MCF).

forest and *Q. mongolica* forest, the results of this study are similar to other related research findings in the same Changbai Mountain range (Zhang et al., 2017; Liu et al., 2023). Although there was no significant temporal change in the soil conservation value in this study, forests during the half-mature to mature stages, especially the *J. mandshurica* forest, exhibited higher soil conservation value, making it the primary management and operational target for improving soil conservation value in the reserve.

In addition, the conservation of nutrient elements by forest trees is also one of the important service functions of forest ecosystems (Fan et al., 2015). Organ biomass is an important basis for estimating the level of tree nutrient content, and due to the differences in the growth rate of different tree species, the current study used the allometric growth equation of various tree species to calculate the organ biomass (Wang, 2006), and based on the weight of the organ biomass of trees with a DBH of 5–100 cm and the organ nutrient content of each tree species, the N, P, and K nutrient elements content (%) of individual trees were calculated (Fan, 2014). There are obvious differences in the nutrient content of different tree species (Eriksson and Rosen, 1994), and there are also significant differences in nutrient contents of different organs of trees (Deng et al., 2019), in the current study, the N and K content of each organ is the highest in leaves, followed by branches, and relatively small in stems and roots, so the difference in forest biomass and organ nutrient content directly determines the N, P, and K nutrient retention capacity of trees. And as the basic element of protein, compared with P and K, N has the highest average content in individuals of different tree species (Liu and Wang, 2018), so the tree nutrient value of N element per unit area of different stand types and age groups is the highest, followed by P and K. As the forest age increases, the overall annual nutrient retention value of the forest shows a trend of first increasing and then significantly decreasing when it reaches the over-mature forest stage. In particular, the near-mature and mature *F. mandshurica* forests and *B. platyphylla* forests should be the primary management targets for enhancing the nutrient retention value of forestry in the reserve.

The average value of provision and support service functions per unit area of forest ecosystem in Sanhu Nature Reserve is 5,670 $\$\cdot ha^{-1}\cdot y^{-1}$, which is higher than the average value per unit area of reserves in China and the world (Taye et al., 2021; Kang et al., 2022), but it is significantly lower than the Shennongjia Nature Reserve (14,896 $\$\cdot ha^{-1}\cdot y^{-1}$) (Wu, 2018), which has very rich biological resources. Affected by tree species composition, ecosystem structure, distribution area, etc., the unit area value of different reserves presents significant differences in terms of forest supply, species conservation, nutrient fixation, and soil conservation (Uddin et al., 2013; Bai et al., 2019; Wang, 2022). Compared with the Ailao Mountain Reserve in Yunnan, the supply value of timber per unit in the Sanhu Reserve is relatively small, because there are more precious wood species in the Ailao Mountain Reserve (Tang, 2021). From the perspective of the entire reserve, the near-mature and mature forests have high provision and support service values, especially the mixed broad-leaved forest. The per unit area service values of *J. mandshurica* forest and mixed broad-leaved forest are relatively high. Therefore, in Jilin Songhuajiang Sanhu National Nature Reserve, management and operation should focus on near-mature and mature mixed broad-leaved forests in order to maintain and enhance the supply and support service values of the forest ecosystem. Additionally, the service functions of *Q. mongolica* forest and *J. mandshurica* forest should be gradually improved.

5. Conclusion

There are significant differences in the provision and support service values of forests with different types and ages. The near-mature *F. mandshurica* forest has a high provision value, with the value peak appearing mainly in the half-mature and mature forest stages. The over-mature *F. mandshurica* forest and mature *Q. mongolica* forest both show high species conservation value. Moreover, with the development of the forest, the species conservation value of *B. platyphylla* forest, *J. mandshurica* forest, and mixed broad-leaved forest shows an increasing trend up to the mature and over-mature forest stages, while the *Q. mongolica* forest maintains continuous growth. In terms of nutrient retention value, mature *B. platyphylla* forest has a significant advantage, and near-mature and mature forests have high nutrient retention capacity. The near-mature *J. mandshurica* forest has a high soil conservation value, with overall high soil conservation value observed from the half-mature to mature forest stages. From the perspective of the entire research area, the soil fertilizer conservation value is the highest, followed by the forest trees supply value and species conservation value, and the mixed broad-leaved forest and *Q. mongolica* forest are the main body of the reserve's provision and support service functions. In addition, near-mature and mature forests in the reserve are the main contributors to the service function value, especially the mixed broad-leaved forest in the reserve. It is of great practical significance to specifically protect and manage forest types with high service value in different forest development stages for promoting the sustainable development of regional forest resources.

Data availability statement

The original contributions presented in this study are included in the article/**Supplementary material**, further inquiries can be directed to the corresponding author.

Author contributions

QL, YC, and CF contributed to conception and design of the study. QL and CF organized the database. FY performed the statistical analysis. QL wrote the first draft of the manuscript. QL, YC, FY, and CF wrote sections of the manuscript. All authors contributed to manuscript revision, read, and approved the submitted version.

Funding

The authors acknowledge the support of the Technology Development Program of Jilin Province (YDZJ202201ZYTS494), the Science and Technology Research Project of the Education Office of Jilin Province (JJKH20220063KJ), the Incubation Programme Project of Youth Innovation Team (Research team on vegetation-soil-microbial interaction effects and synergistic mechanisms in forest ecosystems), the National Key Technology Research and Development Program of the Ministry of Science and Technology of China (2021FY100802-04), and the Doctoral Scientific Research Foundation of Beihua University (Characteristics of Heavy Metal Pollution and Accumulation in Vegetable Soils in the Suburbs of Typical Industrial Cities).

Conflict of interest

The authors declare that the research was conducted in the absence of any commercial or financial relationships that could be construed as a potential conflict of interest.

Publisher's note

Supplementary material

The Supplementary Material for this article can be found online at: https://www.frontiersin.org/articles/10.3389/ffgc.2023.1199304/full#supplementary-material

References

Adger, W., and Weiguang, C. (1995). Total economic value of mexican forests. *AMBIO* 024, 285–295.

Bai, Z., Wang, W., Huan, L. I., Liu, D., Guo, Z., and Liu, H. (2019). Change of forest ecosystem service function and its value in kanas nature reserve. *J. Land. Res.* 11:4.

Beaumont, N. J., Jones, L., Garbutt, A., Hansom, J. D., and Toberman, M. (2014). The value of carbon sequestration and storage in coastal habitats. *Estuar. Coas. Shelf Sci.* 137, 32–40. doi: 10.1016/j.ecss.2013.11.022

Blattert, C., Lemm, R., Thees, O., Lexer, M. J., and Hanewinkel, M. (2017). Management of ecosystem services in mountain forests: review of indicators and value functions for model based multi-criteria decision analysis. *Ecol. Indicat.* 79, 391–409. doi: 10.1016/j.ecolind.2017.04.025

Chang, Y., Zou, T., Yoshino, K., Luo, S., and Zhou, S. (2019). Ecological policy benefit valuation based on public feedback: forest ecosystem services in wuyishan nature reserve, China. *Sci. Total Environ.* 673, 622–630. doi: 10.1016/j.scitotenv.2019.04.076

Chazdon, R. L., Peres, C. A., Dent, D., Sheil, D., Lugo, A. E., Lamb, D., et al. (2009). The potential for species conservation in tropical secondary forests. *Conservat. Biol.* 23, 1406–1417. doi: 10.1111/j.1523-1739.2009.01338.x

Chen, J., Yang, H., Man, R., Wang, W., Sharma, M., Peng, C., et al. (2020). Using machine learning to synthesize spatiotemporal data for modelling DBH-height and DBH-height-age relationships in boreal forests. *Forest Ecol. Manage.* 466:118104. doi: 10.1016/j.foreco.2020.118104

Cheng, X., Van Damme, S., Li, L., and Uyttenhove, P. (2019). Evaluation of cultural ecosystem services: a review of methods. *Ecosyst. Serv.* 37:100925. doi: 10.1016/j.ecoser.2019.100925

Costanza, R., d'Arge, R., de Groot, R., Farber, S., Grasso, M., Hannon, B., et al. (1997). The value of the world's ecosystem services and natural capital. *Nature* 387, 253–260. doi: 10.1038/387253a0

Daily, G. C., and Ehrlich, P. R. (1999). Managing earth's ecosystems: an interdisciplinary challenge. *Ecosystems* 2, 277–280. doi: 10.1007/s100219900075

Deng, S., Shi, K., Ma, J., Zhang, L., Ma, L., and Jia, Z. (2019). Effects of fertilization ratios and frequencies on the growth and nutrient uptake of magnolia wufengensis (magnoliaceae). *Forests* 10:65. doi: 10.3390/f10010065

Eriksson, H. M., and Rosen, K. (1994). Nutrient distribution in a Swedish tree species experiment. *Plant Soil* 164, 51–59. doi: 10.1007/BF00010110

Faccoli, M., and Bernardinelli, I. (2014). Composition and elevation of spruce forests affect susceptibility to bark beetle attacks: implications for forest management. *Forests* 5, 88–102. doi: 10.3390/f5010088

Fan, C. (2014). *Carbon estimation and distribution characteristics of forest vegetation in jilin province. Ph. D, Thesis.* Northeast Forestry University.

Fan, H., Wu, J., Liu, W., Yuan, Y., Hu, L., and Cai, Q. (2015). Linkages of plant and soil C:N:P stoichiometry and their relationships to forest growth in subtropical plantations. *Plant Soil* 392, 127–138. doi: 10.1007/s11104-015-2444-2

Farnsworth, K. D., Lyashevska, O., and Fung, T. (2012). Functional complexity: the source of value in biodiversity. *Ecol. Complexity* 11, 46–52. doi: 10.1016/j.ecocom.2012.02.001

Font, A. R. (2000). Mass tourism and the demand for protected natural areas: a travel cost approach. *J. Environ. Econ. Manage.* 39, 97–116. doi: 10.1006/jeem.1999.1094

Food and Agriculture Organization (2020). *Global forest resources assessment (FRA).* Italy: Food and Agriculture Organization.

Fromm, O. (2000). Ecological structure and functions of biodiversity as elements of its total economic value. *Environ. Res. Econ.* 16, 303–328. doi: 10.1023/A:1008359022814

Gamfeldt, L., Snäll, T., Bagchi, R., Jonsson, M., Gustafsson, L., Kjellander, P., et al. (2013). Higher levels of multiple ecosystem services are found in forests with more tree species. *Nat. Commun.* 4:1340. doi: 10.1038/ncomms2328

Gan, H. Y., Schöning, I., Schall, P., Ammer, C., and Schrumpf, M. (2020). Soil Organic matter mineralization as driven by nutrient stoichiometry in soils under differently managed forest stands. *Front. Forests Global Change* 3:99. doi: 10.3389/ffgc.2020.00099

Goodfellow, S., and Peterken, G. F. (1981). A method for survey and assessment of woodlands for nature conservation using maps and species lists: the example of norfolk woodlands. *Biol. Conservat.* 21, 177–195. doi: 10.1016/0006-3207(81)90090-2

Grytnes, J. A. (2010). Fine-scale vascular plant species richness in different alpine vegetation types: relationships with biomass and cover. *J. Veget. Sci.* 11, 87–92. doi: 10.2307/3236779

Guan, S., Lu, Y., and Liu, X. (2022). Evaluation of multiple forest service based on the integration of stand structural attributes in mixed oak forests. *Sustainability* 14:8228. doi: 10.3390/su14148228

Guo, Z., Xiao, X., Gan, Y., and Zheng, Y. (2001). Ecosystem functions, services and their values – a case study in xingshan county of CHINA. *Ecol. Econ.* 38, 141–154. doi: 10.1016/S0921-8009(01)00154-9

Hanley, N. D. (1993). The contingent valuation of forest characteristics: two experiments. *J. Agric. Econ.* 44, 218–229. doi: 10.1111/j.1477-9552.1993.tb00267.x

He, F., Yang, B., Wang, H., Yan, Q., Cao, Y., and He, X. (2016). Changes in composition and diversity of fungal communities along quercus mongolica forests developments in northeast China. *Appl. Soil Ecol.* 100, 162–171. doi: 10.1016/j.apsoil.2015.12.014

Hettiarachchi, J., and Ranasinghe, D. (2013). "A survey of the market availability and its potential for non-wood forest products, with special reference to medicinal plants and cane," in *Proceedings of international forestry & environment symposium.*

Hidemichi, F., Masayuki, S., and Shunsuke, M. (2017). Decomposition analysis of forest ecosystem services values. *Sustainability* 9:687. doi: 10.3390/su9050687

Jin, X., Ma, J., Cai, T., Sun, X., and University, N. F. (2016). Non-use value assessment for wetland ecosystem service of hongxing national nature reserve in northeast China. *J. Forestry Res.* 27, 1435–1442. doi: 10.1007/s11676-016-0264-8

JPFD. (2003). *Jilin province one-way volume table.* Changchun: Jilin Provincial Forest Department.

Kang, N., Hou, L., Huang, J., and Liu, H. (2022). Ecosystem services valuation in China: a meta-analysis. *Sci. Total Environ.* 809:151122. doi: 10.1016/j.scitotenv.2021.151122

Konarska, K. M., Sutton, P. C., and Castellon, M. (2002). Evaluating scale dependence of ecosystem service valuation: a comparison of NOAA-AVHRR and Landsat TM datasets. *Ecol. Econ.* 41, 491–507. doi: 10.1016/S0921-8009(02)00096-4

Kuuluvainen, T., and Gauthier, S. (2018). Young and old forest in the boreal: critical stages of ecosystem dynamics and management under global change. *Forest Ecosyst.* 5:26. doi: 10.1186/s40663-018-0142-2

Lee, W.-K., Gadow, K., Chung, D.-J., Lee, J.-L., and Shin, M.-Y. (2004). DBH growth model for pinus densiflora and quercus variabilis mixed forests in central Korea. *Ecol. Mod.* 176, 187–200. doi: 10.1016/j.ecolmodel.2003.11.012

Lei, J. (2006). The strategic position of songhua river three lakes protected area in the construction of northeast ecological system. *Forestry Econ.* 3, 57–59.

Li, W., Bai, Z., Jin, C., Zhang, X., Guan, D., Wang, A., et al. (2017). The influence of tree species on small scale spatial heterogeneity of soil respiration in a temperate mixed forest. *Sci. Total Environ.* 590, 242–248. doi: 10.1016/j.scitotenv.2017.02.229

Li, Z., Zhang, Y., Zhu, Q., Tian, S., and Chen, Z. (2011). Evaluation of values of ecosystem service function of the plain forestry in China. *Energy Proc.* 11, 4902–4910.

Liu, F., Feng, C., Zhou, Y., Zhang, L., Du, J., Huang, W., et al. (2022). Effectiveness of functional zones in national nature reserves for the protection of forest ecosystems in China. *J. Environ. Manage.* 308:114593. doi: 10.1016/j.jenvman.2022.114593

Liu, S., and Wang, H. (2018). N,P,and K characteristics of different age groups of temperate coniferous tree species in northwestern China. *J. Forestry Res.* 29:8. doi: 10.1007/s11676-017-0442-3

Liu, Y., Chen, Y., Liu, Y., and Li, Y. (2023). Comprehensive assessment on soil nutrient characteristics and quality of typical forests in zhangguangcai mountains. *Guizhou Agric. Sci.* 51, 28–34.

Ma, S., Qiao, Y., Wang, L., and Zhang, J. (2021). Terrain gradient variations in ecosystem services of different vegetation types in mountainous regions: vegetation resource conservation and sustainable development. *Forest Ecol. Manage.* 482:118856. doi: 10.1016/j.foreco.2020.118856

Musavi, T., Migliavacca, M., Reichstein, M., Kattge, J., Wirth, C., Black, T. A., et al. (2017). Stand age and species richness dampen interannual variation of ecosystem-level photosynthetic capacity. *Nat. Ecol. Evolut.* 1:0048. doi: 10.1038/s41559-016-0048

NFGA (2010). *Technical regulations for inventory for forest management planning and design*. Beijing: National Forestry and Grassland Administration.

NFGA (2020). *Specifications for assessment of forest ecosystem services*. Beijing: National Forestry and Grassland Administration.

Ninan, K. N., and Inoue, M. (2013a). Valuing forest ecosystem services: case study of a forest reserve in Japan. *Ecosyst. Serv.* 5, 78–87. doi: 10.1016/j.ecoser.2013.02.006

Ninan, K. N., and Inoue, M. (2013b). Valuing forest ecosystem services: what we know and what we don't. *Ecol. Econ.* 93, 137–149. doi: 10.1016/j.ecolecon.2013.05.005

Niu, X., Wang, B., Liu, S., Liu, C., Wei, W., and Kauppi, P. E. (2012). Economical assessment of forest ecosystem services in China: characteristics and implications. *Ecol. Complexity* 11, 1–11. doi: 10.1016/j.ecocom.2012.01.001

Odum, H. T., and Odum, E. P. (2000). The energetic basis for valuation of ecosystem services. *Ecosystems* 3, 21–23. doi: 10.1007/s100210000005

Qian, Y. (1999). Study on soil physical properties of desertified land in mosuowan reclamation area. *Arid Zone Res.* 16, 41–46.

Sang, W., and Bai, F. (2009). "Vascular diversity patterns of forest ecosystem before and after a 43-year interval under changing climate conditions in the changbaishan nature reserve, northeastern China," in *Forest ecology: recent advances in plant ecology*, ed. A. G. Van der Valk (Dordrecht: Springer Netherlands), 115–130. doi: 10.1007/978-90-481-2795-5_10

Shengjun, J. I., Geng, Y., Defeng, L. I., and Wang, G. (2009). Plant coverage is more important than species richness in enhancing aboveground biomass in a premature grassland, northern China - science direct. *Agric. Ecosyst. Environ.* 129, 491–496. doi: 10.1016/j.agee.2008.11.002

Smith, D. M., Eade, R., Scaife, A. A., Caron, L. P., Danabasoglu, G., Delsole, T. M., et al. (2019). Loss and damage: the role of ecosystem services. *NPJ Clim. Atmos. Sci.* 2, 8–14.

Song, M., Dong, M., and Jiang, G. (2002). Importance of clonal plants and plant species diversity in the northeast China transect. *Ecol. Res.* 17, 705–716. doi: 10.1046/j.1440-1703.2002.00527.x

Tang, A. (2021). *Evaluation of forest ecosystem service value in ailaoshan national nature reserve*. China: Yunnan Normal University.

Taye, F. A., Folkersen, M. V., Fleming, C. M., Buckwell, A., Mackey, B., Diwakar, K. C., et al. (2021). The economic values of global forest ecosystem services: a meta-analysis. *Ecol. Econ.* 189:107145. doi: 10.1016/j.ecolecon.2021.107145

Tobias, D., and Mendelsohn, R. (1991). Valuing ecotourism in a tropical rain-forest reserve. *J. Hum. Environ.* 20, 91–91.

Uddin, M. S., van Steveninck, E., Stuip, M., and Shah, M. A. R. (2013). Economic valuation of provisioning and cultural services of a protected mangrove ecosystem: a case study on sundarbans reserve forest. Bangladesh. *Ecosyst. Serv.* 5, 88–93. doi: 10.1016/j.ecoser.2013.07.002

Uhde, B., Heinrichs, S., Stiehl, C. R., Ammer, C., Müller-Using, B., and Knoke, T. (2017). Bringing ecosystem services into forest planning – can we optimize the composition of chilean forests based on expert knowledge? *Forest Ecol. Manage.* 404, 126–140. doi: 10.1016/j.foreco.2017.08.021

Villa, F., Bagstad, K. J., Voigt, B., Johnson, G. W., Portela, R., Honzák, M., et al. (2014). A methodology for adaptable and robust ecosystem services assessment. *PLoS One* 9:e91001. doi: 10.1371/journal.pone.0091001

Wang, C. (2006). Biomass allometric equations for 10 co-occurring tree species in Chinese temperate forests. *Forest Ecol. Manage.* 222, 9–16. doi: 10.1016/j.foreco.2005.10.074

Wang, X. (2022). The evaluation of forest ecosystem service function value in guandi mountain state-owned forest region in shanxi province. *Chin. Agric. Sci. Bull.* 38, 49–55.

Weckwerth, W. (2011). Metabolomics and systems biology approaches for the investigation of endophytes – plant- interaction – a vision for their importance in biotechnology and natural product research. *Planta Medica* 77:L12. doi: 10.1055/s-0031-1282090

Wenda, L., Dongxiang, W., and Nan, L. (1999). Market analysis for timber and forest products in China. *J. Forestry Res.* 10, 124–126. doi: 10.1007/BF02855543

Wu, Y. (2001). *Fertilizer Use Guide. Beijing: China Agriculture Press* .

Wu, Y. (2018). *Evaluation on service value of forest ecosystem in daba mountain natural reserve Ph, D. Thesis*. Chongqing Normal University.

Yuan, J., Xin, W., Zhengchun, S., Fei, C., Zhaoyong, H., Xiaofeng, Z., et al. (2015). Impacts of CWD on understory biodiversity in forest ecosystems in the qinling mountains China. *Pakistan J. Bot.* 47, 1855–1864.

Zhang, L., Rong, H., Yang, X. U., and Xingwang, X. U. (2011). Evaluation research of the service value of the forest ecosystem in jiuhua mountain, anhui. *J. Mount. Sci.* 29, 291–298.

Zhang, T., Wang, C., and Zhang, Q. (2017). Vertical variation in stoichiometric relationships of soil carbon, nitrogen and phosphorus in five forest types in the maoershan region northeast China. *Chin. J. Appl. Ecol.* 28, 3135–3143.

Zhang, Y. (2010). The millennium ecosystem assessment follow-up: a global strategy for turning knowledge into action. *J. Natl. Res.* 3, 522–528.

Zhang, Y., Liu, Y., Liu, S., and Zhang, X. (2012). Dynamics of stand biomass and volume of the tree layer in forests with different restoration approaches based on tree-ring analysis. *Chin. J. Plant Ecol.* 36, 117–125. doi: 10.3724/SP.J.1258.2012.00117

frontiers | Frontiers in Forests and Global Change

TYPE Original Research
PUBLISHED 18 July 2023
DOI 10.3389/ffgc.2023.1198143

OPEN ACCESS

EDITED BY
Zishan Ahmad Wani,
Baba Ghulam Shah Badshah University, India

REVIEWED BY
Gajendra Singh,
Uttarakhand Space Application Centre (USAC), India
Rupali Sharma,
Dr. Yashwant Singh Parmar U.H.F, India
Pradeep Singh,
Kumaun University, India

*CORRESPONDENCE
Himanshu Bargali
✉ himanshubargali44@gmail.com
Aseesh Pandey
✉ draseeshpandey@gmail.com

RECEIVED 31 March 2023
ACCEPTED 05 June 2023
PUBLISHED 18 July 2023

CITATION
Bargali H, Bhatt D, Sundriyal RC, Uniyal VP, Pandey A and Ranjan R (2023) Effect of forest fire on tree diversity and regeneration in the forests of Uttarakhand, Western Himalaya, India.
Front. For. Glob. Change 6:1198143.
doi: 10.3389/ffgc.2023.1198143

Effect of forest fire on tree diversity and regeneration in the forests of Uttarakhand, Western Himalaya, India

Himanshu Bargali [1,2]*, Dinesh Bhatt[1], Rakesh Chandra Sundriyal[3], Virendra Pratap Uniyal[4], Aseesh Pandey [2]* and Ram Ranjan[5]

[1]Department of Zoology and Environment Science, Gurukula Kangri (Deemed to be University), Haridwar, India, [2]G. B. Pant National Institute of Himalayan Environment, Kosi-Katarmal, India, [3]Department of Forestry and Natural Resources, Hemvati Nandan Bahuguna Garhwal University (a Central University), Srinagar, India, [4]Wildlife Institute of India, Dehradun, India, [5]Department of Economics, School of Humanities and Social Sciences, Shiv Nadar University, Greater Noida, Uttar Pradesh, India

The objective of this study was to investigate the impact of forest fires on tree diversity and their regeneration in three fire-prone forests of Uttarakhand, India. We used Landsat 5, 7, and 8 satellite imagery to prepare fire frequency maps and the study area was divided into four fire frequency classes. Ten plots were marked in each fire frequency class to assess diversity and regeneration pattern of tree species. A total of 14 tree species belonging to 14 genera and 13 families were sampled during the study period. We found that tree species diversity was higher in areas with low fire frequencies in comparison to the areas with no fire frequency class. We also observed that regeneration of tree species varied significantly across all fire frequency classes and forest types, with increasing dominance of certain fire-tolerant species in areas with frequent fires. Of the 33,678 individuals (tree, sapling, and seedling) recorded in all the fire frequency classes, 12,630 were in Sal Forest, 8,033 were in Chir-pine Forest, and 13,015 were in Mixed Forest. The study suggests that if forest fire incidences continue at current levels, the forests could experience a decline in tree diversity. Although forest fire is a natural occurrence in many ecosystems, the increasing frequency and intensity of fires due to human activities such as land-use change and climate change have disrupted the natural fire regime.

KEYWORDS

fire frequency, forest fire, tree diversity, regeneration, Uttarakhand, Western Himalaya, India

Introduction

Forest fire is a natural ecological disturbance agent that can have diverse effects on ecosystem composition, structure, and function at both the landscape and regional scale (Whelan, 1995; Keane et al., 2002; Negi, 2019; Bargali et al., 2022a). However, anthropogenic activities such as dependency on non-timber forest product and agricultural area expansion are among the primary causes of forest fires, which negatively impact species diversity, nutrient dynamics, and regeneration potential, and also emit greenhouse gases that contribute to global climate warming (Amiro, 2001; Murthy et al., 2006; Bhandari et al., 2012; Chaturvedi et al., 2017; Ray et al., 2019). In the Western Himalayan state of Uttarakhand, India, forest fire is a major issue especially during the dry season and adversely impacts forest ecosystems (Rikhari and Palni, 1999; Babu et al., 2016; Bargali et al., 2020). Long-term impacts of forest fire correspond to both the frequency and seasonality of the fire incidences; however, certain species exhibit adaptations to fire such as thick bark and altered germination timing for post-fire re-establishment of forest ecosystems (Khan and Tripathi, 1989; Bargali, 2018; Fule et al., 2021). Fire frequencies known to affect the density of seedlings and saplings of certain species, as lower densities were observed in high fire frequency zones (Hutchinson et al., 2012; Jhariya et al., 2012). Changes in vegetation structure and successional patterns due to fires can promote the expansion of fire-tolerant tree, grass, and shrub species and replace normal species regeneration patterns (Furley et al., 2008; Ryan and Williams, 2011; Syaufina and Ainuddin, 2011; Negi, 2019). However, studies on the post-fire regeneration of woody species in Himalaya are lacking (Negi, 2019). To address this knowledge gap, the present study aims to (1) analyze forest fire frequency patterns using satellite imagery, (2) examine how tree species diversity responds to fires, and (3) assess how the regeneration of woody species co-occurs with fire frequency classes in the three major fire-prone forests of Uttarakhand, Western Himalaya, India. Quantifying post-fire changes in regeneration and tree diversity in the fire-prone forests of Uttarakhand would be helpful for ecological assessment, sustainable forest management, and forest planning.

Materials and methods

Study site

Uttarakhand is a region located in the Western Himalaya of northern India, spanning from 28°43′N to 31°27′N and 77°34′ to 81°02′ E. It serves as a transitional zone between the Tibetan Plateau in the north, the Upper Gangetic Plains in the south, and the East Himalayan provinces in the western. The region is categorized into three zones: the Himalaya, the Shiwalik, and the Terai area, and has a climate ranging from subtropical to alpine (FSI, 2007). It experiences an annual rainfall of 92.31 mm[1] and a mean annual temperature (MAT) of 13.12–29.27°C (Negi, 2019). Uttarakhand boasts of 45.6% forest cover, including nine forest categories, such as tropical moist deciduous forests, tropical dry deciduous forests, sub-tropical pine forests, Himalayan moist temperate forests, Himalayan dry temperate forests, sub-alpine forests, moist alpine scrub, dry alpine scrub, and tree outside forests Bargali et al. (2022b). The state has a protected area network of six national parks, seven wildlife sanctuaries, and four conservation reserves, covering 7376.33 km^2 (13.79%) of the state's total geographic area (National Wildlife Database Cell). Uttarakhand reported 21,487 forest fire incidence out of the 345,989 incidence in India from November 2020 to June 2021 (Uttarakhand Forest Department). These fires occur annually between November and May due to natural and anthropogenic reasons, such as the accumulation of inflammable materials like dry leaves, twigs, and pine needles (Bahuguna and Upadhyay, 2002; Babu et al., 2016). The purpose of this study was to examine the effect of forest fire frequency on tree diversity and regeneration in three fire-prone forests in Uttarakhand Himalaya: Sal forests (*Shorea robusta* Gaertn.) at Motichur, Haridwar district; Chir-pine forests (*Pinus roxburghii* Sarg.) at Mauna Forest, Nainital district; and mixed forests of Banj-oak (*Quercus leucotrichophora* A.Camus) and Chir-pine (*P. roxburghii*) at Dhaulchina, Almora district. These selected forest types were identified based on their predominant occurrence and widely acknowledged significance in shaping ecosystem functioning. Previous studies have provided evidence of their substantial impact on diverse ecological factors, but limited to species richness, biodiversity, structural patterns, phenological dynamics, tree composition, allocation of biomass, primary productivity, nutrient cycling, accumulation of organic matter, and rates of decomposition (Joshi et al., 2022).

Fire frequency mapping

Forest fire frequency maps were developed for Uttarakhand state using Landsat 5, 7, and 8 satellite images spanning a period of 10 years (2011–2020) (**Table 1**).

The MODIS hotspot data or active fire data (MOD14) from the official website of the Fire Information for Resource Management System (FIRMS) of NASA were downloaded and merged with the shapefile data of fire points. Satellite images of each selected sites were extracted, geo-corrected, and classified into four frequency classes (i.e., no fire, low fire, moderate fire, and high fire frequency classes) (**Figure 1**).

Supervised classification was employed to classify the extracted and geo-corrected satellite images of selected study sites (i.e., Sal Forest, Pine Forest, and Mixed Forest) (**Table 2**).

A fishnet was created using the data management tool in ArcMap software, and the fire points and raster were spatially joined to generate the fire frequency map. A total of 16,206 fire points were recorded and further categorized into four fire frequency classes for the entire state. To exclude fire points that fall on settlements, we overlaid the settlement layer on top of the fire point layer. This ensured that only fire points within forest regions were used in our analysis. The fire frequency further classified into four frequency classes, namely, no fire, low fire, moderate fire, and high fire frequency class as depicted in **Figure 2**. To avoid bias, in each fire frequency class, we have selected 1 ha area for each forest types (**Table 3**).

Validation of fire frequency by forest fringe community

The fire frequency classes (namely, no fire, low fire, moderate fire, and high fire areas) were verified through consultation with the resident communities adjoining to the study sites. Once the validation of fire frequency classes was completed in each forest type, the demarcation of long-term study plots was made. The selection process includes the identification of three

---

[1] https://mausam.imd.gov.in/

TABLE 1 Date/Season of the data used for forest fire mapping.

Satellite	Month/Season
Landsat 5	March 2011–February 2013 (winter and summer)
Landsat 7	March 2013–February 2017 (winter and summer)
Landsat 8	March 2017–February 2020 (winter and summer)

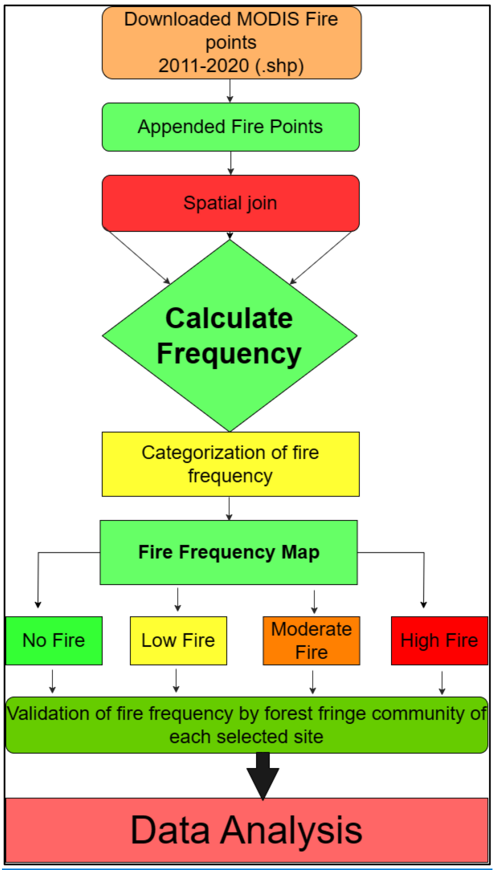

FIGURE 1
Systematic diagram showing the methodology adapted for fire frequency mapping (Bargali et al., 2017).

distinct forest types, and delineation of four fire frequency within each forest. Consequently, we identified a total of twelve study sites, located in different forest type with assigned specific fire frequency class. Our approach was to capture a broad range of fire frequency regimes across three major forest types, ensuring a comprehensive understanding of the relationship between fire and vegetation dynamics.

Field data sampling

Over a period of 2 years (2019–2020), a field study was conducted to collect floristic data from 12 plots (each 1 hectare in size) in selected forests that had undergone significant forest cover loss due to forest fires. Forests were stratified into three types: Sal Forest (SF), Chir-pine forest (C-PF), and Mixed Forest (MF), and selected for quantitative assessment. Stratified random sampling was used to sample plots within each forest type and fire frequency (Bargali et al., 2022a). In total, 120 plots were marked, covering a total area of 12 hectares, with 40 plots in each forest type, equally distributed among three forest types. Within each plot, all living woody trees with > 3 cm diameter at breast height were measured and identified. Voucher specimens were collected for unidentified individuals in the field. The identification process involved using checklists of Uttarakhand, the flora of Uttarakhand, and relevant literature (Osmaston, 1927; Polunin and Stainton, 1984; Pant, 1986). Field vegetation data were gathered in September and October 2020, and GPS (Oregon 700, Garmin) was used to map field sampling points. Collar diameter, girth at breast height, and plant height were measured for all woody plants (> 1 cm DBH) inside the plots. Additionally, two 5 × 5 m subplots were laid on two corners of the plot to enumerate seedlings and saplings. Individuals with > 30 cm CBH were defined as trees, however, individuals with CBH > 10 and < 30 cm were considered as sapling and individuals having CBH < 10 cm were considered as seedlings.

Data analysis

In the present study total number of species across all fire frequency classes was calculated for three growth forms (seedlings, saplings, and trees). Stem density was determined for each growth form in each class, and one-way ANOVA was used to identify significant differences in these factors among the frequency classes. The diversity index of trees was evaluated using the Shannon-Wiener index (H') (Shannon and Wiener, 1963). The study results were presented in terms of stem density and the number of species for all growth forms per fire frequency class. Statistical analyses were conducted using the ORIGIN 2023 software.

Results

Fire points under different fire frequency classes

As per the data collected on fire incidents under various fire frequency classes, there was a consistent reduction in the area affected by fires as the frequency of fires increased (**Figure 2**).

Over the 10 years period from 2011 to 2020, only 115 points (0.71% area) fell into the high fire frequency class (HF), 738 points (4.51% area) fell into the low fire frequency class (LF), 2,979 points (18.21% area) fell into the moderate fire frequency class (MF), and

TABLE 2 District wise area (Sq. km.) in each fire frequency classes.

Forest frequency class	District		
	Almora	Haridwar	Nainital
High fire	112.5	37.5	164.74
Low fire	930.36	351.94	956.88
Moderate fire	341.58	214.64	443.53
No fire	1568.52	1700.93	2362.63

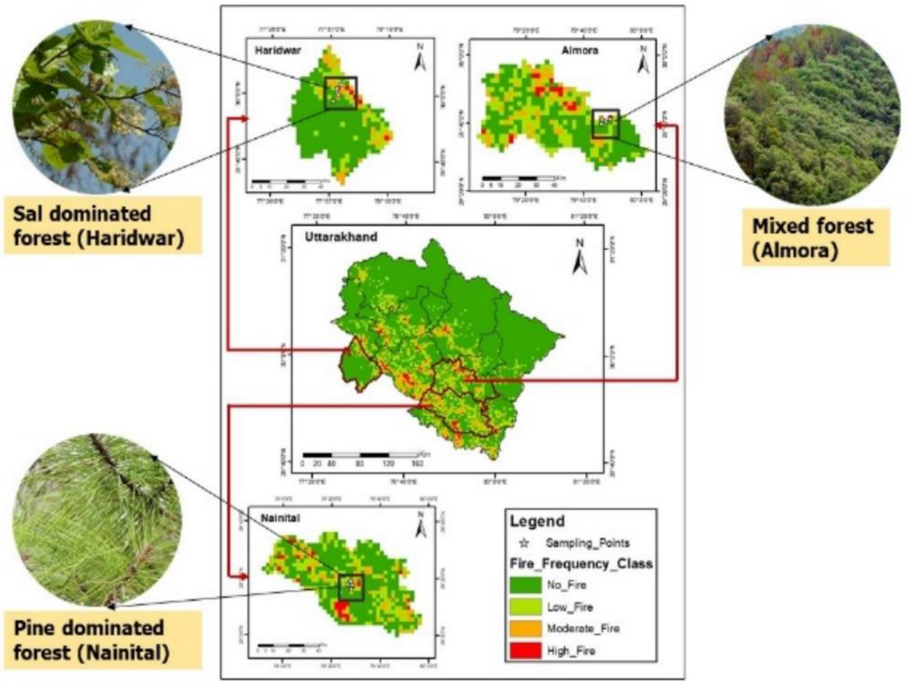

FIGURE 2
Fire frequency map, sampling points, and selected forest types in the studied sites.

12,524 points (76.57% area) fell into the no fire frequency class (NF) (**Figure 2**).

Species abundance and diversity

The study analyzed stem density, species diversity, and Shannon-Wiener values across three forest types: Sal Forest, Chir-Pine Forest, and Mixed Forest. A total of 7,468 stems from 36 tree species belonging to 29 genera and 26 families were observed. Stem density varied across forest types and growth stages, with SF having a density range of 485 to 655 stems ha^{-1} during tree growth, 430 to 880 stems per hectare as saplings, and 1,400 to 2,330 stems per hectare as seedlings. Species diversity was also found to vary by fire class, with SF having the highest diversity, and MiF the lowest. We calculated the Shannon-Wiener (H') values for each forest type and found that they were recorded between 1.54 to 1.93 for SF, 1.21 to 1.34 for C-PF, and 0.16 to 0.26 for MiF (**Figure 3**). Finally, stem diameter distribution showed a reverse J-shaped curve in all fire classes, with lower DBH stems being more prevalent and decreasing with increasing fire frequency (**Figure 4**).

Tree species regeneration

The analysis of the tree data revealed a statistically significant (p-value = 0.0003, R^2 = 0.890) relationship between the number of tree species and fire frequency classes in studied forests (**Figures 5A–D**). The results suggest that fire frequency has a highly significant ($p \leq 0.001$) impact on tree species diversity in these forests. Specifically, the number of tree species is low in forests with HF frequency compared to NF or LF frequency.

The analysis of the sapling data shows that there is a significant (p-value = 0.042, R^2 = 0.852) relationship between the number of sapling species and fire frequency in studied forests (**Figure 5B**). Overall, the data suggests that fire frequency has a significantly positive ($p \leq 0.05$) impact on the number of sapling species in the three forest types. However, fire frequency has shown a non-significant impact on the numbers of seedling species in these forest types.

Sal Forest

The stem density in Sal Forest in different girth classes was compared between the four fire frequency classes: NF, LF, MF, and HF (**Figure 4**). In the 1–10 cm girth class, the highest stem density was recorded in the LF class (2,330 individuals ha^{-1}), followed by NF (2,120 individuals ha^{-1}), MF (1,810 individuals ha^{-1}), and HF (1,400 individuals ha^{-1}). Similarly, in the 11–30 cm girth class, the highest stem density was recorded in the LF class (880 individuals ha^{-1}), followed by NF (780 individuals ha^{-1}), MF (560 individuals ha^{-1}), and HF (430 individuals ha^{-1}). In the 31–60 cm girth class, the highest stem density was recorded in the NF class (180 individuals ha^{-1}), followed by LF (200 individuals ha^{-1}), MF (170 individuals ha^{-1}), and HF (145 individuals ha^{-1}). In the 61–90 cm girth class, the highest stem density was recorded in the NF class (150 individuals ha^{-1}), followed by LF (140 individuals ha^{-1}), MF (120 individuals ha^{-1}), and HF (90 individuals ha^{-1}). In the 91–120 cm girth class, the highest stem density was recorded in the NF class (120 individuals ha^{-1}), followed by LF (125 individuals ha^{-1}),

TABLE 3 Description of selected fire frequency classes, plot studied, burned area, species diversity and stem density test types in the studied sites.

Class code	Fire frequency class	No. of plots	Area selected for study (ha)	No. of individuals (ind. ha^{-1})		
				Tree	Sapling	Seedling
Sal Forest (SF)						
SNF	No fire	10	1	620	780	2,120
SLF	Low fire	10	1	655	880	2,330
SMF	Moderate fire	10	1	560	560	1,810
SHF	High fire	10	1	485	430	1,400
Chir-pine forest (C-PF)						
C-PNF	No fire	10	1	776	480	820
C-PLF	Low fire	10	1	837	660	990
C-PMF	Moderate fire	10	1	720	420	730
C-PHF	High fire	10	1	630	320	650
Mixed Forest (MiF)						
MFNF	No fire	10	1	650	830	1,820
MFLF	Low fire	10	1	720	890	2,200
MFMF	Moderate fire	10	1	480	710	1,910
MFHF	High Fire	10	1	335	640	1,830

SNF, Sal Forest no fire; SLF, Sal Forest low fire; SMF, Sal moderate fire; SHF, Sam High Fire; C-PNF, Chir-pine no fire; C-PLF, Chir-pine low fire; C-PMF, Chir-pine moderate fire; C-PHF, Chir-pine high fire; MFNF, Mixed forest no fire; MFLF, Mixed forest low fire; MFMF, Mixed forest moderate fire; MFHF, Mixed forest high fire.

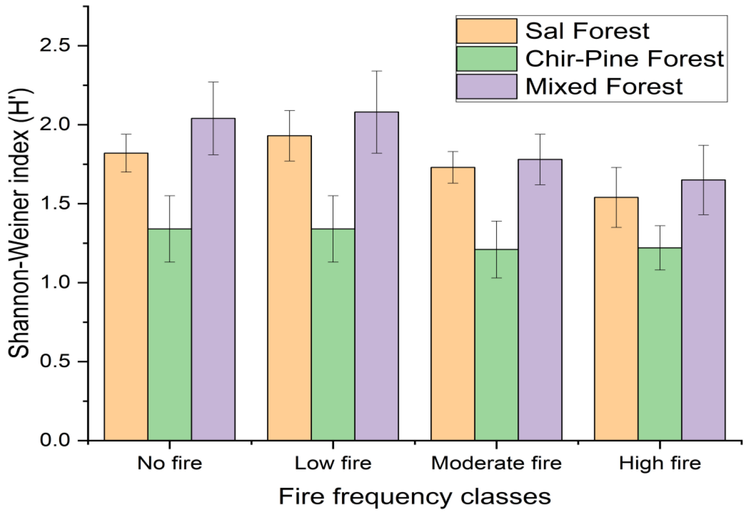

FIGURE 3
Shannon-Weiner index (H') for all the selected forest types and their fire frequency classes.

MF (130 individuals ha^{-1}), and HF (85 individuals ha^{-1}). In the 121–150 cm girth class, the highest stem density was recorded in the NF class (70 individuals ha^{-1}), followed by LF (65 individuals ha^{-1}), MF (70 individuals ha^{-1}), and HF (55 individuals ha^{-1}). In the 151–180 cm girth class, the highest stem density was recorded in the NF class (60 individuals ha^{-1}), followed by MF (50 individuals ha^{-}), LF (70 individuals ha^{-1}), and HF (40 individuals ha^{-1}). In the 180–210 cm girth class, the highest stem density was recorded in the NF class (30 individuals ha^{-1}), followed by LF (35 individuals ha^{-1}), MF (20 individuals ha^{-1}), and HF (20 individuals ha^{-1}). Finally, in the >210 cm girth class, the highest stem density was recorded in the NF class (10 individuals ha^{-1}), followed by LF (20 individuals ha^{-1}), and no stems were recorded in the MF and HF classes. In all fire frequency categories, the density of trees decreases as the girth classes increase *S. robusta* is the most abundant species in all four fire frequency classes, followed by *M. philippensis, S. cumini, B. monosperma*, and *A. marmelos*. The abundance of *S. robusta* is highest in the LF and NF classes, and lowest in the HF class. Conversely, the abundance of *M. philippensis* and *S. cumini* is highest in the HF class. *B. monosperma* shows the highest abundance in the MF class, while *A. marmelos* has the highest abundance in the LF class. In the sapling category, *S. robusta*

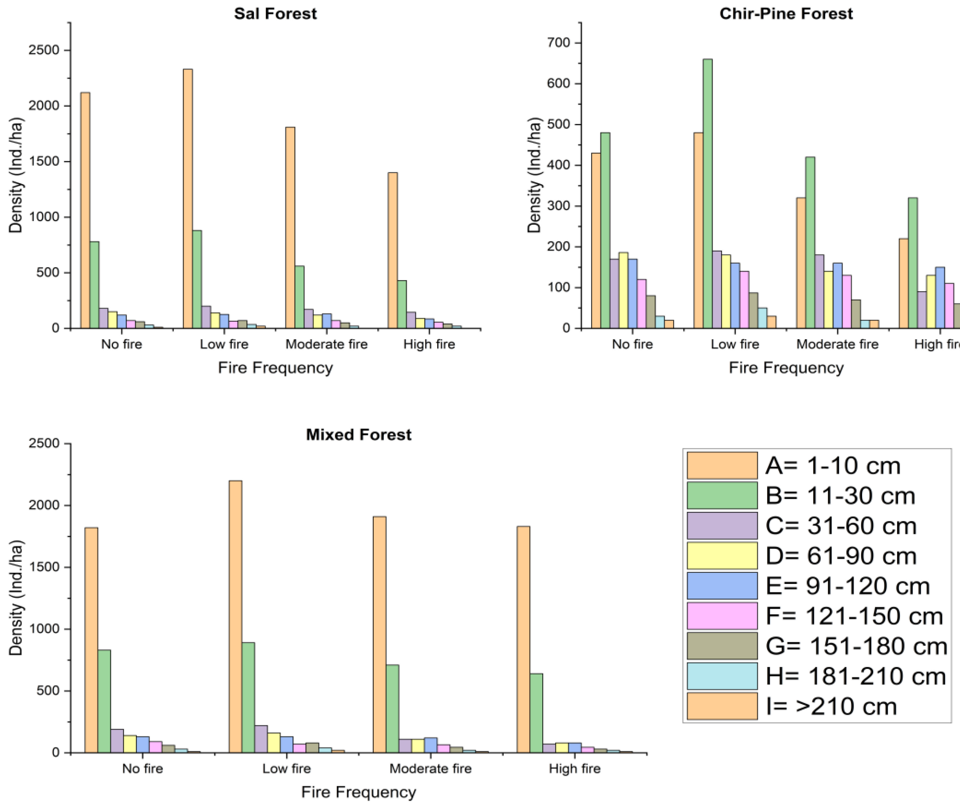

FIGURE 4
Stem diameter class distribution in all the frequency classes of selected forest types.

is again the most abundant species in all four fire frequency classes. However, the abundance of other species differs from the tree category. *M. philippensis* is the second most abundant species, followed by *E. laevis, S. oleosa,* and *C. fistula*. The abundance of *S. robusta* and *M. philippensis* is highest in the NF and LF classes, and lowest in the MF and HF classes. *E. laevis* and *S. oleosa* show the highest abundance in the LF and MF classes, respectively. *C. fistula* is only present in significant numbers in the LF class. In the seedling category, *S. robusta* is again the most abundant species in all four fire frequency classes, followed by *M. philippensis, E. laevis*, and *Schleichera oleosa*. The abundance of *S. robusta* is highest in the NF class and decreases with increasing fire frequency. *M. philippensis* shows the highest abundance in the NF and LF classes and is absent in the MF and HF classes. *E. laevis* shows the highest abundance in the NF and LF classes, while *S. oleosa* is only present in significant numbers in the NF class. The results suggest that *S. robusta* in the Sal forest is the most abundant species across all three growth stages (tree, sapling, and seedling) and all four fire frequency classes (Table 4).

Chir-pine forest

In the Pine Forest, the highest densities across all girth classes were observed in the LF frequency class, followed by NF, MF, and HF frequency classes, respectively. In the 1–10 cm girth class, the stem density was highest in the LF (Figure 4) frequency class with 480 individuals ha^{-1}, followed by the NF frequency class with 430 individuals ha^{-1}. The stem density was lowest in the HF frequency class with 220 individuals ha^{-1}, followed by the MF frequency class with 320 individuals ha^{-1}. In the 11–30 cm girth class, the stem density was highest in the LF frequency class with 660 individuals ha^{-1}, followed by the NF frequency class with 480 individuals ha^{-1}. The stem density was lowest in the HF frequency class with 320 individuals ha^{-1}, followed by the MF frequency class with 420 individuals ha^{-1}. In the 31–60 cm girth class, the stem density was highest in the MF frequency class with 180 individuals ha^{-1}, followed by the NF frequency class with 170 individuals ha^{-1}. The stem density was lowest in the HF frequency class with 90 individuals ha^{-1}. In the 61–90 cm girth class, the stem density was highest in the LF frequency class with 180 individuals ha^{-1}, followed by the MF frequency class with 140 individuals ha^{-1}. The stem density was lowest in the HF frequency class with 130 individuals ha^{-1}. In the 91–120 cm girth class, the stem density was highest in the LF frequency class with 160 Individuals ha^{-1}, followed by the MF frequency class with 160 individuals ha^{-1}. The stem density was lowest in the HF frequency class with 150 individuals ha^{-1}. In the 121–150 cm girth class, the stem density was highest in the LF frequency class with 140 individuals ha^{-1}, followed by the MF frequency class with 130 individuals ha^{-1}. The stem density was lowest in the HF frequency class with 110 individuals ha^{-1}. In the 151–180 cm girth class, the stem density was highest in the NF frequency class with 87 individuals ha^{-1}, followed by the LF frequency class with 70 individuals ha^{-1}. The stem density was lowest in the HF frequency class with 60 individuals ha^{-1}. In the 180–210 cm girth class, the stem density

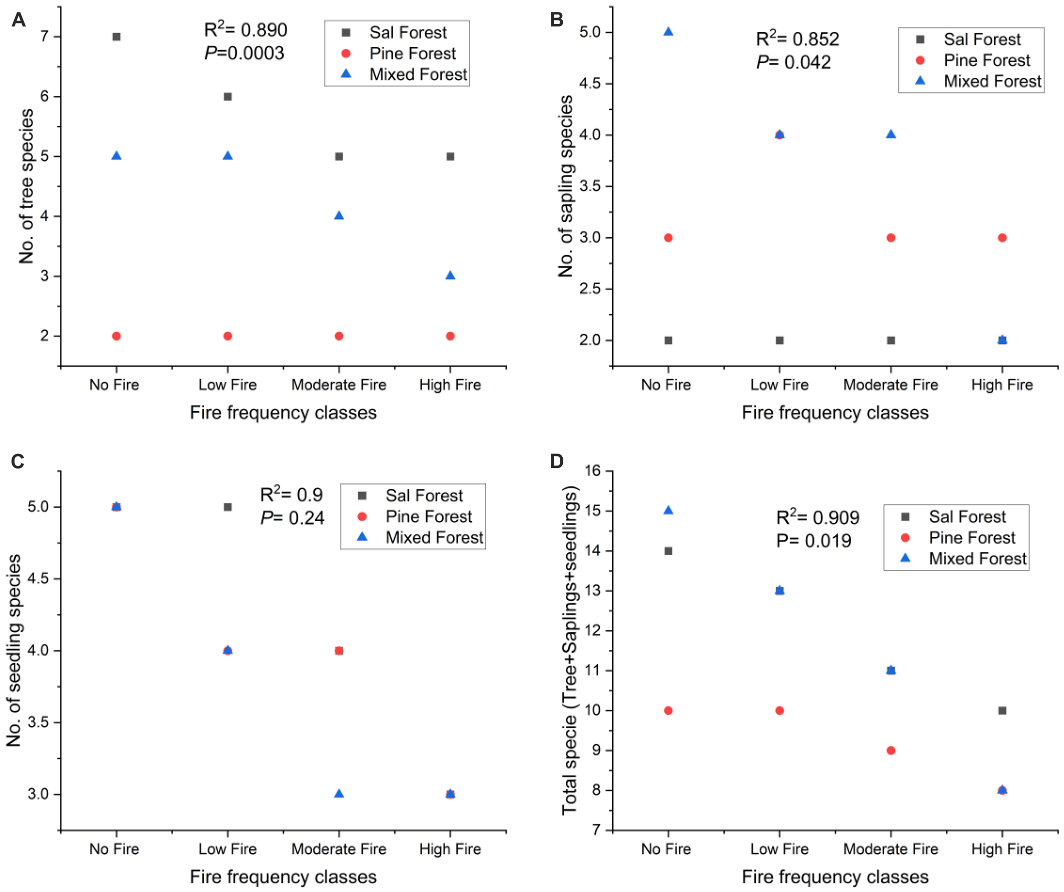

FIGURE 5
Relationship of forest fire frequency classes with **(A)** number of tree species, **(B)** number of sapling species, **(C)** number of seedling species, and **(D)** total number of species (tree + sapling + seedling).

was highest in the NF frequency class with 50 individuals ha^{-1}, followed by the LF frequency class with 30 individuals ha^{-1}. The stem density was lowest in the MF and HF frequency classes with 20 individuals ha^{-1}. In the >210 cm girth class, the stem density was highest in the NF frequency class with 30 individuals ha^{-1}, followed by the LF frequency class with 20 individuals ha^{-1}. The stem density was lowest in the MF and HF frequency classes with 20 and 10 individuals ha^{-1}, respectively. *P. roxburghii* is highly fire-resistant, with 73.68% of trees surviving a NF scenario, 46.18% surviving in LF, 16.12% in MF, and 10.26% in HF. *M. esculenta*, on the other hand, is less fire-resistant, with only 26.31% of trees surviving a no-fire scenario, 28.12% in LF, 14.13% in MF, and 10.16% in HF. *P. roxburghii* saplings showing more fire resistance than *M. esculenta* saplings. Additionally, *P. pashia* is listed as a sapling that is highly resistant to LF but has no saplings recorded on MF and HF classes. *L. ovalifolia* is recorded as a seedling that is moderately fire-resistant, with 24.69% in NF scenario, 14.14% in LF and10.18% in MF, and no seedlings recorded on HF frequency class.

Mixed Forest

In the tree layer the *P. roxburghii* can withstand a high percentage of low frequency fires (NF and LF), but is less tolerant to moderate and high frequency fires (MF and HF). *M. esculenta*, on the other hand, has lower tolerance to low frequency fires but can withstand moderate and high frequency fires to a greater extent (Figure 4). In the sapling category, *P. roxburghii* has a similar trend as in the tree category, showing higher tolerance to low frequency fires and lower tolerance to moderate and high frequency fires. *M. esculenta* has a higher tolerance to all fire frequencies in the sapling category compared to the tree category. *Q. leucotrichophora* has a moderate tolerance to all fire intensities in the sapling category. In the seedling category, *P. roxburghii* has the highest tolerance to all fire frequencies, but *R. arboreum* and *L. ovalifolia* show relatively lower tolerance to moderate and high frequency fires. *M. esculenta* and *Q. leucotrichophora* have moderate tolerance to all fire frequencies in the seedling category.

Discussion

The effect of fire frequency on tree density also varies across forest types. In SF, the tree density decreases with an increase in fire frequency, while in PF, the effect of fire frequency on tree density is less pronounced. In MiF, the tree density also decreases with an increase in fire frequency, but the effect is less severe compared to SF. In the present study, significant differences in species diversity

TABLE 4 Abundance of tree species at different growth stages (tree, sapling, and seedling) across all fire frequency classes.

Forest type (s)	Species	NF	LF	MF	HF
Sal Forest					
Tree					
1.	*Shorea robusta*	33.38	36.25	12.12	6.14
2.	*Mallotus philippensis*	13.35	16.14	14.26	8.24
3.	*Syzygium cumini*	14.3	18.12	16.12	n/p
4.	*Butea monosperma*	9.538	12.06	16.28	8.23
5.	*Aegle marmelos*	7.154	14.8	6.21	n/p
Sapling					
1.	*Shorea robusta*	37.28	38.26	16.23	20.24
2.	*Mallotus philippensis*	37.74	39.24	14.25	10.62
3.	*Ehretia laevis*	12.98	14.21	4.23	n/p
4.	*Schleichera oleosa*	7.98	6.24	2.15	7.34
5.	*Cassia fistula*	3.99	16.26	0.67	0.24
Seedling					
1.	*Shorea robusta*	59.72	52.12	16.14	18.13
2.	*Mallotus philippensis*	16.56	12.26	n/p	3.2
3.	*Ehretia laevis*	10.88	8.2	8.12	n/p
4.	*Schleichera oleosa*	12.48	10.26	n/p	n/p
Pine forest					
Tree					
1.	*Pinus roxburghii*	73.68	46.18	16.12	10.26
2.	*Myrica esculenta*	26.31	28.12	14.13	10.16
Sapling					
1.	*Pinus roxburghii*	23.07	29.29	16.18	6.13
2.	*Myrica esculenta*	30.76	32.23	18.14	12.8
3.	*Pyrus pashia*	46.15	16.14	n/p	n/p
Seedling					
1.	*Pinus roxburghii*	49.38	38.42	14.4	12.5
2.	*Myrica esculenta*	12.34	13.18	10.8	6.18
3.	*Quercus leucotrichophora*	7.4	8.12	n/p	n/p
4.	*Lyonia ovalifolia*	24.69	14.14	10.18	n/p
Mixed Forest					
Tree					
1.	*Pinus roxburghii*	38.35	16.46	8.16	6.1
2.	*Myrica esculenta*	13.69	18.1	6.1	3.2
3.	*Quercus leucotrichophora*	18.26	26.26	4.26	n/p
Sapling					
1.	*Pinus roxburghii*	22.22	28.13	4.82	6.2
2.	*Myrica esculenta*	24.69	26.25	10.12	8.23
3.	*Quercus leucotrichophora*	14.81	16.3	6.25	8.63
Seedling					
1.	*Pinus roxburghii*	43.95	20.18	3.12	4.3
2.	*Myrica esculenta*	9.15	10.16	2.23	1.14
3.	*Quercus leucotrichophora*	13.73	8.3	2.63	2.63
4.	*Rhododendron arboreum*	13.73	6.2	4.23	1.44
5.	*Lyonia ovalifolia*	19.41	2.11	4.23	2.44

were observed in the selected forest types of Uttarakhand. While species diversity increased in the LF frequency. For the SF, the highest tree diversity is observed in the no fire and low fire classes. The tree diversity decreases with increasing fire frequency, and the lowest tree diversity is observed in the high fire frequency class. For the PF, the tree diversity is the same across all fire frequency classes. For the MF, the highest tree diversity is observed in the no fire and low fire classes and the tree diversity decreases with increasing fire frequency. The lowest tree diversity is observed in the high fire class. Our results show that species richness and stand density decreased in high fire frequency class which could be due to the result of the poor regeneration processes that decrease species diversity in higher fire frequency classes. Our results support similar findings reported by Negi (2019), Bisht et al. (2020), Joshi et al. (2022), Bargali et al. (2022a) in different forests of Uttarakhand. Our results also support similar findings reported in the tropical dry deciduous forest of Chhattisgarh (Jhariya et al., 2012), in Mudumalai Tiger Reserve (Kodandapani et al., 2008; Verma and Jayakumar, 2015), and Sathyamangalam Tiger Reserve (Sathya and Jayakumar, 2017). Decreased species richness was also reported by Saha (2002), Saha and Howe (2003) in the dry deciduous forest of Central India. Our results also suggest that the low fire frequency could be beneficial for the regeneration of tree species. This result is concurrent with other experimental studies by Saha and Howe (2003) in the dry deciduous forest of Central India and in the Central Himalayan regions (Pande et al., 2014). According to Kodandapani (2001), mid-frequency fires enhance greater regeneration of seedlings due to the release of chemicals and nutrients locked up in old herbages as well as increasing light intensity, thus allowing rapid seed growth and low mortality rates once they successfully cross from the seedling stage to the sapling stage. Expanded soil supplement and the removal of seed dormancy could also explain the findings regarding the germination of specific tree species (Goldammer, 1988; Saha, 2002).

The density of trees varies across the forest types. SF has the highest tree density followed by PF and MF. The results showed that the highest sapling density values are found in the NF and LF, and lowest in HF frequency class for all three types of forests (Sal, Chir-Pine, and Mixed). This suggests that the absence or low fire are generally beneficial for regeneration of sapling of tree species. Conversely, the lowest sapling density values are generally found in the "High fire" frequency class for all three types of forests. This suggests that high fire frequency has a negative impact on sapling growth. In terms of the moderate fire frequency classes, the results are somewhat variable. For the SF, sapling density is highest in the LF frequency class and lowest in the MF frequency class. For the C-PF, sapling density is highest in the MF frequency class and lowest in the LF frequency class. For the MF forest, sapling density is highest in the LF frequency class and lowest in the MF frequency class. Overall, it appears that sapling density is generally highest in the NF frequency class and lowest in the HF frequency class, with variable responses to LF and MF frequencies depending on the forest type. The benefits of moderate or low disturbance for species regeneration have also been reported by Khan et al. (1987) and Maram and Khan (1998). This is in contrast to studies by Gould et al. (2002), Mondal and Sukumar (2014) in Mudumalai Tiger Reserve which found increasing numbers of seedlings and saplings in a single-burnt class compared to the control class.

Jhariya et al. (2012) reported that seedlings follow a similar trend in all fire frequency classes.

Conclusion

Our study highlights the varying effects of forest fires on tree species recovery in the Sal, Chir-Pine, and Mixed forests of Uttarakhand, Western Himalaya, India. It was observed that low fire event did not have a significant positive impact on the regeneration of species. Our findings suggest that low fire frequency inhibited the regeneration of seedling densities but increased species richness and tree density. On the other hand, high fire frequencies also hinder the growth of regenerating seedlings. Therefore, the recovery of tree species is impacted by all fire frequencies, whether high or low. Across all fire frequency classes, except for low fire frequency, there was less diversity than the control and an increasing dominance of certain fire-tolerant species with increasing fire frequency. In the Sal Forest, *S. robusta* is most abundant in the no fire frequency class but declines with increasing fire frequency. *Mallotus philippensis* is highly abundant in the no fire and low fire frequency classes but not recorded in the moderate fire and high fire classes. In the Pine Forest, low fire frequency class exhibits the highest density across all girth classes, followed by no, moderate, and high fire frequency classes. *P. roxburghii* shows high fire resistance, with survival rates of 73.68% (NF), 46.18% (LF), 16.12% (MF), and 10.26% (HF). *Pyrus pashia* shows high resistance as a sapling to low fire but no presence as saplings in the moderate and high fire frequency classes. In the Mixed Forest, *M. esculenta* exhibits greater tolerance to all fire frequencies as saplings compared to trees, while *Q. leucotrichophora* showed moderate tolerance as saplings. In the seedling category, *P. roxburghii* shows the highest tolerance to all fire frequencies, while *R. arboreum* and *L. ovalifolia* show relatively lower tolerance to moderate and high-frequency fires. *M. esculenta* and *Q. leucotrichophora* exhibit moderate tolerance to all fire frequencies as seedlings. Our study concludes that all fire frequency classes have significant impact on the regeneration of tree species, with low fire frequency being beneficial. The healthy regeneration of species is essential for maintaining plant species diversity and density in any ecosystem. This study provides a valuable baseline dataset for future in-depth studies related to forest fires, and further research is needed to explore the different ecological aspects and effects of fire on forest vegetation in Uttarakhand, Western Himalaya.

Data availability statement

The raw data supporting the conclusions of this article will be made available by the authors, without undue reservation.

Author contributions

HB: conceptualization data collection, methodology, data analysis, writing, software, and visualization. DB: conceptualization, supervision, methodology, validation, and writing—review. RS and VU: conceptualization, supervision, investigation, validation, and writing—review. AP: supervision, investigation, validation, and writing—review. RR: validation and writing—review. All authors contributed to the article and approved the submitted version.

Acknowledgments

The authors express their gratitude to the Director of G. B. Pant National Institute of Himalayan Environment (GBPNIHE) for providing institutional support. We acknowledge the Department of Zoology and Environment Science at Gurukula Kangri (Deemed to be University), Haridwar, for their logistic support. The authors thanks to G. C. S. Negi, former Scientist "G" at GBPNIHE, for his valuable suggestions and inputs.

Conflict of interest

The authors declare that the research was conducted in the absence of any commercial or financial relationships that could be construed as a potential conflict of interest.

Publisher's note

References

Amiro, B. D. (2001). Paired-tower measurements of carbon and energy fluxes following disturbance in the boreal forest. *Glob. Chang. Biol.* 7, 253–268. doi: 10.1046/j.1365-2486.2001.00398.x

Babu, K. V. S., Roy, A., and Prasad, P. R. (2016). Forest fire risk modeling in Uttarakhand Himalaya using Terra satellite datasets. *Eur. J. Remote Sens.* 49, 381–395. doi: 10.5721/EuJRS20164921

Bahuguna, V. K., and Upadhyay, A. (2002). Forest fires in India: policy initiatives for community participation. *Int. For. Rev.* 4, 122–127. doi: 10.1505/IFOR.4.2.122.17446

Bargali, H (2018). Forest fire frequency in Nainital District of Uttarakhand state. Riga: LAP Lambert Academic Publishing.

Bargali, H., Calderon, L. P. P., Sundriyal, R. C., and Bhatt, D. (2022a). Impact of forest fire frequency on floristic diversity in the forests of Uttarakhand, western Himalaya. *Trees Forests People* 9:100300. doi: 10.1016/j.tfp.2022.100300

Bargali, H., Gupta, S., Malik, D. S., and Matta, G. (2017). Estimation of fire frequency in Nainital District of Uttarakhand state by using satellite images. *J. Remote Sens. GIS* 6, 1–5. doi: 10.4172/2469-4134.1000214

Bargali, H., Kumar, A., and Singh, P. (2022b). Plant studies in Uttarakhand, Western Himalaya: A comprehensive review. *Trees Forests People* 8:100203. doi: 10.1016/j.tfp.2022.100203

Bargali, H., Singh, P., and Bhatt, D. (2020). Role of Chir Pine (*Pinus roxburghii* Sarg.) in the forest fire of Uttarakhand Himalaya. *ENVIS Bull. Himalayan Ecol.* 28, 82–85.

Bhandari, B. S., Mehta, J. P., and Semwal, R. L. (2012). "Forest fire in Uttarakhand Himalaya: an overview," in *Glimpses of forestry research in the Indian Himalayan region*, eds G. C. S. Negi and P. P. Dhyani (Almora: G.B. Pant Institute of Himalayan Environment & Development), 167–176.

Bisht, D., Singh, P., and Sundriyal, R. C. (2020). Forest status under fire regime: an ecological assessment in Upper-Kosi watershed in Almora district, Uttarakhand, India. *Indian J. For.* 43, 206–211. doi: 10.54207/bsmps1000-2021-89G23K

Chaturvedi, R. K., Raghubanshi, A. S., Tomlinson, K. W., and Singh, J. S. (2017). Impacts of human disturbance in tropical dry forests increase with soil moisture stress. *J. Veg. Sci.* 28, 997–1007. doi: 10.1111/jvs.12547

FSI (2007). ISFR India State of Forest Report 2007. Dehradun: Forest Survey of India.

Fule, P. Z., Garkoti, S. C., and Semwal, R. L. (2021). Frequent burning in chir pine forests Uttarakhand, India. *Fire Ecol.* 17, 1–11. doi: 10.1186/s42408-021-00106-3

Furley, P. A., Rees, R. M., Ryan, C. M., and Saiz, G. (2008). Savanna burning and the assessment of long-term fire experiments with particular reference to Zimbabwe. *Prog. Phys. Geogr.* 32, 611–634. doi: 10.1177/0309133308101383

Goldammer, J. G. (1988). Rural land-use and wildland fires in the tropics. *Agrofor. Sys.* 6, 235–252. doi: 10.1007/BF02344761

Gould, K. A., Fredericksen, T. S., Morales, F., Kennard, D., Putz, F. E., Mostacedo, B., et al. (2002). Post-fire tree regeneration in lowland Bolivia: Implications for fire management. *Forest Ecol. Manag.* 165, 225–234. doi: 10.1016/S0378-1127(01)00620-X

Hutchinson, T. F., Yaussy, D. A., Long, R. P., Rebbeck, J., and Sutherland, E. K. (2012). Long-term (13-year) effects of repeated prescribed fires on stand structure and tree regeneration in mixedoak forests. *Forest Ecol. Manag.* 286, 87–100. 08.036 doi: 10.1016/j.foreco.2012

Jhariya, M. K., Bargali, S. S., Swamy, S. L., and Kittur, B. (2012). Vegetational structure, diversity and fuel load in fire affected areas of tropical dry deciduous forests in Chhattisgarh. *Vegetos* 25, 210–224.

Joshi, V. C., Bisht, D., Sundriyal, R. C., and Pant, H. (2022). Species richness, diversity, structure, and distribution patterns across dominating forest communities of low and mid-hills in the Central Himalaya. *Geol. Ecol. Landsc.* 1–11. doi: 10.1080/24749508.2021.2022424

Keane, R. E., Ryan, K. C., Veblen, T. T., Allen, C. D., Logan, J. A., Hawkes, B., et al. (2002). *Cascading effects of fire exclusion in the Rocky Mountain ecosystems: a literature review. General Technical Report. RMRSGTR-91*. Fort Collins, CO: U.S. Department of Agriculture. doi: 10.2737/RMRS-GTR-91

Khan, M. L., Rai, J. P. N., and Tripathi, R. S. (1987). Population structure of some tree species in disturbed and protected subtropical forests of north-east India. *Acta Oecol.* 8, 247–255.

Khan, M. L., and Tripathi, R. S. (1989). Effects of stump diameter, stump height and sprout density on the sprout growth of four tree species in burnt and unburnt forest plot. *Acta Oecol.* 10, 303–316.

Kodandapani, N. (2001). Forest fires. *Resonance* 6, 34–41. doi: 10.1007/BF02868242

Kodandapani, N., Cochrane, M. A., and Sukumar, R. (2008). A comparative analysis of spatial, temporal, and ecological characteristics of forest fires in seasonally dry tropical ecosystems in the Western Ghats, India. *Forest Ecol. Manag.* 256, 607–617. doi: 10.1016/j.foreco.2008.05.006

Maram, M. K., and Khan, M. L. (1998). Regeneration status of trees in various categories of forests in Manipur. *J. Hill Res.* 11, 178–182.

Mondal, N., and Sukumar, R. (2014). Characterising weather patterns associated with fire in a seasonally dry tropical forest in southern India. *Int. J. Wildland Fire.* 23, 196–201. doi: 10.1071/WF13002

Murthy, M. S. R., Badarinath, K. V. S., Gharai, B., Rajshekhar, G., and Roy, P. S. (2006). The Indian forest fire response and assessment system (INFFRAS). *Int For Fire News* 34, 72–77. doi: 10.1111/btp.12219

Negi, G. C. S. (2019). Forest fire in Uttarakhand: causes, consequences and remedial measures. *Int. J. Ecol. Environ. Sci.* 45, 31–37.

Osmaston, A. E. (1927). *A forest flora for Kumaon, Allahabad*. Available online at: https://fsi.nic.in/

Pande, R., Bargali, K., and Pande, N. (2014). Impacts of disturbance on the population structure and regeneration status of tree species in a Central Himalayan Mixed-Oak Forest. *India. Taiwan J. For. Sci.* 29, 179–192.

Pant, P. C. (1986). *Flora of Corbett National Park*. Kolkata: Botanical Survey of India, 224.

Polunin, O., and Stainton, A. (1984). *Flowers of the Himalaya*. Oxford: Oxford University Press.

Ray, T., Malasiya, D., Dar, J. A., Khare, P. K., Khan, M. L., Verma, S., et al. (2019). Estimation of greenhouse gas emissions from vegetation fires in Central India. *Clim. Chang. Environ. Sustain.* 7, 32–38. doi: 10.5958/2320-642X.2019.00005.X

Rikhari, H. C., and Palni, L. M. S. (1999). Fire affects ground flora dynamics of forest ecosystem: A case study from Central Himalaya. *Trop. Ecol.* 40, 145–151.

Ryan, C. M., and Williams, M. (2011). How does fire intensity and frequency affect miombo woodland tree populations and biomass? *Ecol. App.* 21, 48–60. doi: 10.1890/09-1489.1

Saha, S. (2002). Anthropogenic fire regime in a deciduous forest of central India. *Curr. Sci.* 82, 1144–1147.

Saha, S., and Howe, H. F. (2003). Species composition and fire in a dry deciduous forest. *Ecology* 84, 3118–3123. doi: 10.1890/02-3051

Sathya, M., and Jayakumar, S. (2017). Post-fire regeneration status of tree species in a tropical dry deciduous forest of Southern India. *J. Trop. For. Sci.* 29, 305–317. doi: 10.26525/jtfs2017.29.3.305317

Shannon, C. E., and Wiener, W. (1963). *The mathematical theory of communities.* Champaign, IL: University of Illinois Press.

Syaufina, L., and Ainuddin, A. N. (2011). Impacts of fire on Southeast Asia tropical forests biodiversity: A review. *Asian J. Plant Sci.* 10, 238–244. doi: 10.3923/ajps.2011.238.244

Verma, S., and Jayakumar, S. (2015). Post-fire regeneration dynamics of tree species in a tropical dry deciduous forest Western Ghats, India. *Forest Ecol. Manag.* 341, 75–82. doi: 10.1016/j.foreco.2015.01.005

Whelan, R. J. (1995). *The ecology of fire*. Cambridge, MA: Cambridge University Press.

frontiers | Frontiers in Forest and Global Change

TYPE Original Research
PUBLISHED 28 September 2023
DOI 10.3389/ffgc.2023.1183509

OPEN ACCESS

EDITED BY
Manfred J. Lexer,
University of Natural Resources and Life Sciences Vienna, Austria

REVIEWED BY
Yan Gao,
Universidad Nacional Autonoma de Mexico, Mexico
Polyanne Gomide,
Universidade Federal de Lavras, Brazil

*CORRESPONDENCE
Ki Hwan Cho
✉ holidaycho@gmail.com

RECEIVED 31 March 2023
ACCEPTED 13 September 2023
PUBLISHED 28 September 2023

CITATION
Dhakal T, Cho KH, Kim S-J and Beon M-S (2023) Modeling decline of mountain range forest using survival analysis.
Front. For. Glob. Change 6:1183509.
doi: 10.3389/ffgc.2023.1183509

Modeling decline of mountain range forest using survival analysis

Thakur Dhakal[1], Ki Hwan Cho[2]*, Su-Jin Kim[3] and Mu-Sup Beon[4]

[1]Department of Life Science, Yeungnam University, Gyeongsan, Republic of Korea, [2]Institute of Natural Science, Yeungnam University, Gyeongsan, Republic of Korea, [3]Division of Forest Ecology, National Institute of Forest Science, Seoul, Republic of Korea, [4]Department of Landscape Architecture, Jeonbuk National University, Jeonju, Republic of Korea

Deforestation is a global issue; however, each deforestation phenomenon occurs within its own local context. Elucidating this context in detail is important to prevent deforestation and maintain sustainable ecosystem management. In this study, we analyzed the land cover changes, forest characteristics, and modeled the forest decline over the last two decades to reveal the pattern and affecting factors of deforestation in the Honam-Jeongmaek mountain range. Forests less than 50-years-old dominate the study area, indicating they were mainly regenerated after the 1970s. Reforestation policies such as planting trees have helped forest regeneration. In the study region, as deforestation occurred, agricultural and residential areas decreased, and barren and grassland increased. We applied the Weibull regression model to determine forest survivorship and covariates. The deforestation risks are significantly different among regions; protected areas lose less forest than non-protected areas but the losses in protected areas were also significant, with approximately 5% from 2000 to 2020. Areas of higher elevation and steep slopes experience less deforestation, whereas areas closer to the mountain ridge are at greater risk. With survival analysis, it is possible to assess the risk of deforestation quantitatively and predict long-term survival of forests. The findings and methods of this study could contribute to better forest management and policymaking.

KEYWORDS

mountain range, deforestation, survival analysis, Weibull regression, land cover change

1. Introduction

Deforestation has been a global issue for decades (Morton et al., 2006; Hosonuma et al., 2012; Yao et al., 2014; Barlow et al., 2016; Sandker et al., 2017). According to the Food and Agriculture Organization (FAO), the world had lost 178 million ha of forest since 1990, with a net loss rate of 4.7 million ha per year between 2010 and 2020 (FAO, 2020). The major causes of deforestation include, industrial agriculture, increasing cattle numbers, timber logging, mining, city expansion and infrastructure, forest fires, paper production, and climate change (Adams et al., 2012; Mon et al., 2012; López-Carr, 2021). Although deforestation is a global phenomenon, the specific patterns in which it occurs and its impact on socio-ecological relationships may vary by local context.

Forests in the Korean peninsula experienced severe depletion during the Korean war, but reforestation has been conducted since the 1960s in South Korea (Kim and Zsuffa, 1994; Park and Lee, 2014; Allison, 2016; Choi et al., 2019). The tree growing stocks increased from 9.6 m^3/ha in 1960 to 126.6 6 m^3/ha in 2010. From 1953 to 2010, forest area in South Korea almost doubled, with a 13-fold increase in the density of trees (Buckingham and Hanson, 2015). Despite a very successful forest regeneration campaign, deforestation continued in some areas and the issue has been receiving more attention. The forest area in South Korea has decreased from 6,551,000 ha in 1990 to 6,287,000 ha in 2020 (FAO, 2020). The overall decreasing ratio is relatively low (4% of forest in 1990), but this ratio varies in different regions (Global Forest Watch, 2021).

Most of the natural forests in Korea are located in mountains; thus, owing to the lack of accessibility, mountain forests are less affected by anthropogenic activities and have continued to grow after regeneration. Mountain forests are an important ecosystem component that plays a key role as a refuge for vulnerable species (Chung et al., 2016, 2018) and an ecological corridor connecting various ecosystems (Choi, 2004; Cho et al., 2008; Hayes, 2010; Chung et al., 2016, 2018). The network of mountain ridgelines has been traditionally conceptualized in Korea and are called "Daegan" and "Jeongmack" (Choi, 2004). The traditional concept of "mountains do not cross water and water does not go over mountains," has been passed down over hundreds of years and is widely accepted as an important geographic idea. The traditional geographic concept, which is aware of the importance of ridge networks, is similar to the modern concept of watersheds. Of note, the traditional concept emphasizes the continuity rather than the divide of watersheds. The mountain network of the Korea peninsular was composed of one main ridgeline, Daegan, Baekdu–Daegan, and several Jeongmacks. The concept has been adapted to the management of mountain ranges. The Baekdu–Daegan is the longest and highest mountain ridgeline range and is protected by a legislative act. Whereas Jeongmacks, a subsidiary of Beakdu–Daegan mountain ranges, are not well protected despite their importance to ecosystem functionality and socio-ecological linkage (Jang et al., 2008; Choi et al., 2014). Owing to the lack of protection laws, the forests on the Jeongmack mountain range are undergoing deforestation, especially around the villages near the ridgeline.

Deforestation monitoring is usually performed using remote sensing imagery (Greenberg et al., 2005; Songer et al., 2008; Sandker et al., 2017; Hadi et al., 2018). In a deforestation analysis study, it is common to create land cover/land use (LULC) maps using satellite images and compare the forest area of the LULC maps in two or more specific times (Sandker et al., 2017; Hadi et al., 2018). This approach quantifies the overall change in forest area; however, it has limitations in analyzing the trend of forest decline and predicting future decline (the time taken for a forest area to be reduced to a certain level).

The factors affecting deforestation have been analyzed using different models, including regression (Rosa et al., 2013; Pir Bavaghar, 2016), machine learning (Mayfield et al., 2020; Larrea-GallegosIan and Vázquez-Rowe, 2021), and survival analysis models (Vance and Geoghegan, 2002; Greenberg et al., 2005). Greenberg et al. (2005) used survival analysis to determine decreases in rainforest area; by using this method, it was not only possible to identify the factors affecting the deforestation rate but also quantify the accelerating deforestation rate. Vance and Geoghenan (2002) applied survival analysis to identify the factors that influence deforestation probability. Although survival analysis is recognized as a promising method to model and predict land cover change (An and Brown, 2008; Wang et al., 2013), it has not been frequently applied in deforestation research.

To date, studies on the temporal pattern of deforestation in South Korea are scarce. Research has mainly focused on the deforestation quantity and its spatial distribution (Jang et al., 2008; Yu et al., 2016). To help ecosystem management, answers to the following questions are essential: (1) how much forest area has been destroyed and how has the rate of deforestation changed over time? and (2) what factors affect deforestation? We believe that survival analysis is a useful statistical method to answer these questions. It models both the overall quantity and pattern change of deforestation over time. This study examined deforestation patterns and trends of the Honam–Jeongamaek mountain forest, which has long been the background of socio–ecological interactions.

2. Methods

2.1. Study area

The study area is the north part of Honam–Jeongmack mountain range, located in the southwestern part of the Korean peninsula (35° 36′ N, 128° 06′ E; Figure 1). One end of the mountain range is connected to the Baekdu–Daegan mountain range, the core ecological axis of the Korean Peninsula, and the other to the Naejangsan national park. The average temperature normals are 10.7 ~ 13.3 and precipitation total normals are 1329.8 ~ 1486.0 mm (Supplementary Table 1). The elevation range of the ridge line is between 166 meters and 1,230 meters above sea level. Among the broadleaf forests, oak forests are the most widespread, and among the coniferous forests, pine forests are the most widespread.

The administrative boundaries of the mountain villages roughly coincide with the 3 km buffer zone on the ridge; therefore, the 3 km buffer zone area was analyzed. The mountain range spans six municipalities. The study area can be divided into three regions according to regional characteristics. The west region of the mountain range (Wangju-gun and Jeongup-si) is connected to a wide range of farmland. This region is also under pressure for development as a large city (Jeonju-si, with a population of 657,432). The northeast region (Jinan-gun and Jangsu-gun) is a typical mountainous area with high elevation. The southeast region is a mixture of mountainous and agricultural areas (Imsil-gun, Sunchang-gun, and Jeongeup-si) and the elevation of the mountain is relatively low compared to the northeast region. Jeongup-si encompasses two regions: the west and southeast regions divided by the ridgeline (Figure 1). Over the past 20 years, Wanju-gun and Jeongup-si have seen an increase in population, while other municipalities have seen a decrease (Supplementary Table 2).

2.2. Data

Global forest change (GFC) data (Hansen et al., 2013) was used for survival analysis because it provides deforestation information. The dataset provides global tree (taller than 5 m in height) cover in 2000, and indications of deforestation from 2000 to 2020 on an annual basis. For this study, the vegetated areas in GFC data are regarded as forests. The data was produced based on the multi-temporal Landsat imagery with a spatial resolution of 30 m. In the GFC data, forest loss was defined as a complete removal of canopy tree cover; forest degradation, such as selective removals, was not characterized as a change (Hansen et al., 2013).

Although GFC data can provide an approximation of forest loss (Galiatsatos et al., 2020), the uncertainties exist in the dataset (Galiatsatos et al., 2020; Shimizu et al., 2020). In addition to modeling long-term deforestation trends based on GFC data,

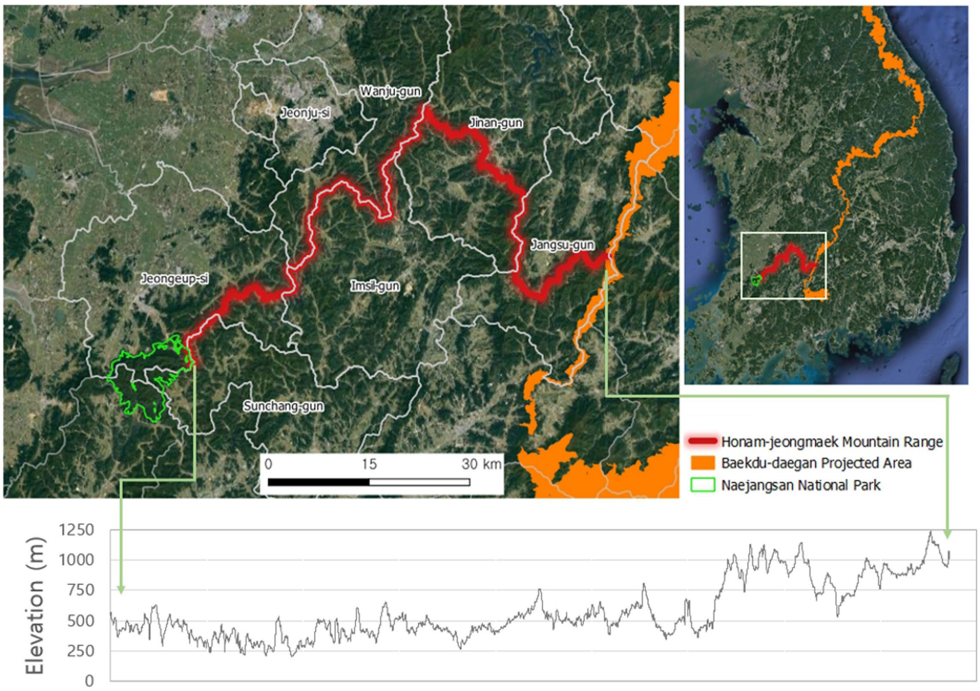

FIGURE 1
The ridgeline of Honam-Jeongmaek mountain range (red line) with elevation profile, and the Baekdu-Daegan protection area (orange area). Image data: Google.

TABLE 1 Specification of used land cover maps.

Published Year	Mapping level	Spatial resolution	Data type
2002	Level 2	5 m	polygon
2007	Level 2	5 m	polygon
2013	Level 2	5 m	polygon
2020	Level 3	1 m	polygon

we used quality-controlled land cover maps for detailed quantitative analysis of land cover change and forest type maps to characterize forests.

Land cover (LC) and forest type (FT) maps were used to identify the characteristics of the forest area. The LC maps are produced and distributed by the Ministry of Environment, South Korea. There are three different levels of LC types: level 1 consists of six LC types, namely, used (built-up) area, agricultural land, forest, grassland, wet land, barren, and water. Level 2 and 3 LC types provide more detailed classifications of land cover. Level 2 and 3 maps were used for analysis (Table 1), which have 22 and 41 LC types, respectively. For consistency, the level 2 LC classification (Supplementary Table 3) was used in the analysis. There are three forest types: broadleaf, coniferous, and mixed forests. Forest type maps are produced and provided by the Korea Forest Service. These maps provide detailed forest information on 42 tree types, decadal age classes, and stand density classes, and have been updated in the last decade. We used the FT map, published in 2015 and updated using aerial images from the early 2010s to identify characteristics of forest stand. Information of accuracy evaluation for each map is not provided, but there is a quality control condition that each map must have an overall accuracy of 95% or higher in order to be published (Environmental Spatial Information Service, 2023).

The Advanced Land Observing Satellite (ALOS) World 3D-30 m (AW3D30) global digital surface model data (Tadono et al., 2016) was used to analyze topographic characteristics such as elevation and slope. The latitude and longitude coordinates were projected onto the Universal Transverse Mercator (UTM) coordinate system (EPSG: 32652). The maps had different projected coordinate systems that were reprojected using the UTM.

2.3. Survival analysis

Survival analysis accounts for the time when an event occurs in addition to the magnitude of that event. It is a useful tool to develop regression models that best fit the relationship between the time of deforestation and covariates. We applied the Weibull regression model for parametric survival analysis, which has advantages of estimating baseline hazard function and modeling the effects of covariates (Lee and Wang, 2003; Zhang, 2016). The parametric survival model is used to predict future trends. In the practical application of survival analysis, it is common to use log transformations for the distribution of time to an event (T), and the relationship between T and the covariates can be expressed as:

$$\ln(T) = \beta_0 + \beta_1 x_1 + \ldots + \beta_p x_p + \sigma\varepsilon$$

where $\beta_0, \ldots, \beta_p$ are the regression coefficients for corresponding covariates; $x_1, \ldots, x_p$, σ is a scale parameter, and ε is the random disturbance term. The Weibull regression model assumes ε follows the

TABLE 2 Covariates used in the Weibull regression analysis.

Variable	Data	Spatial resolution
Region (Northeast, Southeast West)	Categorical	30 m
Protected area (protected, non-protected)	Categorical	30 m
Elevation (m)	Continuous	30 m
Slope (degree)	Continuous	30 m
Distance to ridge (m)	Continuous	30 m

Weibull distribution. The hazard function (the risk of event function, e.g., death or deforestation) at any moment in the Weibull regression model can be expressed with shape parameter λ as:

$$
\begin{aligned}
h(t) &= \lambda t^{\lambda-1} e^{-\lambda(\beta_0+\beta_1 x_1+\ldots+\beta_p x_p)} \\
&= \lambda e^{-\lambda\beta_0} t^{\lambda-1} e^{-\lambda(\beta_1 x_1+\ldots+\beta_p x_p)} \\
&= h_0(t) e^{-\lambda(\beta_1 x_1+\ldots+\beta_p x_p)}
\end{aligned}
$$

The baseline hazard is formulated as $h0(t)=\lambda e-\lambda\beta 0t\lambda-1$. The Weibull regression model can be used to test the relative effect of covariates (hazard ratio) and the change of hazard over time (accelerated failure-time, AFT).

Survival analysis requires the information of start, end, and event times. As the GFC data recorded a deforestation event after 2000, the LC map published in 2002 was used for the base information of the forest at the start time. The LC map is usually created based on the images taken a few years ago; thus, we decided to set 2000 as the start time (year) to maintain consistency with the GFC data. Each raster pixel of the GFC data located in the forest area of the map was considered as an alive forest pixel. The event was defined as forest loss on the GFC data. If a forest pixel had no forest loss indication, it was considered that the forest remained intact until 2020. The intact forest is dealt as right-censored data. We estimated the effect of covariates on survival time based on the Weibull regression model. A total five covariates, two categorical variables, and three continuous variables were used (Table 2). The correlation coefficient between the elevation and slope was 0.29, the correlation coefficient between the elevation and the distance to ridgeline was −0.19, and the correlation coefficient between the slope and the distance to the ridgeline was −0.14 (Supplementary Table 3).

2.4. Software

The quantum geographic information system (QGIS Development Team, 2023) was used for GIS data analysis, and R software (version 4.2.1; R Core Team, 2023) was used for statistical analysis. A Survival analysis was conducted using the “survival” package (version 3.2–10; Therneau and Grambsch, 2000).

3. Results

3.1. Land cover change

Land cover changes over the last two decades are listed in Table 3. The overall change of used (built-up) area was ~15–20 km^2 (Table 2). But detailed LC change analysis revealed larger variation, residential area decreased from 10.3 km^2 in 2002 LC map to 2.5 km^2 in 2020 LC map, while transportation infrastructure area increased from 5.9 to 15.4 km^2 during the same period. The grass and barren land types increased, and majority of the incensement was caused by anthropogenic activity. In the case of grass, the artificial grassland had an area of 77.3 km^2 on the 2020 LC map, while natural meadow had an area of only 0.2 km^2. Similarly, artificial barren land area was 17.0 km^2, while natural barren land was 2.7 km^2 on the 2020 LC map. The water area has been fluctuating around 22 km^2. During the last two decades, the net decrease in forest area was 49.9 km^2. Even in areas with new forests, owing to afforestation activities, the deforestation area increased. Among the areas that were forests on the 2002 LC map, a total forest area of 49.9 km^2 was changed to other land cover types on the 2020 LC map. Most of the decreased area turned into grassland (45.7 km^2), barren land (12.0 km^2) and agricultural land (11.1 km^2) on the 2020 LC map (Table 4). 83% of the new forest grew on agricultural land (12.7 km^2) and grasslands (7.59km^2; Table 4). The area of broadleaf, coniferous, and mixed forest was 386.5, 128.6, and 30.9 km^2, respectively on the 2020 LC map.

The study area includes several types of protected areas, such as national parks, wildlife sanctuaries, and wetlands, among others. The forest area in the protected areas was 113.5 km^2 on the 2002 LC map and 107.2 km^2 on the 2020 LC map. The forest area in the non-protected areas was 510.5 km^2 on the 2002 LC map and 446.9 km^2 on the 2020 LC map.

3.2. Characteristics of forest

We calculated forest area by stand age class in the three regions (within the 3 km buffer from the ridgeline) based on the FT maps (Figures 2, 3). The majority of the forests belong to the stand age 31 to 40 years, implying that these forests were regenerated post the 1970s. The northeast region has the largest forest area but old forests (> 41 years) of the region are relatively small compared to that of other regions. The west region has the largest area of old forests. Pine tree covers the largest area of the coniferous forest. Among the pine tree forests, *Pinus densiflora* dominated forests are the largest (59.4 km^2). The representative planted pine species occupying a large area are the larch (*Larix kaempferi,* 33.9 km^2) and Rigida pine (*Pinus rigida,* 35.1 km^2; Table 5). Oak tree (*Quercus* spp.) covers the largest area (216.5 km^2) of the broadleaf forest, while tulip tree (*Liriodendron tulipifera*) covers the largest area (12.0 km^2) among planted broadleaf trees. Young forests (< 20 years) are dominated by naturally regenerating oak or pine trees (Table 5).

3.3. Survivorship of mountain forest

Hazard ratios (HRs) from the Weibull regression model for the deforestation event are listed in Table 6. The deforestation risk of the

TABLE 3 Land cover area (km^2).

Land cover type	2002	2007	2013	2020	Change (2002–2022)
Used area (built-up area)	19.69	18.35	15.15	21.03	1.34
Residential area	10.29	9.38	5.42	2.51	−7.78
Industrial area	0.33	0.64	0.34	0.17	−0.16
Commercial area	0.75	0.90	1.13	1.29	0.54
Cultural, sports, and recreational area	0.06	0.12	0.31	0.27	0.21
Transportation area	5.90	6.03	6.75	15.40	9.50
Public facilities area	2.36	1.28	1.20	1.39	−0.97
Agricultural Land	114.02	115.97	103.41	79.28	−34.74
Rice paddy field	57.33	56.67	28.94	21.25	−36.08
Field	52.86	55.13	62.69	43.62	−9.24
Facility plantation	0.32	0.47	1.16	1.93	1.61
Orchard	2.57	2.21	7.36	8.85	6.28
Other cultivated area	0.94	1.49	3.26	3.63	2.69
Forest	623.98	617.17	600.16	574.11	−49.87
Broadleaf forest	286.07	285.07	397.78	386.49	100.42
Coniferous forest	250.93	245.96	167.59	154.54	−96.39
Mixed forest	86.98	86.14	34.79	33.08	−53.9
Grass	13.11	16.72	43.28	77.55	64.44
Natural meadow	5.48	5.60	33.20	0.23	−5.25
Artificial grass	7.63	11.12	10.08	77.32	69.69
Wetland	1.53	3.01	5.44	5.66	4.13
Inland wetland	1.53	3.01	5.44	5.66	4.13
Barren	3.51	6.11	8.37	19.74	16.23
Natural barren	0.07	0.16	1.71	2.75	2.68
Artificial barren	3.44	5.95	6.66	16.99	13.55
Water	22.74	21.23	22.75	21.21	−1.53
Inland water	22.74	21.23	22.75	21.21	−1.53

TABLE 4 Land cover change between forest and other land covers (2002–2020; km^2).

Land cover type	Forest to other land cover	Other land cover to forest
Used area (built-up area)	3.68	2.81
Agricultural land	11.10	12.46
Grass	45.72	7.59
Wet land	0.71	0.08
Barren	11.96	0.51
Water	0.78	0.61

west and southeast regions is significantly lower than that of the northeast region (confidence intervals lower than 1). The west region had the lowest deforestation risk (Table 6). If the deforestation trends maintain the current trajectory, the amount of forest (LC map in 2002) in the northeast, west, and southeast regions will decrease by 75, 82.5, and 80%, respectively, by 2040 (Figure 4). The 95% confidence interval of the non-protected area is greater than 1 (Table 6), which means that the risk of deforestation in the non-protected area is significantly higher than that of the protected area. However, forests in the protected areas also undergo deforestation. The loss of forest in protected areas is predicted to reach 10% in 2035, and if unprotected, 20% in the same year. As elevation, slope, and distance to ridge increases, deforestation risk decreases (confidence intervals of the covariates are lower than 1). Figure 5 shows the survival curves of the unprotected forest areas by region. The forest areas in the south and southeast regions are predicted around 80% in 2040. In contrast, the forest areas in the northeast region will decrease by 72% in the same year if the current trend continues without policy changes to protect the forest.

4. Discussion

To understand the characteristics and regional context of deforestation, we conducted two different analyses that related to each

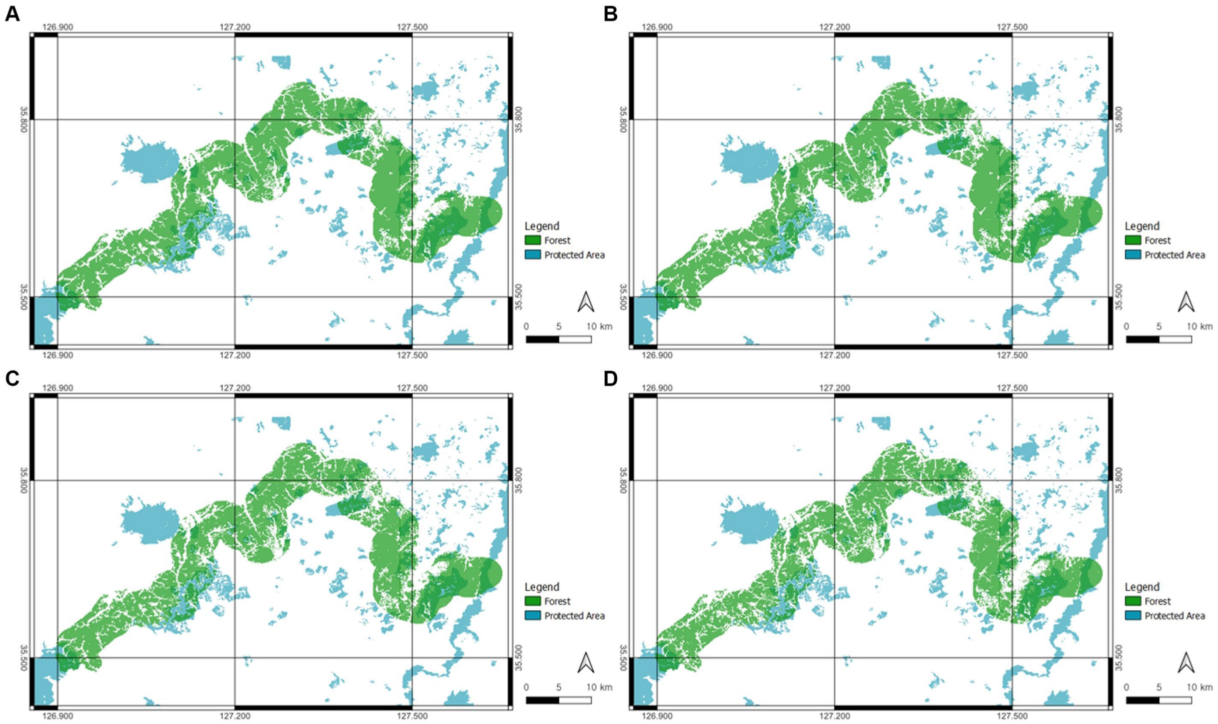

FIGURE 2
Forest in land cover maps within 3 km buffer of mountain ridge and protected area (blue, **A**) 2002, **(B)** 2007, **(C)** 2013 and **(D)** 2020.

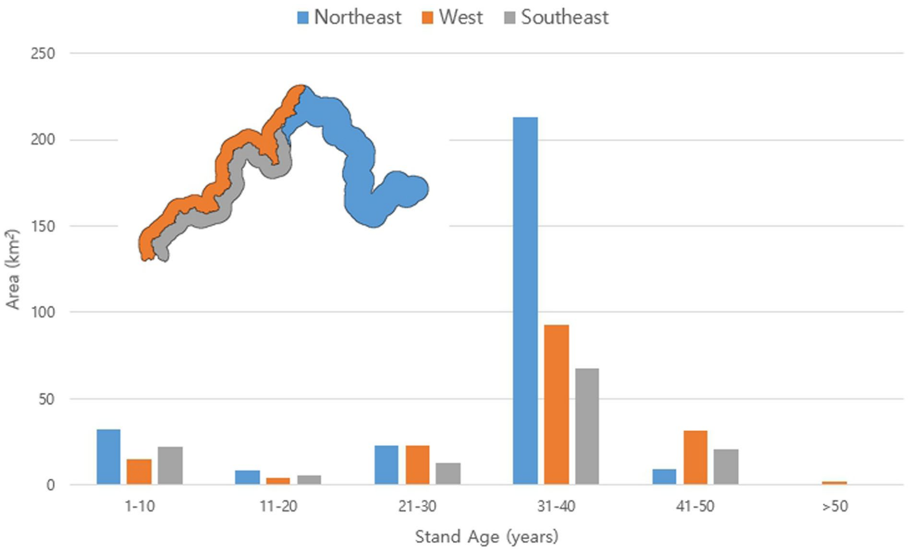

FIGURE 3
Forest areas by stand age of three regions.

other: first, we analyzed land cover change and forest characteristics using maps that are spatially accurate but cover discrete time periods (LC maps) or single period (FT map); second, we used temporally detailed GFC data to model trends in deforestation over time. This approach complements the weaknesses of both datasets, one lacking temporal detail and the other with relatively large uncertainties.

4.1. Land cover change

Urbanization and agricultural expansion have been acknowledged as major driving forces of deforestation (Greenberg et al., 2005; Morton et al., 2006; López-Carr, 2021). The FAO (2020) reported that agriculture has the biggest impact on deforestation (~ 80%), followed

TABLE 5 Stand age and area (km²) of major forest types.

Forest type	Stand age (years)					
	1–10	11–20	21–30	31–40	41–50	>51
Oak forest (*Quercus* spp.)	15.81	3.90	14.63	151.33	30.51	0.36
Pine forest (*Pinus densiflora*)	5.57	0.68	4.16	38.15	10.72	0.04
Rigida pine forest (*Pinus rigida*)	0.03	0.03	0.77	34.15	0.12	0.00
Larch forest (*Larix kaempferi*)	0.52	0.49	4.14	28.42	0.28	0.00
Mixed forest	4.58	0.31	6.56	26.08	1.22	0.00

TABLE 6 Hazard ratios (HR) from the Weibull regression model for the deforestation dataset.

Covariates	Coefficient (β)	HR [exp(β)]	95% Confidence interval	*p* value
Region				<0.001
Northeast	(0.00)	(1.00)		
West	−2.137	0.118	0.115–0.121	
Southeast	−1.313	0.269	0.263–0.275	
Protection				<0.001
Protected	(0.00)	(1.00)		
Non-protected	0.611	1.842	1.796–1.888	
Elevation (m)	−0.004	0.9956	0.9955–0.9956	<0.001
Slope (°)	−0.018	0.982	0.981–0.983	<0.001
Distance to ridge (m)	−0.00006	0.99994	0.99993–0.99995	<0.001
Scale = 0.707				

by construction (15%), and urbanization (~ 5%); however, the driving factors vary by country, geographic region, and era. Contrary to the results of previous studies, the decrease in forest in the study area occurred simultaneously with decreasing agricultural and residential areas. However, the net decreasing rate of agricultural lands is more rapid (−30%) than that of forest areas (−8%; Table 3). The net decreasing rate of residential areas is even more drastic; 10.3 km² of the residential area on the 2002 LC map decreased to 2.5 km² on the 2020 LC map (−75%). However, transportation infrastructure area increased by 2.6 times (from 5.9 to 15.4 km²). This suggests that deforestation may continue to increase even in rural areas with declining populations. Figure 6A shows a constructed road after deforestation in 2003. During the two decades, the areas of barren and grassland have shown a 5.9-and 5.6-fold increase, respectively (Table 3), while 86% of the barren land on the 2020 LC map is artificial. Part of the barren land area is a construction site that is temporarily barren. The grassland areas are more difficult to interpret. Some areas may be sites with grass growth on abandoned land, but some areas may be classified as grassland when seedlings are planted after logging (Figure 6B). The exchange of agricultural land and forest area is worth noting. The changed area from forests to agricultural lands is similar to the area changed from agricultural lands to forests (Table 4). But the conditions under which the change occurs are different: forests with suitable conditions for agriculture are changing to agricultural land. In contrast, the new forests are growing on agricultural land that is difficult to farm, i.e., abandoned farmland. This pattern of forest expansion is found in places where large-scale migration to urban areas takes place (Cervera et al., 2019; Ameztegui et al., 2021).

Post-logging reforestation does not permanently destroy forest areas. However, the planted trees have a different species composition and vertical structure from the surrounding forests, and they take abundant time to obtain functional homogeneity with the surrounding forests. In addition to the amount of forest loss, the decline causes forest fragmentation (Figure 2). Although forest fragmentation analysis was not conducted because it deviates from the subject of this study, a study in Jinan-gun, which is located in the study area, revealed that forest fragmentation around the mountain village is progressing (Kang et al., 2012).

4.2. Characteristics of forest

Government led reforestation policies started in 1973 are supporting the increase of overall growth of forests in South Korea (Bae et al., 2012; Park and Lee, 2014). Forests less than 40-years-old dominate in the study area. Considering that the data from the early 2010s was used to create the FT map, the forests were mainly regenerated after the 1970s. Tree planting carried out as part of the reforestation policies has facilitated forest regeneration, but natural regeneration of *Pinus densiflora* and *Quercus* spp. also occurred in large areas. Naejangsan Natural Park and the surrounding areas were the main habitats of old forests (≥ 41 years old). The lack of old forests in the mountain regions indicates the extensive use of timber and

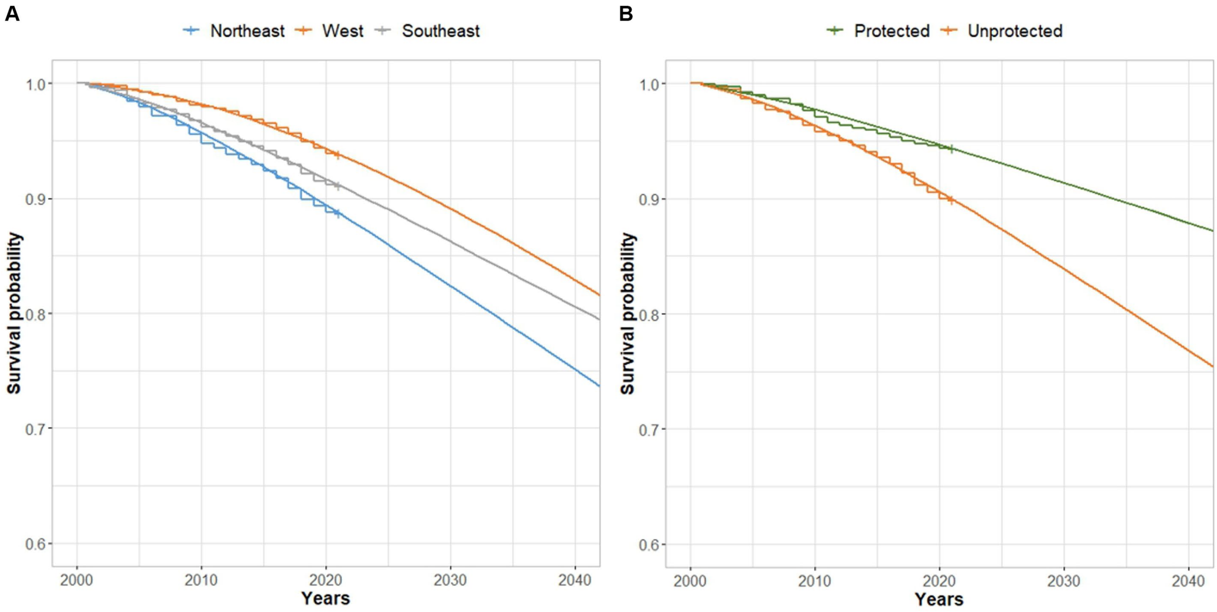

FIGURE 4
Predicted survival curves, based on a Weibull regression model, showing the effect of **(A)** regions and **(B)** protection area.

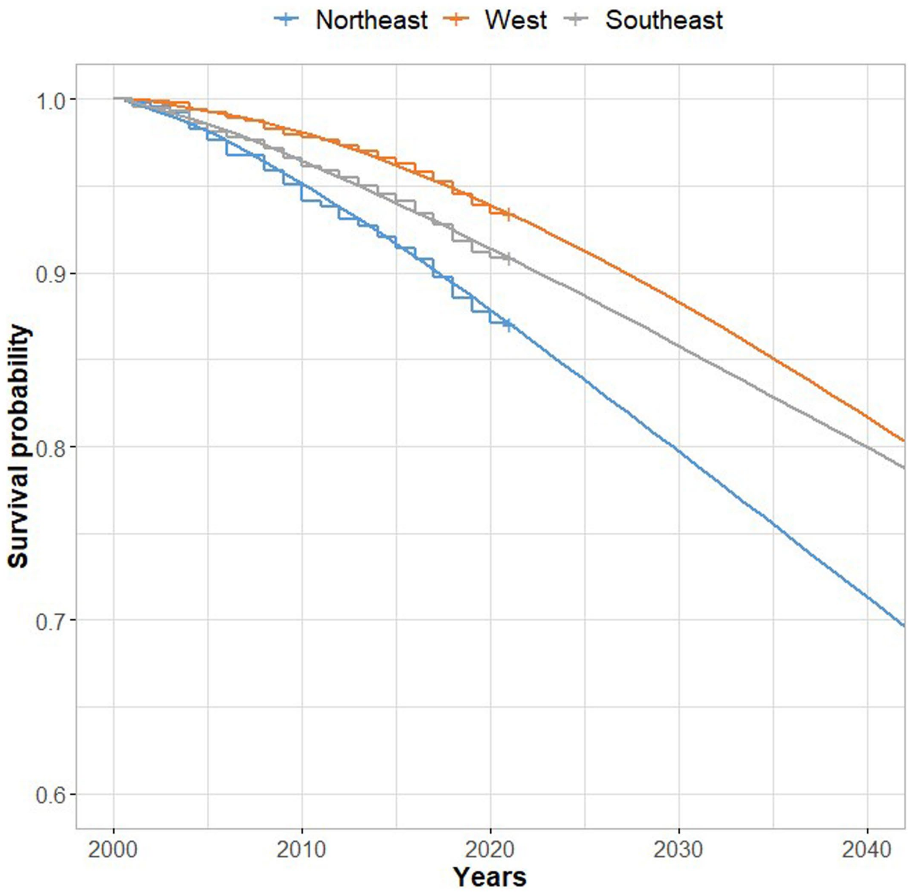

FIGURE 5
Predicted survival curves, based on a Weibull regression, showing the effect on regions of unprotected area.

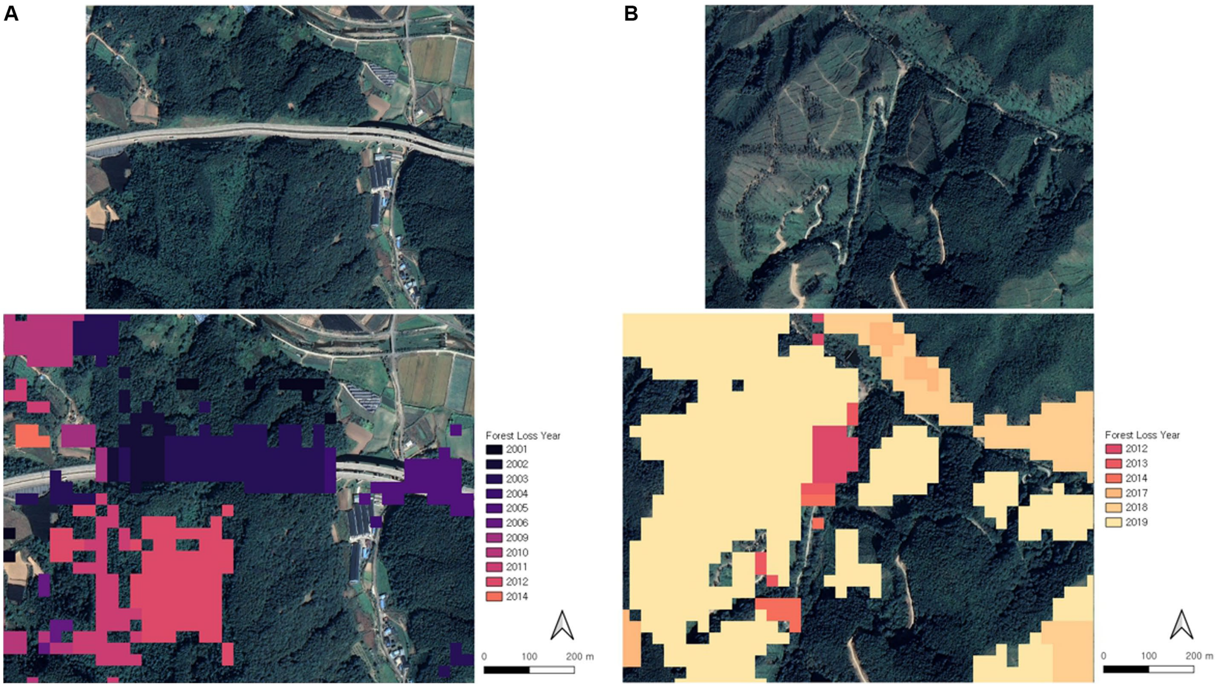

FIGURE 6
Deforestation cases **(A)** constructed infrastructure (35.7734 ° N, 127.4712° E; **B**) post-logging reforestation (35.7411 ° N, 127.4642° E; google satellite images). Image data: Google.

woodland resources by the villagers before the 1970s. Since forest management after Korean War focused on the supply of fuel wood, fast-growing trees were selected as the main reforestation species (Bae et al., 2014). As a result, the larch, rigida pine, and tulip tree occupy the largest area in the afforestation sites. However, due to changing socioeconomic conditions, these species have less economic value currently, as fuel wood is no longer needed. In addition, naturally regenerated forest, especially oak forest, is considered to have low economic value. The forest dominated by these species are used for logging and replanting on a massive scale (Figure 6B). However, logging a matured forest to grow a managed young forest changes the forest structure and undermines habitat continuity and biodiversity (Hagar et al., 2014; Kuuluvainen and Gauthier, 2018).

4.3. Survivorship of mountain forest

Deforestation can be affected by several factors. Forests located near villages and infrastructure are more likely to be removed or degraded than are remote forests (Greenberg et al., 2005; Sharma et al., 2020). Additionally, deforestation can be affected by topographical characteristics such as slope and elevation (Sharma et al., 2020; Feng et al., 2021). We applied the Weibull regression to model the forest survivorship and covariates that affect it. The northeast region has been affected more by deforestation than have the other regions (Figure 4A). As the northeast has the largest forest, the high risk in the region (Table 4) imposes a larger deforestation area (Figure 3).

Protected areas lose less forest than non-protected area, but there has been a loss of ~5% of forest in protected areas over the past 20 years. Since the early 2010s, deforestation rates have decreased due to an increase in protected areas. Not all protected areas area strictly protected as are national parks. Thus, even in protected areas forest loss may occur. Sustainable management of unprotected areas is essential for the conservation of the Jeongmack mountain range; the forest of this area has long been the ground for socio–ecological interactions in Korea. Excessive expansion of protected area can undermine forest use and the socio–ecological interactions. Temporal deforestation caused by logging and planting need to be regulated in a more organized manner. Therefore, it is necessary to expand the forestry direct payment project, which started in 2022, to motivate the preservation of forests without damaging them.

In contrast, the areas of higher elevation and steep slope are less affected by deforestation because the high elevation and steep slopes impose restrictions on land use. Notably, however, as the distance to the ridge decreases, the risk of deforestation increases (Table 6); that is, the closer the area to the ridge, the greater the risk of deforestation. Incidentally, there are many villages on the mountain range. The original villages were located on the periphery of the mountain range owing to the mild habitat condition. Thus, new developments accompanying deforestation occur mainly in undeveloped areas such as forest near mountain ridges. However, if the ridge area elevation is high, the area would have a low risk of deforestation because the elevation factor (coefficient: −0.004) compensates for the increased risk owing to the distance factor (coefficient: −0.00006) at the same unit meter.

Unplanned forest destruction or unauthorized deforestation, such as wildfires or illegal logging, are regularly monitored by the authorities. However, assessing the deforestation risk and preparing preemptive countermeasures based on the evaluation is difficult with

FIGURE 7
Estimated deforestation risk in 2022.

only monitoring. However, survival analysis makes it possible to assess the risk of deforestation quantitatively and predict long term deforestation based on the covariates and estimated risk. Figure 7 shows the deforestation risk in 2022 calculated based on the Weibull regression results. The value changes depending on the year of prediction. The northern part of the mountain range is at a high deforestation risk, which has a relatively low elevation and gentle slope. The findings and method of this study could contribute to better forest management in Jeongmack mountain range, South Korea, but it is not restricted to this area.

5. Limitations of the study

There are several weaknesses and potential limitations to this study. The analyses are based on the published datasets. We have to admit no accuracy assessment of the GFC dataset has been conducted on a regional scale. The LC maps and FT map are quality controlled GIS data. However, the datasets have uncertainty related to the weakness in dating. Given the time it takes to create these data, there may be a time lag of one to 2 years between the information used and when the data is available. In contrast, GFC data provides continuous information over time, but has high accuracy uncertainty (Galiatsatos et al., 2020; Shimizu et al., 2020). Galiatsatos et al. (2020) found that the annual accuracy varies with the availability of cloud-free imagery. If cloud-free imagery is not available for the year in which deforestation occurs, deforestation detection is postponed until the next year in which imagery is available. Shimizu et al. (2020) reported a scale issue, the GFC dataset tend to miss forest disturbances smaller than 3 ha. Counting for the limitation of the GFC dataset, the results might underestimate the deforestation area and hazard ratios. Overall, including spatial and temporal accuracy assessments will improve the reliability of deforestation analysis.

It is worth noting that the survival analysis did not take into account the time-varying covariates. The covariates used in the research were all static; however, some covariates (e.g., distance to built-up area) vary over time and they can affect the deforestation risk. The time varying covariates of survival analysis models can provide in-depth information for assessing deforestation risk. The use of additional factors such as population change, economic growth, and climatic conditions will improve the performance of the model.

Data availability statement

The original contributions presented in the study are included in the article/Supplementary material, further inquiries can be directed to the corresponding author.

Author contributions

The study was designed by KC and M-SB. Data collection and analysis were conducted by S-JK, KC, and TD. The manuscript writing was performed by KC and TD. All authors contributed to the article and approved the submitted version.

Funding

This study was supported by National Institute of Forest Science, Republic of Korea, through the 'Systematization of forest space management in Baekdudaegan, Jeongmack and development of conservation and restoration systems by zone'. This research was partly supported by the Basic Science Research Program through the National Research Foundation of Korea (NRF) [2020R1I1A1A01067345], funded by the Ministry of Education.

Conflict of interest

Publisher's note

Supplementary material

The Supplementary material for this article can be found online at: https://www.frontiersin.org/articles/10.3389/ffgc.2023.1183509/full#supplementary-material

References

Adams, C., Chamlian Munari, L., Van Vliet, N., Sereni Murrieta, R. S., Piperata, B. A., Futemma, C., et al. (2012). Diversifying incomes and losing landscape complexity in Quilombola shifting cultivation communities of the Atlantic rainforest (Brazil). *Hum. Ecol.* 41, 119–137. doi: 10.1007/s10745-012-9529-9

Allison, H. (2016). The fall and rise of South Korea's forests. *Q. J. For.* 110, 37–41.

Ameztegui, A., Morán-Ordónez, A., Márquez, A., Blázquez-Casado, Á., Pla, M., Villero, D., et al. (2021). Forest expansion in mountain protected areas: trends and consequences for the landscape. *Landsc. Urban Plan.* 216:104240. doi: 10.1016/j.landurbplan.2021.104240

An, L., and Brown, D. G. (2008). Survival analysis in land change science: integrating with GIScience to address temporal complexities. *Ann. Assoc. Am. Geogr.* 98, 323–344. doi: 10.1080/00045600701879045

Bae, J. S., Joo, R. W., and Kim, Y. S. (2012). Forest transition in South Korea: reality, path and drivers. *Land Use Policy* 29, 198–207. doi: 10.1016/j.landusepol.2011.06.007

Bae, J. S., Lee, K. H., Lee, Y. G., Youn, H. J., Park, C. R., Choi, H. T., et al. (2014). Lessons Learned from the Republic of Korea's National Reforestation Programme. Korea Forest Service, Daejeon, Republic of Korea. Available at: https://www.cbd.int/ecorestoration/doc/Korean-Study_Final-Version-20150106.pdf.

Barlow, J., Lennox, G. D., Ferreira, J., Berenguer, E., Lees, A. C., Mac Nally, R., et al. (2016). Anthropogenic disturbance in tropical forests can double biodiversity loss from deforestation. *Nature* 535, 144–147. doi: 10.1038/nature18326

Buckingham, K., and Hanson, C. (2015). *The restoration diagnostic case example South Korea*. South Korea: World Resources Institute.

Cervera, T., Pino, J., Marull, J., Padró, R., and Tello, E. (2019). Understanding the long-term dynamics of forest transition: from deforestation to afforestation in a Mediterranean landscape (Catalonia, 1868–2005). *Land Use Policy* 80, 318–331. doi: 10.1016/j.landusepol.2016.10.006

Cho, K. H., Hong, S. K., and Cho, D. S. (2008). Ecological role of mountain ridges in and around Gwangeung Royal Tomb forest in Central Korea. *Journal of Plant Biology* 51, 387–394. doi: 10.1007/BF03036058

Choi, Y. K. (2004). "Baekdudaegan, the central Axis of the Korean peninsular: the path toward management strategies regarding to its concepts" in *Ecological issues in a changing world*. eds. S. K. Hong, J. A. Lee, B. S. Ihm, A. Farina, Y. Son and E. S. Kim (Dordrecht: Springer), 355–383.

Choi, G., Jeong, Y., and Kim, S. I. (2019). Success Factors of National-Scale Forest Restorations in South Korea, Vietnam, and China. *Sustainability* 11, 1–17. doi: 10.3390/su11123488

Choi, S. M., Kweon, H. K., Lee, J. W., Choi, Y. H., and Choi, T. J. (2014). A study on deterioration of Ridge Trail in Jeongmaek. *Korean Journal of Environment and Ecology* 28, 450–456. doi: 10.13047/KJEE.2014.28.4.450

Chung, M. Y., López-Pujol, J., and Chung, M. G. (2016). Is the Baekdudaegan "the southern Appalachians of the east"? *A comparison between these mountain systems, focusing on their role as glacial refugia, Korean Journal of Plant Taxonomy* 46, 337–347. doi: 10.11110/kjpt.2016.46.4.337

Chung, M. Y., Son, S., Suh, G. U., Herrando-Moraira, S., Lee, C. H., López-Pujol, J., et al. (2018). The Korean Baekdudaegan Mountains: a glacial refugium and a biodiversity hotspot that needs to be conserved. *Front. Genet.* 9, 1–7. doi: 10.3389/fgene.2018.00489

Environmental Spatial Information Service. (2023). *Land cover mapping guidelines*. Available at: https://egis.me.go.kr/bbs/landcover.do (Accessed May 24, 2023).

FAO. (2020). *Global forest resources assessment 2020 in Main report*. Rome: Food and Agriculture Organization of the United Nations.

Feng, Y., Ziegler, A. D., Elsen, P. R., Liu, Y., He, X., Spracklen, D. V., et al. (2021). Upward expansion and acceleration of forest clearance in the mountains of Southeast Asia. *Nature Sustainability* 4, 892–899. doi: 10.1038/s41893-021-00738-y

Galiatsatos, N., Donoghue, D. N., Watt, P., Bholanath, P., Pickering, J., Hansen, M. C., et al. (2020). An assessment of global forest change datasets for national forest monitoring and reporting. *Remote Sens.* 12:1790. doi: 10.3390/rs12111790

Global Forest Watch. (2021). *South Korea deforestation rates & statistics*. Available at: https://www.globalforestwatch.org/dashboards/country/KOR/ (Accessed July 2, 2022).

Greenberg, J. A., Kefauver, S. C., Stimson, H. C., Yeaton, C. J., and Ustin, S. L. (2005). Survival analysis of a neotropical rainforest using multitemporal satellite imagery. *Remote Sens. Environ.* 96, 202–211. doi: 10.1016/j.rse.2005.02.010

Hadi, K., Krasovskii, A., Maus, V., Yowargana, P., Pietsch, S., Rautiainen, M., et al. (2018). Monitoring deforestation in rainforests using satellite data: a pilot study from Kalimantan, Indonesia. *Forests* 9, 1–26. doi: 10.3390/f9070389

Hagar, J. C., Eskelson, B. N. I., Haggerty, P. K., Nelson, S. K., and Vesely, D. G. (2014). Modeling marbled murrelet (*Brachyramphus marmoratus*) habitat using LiDAR-derived canopy data. *Wildl. Soc. Bull.* 38, 237–249. doi: 10.1002/wsb.407

Hansen, M. C., Potapov, P. V., Moore, R., Hancher, M., Turubanova, S. A., Tyukavina, A., et al. (2013). High-resolution global maps of 21st-century forest cover change. *Science* 342, 850–853. doi: 10.1126/science.1244693

Hayes, P. (2010). Sustainable security in the Korean peninsula: envisioning a northeast Asian biodiversity corridor. *The Korean Journal of International Studies* 8, 197–229.

Hosonuma, N., Herold, M., Sy, V. D., Fries, R. S. D., Brockhaus, M., Verchot, L., et al. (2012). An assessment of deforestation and forest degradation drivers in developing countries. *Environ. Res. Lett.* 7:044009. doi: 10.1088/1748-9326/7/4/044009

Jang, G. S., Jeon, S. W., and Kim, S. S. (2008). Analyzing characteristics of forest damage withing the Geum-Buk mountain range. *Journal of the Korean Institute of Landscape Architecture* 36, 55–63.

Kang, W., Koh, I., Park, C. R., and Lee, D. (2012). An analysis of changes in forest fragmentation and morphology in surrounding landscapes of maeulsoops and Jinan-gun. *Korean J Ecol Environ.* 26, 941–951.

Kim, K. H., and Zsuffa, L. (1994). Reforestation of South Korea: the history and analysis of a unique case in forest tree improvement and forestry. *For. Chron.* 70, 58–64. doi: 10.5558/tfc70058-1

Kuuluvainen, T., and Gauthier, S. (2018). Young and old forest in the boreal: critical stages of ecosystem dynamics and management under global change. *Forest Ecosystems* 5, 1–15. doi: 10.1186/s40663-018-0142-2

Larrea-GallegosIan, G., and Vázquez-Rowe, I. (2021). Exploring machine learning techniques to predict deforestation to enhance the decision-making of road construction projects. *J. Ind. Ecol.* 26, 225–239. doi: 10.1111/jiec.13185

Lee, E. T., and Wang, J. W. (2003). *Statistical methods for survival data analysis*. Wiley Series in Probability and Statistics, Wiley, New York.

López-Carr, D. (2021). A review of small farmer land use and deforestation in tropical Forest Frontiers: implications for conservation and sustainable livelihoods. *Land* 10, 1–23. doi: 10.3390/land10111113

Mayfield, H. J., Smith, C., Gallagher, M., and Hockings, M. (2020). Considerations for selecting a machine learning technique for predicting deforestation. *Environ. Model Softw.* 131:104741. doi: 10.1016/j.envsoft.2020.104741

Mon, M. S., Mizoue, N., Htun, N. Z., Kajisa, T., and Yoshida, S. (2012). Factors affecting deforestation and forest degradation in selectively logged production forest: a case study in Myanmar. *For. Ecol. Manag.* 267, 190–198. doi: 10.1016/j.foreco.2011.11.036

Morton, D. C., DeFries, R. S., Shimabukuro, Y. E., Anderson, L. O., Arai, E., Espirito-Santo, F. D. B., et al. (2006). Cropland expansion changes deforestation dynamics in the southern Brazilian Amazon. *PNAS* 103, 14637–14641. doi: 10.1073/pnas.0606377103

Park, M., and Lee, H. (2014). Forest policy and law for sustainability within the Korean peninsula. *Sustainability* 6, 5162–5186. doi: 10.3390/su6085162

Pir Bavaghar, M. (2016). Deforestation modelling using logistic regression and GIS. *J. For. Sci.* 61, 193–199. doi: 10.17221/78/2014-JFS

QGIS Development Team. (2023). *QGIS geographic information system*. Open Source Geospatial Foundation Project. Available at: http://qgis.osgeo.org

R Core Team. (2023). *R: A language and environment for statistical computing*. R Foundation for Statistical Computing, Vienna, Austria. Available at: https://www.R-project.org/

Rosa, I. M., Purves, D., Souza, C. Jr., Ewers, R. M., et al. (2013). Predictive modelling of contagious deforestation in the Brazilian Amazon. *PLoS One* 8:e77231. doi: 10.1371/journal.pone.0077231

Sandker, M., Finegold, Y., D'Annunzio, R., and Lindquist, E. (2017). Global deforestation patterns: comparing recent and past forest loss processes through a spatially explicit analysis. *Int. For. Rev.* 19, 350–368. doi: 10.1505/146554817821865081

Sharma, P., Thapa, R. B., and Matin, M. A. (2020). Examining forest cover change and deforestation drivers in Taunggyi District, Shan State, Myanmar. *Environ. Dev. Sustain.* 22, 5521–5538. doi: 10.1007/s10668-019-00436-y

Shimizu, K., Ota, T., and Mizoue, N. (2020). Accuracy assessments of local and global Forest change data to estimate annual disturbances in temperate forests. *Remote Sens.* 12:2438. doi: 10.3390/rs12152438

Songer, M., Myint, A., Senior, B., DeFries, R., and Leimgruber, P. (2008). Spatial and temporal deforestation dynamics in protected and unprotected dry forests: a case study from Myanmar (Burma). *Biodivers. Conserv.* 18, 1001–1018. doi: 10.1007/s10531-008-9490-5

Tadono, T., Nagai, H., Ishida, H., Oda, F., Naito, S., Minakawa, K., et al. (2016). Generation of the 30 M-mesh global digital surface model by Alos prism. *ISPRS – Int. Arch. Photogramm. Remote Sens. Spatial Inf. Sci.* XLI-B4, 157–162. doi: 10.5194/isprsarchives-XLI-B4-157-2016

Therneau, T. M., and Grambsch, P. M. (2000). *Modeling survival data: Extending the cox model*. Springer: New York.

Vance, C., and Geoghegan, J. (2002). Temporal and spatail modeling of tropical deforestation: a survival analysis linking satellite and household survey data. *Agric. Econ.* 27, 317–332.

Wang, N., Brown, D. G., An, L., Yang, S., and Ligmann-Zielinska, A. (2013). Comparative performance of logistic regression and survival analysis for detecting spatial predictors of land-use change. *Int. J. Geogr. Inf. Sci.* 27, 1960–1982. doi: 10.1080/13658816.2013.779377

Yao, Y., Liang, S., Cheng, J., Lin, Y., Jia, K., and Liu, M. (2014). Impacts of deforestation and climate variability on terrestrial evapotranspiration in subarctic China. *Forests* 5, 2542–2560. doi: 10.3390/f5102542

Yu, J., Choi, W., Lee, S., and Choi, J. (2016). Forest degradation and spatial distribution of Forest land development. *Journal of the Korea Society of Environmental Restoration Technology* 19, 101–110. doi: 10.13087/kosert.2016.19.6.101

Zhang, Z. (2016). Parametric regression model for survival data: Weibull regression model as an example. *Ann Transl Med* 4:484. doi: 10.21037/atm.2016.08.45

frontiers | Frontiers in Forest and Global Change

TYPE Original Research
PUBLISHED 28 September 2023
DOI 10.3389/ffgc.2023.1206677

OPEN ACCESS

EDITED BY
Zishan Ahmad Wani,
Baba Ghulam Shah Badshah University, India

REVIEWED BY
Zeeshan Ahmad,
Quaid-i-Azam University, Pakistan
Shreekar Pant,
Baba Ghulam Shah Badshah University, India

*CORRESPONDENCE
Gopal Singh Rawat
✉ gsrawa59@gmail.com
Surendra Singh Bargali
✉ surendrakiran@rediffmail.com

RECEIVED 16 April 2023
ACCEPTED 12 September 2023
PUBLISHED 28 September 2023

CITATION
Bisht S, Bargali SS, Bargali K, Rawat YS and Rawat GS (2023) Dry matter dynamics and carbon flux along riverine forests of Gori valley, Western Himalaya.
Front. For. Glob. Change 6:1206677.
doi: 10.3389/ffgc.2023.1206677

Dry matter dynamics and carbon flux along riverine forests of Gori valley, Western Himalaya

Soni Bisht[1], Surendra Singh Bargali[1]*, Kiran Bargali[1],
Yashwant Singh Rawat[1] and Gopal Singh Rawat[2]*

[1]Department of Botany, Kumaun University, Nainital, India, [2]Wildlife Institute of India, Dehradun, India

Introduction: Riverine forests in the Himalaya represent a biodiverse, dynamic, and complex ecosystem that offers numerous ecosystem services to local and downstream communities and also contributes to the regional carbon cycle. However, these forests have not been assessed for their contribution to dry matter dynamics and carbon flux. We studied these parameters along three classes of riverine forests in eastern Uttarakhand, dominated by *Macaranga, Alnus*, and *Quercus-Machilus* forest.

Methods: Using volume equations, we assessed tree biomass, carbon storage, and sequestration in the study area.

Results: The total standing tree biomass in *Macaranga*, *Alnus*, and *Quercus-Machilus* forest ranged from 256.6 to 558.1 Mg ha^{-1}, 460.7 to 485.8 Mg ha^{-1}, and 508.6 to 692.1 Mg ha^{-1}, respectively. A total of 77.6–79.6% of vegetation biomass was stored in the aboveground biomass and 20.4–22.4% in belowground plant parts across the riverine forests. The carbon stock in *Macaranga* forest ranged from 115.5 to 251.1 Mg ha^{-1}, in *Alnus* forest from 207.3 to 218.6 Mg ha^{-1}, and in *Quercus-Machilus* forest from 228.9 to 311.4 Mg ha^{-1}. The mean annual litterfall was accounted maximum for *Quercus-Machilus* forest (5.94 $\pm$ 0.54 Mg ha^{-1} yr.$^{-1}$), followed by *Alnus* (5.57 $\pm$ 0.31 Mg ha^{-1} yr.$^{-1}$) and *Macaranga* forest (4.67 $\pm$ 0.39 Mg ha^{-1} yr.$^{-1}$). The highest value of litterfall was recorded during summer (3.40 $\pm$ 0.01 Mg ha^{-1} yr.$^{-1}$) and the lowest in winter (0.74 $\pm$ 0.01 Mg ha^{-1} yr.$^{-1}$). The mean value of net primary productivity and carbon sequestration was estimated to be highest in *Quercus-Machilus* forest (15.8 $\pm$ 0.9 Mg ha^{-1} yr.$^{-1}$ and 7.1 $\pm$ 0.9 Mg C ha^{-1} yr.$^{-1}$, respectively) and lowest in *Alnus* forest (13.9 $\pm$ 0.3 Mg ha^{-1} yr.$^{-1}$ and 6.1 $\pm$ 0.3 Mg C ha^{-1} yr.$^{-1}$, respectively).

Discussion: The results highlight that riverine forests play a critical role in providing a large sink for atmospheric CO$_2$. To improve sustainable ecosystem services and climate change mitigation, riverine forests must be effectively managed and conserved in the region.

KEYWORDS

biomass, litterfall, productivity, riverine, sequestration, volume equation

1. Introduction

Riverine forests play a significant role in ecosystem processes, including energy flow and carbon dynamics (Allan et al., 2021). These forests are also known to serve as important bio-corridors for the movement of a variety of faunal groups during various seasons (Rawat, 2017). They are a productive ecosystem and are hotspots for epiphytic orchids and agricultural output (Marwah et al., 2021). Riverine forests hold discrete ecological traits because of their interaction with the aquatic ecosystem. Thus, their borders can be identified by variations in soil conditions, vegetation, and other elements that represent this aquatic–terrestrial interaction (Naiman et al., 2000). The riverine forests all over the Himalayan region are susceptible to natural (floods and landslides), anthropogenic, and climatic fluctuations (Bookhagen and Burbank, 2010). Despite the importance of these forests, overexploitation, unrestricted grazing, fuel wood collection, agricultural development, boundary disputes, developmental projects, and linear infrastructures pose a serious threat to these ecosystems (Merawi, 2016; Rajpara et al., 2022).

The riverine forests in the Himalayan region are represented by a number of early and mid-seral communities such as *Acacia catechu–Dalbergia sissoo* along foothills, *Drypetes roxburghii–Toona ciliata*, *Duabanga grandiflora–Terminalia myriocarpa* (eastern Himalaya), *Macaranga pustulata*, *Alnus nepalensis*, *Debregeasia hypoleuca*, *Hippophae salicifolia*, *Salix* species, and *Populus ciliata*, etc., at higher elevations (Champion and Seth, 1968; Rawat, 2017). Of these, most dominant forest formations, especially between 900 and 2,200 m above sea level, are formed by *Macaranga pustulata* and *Alnus nepalensis*. These species form early successional stages (Dhar et al., 1997), colonizing freshly eroded river banks and landslide areas. In Central and Eastern Himalaya, the following communities of riverine forests become more prevalent: *Macaranga* forests (below 1,000 m), *Alnus* forests between 1,000 and 2000 m, and *Quercus-Machilus* forests between 1,500 and 2,200 m asl. The alder forest frequently forms pure stands in landslide-prone areas, although it also occurs mixed with other late successional species in the Himalayan region (Joshi and Garkoti, 2021). It is primarily found close to moist habitats and can fix atmospheric nitrogen through symbiotic interaction with gram-positive *Frankia*, allowing it to survive exceptionally hard climatic conditions and hasten the natural succession (Crisafulli et al., 2015; Joshi and Garkoti, 2021). Due to their crucial role in socioeconomic advantages, ecological functioning, and soil conservation, the local communities depend on these forests for their sustenance needs (Bisht et al., 2022a).

The dry matter dynamics is a key indicator from the energy fixation and flux of biological materials point of view (Anderson, 1971). According to the Intergovernmental Panel on Climate Change, carbon stored in a forest ecosystem is divided into three main pools, i.e., biomass, litter, and soil. The carbon pools in a forest ecosystem are influenced by topography, forest structure, tree species composition, species diversity, age structure, edaphic conditions, and human-induced disturbances (Arasa-Gisbert et al., 2018; FSI, 2021). The current total carbon pool in the forested zone of the Indian Himalayan Region is about 103.9 Mg ha^{-1}, of which 23% is in the sub-tropical forests (FSI, 2021). Among the edaphic factors, the nutrient content in the soil may affect parameters such as tree growth and basal area and thus consequently influence the structure of plant communities (Becknell and Powers, 2014) and carbon storage. To formulate viable strategies to increase the soil carbon, it is critical to include soil restoration, forest regeneration, and nutrient management (Sagar and Singh, 2005; Lal, 2015). The majority of organic matter elaborated by plants through photosynthesis is returned to the soil as litter. The litterfall results in seasonal or constant input of organic matter and nutrients to the forest floor and represents one of the most important pathways for the transfer of energy, affecting the growth and development of the vegetation and soil pool (Mfilinge et al., 2002).

There is a paucity of literature on the structure and functioning of these forests from the region. Therefore, the assessment of riverine forests, including their conservation status and potential for carbon flux, standing biomass, productivity, and carbon accumulation, is critical for long-term conservation planning and national accounting of the United Nations convention on climate change. Since forests sequester carbon from the atmosphere as part of the growth process, any increase in the biomass constitutes a sink that reduces the build-up of atmospheric carbon dioxide. This emphasizes the importance of forest ecosystems in the global carbon cycle and the necessity to accurately evaluate the amount of carbon stored in forest ecosystems (Pan et al., 2011). Interestingly, this is the first study on the dynamics of dry matter and carbon flux in riverine forests from the Gori valley, Western Himalaya. There is no prior literature on forest biomass and accumulation of carbon for this region. This stimulated the estimation of productivity and sequestration to understand the functioning of the riverine forest ecosystem. The information obtained from this study will significantly contribute to the dry matter dynamics and carbon cycle across the globe. Furthermore, it will benefit forest officials and ecologists for the conservation and restoration of riverine habitats. Thus, the present study was conducted to address the following questions: (1) How does the altitude affect phytosociological parameters in the region? (2) What is the pattern of biomass and net primary productivity in the riverine forests? (3) What is the magnitude of litterfall? (4) How do the carbon stock and sequestration potential vary in the riverine forests of Kumaun Himalaya, India?

2. Materials and methods

2.1. Study area

The study was carried out in the Gori watershed of the eastern Kumaun region, encompassing an area of 1920 km^2 (Figure 1). Out of the 11 micro-watersheds, 6 (Dogrigad, Ghosigad, Painagad, Madkani river, Dhuratoli, and Patmoligad) were selected for the study after a reconnaissance survey. These study sites were located at 29°45′11.03 to 30°20′56.20 N and 80°22′49.90 to 80°11′41.34 E between 900 and 2,200 m asl in Pithoragarh district of Uttarakhand state. All the sampling was done within a 500 m distance of rivers and rivulets. The riverine forests in the study area are represented by two early seral communities (*Macaranga* and *Alnus*) and two more stable and climax communities (*Toona-Engelhardia* and *Quercus-Machilus*). Around 25.5% (489.2 km^2) of the geographical study area consists of forest, with broadleaf deciduous forest (*Macaranga, Alnus*) and broadleaf evergreen forest (*Quercus-Machilus*) occupying a 25.1 and 36.3 km^2 area, respectively. The area forms a transition zone between eastern (*M. pustulata*) and western (*Pinus roxburghii* and *Q. semecarpifolia*) Himalayan forests and comprises an exceptional diversity of orchid flora (Bisht and Adhikari, 2014). However, *Toona-Engelhardia* patches along the Gori river have disappeared from lower altitudes due to linear infrastructure and development projects.

2.2. Climate

The annual climate of the area is monsoon type, which can be divided into three prominent seasons, i.e., winter (October to February), summer (March to mid-June), and rainy season (mid-June to September). The mean maximum monthly temperature ranges from 15.1°C (January) to 30.4°C (June), and the minimum temperature ranges from 2.6 (January) to 18.8 (July). The average annual precipitation is 793.6 mm, and the annual mean relative humidity is 51.2% (Figure 2).

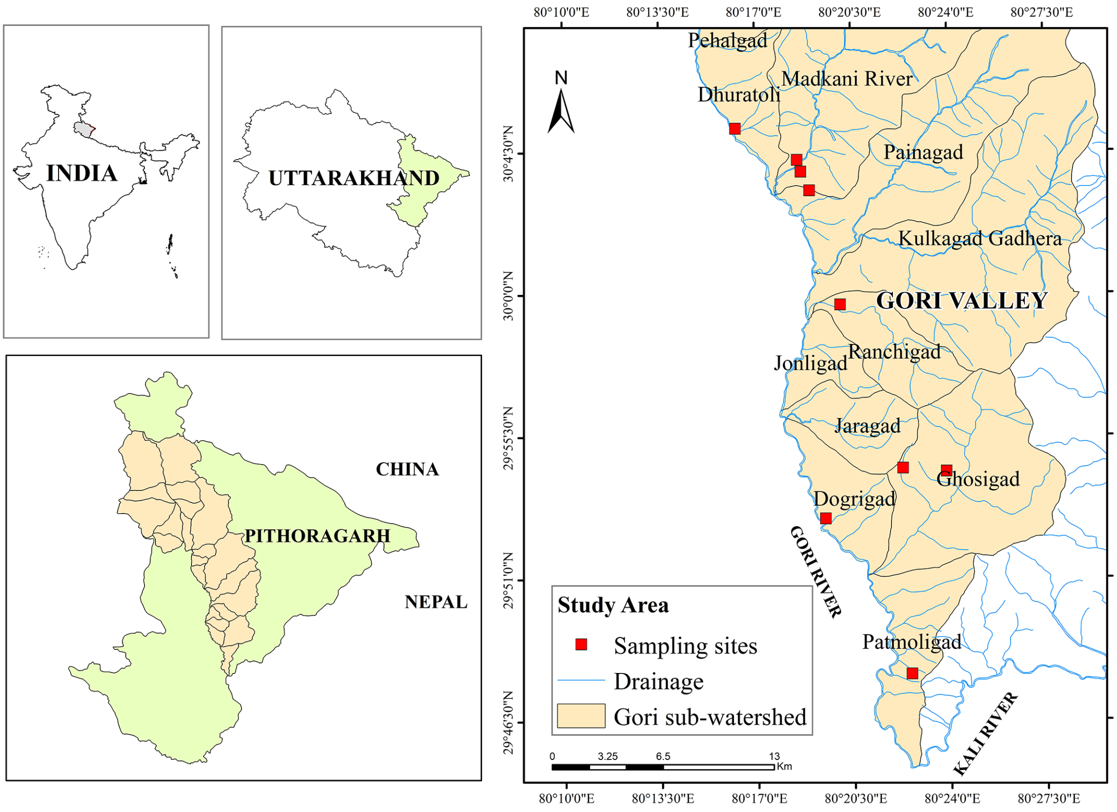

FIGURE 1
Map of study area showing sampling points and micro-watersheds in Gori valley, Western Himalaya.

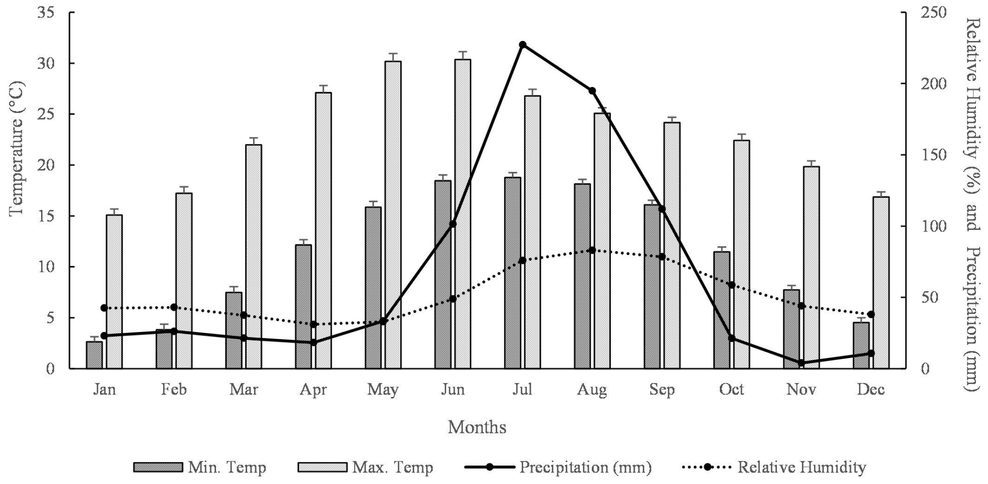

FIGURE 2
Meteorological data of the study area from 1981 to 2019 (Source: https://power.larc.nasa.gov, accessed on 6 June 2022).

2.3. Geology

The dominant rock types include phyllites, schists, gneisses, siltstone, and basic intrusive rocks belonging to the Vaikrita Group, especially in the Gori valley (Dumka, 2011; Ali et al., 2013). Between Baram and Baikot, a steeply dipping NNWSSE (western syncline) trending fault coincides with the thrust, defining the base of the Chhiplakot Klippe. Significantly, a subvertical slab of coarse-grained, unmetamorphosed granite with accompanying quartz porphyry and felsite is emplaced along the fault zone, bringing about contact metamorphism in the Precambrian to Lower Paleozoic dolomite and carbonaceous slate of the Tejam zone. Its mylonitized and greatly shared border along the wide valley bears testimony to the post-emplacement movement along the fault. There is yet another similar granitic body right within the same sedimentary, between dolomites and carbonaceous slates, discernible in the tract further downstream in the valley between Toli and Chiphaltara (Valdiya, 1976).

2.4. Soil sampling

2.4.1. Data collection

The soil samples from each forest site were collected from three depths (0–10, 10–20, and 20–30 cm) in triplicate with the help of a soil corer of known volume. The collected soil samples were systematically mixed and packed separately in zip lock bags and instantly transferred to the laboratory. Manual removal of coarse items such as stones, roots, and litter were carried out. The soil balls were crushed to separate the soil particles, and then, field damp soil samples were sieved with a 2 mm mesh and air dried to test the soil physico-chemical characteristics. The soil moisture (Mo) was determined gravimetrically by drying the soil samples in an oven to constant weight. The weight of the fresh soil and the oven dry weight of the same soil sample was expressed as a percentage of the difference of the moisture content (Jackson, 1958). The water-holding capacity (WHC) of the soil samples was measured by using the formula following Piper (1950). The bulk density (BD) was estimated with the help of a special mental core cylinder of known volume.

The soil pH was measured using a digital soil pH meter (Systronic-μ pH system 361) with ±0.05 accuracy. The soil water suspension was conducted in the ratio of 1:2. The instrument was calibrated with a standard buffer solution of pH 4, 7, and 9.2 before measurement. The soil organic carbon (OC) was determined using the Walkley and Black (1934) titration method following Jackson (1958). Nitrogen (N) was estimated using Kjeltec-2300 following the micro-Kjeldahl application of Peach and Tracey (1956) and Misra (1968). Available phosphorus (P) was estimated following the Olsen et al. (1954) method and potassium (K) by Flame Photometer after proper digestion of the samples. The factor of 1.724 was used to convert the OC into soil organic matter (SOM; Jackson, 1958; Misra, 1968). The value of organic carbon and SOM were determined by multiplying the values of carbon (%) with factors of 1.3 and 1.724, respectively.

2.5. Growing stock and biomass estimation

Nine forest sites were assessed for biomass and carbon stock based on altitudinal gradient. Within each site, 10 quadrats of a 10×10 m size were laid randomly with a replicate of three. All individual trees were measured for circumference at breast height (cbh) at 1.37 m from the ground (Singh et al., 1997). Following Curtis and McIntosh (1950), Misra (1968), and Mueller-Dombois and Ellenberg (1974), the data were analyzed for density and the basal area of the tree species for distinct forest types. The species diversity index was computed using the Shannon–Weiner diversity Index (Shannon and Weaver, 1949), and richness was considered as the total number of species in the sampled site (Wani and Pant, 2023). The forest types were identified using TWINSPAN.

The growing stock volume (GSV) equations (FSI, 1996, Table 1) were used to estimate aboveground biomass (Sharma et al., 2010; Dimri et al., 2017; Bisht et al., 2023) since allometric equations were not available for each species. The estimated GSV (m^3 ha^{-1}) was multiplied by the appropriate biomass expansion factor (Brown et al., 1999) to convert into aboveground biomass (AGB), i.e., stems, branches, twigs, and leaves. In addition, the equation of Cairns et al. (1997) was used to estimate belowground biomass (BGB), which reflects the biomass of root components.

TABLE 1 List of volume equations used for different tree species in the study sites based on Forest Research Institute and Forest Survey of India.

Tree species	Volume equations
Hardwood	
Acer acuminatum Wall. ex D.Don	$V=-0.162945+3.109717*D$
Alnus nepalensis D. Don	$V=0.0741-1.3603*D+10.9229*D^2$
Bauhinia variegata L.	$V=-0.04262+6.09491*D^2$
Betula alnoides Buch. -Ham.ex D. Don	$V=-0.12110+1.58826*D+1.96643*D^2$
Bombax ceiba L.	$V=0.136196-2.07674*D+10.1566*D^2$
Celtis australis L.	$\sqrt{V}=0.03629+3.95389*D-0.84421*\sqrt{D}$
Desmodium oojeinense (Roxb.) H. Ohashi	$V=0.025941-0.832619*D+8.285841*D^2$
Engelhardia spicata Bl.	$\text{Log}_e V=2.535662+2.519379 \log_e D$
Ficus neriifolia Sm.	$\sqrt{V}=0.03629+3.95389*D-0.84421*\sqrt{D}$
Ficus rumphii Bl.	$\sqrt{V}=0.03629+3.95389*D-0.84421*\sqrt{D}$
Grewia optiva J. R. Drumm. ex Burret	$V=-0.01611+4.90810*D^2$
Lyonia ovalifolia (Wall.) Drude.	$V=0.03468-0.56878*D+4.72282*D^2$
Macaranga pustulata King ex Hook.f.	$V=0.13333-2.18825*D+13.12678*D^2$
Machilus odoratissima Nees	$V=6.678*D*D-0.240*D-0.024$
Mallotus philippensis (Lam.) Mull. Arg.	$V=0.14749-2.87503*D+19.61977*D^2-19.11630*D^3$
Persea duthiei (King) Kosterm.	$V=6.678*D*D-0.240*D-0.024$
Pyrus pashia Buch. -Ham. ex D.Don	$V=0.046-0.646*D+4.272*D^2$
Quercus floribunda Lindl. ex *A. Camus*	$V=0.0988-1.55471*D+10.16317*D^2$
Quercus glauca Thunb.	$\sqrt{V}=0.04430-0.84266*D+6.362390*D^2+2.27556*D^3$
Quercus leucotrichophora A.Cam. ex Bah.	$\sqrt{V}=0.240157+3.820069*D-1.39452*\sqrt{D}$
Rhododendron arboreum Sm.	$V=0.06007-0.21874\sqrt{D}+3.63428*D^2$
Sapium insigne (Royle) Trim.	$V=-0.06440+0.48094*D+4.61818*D^2$
Shorea robusta Gaertn.	$\sqrt{V}=0.03085-0.77794*D+8.42051*D^2+5.91067*D^3$
Symplocos chinensis (Lour.) Druce	$V=-0.212798+3.288996*D+0.046417*\sqrt{D}$
Syzygium cumini (L.) Skeels.	$\log_e V=2.132776+2.479397*\log_e D$
Toona ciliata M. Roem.	$V=-0.27525+3.0319*D$
Rest of the species	$V=0.007602-0.033037*D+1.868567*D^2+4.483454*D^3$
Softwood	
Pinus roxburghii Sarg.	$\sqrt{V}=0.05131+3.9859*D-1.0245*\sqrt{D}$

*V-volume (m^3) under bark, D-diameter at breast height (1.37 m) over bark in meters.

The sum of AGB and BGB yielded the total biomass for trees (TB, Mg ha^{-1}).

2.6. Estimation of litterfall and net primary productivity

The litterfall was estimated annually by placing five litter traps at different locations at each forest site. Each wooden trap was 0.5×0.5×0.15 m in size and fitted with a nylon net at the bottom. The litter from each trap was collected in a zip-lock bag season wise, i.e., winter (October to February), summer (March to May), and rainy season (June to September). The samples were then brought to the laboratory and oven-dried at 80°C. Half of the oven-dried weight of the collected litter from each site was considered its carbon content (Verma and Jain, 2017).

For the estimation of productivity in each forest, 1/4th of the trees were marked in the year 2017, and their cbh was remeasured in each sampling plot in the subsequent year, i.e., 2018. The net change in biomass ($\Delta B = B_2$-B_1) yielded annual biomass accumulation. Annual litterfall was added to the aboveground biomass accumulation, and one-fifth of the leaf litter was added to the belowground biomass accumulation as mortality in fine roots (Orlov, 1968; Ogino, 1977). The latter value equaled net primary productivity. The biomass accumulation ratio (BAR), a measure of biomass to net primary productivity, was used to characterize the production condition in the forest communities (Whittaker, 1975).

2.7. Estimation of carbon stock and sequestration

For the total carbon stock (TC, Mg C ha^{-1}), we multiplied TB with species-specific carbon factor, where the C factor of 46% was used for forest types in which all conifers collectively constituted more than half of the forest composition. The C was taken as 45% for forest types where conifers and broadleaf species coexisted or where broadleaf species constituted more than half of the total (Manhas et al., 2006). Net change in carbon stock (ΔC) was calculated by subtracting the carbon stock of two consecutive years. Annual accumulation of carbon in the litter was added to ΔC to obtain the carbon sequestration potential (CSP) at each site (Awasthi et al., 2022).

3. Results

3.1. Phytosociological attributes

All riverine forests occurred within a 15–50° slope along the river or stream. A total of 43 tree species belonging to 37 genera and 27 families were recorded along the altitudinal gradient. Among these, most were angiosperms (97.7%). The three forest types identified near the riverine habitat were *Macaranga* (890–1,500 m), *Alnus* (1355–1,645 m), and *Quercus-Machilus* (1865–2,195 m) forest. The tree density was at the maximum in *Quercus-Machilus*, ranging from 510 to 790 individuals ha^{-1}, followed by *Alnus* (480,630 individuals ha^{-1}) and *Macaranga* forest (470–640 individuals ha^{-1}). The total basal area was highest in *Quercus-Machilus* forest, ranging from 31.4 to 51.4 m^2 ha^{-1}, followed by *Alnus* forest (26.8–39.5 m^2 ha^{-1}) and *Macaranga* forest (11.7–27.2 m^2 ha^{-1}). The tree diversity was highest in *Macaranga* forest site 2 (2.09), and it was lowest in *Alnus* forest site 1 (0.32). In terms of tree richness, *Macaranga* forest site 2 had the maximum (14 spp.) and *Alnus* forest site 1 and 3 (4 spp. each) had the minimum number of species (Table 2).

3.2. Soil properties

Across the sampled sites, soil was slightly acidic in nature, and pH varied between 5.3 ± 0.1 (*Alnus* site 3) and 6.4 ± 0.1 (*Quercus-Machilus* site 1). The soil moisture ranged from 17.7 ± 1.9% (*Quercus-Machilus* site 2) to 31.4 ± 1.1% (*Macaranga* site 2). The water-holding capacity varied between 28.3 ± 1.6% (*Quercus-Machilus* site 2) and 33.9 ± 1.5% (*Macaranga* site 2). The bulk density ranged from 0.39 ± 0.05 to 0.72 ± 0.04 g cm^{-3} at *Macaranga* site 3 and *Quercus-Machilus* site 1, respectively (Table 3).

TABLE 2 Description and characteristics of riverine forest communities in the study area.

Forest types	Site	Altitude (m)	Micro-watershed	Dominant species	Co-dominant species	CC (%)	Density (individuals ha^{-1})	Total basal area (m^2 ha^{-1})	H	TR
Macaranga	1	890	Dogrigad	*M. pustulata*	*Engelhardia spicata, Sapium insigne, Toona ciliata, Bombax ceiba, Mallotus philippinensis*	30	530	11.7	1.24	6
	2	1,125	Patmoligad			55	470	27.0	2.09	14
	3	1,500	Painagad			60	640	27.2	1.58	8
Alnus	1	1,355	Dhuratoli	*A. nepalensis*	*Carpinus viminea, Lyonia ovalifolia, Q. leucotrichophora, E. spicata*, etc.	60	580	39.5	0.32	4
	2	1,500	Madkani river			55	480	26.8	1.52	9
	3	1,645	Madkani river			30	630	38.2	0.36	4
Quercus-Machilus	1	1865	Ghosigad	*Quercus leucotrichophora, Neolitsea cuipala*	*Persea duthiei, Neolitsea pallens, Betula alnoides, Pyrus pashia, Machilus odoratissima*, etc.	55	510	47.4	1.67	10
	2	2065	Madkani river			40	790	51.4	1.80	9
	3	2,195	Dogrigad			15	780	31.4	1.81	10

CC, canopy cover; H, diversity; TR, tree richness.

TABLE 3 Soil physico-chemical properties in different riverine forests.

Site	Mo (%)	WHC (%)	BD (g cm^{-3})	pH	OC (%)	*N* (%)	*P* (Kg ha^{-1})	*K* (Kg ha^{-1})	SOM (%)	SCS (Mg C ha^{-1})
M1	24.6 ± 1.5	28.6 ± 1.0	0.46 ± 0.04	5.5 ± 0.1	1.98 ± 0.11	0.16 ± 0.02	19.6 ± 0.9	105.4 ± 5.0	3.4 ± 0.2	9.0 ± 0.3
M2	31.4 ± 1.1	33.9 ± 1.5	0.44 ± 0.06	5.5 ± 0.1	2.72 ± 0.15	0.18 ± 0.01	22.6 ± 1.2	116.4 ± 9.6	4.7 ± 0.3	11.8 ± 1.1
M3	27.0 ± 1,1	29.1 ± 0.8	0.39 ± 0.05	5.4 ± 0.1	2.23 ± 0.10	0.17 ± 0.03	22.3 ± 1.1	124.8 ± 10.7	3.9 ± 0.2	8.7 ± 0.7
A1	26.0 ± 1.4	31.2 ± 1.4	0.53 ± 0.07	5.5 ± 0.0	2.93 ± 0.19	0.19 ± 0.01	19.0 ± 1.8	107.4 ± 17.8	5.0 ± 0.3	15.2 ± 1.2
A2	24.3 ± 1.7	31.0 ± 1.5	0.44 ± 0.06	5.4 ± 0.1	2.86 ± 0.16	0.20 ± 0.01	19.9 ± 1.3	118.1 ± 14.6	4.9 ± 0.3	12.4 ± 1.0
A3	21.4 ± 1.2	28.4 ± 2.7	0.42 ± 0.07	5.3 ± 0.1	3.10 ± 0.15	0.24 ± 0.02	21.5 ± 1.8	149.7 ± 37.5	5.3 ± 0.3	12.7 ± 1.5
B1	19.1 ± 1.8	31.2 ± 1.2	0.72 ± 0.04	6.4 ± 0.1	2.81 ± 0.14	0.16 ± 0.01	11.0 ± 1.5	143.7 ± 25.0	4.8 ± 0.2	18.4 ± 1.0
B2	17.7 ± 1.9	28.3 ± 1.6	0.65 ± 0.06	6.2 ± 0.2	3.66 ± 0.17	0.19 ± 0.02	13.8 ± 1.4	152.0 ± 12.4	6.3 ± 0.3	22.9 ± 1.1
B3	18.5 ± 1.9	30.5 ± 1.0	0.64 ± 0.06	6.0 ± 0.2	3.15 ± 0.14	0.18 ± 0.01	15.4 ± 0.8	176.4 ± 13.7	5.4 ± 0.2	13.2 ± 1.5

M, Macaranga forest; A, Alnus forest; B, Quercus-Machilus forest, and numeric after alphabet denotes site 1, 2, and 3 in each forest type, Mo-moisture, WHC-water-holding capacity, BD-bulk density, OC-organic carbon, N-total nitrogen, P-available phosphorus, K-available potassium, SOM-soil organic matter, SCS-soil carbon stock.

TABLE 4 Aboveground biomass (AGB), belowground biomass (BGB), total biomass (TB), net primary productivity (NPP), biomass accumulation ratio (BAR), aboveground carbon stock (AGC), belowground carbon stock (BGC), total carbon stock (TC), and carbon sequestration potential (CSP) along the altitudinal gradient in riverine forests.

Forest	Macaranga			Alnus			Quercus-Machilus		
Sites	1	2	3	1	2	3	1	2	3
AGB (Mg ha^{-1})	198.1	397.9	435.6	377.2	361.4	389.4	544.2	526.0	393.8
BGB (Mg ha^{-1})	58.6	116.3	122.5	92.6	99.3	96.4	147.9	144.6	114.8
TB (Mg ha^{-1})	256.6	514.2	558.1	469.8	460.7	485.8	692.1	670.7	508.6
NPP (Mg ha^{-1} yr.$^{-1}$)	12.76	14.79	14.52	12.93	13.67	14.99	11.98	18.78	16.78
BAR	20.12	37.73	35.41	35.63	34.36	32.41	57.75	35.72	30.30
AGC (Mg C ha^{-1})	89.1	179.0	196.0	169.7	162.6	175.2	244.9	236.7	177.2
BGC (Mg C ha^{-1})	26.4	52.3	55.1	41.7	44.7	43.4	66.6	65.1	51.7
TC (Mg C ha^{-1})	115.5	231.4	251.1	211.4	207.3	218.6	311.4	301.8	228.9
CSP (Mg ha^{-1} yr.$^{-1}$)	5.7	6.6	6.4	5.7	6.0	6.6	5.4	8.4	7.4

The organic carbon, total nitrogen, available phosphorus, and available potassium ranged from 1.98 ± 0.11% (*Macaranga* site 1) to 3.66 ± 0.17% (*Quercus-Machilus* site 2), 0.16 ± 0.02% (*Macaranga* site 1 and *Quercus-Machilus* site 1) to 0.24 ± 0.02% (*Alnus* site 3), 11.0 ± 1.5 Kg ha^{-1} (B1) to 22.6 ± 1.2 Kg ha^{-1} (*Macaranga* site 2), and 105.4 ± 5.0 Kg ha^{-1} (*Macaranga* site 1) to 176.4 ± 13.7 Kg ha^{-1} (*Quercus-Machilus* site 3), respectively (Table 3). The soil organic matter and soil carbon stock ranged from 3.4 ± 0.2% (*Macaranga* site 1) to 6.3 ± 0.3% (*Quercus-Machilus* site 2) and 8.7 ± 0.7 Mg C ha^{-1} (*Macaranga* site 3) to 22.9 ± Mg C ha^{-1} (*Quercus-Machilus* site 2), respectively.

3.3. Biomass, litterfall, and net primary productivity

The tree biomass ranged from 256.6–558.1 Mg ha^{-1} in *Macaranga* forest to 460.7–485.8 Mg ha^{-1} in *Alnus* forest and 508.6–692.1 Mg ha^{-1} in *Quercus-Machilus* forest (Table 4). Of the total biomass, the aboveground biomass (544.2 Mg ha^{-1}) and belowground biomass (147.9 Mg ha^{-1}) contributed the maximum in *Quercus-Machilus* forest site 1. However, aboveground biomass (198.1 Mg ha^{-1}) and belowground biomass (58.6 Mg ha^{-1}) recorded the minimum for *Macaranga* forest site 1. The dominant tree species in *Alnus* forest contributed 62–88% to total biomass. However, *Macaranga* and *Quercus-Machilus* forest contributed only 23–45% to total biomass. The total annual litterfall ranged from 4.01–5.35 Mg ha^{-1} yr.$^{-1}$ in *Macaranga* forest to 4.99–6.07 Mg ha^{-1} yr.$^{-1}$ in *Alnus* forest and 4.91–6.72 Mg ha^{-1} yr.$^{-1}$ in *Quercus-Machilus* forest (Table 5). Mean litterfall was recorded highest in *Quercus-Machilus* forest (5.94 ± 0.54 Mg ha^{-1} yr.$^{-1}$), followed by *Alnus* forest (5.57 ± 0.31 Mg ha^{-1} yr.$^{-1}$) and *Macaranga* forest (4.67 ± 0.39 Mg ha^{-1} yr.$^{-1}$). The maximum mean annual litterfall was accounted for the summer season (3.00 ± 0.25 Mg ha^{-1} yr.$^{-1}$) in *Quercus-Machilus* forest. However, it was observed at minimum during the winter season (0.76 ± 0.05 Mg ha^{-1} yr.$^{-1}$) for *Macaranga* forest. The net primary productivity ranged from 12.76–14.79 Mg ha^{-1} yr.$^{-1}$ in *Macaranga* forest to 12.93–14.99 Mg ha^{-1} yr.$^{-1}$ in *Alnus* forest and 11.98–18.78 Mg ha^{-1} yr.$^{-1}$ in *Quercus-Machilus* forest. Moreover, the biomass accumulation ratio varied between 20.12 and 57.75 for riverine forests in the sampled sites.

3.4. Carbon stock and sequestration potential

The carbon stock ranged from 115.5–251.1 Mg C ha^{-1} in *Macaranga* forest to 207.3–218.6 Mg C ha^{-1} in *Alnus* forest and 228.9–311.4 Mg C ha^{-1} in *Quercus-Machilus* forest. Of the total

TABLE 5 Seasonal pattern of litterfall (Mg ha^{-1} yr.$^{-1}$) in three distinct sites of different forests.

Forest	Site	Winter	Summer	Rainy	Total	Average
Macaranga	1	0.74 ± 0.01	1.79 ± 0.02	1.48 ± 0.00	4.01	4.67 ± 0.39
	2	0.85 ± 0.00	2.61 ± 0.01	1.89 ± 0.03	5.35	
	3	0.68 ± 0.02	2.44 ± 0.01	1.54 ± 0.01	4.66	
Alnus	1	0.88 ± 0.04	2.70 ± 0.01	2.06 ± 0.02	5.64	5.57 ± 0.31
	2	1.07 ± 0.00	2.34 ± 0.03	1.58 ± 0.02	4.99	
	3	1.32 ± 0.01	2.97 ± 0.01	1.78 ± 0.00	6.07	
Quercus-Machilus	1	0.90 ± 0.02	2.53 ± 0.00	1.48 ± 0.01	4.91	5.94 ± 0.54
	2	1.25 ± 0.02	3.40 ± 0.01	2.07 ± 0.01	6.72	
	3	0.94 ± 0.01	3.06 ± 0.02	2.18 ± 0.04	6.18	

carbon stock, the aboveground carbon was estimated to be highest in *Quercus-Machilus* forest site 1 (244.9 Mg C ha^{-1}) and lowest in *Macaranga* forest site 1 (89.1 Mg C ha^{-1}). In addition, belowground carbon was recorded at the maximum in *Quercus-Machilus* forest site 1 (66.6 Mg C ha^{-1}) and the minimum in *Macaranga* forest site 1 (26.4 Mg C ha^{-1}). The carbon sequestration potential ranged from 5.7–6.6 Mg C ha^{-1} yr.$^{-1}$ (*Macaranga* forest) to 5.7–6.6 Mg C ha^{-1} yr.$^{-1}$ (*Alnus* forest) and 5.4–8.4 Mg C ha^{-1} yr.$^{-1}$ (*Quercus-Machilus* forest).

4. Discussion

The dry matter dynamics and the carbon flux of the forest are influenced by the structural and functional characteristics of the forest stand. The tree density ($r = 0.73$) and total basal area ($r = 0.71$) increased with increasing altitude in the riverine forests. In the present study, the density and total basal area in riverine forests were reported to be higher in contrast to previous studies (Rawal and Pangtey, 1994; Dhar et al., 1997). The richness and diversity across the sites were observed to be lesser than the values reported by Dhar et al. (1997) in Kumaun Himalaya. A higher tree density in *Alnus* forest was recorded, while slightly lesser tree diversity and richness were recorded when compared with the values recorded by Gairola et al. (2011) in Garhwal Himalaya. In addition, lower tree density, richness, and diversity in broadleaf forest were recorded compared to the values observed by Gairola et al. (2011).

The physico-chemical characteristics of soil vary within space and time due to variation in topography, climate, weathering processes, vegetation cover, microbiological activity, season, and other biotic and abiotic factors (Bargali et al., 2019; Manral et al., 2020). Therefore, soil characteristics vary over relatively small distances throughout the Himalayan region, and species composition plays an important role in the formation of soil organic matter and influences soil-forming processes (Bargali et al., 2018). All the forest communities showed distinct soil physico-chemical characteristics in the present study. It was observed that soil organic carbon was significantly correlated ($r = 0.80$, $p < 0.05$) with the total basal area of the forest. The higher concentration of soil nutrients in *Alnus* forest was due to its nitrogen-fixing ability and nutrient-rich litter, which enhances the physico-chemical and biological characteristics of the soil (Awasthi et al., 2022). Alder, once established in degraded land, improves the physicochemical properties of soil (Perakis and Pett-Ridge, 2019; Joshi and Garkoti, 2021). Moreover, alder develops clustered roots that release phosphorus and carboxylates and other important elements available in the soil (Lambers et al., 2019). However, the soil in broadleaf forests is often deep and fertile and has a thick layer of humus.

Litterfall serves as a conduit between the tree canopy and the soil below, contributing nutrients gathered from the biomass and affecting the productivity of the forest (Pitman, 2013). Seasonality plays a key role in the fluctuation of litterfall. Both anthropogenic and natural factors, including climate change, may have an impact on litterfall output and seasonal progression. In the present study, the lower values of litterfall were due to lower tree density ($r = 0.69$), lower total basal area ($r = 0.72$), and other site conditions (Table 6). The amount of litterfall in any ecosystem shows a linear relationship with the canopy cover, tree size, tree density, and basal area of the forest (Navarroa et al., 2013). With an increase in annual litterfall input, the soil organic carbon ($r = 0.96$) and soil carbon stock ($r = 0.69$) have significantly increased in the forest sites. The litter of *Alnus* is nitrogen rich, which promotes soil carbon (Bissonnette et al., 2014; Perakis and Pett-Ridge, 2019) and thus markedly benefits soil fertility. The annual litterfall in the present study was estimated to be higher than the values reported by Sharma and Ambasht (1987) in eastern Himalaya, due to higher values of tree density and total basal area. According to Chen et al. (2014), litterfall peaks in the monsoon and summer seasons for temperate broadleaf forests. The peak litterfall production during the summer season reported in this study is an indication of the tree's physiological response to increased temperature.

Forest structure and composition had a substantial effect on biomass, carbon stock, and soil organic carbon. The tree biomass of the forest depends upon vegetation structure, species composition, and stand age (Bisht et al., 2022b). In terms of forest communities, *Quercus-Machilus* forest had the highest aboveground biomass, indicating a greater number of individuals with higher girth class. Moreover, *Macaranga* forest, with lower density and total basal area, had the lower aboveground biomass in the forest sites. The total biomass in *Alnus* and *Quercus-Machilus* forest was recorded to be higher compared to the values recorded by Singh and Singh (1987), Rikhari et al. (1997), Gairola et al. (2011), and Joshi and Garkoti (2021) in Uttarakhand Himalaya, which might be due to variation in species composition and girth class size. The value of tree biomass falls within the range reported

TABLE 6 Pearson's correlation matrix for different environmental variables in the study area.

	TBA	H	TR	OC	N	P	K	SOM	SCS	TC	LF	CSP
TD	0.40	0.05	−0.14	0.56	0.16	−0.34	0.74[b]	0.58	0.39	0.32	0.69[b]	0.81[b]
TBA		−0.07	−0.01	0.80[b]	0.26	−0.63	0.51	0.80[b]	0.89[a]	0.85[a]	0.72[b]	0.36
H			0.92[a]	0.01	−0.56	−0.26	0.23	0.03	0.11	0.35	−0.01	0.36
TR				0.08	−0.42	−0.15	0.17	0.10	0.10	0.39	0.06	0.25
OC					0.51	−0.47	0.64	0.99[a]	0.81[b]	0.60	0.96[a]	0.68[b]
N						0.33	0.23	0.50	0.07	−0.02	0.52	0.26
P							−0.54	−0.46	−0.77[b]	−0.57	−0.33	−0.17
K								0.64	0.43	0.52	0.68[b]	0.63
SOM									0.80[b]	0.61	0.96[a]	0.70[b]
SCS										0.72[b]	0.69[b]	0.45
TC											0.53	0.37
LF												0.79[b]

[a]Significant at 0.01 and [b]at 0.05; figures with no subscript are not significant; TD-tree density, TBA-total basal area, H-diversity, TR-tree richness, OC-organic carbon, N-nitrogen, P-phosphorus, K-potassium, SOM-soil organic matter, SCS-soil carbon stock, TC-total carbon stock, LF-litterfall, CSP-carbon sequestration potential.

by Sharma et al. (1998) in *Alnus* forest. Moreover, the tree biomass in the present study was recorded to be higher than the riverine *Shorea robusta* and riverine *A. catechu* forest of Sharma et al. (2010) and Sajad et al. (2021). In the Himalayan region, very few studies have been conducted on dry matter dynamics of riverine forests.

The net primary productivity is the key indicator of concern from the forest management and sustainability point of view. The productivity of the forest ecosystem depends upon the population dynamics, forest structure, species composition, growth traits, and rate of increment in given environmental and site conditions. The NPP reported for *Alnus* forest falls within the range reported by Singh and Singh (1987) and Rikhari et al. (1997). Furthermore, a key indicator of the potential age of the dominating species and the harshness of the environment, which measures the accumulation of primary persistent material, is the biomass accumulation ratio (Whittaker, 1975). The BAR in *Quercus-Machilus* forest was recorded at 41.3 ± 8.4, which was higher than the value (28.3 ± 1.9) reported by Singh et al. (1994) in Kumaun Himalaya. For *Alnus* plantation, the value falls within the range reported by Sharma et al. (1998). As the altitude rises, the mean value of the BAR increased due to larger amount of biomass production in the riverine forests.

The process of absorbing and exporting carbon varies considerably in forest ecosystems, depending on forest density, soil, and carbon stock. The carbon flux varies with the size, age, and species composition of trees in the forest ecosystem (Covey et al., 2012). The total carbon stock of the *Alnus* and *Quercus-Machilus* forest was higher than the values observed previously (Rikhari et al., 1997; Gairola et al., 2011). The carbon stock in the present study was higher than that of the riverine *S. robusta* and *A. catechu* forest recorded by Sharma et al. (2010). The significant relation between total basal area and carbon stock ($r = 0.85$) indicates that an increase in the stand basal area led to an increase in the carbon stock of the forest ecosystem. Carbon sequestration potential showed strong correlation with the tree density of the forest sites ($r = 0.81$, $p < 0.01$). According to Gera (2012), the variations in the sequestration potential can be attributed to the mean annual increment, which varies with forest site, age, density, and plantation. The present study reveals that soil is the largest pool of forest carbon, contributing 48.2–50.6%, followed by aboveground carbon (38.7–39.5%) and belowground carbon (10.1–11.6%, Figure 3).

5. Conclusion

It was observed that as altitude increased, there was a significant increase in both tree density and total basal area within riverine forests. The highest values for these parameters were documented in the *Quercus-Machilus* forest, while the lowest values were observed in the *Macaranga* forest. Similarly, tree biomass and productivity exhibited their peak values in the *Quercus-Machilus* forest (692.1 Mg ha^{-1}) and their lowest values in the *Macaranga* forest (66.91 Mg ha^{-1}). The annual litterfall demonstrated a seasonal variation, with higher levels during the summer (3.40 ± 0.01 Mg ha^{-1}) and lower levels in the winter (0.74 ± 0.01 Mg ha^{-1}), ranging from 4.01 Mg ha^{-1} in the *Macaranga* forest to 6.72 Mg ha^{-1} in the *Quercus-Machilus* forest. This investigation unveiled that the *Quercus-Machilus* forest not only stores a substantial amount of carbon (280.7 ± 26.0 Mg ha^{-1} yr.$^{-1}$) but also sequesters carbon effectively (7.1 ± 0.9 Mg C ha^{-1} yr.$^{-1}$) compared to the *Macaranga* and *Alnus* forests. In conclusion, the research indicates that a greater litterfall and higher forest density in riverine habitats exert a more pronounced influence on soil organic carbon content. Additionally, it was observed that *Alnus* forests significantly enhanced the nitrogen content in the forest ecosystem, positively affecting soil fertility.

This study contributes to our comprehension of carbon storage and fluxes within riverine forests in the Western Himalaya. Carbon offset programs such as REDD+ offer abundant opportunities and resources for the conservation of these forests, allowing for the retention of carbon reserves while simultaneously delivering supplementary ecosystem services to local communities. Consequently, it is advisable to contemplate the utilization of riverine forests for the restoration of deteriorated sites in the Western Himalaya, and the implementation of alder-based

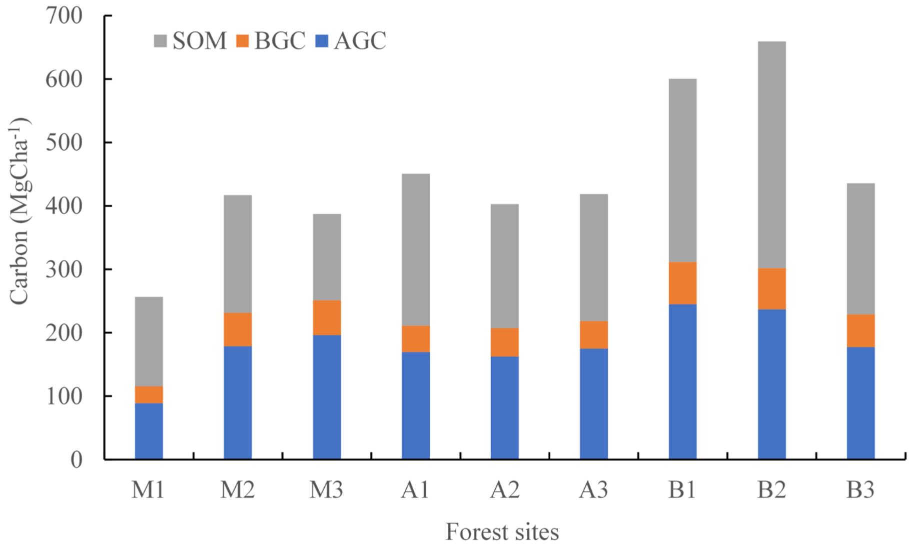

FIGURE 3
Density of carbon in soil and tree biomass in riverine forests of different sites (M-*Macaranga* forest, A-*Alnus* forest, B-*Quercus*-*Machilus* forest, and numeric after alphabet denotes site 1, 2, and 3 in each forest type, SOM-soil organic matter, AGC-aboveground carbon, and BGC-belowground carbon; for details, see Table 4).

restoration initiatives should be examined as a potential means to enhance carbon storage within ecosystems. This should be viewed as an integral element of climate change mitigation strategies and forest ecosystem management.

Data availability statement

The original contributions presented in the study are included in the article/supplementary material, further inquiries can be directed to the corresponding authors.

Author contributions

SB collected data, performed analysis, and prepared the manuscript. YR and SSB conceptualized. KB and GR finally reviewed the paper. All authors contributed to the article and approved the submitted version.

Funding

NMHS is duly acknowledged for providing funding for the project, Mainstreaming landscape approach for biodiversity conservation, improved livelihoods and ecosystem health in Kailash Sacred Landscape part of India, received by SB and GR.

Acknowledgments

The authors acknowledge the Director and Dean, Wildlife Institute of India, for providing the necessary facilities. The authors thank the Project Coordinator of the project “Mainstreaming Landscape Approach to Biodiversity Conservation, Livelihoods and Ecosystem Health in Kailash Sacred Landscape India” for encouragement. The authors are immensely grateful to the Uttarakhand State Forest Department for their permits to work in the high-altitude zones of the study area and are also thankful to the villagers and field assistants for their help.

Conflict of interest

The authors declare that the research was conducted in the absence of any commercial or financial relationships that could be construed as a potential conflict of interest.

Publisher's note

References

Ali, S. N., Biswas, R. H., Shukla, A. D., and Juyal, N. (2013). Chronology and climatic implications of late quaternary glaciations in the Goriganga valley, central Himalaya, India. *Quat. Sci. Rev.* 73, 59–76. doi: 10.1016/j.quascisrev.2013.05.016

Allan, J. D., Castillo, M. M., and Capps, K. A. (2021). “Carbon dynamics and stream ecosystem metabolism” in *Stream ecology: structure and function of running Waters*. eds. J. D. Allan, M. M. Castillo and K. A. Capps (Heidelberg: Springer Netherlands), 421–452.

Anderson, F. (1971). “Methods and preliminary results of estimation of biomass and primary production in south Swedish mixed deciduous woodland” in *Proceedings of Brussels symposium on productivity of forest ecosystems*. ed. P. Duvigneaud (Paris: Unesco), 281–288.

Arasa-Gisbert, R., Vayreda, J., Rom an-Cuesta, R. M., Villela, S. A., Mayorga, R., and Retana, J. (2018). Forest diversity plays a key role in determining the stand carbon stocks of Mexican forests. *For. Ecol. Manag.* 415–416, 160–171. doi: 10.1016/j.foreco.2018.02.023

Awasthi, P., Bargali, K., Bargali, S. S., and Jhariya, M. (2022). Structure and functioning of *Coraria nepalensis* dominated shrublands in degraded hills of Kumaun Himalaya. I. Dry matter dynamics. *Land Degrad. Dev.* 33, 1474–1494. doi: 10.1002/ldr.4235

Bargali, K., Manral, V., Padalia, K., Bargali, S. S., and Upadhyay, V. P. (2018). Effect of vegetation type and season on microbial biomass carbon in central Himalayan forest soils, India. *CATENA* 171, 125–135. doi: 10.1016/j.catena.2018. 07.001

Bargali, S. S., Padalia, K., and Bargali, K. (2019). Effects of tree fostering on soil health and microbial biomass under different land use systems in central Himalaya. *Land Degrad. Dev.* 30, 1984–1998. doi: 10.1002/ldr.3394

Becknell, J. M., and Powers, J. S. (2014). Stand age and soils as drivers of plant functional traits and aboveground biomass in secondary tropical dry forest. *Can. J. For. Res.* 44, 604–613. doi: 10.1139/cjfr-2013-0331

Bisht, S., and Adhikari, B. S. (2014). *Dendrobium longicornu*: an addition to the orchid flora of Western Himalaya. *Richardiana* 14, 157–168.

Bisht, S., Bargali, K., Bargali, S. S., Rawat, P. S., and Rawat, Y. S. (2022a). Carbon Pool in *Quercus lanuginosa* (D. Don) Forest of Askot wildlife sanctuary, Western Himalaya in relation to stand attributes. *Indian Forester* 148, 709–717. doi: 10.36808/if/2022/v148i7/168610

Bisht, S., Bargali, S. S., Bargali, K., Rawat, G. S., Rawat, Y. S., and Fartyal, A. (2022b). Influence of anthropogenic activities on Forest carbon stocks-a case study from Gori Valley, Western Himalaya. *Sustainability* 14:16918. doi: 10.3390/su142416918

Bisht, S., Rawat, G. S., Bargali, S. S., Rawat, Y. S., and Mehta, A. (2023). Forest vegetation response to anthropogenic pressures: a case study from Askot wildlife sanctuary, Western Himalaya. *Environ. Dev. Sustain.* 1, 1–25. doi: 10.1007/s10668-023-03130-2

Bissonnette, C., Fahlman, B., Peru, K. M., Khasa, D. P., Greer, C. W., Headley, J. V., et al. (2014). Symbiosis with Frankia sp. benefits the establishment of *Alnus viridis* spp. *Crispa* and *Alnus incana* spp. Rugosa in tailings sand from the Canadian oil sands industry. *Ecol. Eng.* 68, 167–175. doi: 10.1016/j.ecoleng.2014.03.06

Bookhagen, B., and Burbank, D. W. (2010). Toward a complete Himalayan hydrological budget: spatiotemporal distribution of snowmelt and rainfall and their impact on river discharge. *J. Geophys. Res.* 115:F03019. doi: 10.1029/2009JF001426

Brown, S. L., Schroeder, P., and Kern, J. S. (1999). Spatial distribution of biomass in forests of the eastern USA. *For. Ecol. Manag.* 123, 81–90. doi: 10.1016/S0378-1127(99)00017-1

Cairns, M. A., Brown, S., Helmer, E. H., and Baumgardner, G. A. (1997). Root biomass allocation in the world's upland forests. *Oecologia* 111, 1–11. doi: 10.1007/s004420050201

Champion, H. G., and Seth, S. K. (1968). *A revised survey of the Forest types of India*. New Delhi: Goverment of India Publications.

Chen, H., Gurmesa, G. A., Liu, L., Zhang, T., Fu, S., Liu, Z., et al. (2014). Effects of litter manipulation on litter decomposition in a successional gradient of tropical forests in southern China. *PLoS One* 9:e99018. doi: 10.1371/journal.pone.0099018

Covey, K. R., Orefice, J., and Lee, X. (2012). "The physiological ecology of carbon science in Forest stands" in *Managing Forest carbon in a changing climate*. eds. M. S. Ashton, M. L. Tyrrell, D. Spalding and B. Gentry (Heidelberg: Springer Netherlands), 31–49.

Crisafulli, C. M., Swanson, F. J., Halvorson, J. J., and Clarkson, B. D. (2015). "Volcano ecology: disturbance characteristics and assembly of biological communities" in *The encyclopedia of volcanoes*. ed. H. Sigurdsson. *2nd* ed (Cambridge, MA: Academic Press), 1265–1284.

Curtis, J. T., and McIntosh, R. P. (1950). The interrelations of certain analytical and synthetic phytosociological characters. *Ecology* 31, 434–455. doi: 10.2307/1931497

Dhar, U., Rawal, R. S., and Samant, S. S. (1997). Structural diversity and representativeness of forest vegetation in a protected area of Kumaun Himalaya, India: implications for conservation. *Biodivers. Conserv.* 6, 1045–1062. doi: 10.1023/A:1018375932740

Dimri, S., Baluni, P., and Sharma, C. M. (2017). Biomass production and carbon storage potential of selected old-growth temperate forests in Garhwal Himalaya, India. *Proc. Natl. Acad. Sci. India B Biol. Sci.* 87, 1327–1333. doi: 10.1007/s40011-016-0708-0

Dumka, R. K. (2011). Determination of crustal strain field in Kumaun Himalaya using global positioning system (GPS). *Geodesy* 13, 978–973.

FSI. (1996). *Volume equations for forests of India*, Forest Survey of India, Ministry of Environment and Forests, Government of India: Nepal and Bhutan.

FSI. (2021). *The state of forest report. Forest survey of India*. Dehradun: Ministry of Environment and Forests.

Gairola, S., Sharma, C. M., Ghildiyal, S. K., and Suyal, S. (2011). Live tree biomass and carbon variation along an altitudinal gradient in moist temperate valley slopes of the Garhwal Himalaya (India). *Curr. Sci.* 100, 1862–1870.

Gera, M. (2012). Poplar culture for speedy carbon sequestration in India: A case study from Terai region of Uttarakhand. *ENVIS Forest. Bull.* 12, 75–83.

Jackson, M. L. (1958). *Soil chemical analysis*. Prentice Hall, Inc., Englewood Clift, NJ.

Joshi, R. K., and Garkoti, S. C. (2021). Dynamics of ecosystem carbon stocks in a chronosequence of nitrogen-fixing Nepalese alder (*Alnus nepalensis* D. Don.) forest stands in the Central Himalayas. *Land Degrad. Dev.* 32, 4067–4086. doi: 10.1002/ldr.3901

Lal, R. (2015). Restoring soil quality to mitigate soil degradation. *Sustainability* 7, 5875–5895. doi: 10.3390/su7055875

Lambers, H., Nascimento, D. L., Oliveira, R. S., and Shi, J. (2019). Do cluster roots of red alder play a role in nutrient acquisition from bedrock? *Proc. Natl. Acad. Sci.* 116, 11575–11576. doi: 10.1073/pnas.1905336116

Manhas, R. K., Negi, J. D. S., Kumar, R., and Chauhan, P. S. (2006). Temporal assessment of growing stock, biomass and carbon stock of Indian forests. *Clim. Chang.* 74, 191–221. doi: 10.1007/s10584-005-9011-4

Manral, V., Bargali, K., Bargali, S. S., and Shahi, C. (2020). Changes in soil biochemical properties following replacement of Banj oak forest with Chir pine in central Himalaya, India. *Ecol. Proc.* 9:30. doi: 10.1186/s13717-020-00235-8

Marwah, G., Bisht, S., and Rawat, G. S. (2021). Patterns of distribution among epiphytic orchids and environmental factors in Gori valley, western Himalaya. *Orchid Soc. India* 35, 159–167.

Merawi, E. (2016). Identification of ecological threats, pressure and their relative severity of Temcha riverine forest, north west, Ethiopisa. *Am. J. Agric. For.* 4, 64–68. doi: 10.11648/j.ajaf.20160403.12

Mfilinge, P., Atta, N., and Tsuchiya, M. (2002). Nutrient dynamics and leaf litter decomposition in a subtropical mangrove forest at Oura Bay, Okinawa, Japan. *Trees* 16, 172–180. doi: 10.1007/s00468-001-0156-0

Misra, R. (1968). *Ecological work book*. Oxford and IBH Publishing Company, Calcutta.

Mueller-Dombois, D., and Ellenberg, E. (1974). *Aims and methods of vegetation ecology*. New York: John Wiley and Sons.

Naiman, R. J., Bilby, R. E., and Bisson, P. A. (2000). Riparian ecology and management in the Pacific coastal rain forest. *Bioscience* 50, 996–1011. doi: 10.1641/0006-3568(2000)050[0996:REAMIT]2.0.CO;2

Navarroa, F. B., Romero-Freireb, A., Del Castillob, T., Forondac, A., Jiméneza, M. N., Ripolla, M. A., et al. (2013). Effects of thinning on litterfall were found after years in a *Pinus halepensis* afforestation area at tree and stand levels. *For. Ecol. Manage.* 289, 354–362. doi: 10.1016/j.foreco.2012.09.026

Ogino, K. (1977). A beech forest at Ashiu-biomass, its increment and net production. *Primary Productivity of Japanese Forests*, 172–186.

Olsen, S., Cole, C., Watanabe, F., and Dean, L. (1954). *Estimation of available phosphorus in soils by extraction with sodium bicarbonate*. U.S.: Department of Agriculture Circular.

Orlov, A. J. (1968). *Development and life duration of pine feeding roots*. Productivity Studies in Root Systems and Rhizosphere Organisms. USSR, Leningrad, 139–145.

Pan, Y., Birdsey, R. A., Fang, J., Houghton, R., Kauppi, P. E., Kurz, W. A., et al. (2011). A large and persistent carbon sink in the World's forests. *Science* 333, 988–993. doi: 10.1126/science.1201609

Peach, K., and Tracey, M. (1956). *Modern methods of plant analysis*. Springer, Adelaide.

Perakis, S. S., and Pett-Ridge, J. C. (2019). Nitrogen-fixing red alder trees tap rock-derived nutrients. *Proc. Natl. Acad. Sci.* 116, 5009–5014. doi: 10.1073/pnas.1814782116

Piper, C. (1950). *Soil and plant analysis*. New York: The university of Adelaide, Academic Press.

Pitman, R. M. (2013). "Litterfall–biomass, chemistry, leaf area, and links with wider ecosystem functioning" in *Developments in environmental science*. eds. M. Ferretti and R. Fischer (Amsterdam, Netherlands: Elsevier), 251–264.

Rajpara, M. N., Rajparb, A. H., and Zakaria, M. (2022). Riverine forest as a significant habitat to harbor a wide range of bird species. *Braz. J. Biol.* 84:e256160. doi: 10.1590/1519-6984.256160

Rawal, R. S., and Pangtey, Y. S. P. (1994). High altitude forest in a part of Kumaun, central Himalaya. *Proc. Indian Natl. Sci. Acad.* B60, 557–564.

Rawat, G. S. (2017). "The Himalayan vegetation along horizontal and vertical gradients" in *Bird Migration in the Himalaya*. eds. H. T. Prins and T. Namgail (Cambridge, UK: Cambridge University Press), 189–204.

Rikhari, H. C., Adhikari, B. S., and Rawat, Y. S. (1997). Woody species composition of temperate forests along an elevational gradient in Indian central Himalaya. *J. Trop. For. Sci.* 10, 197–211.

Sagar, R., and Singh, J. S. (2005). Structure, diversity, and regeneration of tropical dry deciduous forest of northern India. *Biodivers. Conserv.* 14, 935–959. doi: 10.1007/s10531-004-0671-6

Sajad, S., Haq, S. M., Yaqoob, U., Calixto, E. S., and Hassan, M. (2021). Tree composition and standing biomass in forests of the northern part of Kashmir Himalaya. *Vegetos* 34, 857–866. doi: 10.1007/s42535-021-00234-w

Shannon, C. E., and Weaver, W. (1949). *The mathematical theory of communication*. University of Illinois Press, Urbana, USA.

Sharma, E., and Ambasht, R. S. (1987). Litterfall, decomposition and nutrient release in an age sequence of *Alnus nepalensis* plantation stands in the eastern Himalaya. *J. Ecol.* 75, 997–1010. doi: 10.2307/2260309

Sharma, C. M., Baduni, N. P., Gairola, S., Ghildiyal, S. K., and Suyal, S. (2010). Tree diversity and carbon stocks of some major forest types of Garhwal Himalaya, India. *For. Ecol. Manag.* 260, 2170–2179. doi: 10.1016/j.foreco.2010.09.014

Sharma, E., Sharma, R., and Pradhan, M. (1998). Ecology of Himalayan alder (*Alnus nepalensis* D. Don). *Proc. Indian Natl. Sci. Acad.* 64, 59–78.

Singh, S. P., Adhikari, B. S., and Zobel, D. B. (1994). Biomass, productivity, leaf longevity, and Forest structure in the central Himalaya. *Ecol. Monogr.* 64, 401–421. doi: 10.2307/2937143

Singh, S. P., Rawat, Y. S., and Garkoti, S. C. (1997). Failure of brown oak (*Quercus semecarpifolia*) to regenerate in central Himalaya: a case of environmental semisurprise. *Curr. Sci.* 73, 371–374.

Singh, J. S., and Singh, S. P. (1987). Forest vegetation of the Himalaya. *Bot. Rev.* 53, 80–192. doi: 10.1007/BF02858183

Valdiya, K. S. (1976). Himalayan transverse faults and folds and their parallelism with subsurface structures of north Indian plains. *Tectonophysics* 32, 353–386. doi: 10.1016/0040-1951(76)90069-X

Verma, S., and Jain, A. (2017). Carbon stock in biomass and litter in different plantation of tropical Forest research institute, Jabalpur. *J. Tree Sci.* 36, 29–33. doi: 10.5958/2455-7129.2017.00003.6

Walkley, A., and Black, C. A. (1934). An examination of Degtjareff methods for determining soil organic matter and a proposed modification of the chronic acid titration methods. *Soil Sci.* 37, 29–38. doi: 10.1097/00010694-193401000-00003

Wani, Z. A., and Pant, S. (2023). Assessment of floristic diversity and community characteristics of Gulmarg wildlife sanctuary, Kashmir Himalaya. *Geol. Ecol. Landsc.* 1–21, 1–21. doi: 10.1080/24749508.2023.2196767

Whittaker, R. H. (1975). *Communities and ecosystem*. *2nd Edn.* Macmillan Publ. Co., New York, 385.

Frontiers in
Forests and Global Change

Informs and promotes sustainable management of the world's forests

An innovative journal that places forests at the forefront of attention for scientists, policy makers and the public. It advances our understanding of how forests 'work', spanning from molecules to ecosystems to the biosphere.

Discover the latest Research Topics

See more →

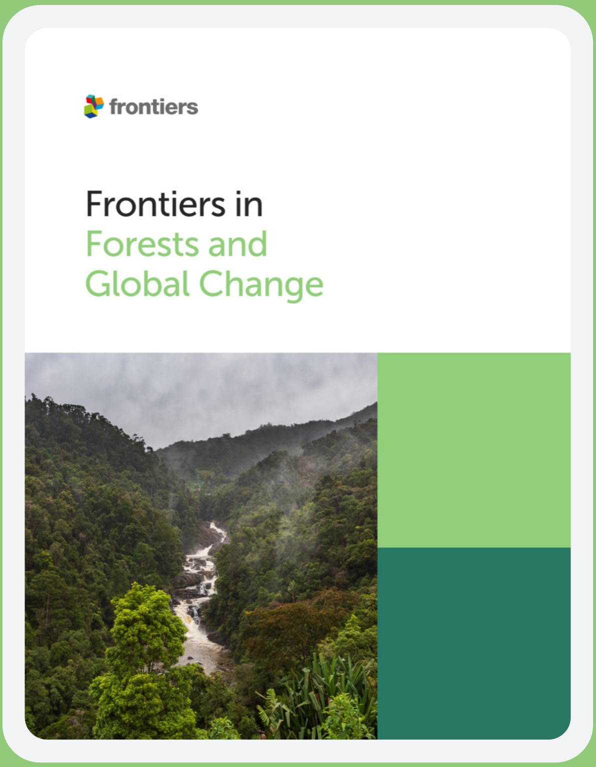

Frontiers

Avenue du Tribunal-Fédéral 34
1005 Lausanne, Switzerland
frontiersin.org

Contact us

+41 (0)21 510 17 00
frontiersin.org/about/contact

frontiers | Research Topics